182
117

DETERMINING PARAMETERS FOR STIFF CLAYS AND RESIDUAL SOILS USING THE SELF-BORING PRESSUREMETER

by

Philippe Mayu

Dissertation submitted to the Faculty of the

Virginia Polytechnic Institute and State University

in partial fulfillment of the requirements for the degree of

Doctor of Philosophy

in

Civil Engineering

APPROVED:

G.W Clough

J.M.Duncan

R.M.Jones

J.H.Hunter

R.D.Krebs

March, 1987

Blacksburg, Virginia

DETERMINING PARAMETERS FOR STIFF CLAYS AND RESIDUAL SOILS USING THE SELF-BORING PRESSUREMETER

by

Philippe Mayu

G.W Clough

Civil Engineering

(ABSTRACT)

As testing stiff soils in the laboratory often leads to information which is not consistent with field performance, research was undertaken to determine in situ the soil properties. Among the devices which generated interest is the self-boring pressuremeter (SBPM).

In this research, two stiff soils of the Commonwealth of Virginia were tested: A residual soil found in Blacksburg and a very stiff, non- fissured and sensitive clay, of marine origin, known as the Miocene clay of the downtown Richmond area.

Testing the residual soil of Blacksburg with the SBPM led to the following new operational approaches: (1) a systematic use of a steel-sheath known as "Chinese lantern" to protect the membrane of the probe, (2) the development of a loading frame providing adequate reaction when self-boring in stiff soils, (3) the development of a new calibration unit for the SBPM which allows to calibrate the probe under conditions more like those encountered in stiff soils and, (4) the development of a high capacity computerized data acquisition system.
Testing the residual soil also allowed to establish a sound data base for this soil.

In the Miocene clay, the laboratory test results indicate that conventional sampling technique which consists in pushing Shelby tubes disturbs significantly the soil and leads to scattered test results. In contrast, tests performed on samples taken from high quality block samples indicate consistent behavior patterns.

SBPM test results in the Miocene clay indicate that the clay exhibits high lateral stresses. They also indicate the existence of an anisotropic state of lateral stress which can be explained from the regional topography. The soil parameters interpreted from the SBPM test

results in the Miocene clay compare well with the soil parameters determined in the laboratory on the block samples.

Acknowledgements

The author is indebted to his advisor, Professor G. Wayne Clough for his interest, guidance and constructive criticism throughout the preparation of this dissertation.

The author wishes to express his sincere thanks and appreciation to Professors J. M. Duncan, J. H. Hunter, R. M. Jones and R. D. Krebs for serving on his dissertation committee, reviewing the manuscript and offering valuable suggestions.

The author is specially gratful to Dr. J. Benoit for his help during this research. He would like also to express all his thanks to Drs. R. Bachus, B. Clarke, G. M. Denby and J. M. O. Hughes for providing assistance and advice.

The author is indebted to Dr. R. E. Martin, E. G. Drahos and the personnel of Schnabel Engineering Associates for their help during the testing programs in Richmond.

The author would like to express his appreciation to Le Fonds National Suisse Pour La Recherche Scientifique for awarding him a two years grant at the beginning of his PhD program.

Finally, the author would like to thank sincerely all his collegues and the personnel of the Civil Engineering Department at Virginia Tech for their help throughout this research program.

This research was supported by the National Science Foundation under the NSF Grant No. MSM-8414478.

Table of Contents

List of Illustrations

List of Tables

Chapter 1

INTRODUCTION

Historically, prediction of geotechnical performance in stiff soils has been prone to a considerable amount of guesswork and empiricism. There are many reasons for this. A major one is that in stiff soils, the conventional approach of making a boring, taking samples, and testing them in the laboratory often leads to information that is not consistent with field performance. This approach can fail in some stiff soils simply because it is not possible to take a representative sample. The residual soils of the Southeastern Piedmont present this problem since they have a structure that is damaged in the process of sampling or extruding the soil from the sample tube. On the other hand, stiff clays, such as those found in the Washington D.C. area, contain fissures that cause the soil to fail in a laboratory test in a manner that is not applicable to field loading.

These and other problems with conventional geotechnical testing technology have led to research into the use of in-situ testing for stiff soils. One such device that has generated interest in this regard is the pressuremeter. In its simplest form, the pressuremeter is a device which is lowered into a predrilled hole at the test depth, and used to expand a cylindrical membrane against the sides of the hole. The most common form of this approach is referred

to as the Menard pressuremeter test after the inventor of the probe, Louis Menard (1955). The resulting cavity expansion curve from the test is used to determine the lateral pressure in the soil, the soil stiffness, and the strength of the soil. This approach to determining design parameters for stiff soils is finding widening use in the U.S. Locally, it has been introduced in general practice in the Richmond, Virginia area.

In spite of its appealing nature, the Menard pressuremeter approach has its drawbacks. Foremost among these is the fact that the results of the test are influenced by the manner in which the hole is prepared. Hole preparation is a problem in that it is almost impossible to guarantee that the hole will have the same characteristics because different drillers are employed and different soil conditions are encountered. An additional drawback occurs in that inevitably some soil disturbance is induced when the stresses are removed from the soil as the hole is opened. In an attempt to obviate these drawbacks, the self-boring pressuremeter (SBPM) was invented in 1972 (Jezequel, Le Mehaute and Le Mee (1970), Wroth and Hughes (1972)). A sketch of the English version of the SBPM is shown in Fig. 1.1. This probe is intended to drill by itself into the ground, while keeping intimate contact with the soil and avoiding any stress relief. After reaching a test depth, a cylindrical membrane is expanded as in the Menard test. However, the SBPM has the added advantage that test parameters can be monitored automatically through the use of electronic systems and automated data aquisition units. This type of operation also allows monitoring the membrane movement at more than one point. The redundancy in this approach permits a check on the behavior of the membrane, and provides insight to any nonuniformities in the stress field or soil stiffness or strength around the probe.

The experiences to date with the SBPM in stiff soils has been mixed, and not many opportunities have emerged where the probe could be used. Results with the SBPM have generally shown soil stiffness values and strengths that are higher than those obtained with conventional laboratory testing. In only a few instances have the higher design parameters been applied in practice, since there is a natural reluctance on the part of the practicing engineer to use what might be interpreted as unconservative information. It remains to establish

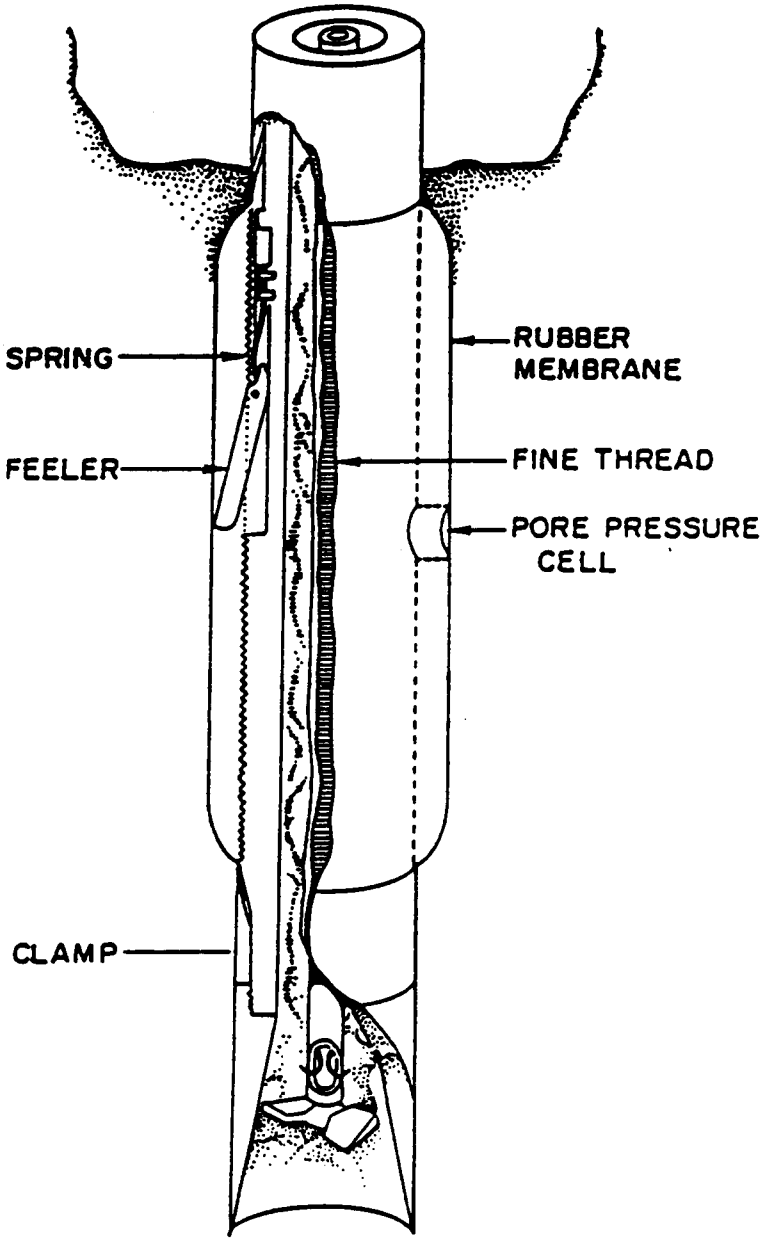

FIGURE 1.1 SKETCH OF THE ENGLISH SELF-BORING PRESSUREMETER (AFTER WROTH AND HUGHES, 1974)

that the parameters obtained from the SBPM test are realistic. If it can be done, then the economics of design in stiff soils can be significantly improved. It is the objective of this investigation to develop information which will serve to evaluate the SBPM in stiff soils.

This study is primarily experimental in nature, and involves two sites in the Commonwealth of Virginia. The first of these is just outside the Blacksburg town limits in a residual soil environment. The residual soil, a product of weathering of the parent rock, was tested over a depth of 9 M. It is heterogeneous in nature but stiff, with zones of cohesive material, of nearly non-plastic silty sand, and of rock in an advanced state of weathering. The Blacksburg site was chosen for several reasons. First, it consisted of a residual soil, which provided the opportunity to test this material which is important to geotechnical engineering in the southeastern portion of the United States. Second, it was conveniently located relative to Virginia Tech, and allowed the investigator to test without incurring the costs associated with a remote site. Third, because of its proximity to Virginia Tech, and the support facilities there, experimentation could be done with the equipment, and changes could be made relatively easily.

The testing at Blacksburg site led to a number of new operational approaches to the work:

1. After experience showed that the normal, unreinforced pressuremeter membrane was frequently damaged during insertion, all subsequent testing was conducted using a flexible steel-sheathed protective covering over the membrane. The steel-sheath covering is given the name "Chinese lantern", because of the fact that it has numerous small slits down it so the sheath can expand easily under pressure.

2. Given that the reaction of the weight of the insertion equipment proved inadequate to advance the probe, a new adjustable frame was devised which could be connected to anchors drilled into the ground. The new frame served to hold the insertion equipment down, and allow the probe to advance properly.

3. Concern over the high pressures found necessary to expand the probe in stiff soils led to development of a special calibration unit for the probe where it could be expanded under high pressures, and thus calibrated under conditions more like those encountered in the field.

4. In a related vein to 3., the fact that high pressures were involved also caused redesign and fabrication of a new pressure panel control unit for the pressuremeter.

5. Finally, a new, high capacity data acquisition system was developed during the course of this work.

Part of the testing at Blacksburg site was devoted to checking out the new operating systems. However, considerable work was also done after the systems were found to be working so that a sound pressuremeter data base could be established for the soil. Over fourty tests were conducted in nine holes at the site. Among these tests, twenty two gave meaningful results for properties of the soil.

To establish a conventional information base for the residual soils, three holes were augered using a drill rig, and Standard Penetration Testing was performed in each one. Classification tests were performed on the split spoon samples obtained in this operation. Few more sophisticated tests could be conducted since the soils from the split spoon samples were disturbed, and it was not possible to push Shelby tubes for any length into the soil to obtain better quality samples because of the high resistance of the soil to penetration, and the relatively low reaction in the drill rig which was available. Nonetheless, a limited number of strength and deformation tests were performed on the samples which were in hand, to gain some basic idea of the behavior of the soil. In future work for the larger project which is being done by Professor G. W. Clough, adviser of this investigation, other approaches are to be undertaken to add to the conventional data base for the soil.

The second site for this work is located in the downtown Richmond area, where a stiff clay deposit is found that forms the bearing layer for most deep foundations of the larger structures

built in Richmond. The soil is unique in that it is very stiff, but it is also sensitive and does not contain fissures except in isolated instances. Evidence also exists for high lateral stresses in the clay. For example, drillers report that boreholes often squeeze inward in short periods of time. Additionally, it is frequently observed that samples of the clay disc, or form horizontal cracks as they are pushed from the sample tubes. The latter behavior was seen in the investigation.

Both laboratory and SBPM tests were conducted for the Miocene clay. In addition, valuable results are available for this material in the form of Menard pressuremeter results through the consulting firm Schnabel Engineering Associates. The Schnabel firm has pioneered the use of pressuremeter testing in the Miocene clay, and has used the information from such work to help choose design parameters for the clay.

As opposed to the Blacksburg residual soil, quality samples for laboratory testing could be obtained for the Miocene clay. Sampling was done in two ways. First, Shelby tubes were pushed into the soil in the conventional manner using a drill rig. Second, the opportunity arose to cut block samples of the clay from the bottom of large diameter holes drilled for pier foundations. These latter samples allowed testing of Miocene clay in what is believed to be a nearly undisturbed state, while the Shelby tube samples provided for testing of the soil as it would be done in normal practice. The laboratory testing program was undertaken using different samples to classify the soil, and to determine as accurately as possible the strength and deformation characteristics of the soil.

The final SBPM testing program for the Miocene clay was not as extensive as originally planned. In the course of this work, several modifications were required in the procedure used so that adequate reaction could be obtained to advance the probe in the very stiff clays. Eventually, a method was adopted to work with a drill rig, and this posed problems in that the high cost of using the rig and the drill crew forced a shortened testing program. However, in any event, six successful SBPM were conducted, and the results of the tests provide a base for comparison to the laboratory testing effort and the data available from the Menard pressuremeter. The comparisons allow for important conclusions to be drawn relative to the

impact of sample and test quality on design parameters for Miocene clay. Also, the SBPM test data show that the lateral stresses in the clay are, as suspected, very high, and appear to be characteristic of an anisotropic stress field that can be explained in terms of the Richmond area topography.

A review of the existing experience with the SBPM in stiff soils is presented in Chapter 2 of this study. The limitations of this experience and the specific problems associated to the stiff soils are also underlined.

In Chapter 3 and Chapter 4, the soil investigation and the laboratory testing programs are described for the Miocene clay and for the residual soil, respectively. The soil parameters derived from the laboratory testing programs are also presented in these chapters.

The SBPM probe used for this study is presented in Chapter 5. Details on the equipment and on the self-boring techniques used in the soils tested are given in this chapter. The special calibrations of the probe and the testing procedures in the field are also described.

In Chapter 6, the results and the interpretation of the SBPM tests performed in the Miocene clay are described and the soil properties derived from these tests are compared to the laboratory parameters and to the Menard pressuremeter data.

The results of the SBPM tests performed in the residual soils and the soil properties interpreted from the tests are presented in Chapter 7. Finally, a summary and conclusion to this research is given in Chapter 8.

Chapter 2

BACKGROUND

2.1 STIFF SOILS

2.1.1 Introduction

The consistency of a cohesive soil is commonly measured in terms of its undrained shear strength. Based on correlation with the unconfined compression strength, a cohesive soil is stiff when its undrained shear strength is at least 49 KN/M2 (7 psi). If normally consolidated, such a soil is found under a minimum cover of 15 M (50 ft) of soil. When found near the ground surface, the stiffness of the soil is generally due to overconsolidation by unloading, dessication or/and by cementation. Stiff cohesive soils are very often fissured, and some types of these soils are "structured".

2.1.2 Role of fissures

Fissures are part of the structure of the stiff cohesive soils. They have different origins depending on the type of soil. Fissures in a dessicated clay or in a residual soil come from shrinkage during dessication and from weathering. Fissures in a mass of cohesive soil which has been unloaded comes from the failure of the soil which occurs as the soil is unloaded.

Skempton (1977) gives rules to design slopes in stiff fissured clays. For a slope design and any other work which lead to stress relief in the soil mass, fissures play an important role in the behavior of the soil. They open as the stresses in the soil are relieved and allow the water to penetrate and soften the soil mass.

The issue of this research is the study of the geotechnical properties of stiff soils in a confined state of stress. Under these conditions, fissures stay normally closed and the properties of the soil are not altered with time by the presence of the fissures.

Fissures in a large mass of soil are part of the continuum. When an attempt is made to characterize the continuum by laboratory tests on small soil samples, fissures become a problem. As an example, Lo (1970) studied the effect of the fissures on the measured undrained shear strength of the soil. He defined two extreme values of strength, the undrained shear strength of the intact soil without fissures, and the strength along a fissure. Considering the fact that fissures are randomly oriented and not continuous, he defined the operational strength as the overall strength of the soil. He proposes a relationship between the operational strength of the soil and the area of failure, and other soil parameters which can be determined. This relationship was established for Brown London Clay (Fig. 2.1). The curve proposed by Lo fits the test data well, showing a clear dependency of the area of failure upon the undrained shear strength of the soil. The smaller the size of the sample, the smaller the area of failure, the less numerous the fissures, in particular the one with the same orientation as the failure area and the larger the undrained shear strength measured. On the other hand, the larger the area of failure, the less important the fissures, as they are part of a continuous

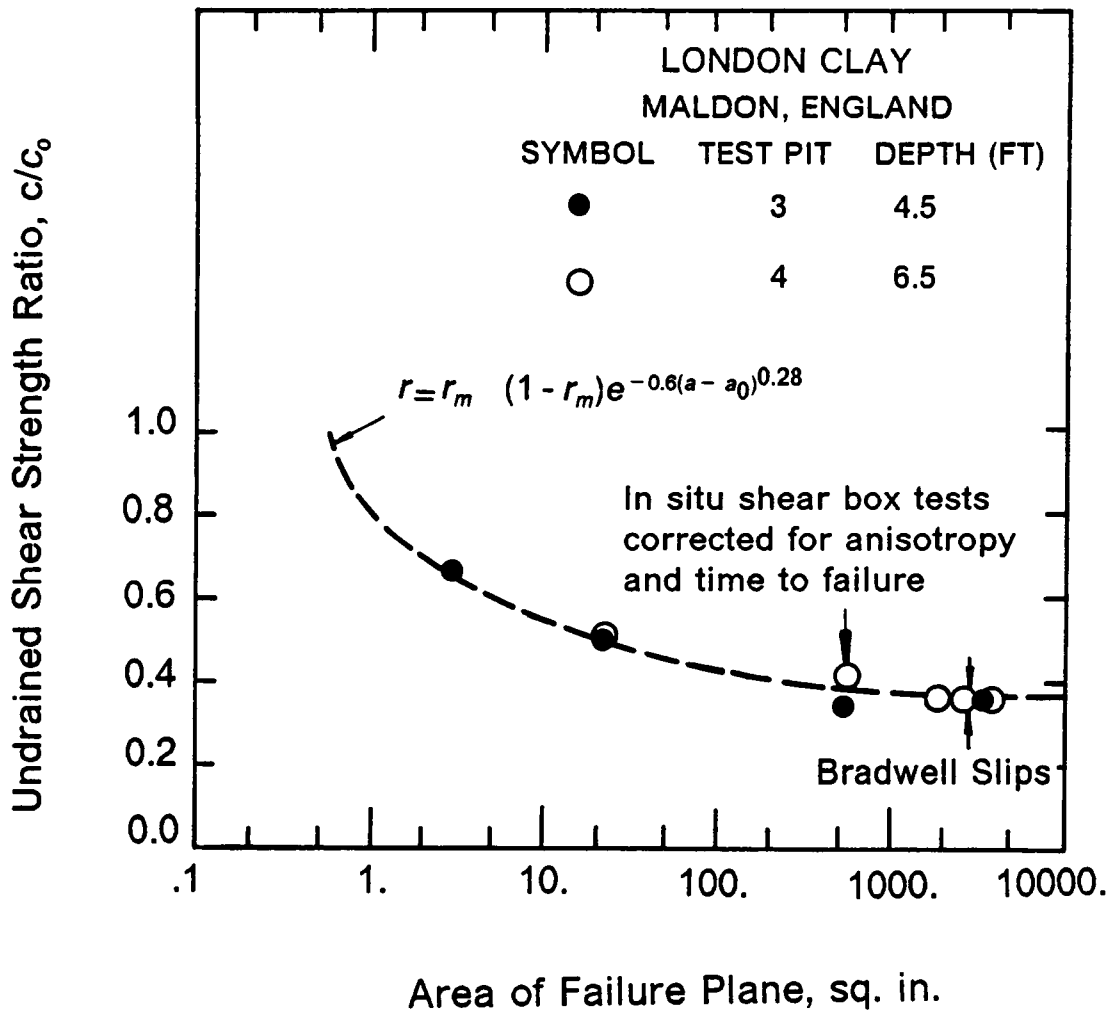

FIGURE 2.1 STRENGTH-SIZE RELATION OF LONDON CLAY

(AFTER LO, 1970)

mass of soil. For Brown London Clay (Fig. 2.1), the undrained shear strength of the soil becomes independent of the size of the area of failure for areas of failure larger than 0.008 M2 (500 sq in).

2.1.3 Structure

A clay is called structured when bonds between the clay particles exist, like a cementation for a sand. Little is known about the development of these bonds but it is assumed that recrystallisation occurs at the points of contact between the clay particles. The bonds, called diagenetic bonds, develop after the secondary consolidation of the soil took place. Their development is affected by factors like time, temperature, nature of the clay mineral and pore fluid and by the consolidation pressure.

The differences between a structured stiff clay with strong diagenetic bonds and a non structured stiff clay are best seen when the two clays are tested in consolidated undrained conditions (CU test) in a triaxial apparatus. The typical response of the two clays is given in Fig. 2.2. The structured clay, in continuous line, shows a very brittle behavior with a sharp peak at a strain generally less than 1%. Before the peak, the soil sample is uniformly strained. As fracture of the sample occurs, the strain measured which follows the peak of stress is in fact a combination of a true strain of the soil and a displacement along the failure surface. For large strains (typically 10-15%), the residual strength of the soil on the failure surface is reached. Consequently, the strength measured does not change with the increasing strain. The excess pore pressure generated during the shearing of the structured clay are positive throughout the test. They follow directly the level of stress in the soil sample and, therefore, the shape of the curve excess pore pressure versus strain is similar to shape of the curve shear stress versus strain. The excess pore pressure developed when stressing the soil are positive and result from the compression of the soil skeleton. The bonds between particles are strong enough to minimize relative displacements between particles.

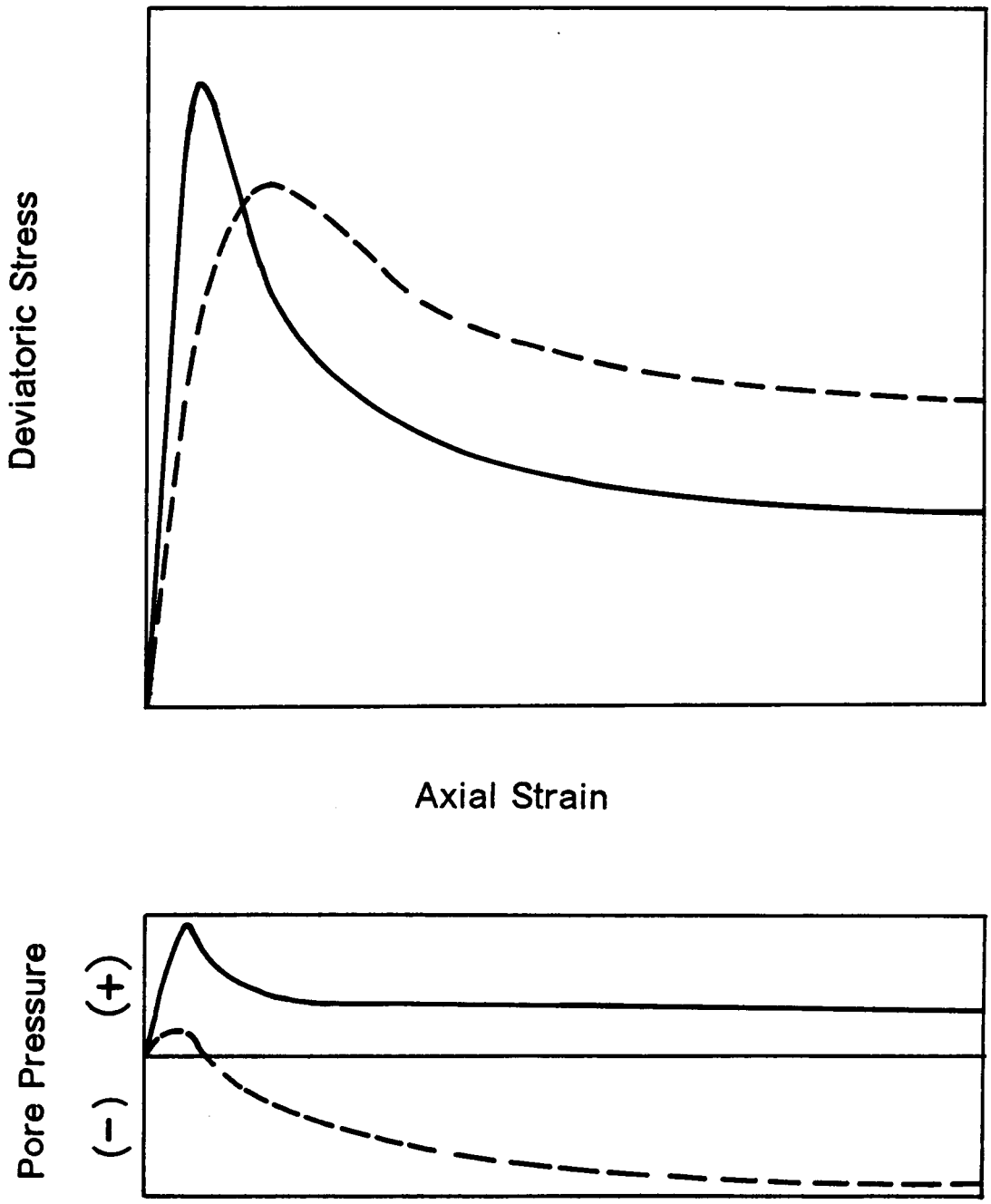

Note: The two clays are tested at similar consolidation pressures

FIGURE 2.2 TYPICAL RESPONSES OF STIFF SOILS UNDER CU TRIAXIAL TESTS

The non-structured stiff clay behaves like a dense sand. It is a material with a compact arrangement of the soil particles but with weak bonds between them. This clay, when sheared, shows also a peak on the shear stress versus strain curve. The peak is not so sharp as for the structured clay and it occurs at larger strains (typically at 2 to 3% strain). The definition of strain before and after peak is the same as before: fairly uniform strain through the sample before peak and combination of true strain and displacement along the failure surface after peak. The residual strength of the soil is reached for large strains (typically 10%) as for the structured clay. Excess pore pressure response of the stiff non-structured clay to shearing is similar to the response of a dense sand. The two materials are particle materials and they follow the "critical state" behavior. As they are in a compact particle arrangement and sheared under undrained conditions, negative excess pore pressures are developed.

The two examples shown in Fig. 2.2 have been chosen in order to illustrate two extreme cases. In reality, most structured clays are fissured and have zones of weak bonds which influence the strength of the soil determined in a laboratory test, and hence the development of excess pore pressures during shearing. The resulting behavior is therefore between the two extreme behavior types described in Fig. 2.2.

2.1.4 Normalized behavior

The idea of normalizing soil behavior was initiated by D. W. Taylor at MIT (1955). Later this was extended at Imperial College, London, through the results of experimental work done on remolded clays (Parry 1960, Henkel 1960). Further research by Ladd and his associates brought the concept to fruition. Ladd et al. (1977) give a review of the work done on normalization of the soil behavior. It was found that soils tested at the same overconsolidation ratio (OCR) but at different maximum past pressures exhibit very similar strength and stress-strain characteristics when normalized with respect to the consolidation stress. Fig. 2.3 gives an example of the normalization process. The stress-strain curves of two samples of clay con-

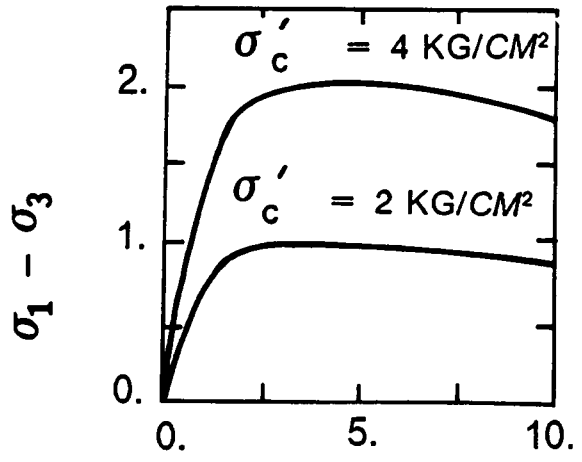

a) TRIAXIAL COMPRESSION TEST DATA

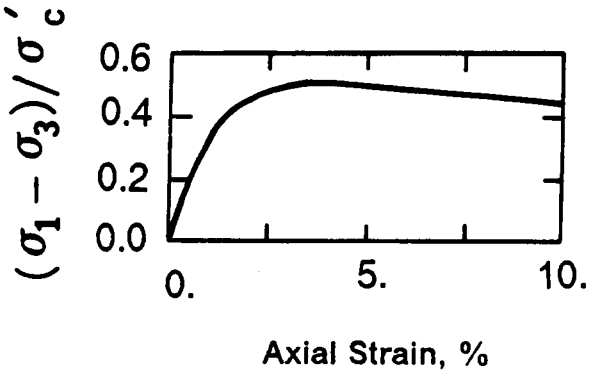

b) NORMALIZED PLOT OF TRIAXIAL TEST DATA

FIGURE 2.3 EXAMPLE OF NORMALIZED BEHAVIOR
(AFTER LADD ET AL., 1977)

solidated at 196 and 392 KN/M2 (28 and 57 psi) are indicated in Fig. 2.3a. When these two curves are normalized by their respective consolidation stress, they become a single curve as shown in Fig. 2.3b and the stress-strain behavior of the soil has been normalized with respect to the consolidation stress.

The concept of normalized behavior has significance beyond simply being a convenient way of presenting test results since it enables a systematic evaluation of the importance of the stress history on the strength-deformation properties of a clay. A second example of normalized behavior is given in Fig. 2.4. In this figure, normalized stress-strain and strength data for resedimented Boston Blue Clay are presented as a function of OCR. Ladd and Foott (1974) went one step further in the use of the normalized soil behavior concept by integrating the concept in a complete design procedure called SHANSEP (Stress History and Normalized Soil Engineering Properties).

It must be underlined that the SHANSEP procedure to normalize the soil behavior applies only to cohesive soils which maintain their basic structure during loading beyond the in-situ stresses and into the virgin compression range. It does not apply to structured soils since their structure is drastically altered when they are loaded beyond their "apparent" maximum past pressure.

2.1.5 Residual soils

The residual soil is formed through chemical weathering of the parent rock. Experimental investigations have confirmed that water is the most important agent of chemical weathering, acting through the processes of dissolution and hydrolysis. The progress of chemical weathering in a given rock body is influenced by three principal factors: Oxydation, pH and drainage.

Oxydizing conditions convert Fe^{++} to Fe^{+++}. It affects the Fe^{++} whithin the silicate minerals and the leached-out Fe^{++} in solution. This conversion participates in the disruption

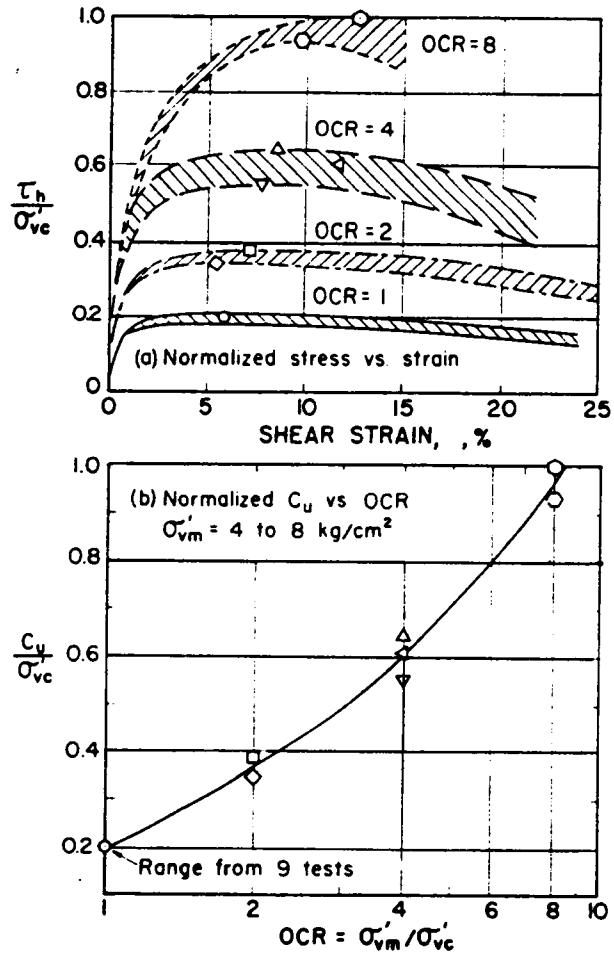

FIGURE 2.4 NORMALIZED CKoU DIRECT SIMPLE SHEAR TEST DATA FOR BOSTON BLUE CLAY (AFTER LADD AND FOOTT, 1974)

of the crystal lattice. The insoluble Fe^{+++} hydroxides tend to remain in the zone of weathering leading to a residual concentration of iron in the weathering profile.

Low pH promotes hydrolysis of silicates minerals by providing additional H^{+} ions which enter the crystal lattice, displacing metal cations and disrupting the silicate framework. The quantity of water passing through the zone of weathering influences the nature of the secondary minerals which form during weathering. Where there is a large amount of water entering the zone of weathering and drainage is good, even poorly soluble products of hydrolysis may be leached out, ultimately leaving an insoluble residue largely of Fe^{+++} and Al hydroxides. Where drainage is impeded, or where there is insufficient water to leach out all the products of weathering, clays will be the stable secondary minerals.

The engineering properties of the residual soils are controlled by the weathering profile which is the sequence of the layers of material with different physical properties developed in place above the unweathered rock. The weathering profile consists generally in a three fold division of (1) residual soil, (2) weathered rock and (3) relatively unweathered, fresh bedrock. Factors such as rainfall, groundwater conditions and nature of the rock shape the weathering profile.

In their study of the slope stability in residual soils, Deere and Patton (1971) reviewed some of the features of the weathering profile controlled by the parent rock.

Several classifications of the weathering profile were proposed for different environmental conditions. Among them is the work by Sowers (1963) and Sowers and Richardson (1983) on the properties of the residual soils found in the Piedmont and Blue Ridge of the Southeast of the United States.

2.2 Summary stiff soils

To summarize, stiff soils are generally overconsolidated, and if cohesive, they are often fissured, especially near the ground surface where the effect of unloading, dessication and weathering of the soil are likely maximized.

Fissures generally do not affect the behavior of the soil if the soil mass is in a confined state of stress. If the soil mass is unconfined like in the case of slopes or excavations, fissures play an important role because they open as a consequence of the reduction of the confinment and create a path to the water which penetrate and soften the soil mass.

Laboratory testing on samples of fissured stiff soil can be misleading because of disturbance which takes place during sample extrusion, because of fissures which can control the behavior of a small size sample.

Stiff soils which have developed interparticle bonds during their formation are called structured. They are generally more brittle than the non-structured soils and can have a distinctive behavior if the bonds are well developed.

Attempts have been made to normalize the behavior of the cohesive soils. Normalized behavior allows to evaluate systematically the importance of the stress history on the strength deformation properties of a clay.

2.3 PRESSUREMETER

2.3.1 History of the pressuremeter

A pressuremeter is a cylindrical probe with a membrane. It is used in-situ by expanding the membrane against the surrounding soil. The first pressuremeter was developed by Kogler in 1933 but was never successfully marketed.

The first practical pressuremeter is attributed to Menard (1957) and his version of the test has found a growing acceptance in geotechnical practice in the United States. The Menard pressuremeter is placed in a predrilled hole. The results from the test, called the pressuremeter curve consist of a pressure-volume relationship. Soil parameters which can be derived from the pressuremeter curve are lateral earth pressure, shear strength, soil stiffness and coefficient of consolidation (advanced probes). Tests can be performed over a wide range of depths.

Over the past decade, new versions of pressuremeters have been developed, including the self-boring, the pushed-in, the high pressure and the pavement probes. Of these new probes, the self-boring pressuremeter (SBPM) has attracted the greatest interest. This probe was developed almost simultaneously by workers in France and England. It has the capability to drill itself in the ground, presumably with little disturbance to the surrounding soil.

A schematic view of the English probe was shown in Fig. 1.1. The pressuremeter advances in the ground by means of a thrust acting downwards and applied from the ground surface to the drill rods. As the soil is forced into the bottom of the sharp edge cutting shoe, it is chopped into small pieces by the rotating cutter. The pieces of soil are then flushed to the surface of the ground through the annulus between the drill rods and the cutter rods.

When the test depth is reached, drilling is stopped and pore pressures in the soil are monitored using the pore pressure cells set into the sides of the probe.

Following the stabilization short period of the pore pressures, the test is performed by expanding the cylindrical membrane around the probe. As pore pressures can be monitored with the self-boring probe, both, drained and undrained soil responses are defined.

The English self-boring pressuremeter is known as the Camkometer, and the French probe is referred to as the PAF probe. Descriptions of the two SBPMs are given respectively by Wroth and Hughes (1972) for the Camkometer and by Baguelin et al. (1972) for the PAF. A comparison of the main features of the two probes is given in Tab. 2.1. The advantages of the English probe over the French one are:

1. A large length versus diameter ratio (6 compared to 2 or 4) which approximates better the plane strain conditions.

2. A real measurement of displacements which allows to observe anisotropy, heterogeneity and disturbance rather than a measurement of volume like for the PAF, which smears all the factors.

2.3.2 Pressuremeter curve

The pressuremeter curve of what is considered as a good quality test in clay is presented in Fig. 2.5. The pressure ψ applied to the inside of the probe is plotted against the strain ε which is the observed expansion of the membrane divided by its initial radius. The pressure ψhas been corrected for the small strength of the membrane. This correction is represented in Fig. 2.5 by the difference between the ordinates of points O and I. As the test starts, there is no nitrogen pressure in the probe and the membrane fits tightly the rigid body of the instrument. In theory, as the pressure is increased inside the probe, no expansion of the membrane should be detected until the applied pressure ψ is equal to the in-situ total lateral stress in the ground in contact with the pressurenmeter. This particular pressure which

TABLE 2.1 COMPARISON BETWEEN THE ENGLISH AND THE FRENCH SBPM

Item	English SBPM	French SBPM
Name	Camkometer	Pressiometre Auto-Foreuse (PAF)
Body type	Rigid (single unit)	Flexible (cellular)
Probe dimens.	L / D = 6	L / D = 2 or 4
Pressurizing medium	Nitrogen	water
Pressure measurement	At probe level	At ground level
Strain measurement	By 3 tracking arms set set at mid probe, 120 degrees apart	By volume change of water
Cutter drive unit	At ground surface	At top of probe
Cutter position	Adjustable at all time	Adjusted prior to insertion

Note : L = Length of the probe, D = Diameter of the probe

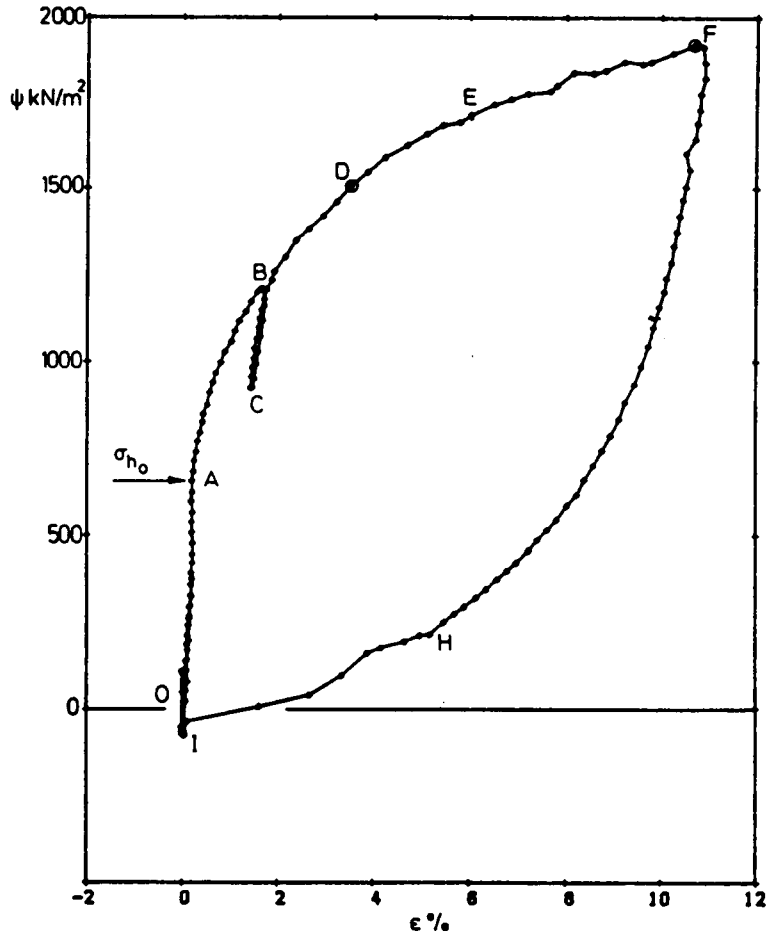

FIGURE 2.5 RESULTS OF A PRESSUREMETER TEST IN BARTOON CLAY, ZEEBRUGGE (AFTER WROTH, 1982)

equilibrates pressure inside and outside the probe is known as lift-off pressure. It is represented by point A in Fig. 2.5.

The shear modulus of the soil can be measured by inserting in the expansion curve OF one or several unloading-reloading cycles such as BCB. If the soil behaves elastically during the unloading-reloading cycle, BC will be a straight line of gradient 2G, G being the shear modulus.

The unloading curve FO at the end of the expansion curve is generally monitored. Its shape gives a good indication of the nature of the soil. This is useful when testing in unknown soils or in soils with thin layers of different soils.

Details on the interpretation of the test results are given in a subsequent chapter.

2.4 RESULTS FROM PREVIOUS TESTING IN STIFF SOILS

Key investigations of stiff soil using a SBPM are documented in Tab. 2.2. Most of the work was carried out using either the English probe or the French version described above. No investigation of residual soil has been reported in the litterature.

2.4.1 Modulus values

One of the most important parameters that can be derived from a testing program in stiff soils is the modulus of the soil. Generally, the governing constraint when designing a retaining wall or a foundation in stiff soils is movements and, as a result, an accurate determination of the modulus of the soil is needed.

As there is no standard modulus definition from the pressuremeter or laboratory tests, the way the modulus is chosen should be clearly defined. Modulus values are derived in

TABLE 2.2 REVIEW OF SELF-BORING PRESSUREMETER WORK IN STIFF SOILS

REFERENCE	TYPE OF CLAY LOCATION	SOME PROPERTIES OF THE CLAY	PROBE USED NUMBER OF TESTS	REMARKS		
				SHEAR STRENGTH	MODULUS	AT REST PRESSURE COEFFICIENT, K_o
Windle D. and Wroth C.P. (1977)	heavily overconsolidated fissured clay two sites : Gault clay, Cambridge London clay, Hendon	Gault clay w_n = 25 - 30% LL = 70 - 75 PI = 40 - 53 s_u (1) = 70-160 KN/m^2 London clay w_n = 26 - 30% LL = 60 - 80 PI = 34 - 50 s_u (1) = 200-350 KN/m^2	Camkometer (English SBPM)	Gault clay marked effect of loading rate on peak shear strength interperpreted from SBPM tests London clay good correlation between residual shear strength interpreted from SBPM tests and Dutch cone test result	Gault clay E_u = 40-100 MN/m^2 values of E_u independent on the rate of loading London clay E_u = 40-100 MN/m^2 (about 4.0 times the values obtained in laboratory from UU triaxial compression tests	Gault clay K_o = 3 - 4 London clay K_o = 1.6 - 3.6
Jamiolkowski M. and Lancellotta R. (1977)	very stiff slightly fissured clay Montalto di Castro (Italy)	w_n = 22 - 27% LL = 45 - 60 PI = 30 - 35 s_u (1) = 220-350 KN/m^2 O.C.R. = 3.4 (1) From laboratory tests	PAFSOR (French SBPM) 12 tests	values of strength interpreted from SBPM test results 2.0-2.5 times larger than values from UU triaxial compression tests	E_u values interpreted from SBPM tests are 2.0-3.0 times the values obtained in laboratory	

TABLE 2.2 REVIEW OF SELF-BORING PRESSUREMETER WORK IN STIFF SOILS

REFERENCE	TYPE OF CLAY LOCATION	SOME PROPERTIES OF THE CLAY	PROBE USED NUMBER OF TESTS	REMARKS		
				SHEAR STRENGTH	MODULUS	AT REST PRESSURE COEFFICIENT, K_o
Law K.T. and Eden W.J. (1980)	stiff sensitive clay Leda clay, NRCC, Ottawa	w_n = 80% LL = 54 PI = 29 OCR = 2.2 Sensitivity = 50	Camkometer (English SBPM)	-oversized cutting shoe leads to over-estimate shear strength by 80%	oversized cutting shoe leads to over-estimate modulus by 30%	
Eden W.J. and Law K.T. (1980)	See Law K.T. and Eden W.J. (1980)			shear strength interpreted from SBPM tests 20-40% higher than values given by field vane tests. UU triaxial compression tests give intermediate values between those of the pressuremeter and the field vane		
Denby G.M., Costa C.A., Clough G.W. and Davidson R.R. (1981)	stiff to hard over-consolidated clay with fissures, slickensides shear zones Seattle	Units B & D / Unit E w_n = 24% / 33% LL = 47 / 59 PI = 22 / 27 s_u (1) = 100-200 KN/m^2 OCR = 4.6 (1) From Laboratory tests	Camkometer (English SBPM)	shear strength interpreted from SBPM tests lies in the upper range of the UU strength data	initial tangent modulus interpreted from SBPM tests 2 times moduli obtained from unload/reload UU triaxial tests	good agreement between K_o values from SBPM test and laboratory values Units B & D K_o = 0.8-1.3 Unit E K_o = 1.6-2.2

TABLE 2.2 REVIEW OF SELF-BORING PRESSUREMETER WORK IN STIFF SOILS

REFERENCE	TYPE OF CLAY LOCATION	SOME PROPERTIES OF THE CLAY	PROBE USED NUMBER OF TESTS	REMARKS		
				SHEAR STRENGTH	MODULUS	AT REST PRESSURE COEFFICIENT, K_o
Dalton J.C.P. and Hawkins P.G. (1982)	heavily overconsolidated fissured clay Gault clay, Cambridge	see Windle and Wroth (1977)	Camkometer (English SBPM)			SBPM tests results indicate anisotropy with respect to K_o values in the horizonal plane
Johnson G.W. (1982)	stiff clay, 2 sites in the vicinity of University of Texas at Austin	w_n = 16 - 25% other data not available	Texas Self-Boring Pressuremeter 4 tests	shear strength interpreted from SBPM tests 2.0-3.0 times values obtained in laboratory from UU triaxial compression tests	good correlations between initial shear modulus interpreted from SBPM tests and modulus values determined from seismic cross-hole tests	
Ghionna V., Jamiolkowski M., Lacasse S., Ladd C.C., Lancellotta R. and Lunne T. (1983)	hard clay, possibly micro-fissured Taranto clay (Italy)	w_n = 23% LL = 60 PI = 24 - 30 $s_u^{(1)}$ = 250-400 KN/m^2 OCR = 20 - 30 (1) From laboratory tests	Camkometer (English SBPM)	shear strength interpreted from SBPM tests 2.0-3.0 times values obtained in laboratory from UU triaxial compression tests	modulus interpreted from SBPM tests are 4.0-10.0 times modulus obtained in laboratory from UU compression triaxial tests and simple shear tests	unreasonable values of K_o interpreted from SBPM test results K_o varies between 3.0-6.0 between 8.0-16.0 m depth

TABLE 2.2 REVIEW OF SELF-BORING PRESSUREMETER WORK IN STIFF SOILS

REFERENCE	TYPE OF CLAY LOCATION	SOME PROPERTIES OF THE CLAY	PROBE USED NUMBER OF TESTS	REMARKS		
				SHEAR STRENGTH	MODULUS	
Mahar L.J. and O'Neill M.W. (1983)	two clays overconsolidated by dessication Beaumont formation closely spaced fissures and slickensides depth = 0-26 ft Montgomery formation fissures, slickensides and sand seams depth > 26 ft Houston, Texas	Beaumont form. w_n = 20 - 30% LL = 40 - 80 PI = 30 - 60 γ_T = 126 pcf s_u(1)=30-150 KN/m^2 Sensitivity=0.5-1.5 OCR > 6.0 Montgomery form. w_n = 15 - 25% LL = 25 - 30 PI = 5 - 15 γ_T = 133 pcf s_u(1)=50-220 KN/m^2 Sensitivity = 2.0 OCR = 4.0 - 6.0 (1)From Laboratory tests	Texas Self-Boring Pressuremeter 8 tests	Beaumont form. values of shear strength from SBPM are same order as UU triaxial but 1.5 times larger than values from NSP(1) tests and 1.1 to 2.0 times smaller than values from CPT(2) tests Montgomery form. values of shear strength from SBPM 1.0 to 4.0 times larger than values from UU triaxial but 1.1 to 1.5 times larger than values from the NSP(1) approach and 1.1 to 2.0 times smaller than values from CPT(2) tests	for both formations, values of E_u from UU tests random and scattered. values from cross-hole technique are 5.0-10.0 times larger than values from SBPM. Values from NSP(1) and CIU(3) tests are 2.0-3.0 times smaller than values from SBPM (1)NSP=normalized strength parameters (2)CPT=cone penetrometer with N_c=9 (3)CIU=undrained triaxial test istropically consolidated	Beaumont form. K_o = 2.0 - 3.0 values of K_o from SBPM 1.5-2.0 larger than values interpreted from laboratory tests. Montgomery form. K_o = 0.8 - 1.2 generally good agreement between K_o values from SBPM and laboratory tests

laboratory from unconsolidated undrained triaxial tests (UU tests) and from isotropically or anisotropically consolidated undrained triaxial tests (CIUC or CK_oUC tests).

In CIUC or K_oUC tests, the soil is generally reconsolidated to stresses which are close to the field stresses. In UU tests, modulus values are derived from small unloading-reloading cycles during the test itself. In CIUC or CK_oUC tests, modulus values can be estimated the same way. It is also estimated from the slope of tangents to the test curve at different strains or from the slope of the secant passing by the origin and the point of 50% shear strength on the test curve. In pressuremeter tests, modulus is derived from small unloading-reloading cycles in the expansion part of the pressuremeter curve. It is also derived from the slope of the pressuremeter curve at the point of lift-off pressure (initial modulus) and from the slope of the secant passing through the point on the pressuremeter curve corresponding to the mobilization of 50% of the shear strength of the soil, to be consistent with the laboratory definition.

The data in Tab. 2.2 indicate that modulus values from SBPM are consistently higher than those from laboratory. The moduli determined from the pressuremeter are typically 2 to 4 times the moduli determined from laboratory tests. The study of the Taranto clay reported by Ghionna and al (1982) illustrates this well. Secant moduli were determined at 50% of the peak strength on the stress strain curve of undrained triaxial and direct simple shear tests performed on samples consolidated anisotropically to field state of stress. To be consistent with the laboratory definition, the secant modulus on the pressuremeter curve was determined from the slope of the secant passing from the point of lift-off pressure to the point on the pressuremeter curve which corresponds to 50% of the peak strength when the method proposed by Prevost and Hoeg (1975) is used to determine the stress strain curve from the pressuremeter curve. Comparing the two sets of moduli, the authors find that the modulus from the pressuremeter test is 4 times the modulus from the laboratory tests.

Because similar findings exist for the undrained shear strength for which the SBPM results seem to be in the wrong, it is justified to suspect the SBPM modulus data. However, the following points are pertinent to the modulus issue:

1. As mentioned before, fissuring in stiff soils has often a predominent role in behavior of laboratory samples. A similar effect does not normally occur in the pressuremeter test because a large volume of soil is tested in place. The pressuremeter type of situation is most likely more representative of the one existing under large foundation units or behind securely supported retaining structures.

2. In soft clays, SBPM tests usually underestimate modulus values relatively to laboratory test results because of disturbance during insertion, an effect not so prominent in stiff soils.

3. Research at the university of Texas by Johnson (1982) under the direction of Reese and Stokoe has shown that SBPM modulus values are in the line with those from crosshole seismic tests.

4. In recent consulting work using finite element method performed by G.W.Clough, adviser for this research, success has been achieved in prediction of movements of several deep excavations in Seattle clay using pressuremeter modulus values.

Other pertinent findings have been reported on modulus values:

1. Windle and Wroth (1977) observed that modulus obtained from unloading-reloading cycles during pressuremeter tests is independent on the rate of unloading-reloading used for the cycle. Also, they found that values of modulus derived from cycles performed on the expansion part of the pressuremeter curve are consistently higher than modulus values derived from cycles on the unloading part of the same curve.

2. Law and Eden (1980) report that disturbances of the soil caused by an oversized cutting shoe can lead to an overestimation of the soil modulus by 30% with respect to values obtained from pressuremeter test results when the cutting shoe has the same diameter as the probe itself.

The general conclusion from the preceeding remarks is that the higher modulus values from the SBPM may be correct, albeit for some fortuitous combination of factors which are not clear at this time.

There are several studies relative to the modulus issue which appear to be fruitful. The first involves an assessment of exactly how the modulus from the pressuremeter should be determined, i.e., from the primary loading curve or from an unload-reload cycle. The second concerns investigation of how the unload-reload response varies with the number of cycles and at what point in the test unloading is accomplished. In the proceedings of the Workshop held at Virginia Tech in 1983 and published by Clough and Silver (1984), Wroth suggested that degradation in the unload-reload modulus as the loading is increased may be indicative of strain softening in stiff clays. Of course, for research in that direction, field derived modulus values must be compared to results of carefully performed laboratory tests and wherever possible, modulus values back-calculated from field data.

2.4.2 In-situ lateral stresses

The direct measurement of the existing in-situ lateral stresses is certainly one of the most important capabilities of the SBPM. No device could accomplish such a task before. This capability is of particular interest when working in stiff soils which are known to have high locked-in lateral stresses.

In absence of SBPM test results, determination of the lateral stresses rely generally on empirical correlations such as the correlation developed by Brooker and Ireland (1965) which links the coefficient of lateral earth pressure of the soil to the overconsolidation ratio (OCR) and the plasticity index or the angle of internal friction of the soil. It is well known that such correlations work with normally consolidated (NC) soils or slightly overconsolidated (OC) soils (OCR $<$ 5). For higher OCR and for soils which are fissured or structured, these correlations might be misleading and a direct measurement of the lateral stresses becomes necessary.

SBPM values of lateral stresses are generally compared to values obtained from empirical correlations as there is no other way to assess the SBPM performance. Opinions on the SBPM ability to measure proper values are then formed from this comparison. For exemple, Denby et al. (1982) working in the Seattle clay found good agreement between lateral stress measurements in-situ with SBPM, laboratory values with the stressmeter and values from the correlation by Brooker and Ireland. Windle and Wroth, working in the London clay, find also good agreement between SBPM values and values derived by Bishop et al. (1965) using the methode of estimating K_o proposed by Skempton (1961). On the other hand, Ghionna et al. (1983) conclude from their investigation of the Taranto clay that the values of K_o derived from SBPM tests are too high relative to "expected" behavior from laboratory testing.

The question which arises is: In stiff soils, should we rely on comparisons to correlations to judge the quality of the lateral stresses measurements of the SBPM or should we rather try to rely on other means such as back calculated values from instrumented case histories?

One of the grieves Ghionna et al. (1983) have towards the SBPM is the measurement of different lateral stresses in different directions. Dalton and Hawkins (1982) first reported this type of response and carefully confirmed that no equipment problem produced the effect. Recently, Benoit (1983), working in soft clay using a micro-computer data acquisition system allowing detailed records found a variation in horizontal lateral pressures measured by the SBPM similar to the one reported by Dalton and Hawkins (1982).

More experience is needed in the measurement of lateral horizontal pressures in stiff soils. Use of micro-computer data acquisition systems will give accurate measurements. As the results of the SBPM tests are sometimes in conflict with the conventional thinking and as there is no direct way to control the validity of these tests, any new experience with the SBPM brings a valuable piece of information.

2.4.3 Undrained shear strength

In both, soft and stiff clays, many investigators have found that the SBPM yield undrained shear strengths which are higher than those from the laboratory tests. For stiff clays, in particular, Jamiolkowski and Lancellotta (1977), Johnson (1982) and Ghionna et al. (1983) find ratios of 2 to 4 between SBPM strength values and UU strength values in laboratory. On the other hand, Denby and al (1981) find SBPM values of the same order as the upper values obtained from UU tests. Mahar and O'Neil (1983) working with two different clays find in one case similar results between SBPM and UU tests and, in an other case, they find a ratio of 1 to 4 between the two strengths. Law and Eden (1980) who studied the effect of soil disturbance using an oversized cutting shoe found that forced disturbance increases by 80% the interpreted value of the undrained shear strength.

As opposed to the situation with the modulus, many of the high values of shear strength in stiff clays seem to definitively overestimate the actual strength. Part of the problem often lies in the fact that these materials are fissured and laboratory results are very scattered. Also, properties of stiff soils in a confined or unconfined state of stress are different and should be chosen accordingly.

A stiff clay where fissures are not developed would be an approriate medium to carry SBPM tests and laboratory tests and compare the different results.

2.4.4 Coefficient of consolidation

The coefficient of consolidation, c_v, can be derived from the results of a SBPM test if after an initial stage of shear loading, a holding test is performed with measurement of the pore pressure dissipation (see Clarke et al. (1979)). This requires accurate measurement of the pore pressures in the field, a task not easily accomplished. Very few have attempted this

version of the pressuremeter test. In soft clays, Clarke et al. (1979) and Benoit (1983) have reported holding test results. In both cases, the coefficients of consolidation are considerably higher (from 10 to 100 times) than the values determined in laboratory with the conventional oedometer test. Natural anisotropy of clays is at the origin of these differences.

It is desirable to carry out SBPM holding tests in stiff clays as well as a series of high quality tests in the laboratory to determine c_v values.

2.4.5 Summary on SBPM experience in stiff soils

It is well known that results of laboratory tests in stiff soils are very scattered, mainly because of the limited size of the samples tested which gives importance to fissures and disturbance in the soil.

The inability of measuring representative soil properties in the laboratory leads to the use of in-situ testing equipments such as the SBPM. Without any question, the SBPM is a good way to determine soil properties of confined masses of stiff soils. By self-boring, disturbance is minimized and the expansion of the membrane of the probe during testing involves a large mass of soil.

Experience with the SBPM in stiff soils is limited at this date, mainly because design in soft soils is generally more critical and attention has been focused on this type of soils. Also, by the very nature of the soil itself, testing in stiff soils involve problems which do not exist when testing soft soils. The SBPM has yet to prove it can yield data for stiff soils which are consistently reasonable. For that reason, a well designed laboratory, field and analytical research program is necessary.

Chapter 3

MIOCENE CLAY : SITE INVESTIGATION AND DETERMINATION OF PROPERTIES

3.1 INTRODUCTION

Two stiff soils were investigated for this research:

1. a Miocene clay of marine origin overconsolidated by erosion found in the Richmond area, Virginia and

2. a residual soil overconsolidated by dessication, found in the vicinity of the campus of Virginia Tech

This chapter presents the general characteristics of the Miocene clay and the results of the site investigation and the laboratory testing program performed on this soil. Chapter 4

gives similar results for the residual soil. Self boring pressuremeter tests results in the Miocene clay are given in Chapter 6.

3.2 GENERAL CHARACTERISTICS OF THE SITES

3.2.1 Locations.

Samples of the Miocene clay were taken from two sites, both situated in downtown Richmond, Virginia. The two sites are indicated in Fig. 3.1. One site, known as 6th Street Festival Market Place, is located at the intersection of Broad Street and 6th Street. The other site, known as Exhibition Center is situated at the intersection of Marshall Street and 5th Street. The ground level at the 6th Street Festival Market Place site is at elevation 180, and the top of the Miocene clay formation is found under 12 M (40 ft) of cover. At the Exhibition Center site, the ground level is at elevation 171, and the top of the Miocene clay formation is found under 9 M (30 ft) of cover.

3.2.2 Geology

The subsoils of the Richmond area have been studied by Casagrande (1966), Martin and De Stephen (1983) and Martin and Drahos (1986). The typical sequence of geological formations encountered is as given in Fig 3.2. On the left side of the figure, the formations found several miles northwest of Richmond are given. On the right side is shown the subsoil profile encountered in the downtown area, in the vicinity of the two sites studied for this work. In the downtown area, granite bedrock is found approximatively at El. 20, i.e., 45 M (150 ft) below the

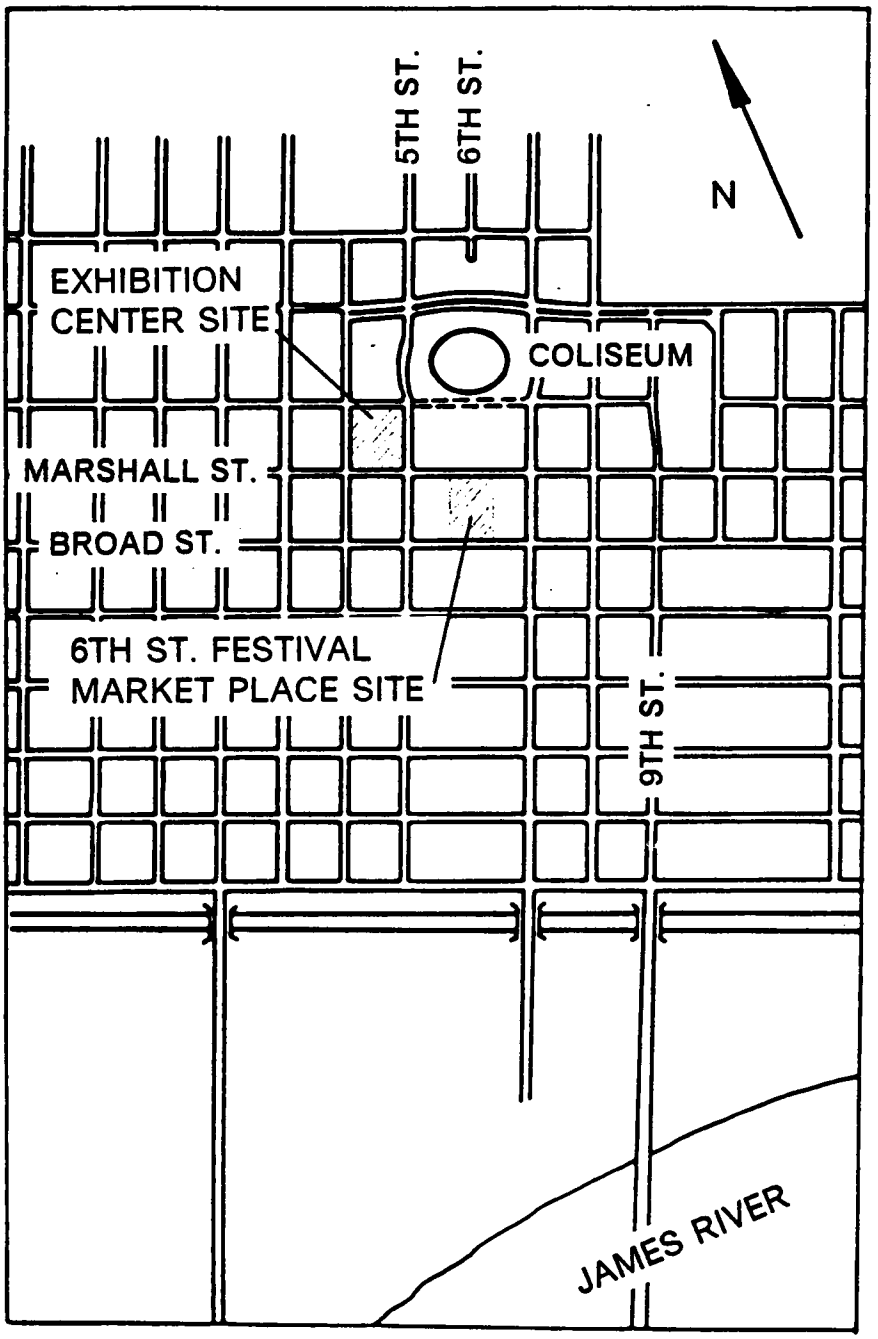

FIGURE 3.1 LOCATION OF THE TWO SITES

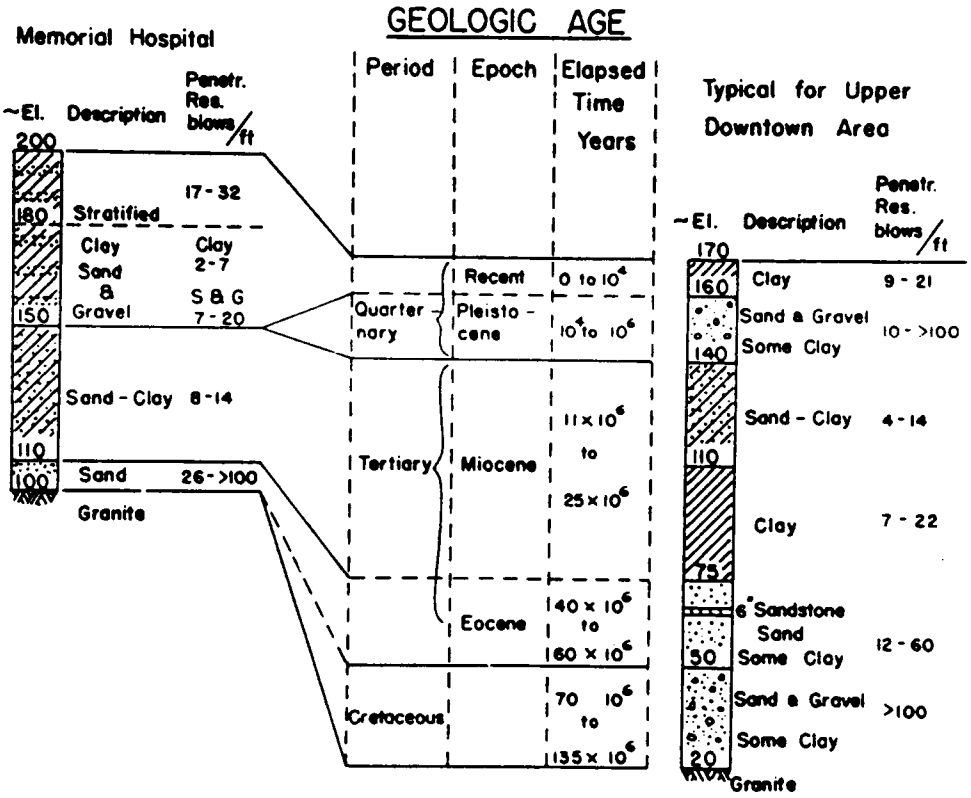

FIGURE 3.2 GEOLOGICAL SEQUENCE OF THE RICHMOND AREA

(AFTER CASAGRANDE, 1966)

ground surface. Layers of very compact sands and gravels immediately overly the rock. These materials are coarse alluvial of Cretaceous age, somewhere in the range of 70 000 000 to 135 000 000 years old. Above the Cretaceous sand is found successively deposits from the Eocene and Miocene epochs, of the Tertiary Period. The Eocene deposits, 40 000 000 to 60 000 000 years old are mainly sand, slightly clayey containing locally sandy clay. The Miocene deposits, 11 000 000 to 25 000 000 years old consist of a thick layer of dark grey marine clay. In the downtown area, this deposit is typically 21 M (70 ft) thick. This is the soil of interest to this work. It was preloaded by a substantial weight of overlying deposits that was later eroded. This soil is only slightly fissured, very stiff but also sensitive.

Formations of the Quaternary Period overlay the Miocene clay. They consist in Pleistocene and Recent deposits of sandy and silty nature.

3.3 SITE INVESTIGATION - DRILLING AND SAMPLING

3.3.1 Soil conditions

The soil conditions at the Richmond sites are determined from the logs of the borings B101 and B114 for the Exhibition Center site, and B202 and B203 for the 6th Street Festival Market Place site in which samples were taken to be tested in laboratory. The logs of these borings are given in Appendix A. From the ground surface, the following layers are encountered at the 6th Street Festival Market Place location:

1. a fill, 2.1 M (7 ft) to 3.9 M (13 ft) thick, made of reddish brown clayey silt or silty clay with some fine sand, classified CH or MH according to USCS.

2. a succession of layers of brown clayey sand or gravel and sandy clay, 8.7 M (29 ft) to 9.0 M (33 ft) thick, classified SM, SC, CL or GC according to USCS.

3. a layer of grey brownish silty clay with some sand, 1.5 M (5 ft) to 2.4 M (8 ft) thick, classified CL according to USCS.

4. a layer of dark grey clay with trace of fine sand, classified CH according to USCS. This soil is the soil of interest for this study. It was investigated over a depth of nearly 9 M (30 ft) by the borings.

A very similar soil sequence is found at the Exhibition Center location to that just described, but the thickness of the layers vary slightly. Details on the nature and the thickness of the layers can be obtained from the logs of the borings given in the Appendix A.

3.3.2 Water conditions

The water table at both sites is perched at the top of layers of low permeability at a depth which varies from point to point. Typically, it is found at a depth of 4.2 M (14 ft) to 7.2 M (24 M) at the Exhibition Center location and at a depth of 5.1 M (17 M) to 10.2 M (34 ft) at the 6th Street Festival Market Place.

3.3.3 Sampling

The location and the depth of the samples taken for laboratory testing are indicated in Table 3.1. Nine samples were obtained by pushing 0.08 M (3 in) diameter Shelby tubes. To

TABLE 3.1 LOCATION OF THE SAMPLES OF THE MIOCENE CLAY TESTED IN THE LABORATORY

Location	Depth of Sample, M (ft)	Site
B101	17.7-18.3 (59-61)	
B101	19.2-19.8 (64-66)	Exhibition Center
B114	17.1-17.7 (57-59)	
B114	21.2-21.8 (70.5-72.50)	
Pier A.5	16.8 (56) 1 sample	Exhibition Center
Pier 8	16.8 (56) 4 samples	
B202	20.1-20.7 (67-69)	
B202	21.6-22.2 (72-74)	
B203	16.2-16.9 (54-56)	6th Street Festival Market Place
B203	17.4-18.0 (58-60)	
B203	18.6-19.2 (62-64)	

Note: Shelby tubes were pushed in the borings B101, B114, B202 and B203. Block samples were hand excavated in the bottom of the piers A.5 and 8.

extrude the soil, the tubes were split lengthwise as jacking out the samples from the tubes provoked a closely spaced horizontal fissuration of the soil.

Five block samples, 0.15 M (6 in) diameter and 0.13 to 0.20 M (5 to 8 in) long were also obtained from the bottom of piers A.5 and 8 of the Exhibition Center project. The top picture in Fig. 3.3 shows the pier A-5 during concrete pouring, just after the block sample shown at the bottom of the figure was hand excavated. The author was allowed by the contractor to go down at the bottom of the piers, into the bell to hand excavate samples. The tools used to excavate the block samples are a small pick, a chimney pipe section 0.15 M (6 in) diameter and 0.20 M (8 in) long which is welded along the split, a small square board, 0.2 M by 0.2 M (8 in by 8 in) and a rectangular steel blade sharpened on one side and equipped with a wood handle on the opposite side, as shown in in the lower picture of Fig 3.3.

The first step in excavating a block sample consists in digging a trench 0.2 M (8 in) deep with the pick all the way around a block of intact soil at the bottom of the pier. Typically, the block has a square plane cross section 0.2 M by 0.2 M (8 in by 8 in). When the trench is excavated, the section of chimney pipe is placed on the top of the block of soil and the soil around it is shaved vertically, and vertical pressure is applied to the chimney pipe using the small square board. Progressively, by trimming the soil and by applying pressure on the pipe, the block sample is carved and the pipe penetrates down around the soil. When the pipe is filled with soil, pick and blade are used to create access at the base of the pipe, and to cut the soil horizontally at that level. After the block sample is brought back to the ground level, it is extruded from the chimney pipe, rolled in a fabric type cheese cloth placed on a board and inside of a PVC pipe section 0.18 M (7 in) diameter. Hot wax is poured over the block sample to fill all the spaces between it and the pipe section. A few small pieces of solid wax were placed between the block sample and the bottom board to allow the wax to flow all around the block sample. Pouring ceased when the block sample was covered by about 0.03 M (1 in) of wax. After half an hour of cooling time, the wax solidified and the combination PVC pipe and wax provided an excellent protection of the sample. In the laboratory, the block sample was

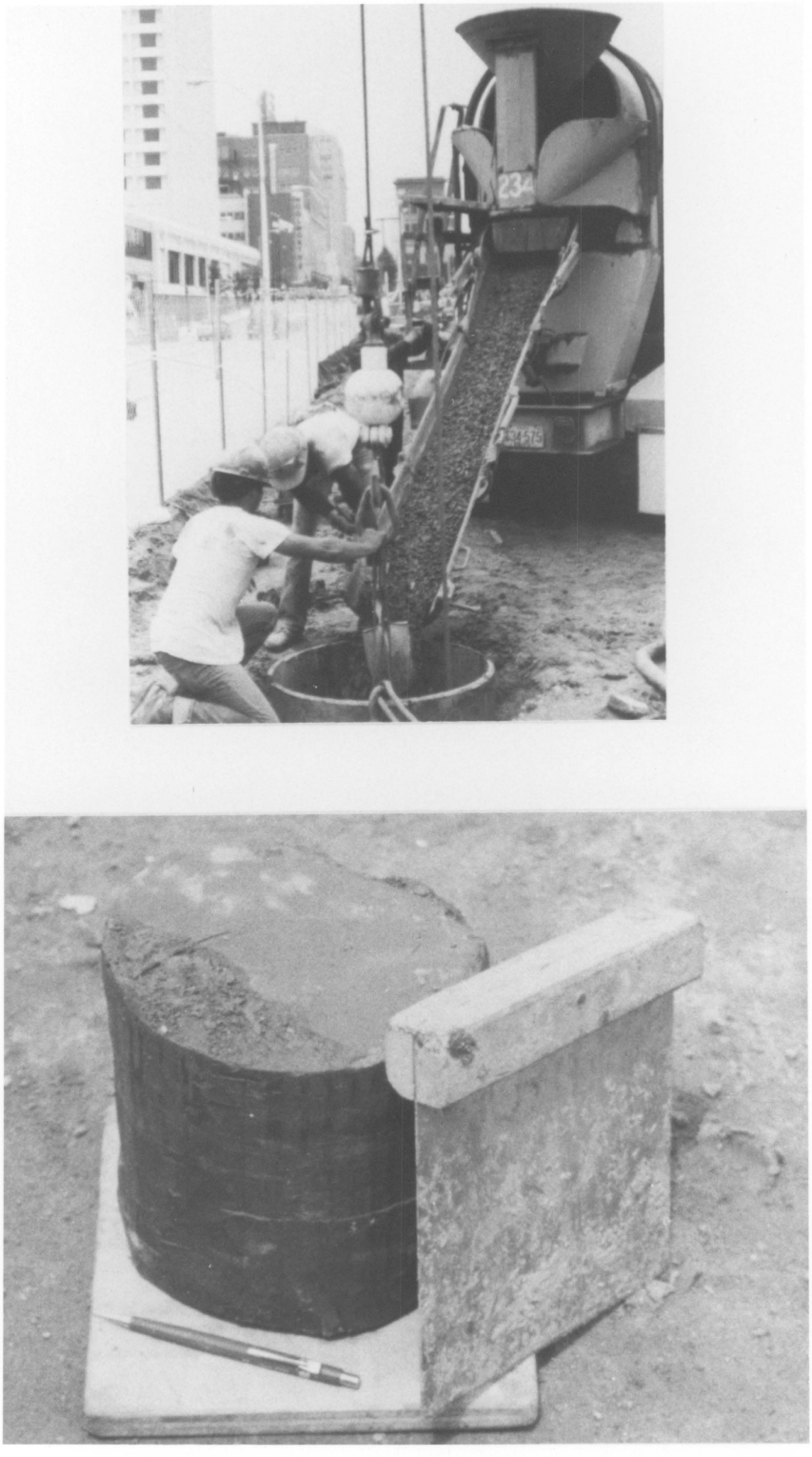

FIGURE 3.3 BLOCK SAMPLING TECHNIQUE

stored in a humid room until it was used for testing. No change of the soil water content was observed during storage.

3.4 LABORATORY TESTING PROGRAM

Thirty three determinations of natural water content, twenty three determinations of Atterberg limits and sixteen determinations of total unit weight were obtained, for the Miocene clay.

Eight unconsolidated undrained (UU) tests were conducted on undisturbed samples in the triaxial apparatus to determine the undrained shear strength of the soil, and four UU tests were performed on remolded soil to assess its sensitivity. Sixteen isotropically consolidated undrained (ICU) tests were conducted on undisturbed samples in a triaxial apparatus to observe the development of pore pressures during shearing and to determine the drained shear strength parameters of the clay. Six stress controlled consolidation tests and three strain controlled consolidation tests were performed to determine the compressibility of the soil.

3.5 RESULTS OF CLASSIFICATION TESTS

One of the hand excavated block samples is shown in the photograph in Fig. 3.3. The block is approximatively 6 in (0.15 M) diameter by 7 in (0.18 M) high. The clay is dark gray, shiny when shaved with the blade shown in the figure. The soil has a hard consistency and cannot be marked by pressing the thumb against the sample. According to Martin and De Stephen (1983), the soil is not slickensided but contains occasional fissures which extend several meters and are randomly oriented. Over several centimeters on both sides of the fissures, the soil has generally a distinctive tan color due to weathering.

The clay mineralogy of the soil from the block sample A-5 was performed by Professor L. Zelazny of the Agronomy Department at Virginia Tech. The results of the analysis indicate the following composition:

Mica:	25%
Kaolinite:	10%
Smectite:	55%
Quartz:	1%
Interstratified Phyllosilicates:	9%

Results of the identification tests are given in Table 3.2 and the values of the Atterberg limits reported on the plasticity chart are given in Fig 3.4. Similar properties are found at the two sites. If the two top samples taken in boring B203 are not considered, the liquid limit varies generally between 65 and 80, the plastic limit between 30 and 40 and the natural water content between 45 and 50%. The total unit weight of the soil typically varies between 109.2 and 115.4 pcf (17.2 and 18.2 KN/M2). The soil, when classified according to USCS, is situated at the border of MH-OH and CH. Its natural water content is nearer the plastic limit than the liquid limit, a sign that the soil is overconsolidated. The tests run on the two top samples taken from the boring B203 indicate locally a lower plasticity, with a liquid limit varying between 44 and 55, a plastic limit between 28 and 29 and a natural water content between 32 and 44%. At this location, the soil is classified ML or OL according to USCS.

Casagrande (1966) reports identification test results performed between El. 43 and El. 23 at different sites in the downtown Richmond area. From the test results, he differentiates the Upper Miocene clay, found between El. 43 and El. 33.5, from the Lower Miocene clay, found below El. 33.5. The Upper Miocene clay is characterized by a liquid limit and a plasticity index which vary between 40 and 60 and between 20 and 40 respectively. The Lower Miocene clay is characterized by a liquid limit and a plasticity index which vary between 60 and 120 and

TABLE 3.2 RESULTS OF THE IDENTIFICATION TESTS ON THE MIOCENE CLAY

Location	Aver. Depth M (ft)	Nat. Water Content, Percent	Liquid Limit	Plastic Limit	Total Unit Weight, KN/M3 (pcf)
B114	21.5 (71.5)	55, 69 32	109 55	50 28	15.5 (98.5)
B114	17.4 (58.0)	46, 47 47	68 63	42 38	17.1 (108.5) 17.3 (109.8)
B101	19.5 (65.0)	45, 50 47, 49	74 70	40 36	
B101	17.9 (59.5)	46, 50 46, 47	64 68	41 40, 36	 17.1 (108.5)
B202	20.4 (68.0)	49, 47 41, 45 48 48 44	77 77 78 70 65	40 35 38 35 38	17.7 (112.3) 17.2 (109.2) 17.2 (109.2) 17.3 (109.8) 17.1 (108.5)
B202	21.9 (73.0)	72 46 44 48	 60 68	37 34 41	 17.4 (110.4) 17.1 (108.5)
B203	16.5 (55.0)	44 38	50	28	 18.7 (119.1)
B203	17.7 (59.0)	32 37 33 38 39	 55 39 46 44	 29 29 28 28	 18.2 (115.4) 18.1 (114.8) 17.4 (110.4) 17.3 (109.8)
B203	18.9 (63.0)	49 45	81 68	35 31	
8 8	16.8 (56.0) 16.8 (56.0)	50, 51 49	74 72	48 43	 18.0 (114.2) 17.2 (109.2)

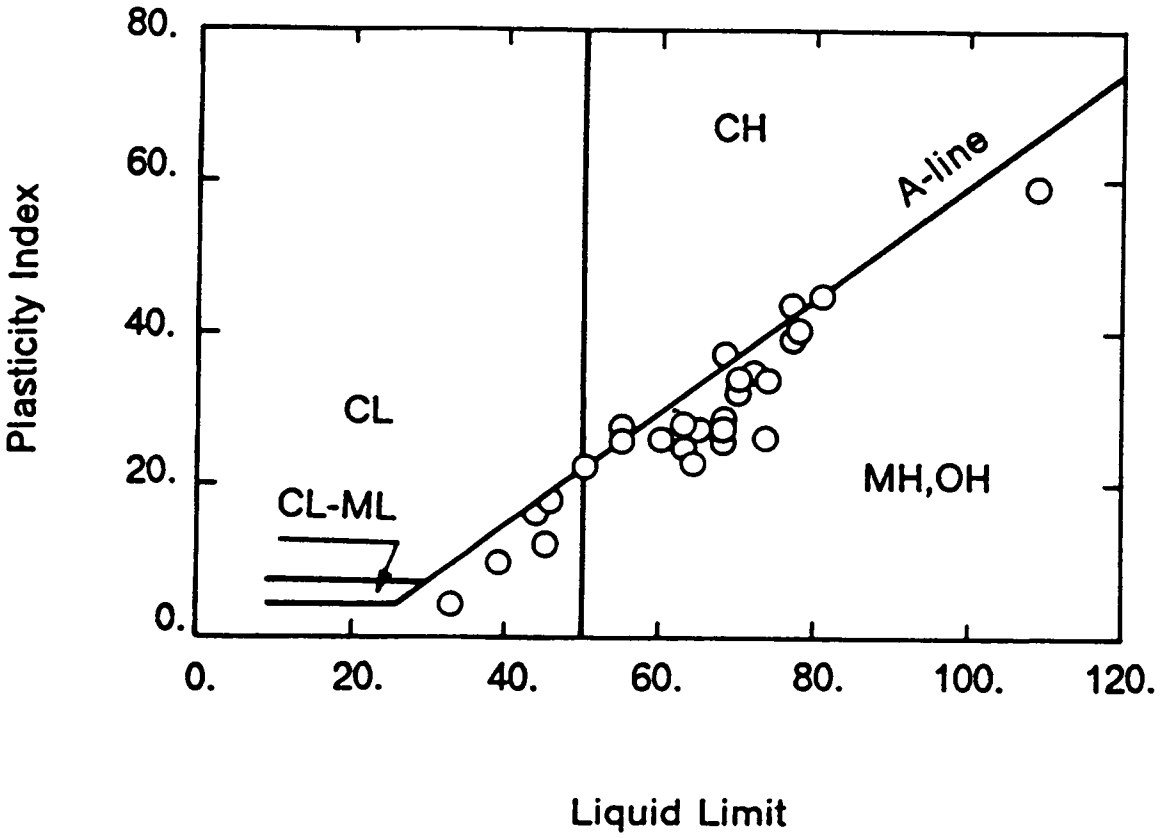

FIGURE 3.4 PLASTICITY OF THE MIOCENE CLAY

between 40 and 80 respectively. Both clays are classified CH according to USCS. Casagrande (1966) also reports Atterberg test results performed on oven-dried samples. For both clays, oven-drying typically reduces the liquid limit by 30 percent and the plasticity index by 50 percent.

The soil samples tested in this study were taken between El. 20 and El. 17, which corresponds to the transition zone between the Upper Miocene clay and the Lower Miocene clay. If classified in terms of their liquid limit, the samples tested fall into both ranges of liquid limits covered by the Upper and Lower Miocene clays. However, on the plasticity chart, the plasticity of the soil samples tested in this study is generally lower than the one reported by Casagrande.

For purpose of comparison, it is useful to consider the Leda clay of Canada. This soil is a well known stiff clay of strong sensitivity. It forms an extreme case against which the Miocene clay can be contrasted.

Typical liquid and plastic limits of the sensitive Leda clays are 60 and 25 respectively, which situate these clays at the boundary of MH and CH in the plasticity chart. A significant difference exists between the Miocene clay and Leda clays in the classification results. The natural water content of the Richmond clay is between the plastic and liquid limits, and generally in the vicinity of the plastic limit. On the contrary, the natural water content of Leda clays, which varies typically between 60 and 90%, is near the liquid limit and often exceeds it.

3.6 CONSOLIDATION TESTS

A total of nine oedometer tests were performed on samples of the Miocene clay. Details on the origin of the samples and on the type of tests are given in Table 3.3.

TABLE 3.3 GENERAL CHARACTERISTICS OF THE OEDOMETER TESTS PERFORMED ON THE MIOCENE CLAY

Location	Depth, M	Type of Test	Type of Sample
B203	16.2 - 16.8	stress controlled	Tube
B114	17.1 - 17.7	stress controlled	Tube
B114	17.1 - 17.7	stress controlled	Tube
B114	17.1 - 17.7	stress controlled, remolded(2)	Tube
Pier 8	16.8	stress controlled	Block
Pier 8	16.8	stress controlled	Block
B202	20.1 - 20.7	strain controlled	Tube
B202	20.1 - 20.7	strain controlled	Tube
B202	20.1 - 20.7	strain controlled	Tube

Notes:

(1) vertical loading means that the direction of loading in the oedometer test is the vertical in the field. Similarily, horizontal loading means that the direction of loading in the oedometer test is the horizontal direction in the field.

(2) test performed on remolded soil

Six of the nine tests are conventional stress controlled tests and the other three are strain controlled tests. The samples tested are 0.06 M (2.5 in) in diameter and 0.02 M (0.9 in) thick. Vertical stresses as high as 4600 KN/M2 (48 tsf) were applied to the samples. The samples were placed in frames equipped with hydraulic loaders which can be used either as stress or strain controlled units. They were found especially convenient when used in stress controlled tests at higher stress levels. The conventional stress controlled consolidation tests were performed on specimens taken from Shelby tubes and block samples to determine the preconsolidation pressure, the compression index, the recompression index and the coefficient of consolidation of the soil. One test was performed on remolded soil to examine the effect of disturbance on the compressibility properties of the clay. The sample of remolded soil was prepared by kneading the soil in the sampler ring with a Harvard miniature compactor.

Strain controlled tests were conducted on samples loaded in the vertical and horizontal directions to determine the coefficient of consolidation, c_v in these two directions.

One advantage of the strain controlled test over the stress controlled test when determining the preconsolidation pressure is the development of a large number of data points. This allows one to accurately construct the e-log p curve, as the average vertical effective pressure in the sample can be determined at any time during the test. A complete mapping of the transition between recompression and virgin compression on the e-log p curve and a precise definition of the preconsolidation pressure is possible using these results.

The strain controlled tests were run according to the procedure described by Smith and Wahls (1969), where drainage during loading occured only at the top of the sample. A pressure transducer monitored the excess pore pressure at the base of the sample. The rate of displacement of the loading piston was fixed at the beginning of the test. In this study, typical rates varied between 1.3 10^{-2} and 1.3 10^{-1} % per minute. During the test, the vertical compression of the sample, the total vertical stress applied to the sample and the excess pore pressure at the base of the sample was monitored. In this study, typical ratios varied between 0.25 and 0.45.

Smith and Wahls (1969) derive the two following expressions to determine the average vertical effective stress $\overline{\sigma'}_1$ in the sample and the coefficient of consolidation c_v:

$$\overline{\sigma'}_1 = \sigma_1 - \alpha u_b$$

$$c_v = \frac{rH^2}{a_v u_b}\left(\frac{1}{2} - \frac{b}{r}\left(\frac{1}{12}\right)\right)$$

with

σ_1	the total vertical stress applied to the sample
u_b	the excess pore pressure at the base of the sample
α	the ratio u/u_b where u is the average excess pore pressure in the sample
b/r	dimensionless ratio which characterizes the variation of the void ratio with depth
H	the height of the sample
a_v	the coefficient of compressibility

$\overline{\sigma'}_1$ and c_v can be determined at any time during the test provided u_b and the compression of the sample are monitored.

To perform oedometer strain controlled tests, the soil must seal the gaps existing between the sample and the oedometer ring for the excess pore pressure to build up at the base of the sample during loading. In the case of the Miocene clay, the gaps remained opened as

the clay is hard and they served as drainage paths during loading. As a consequence, the control of drainage was lost and the interpretation of the test results according to Smith and Wahls was not possible. In this study, two of the three strain controlled tests performed encountered this problem.

In Fig. 3.5, results of three stress controlled oedometer tests are compared. The tests were performed on different types of samples: a sample of remolded soil at the top of the figure, a sample taken from the center of a Shelby tube, and a sample trimmed from a block sample. For reference, the field compressibility of the soil has been estimated as per Schmertmann (1955) and reconstructed for the two lower oedometer curves. It is also indicated on the oedometer curve of the remolded soil.

The following remarks can be made based on the results:

1. The oedometer curve from the block sample indicates very little disturbance. It closely follows the reconstructed field compressibility, a sign of the excellent quality of the sample tested.

2. The test which uses the Shelby tube sample indicates some degree of disturbance. Its oedometer curve is situated between the completly remolded soil oedometer curve at the top of the figure and the curve of the most undisturbed sample at the bottom of the figure.

3. The initial void ratio of the remolded soil is much lower than the initial void ratio of the undisturbed soil of the block samples (1.167 against 1.300). This effect of remolding on the initial void ratio is characteristic of sensitive clays. Remolding destroys the strong interparticle bonds of the loose assemblage and leads to a collapse of the structure of the soil with a substantial reduction of the volume of the voids.

4. The oedometer curve of the remolded soil is very flat and shows no break at the preconsolidation stress level.

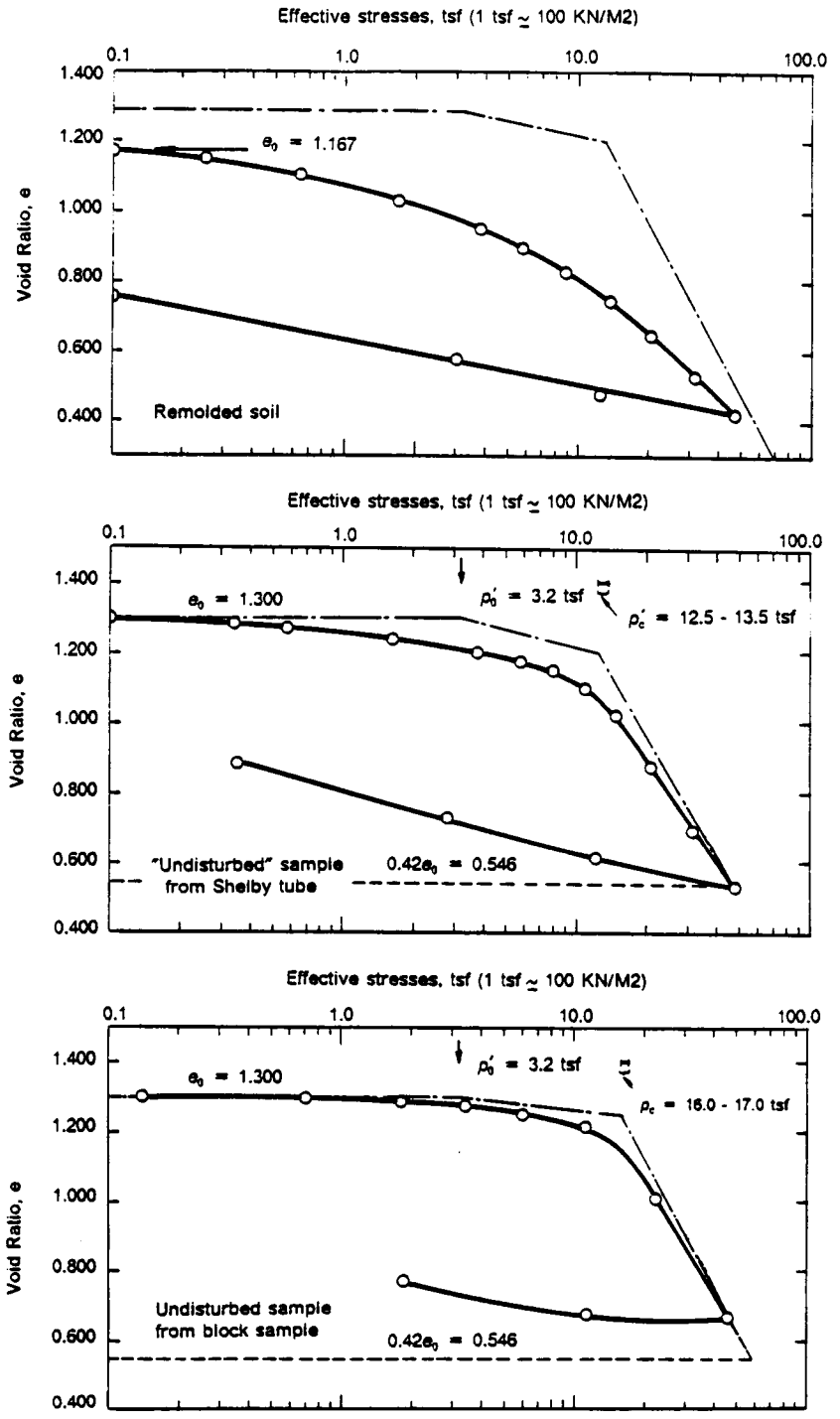

FIGURE 3.5 TYPICAL OEDOMETER TEST RESULTS

5. Disturbance leads to an underestimation of the preconsolidation pressure p'_c. The preconsolidation pressure is estimated as 1250-1350 KN/M2 (12.5-13.5 tsf) for the Shelby tube sample, and 1600-1700 KN/M2 (16.0-17.0 tsf) for the block sample.

6. The slope of the virgin curve, C_c is not affected by a moderate degree of disturbance of the soil such as that for the Shelby tube sample.

Detailed results of all of the oedometer tests are given in Appendix B and the typical compressibility parameters of the Miocene clay interpreted from them are presented in Table 3.4. The compression index, C_c, is determined using the method proposed by Schmertmann (1955) by reconstructing the field compressibility from the laboratory e - log p curve. Results of five tests out of six given in Table 3.4 indicate consistent values of C_c and C_r, for stress controlled tests or strain controlled tests. Typical C_c values are 1.2 to 1.5 and C_r values 0.14 to 0.16. The values of C_r are higher than the ones obtained from the correlation developed by Skempton (1944):

$$C_c = 0.009(LL - 10)$$

where LL is the liquid limit.

This correlation was developed for non sensitive soils and it underestimates the real value of C_c in the case of the Miocene clay. The one test which indicates an unusually low C_c value was from a test on a sample from a Shelby tube. It apparently reflects a significant degree of disturbance.

The preconsolidation pressure, p'_c is determined using the method proposed by Casagrande (1936). Typical values are given in Table 3.4. They vary between 1.3 and 1.6 MN/M2 (13 and 16 tsf).

The overconsolidation ratio, OCR, varies between 4 and 5. It is calculated assuming a uniform cover of total unit weight equal 19.6 KN/M3 (125 pcf) and no water table. The coefficients of consolidation c_v calculated from the results of the stress and strain controlled tests

TABLE 3.4 COMPRESSIBILITY PROPERTIES OF THE MIOCENE CLAY

Location	Average Depth, M	Compression Index, Cc (1)	Recompression Index, Cr (2)	Precons. Pressure, MN/M2 (tsf) (3)	OCR
B203	16.5	0.4	0.04	0.9 (9.2)	2.8
B114	17.4	1.3-1.4	0.14	1.5 (15.0)	4.7
B114	17.4	1.2	0.16	1.3 (13.0)	4.1
Pier 8	16.8	1.2-1.3	0.07	1.6 (16.0)	5.0
Pier 8	16.8	1.2	0.14	1.4 (14.0)	4.4
B202 (4)	20.4	1.5		1.4 (14.0)	3.4

Notes:

(1) Compression index from field compressibility reconstructed according to Schmertmann (1955).

(2) Recompression index from average slope of the unloading part of the e-log p curve.

(3) Preconsolidation pressure according to Casagrande (1936).

(4) Strain controlled test. The two other similar tests were not interpreted for the reasons mentioned in the text.

are given in Fig 3.6 as a function of the change of void ratio of the soil. Typical values of c_v are 10^{-1} to $10^{-2} cm^2/s$ when the change of void ratio is less than 0.1 and 5 $10^{-4} cm^2/s$ when it reaches 0.4.

Silvestri et al. (1985) report results of oedometer tests in Leda clays. The compression index C_c varies from 3.0 to more than 5.0, the recompression index C_r from 0.01 to 0.09 and the preconsolidation pressure from 85 to 150 KN/M2 (0.9 to 1.5 tsf). The C_c values are approximately double those for the Richmond clay. By the same token, the initial void ratio of Leda clays is typically 2.10 to 2.50, nearly twice the initial void ratio of the Miocene clay, explaining the large difference in the compression indices.

3.7 UNDRAINED UNCONSOLIDATED TESTS

Twelve UU tests were performed; four on Shelby tube samples, four on block samples and four on samples of remolded soil. Detailed results are given in Appendix C.

The samples tested have a diameter of 0.04 M 1.4 in) and a ratio length to diameter which varies between 2 and 3. The remolded samples were prepared in a forming jacket by kneading the soil with a Harvard miniature penetrometer, while keeping the water content unchanged.

Standard testing procedures were used. The rate at which the samples were sheared varies between 0.2%/min and 0.5%/min. The corresponding time to failure for a sample failing at 2% axial strain is of the order of 10 minutes.

Typical results are given in Fig 3.7. From the top to the bottom of the figure are given successively the stress- strain curves for a sample of remolded soil, a Shelby tube sample, and a sample taken from an undisturbed block . The horizontal scale is the same for the three diagrams but the vertical scale is divided by two when switching diagrams from the top to bottom. One immediately observable difference in the results is in the shape of the stress-

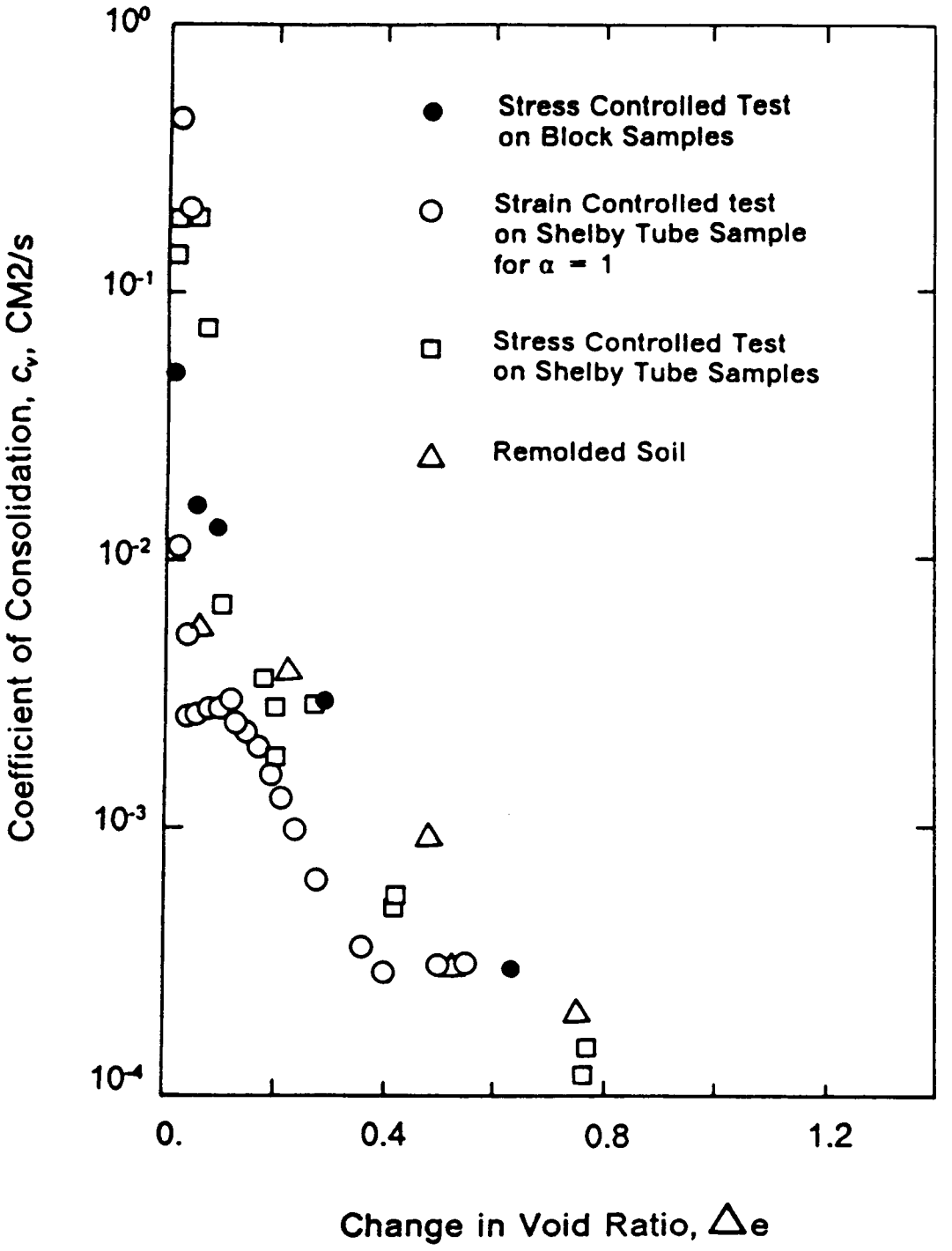

FIGURE 3.6 COEFFICIENT OF CONSOLIDATION VERSUS CHANGE OF VOID RATIO

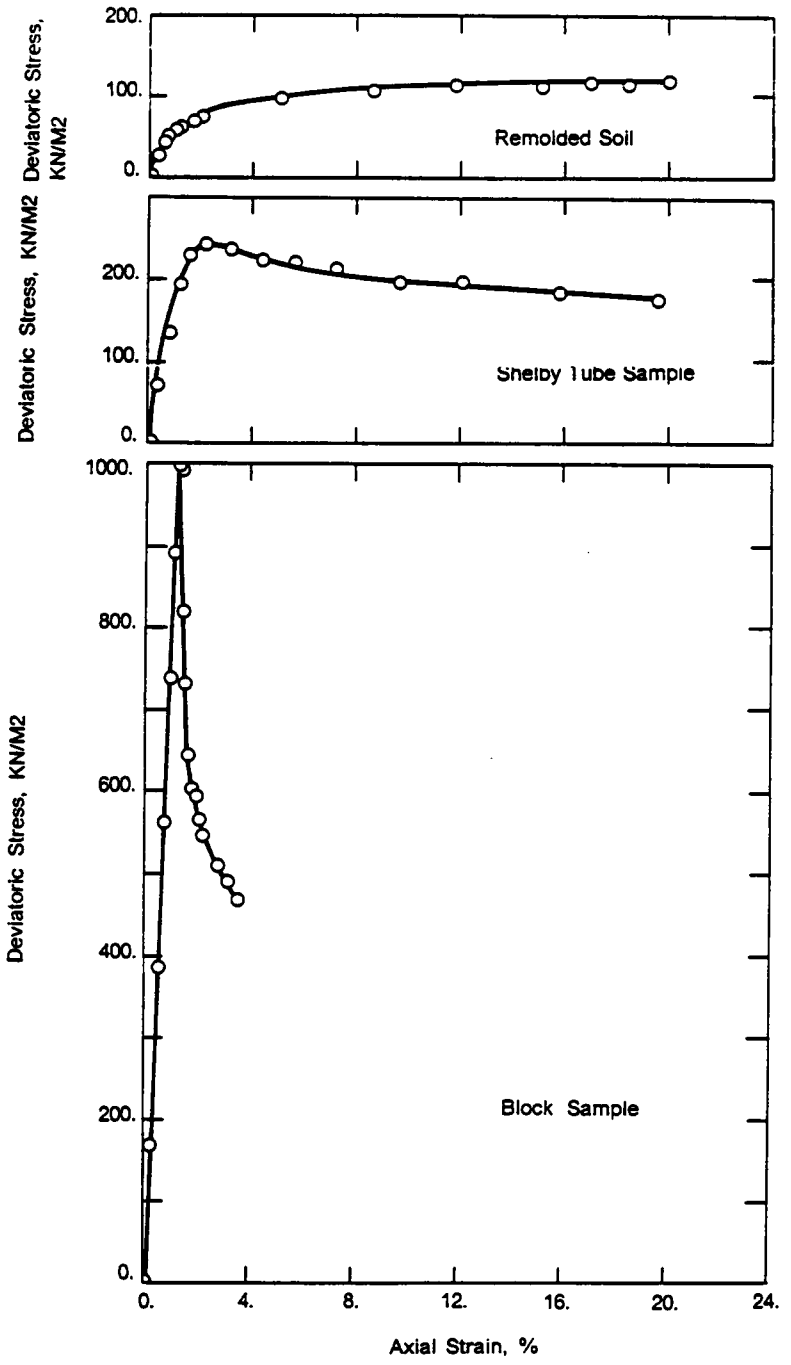

FIGURE 3.7 TYPICAL UU TRIAXIAL TEST RESULTS

strain curve. The test result on the remolded soil does not show a clear peak while that for the sample taken from the Shelby tube has a peak at 2 to 3% axial strain followed by a modest decline. The result on the sample trimmed from the block sample has a sharp peak at 1% axial strain and a significant loss of strength after the peak. Importantly, the peak strength of the soil of the Shelby tube is twice the maximum strength of the remolded soil and the peak strength of the soil from the block sample is four times the peak strength of the soil of the Shelby tube.

Results of all the tests are summarized in Table 3.5. They indicate that three of the four tests on Shelby tube samples have a maximum shear strength between 114.6 KN/M2 (16.6 psi) and 121.9 KN/M2 (17.7 psi). The four tests performed on specimens trimmed from block samples indicate much higher peak strengths with one value of 274 KN/M2 (39.7 psi) and three of 500 KN/M2 (72.5 psi), results which are 2 to 4 times higher than the strengths measured on Shelby tube samples. The shear strength measured from tests on remolded soil varies between 62.1 KN/M2 (9 psi) and 76.9 KN/M2 (11.1 psi), values only 1/5 to 1/8 of those of the block samples.

Mohr envelopes for maximum undrained shear strengths for the Shelby tube and remolded samples are given in Fig. 3.8. They are compared to the Mohr circles at failure for the four tests on the block samples. All of the envelopes follow conventional " $\Phi = 0$ " concepts for saturated clays; however, the undrained shear strengths are very different depending upon the method of sample preparation, with the cohesion values of the block samples by far the highest.

Casagrande (1966) reports results of four unconfined UU triaxial tests, two performed on Upper Miocene clay samples and two on Lower Miocene clay samples. The two test results performed on the Upper Miocene clay indicate undrained shear strength values of 220 and 245 KN/M2 (32 and 35.5 psi) with axial strains at failure equal to 5 and 7 percent. The two test results performed on the Lower Miocene clay indicate undrained shear strength values of 319 and 441 KN/M2 (46 and 64 psi) with axial strains at failure equal to 1.5 and 2 percent. From these test results, only the highest undrained shear strength value (441 KN/M2) from the test

TABLE 3.5 RESULTS OF UU TRIAXIAL TESTS ON THE MIOCENE CLAY

Location	Depth, M	Confining Pressure, KN/M2 (psi)	Peak Shear Strength, KN/M2 (psi)	Residual Shear Strength, KN/M2 (psi)
B203	17.4 - 18.0	69.0 (10.0)	79.0 (11.5)	61.2 (8.9)
B203	17.4 - 18.0	207.1 (30.0)	115.1 (16.7)	-
B203	17.4 - 18.0	345.2 (50.0)	114.6 (16.6)	-
B203	17.4 - 18.0	483.0 (70.0)	121.9 (17.7)	85.7 (12.4)
PIER 8	16.8	345.2 (50.0)	500.0 (72.5)	-
PIER 8	16.8	414.0 (60.0)	274.0 (39.7)	-
PIER 8	16.8	143.0 (20.0)	486.0 (68.0)	< 275.0 (39.0)
PIER 8	16.8	286.0 (40.0)	475.0 (66.0)	< 200.0 (28.0)

SHELBY TUBE SAMPLES AND BLOCK SAMPLES

Location	Depth, M	Confining Pressure, KN/M2 (psi)	Peak Shear Strength, KN/M2 (psi)	Residual Shear Strength, KN/M2 (psi)
B101	17.7 - 18.0	69.0 (10.0)	-	73.8 (10.7)
B101	17.7 - 18.0	207.1 (30.0)	-	56.3 (8.2)
B101	17.7 - 18.0	207.1 (30.0)	-	76.9 (11.1)
B101	17.7 - 18.0	345.2 (50.0)	-	75.9 (11.0)

REMOLDED SOIL

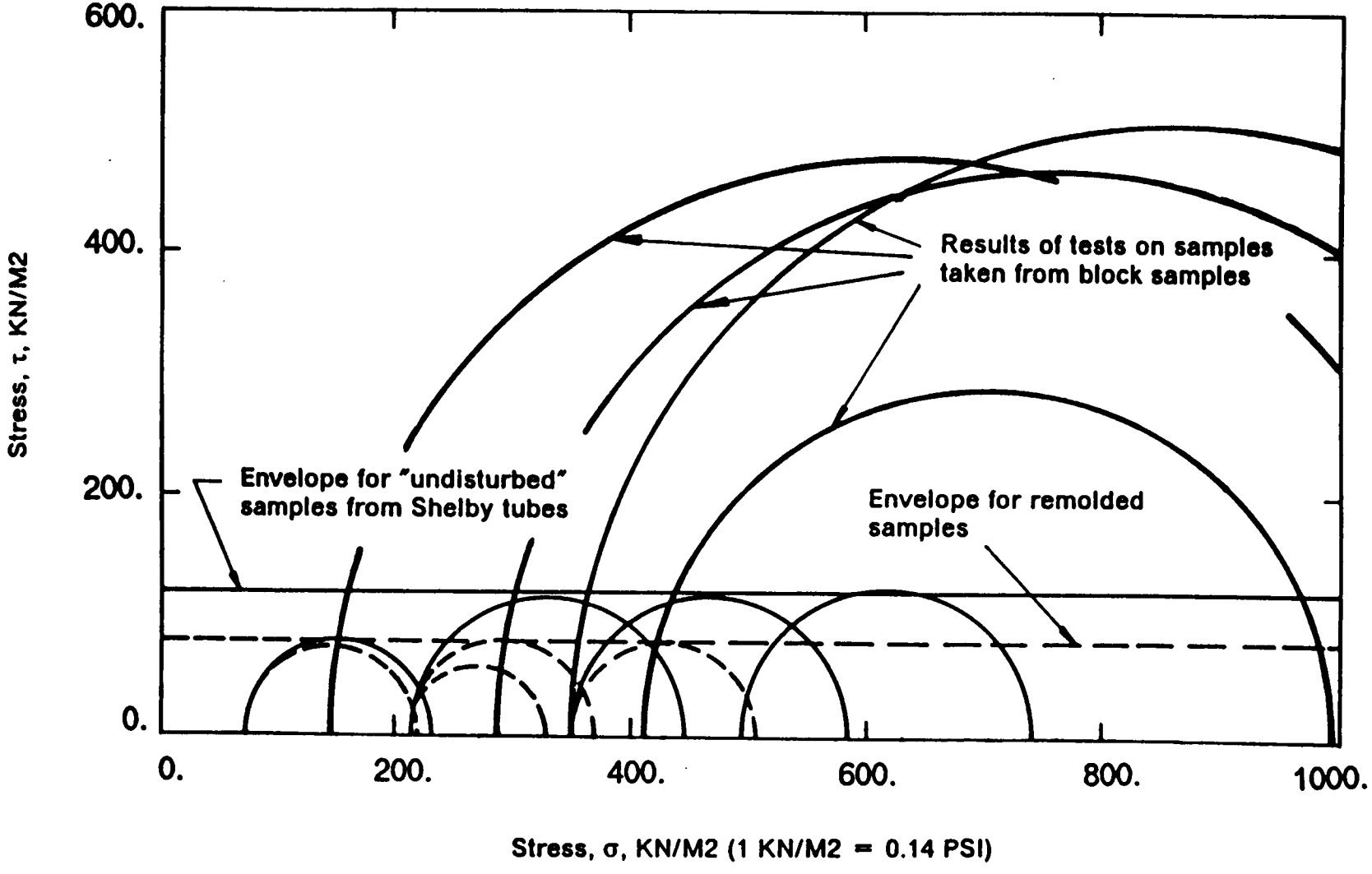

FIGURE 3.8 UNDRAINED SHEAR STRENGTHS

performed on the Lower Miocene clay agrees with the values of undrained shear strength reported in this study. The other values are typically 1.5 to 2 times lower and the axial strains at failure for these tests suggest that the soil was disturbed when it was tested.

Martin and De Stephen (1983) communicate undrained shear strength values from tests on Shelby tube samples ranging between 240 and 442 KN/M2 (33.6 and 61.9 psi).

The sensitivity of the clay, defined as the ratio between its undrained shear strength when undisturbed and its undrained shear strength when remolded averages 7 considering tests on specimens trimmed from block samples.

Casagrande (1966) reports values of sensitivity of 4 and 7 when determined from the UU triaxial test results on the Upper Miocene clay and from 10 to 22 when determined from the UU triaxial test results on the Lower Miocene clay. He does not report how the remolded soil samples used to determine the sensitivity of the soil were prepared and tested.

The results of the undrained shear strength tests can be summarized as follows:

1. Three of four tests on samples taken from the block samples give values of undrained shear strength which vary between 475 and 500 KN/M2 (66.0 and 72.5 psi). This consistency in the results

2. Four tests performed on Shelby tube samples give undrained shear strength values which vary between 79.0 and 121.9 KN/M2 (11.5 and 17.7 psi). These values are also consistent and typically 4 times smaller than those obtained from the block samples.

3. The sensitivity of the clay is 7.

3.8 COMPARISION OF UU TEST RESULTS FOR THE MIOCENE CLAY TO LEDA CLAYS

Crawford (1965) reports the results of a series of unconfined compression tests performed on samples of Leda clay trimmed from undisturbed blocks of soil. The results of the tests indicate a brittle type of behavior during shear with peak values of deviatoric stresses varying between 245 and 441 KN/M2 (36 and 64 psi) occuring at axial strains less than 1%.

Crawford and Eden (1965) report undrained shear strength and sensitivity values of Leda clays from field vane shear tests performed at thirteen different sites. The undrained shear strength varies between 50 and 200 KN/M2 (7 and 29 psi). The sensitivity varies between 10 and 25 but can reach occasionnaly values as high as 500.

From the preceeding results it appears that Leda clays and the Richmond clay have similar behaviors when tested in UU or UC test conditions. They show a brittle response with a peak of shear strength at an axial strain generally less than 1%. Leda clays are much more sensitive than the Richmond clay. The main reason for this difference comes from the fact that Leda clays have a natural water content generally at the liquid limit and, when remolded, these clays behave like viscous fluids. This is not the case for the Miocene clay which has a natural water content situated between the plastic and liquid limits, generally in the vicinity of the plastic limit.

3.9 INTERPRETATION OF ICU TESTS

Six ICU triaxial tests were performed on specimens taken from 0.08 M (3 in) diameter Shelby tubes, ten similar tests were run on samples trimmed from the block samples and three tests were performed on remolded soil samples. The samples tested have a diameter

of 0.04 M (1.4 in) and a ratio length to diameter which varies between 2 and 3. Each test follows three consecutive phases: saturation, consolidation and shear.

Saturation is performed by applying back pressure and cell pressure so that a net effective confining pressure of 13.8 to 34.5 KN/M2 (2 to 5 psi) is applied to the sample. Saturation is controlled by checking the ratio Δu / $\Delta\sigma_{cell}$, known as the B parameter, where Δu is the increase of the excess pore pressure in the sample generated by the change of cell pressure $\Delta\sigma_{cell}$. Typically, B is determined every two hours by measuring the increase of pore pressure generated by an increase of cell pressure of 35 KN/M2 (5 psi). After B is checked, the back pressure is increased by 35 KN/M2 (5 psi) in order to maintain the same difference between the cell pressure and the back pressure which was initiated at the beginning of the saturation phase. Saturation is considered complete when B reaches at least 0.97.

Consolidation follows saturation. In this phase, the consolidation pressure is applied to the sample and changes of volume are measured during drainage.

Drainage during consolidation occurs at the bottom and top of the sample. Filter paper are spaced every 0.006 M (0.25 in) around the sample and are in contact with the top and bottom porous caps to accelerate the drainage during consolidation and the equalization of the excess pore pressures between the center and the extremities of the sample during saturation and shear. Finally, shearing of the sample is performed under undrained conditions. The rate of shear is chosen such that a uniform excess pore pressure develops throughout the sample in order that measurements made with a pressure transducer at the base of the sample are representative of the pore pressures existing in the center of the sample. The vertical force applied to the sample and the excess pore pressures that develop are monitored with the displacement of the piston.

The time versus volume change curve during the consolidation phase of a ICU test using a consolidation pressure of 242 KN/M2 (35 psi) is given in Fig. 3.9. It indicates that 50% of the consolidation occurs before 0.1 minute and that 90% of the consolidation is reached within 10 minutes. This fast rate of consolidation is typical for stiff clays. The method proposed by Gibson, as reported by Bishop and Henkel (1962), is used to determine the rate at which the

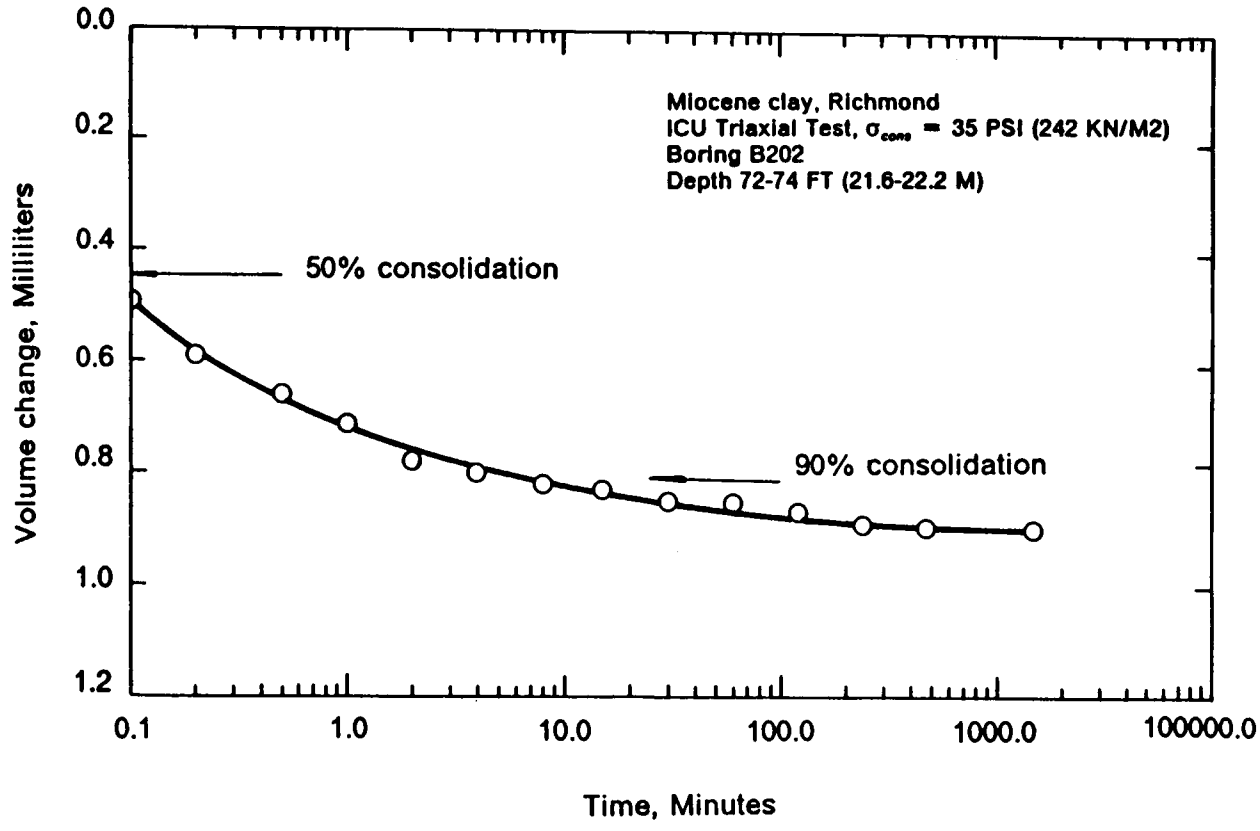

FIGURE 3.9 RATE OF VOLUME CHANGE DURING THE CONSOLIDATION PHASE OF AN ICU TRIAXIAL TEST

sample should be sheared to have a uniform excess pore pressure in the sample. It relates the time factor T to the percentage of equalization between the excess pore pressure at the center of the sample and at its extremities. Typically, if 95% equalization is expected when failure of the sample occurs, and if the sample is drained at its two extremities, then

$$T_{95} = \frac{c_v t}{h^2} = 1.67$$

with

c_v the coefficient of consolidation

h the drainage path length

t the time to failure

At the beginning of the testing program, it was assumed that the changes of void ratio, Δe, during the consolidation phase of the ICU tests was smaller than 0.1. According to Fig. 3.6, a typical value of the coefficient of consolidation for this range of void ratio changes is 10^{-2} cm^2/s. The subsequent testing program confirmed the assumption. Accordingly, time to failure in an ICU test should be 2400 seconds in order to have at failure 95% equalization of excess pore pressure between the extremities and the center of the sample. Assuming that failure occurs at 1% axial strain and that 0.08 M (3 in) is the typical length for the samples, the rate of strain should be 1.2% per hour. This is a conservative estimate as no account is made for the filter paper strips at the periphery which accelerate the equalization of the pore pressures between the center and the extremities of the sample. For this study, all the tests were sheared at strain rates varying between 1% and 2% per hour.

Typical tests results are given in Fig. 3.10. From the top to the bottom of the figure, the stress strain curves and excess pore pressure strain curve are given for a sample of remolded

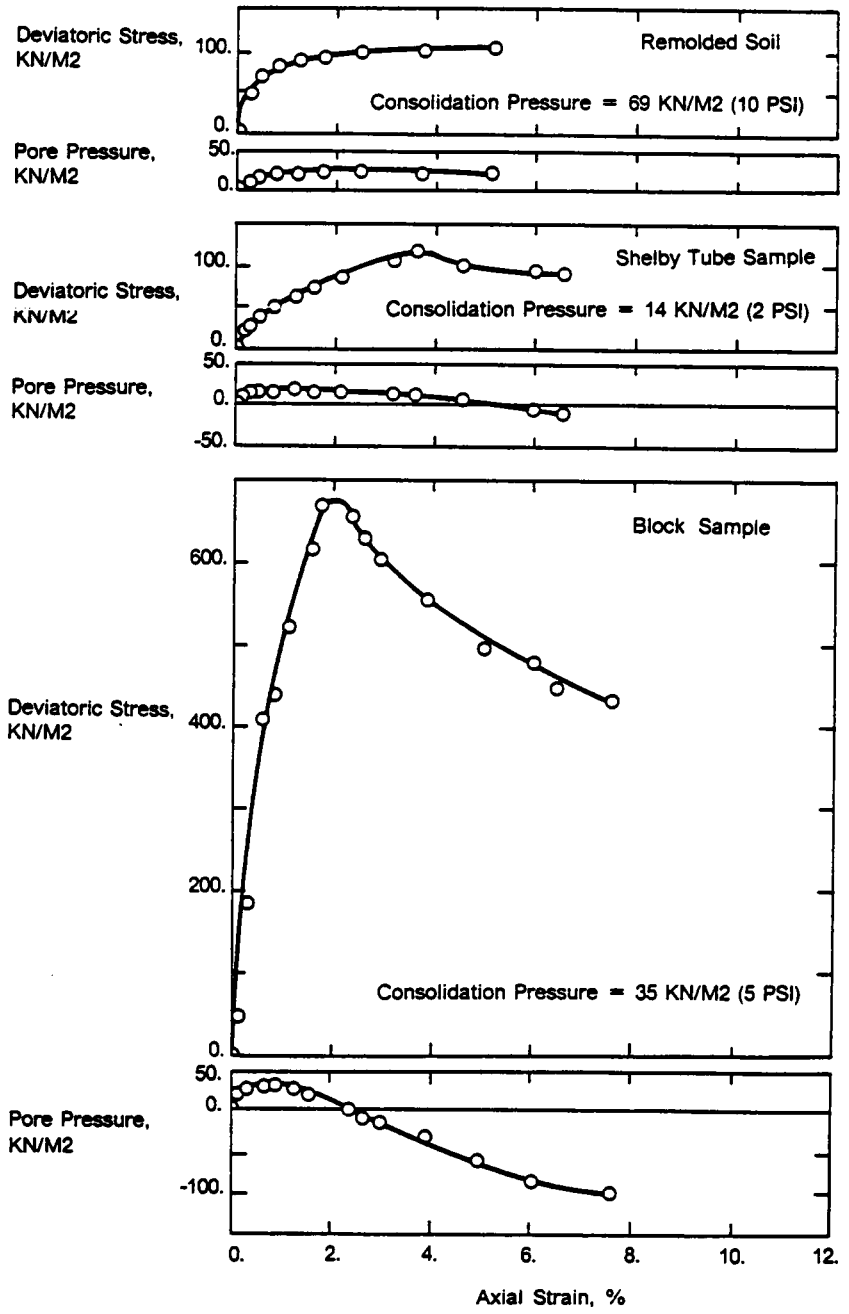

FIGURE 3.10 TYPICAL ICU TRIAXIAL TEST RESULTS

soil, for a Shelby tube sample and for a sample taken from a block sample. Consolidation pressures of 14 to 69 KN/M2 (2 to 5 psi) were used in the three tests.

Similar to the UU tests results, one immediately observable difference in the results is in the shape of the stress strain curve. The test result on the remolded soil does not show a clear peak. The test result on the Shelby tube sample has a peak at 3 to 4% axial strain followed by a small decline to a residual strength at 6 to 7% axial strain which is of the order of 80% of the peak strength. The test result of the sample taken from the block sample has a sharp peak at less than 2% axial strain, and a significant loss of strength after the peak.

The excess pore pressures during shear also show observable differences. The results on remolded soil indicate the development of positive pore pressures throughout with stationary values from 1% axial strain to the end of the test. The results on the Shelby tube sample indicate positive pore pressures between 0 and 5% axial and negative from 5% axial strain to the end of the test at 7% axial strain. Results on the block sample indicate the development of a small positive pore pressure between 0 and 2% axial strain followed by a continuously increasing negative pore pressure until the end of the test. According to Fig. 3.10, the negative pore pressure at failure in the block sample is nearly twenty times the negative pore pressure at failure in the Shelby tube sample. The results shown in Fig. 3.10 indicate that disturbance of the soil delays and limits the development of negative pore pressures during shear for samples consolidated to small consolidation pressures.

Detailed results of the ICU tests are given in Appendix D and summarized in Table 3.6. They indicate that the excess pore pressures at failure as well as the parameter A at failure, A_f, increase with the consolidation pressure, when failure is defined as the peak of deviatoric stress. Also, as the excess pore pressures developed at failure are generally large, the minor effective principal stresses are small and can even be negative such as for the test on a Shelby tube sample B202 consolidated at 242 KN/M2 (35 psi) for which σ'_3 at failure is -24 KN/M2 (-3.4 psi).

The soil structure is not stable when the consolidation pressure reaches 690 KN/M2 (100 psi). The three samples taken from the block samples and consolidated at this level of pres-

TABLE 3.6 RESULTS OF ICU TESTS ON THE MIOCENE CLAY

Location	Depth, M	Consolidation Pressure, KN/M2 (psi)	Deviatoric Stress at Failure, KN/M2 (psi)	Excess Pore Pressure at Failure, KN/M2 (psi)	Af (3)
Pier 8	16.8	35 (5)	333 (48)	9 (1)	0.03
Pier 8	16.8	69 (10)	647 (94)	45 (7)	0.07
Pier 8	16.8	69 (10)	767 (111)	44 (6)	0.06
Pier 8	16.8	207 (30)	814 (118)	191 (28)	0.24
Pier 8	16.8	337 (48)	837 (121)	289 (42)	0.35
Pier 8	16.8	504 (73)	796 (115)	389 (56)	0.49
Pier 8	16.8	587 (85)	787 (114)	497 (72)	0.63
Pier A-5	16.8	690 (100)	821 (119)	587 (85)	0.71
Pier A-5	16.8	787 (114)	773 (112)	690 (100)	0.89
Pier A-5 (4)	16.8	814 (118)	856 (124)	152 (22)	0.18

BLOCK SAMPLES

B114	21.6	14 (2)	108 (16)	9 (1)	0.09
B101	19.6	35 (5)	177 (26)	-49 (-7)	-0.28
B202	21.9	138 (20)	157 (23)	98 (14)	0.63
B202 (1)	21.9	242 (35)	706 (102)	264 (38)	0.37
B202	21.9	393 (57)	814 (118)	353 (51)	0.43
B202	21.9	469 (68)	648 (94)	402 (58)	0.62

SHELBY TUBE SAMPLES

TABLE 3.6 RESULTS OF ICU TESTS ON THE MIOCENE CLAY

Location	Depth, M	Consolidation Pressure, KN/M2 (psi)	Deviatoric Stress at Failure, KN/M2 (psi)	Excess Pore Pressure at Failure, KN/M2 (psi)	Af (3)
Pier 8	16.8	69 (10)	109 (16)	23 (3)	0.21
Pier 8	16.8	207 (30)	217 (31)	84 (12)	0.39
Pier 8 (2)	16.8	504 (73) 173 (25)	308 (45)	14 (2)	0.05

REMOLDED SOIL

Notes:

(1) The excess pore pressure at failure is larger than the consolidation pressure, then < 0.
(2) Sample consolidated at 504 KN/M2 but sheared at 173 KN/M2.
(3) Af is computed at the peak of the deviatoric stress.
(4) Collapse of the soil structure resulting from creep during consolidation.

sure were subjected to creep which , ultimately, led to the collapse of the soil structure. Such a phenomenon happened to the sample consolidated to 814 KN/M2 (118 psi) which went through a drastic volume change, after eight hours of consolidation. This additional volume change was nearly four times the initial volume change which occured during the first eight hours of consolidation. A value of the parameter A at failure, A_f, equal to 0.18 witnesses the complete changes of the soil structure which results from such a collapse. To avoid this problem with the two other samples consolidated to similar consolidation pressures, consolidation time was limited to two hours.

The results of the tests performed on the block samples are shown in Fig. 3.11 in terms of the ratio of the effective principal stresses σ'_1 / σ'_3. The figure indicates sharp and high peak values of σ'_1 / σ'_3 for the lower consolidation stresses. As the consolidation stress increases, the curve σ'_1 / σ'_3 versus axial strain flattens and the peak values of σ'_1 / σ'_3 decrease.

Typical values for σ'_1 / σ'_3 are 170 for a consolidation pressure of 35 KN/M2 (5 psi) and 18 for a consolidation pressure of 337 KN/M2 (48 psi).

Comparison between the results in Fig. 3.11 and the individual deviatoric stress strain curves given in Appendix D indicate that peak ratios σ'_1 / σ'_3 and peak deviatoric stresses occur generally at similar axial strains.

Three test results are compared in Fig. 3.12. The tests were performed at similar consolidation pressures on a sample of remolded soil, on a Shelby tube sample and on a sample taken from a block sample. Results of the tests are expressed in the figure in terms of the ratio of the effective principal stresses versus the axial strain. The difference between the results is striking. The σ'_1 / σ'_3 ratio in the case of the block sample has a peak of magnitude 50 at an axial strain of 1.5%. The two other samples have a very flat response with values of ratio varying between 3 and 5 at the maximum axial strain.

The stress paths of the tests performed on block samples are represented on a p'q diagram in Fig. 3.13, where

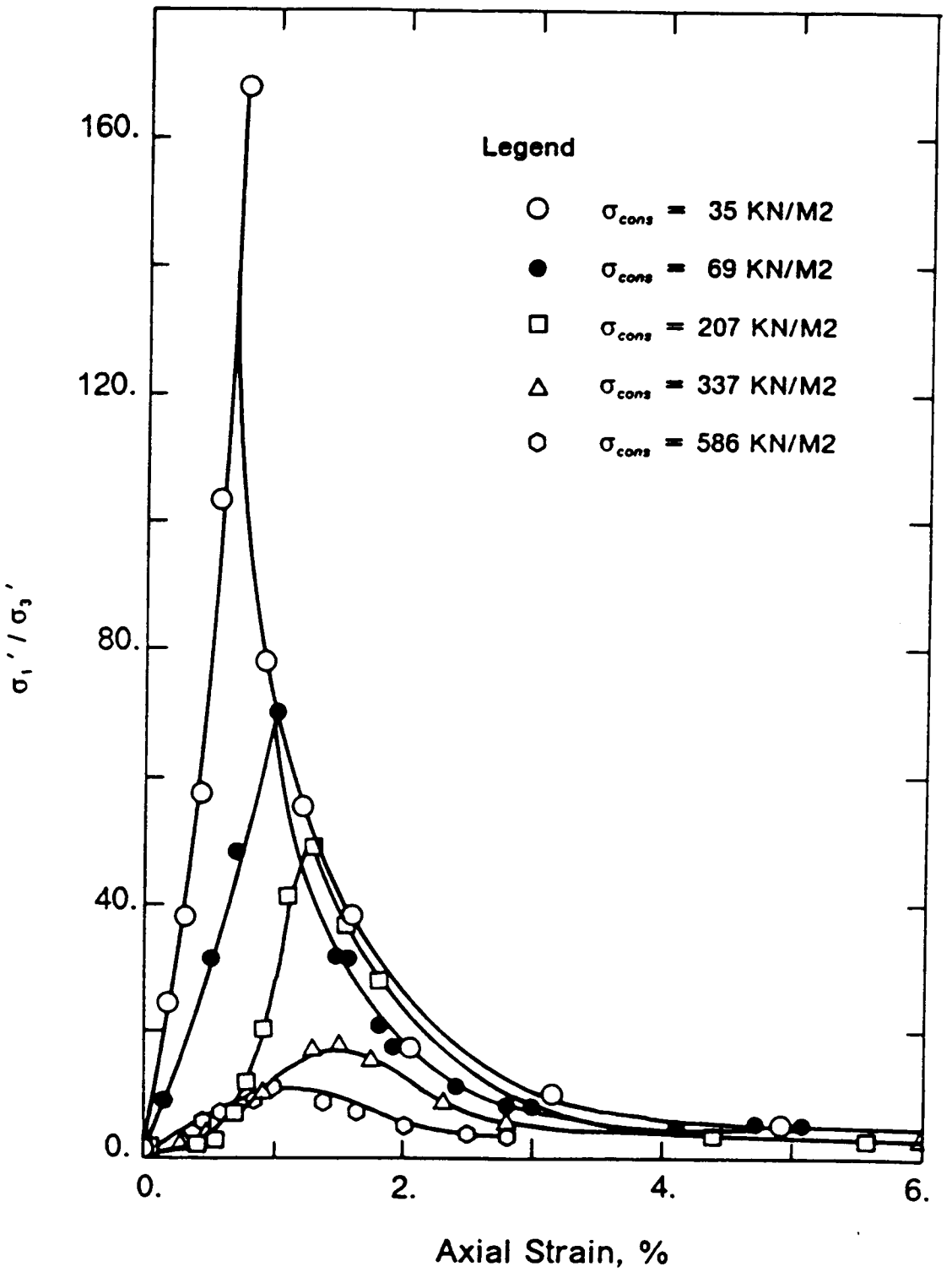

FIGURE 3.11 EFFECTIVE STRESS RATIO VERSUS AXIAL STRAIN FOR THE BLOCK SAMPLES

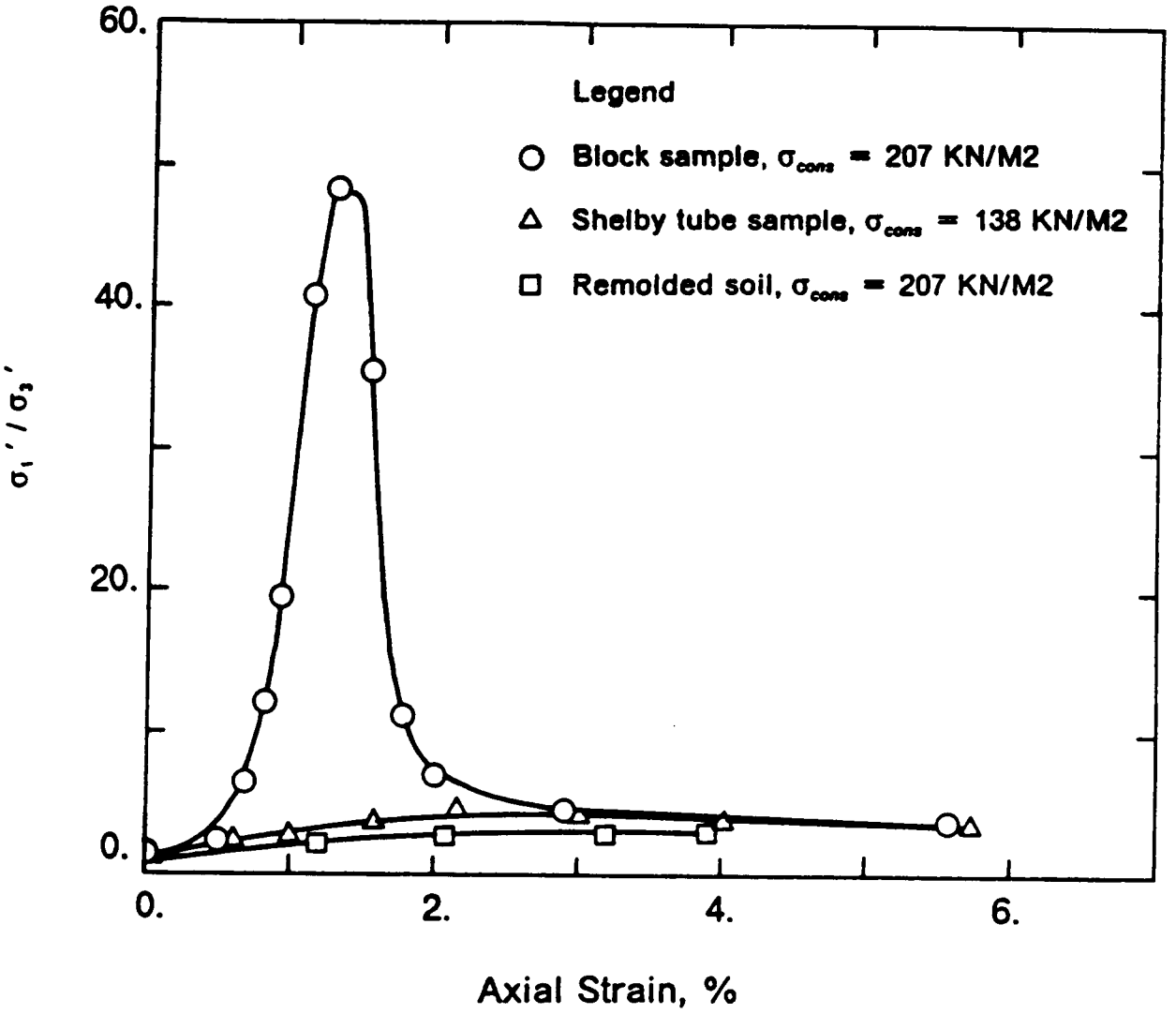

FIGURE 3.12 EFFECTIVE STRESS RATIO VERSUS AXIAL STRAIN FOR DIFFERENT TYPES OF SAMPLES

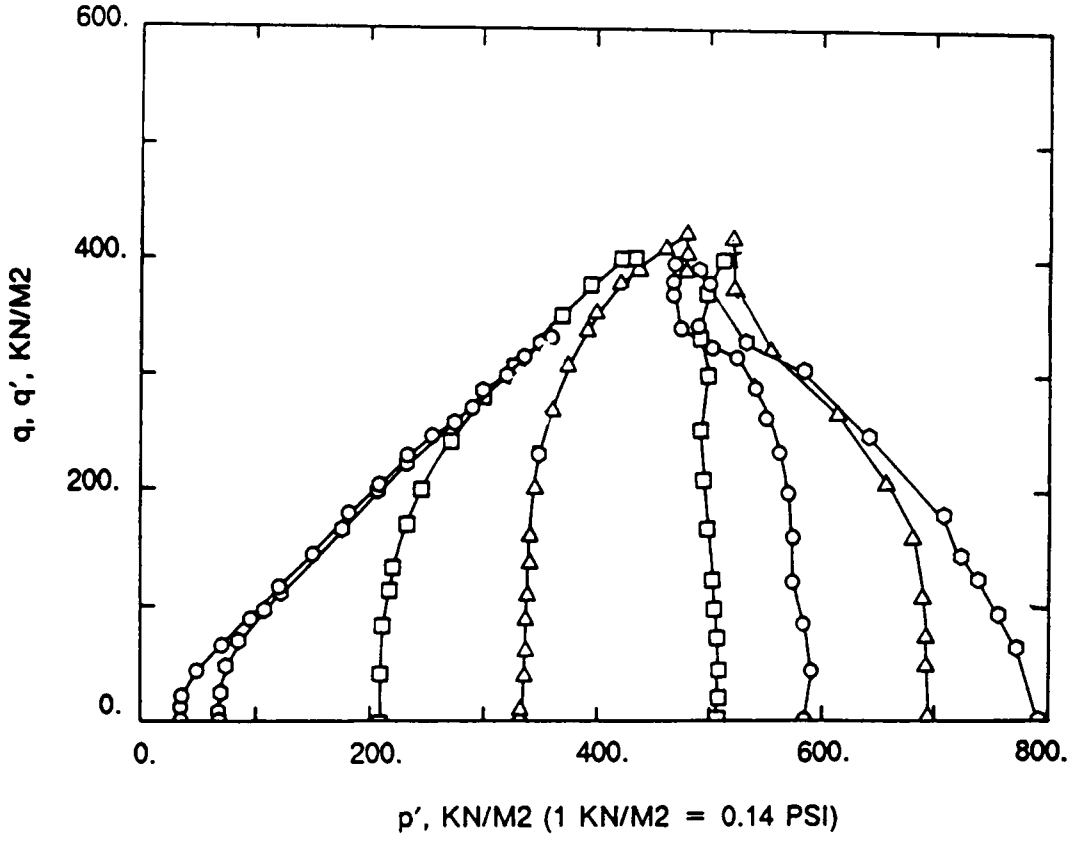

FIGURE 3.13 STRESS PATHS FOR ICU TESTS ON BLOCK SAMPLES

$$p' = (\sigma'_1 + \sigma'_3)/2$$

$$q' = q = (\sigma'_1 - \sigma'_3)/2 = (\sigma_1 - \sigma_3)/2$$

The stress paths start from an isotropic state of consolidation on the p′ axis. On this axis, from the left to the right, the consolidation pressures increase from 35 KN/M2 (2 psi) to 787 KN/M2 (114 psi). All the stress paths show a consistent pattern. At consolidation pressures less than 400 KN/M2 (60 psi), they curve to the right, between 400 and 600 KN/M2 (60 and 87 psi) they are nearly vertical and for consolidation pressures higher than 600 KN/M2 (87 psi) which corresponds to an OCR equal to 2.5, they start to curve to the left. Lo and Morin (1972) report test results on Leda clay samples for which the stress paths also start to curve to the left at an OCR value of 3 approximatively.

At failure, the stress paths follow a common envelope, nearly linear and inclined 44 degrees approximatively with the p′ axis for consolidation pressures less than 400 KN/M2 (60 psi) which curves down at higher consolidation pressures. If no cohesion is assumed, the drained friction angle, Φ', computed from the test results on the block samples given in Table 3.6 and from the slope of the failure envelope on the p′ q diagram given in Fig. 3.13 varies from 70 degrees for consolidation pressures of the order of 70 KN/M2 (10 psi) to 50 degrees for consolidation pressures of the order of 400 KN/M2 (60 psi). These high values come from the fact that the OCR of the soil at a consolidation pressure of 400 KN/M2 (600 psi) is still of the order of 3 to 4. When the consolidation pressure reaches the preconsolidation pressure of the soil, the failure envelope should flatten to reach an angle of the order of 25 degrees. Another way to look at the influence of the sampling method on the response of the soil consists in comparing the different stress paths for similar consolidation pressures and different sampling techniques. This is done in Fig. 3.14 where the stress paths of the tests performed on samples of remolded soil and on Shelby tube samples are superimposed to the stress paths from the tests on the block samples which were presented in Fig. 3.13. Some of the new stress paths follow the same trend as the former ones but, clearly, the consistency in behavior found with the block samples is lost.

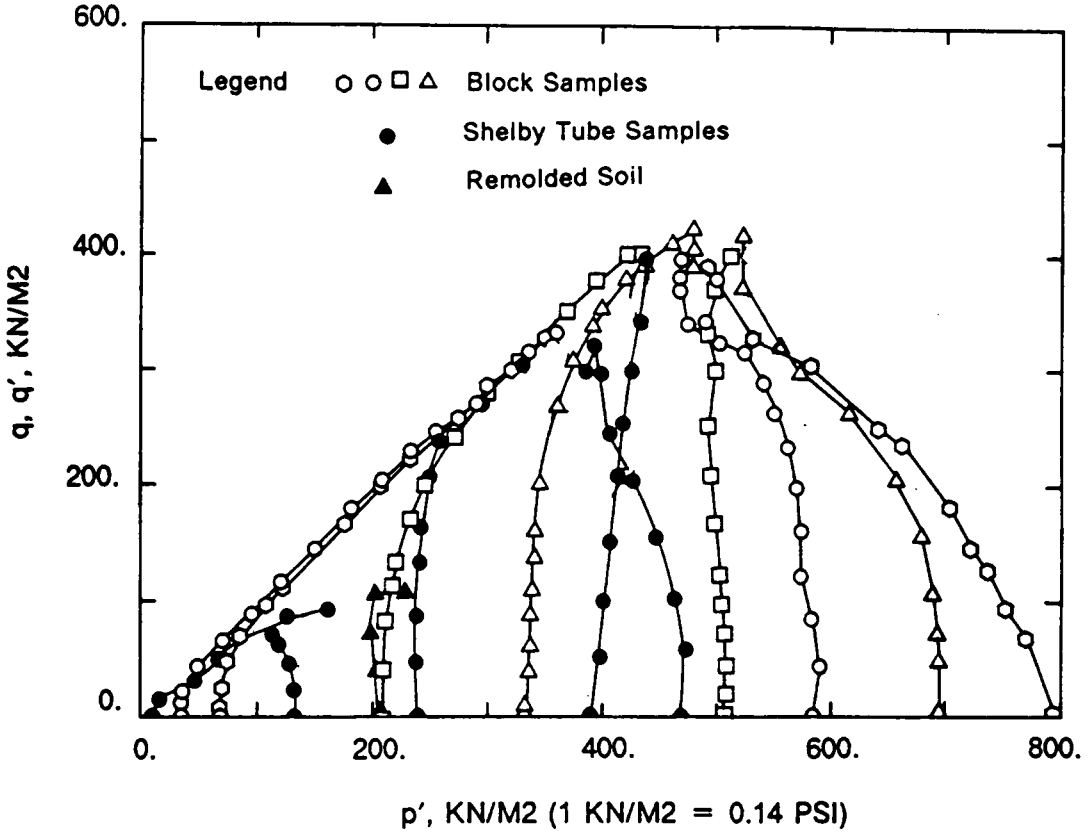

FIGURE 3.14 EFFECTIVE STRESS PATHS FOR ICU TESTS ON DIFFERENT TYPES OF SAMPLES

The A_f parameter for failure defined at peak of the deviatoric stress is plotted versus the consolidation pressure in Fig. 3.15 for the tests performed on the different types of samples. The results of the tests on the block samples show clearly a linear relationship between A_f and the consolidation pressure which goes through the origin and has a slope, given by the ratio of the consolidation pressure by A_f equal to 924 KN/M2. Some of the results of the tests performed on the Shelby tube samples show the same trend as the results of the tests on the block samples but the overall picture is more scattered. The two results from the tests on remolded soil indicate values of A_f about twice those obtained on the block samples at equivalent consolidation pressures. However, since at failure the deviatoric stress for the block samples is 4 to 6 times the deviatoric stress for the remolded soil, the excess pore pressure at failure in the case of block samples is 2 to 3 times the excess pore pressure of the samples of remolded soil. The post peak values of the A_f parameter are similar to the values of A_f at peak except for consolidation pressures less than 70 KN/M2 (10 psi) for which the values of the Af parameter post peak become negative.

The relationship between the ratio of the undrained shear strength, s_u, to the consolidation pressure σ_{cons} , is plotted versus the overconsolidation ratio (OCR) in Fig. 3.16. It is compared to similar relationships established for remolded Weald clay by Henkel (1956) and for Leda clays from the results of tests published by the different authors mentioned in the figure. The response of Weald clay is typical for a non sensitive clay. Its undrained strength ratio s_u / σ_{cons} is unity for an OCR of 10 and reaches 2 for an OCR of 50.

The Miocene clay shows a much higher undrained strength ratio. If the OCR for the Miocene clay is defined as the ratio of a preconsolidation pressure of 1.5 MN/M2 (15 tsf) by the isotropical consolidation pressure in the ICU tests, then, for an OCR of 10, the undrained strength ratio is approximatively 2.5 and it is greater than 6 for an OCR of 50. When slightly overconsolidated or normally consolidated, the Miocene clay and Weald clay have a similar undrained strength ratio.

The results of the tests on Leda clays indicated in Fig. 3.16 are similar to the results obtained from the tests on the Miocene clay. Also, UU and ICU results for the Miocene clay

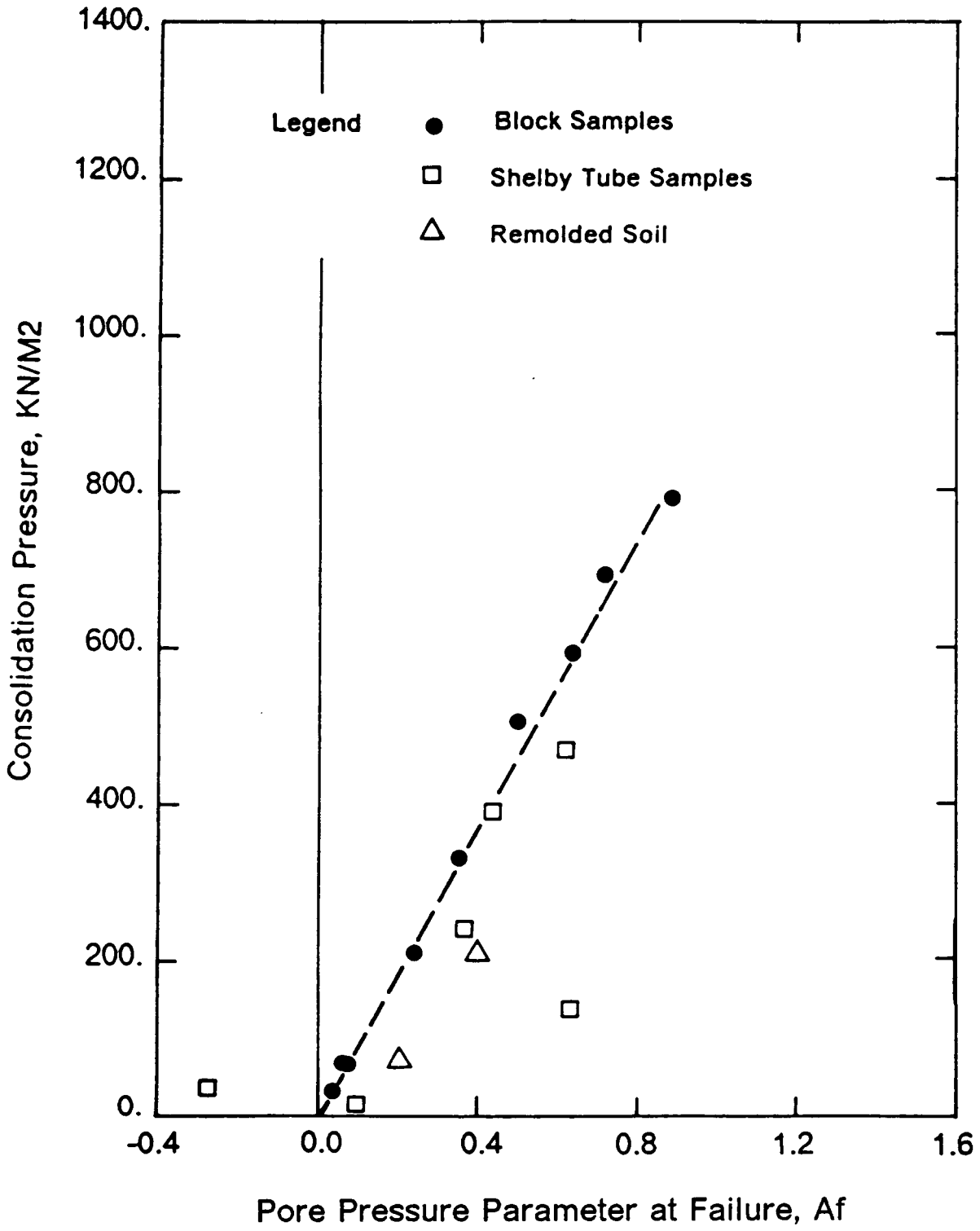

FIGURE 3.15 Af PARAMETER VERSUS THE CONSOLIDATION PRESSURE FOR DIFFERENT TYPES OF SAMPLES

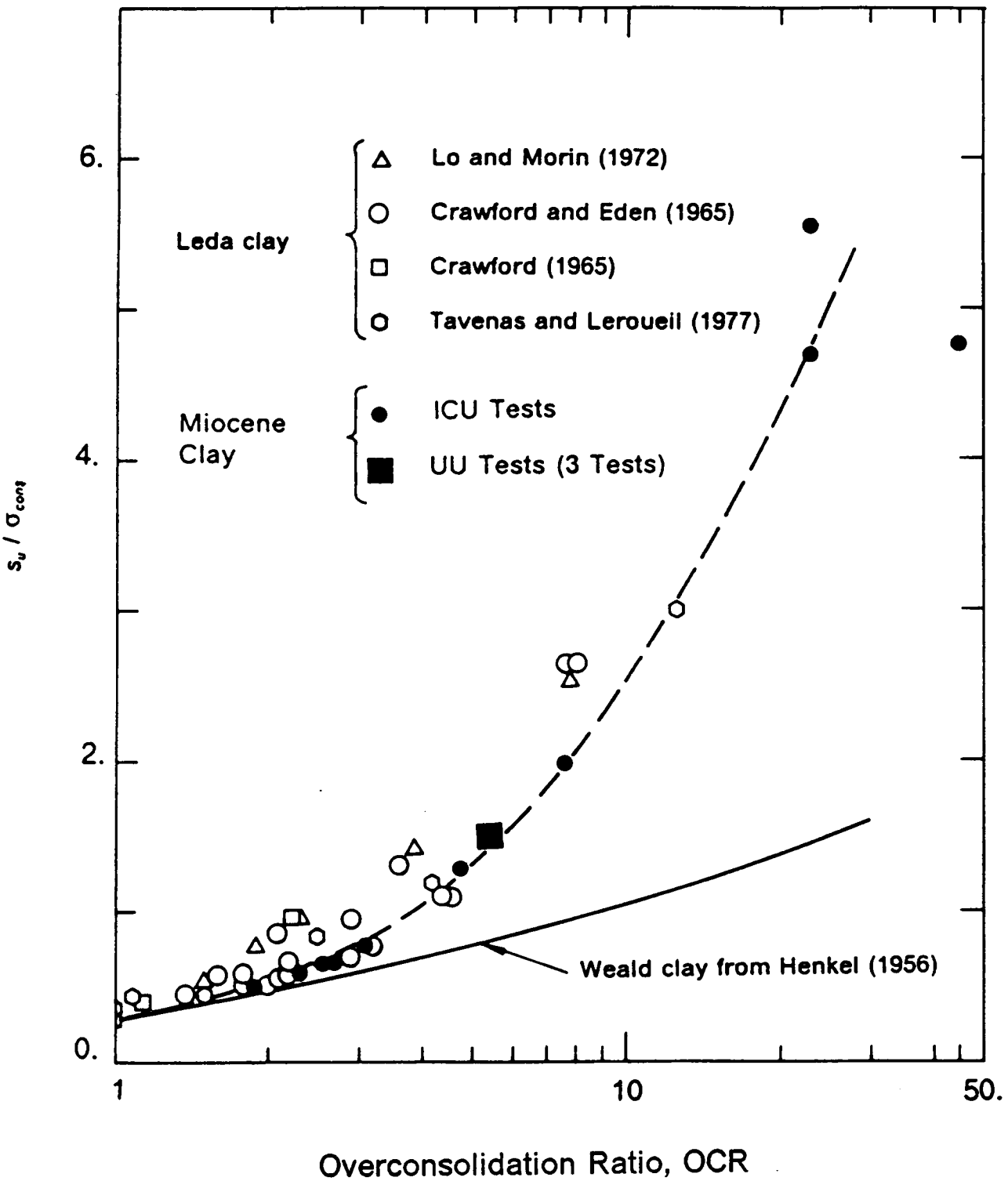

FIGURE 3.16 UNDRAINED STRENGTH RATIO VERSUS OCR

follow the same trend on the figure, indicating that the changes of effective stresses in the soil occuring during the consolidation phase of the ICU tests does not alter the structure of the soil.

A_f values for the Miocene clay are plotted versus OCR in Fig. 3.17 with results for Weald and Leda clays. Values for Weald clay range from 0.9 when normally consolidated to -0.4 when overconsolidated to an OCR of 20. Leda clays never exhibit negative A_f values. Typical A_f values for these clays vary from 0.8 when normally consolidated to 0.10 when overconsolidated to an OCR of 10. The Miocene clay and Leda clays follow a similar trend for OCR values greater than 4. Towards the lower values of OCR, the two soils have trends which diverge. When the OCR is 2, A_f values for the Miocene clay is twice the value obtained for Leda clays.

The nature and strength of the interparticle bonds which depend on the history of the soil are at the origin of the difference of behavior of the Miocene and Leda clays. Leda clays are young Quaternary deposits originated from the retreat of the glaciers. They are presently found at the ground surface and were covered by 10 to 20 M (33 to 66 ft) of sand deposits which were eroded before the clays were fully consolidated under their load. Leda clays tested in laboratory is brittle if overconsolidated. It loses its brittleness when normally consolidated as the interparticle bonds are progressively destroyed. The high sensitivity of Leda clays is exhibited by the fact that it behaves like a viscous fluid when disturbed as its natural water content is at liquid limit or higher. The Miocene clay of Richmond is a much older deposit dating from the Tertiary Period. It is presently found under 15 M (45 ft) of cover but once, it was consolidated under 75 M (250 ft) of soil. In such an environment of time and pressure, very strong diagenetic bonds developed between the particles which reflect the brittleness of the material. The sensitivity of the Miocene clay is lower than the sensitivity of Leda clays but it is more brittle as the collapse of the soil structure occurs more suddenly and lead to the development of higher excess pore pressures at failure.

The normalized behavior on a (s_u / σ_{cons})OC / (s_u / σ_{cons})NC versus OCR diagram is presented for several soils in Fig. 3.18, where (s_u / σ_{cons})NC and (s_u / σ_{cons})OC are the undrained shear strength ratios when the soil is normally consolidated and overconsolidated

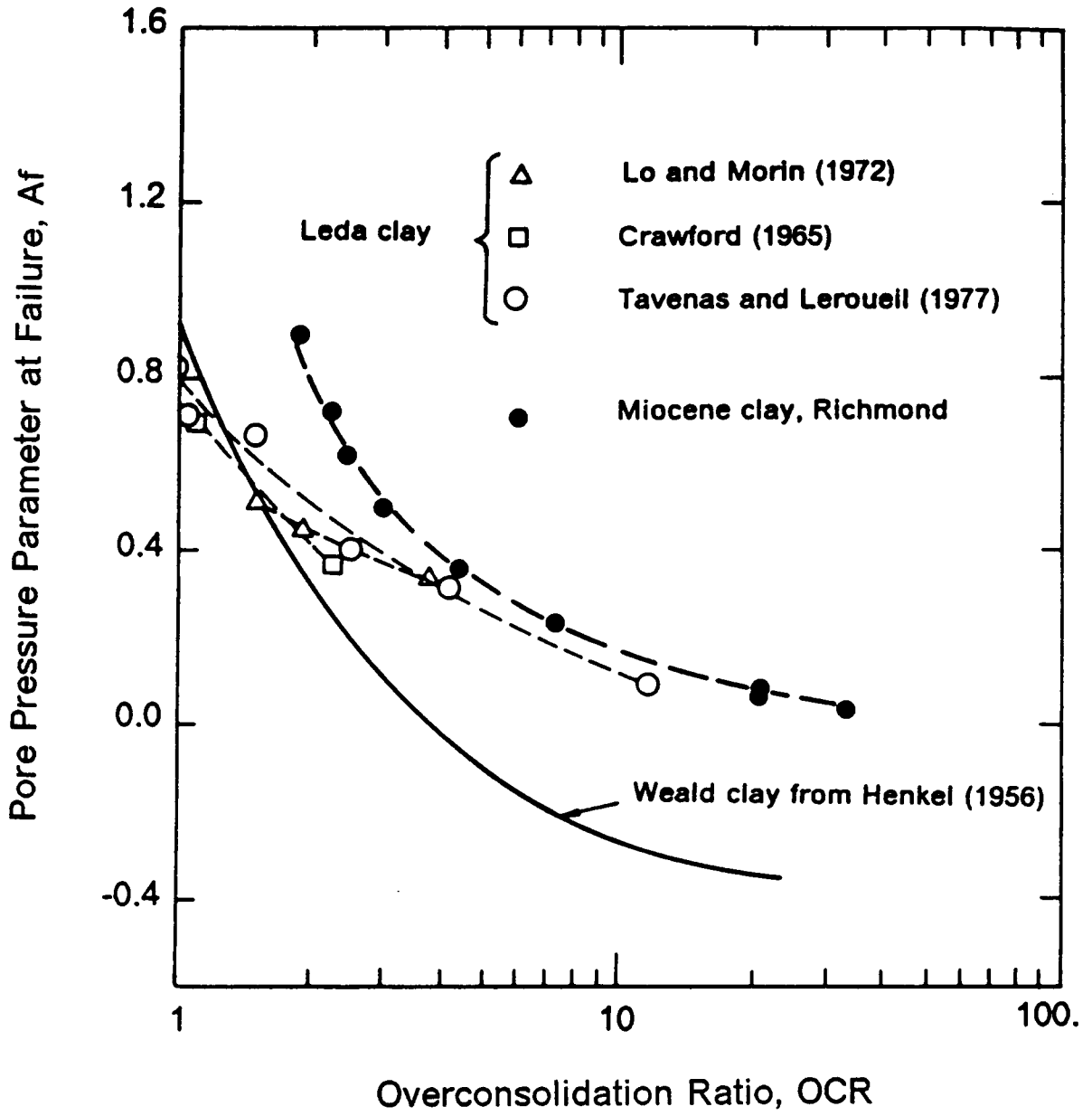

FIGURE 3.17 Af PARAMETER VERSUS OCR

respectively. Six of the soils are clays of low to medium sensitivity reported by Ladd et al. (1977) for which the SHANSEP procedure was used to normalize the soil behavior. Data are also shown for Leda clays and the tests of this investigation.

The normalized plot for the Miocene clay is established from the test results on the block samples. The Miocene clay results indicate a consistent pattern which departs from the group of clays reported by Ladd et al. (1977). Typically, for an OCR of 6, the ratio (s_u / σ_{cons})OC /(s_u / σ_{cons})NC is 1.5 larger for the Miocene clay as compared to the group of the other clays.

Data points on Leda clays are also indicated in Fig. 3.18. They were determined from the test results on block samples reported by Lo and Morin (1972) and Tavenas and Leroueil (1977). Like the Miocene clay, Leda clays depart from the other clays.

3.10 SUMMARY OF THE PROPERTIES OF THE MIOCENE CLAY

The Miocene clay is a medium gray, hard and generally non-fissured clay of marine origin, at the border of MH-OH and CH when classified according to USCS.

Sampling technique proved to be of primary importance in the determination of the properties of the soil in the laboratory. The technique which consists in pushing tubes disturbes the soil , giving undrained shear strength values which are typically half the values obtained from the tests on the block samples. Furthermore, the tests run on the samples from the tubes are scattered and do not show a consistent behavior of the soil. Tests on high quality block samples hand excavated indicate consistency in the results and in the behavioral pattern.

Results of oedometer tests indicate that the field compression index, C_c, varies typically between 1.2 and 1.5 and the recompression index, C_r, between 0.14 and 0.16. The preconsolidation pressure varies between 1.3 and 1.6 MN/M2 (13 and 16 tsf) and the OCR between 4 and 5.

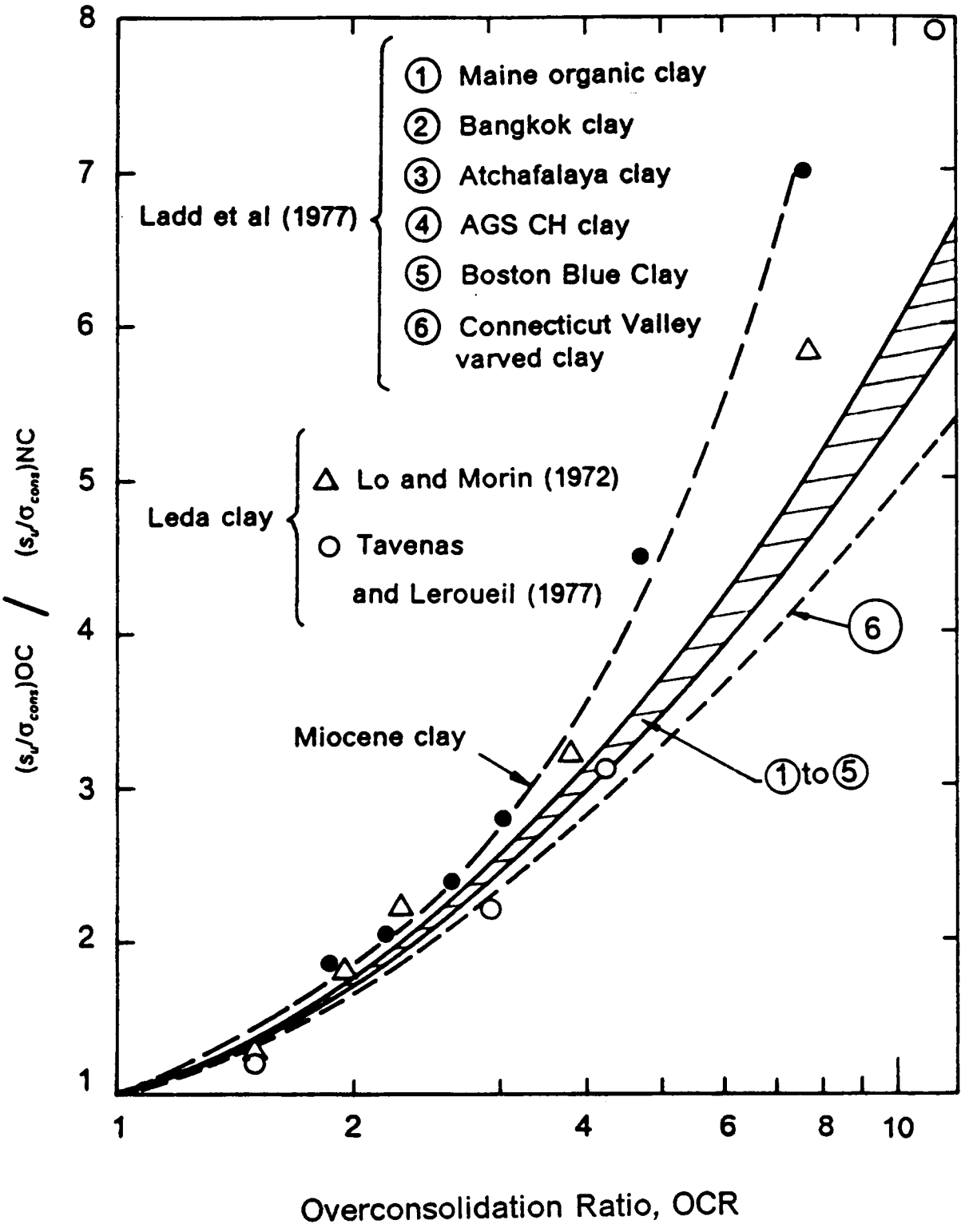

FIGURE 3.18 NORMALIZED BEHAVIOR

The undrained shear strength determined from UU tests is typically 500 KN/M2 (72.5 psi). The sensitivity of the soil is of the order of 7.

ICU tests results on the Miocene clay and on Leda clays were compared in terms of the parameters A_f, OCR, the undrained shear strength ratio and a normalized diagram. The two clays have generally similar types of behavior but the Miocene clay shows trends which depart more from the non sensitive soils than Leda clays. It is believed that this particular behavior is due to the brittleness of the clay.

Chapter 4

RESIDUAL SOIL : SITE INVESTIGATION

DETERMINATION OF THE PROPERTIES

4.1 INTRODUCTION

The second soil investigated in this study is a residual material derived by weathering in place.

This chapter presents the general characteristics of the soil and the results of the site investigation and laboratory testing program.

4.1.1 Site location

The site at which the residual soil is located is situated three miles northwest of the campus of Virginia Tech, in an area known as Kipp's farm. The ground level at the site is at

elevation 612 M (2040 ft) and the residual soil is found from the ground surface to a depth which varies from 3 M (10 ft) to more than 6 M (20 ft). The parent rock underlies the residual soil.

4.1.2 Geology

The area of South Western Virginia in which is situated Blacksburg is one of prominent Appalachian overthrusting. Overthrusting took place after the deposition of the Mississippian strata. This is the reason that the Elbrook and Rome Formations of the Cambrian System overlay the younger formations of the Mississippian System. Deep folding both, preceeded and followed overthrusting.

At the testing site, which is situated in the overthrusting area, the Elbrook and Rome Formations outcrop. The Elbrook Formation mainly consists of interbedded sandy and fine grained dolomite containing thin lenses of fine to medium grained size sandstone. The upper unit consists of a limestone layer.

The Rome Formation consists of interbedded mudstone, fine grained sandstone and siltstone and fine grained dolomite. The upper unit consists of finely laminated dolomite. These rocks have been weathered from the ground surface to form the layer of residual soil several meters thick which was tested.

4.2 SITE INVESTIGATION - DRILLING AND SAMPLING

4.2.1 Soil conditions

The soil conditions at the site are determined from the logs of three borings, SPT1, SPT2 and SPT3 given respectively in Fig. 4.1, Fig. 4.2 and Fig. 4.3 in which SPT test profiles were performed to a depth of 6.4 M (21 ft).

Because of its nature, the soil has no definite stratigraphy. It is generally classified as a medium dense, yellow-red sandy silt to silty sand. In some cases, the soil is more plastic, and in this condition it is classed as an ML to MH material with a stiff consistency. The MH zones were encountered generally near the ground surface and at the bottom of the borings. The Atterberg limits determined from samples taken in these zones are given in the plasticity chart in Fig. 4.4. The liquid limit varies generally between 50 and 70 and the plasticity index between 10 and 30. Two samples taken near the ground surface exhibit liquid limit of 90 and 95 and plasticity indices of 40 and 55.

Parent rock was encountered at the bottom of the boring SPT1, 6.5 M (21.3 ft) deep. It was not encountered in the borings SPT2 and SPT3 which both were 6.9 M (23 ft) deep. Also, zones of weathered rock were found nearby, during the self-boring pressuremeter testing program, at depths varying between 3 M and 6 M (10 ft and 20 ft).

4.2.2 Water conditions

No water table was found in any of the borings for the investigation. Other local soil investigations indicate that the seepage water is collected at the contact between the soil and

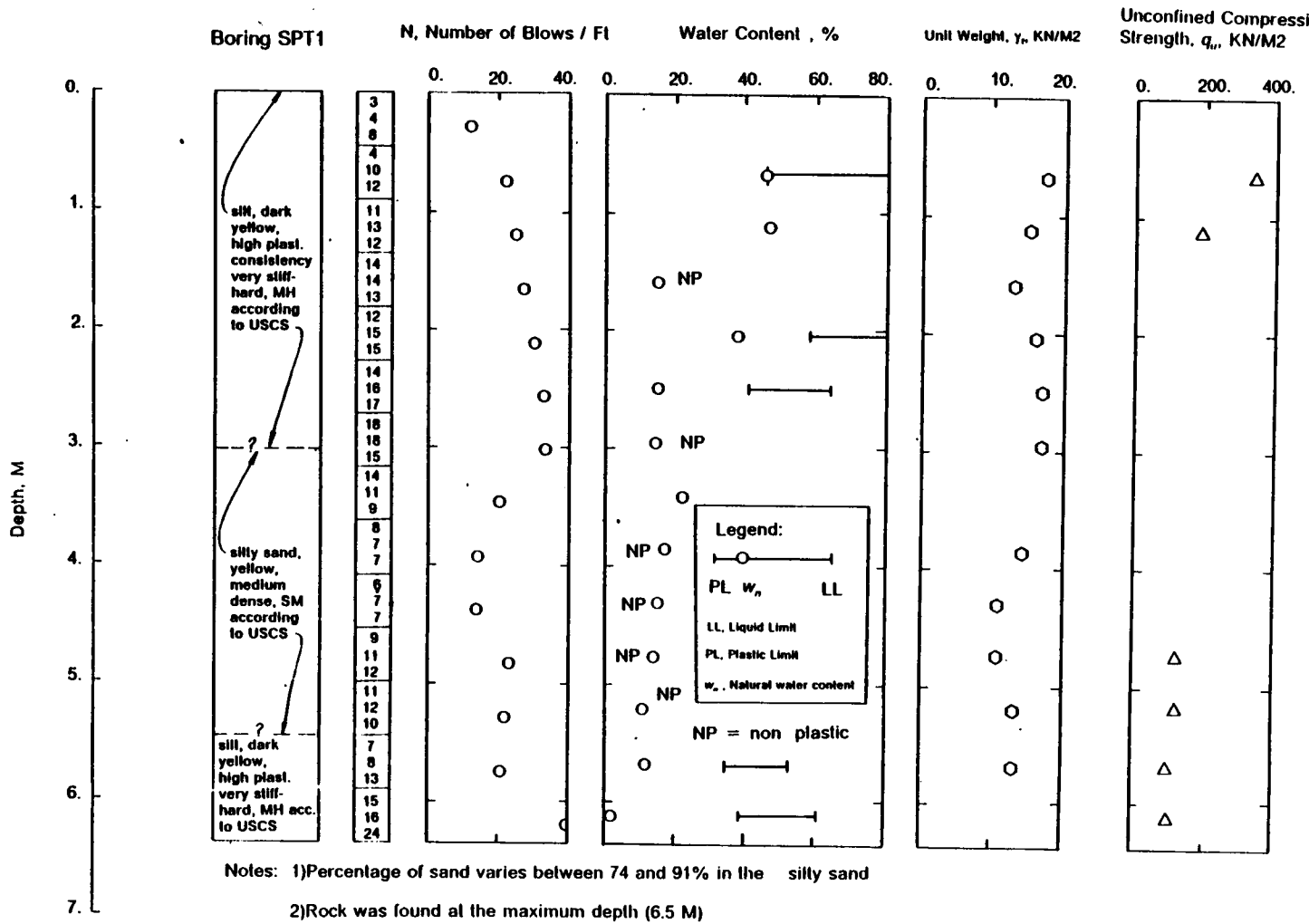

Notes: 1)Percentage of sand varies between 74 and 91% in the silty sand

2)Rock was found at the maximum depth (6.5 M)

FIGURE 4.1 LOG OF BORING SPT1

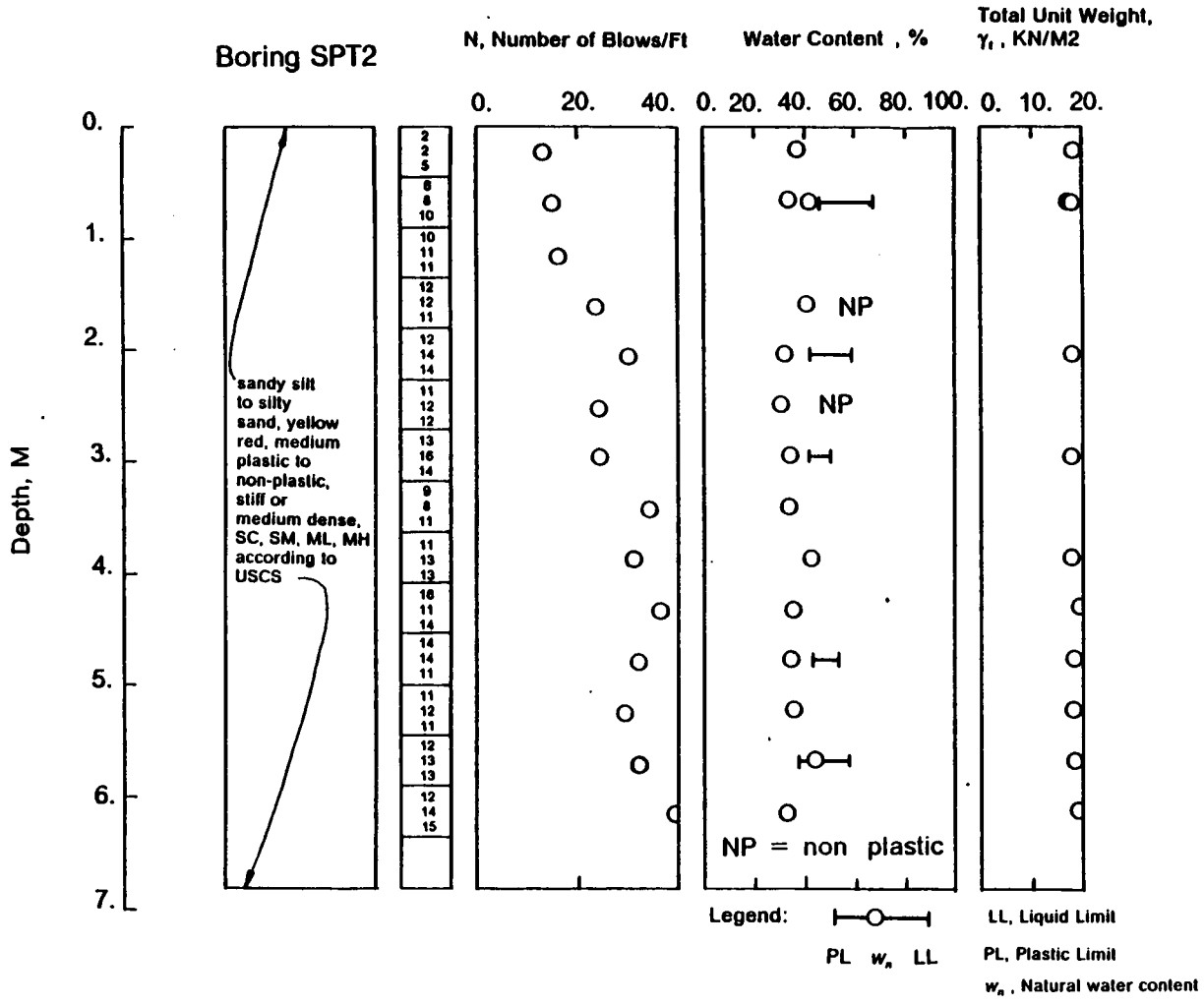

FIGURE 4.2 LOG OF BORING SPT2

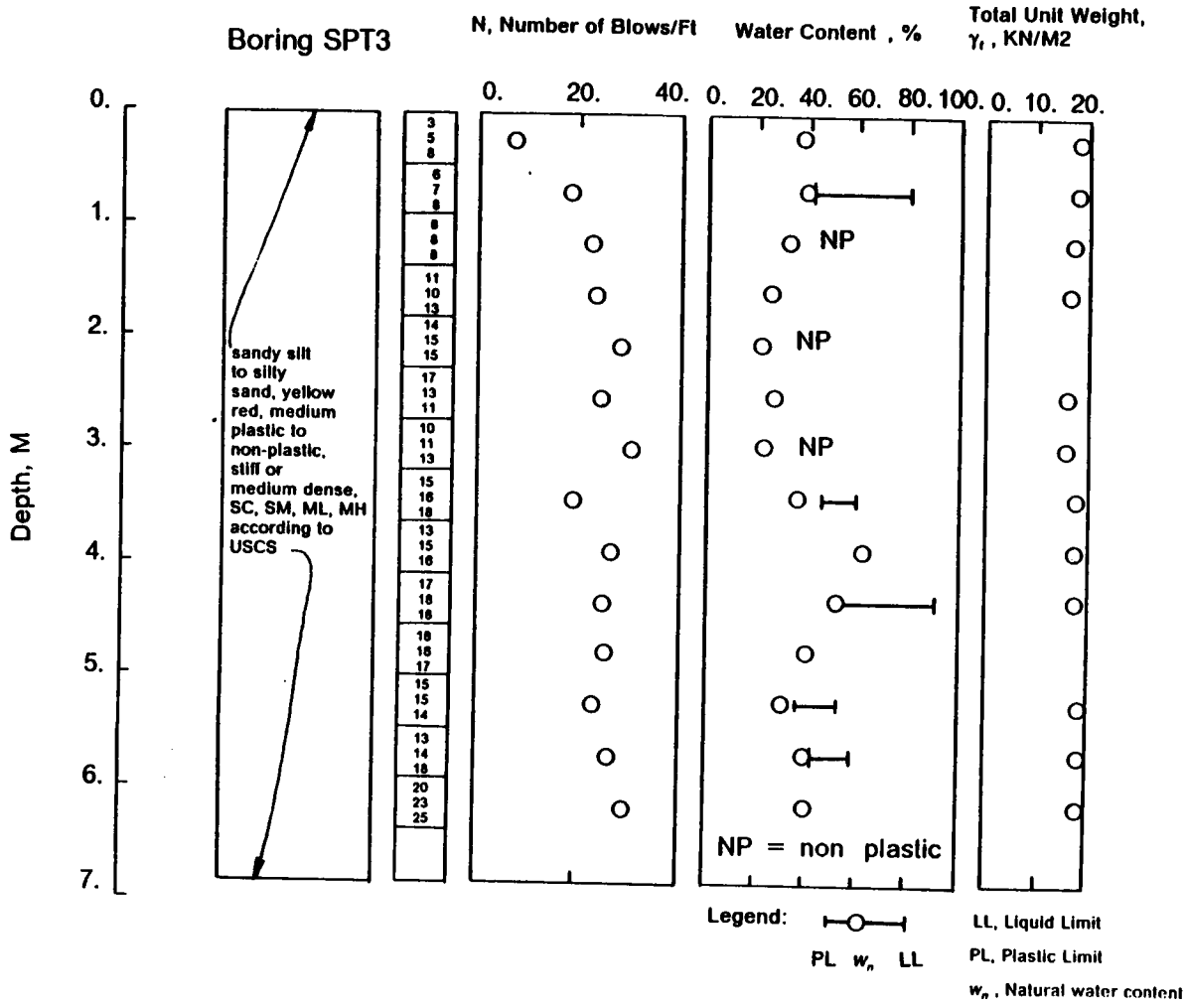

FIGURE 4.3 LOG OF BORING SPT3

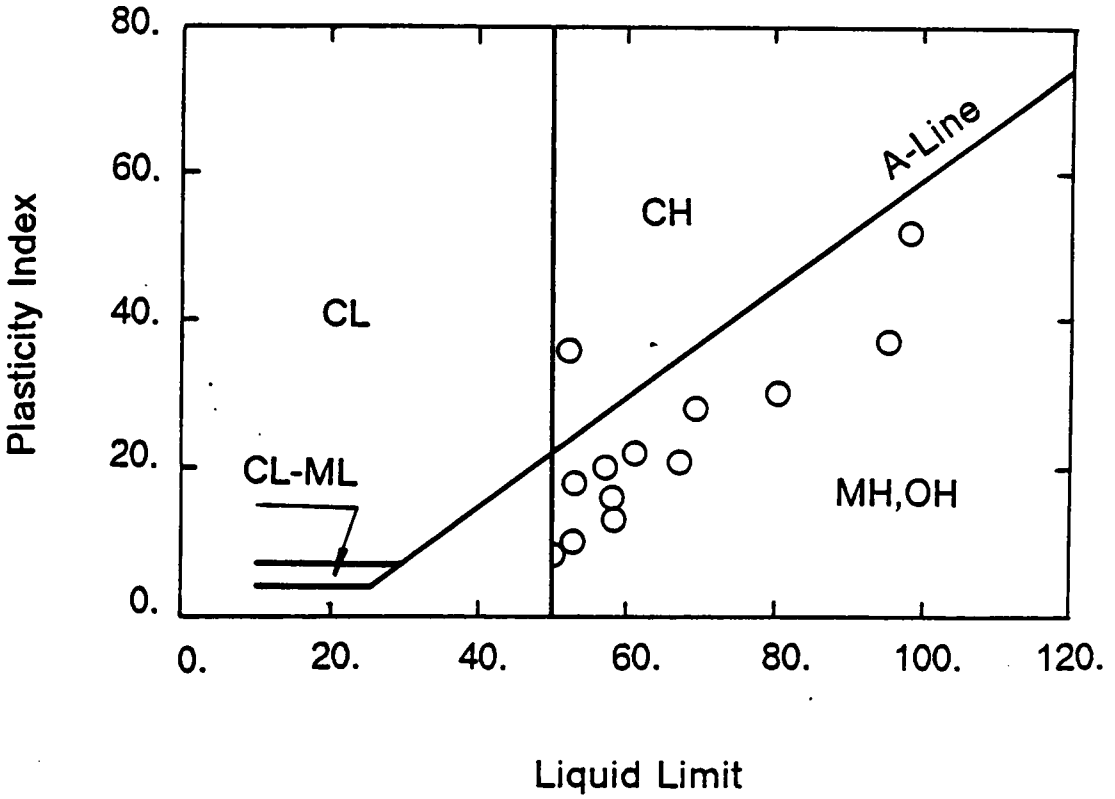

Note: The soil with a liquid limit > 80 is found near the ground surface. For depths > 2.4 M the soil has typically a liquid limit < 60 or is non plastic.

FIGURE 4.4 PLASTICITY OF RESIDUAL SOIL

its parent rock where it forms a water table. Such a contact was not encountered at the site in this work.

4.3 TESTING PROGRAM AND SOIL PROPERTIES

4.3.1 Laboratory and field testing program

A continuous Standard Penetration Test (SPT) profile was performed in the borings SPT1, SPT2 and SPT3. The number of blows per foot, N, was measured and identification tests were performed in laboratory on the samples of soil taken in the split spoon sampler.

N values versus depth are given in Fig 4.5 for the three borings. From the ground surface to 3 M (10 ft), the N values in the three borings are similar and vary from 10 at the ground surface to 30 at a depth of 3 M (10 ft). Below this depth, N is fairly constant but it varies from boring to boring with values of the order of 15 in the boring SPT1 to values of the order of 30 in the boring SPT2.

In the laboratory, fifteen determinations of Atterberg limits, twenty six determinations of natural water content, ten determinations of content of sand and thirty four estimations of total unit weights were made on the samples taken from the split spoon sampler. Six unconfined compression tests and several measurements with the pocket penetrometer were also performed. In addition, two stress controlled oedometer tests were realized on samples taken from Shelby tubes which were pushed in the ground.

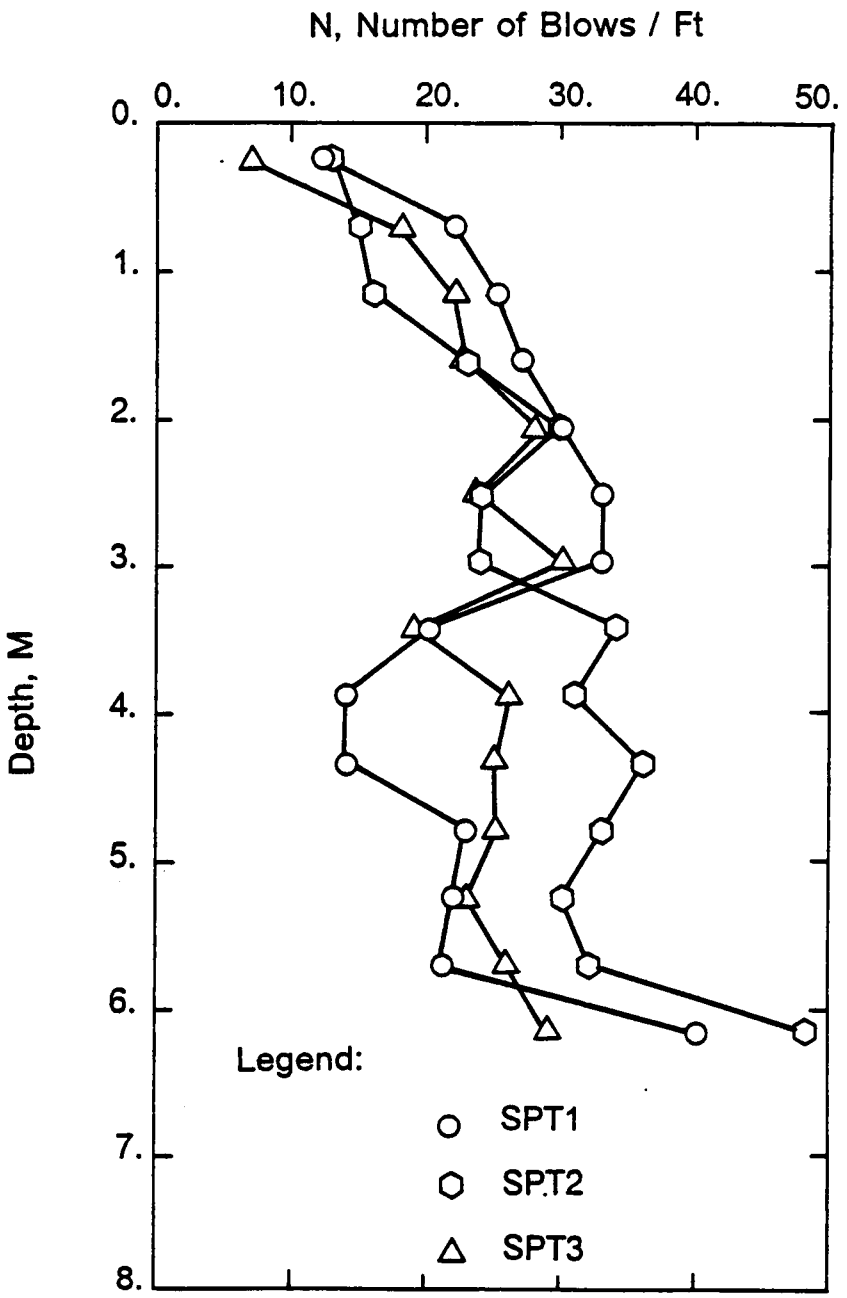

FIGURE 4.5 STANDARD PENETRATION TEST RESULTS

4.3.2 Physical properties

Variations with depth of the natural water content and Atterberg limits are given in Fig. 4.6 for the three borings. The percentage of sand is also indicated on the figure. The plasticity of the soil is low to essentially non existent over most of the investigated depth, especially between 2.1 M (7 ft) and 7 M (23 ft) deep.

The water content in the non-plastic zones is apparently influenced by the rainfall and the quantity of seepage. Boring SPT1 was performed during a dry period. The water content is low, nearly constant with depth, varying generally between 10 and 20%. The two borings SPT2 and SPT3 were performed during a wet period. They exhibit higher water contents which vary between 20 and 40%. In the plastic zones, the natural water content is situated in the vicinity of the plastic limit, a sign that the soil is overconsolidated.

The percentage of sand measured on non-plastic soil samples varies between 44 and 64% in the borings SPT2 and SPT3. In the boring SPT1, it varies between 75 and 92%.

4.3.3 Compressibility properties

Two stress controlled oedometer tests were performed on samples of residual soil classified MH which were obtained by pushing Shelby tubes at a depth of 0.9 M (3 ft) with the loading frame used with the self-boring pressuremeter. Attempts to sample the soil deeper using the same frame or the drill rig from the University were unsuccessful because the high stiffness of the soil and its non cohesive nature.

The results of the two oedometer tests are given in Fig. 4.7 and Fig. 4.8. The preconsolidation pressure interpreted from the oedometer curve by the Casagrande method varies between 200 and 300 KN/M2 (2 and 3 tsf). The resulting overconsolidation ratio (OCR) varies between 10 and 16.

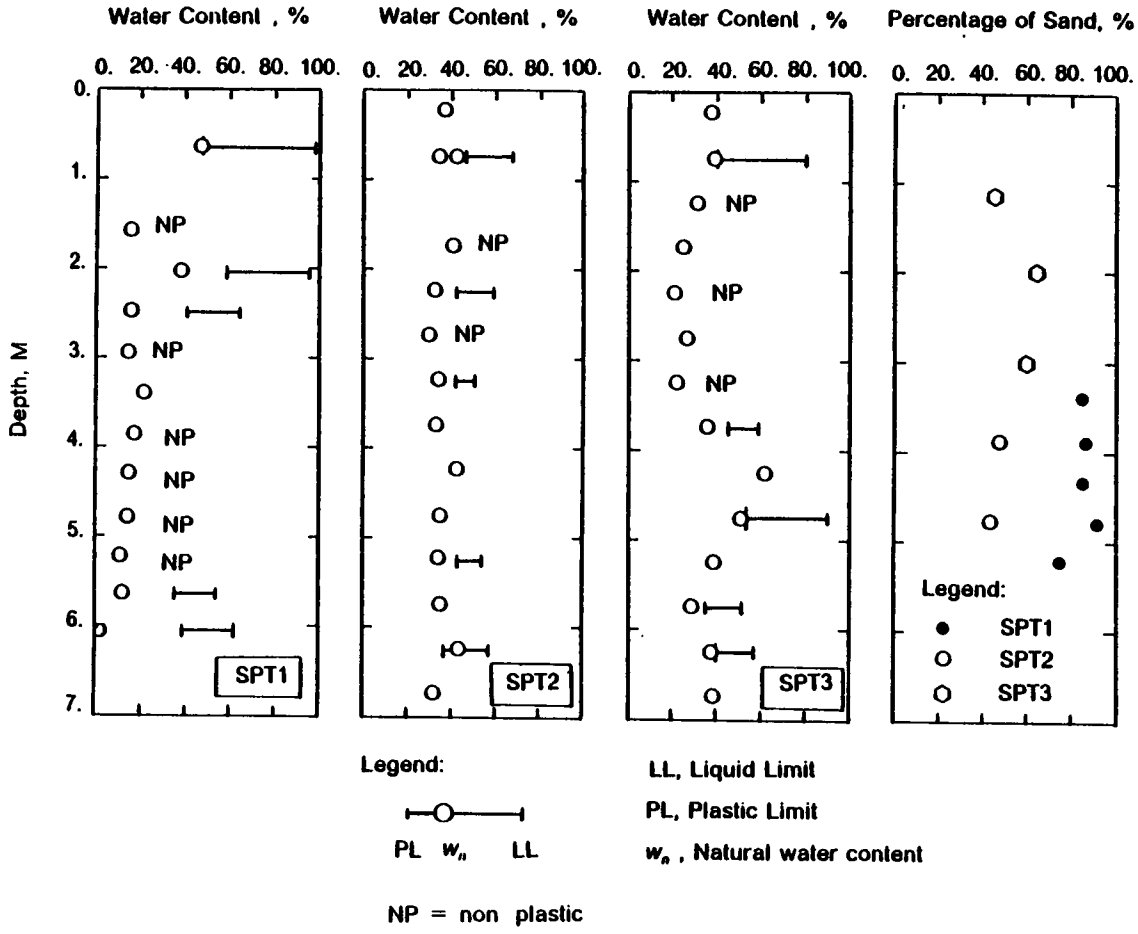

FIGURE 4.6 PLASTICITY AND WATER CONTENT PROFILES

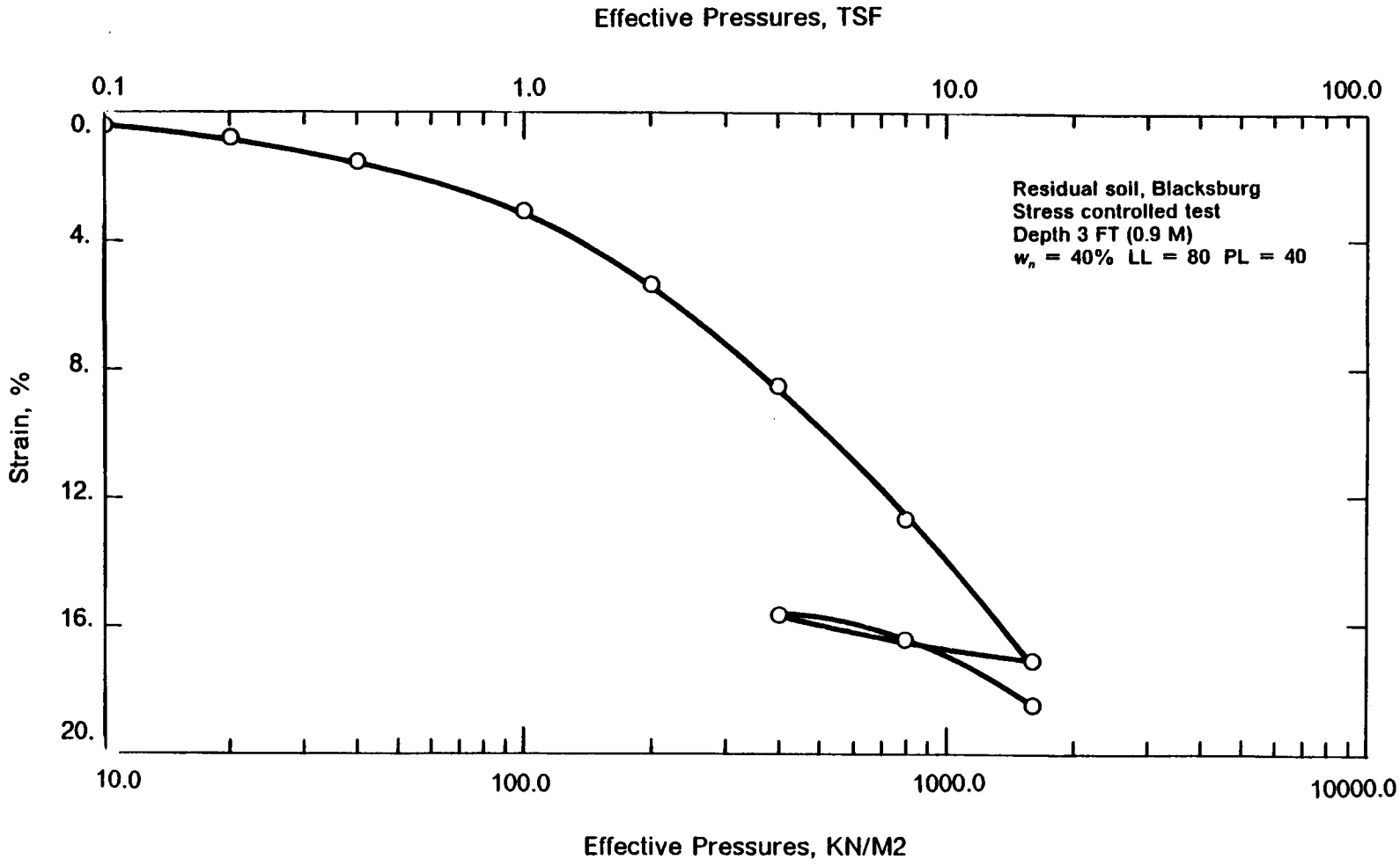

FIGURE 4.7 OEDOMETER TEST RESULT

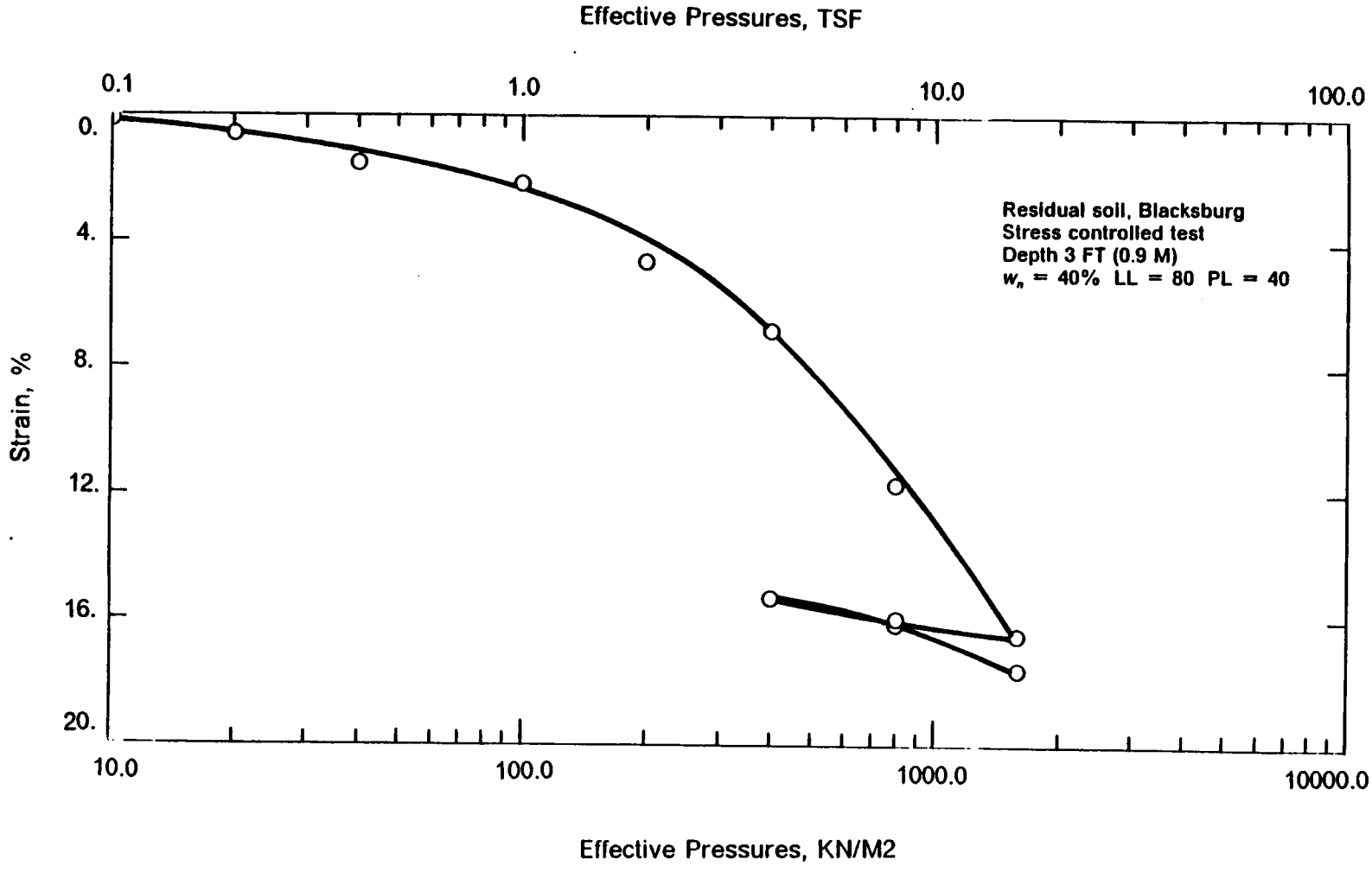

FIGURE 4.8 OEDOMETER TEST RESULT

The compression index, C_c, interpreted from the test curves varies between 0.33 and 0.39. The reconstructed field compressibility, using the Schmertmann method gives values for C_c varying between 0.50 and 0.70. These values are nearly twice the values obtained directly from the test curves, a sign that there is disturbance of the soil due to the sampling process. The values of C_c from the reconstructed field compressibility compare well with the value of 0.63 obtained from the correlation proposed by Skempton:

$$C_c = 0.009(LL - 10)$$

where LL is the liquid limit.

4.3.4 Strength properties

A lower bound of the undrained shear strength of the soil can be estimated from the unconfined compression (UC) test results and from the measurements with the pocket penetrometer performed on the cohesive samples recovered by the split spoon sampler. The variation of the unconfined compression strength with depth is given in Fig 4.9. The undrained shear strength decreases with depth. Typical values are 200 to 400 KN/M2 (1.9 to 3.8 tsf) near the ground surface and 100 to 200 KN/M2 (1.0 to 1.9 tsf) at a depth of 6 M (20 ft).

The interpretation of the self boring pressuremeter tests performed in the free draining residual soil of low plasticity requires the knowledge of the angle of friction of the soil at no volume change, Φ_{cv}. To determine this angle, three direct shear tests were performed on dry remolded samples. The soil was placed in the direct shear test apparatus without control of its initial density as it was assumed that the residual shear strength at constant volume is independant of the placement density but only controlled by the normal stress to the failure plane. The normal pressures to the shear plane were 49, 98 and 196 KN/M2 (0.5, 1.0 and 2.0

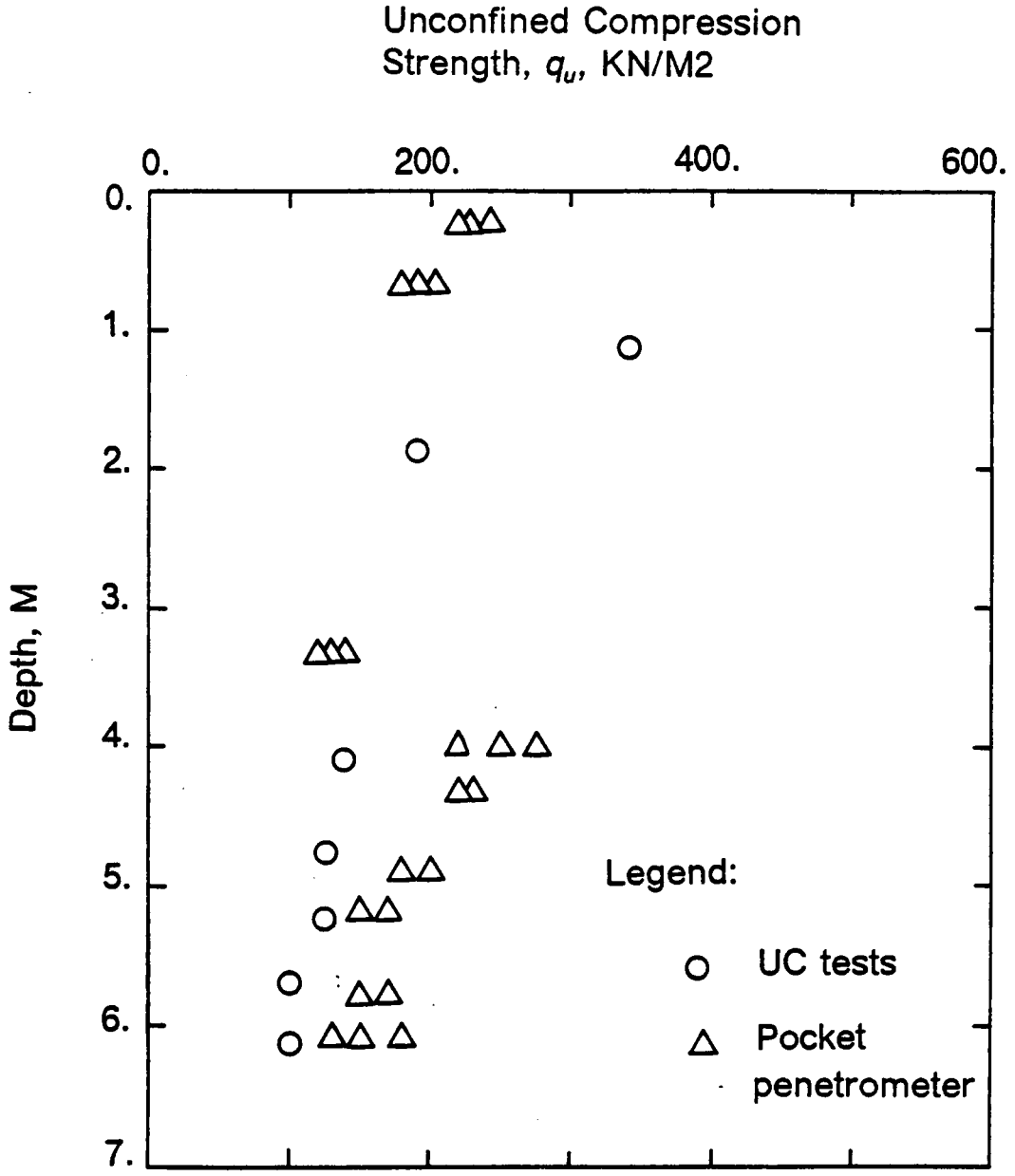

Note: Samples taken from the SPT split spoon sampler

FIGURE 4.9 UNCONFINED COMPRESSION TEST RESULTS

tsf). The results of the three tests are given respectively in Fig. 4.10, Fig. 4.11 and Fig. 4.12. Shearing was alternate and was carried out over 0.015 M (0.6 in) in each direction.

The failure envelope at constant volume is given in Fig. 4.13. Under these conditions, the cohesion of the soil $c_{cv} = 0$ and the friction angle $\Phi_{cv} = 36$ degrees.

4.3.5 Summary of the properties of the residual soil

The residual soil investigated covers the parent rock at least over 7 M (23 ft). It is generally a silty fine sand of low to non existent plasticity except near the ground surface and at the maximum depth investigated where the soil is classified MH according to USCS.

The soil has been indurated by dessication and cementation. Sampling by pushing Shelby tubes was found not possible beyond 1 M (3.3 ft) deep as the soil is very stiff and nearly without plasticity.

SPT tests were performed continuously over a depth of 7 M (23 ft). Typically, N varies from 10 to 30 blows/ft between the ground surface and 3 M (10 ft) deep and remains constant between 3 M (10 ft) and 7 M (23 ft).

Few tests were performed in the laboratory, besides the identification tests as good quality sampling was not possible. Oedometer test results indicate that the preconsolidation pressure and the OCR at 0.9 M (3 ft) deep are 200 to 300 KN/M2 (2 to 3 tsf) and 11 to 16 respectively.

UC tests on disturbed samples provide a lower bound of the undrained shear strength of the cohesive soil which typically varies from 300 KN/M2 (3 tsf) at the ground surface to 150 KN/M2 (1.5 tsf) at 6 M (20 ft) deep.

The direct shear tests carried out on dry remolded soil at large displacements indicate a friction angle at constant volume, Φ_{cv} equal to 36 degrees.

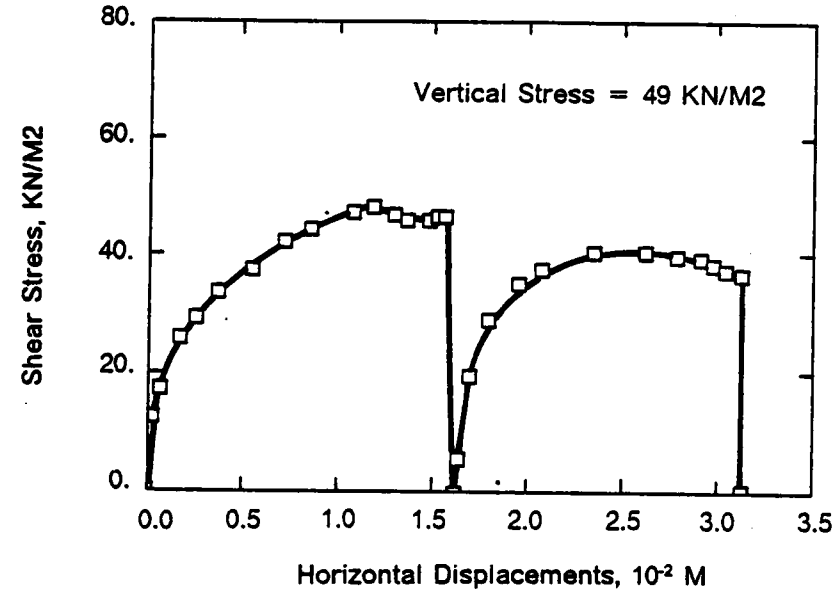

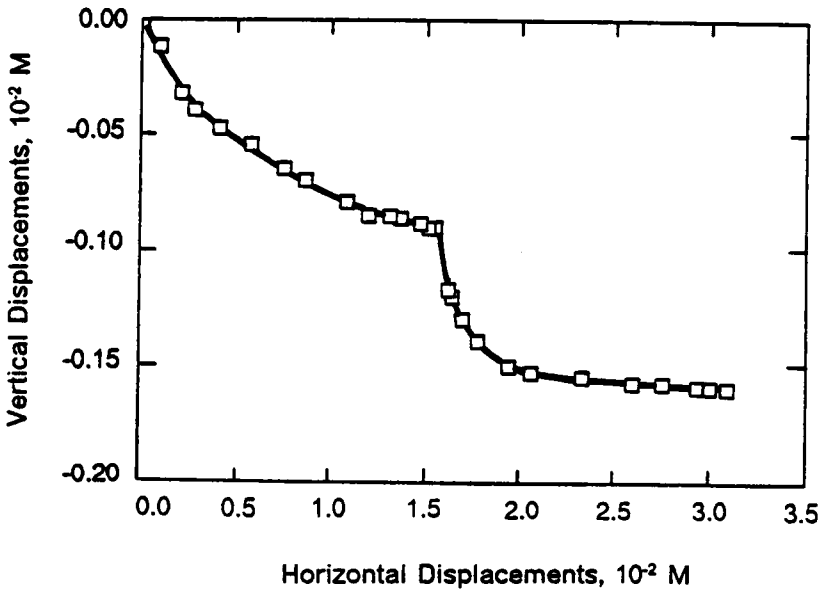

FIGURE 4.10 DIRECT SHEAR TEST RESULTS

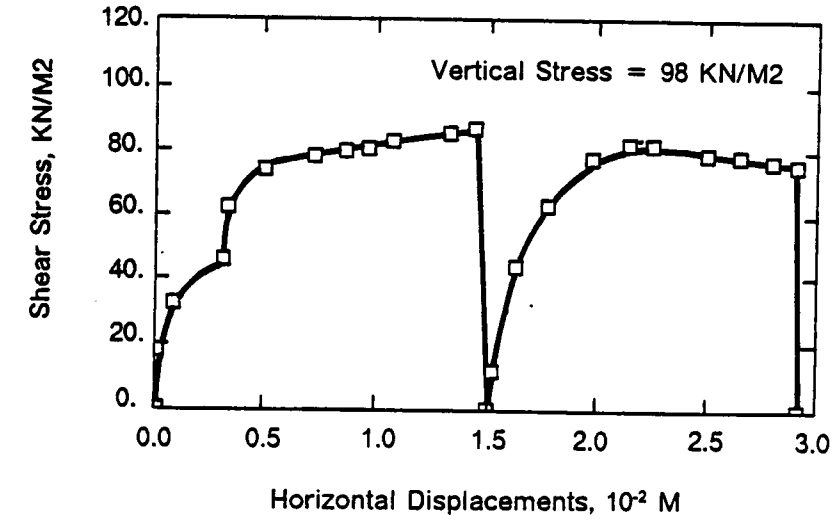

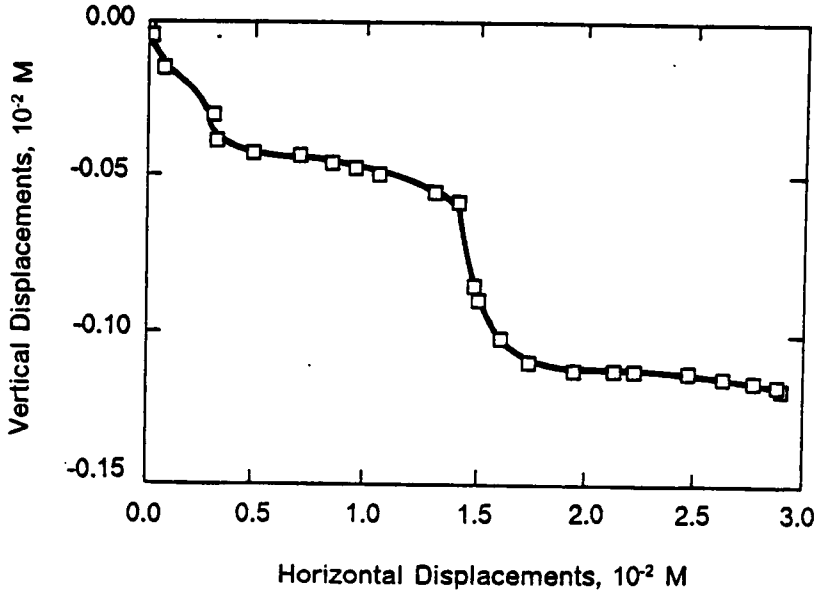

FIGURE 4.11 DIRECT SHEAR TEST RESULTS

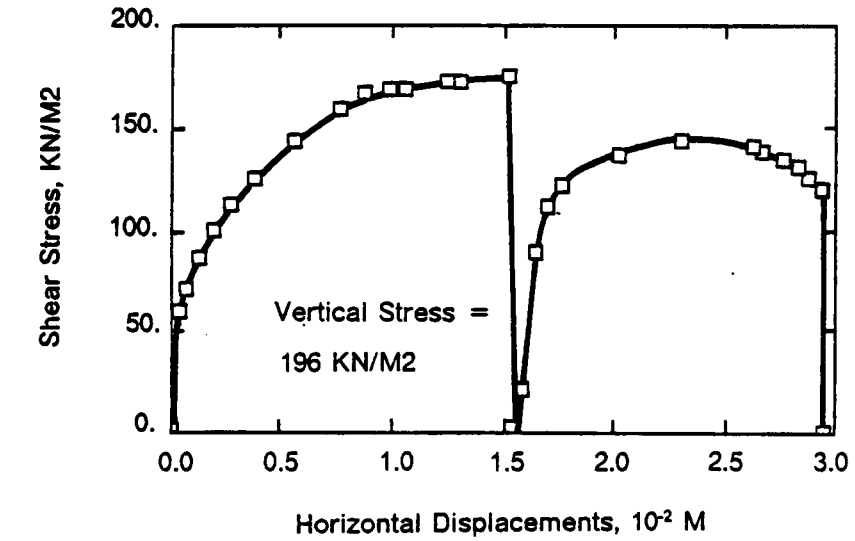

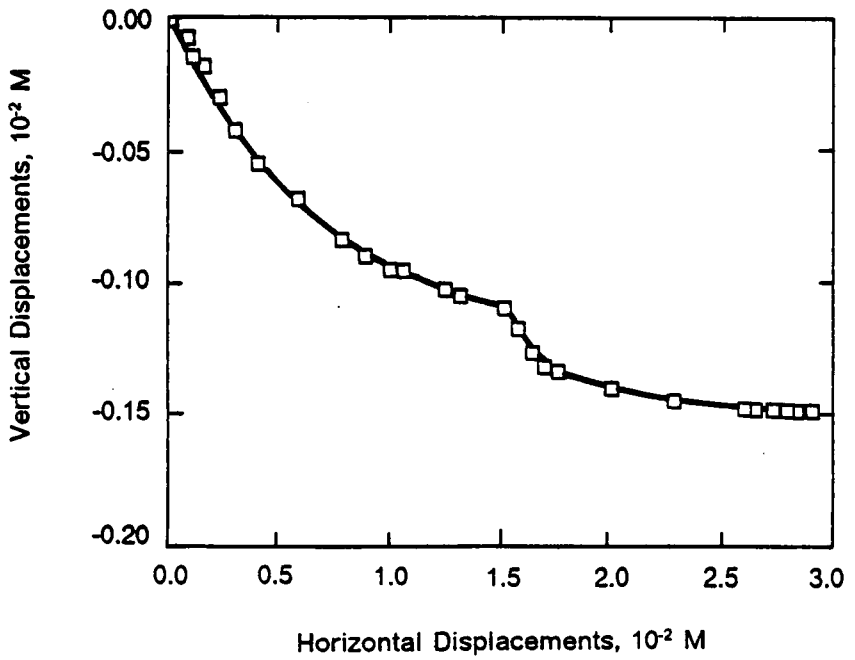

FIGURE 4.12 DIRECT SHEAR TEST RESULTS

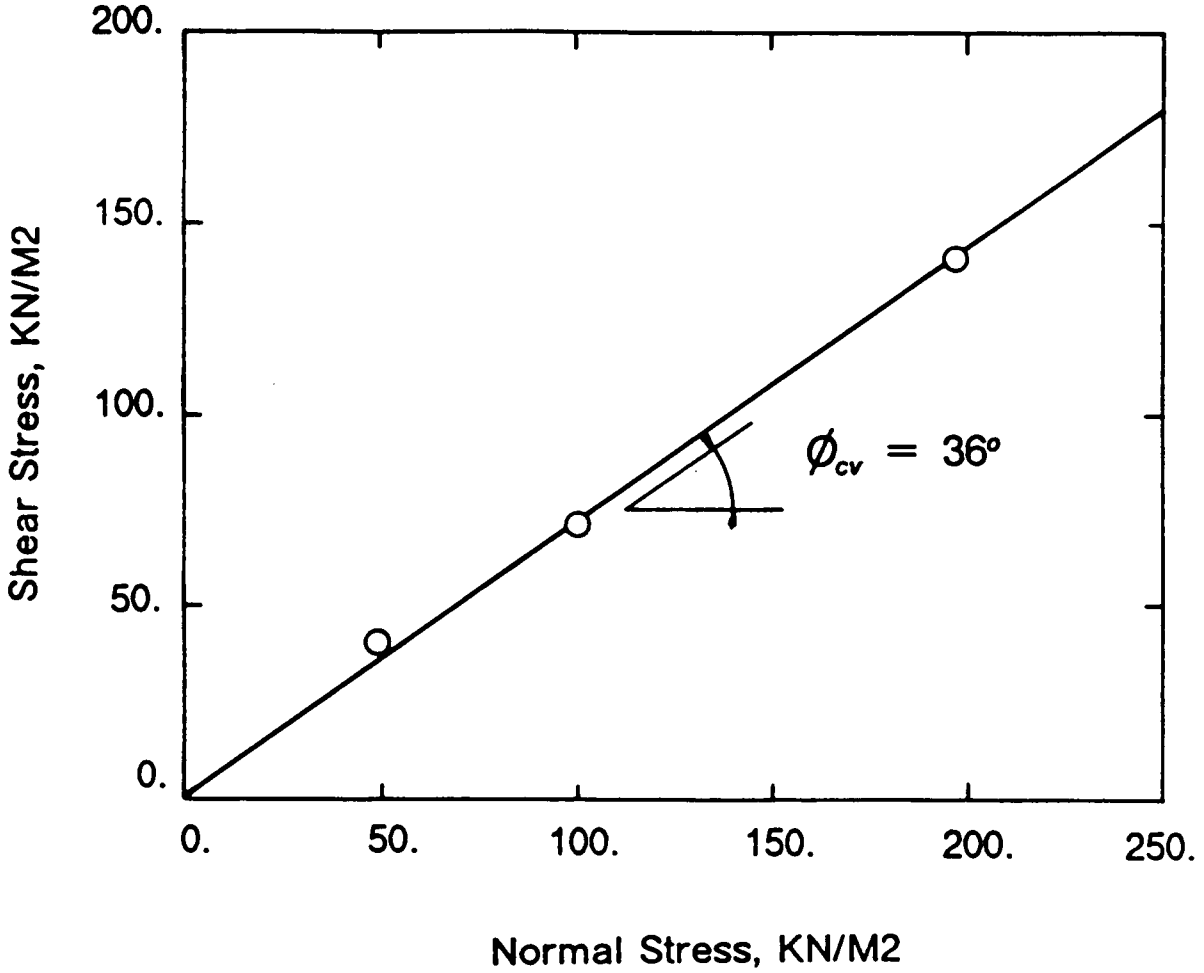

FIGURE 4.13 MOHR-COULOMB ENVELOPE AT CONSTANT VOLUME

Chapter 5

EQUIPMENT, SELF-BORING AND TESTING PROCEDURES

5.1 INTRODUCTION

The pressuremeter used for this study was developed by the English company Cambridge Insitu. The probe was used previously by Benoit (1983) to test the San Francisco Bay Mud, as reported by Benoit and Clough (1986).

The use of the self-boring pressuremeter involves a drilling phase using the self-boring technique and a testing phase. Two different processes were used in this study for the self-boring phase. One relied upon the loading equipment developed originally by Denby (1978) for testing soft clays, with modifications for working in stiff soils. This was used in testing the residual soils near the Virginia Tech campus. An alternative process employed a drill rig to assist in the self boring procedure. This was used to test the Miocene clay of Richmond.

Actual loading of the soil is essentially a pressure control operation. It necessitates a panel to monitor the rate of increase or decrease of the pressure in the probe and a computerized data acquisition system to store the readouts of the different measuring cells. The control panel and the data acquisition system are two new items added to the existing equipment for this study.

5.2 TESTING EQUIPMENT

5.2.1 Self-boring pressuremeter

A detailed description of the pressuremeter used is given by Benoit (1983). The instrument has a diameter of 8.2 CM (3.2 in) and is approximatively 1 M (3.3 ft) long. The pressuremeter module is 0.5 M (1.8 ft) long, the ratio between the pressuremeter module and the diameter is of the order of 6. The lower end of the probe is equipped with a cutting shoe which has a similar function to a shield in tunneling: it must provide support for the excavation work and it must prevent loosening of the surrounding soil. The thrust necessary to move the probe downwards is applied through the external rods attached at the top of the probe. Following the comparison with tunneling, the excavation work is done by a rotating cutter inside the cutting shoe which is supported by an inner rod. Water under pressure is used to bring the mucking back to the ground surface by circulating downwards through the inner rods and flowing back to the ground surface in the annulus situated between the inner rod and the outer rod, loaded with the fragments of soil cut by the cutter.

The probe is equipped with three arms called Arm1, Arm2 and Arm3, two pore pressure cells called PPA and PPB and a total pressure cell. The arms are placed 120 degrees apart along the center perimeter of the inflating section. They are spring loaded by cantilever

beams equipped with strain gauges and measure the radial displacement of the membrane during the expansion test.

The two pore pressure cells PPA and PPB measure the pore water pressure in the soil at the contact with the probe in the vicinity of the arms. They consist in strain gauges mounted on diaphragms which are differentially loaded by the inflating pressure inside the probe and the soil water pressure in the outside.

The total pressure cell is placed inside the pressuremeter and measures the actual pressure existing in the probe.

Testing stiff soils necessitated changes in the set up of the probe. The 0-690 KN/M2 (0-100 psi) pressure cells used by Benoit (1983) were replaced by cells with a pressure range of 0-2760 KN/M2 (0-400 psi). The membrane used was a thick adiprene membrane, and in subsequent stages it was protected by a chinese lantern consisting in a sheath made of stainless steel blades glued side by side on a thin rubber membrane.

The probe equipped with a chinese lantern is shown in the bottom picture in Fig. 5.1. Holes (1) were drilled through the steel blades, in front of the pore pressure cells to allow the measurement of the water pressure. The cutter used for self-boring in the Miocene clay (2) has a straight blade sharpened on the leading edge. It is shown inside the cutting shoe, attached to the inner rod, ready to be used for self-boring. The cutter used to test the residual soil (3) is shown in the figure, on the left side of the cutting shoe. It has a smaller diameter and the cutting edge has a spiral shape. A coaxial cable (4) attached to the pressuremeter contains the line of pressurized nitrogen used to expand the membrane and the electrical wires going to and from the different measuring devices. The pressure in the cable is regulated from the control panel. The electrical signals sent by the measuring devices are interpreted and stored by the computarized data acquisition system.

The top picture in the figure shows typical cuttings of the Miocene clay recovered at the ground surface.

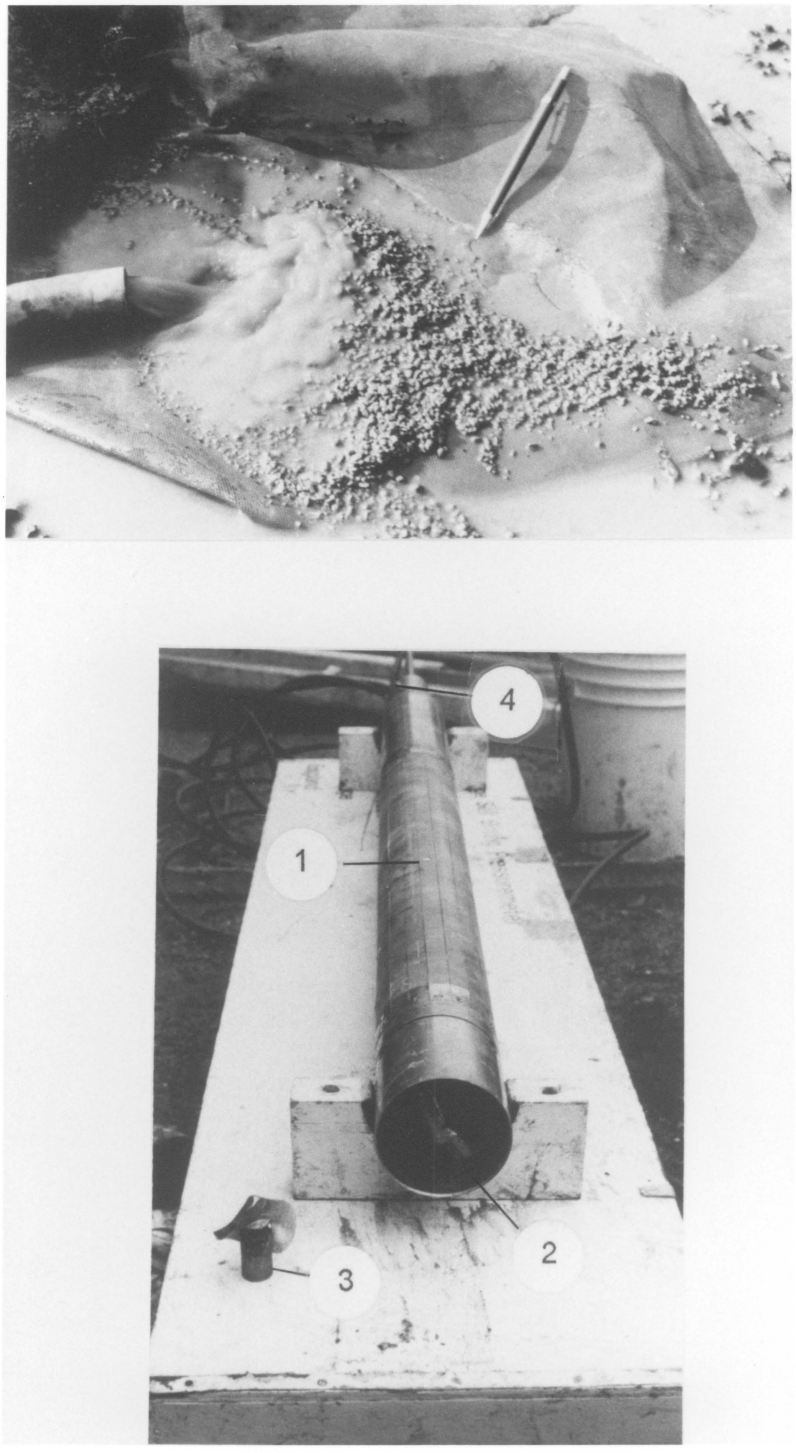

FIGURE 5.1 CUTTINGS OF MIOCENE CLAY (TOP PICTURE)
PROBE EQUIPPED WITH A CHINESE LANTERN (BOTTOM PICTURE)

5.2.2 Control panel

The control panel used for this study is very similar to the one described by Benoit (1983). It is also equipped with a precision valve to regulate the rate of increase of pressure. The pressure lines were replaced by new ones which sustain pressures as high as 3450 KN/M2 (500 psi) and, in addition, it is equipped with a precision valve to control the rate of decrease of pressure in order to perform unloading-reloading cycles.

5.2.3 Data acquisition systems

Two computerized data acquisition systems were used. The first consists in an ISAAC 2000 manufactured by Cyborg and an IBM Personal Computer. The ISAAC 2000 is equipped with a 16 bit A/D converter (board I-150) linked to an extension box in which are stacked the 16 channel multiplexer cards (I-160 boards) to which are attached the wires of the different measuring devices. In the process of storing the data, a software was developed to preset independently for every channel the gain factor by which the electrical signal is multiplied, the time lag between two consecutive measures, the number of samples taken and averaged by measure and the rate of sampling. This data acquisition system was used to perform the tests T1 to T16. Unfortunately, this unit malfunctioned after test T16, and another system was used to carry out the tests T17 to T22 and R1 to R5. It consists in a series of 12 bit A/D converter boards (DASH-8 boards) manufactured by Metrabyte Corporation, an IBM Personal Computer with 640 K memory and a menu drive software known under the name of LABTECH NOTE-BOOK manufactured by Laboratories Technologies Corporation. The multiplexers and the connectors for the measuring devices are situated on the A/D coverter boards which individually support 32 channels. A single gain factor is preset per A/D board, the reason for having 2 to 3 of them when signals of different level are recorded simultaneously. The gain factor

and the time lag between two consecutive measures are the main parameters which are preset for every channel. With the two systems, data are continuously stored in the buffer of the computer and simultaneously dumped on a diskette.

5.3 SELF-BORING EQUIPMENT

5.3.1 Loading frame

The loading frame was developed by Denby (1978) to test the soft clay of the San Francisco Bay. It was subsequently modified and Benoit (1983) gives a detailed description of the different components of the basic system. A picture of the equipment is given in Fig. 5.2. It consists mainly in a hydraulic ground frame (1), a cutter drive unit (2), a hydraulic power unit (3), a water pump (4) and a command table (5). The hydraulic ground frame is equipped with two 10 t jacks which displace vertically a U shape frame. The transverse beam of the U is equipped with a block and wedges which grip the EX casing attached to the pressuremeter and provide to the probe the necessary thrust for the self-boring operation.

Benoit (1978) needed only two sand bags placed on the legs of the loading frame to provide an adequate reaction for self-boring to a depth of 13 M (43 ft) in the San Francisco Bay Mud. However, this was not sucessful in stiff soils like those tested in this work. An assemblage of beams and anchors was developed to provide the necessary reaction for the self-boring operation. The set-up sequence of the frame-beams-anchors system is shown in Fig. 5.3. It includes the following steps:

1. Placement of two anchors 2.4 M (8 ft) apart and dig a prehole at mid-distance. The anchors used were either auger sections 10 to 20 CM (4 to 8 in) diameter and 4.5 to 6.0 M (15 ft to 20 ft) long driven by a drill rig, or anchors 3.0 to 4.5 M (10 to 15 ft) long used by

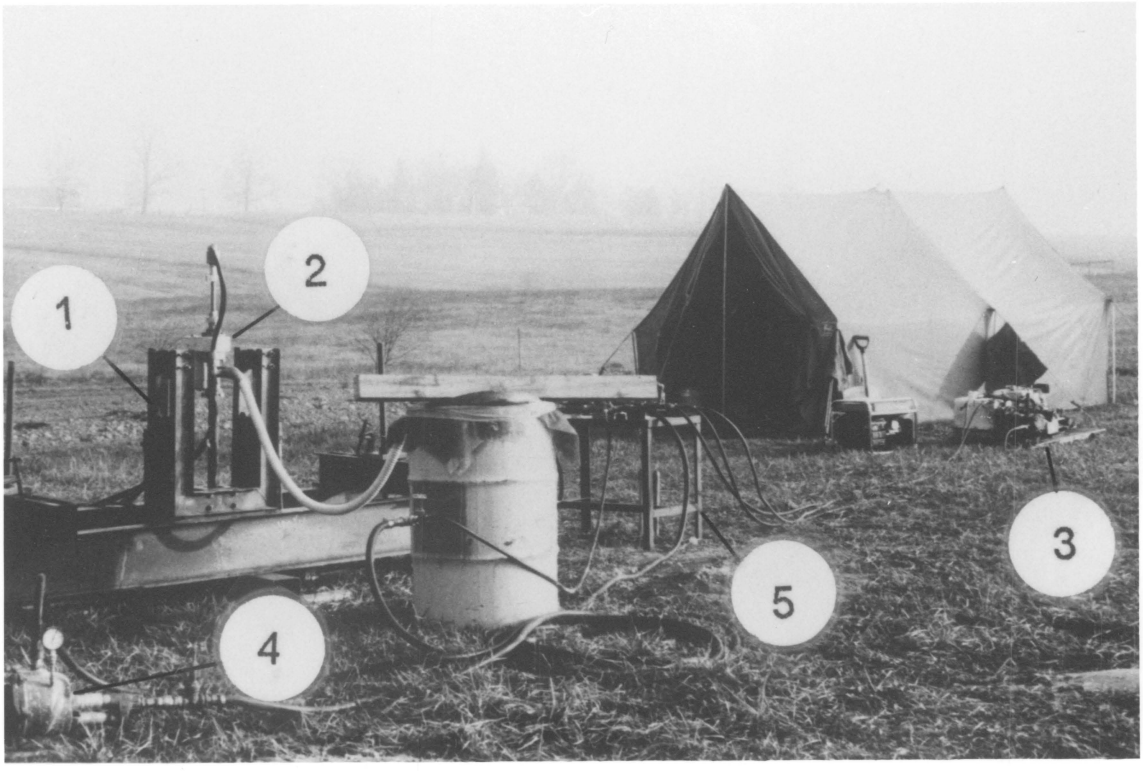

FIGURE 5.2 LOADING FRAME AND EQUIPMENT TO SELF-BORE

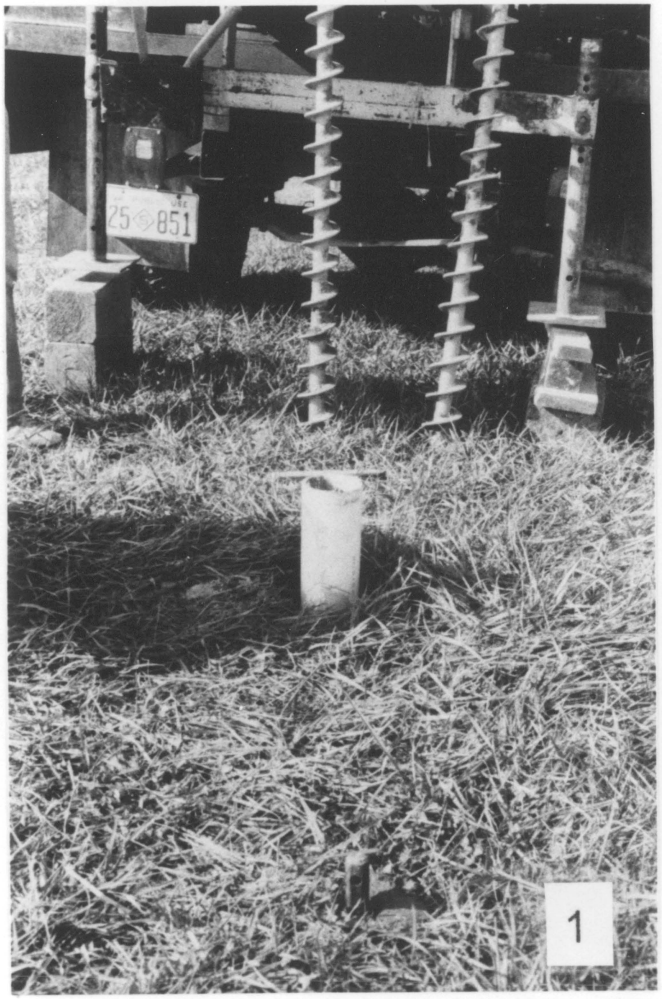

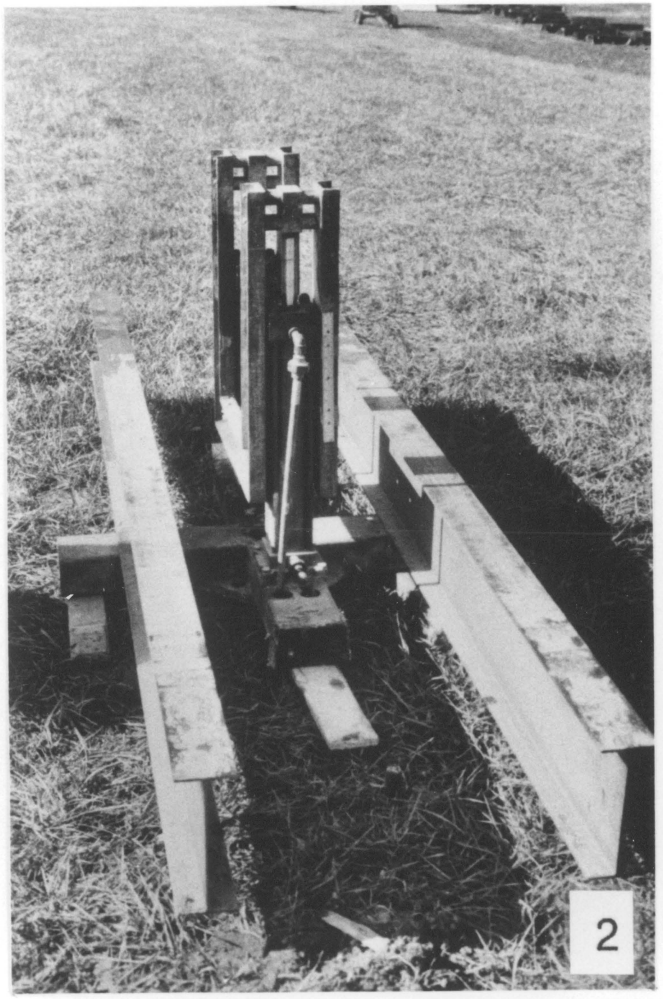

FIGURE 5.3 LOADING FRAME SET-UP FOR SELF-BORING IN STIFF SOILS

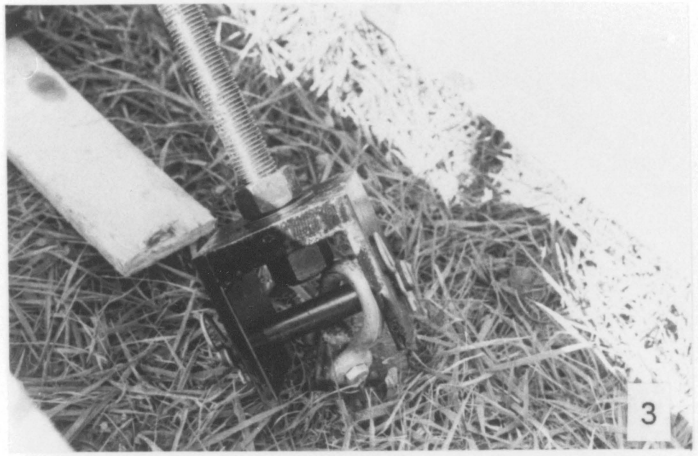

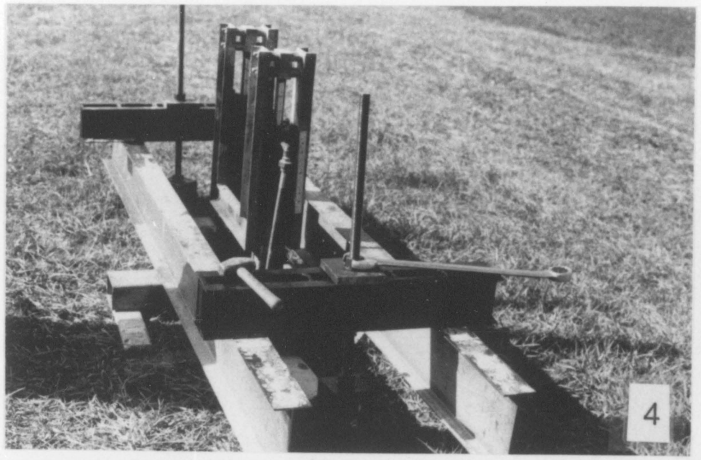

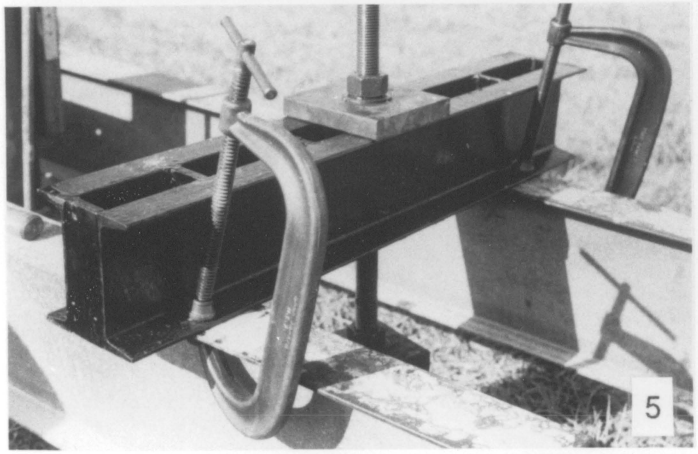

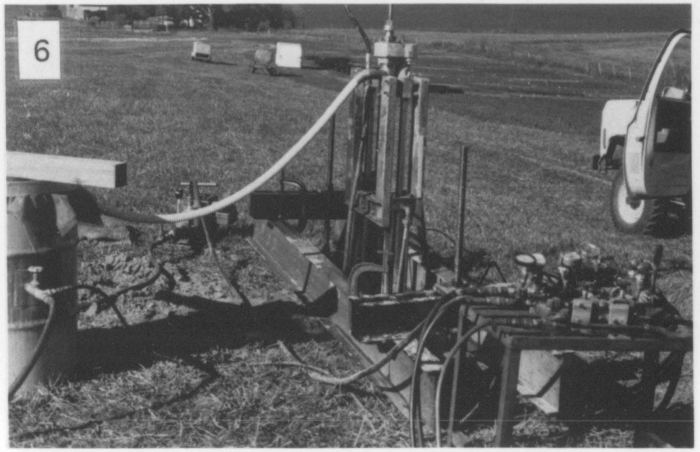

FIGURE 5.3 (CON'D) LOADING FRAME SET-UP FOR SELF-BORNING IN STIFF SOILS

the utility companies. A prehole 1 M (3.3 ft) deep is made with a post digger and cased with a 10 CM (4 in) inside diameter PVC tubing if self-boring starts from the ground surface. If the soil is situated under other soil layers, a drill rig should be used to reach the top of the layer to be tested, the hole should be cased with a 100 MM (4 in) inside diameter casing and the coarse soil particles that might fill the bottom of the hole should be removed by pushing tube samplers.

2. Centering the U frame on the prehole, leveling it with blocks of wood followed by placement of the two longitudinal beams on the legs of the frame.

3. Attaching the clevises to the head of the anchors (auger sections in the figure) and passing pins of the threaded rod through the clevises.

4. Placing the transversal beams on the longitudinal beams and screw the nuts on the repartition plates. Screwing is done evenly at the two anchors to maintain the longitudinal beams leveled and is pursued until the transversal beams prestress the longitudinal beams against the feet of the U frame.

5. Placing C clamps on the flanges of the longitudinal and transversal beams, at their intersection to provide some stiffness to their connection.

6. Completing the set up for testing.

5.3.2 Cutter drive unit

The second main element of the self-boring equipment is the cutter drive unit. It is placed on the top of the EX casing. Its function is to rotate the cutter and to maintain it in a fixed position with respect to the edge of the cutting shoe during the self-boring operation. The

cutter position is an important parameter. Improper positioning of the cutter can lead to disturbance of the soil around and in front of the cutting shoe by stress relaxation if the cutter is placed too far out in the direction of the edge of the cutting shoe or by overstressing if, in the contary, the cutter is kept too far inside the cutting shoe. Proper cutter positioning is a matter of experience. Fig.5.4 gives a chart developed by Clarke (1981) which defines the position the cutter for cohesive soils in terms of the ratio s_u / σ'_v, where s_u is the undrained shear strength and σ'_v the vertical effective stress and in terms of the position of the water table.

5.3.3 Auxillary equipment

The hydraulic power unit activates the two jacks of the loading frame and the cutter drive unit. It is constituted by two pumps mounted on a sleigh which are belt driven by a gas engine and a 15 liters (4 gallons) tank of hydraulic fluid. Detailed description of the equipment is given by Benoit (1983).

The water pump (4), shown in Fig. 5.3, is a Myers HC 100 equipped with a gasoline engine Briggs and Stratton 3HP. It pressurizes the water up to 690 KN/M2 (100 psi).

The command table (5) in Fig. 5.3 is used to initiate the different steps in the self-boring operation and to control the pressures in the lines. Manual valves command the displacement of the jacks, the rotation of the cutter drive unit and the circulation of the water. Precision valves allow to regulate the rate of displacement of the jacks and the speed of rotation of the cutter drive unit. More detailed information on the set-up of the table is given by Denby (1978) and Benoit (1983).

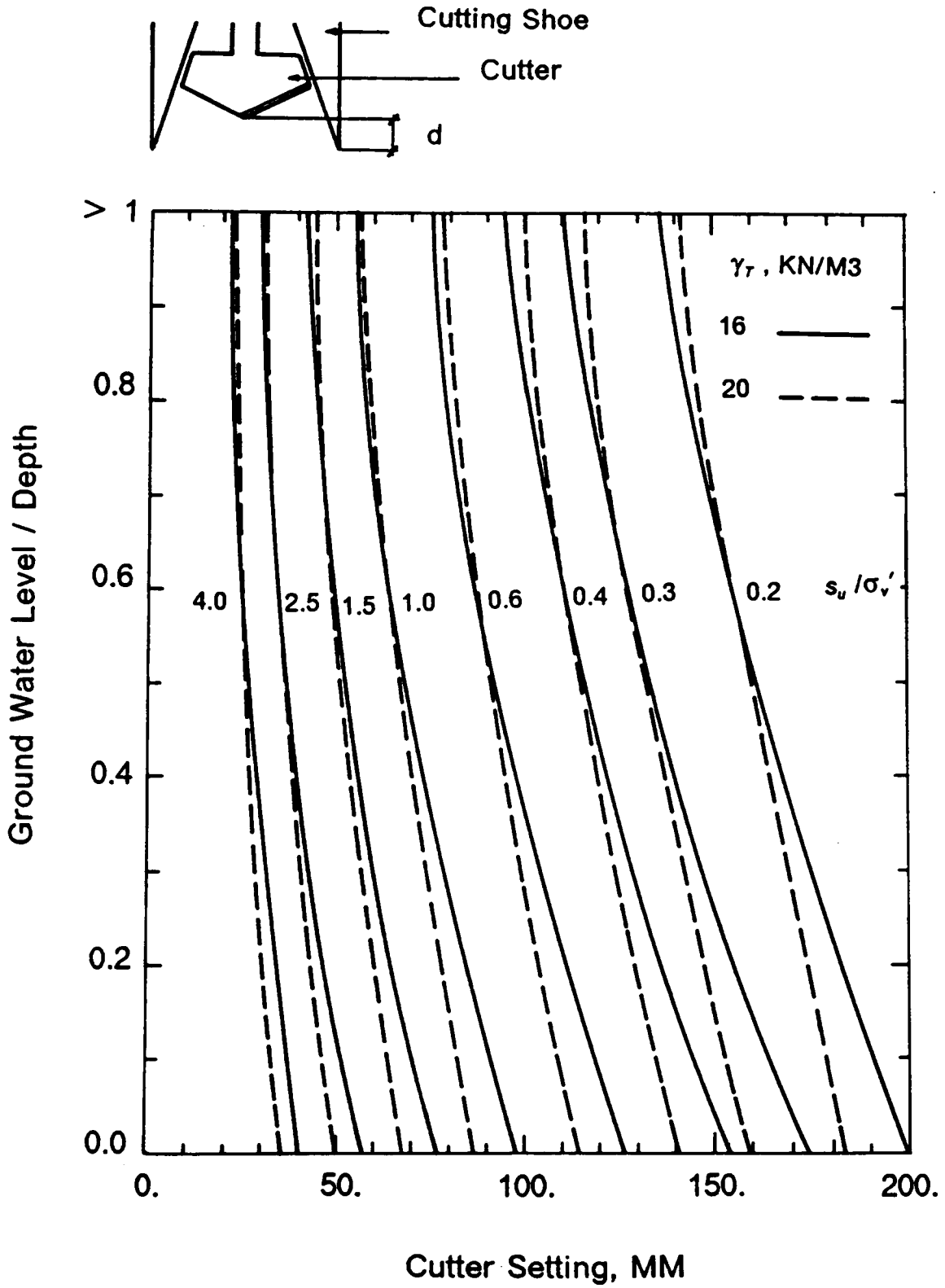

FIGURE 5.4 CUTTER SETTING IN COHESIVE SOILS
(AFTER CLARKE, 1981)

5.3.4 Drill rig

The drill rig is particularily useful for the self-boring operation in very stiff soils, especially when found under several meters of cover since it is equipped with stronger rods than the EX casing used with the loading frame, it provides in such soil conditions an adequate thrust to the self-boring operation and a safe system for the retrieval of the probe.

The system used to self-bore in the Miocene clay is shown in the top picture in Fig. 5.5. The drill rig is an Acker 450 mounted on tracks and capable of delivering a vertical thrust of the order of 22 KN (5000 lbs). The rods to transmit the thrust to the pressuremeter are N rods with a 60.3 MM (2 3/8 in) outside diameter and a 50.8 MM (2 in) inside diameter. The water pump used to bring back the soil cuttings to the ground surface is the same pump as the one used with the loading frame. It is supplied with a 950 liters (250 gallons) water tank mounted on a truck.

The coupling of the rods to the drill rig is shown in the bottom picture in Fig. 5.5. Through this coupling, the drill rig transmits the thrust to the N rods and the rotation to the inner rods. The following pieces compose the coupling:

1. A drill rod adapter (2). Its top extremity has a hexagonal head linked to the chuck of the drill rig (1) and secured with a hairpin clip (3). The inner rod which rotates the cutter is screwed in the lower extremity of this drill rod adapter. Ball bearings are mounted between the shaft of the drill rod adapter and the outer ring which supports the water inlet (4) for the water supply line to remain fixed when the cutter is rotated.

2. A cylinder spacer (5) which covers the shaft of the drill rod adapter (2). Its function is to transmit the thrust downwards.

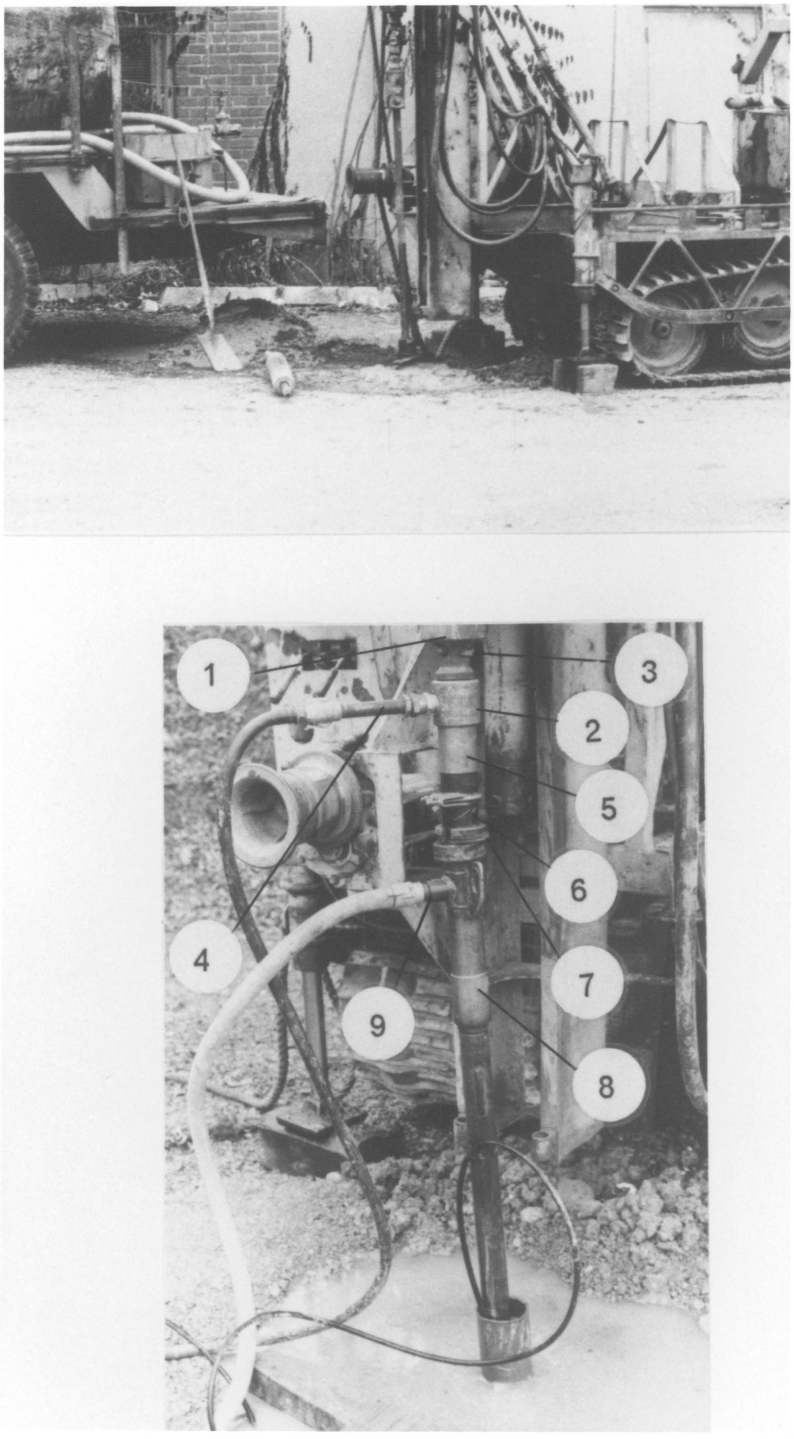

FIGURE 5.5 DRILL RIG (TOP PICTURE)
DETAIL OF THE COUPLING BETWEEN RODS AND DRILL RIG (BOTTOM PICTURE)

3. A split bushing (6). When removed, its space provides access to screw the inner rod. In the figure, tape was wrapped around the split bushing to limit the loss of water through the split on the return.

4. A set of adjusting shims (7) to position the cutter with respect to the cutting shoe.

5. A lower adapter (8) to the N rods which supports the water outlet (9). A slave bearing is cased in the top part of the adapter to prevent the transmission of any torque to the N rods.

Setting up the system for the self-boring operation involves the following steps:

1. Disconnect the upper drill rod adapter (2) from the drill rig chuck (1)

2. Remove the split bushing (6) and screw the inner rod at the bottom face of the drill rod adapter (2)

3. Replace the split bushing (6)

4. Pull upward the split bushing to its uppermost position. In this reference position, the cutter is at its innermost location inside the cutting shoe, in contact with its wall. Substracting the distance the cutter should be moved forward to be in the self-boring position from the space existing between the base of the split bushing (6) and the top of the lower drill rod adapter (8) gives the thickness of the adjusting shims (7) to be placed.

5.4 DRILLING PROCEDURES

5.4.1 Loading frame

The loading frame was used to self bore in the residual soil described in Chapter 4. Self-boring and testing started from the ground surface. At each new location, the loading system was set up according to the procedure shown in Fig. 5.3. The probe was inserted within the prehole dug with a post digger. The arm 1 was systematically oriented toward the North. Before drilling starts, the cutter drive unit was placed on the top of the EX casing and the cutter was positioned with respect to the edge of the cutting shoe. The next step was to control that the hydraulic circuits are idle on the command table and to start the engines of the hydraulic power unit and the water pump. Then, the following sequence of operations was performed:

1. The wedges which grip the EX casing were removed.

2. The U frame was lifted by the jacks to its uppermost position.

3. The wedges were hammered back into position.

4. Simultaneously, the valve of the water line was openend as the valve of the idle circuit was closed.

5. The rotation of the cutter drive was started.

6. The downward displacement of the jacks was initiated.

The sequence of operations listed above was repeated three times to complete the self-boring distance between two consecutive tests as the tests are generally 1 M (3.3 ft) distant and as the run of the jacks is limited to 0.35 M (14 in).

The sequence of operations was performed in the reverse order when self-boring was stopped. The set up of the probe for testing the residual soil and the drilling parameters during the self-boring phase are given in Tab. 5.1. Self-boring was performed to a depth of 9 M (27 ft) at a rate of 2.5 CM (1 in) per minute. The cutter tip was positioned 8 to 15 MM (0.3 to 0.6 in) above the edge of the cutting shoe. During self-boring, the cutter was rotated at 60 to 70 rpm by the cutter drive unit. The water pressure varied between 414 and 552 KN/M2 (60 and 80 psi). Typical jack pressures and corresponding thrust were respectively 2760 KN/M2 (400 psi) and 2.8 KN (630 lbs) near the ground surface. At greater depths, and when localized zones of weathered rock were encountered, the jack pressure and the corresponding thrust were respectively 6900 KN/M2 (1000 psi) and 7.0 KN (1570 lbs).

Identification of the soil crossed by the probe could be made by inspecting the soil cuttings. Self-boring in the zones of cohesive soil produced soft, yellow-brown cuttings, typically 5 MM (0.2 in) long. No cuttings were generally recovered when self-boring was done through the nearly non plastic silty sand. Self-boring in the weathered rock produced small, hard and sharp edge cuttings generally 2 MM (0.01 in) long.

5.4.2 Drill rig

The drill rig was used to self-bore in the Miocene clay described in Chapter 3.

The use of a drill rig requires a similar sequence of operations to the one described for the loading frame. The water pump is started at first, then follows the rotation of the drill rig chuck which drives the cutter and finally, the pressure in the jack which applies the thrust is adjusted to reach the proper rate of advance of the probe. It is recommended to equip the jack with a pressure gauge and to monitor the its pressure during the self-boring operation.

TABLE 5.1 PARAMETERS FOR SELF-BORING WITH THE LOADING FRAME IN THE RESIDUAL SOIL

Parameter	Value
Testing depth	0-9 M (0-27 ft)
Membrane	Adipren, with and without chinese lantern
Cutter position (cutter tip with respect to cutting shoe	8-15 MM (0.3-0.6 in)
Rate of self-boring	25 MM/min (1 in/min)
Cutter rotation	60-70 rpm
Water pressure	414-552 KN/M2 (60-80 psi)
Jack pressure	2070-6900 KN/M2 (300-1000 psi)
Thrust on probe	2.1-7.0 KN/M2 (470-1570 KN/M2)

The jack pressure is a valuable index which characterizes the stiffness of the soil layers encountered by the probe. Its monitoring also prevents clogging of the probe as the thrust to push the probe increases drastically when the cutter is caught and does not function anymore. It is also strongly advised to place a spring loaded friction or drive clutch at the connection between the drill rig and the inner rod in order to limit the maximum torque transmitted by the drill rig to this rod. Twice, the inner rod was sheared during self-boring the Miocene clay because of the lack of control on the torque applied by the drill rig on the inner rod when the cutter was caught in very stiff soil. Typical parameters characterizing the set-up of and the self-boring operation with the drill rig in the Miocene clay are given in Tab. 5.2. With the exception of the vertical thrust which in the Miocene clay is twice the one in the residual soil, the self-boring and set-up parameters in the Miocene clay are similar to the parameters given previously for the residual soil in Tab. 5.1.

The testing depths varied between 0 and 7 M (0 and 23 ft). The position of the tip of the cutter inside the edge of the cutting shoe varied between 12 and 17 MM (0.5 and 0.7 in), the rate of advance varies between 2.5 and 10 CM (1 and 4 in) per minute, the cutter was rotated at 50 to 60 rpm and the water pressure was constantly at 690 KN/M2 (100 psi). The thrust applied to the probe by the drill rig varied between 6.2 KN (1400 lbs) and 12.4 KN (2800lbs) from the top to the bottom of the zone tested.

5.5 TESTING PROCEDURES

5.5.1 Introduction

Testing involved a preliminary calibration in the laboratory to control the good performance of the probe and to determine the correlation constants of the different measuring devices.

TABLE 5.2 PARAMETERS FOR SELF-BORING WITH THE DRILL RIG IN THE MIOCENE CLAY

Parameter	Value
Testing depth	0-7 M (0-23 ft)
Membrane	Adipren, with chinese lantern
Cutter position (cutter tip with respect to cutting shoe)	12-15 MM (0.5-0.7 in)
Rate of self-boring	25-100 MM/min (1-4 in/min)
Cutter rotation	50-60 rpm
Water pressure	690 KN/M2 (100 psi)
Jack pressure	1380-2760 KN/M2 (200-400 psi)
Thrust on probe	6.1-12.4 KN/M2 (1400-2800 KN/M2)

In the field, similar testing procedures were used in the residual soils and in the Miocene clay. They consisted in increasing or decreasing the pressure in the probe at a constant rate. As the residual soil is generally a non saturated fine silty sand, the pressuremeter tests performed in this soil are classified as drained tests. On the contrary; the tests performed in the Miocene clay are classified as undrained as the soil is a saturated clay.

5.5.2 Calibration

Conventional calibration techniques of the self-boring pressuremeter are described by Benoit (1983). They involve the calibration of the three arms and the calibration of the total pressure cell and the two pore pressure cells. The calibration must be performed with the same electrical circuits and loads as the ones used for testing, i.e. with the computer and the data acquisition system. The calibration of the arms is performed without membrane. Each arm is successively calibrated. The displacement of the arm between two consecutive measures is controlled by a Vernier and a linear correlation between the readout in millivolts and the displacement in millimeters or inches is established.

To perform the calibration of the total pressure cell and the pore pressure cells, the pressuremeter is equipped with a membrane. Holes are perforated in the membrane straight to the the pore pressure cells and the caps of the pore pressure cells are placed. The pressuremeter is placed in a calibration sleeve provided by the manufacturer which is a thick wall pipe. The pressure in the probe is incresed by steps and readouts of the three pressure cells are made. Linear correlations are determined between the readouts in millivolts and the applied pressure in the probe.

The different pressure cells used for the testing program of this study are given in Tab. 5.3. The table indicates also the calibration constants of the measuring devices for the different series of tests performed.

TABLE 5.3 RANGES AND CALIBRATION CONSTANTS OF THE MEASURING CELLS

Soil	Residual soil				Miocene clay
Tests		T1	T2-T16	T17-T22	R1-R5
Total pressure cell	Range KN/M2 (psi)	0-27600 (0-400)	0-6900 (0-100)	0-27600 (0-400)	0-27600 (0-400)
	Cali-bration KN/M2/mv (psi/mv)	-11.73 (-1.10)	-1.64 (-0.24)	-9.53 (-1.38)	-9.53 (-1.38)
Pore pressure cell A	Range KN/M2 (psi)	-	-	-	0-27600 (0-400)
	Cali-bration KN/M2/mv	-	-	-	10.14 (1.47)
Arms	Arm 1 MM/mv (in/mv)	0.021 (0.82)	0.021 (0.82)	0.020 (0.80)	0.020 (0.80)
	Arm 2 MM/mv (in/mv)	0.021 (0.82)	0.021 (0.82)	0.022 (0.85)	0.022 (0.85)
	Arm 3 MM/mv (in/mv)	0.022 (0.85)	0.022 (0.85)	0.022 (0.85)	0.022 (0.85)

In response to Jamiolkowski et al (1977) who addressed the existence of compliance of the measuring arms when testing with the pressuremeter, a new type of calibration was initiated. It uses a pressure tank shown in Fig. 5.6 which was specially made for this study. The tank allows simulation of a test conducted under pressure. To do this, the pressuremeter is placed in the tank which is sealed and pressurized at a known pressure. Then, the probe is pressurized by steps or continuously to simulate a real test. The readouts of the measuring devices are monitored and the loading is stopped when a radial strain of the order of 10% is reached. This simulated test allows to:

1. Determination if there is compliance of the strain arms before lift-off.

2. Determination of the stiffness of the system membrane-chinese lantern at lift-off for different magnitudes of lift-off pressures and for different radial strains.

3. Study of the effect of repeated expansion on the stiffness of the membrane and chinese lantern.

4. Check of the calibrations performed in the calibration sleeve

Results of a test in the pressure tank are shown in Fig. 5.7. In this figure, the radial strain measured by Arm1 versus the pressure in the pressuremetre is given successively for a tank pressure of 483 KN/M2 (70 psi) and 621 KN/M2 (90 psi). Similar results were obtained for the two other arms. The figure indicates that no compliance occurs before lift-off as the portion of the test is perfectly vertical before that point. After lift-off, the pressuremeter curve is linear, slightly inclined with the horizontal.

The results of two series of tests performed in the calibration tank, before and after the SBPM tests were conducted in Richmond, are given in Fig. 5.8. In the figure, the lift-off pressures of the individual strain arms are plotted against the tank pressure.

From the test results, it can be concluded that:

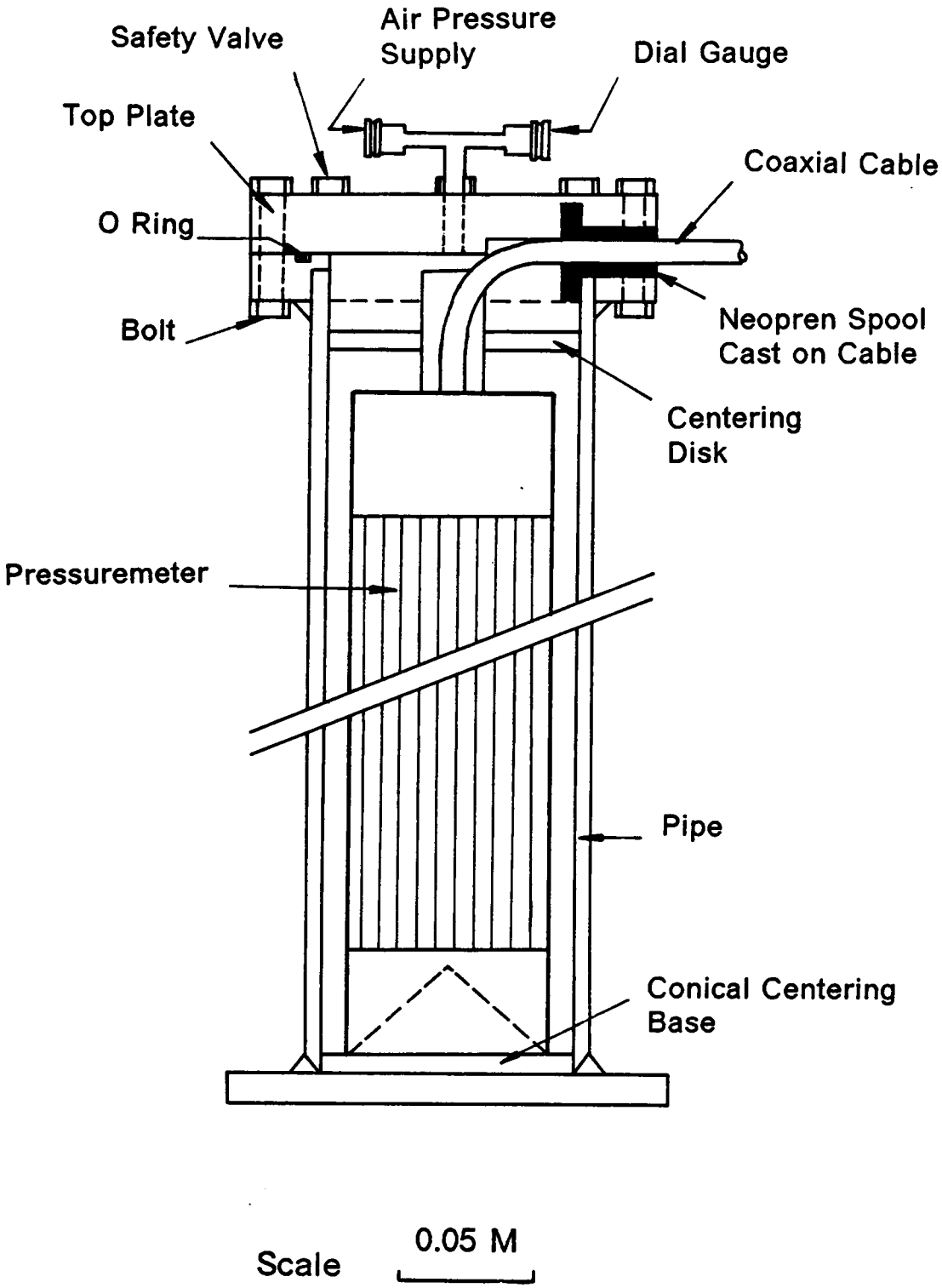

FIGURE 5.6 CALIBRATION TANK

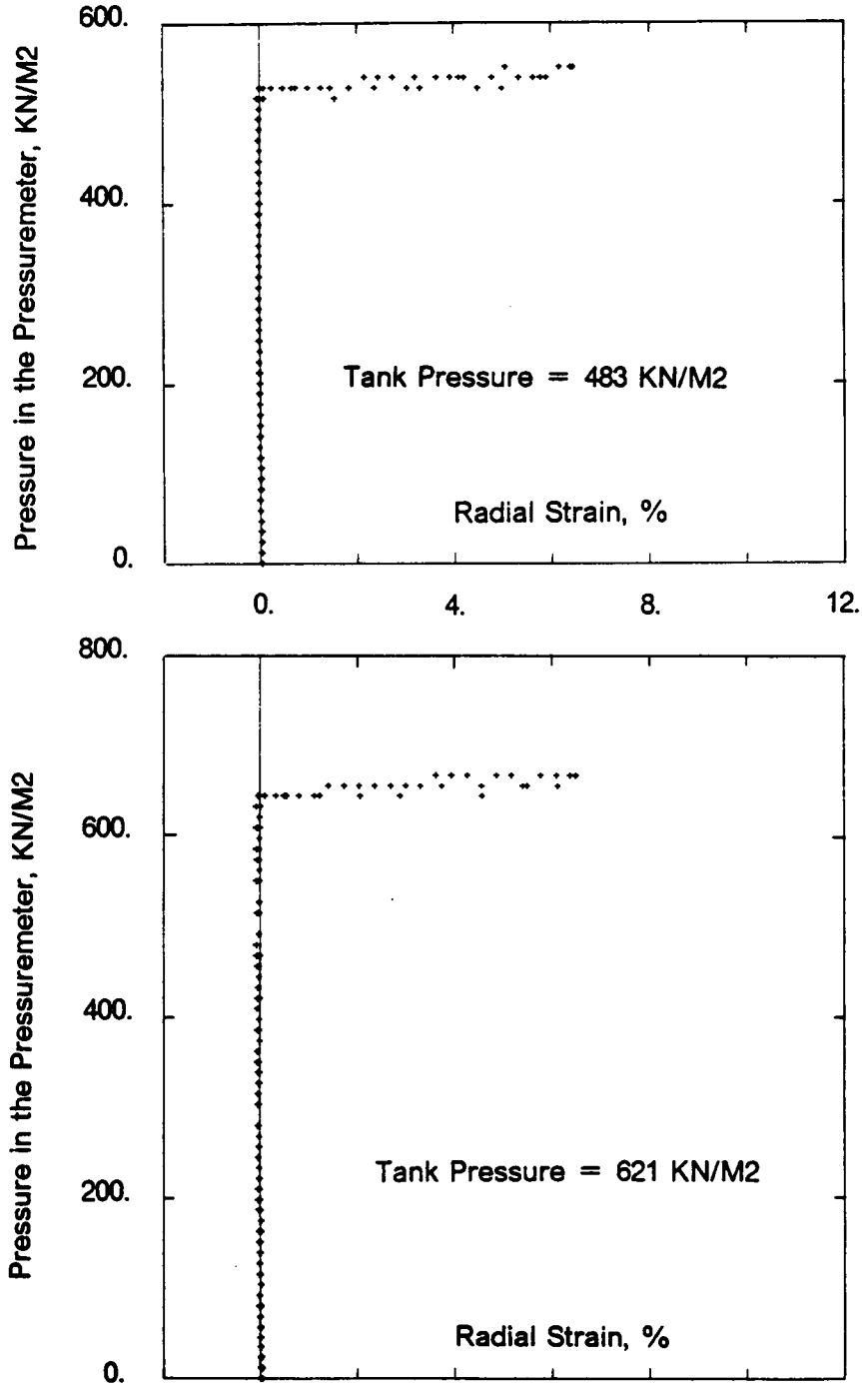

FIGURE 5.7 SIMULATED PRESSUREMETER TEST IN THE CALIBRATION TANK

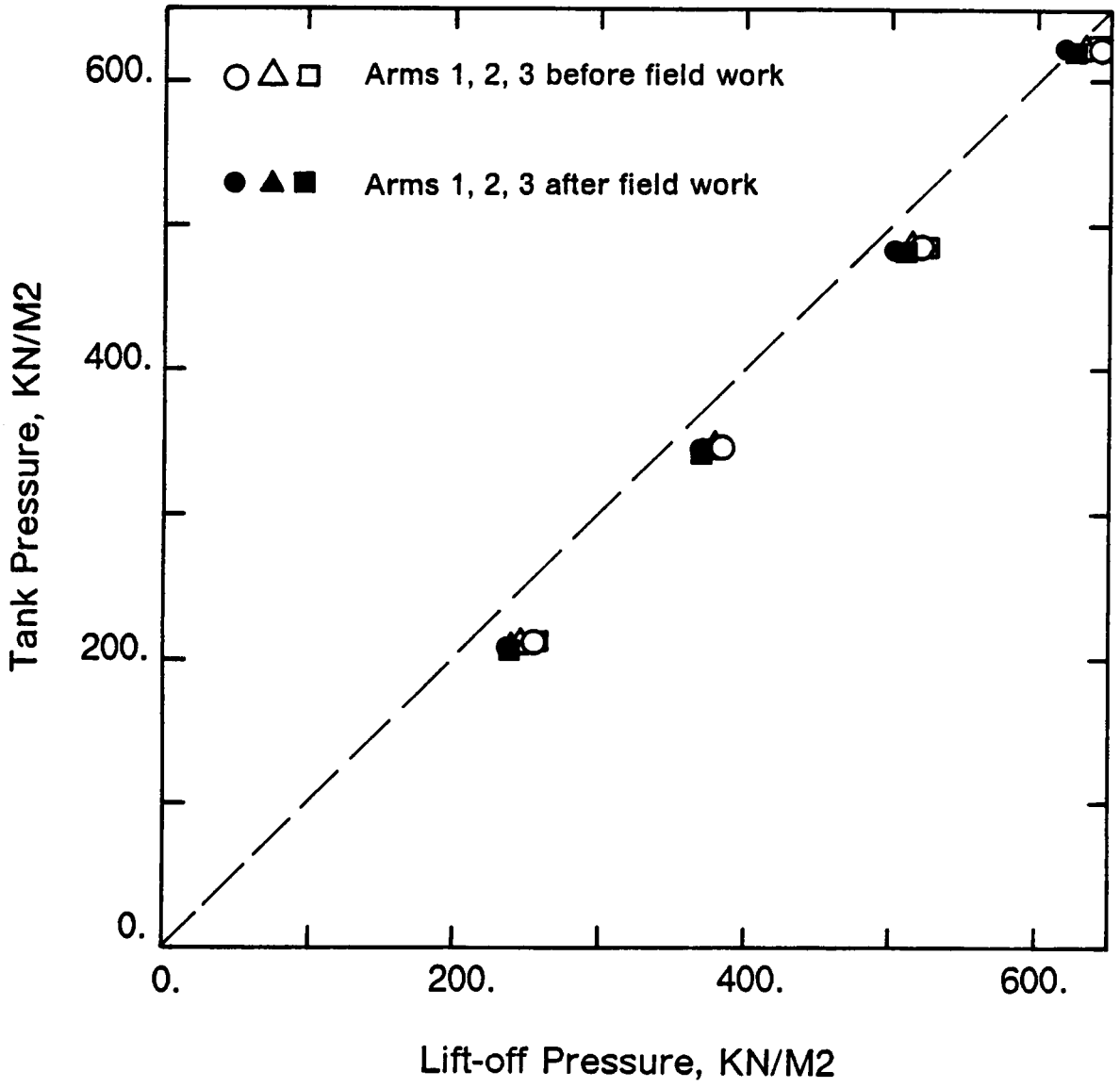

FIGURE 5.8 LIFT-OFF PRESSURE VERSUS TANK PRESSURE

1. The horizontal distances between the individual lift-off points, and the points on the line inclined 45 degrees with the axes, where the lift-off pressure equals the tank pressure, determine the stiffness of the membrane and the chinese lantern at lift-off. It is generally less than 35 KN/M2 (5 psi) and decreases as the tank pressure increases.

2. Lift-off occurs simultaneously for the three strain arms, before and after the SBPM testing program in Richmond. This indicates that the strain arms are capable of recording that the membrane lifts-off simultaneously in all directions when the probe is placed in a uniform stress field.

3. The lift-off pressures recorded by the individual strain arms versus the tank pressure are identical before and after the SBPM tests were performed in Richmond. This implies that the probe was not subjected to malfunction when it was used to test the Miocene clay in Richmond.

The calibration of the total pressure cell using the calibration sleeve and the pressurized tank are compared in Fig. 5.9. The two calibrations are identical as they have the same slope on the diagram pressure versus millivolt readings. They are equal to -9.53 KN/M2/MV (-1.38 psi/MV).

The results of the calibration of the pore pressure cell PPA are shown in Fig. 5.10. Two calibrations were performed: The first one with the pressuremeter placed in the calibration sleeve and pressurized internally between 0 and 1380 KN/M2 (0 and 200 psi). The second was performed by placing the pressuremeter in the calibration tank which was pressurized by steps up to 552 KN/M2 (80 psi). The output readings of the pore pressure cell under these two pressure environments are indicated in Fig. 5.10. They show that the calibration constant of the cell is identical for the two types of calibrations and is equal to 10.14 KN/M2/MV (1.47 psi/MV).

In Fig. 5.11, the stiffness of the system membrane-chinese lantern at lift-off and during expansion is given in terms of the tank pressure. The stiffness at lift-off is influenced by the

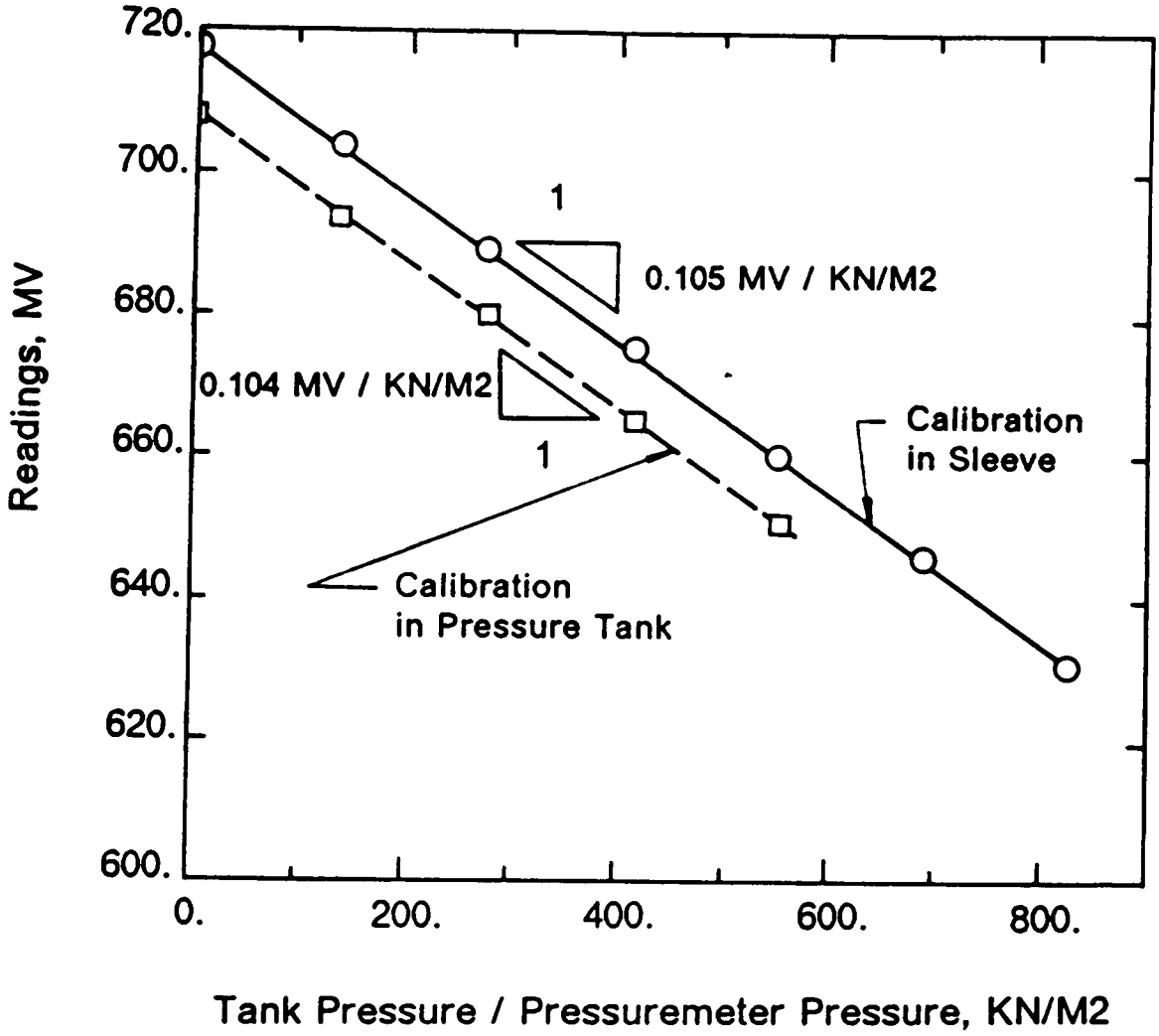

FIGURE 5.9 CALIBRATION OF THE TOTAL PRESSURE CELL

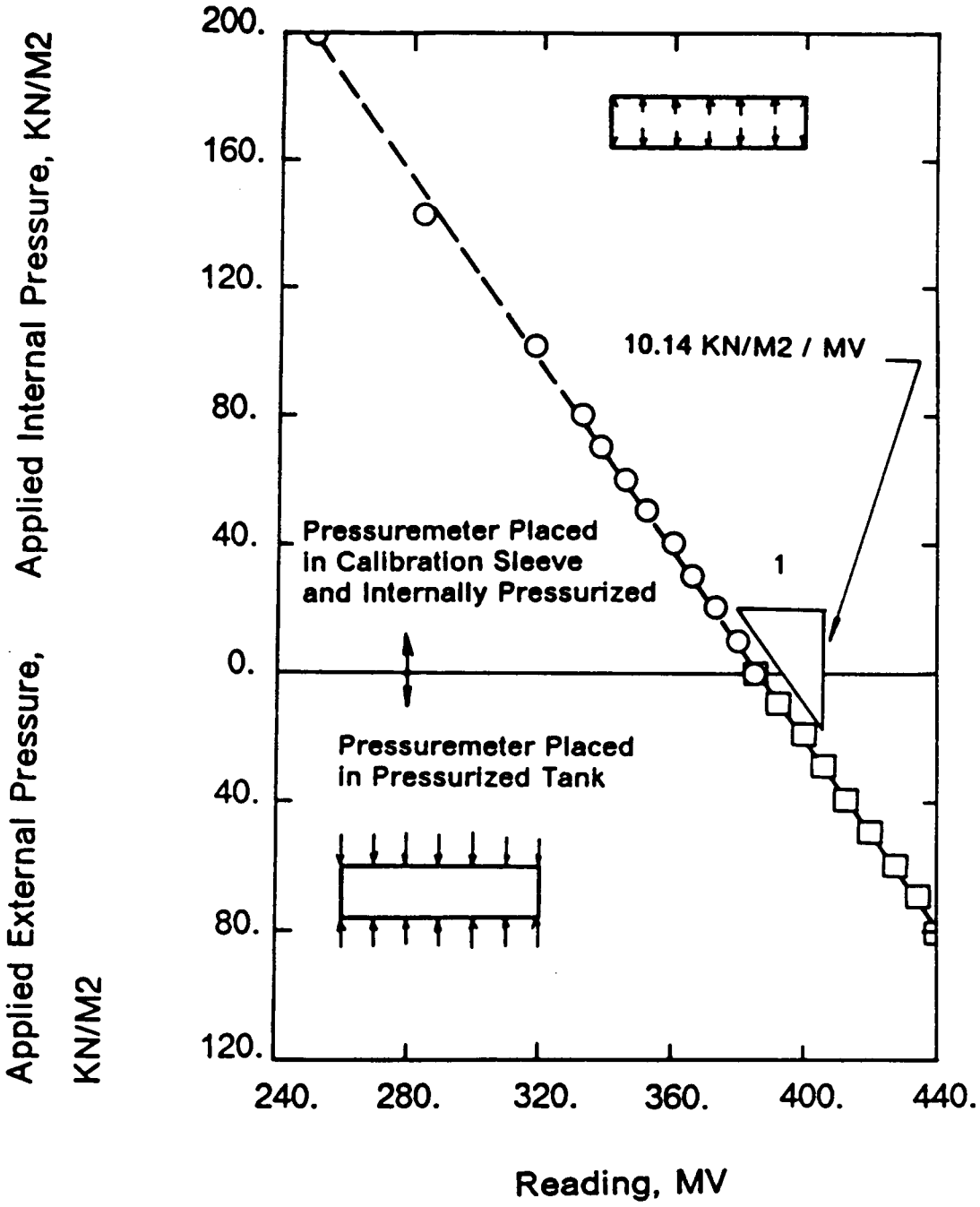

FIGURE 5.10 CALIBRATION OF THE PORE PRESSURE CELL PPA

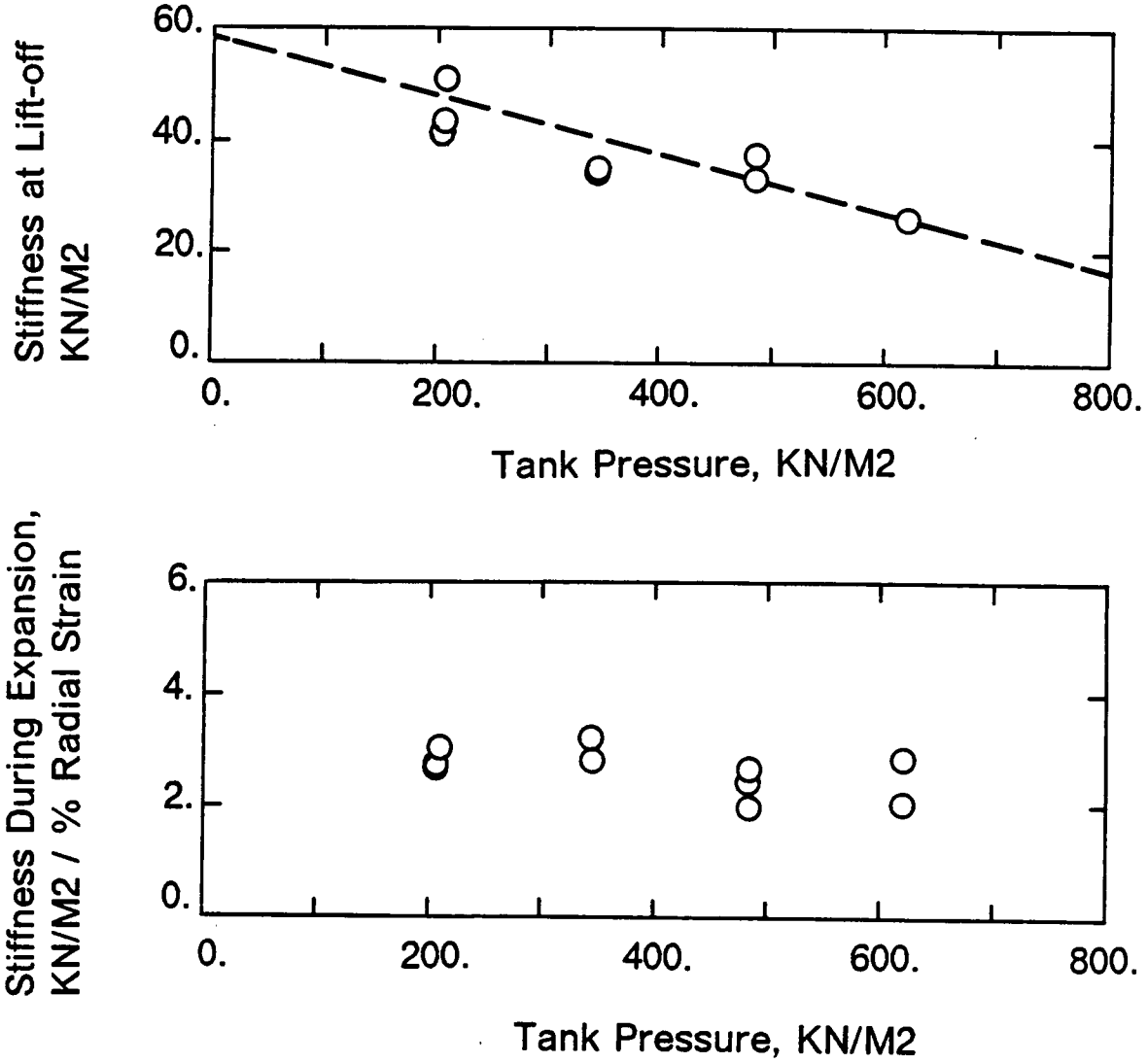

Note: The stiffnesses are the average of the values measured by Arm1, Arm2 and Arm3

FIGURE 5.11 STIFFNESS OF THE MEMBRANE AND CHINESE LANTERN VERSUS TANK PRESSURE

magnitude of the surrounding tank pressure. Typically, the stiffness at lift-off varies between 48 KN/M2 (7 psi) for a tank pressure of 200 KN/M2 (30 psi) to 26 KN/M2 (3.8 psi) for a tank pressure of the order of 620 KN/M2 (90 psi). As an example, the probe situated 5M (16.5 ft) deep in a normally consolidated clay with the water table at the ground surface would be surrounded by a total lateral soil pressure equal to 90 KN/M2 (13 psi). According to Fig. 5.11, in this condition the stiffness of the membrane-chinese lantern system at lift-off is 55 KN/M2 (8 psi) and it represents 60% of the total lateral soil pressure. On the contrary, the probe situated 20 M (66 ft) deep in a stiff clay, above the water table would be surrounded by a total lateral soil pressure equal to 350 KN/M2 (51 psi). According to Fig. 5.11, in this condition, the stiffness of the membrane-chinese lantern system at lift-off is 40 KN/M2 (5.8 psi) and it represents 11% of the total lateral soil pressure.

According to the results shown in the lower diagram in Fig. 5.11, the stiffness of the system membrane-chinese lantern during expansion is not affected by the magnitude of the tank pressure. Typical values of the stiffness during expansion are 2 to 3 KN/M2 (0.3 to 0.4 psi) per percent of radial strain.

In Fig. 5.12, the stiffness of the system membrane-chinese lantern at lift-off and during expansion is expressed in terms of the number of expansion cycles performed. A new membrane was placed on the pressuremeter for the first cycle and the pressure in the tank was maintained constant and equal to 207 KN/M2 (30 psi). The results indicated in the figure do not show any correlation at lift-off or during expansion between the number of expansion cycles and the stiffness of the system membrane-chinese lantern.

5.5.3 Testing procedure

Similar testing procedures were used in the Miocene clay and in the residual soil. The tests were run under a constant stress rate. In the Miocene clay, attempt was made to ap-

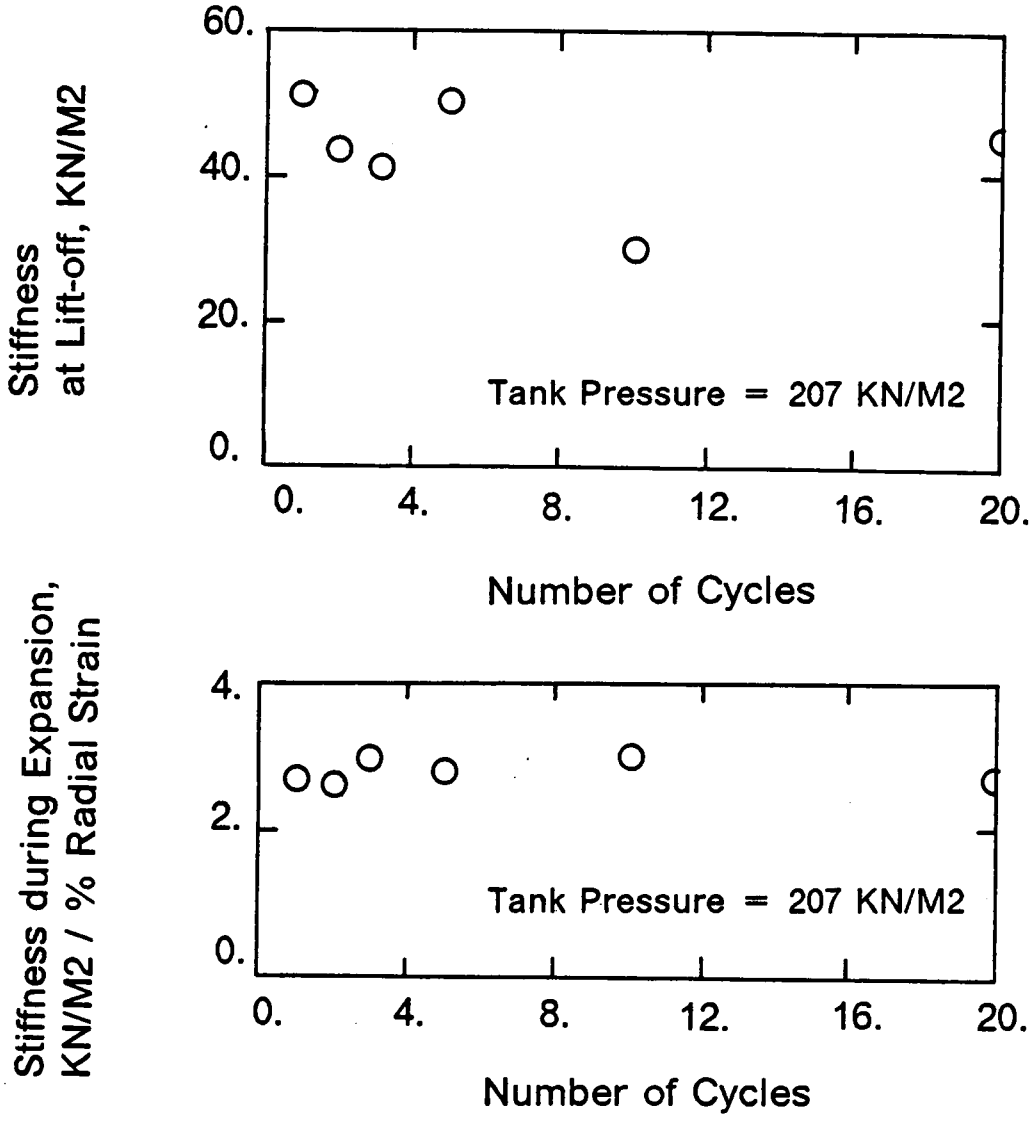

FIGURE 5.12 STIFFNESS OF THE MEMBRANE AND CHINESE LANTERN SYSTEM VERSUS THE NUMBER OF EXPANSION CYCLES

proach undrained conditions by using stress rates varying between 69 and 138 KN/M2 (10 and 20 psi) per minute which led to radial strain rates of the order of 0.5 to 1.0% per minute.

In the case of the residual soils, tests were run under drained conditions as the soil is mostly a non saturated nearly non plastic silty sand. Rates used to test these soils vary typically between 21 and 69 KN/M2 (3 and 10 psi) per minute.

A schematic pressuremeter curve is given in Fig. 5.13. The loading part OD can be monotonic or it can contain unloading reloading cycles such as BC at different strain levels. Similarily, the unloading part can be monotonic or it can contain reloading-unloading cycles such as EF at different strain levels. The purpose of the cycles BC and EF is to determine the elastic modulus of the soil. Wroth (1982) established theoretical relationships for cohesive and friction materials which give the maximum size of the cycles BC to avoid the soil to yield during unloading. These expressions are given in Fig. 5.14. In the case of an elastic perfectly plastic cohesive material, the unloading cycle BC in Fig 5.12 (or PX in Fig. 5.14) should be less than $2s_u$ ($2c_u$ in Fig. 5.14) where s_u is the undrained shear strength of the soil.

In the case of a cohesionless soil, the amplitude of an unloading cycle should be less than

$$\left(\frac{2 \sin \Phi'}{1 + \sin \Phi'}\right)\sigma'_r$$

where Φ' is the effective angle of friction of the soil and σ'_r the effective radial stress reached prior the beginning of the unloading-reloading cycle. Typical unloading-reloading cycles in the Miocene clay and the residual soil had a magnitude varying typically between 104 and 207 KN/M2 (15 and 30 psi).

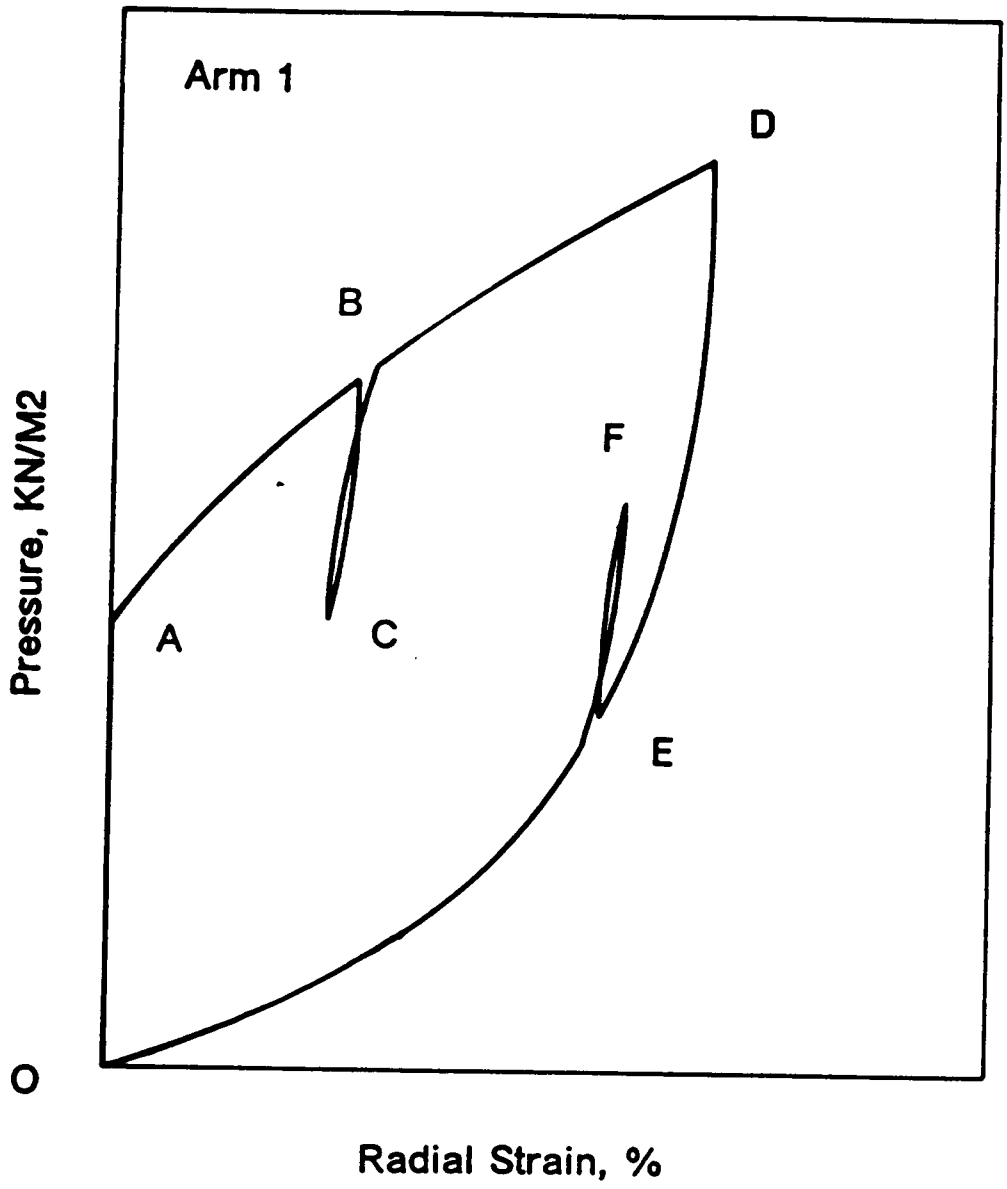

FIGURE 5.13 SCHEMATIC PRESSUREMETER CURVE

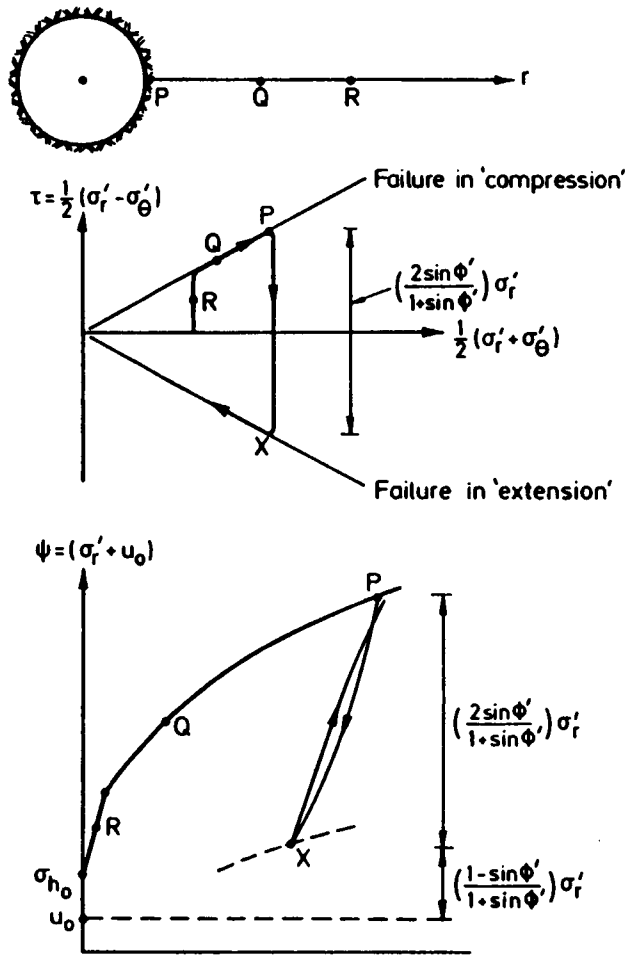

Cohesionless Soil

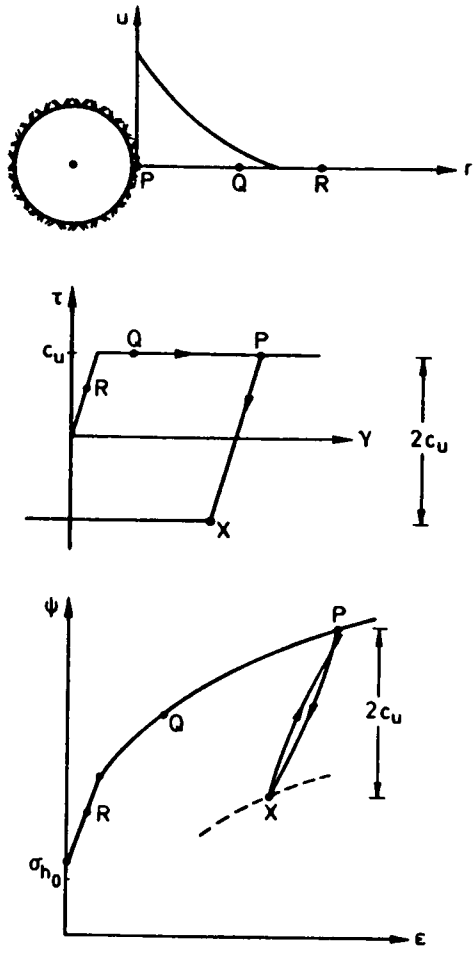

Elastic Perfectly Plastic
Cohesive Soil

FIGURE 5.14 AMPLITUDE OF UNLOAD-RELOAD CYCLES (AFTER WROTH, 1982)

Chapter 6

SELF-BORING PRESSUREMETER TESTS IN THE MIOCENE CLAY

6.1 INTRODUCTION

A total of six tests, termed R1 to R6 were performed in the Miocene clay in Richmond, at the two different sites indicated in Fig. 6.1. The first intention was to perform a profile of SBPM tests at the Coliseum site which is close to the Exhibition Center site where the block samples tested in the laboratory were taken. However, only the test R6 was successfully performed at the Coliseum site as the load frame and the EX casings which were used to self bore were inappropriate to transmit the necessary thrust for the self-boring operation to the probe 17 M (51 ft) in the ground. Subsequently, the remaining testing was conducted in the parking lot of Schnabel Engineering Associates which is situated at the intersection of Canal Street and Foushee Street. At that site, known as the Schnabel Center site, the Miocene clay

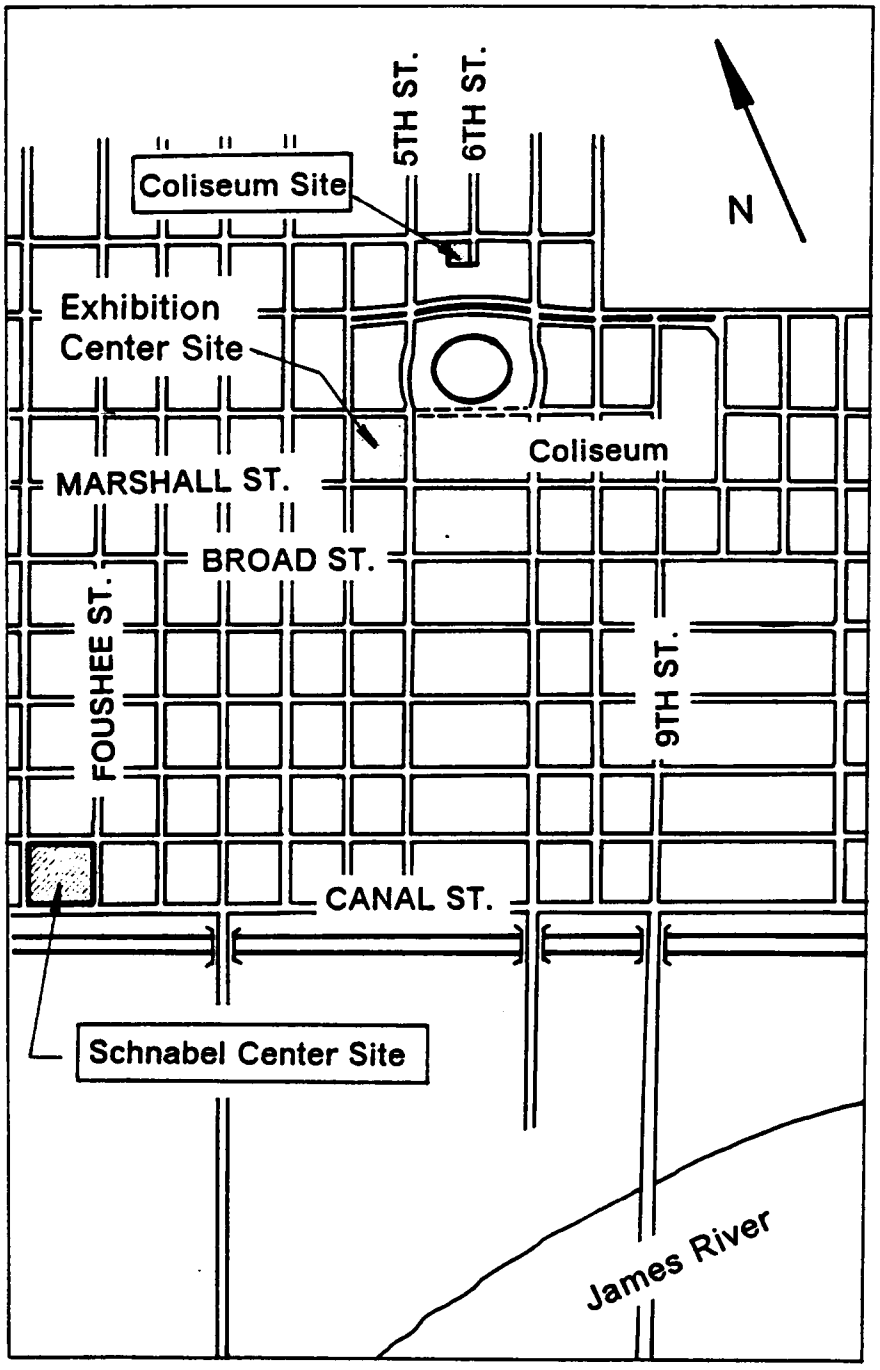

FIGURE 6.1 SBPM TESTING SITES

is very near the surface, which reduces the need for high reaction forces. Five tests termed R1 to R5, were successfully performed at the Schnabel Center site.

6.2 DESCRIPTION OF THE SITES

6.2.1 Schnabel Center Site

A plane view of the Schnabel Center site is given in Fig. 6.2. The site is situated in a zone where the original cover over the Miocene clay has been largely removed by erosion by the James River, and excavation for local construction activity. The location of testing is situated 12 M (40 ft) from the foot of a slope which is about 6.6 M (22 ft) high and inclined approximatively 40 degrees with the horizontal. The tests R1 to R5 were performed in the same hole, at depths between 1 and 7 M (3 and 23 ft) at a location where the Miocene clay is found under 0.6 M (2 ft) of cover. Arm1 of the probe was oriented towards north before the beginning of the self-boring operation for the first test. Arms 2 and 3 were oriented 120° from Arm1 as indicated in Fig. 6.2.

6.2.2 Coliseum site

A laboratory testing program of limited extent was conducted on clay samples from two Shelby tubes, one taken between 3.0 and 3.5 M (10 and 12 ft) depth in a boring distant 6 M (20 ft) from the location of the tests R1 to R5 and the other one between 6.9 and 7.5 M (23 and 25 ft) in the same boring as the tests R1 to R5. The laboratory testing was done in order to determine if the properties of the clay at the Schnabel Center site are similar to those deter-

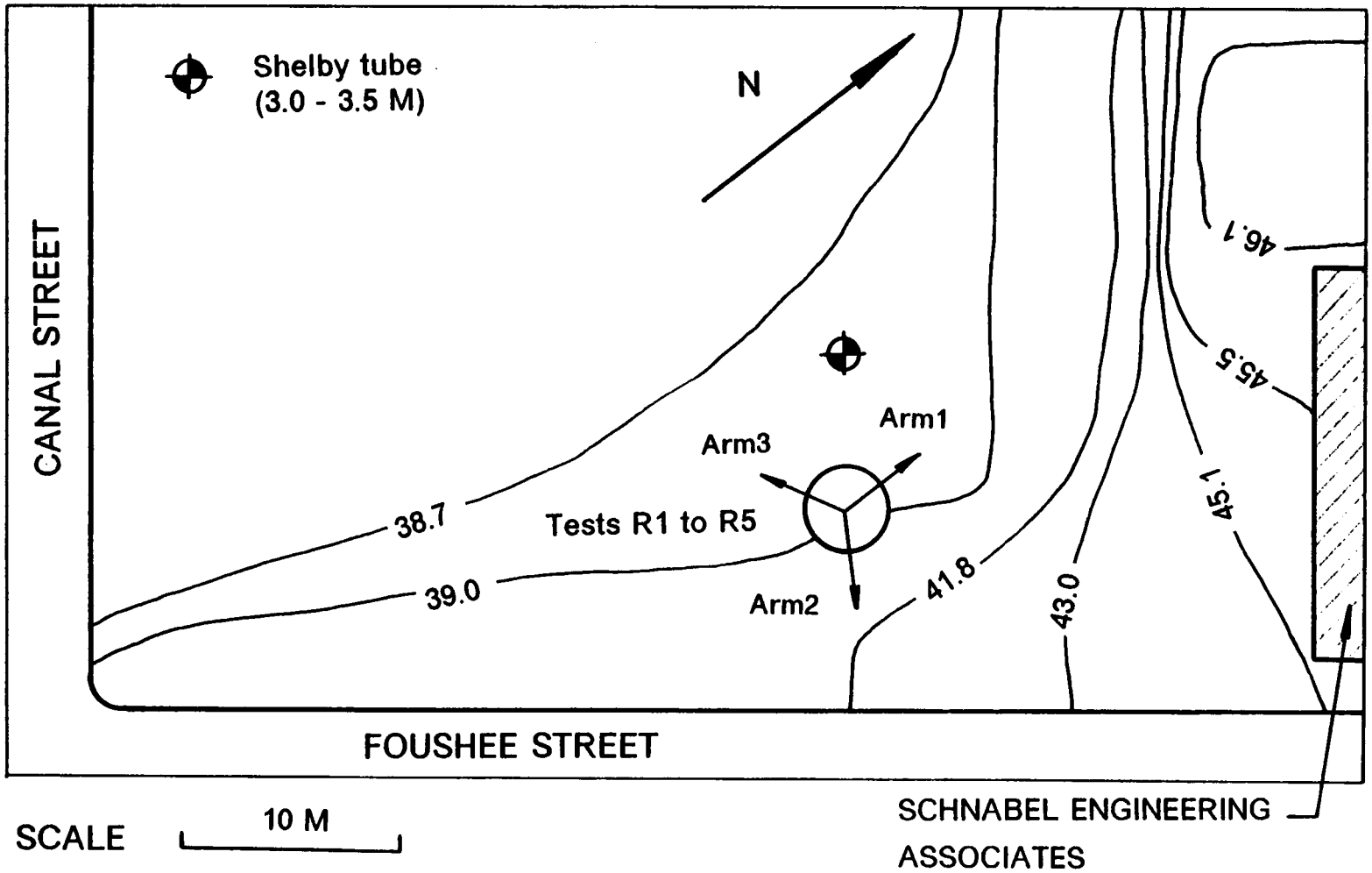

FIGURE 6.2 SCHNABEL CENTER SITE

mined in the detailed testing described in Chapter 3. The work consisted of identification tests, including two Atterberg limits, four natural water contents and three unit weights. Three UU triaxial tests were also performed. Tab. 6.1 gives a comparison of the data from the tests on the Shelby tube samples from the Schnabel Center site to the ranges of parameters determined for the Miocene clay in Chapter 3. The Atterberg limits and the natural water contents fall well within the previous data ranges, while the unit weights for the Schnabel Center site clay are on the low end of those measured previously. The undrained shear strengths for the Schnabel Center site show one higher value than those determined earlier, otherwise the results from the two test sites are very similar. Overall, the Miocene clay at the Schnabel appears to have essentially the same properties as described for the soil in Chapter 3.

Test R6 was performed 15.4 M (50.5 ft) deep, at the top of the Miocene clay formation. Arm1 of the probe was oriented towards north, as was done for the tests R1 to R5. The site is the section of the Coliseum parking lot situated at the intersection of Jackson Street and 6 th Street. At that location, the Miocene clay is found under 12 M (40 ft) of cover.

6.3 BASIC PRESSUREMETER TEST DATA

The raw results of the six self-boring pressuremeter (SBPM) tests are presented in Appendix E. As an example, the results of the test R4 are shown in Fig. 6.3 where the pressuremeter curves recorded by the three arms are given in millivolts. The first part of the pressuremeter curve is vertical until the pressure in the probe equilibrates the total lateral soil pressure and the stiffness of the membrane and chinese lantern system. At that point, known as lift-off, the expansion starts. The pressure versus displacement is monitored during loading and unloading. Two load-unload cycles, one conducted during loading and one during unloading are used to determine the soil modulus. At the point of complete unloading when

TABLE 6.1 RESULTS OF THE LABORATORY TESTING PROGRAM AT SCHNABEL CENTER SITE

Depth, M	Natural Water Content, Percent	Liquid Limit	Plastic Limit	Total Unit Weight, KN/M3
3.0 - 3.6	51	73	34	
6.9 - 7.5	57, 64, 65	92	45	14.5, 15.2, 15.8
From Chapter 3	32 - 72	44 - 109	28 - 48	15.5 - 18.7

IDENTIFICATION

Depth, M	Confining Pressure KN/M2 (psi)	Peak Shear * Strength, KN/M2 (psi)	Axial Strain, at Failure, Percent
6.9-7.5	207 (30)	221 (32.0)	2.0
6.9-7.5	276 (40)	131 (19.0)	2.3
6.9-7.5	345 (50)	110 (16.0)	1.1
From Chapter 3	207 - 483 (30 - 70)	115 - 122 (16.7-17.7)	2.5 - 4.0

* UNDRAINED SHEAR STRENGTHS FROM SHELBY TUBE SAMPLES

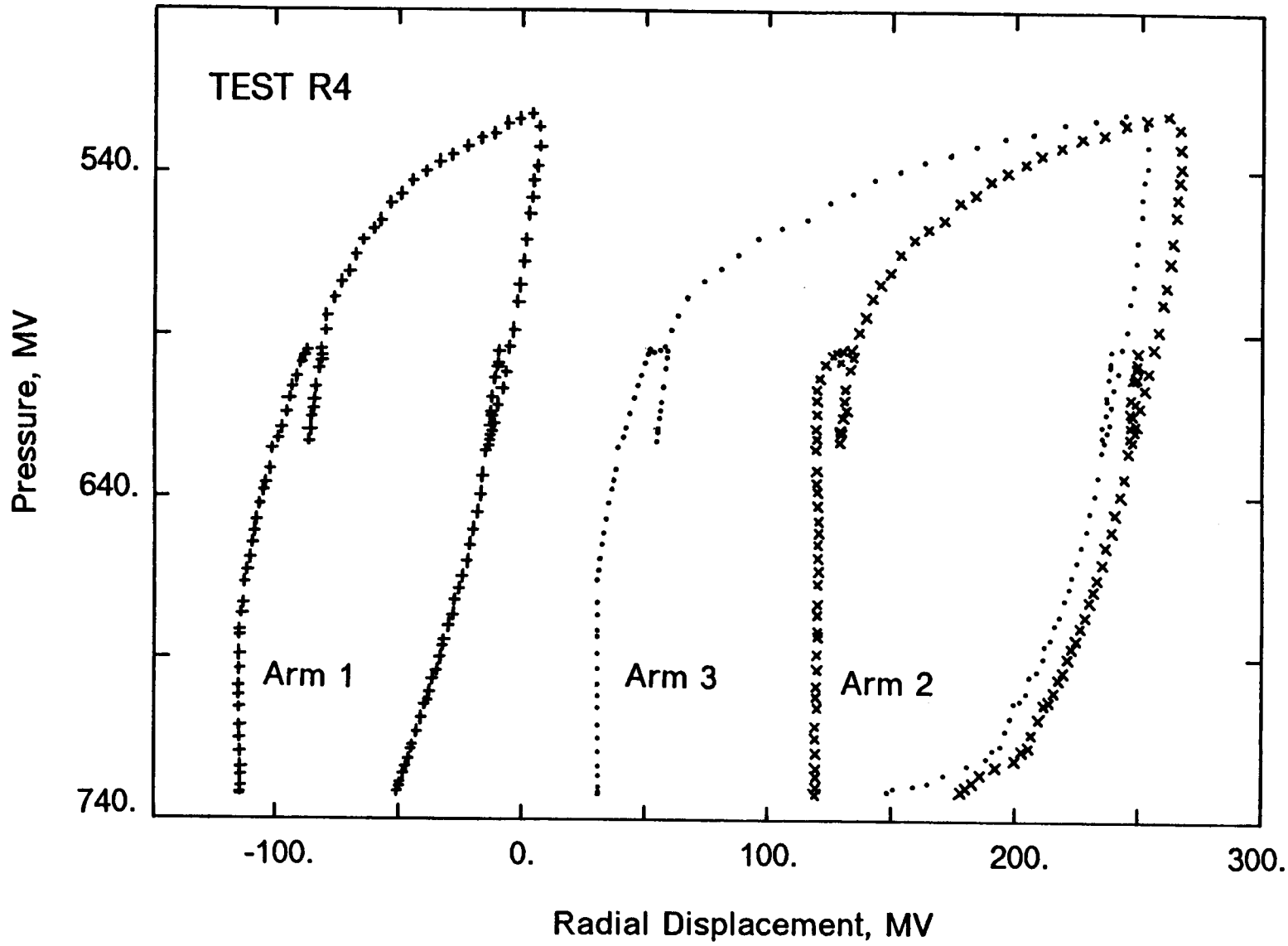

FIGURE 6.3 RAW RESULTS OF THE TEST R4

all stress is removed, the membrane remains displaced from its original position. This is caused by adhesion with the surrounding soil.

In this chapter, the lateral pressures, the undrained shear strength and the elastic modulus of the soil interpreted from the SBPM tests results are presented. They are compared to the values obtained with the Menard pressuremeter and the results of the laboratory testing program.

6.4 HORIZONTAL TOTAL STRESSES

6.4.1 Test Results

The observational method was used to determine the lateral pressures in the ground from the raw test data. This method consists in determining visually from the pressuremeter curves the pressure at which every arm lifts off and to correct it for the stiffness of the system membrane chinese lantern.

As an example, the raw data of the expansion part of the test R1 are plotted in Fig. 6.4 for the three arms. The observational method gives values of 39.5, MV, 95.7 MV and 53.3 MV for Arms 1, 2 and 3 respectively. This converts to 380 KN/M2 (55 psi), 918 KN/M2 (133 psi) and 511 KN/M2 (74 psi) respectively using the calibration constant for the total load cell given in Tab. 5.3. The correction for the stiffness of the membrane chinese lantern system is estimated as 27 KN/M2 (3.9 psi) using Fig. 5.10. After correcting the lift-off pressures for the stiffness of the membrane-lantern stiffness, the total lateral pressures in the ground measured by Arms1, 2 and 3 are respectively 353 KN/M2 (51.2 psi), 891 KN/M2 (129.1 psi) and 484 KN/M2 (70.1 psi).

As apparent from the data given in Fig. 6.4, the test R1 yields lateral pressures from the three arms which are not the same. This implies that the stresses in the horizontal plane in the ground are not isotropic. On one hand, this phenomenon could possibly be attributed to

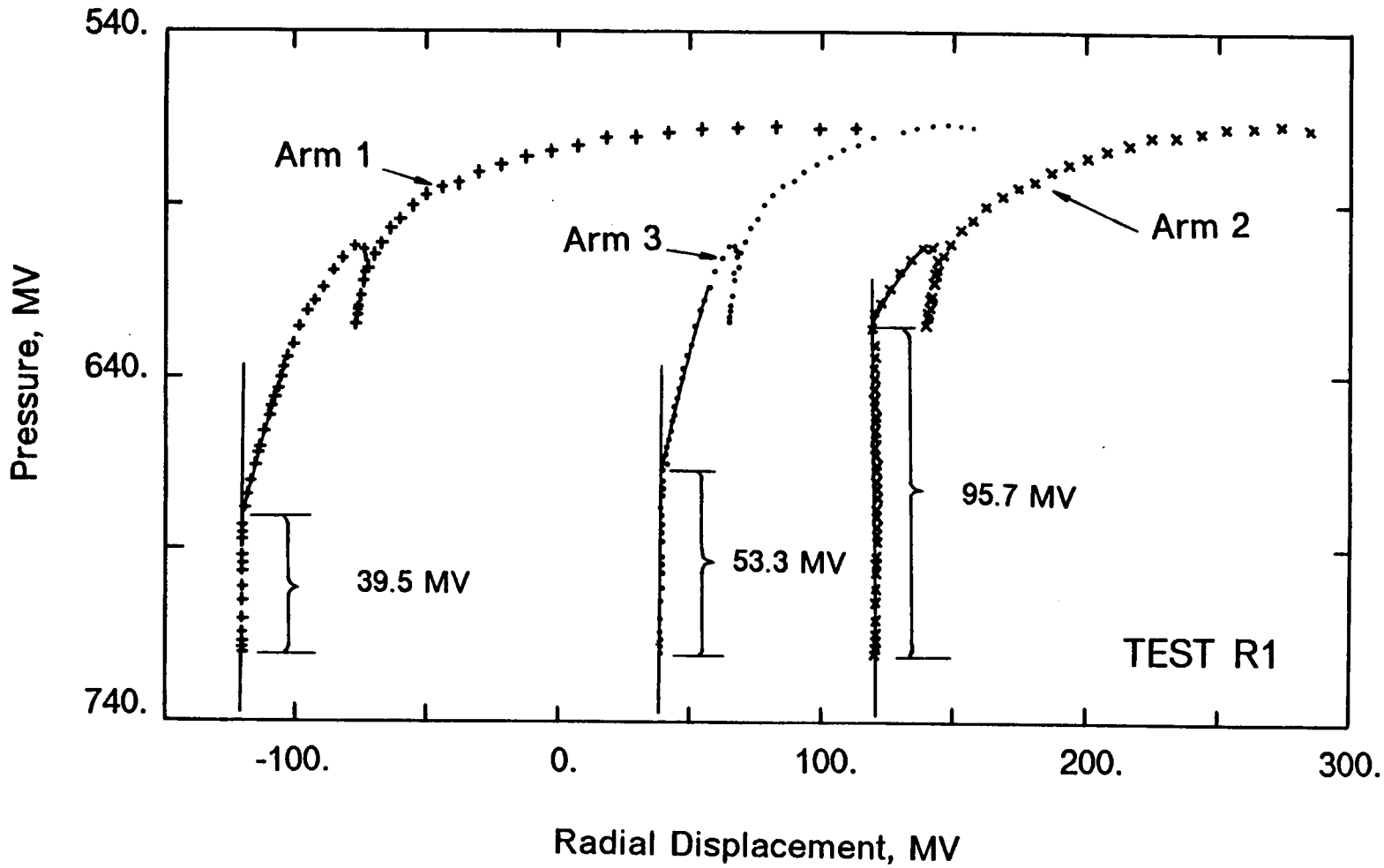

FIGURE 6.4 DETERMINATION OF THE LIFT OFF PRESSURE FROM THE RESULTS OF TEST R1

a malfunction of the equipment. However, it will be remembered that the tests performed in the calibration pressure tank showed that the arms in the pressuremeter lifted off in exact conformance with the stress field in the tank, and that since the stress field in the tank was isotropic, all the arms lifted off at precisely the same time. This was true in tank testing both before and after the field work. Thus, it would appear unlikely that the behavior of the arms in the field tests can be attributed to mechanical malfunction. In support of this conclusion, it can be seen in Appendix E that all of the tests in Richmond showed unequal lift off of the strain arms, and this is not something that occuring in only one test.

In Figs. 6.5 and 6.6, the lateral pressures interpreted from the three strain arms for the six tests in Richmond are plotted versus elevation and depth respectivelly. The elevation plot is made to determine if there is any consistency of lateral stresses with elevation within the Miocene clay deposit. The depth plot is used to determine if the results are more dependent on the amount of overburden above the test location rather than elevation. As can be seen in Fig. 6.6, there is consistency in the results of the tests from the two sites with depth. In study of the lateral stress values in Fig. 6.5 and 6.6, the following trends stand out:

1. The lateral stresses determined by the three strain arms are not the same, and are different by a significant amount.

2. At the Schnabel Center site, where five tests were performed in one hole, and the probe was held in one orientation throughout, the relative positions of the stresses determined from the three arms are consistent. Arm2 always gave the highest stress, followed by the values from Arm3 and Arm1.

3. The lateral stresses determined by any of the arms is higher than the vertical overburden.

Of these findings, the anisotropy in the measured lateral stresses is perhaps the most surprizing. In conventional geotechnical literature, soil deposits are usually assumed to have one value of lateral stress. This reflects the fact that only recently has the equipment been

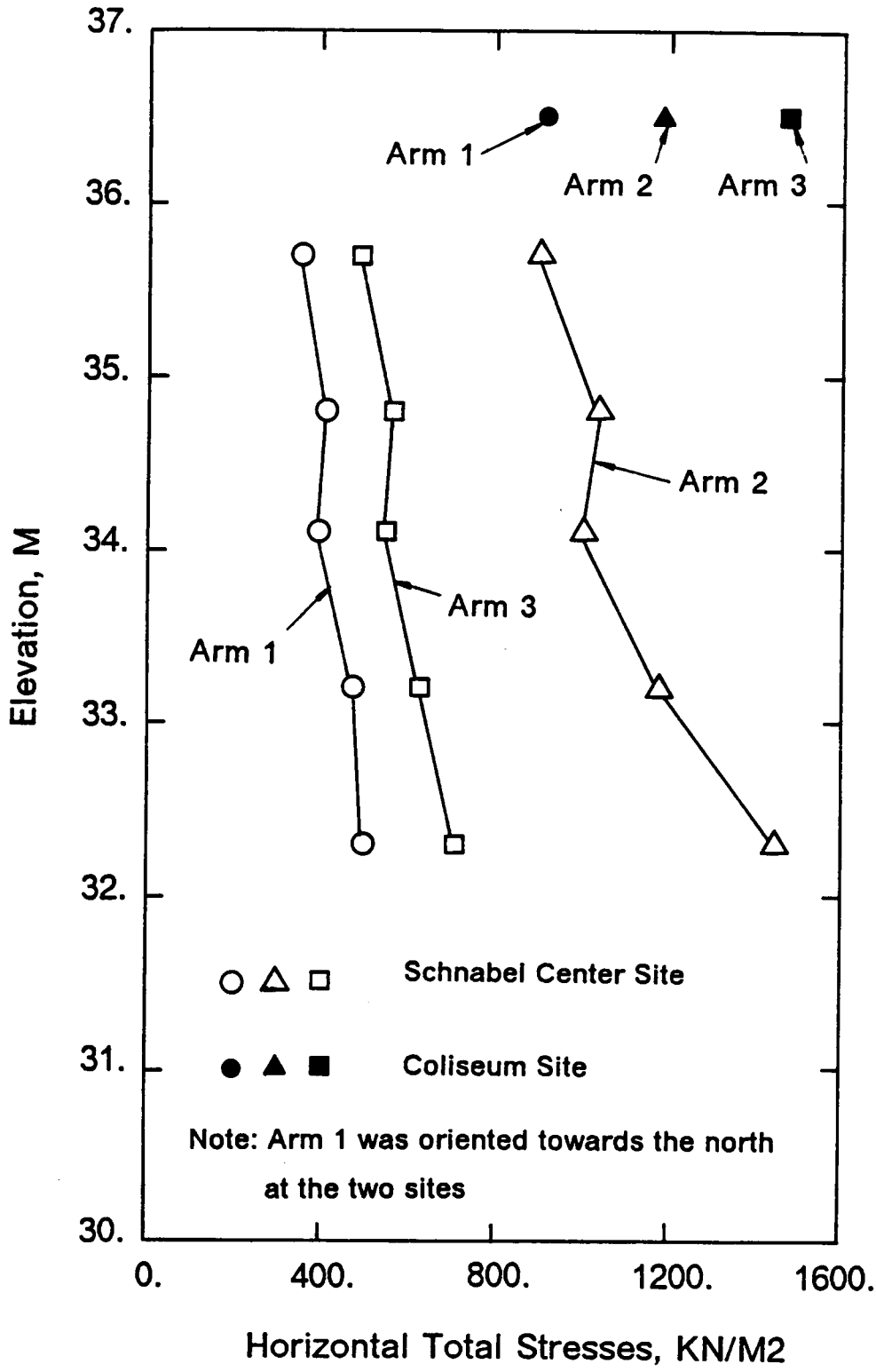

FIGURE 6.5 LATERAL PRESSURES VERSUS ELEVATION

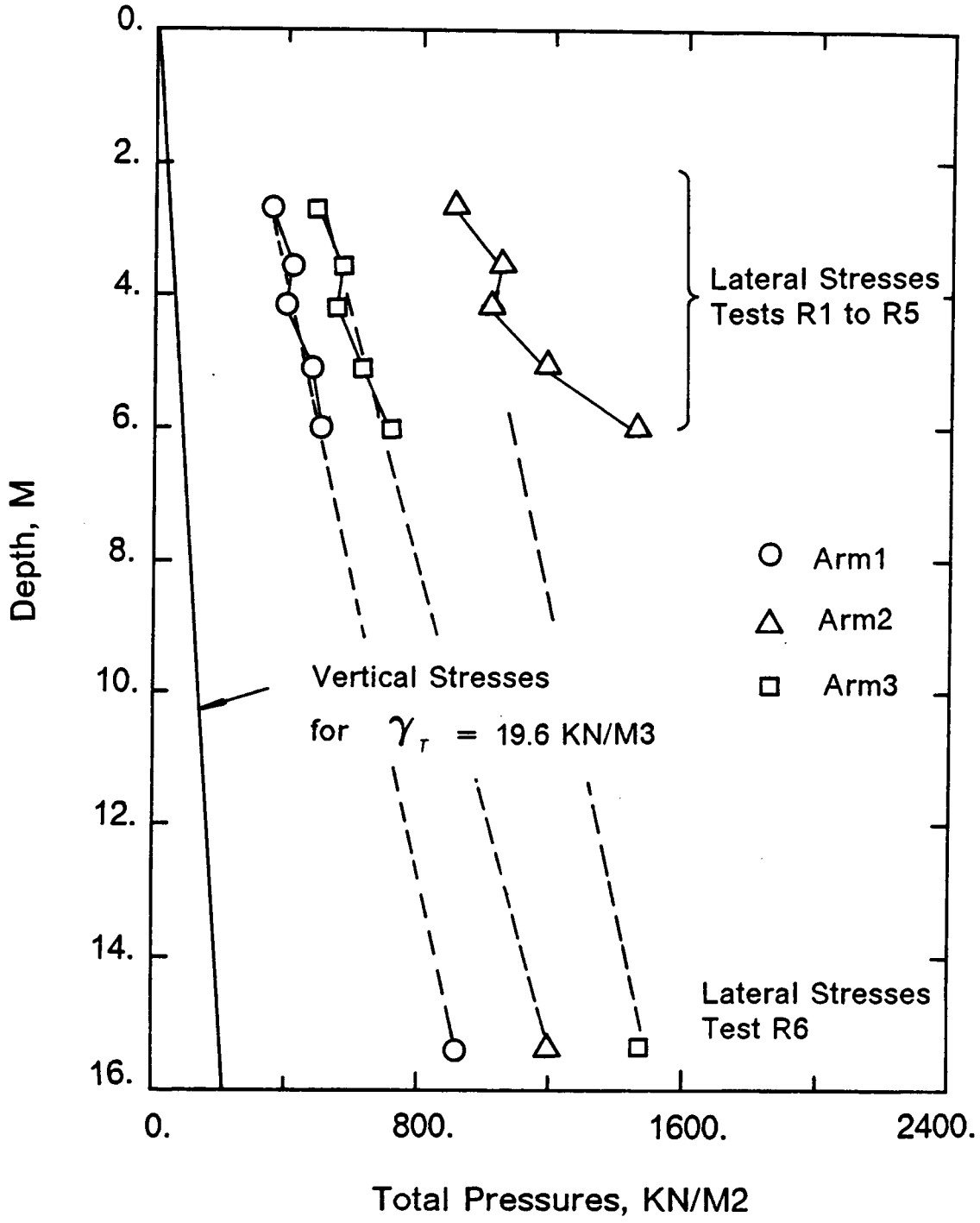

FIGURE 6.6 LATERAL PRESSURES VERSUS DEPTH

available to measure differences that might exist in lateral stresses. However the phenomenon of anisotropy in lateral stresses has been observed by a number of investigators using self-boring pressuremeters equipped like the one for this investigation so that the three strain arms can be monitored independently. Dalton and Hawkins (1982) were the first to identify anisotropic lateral stresses. In their case the tests were carried out in a stiff clay at a site with level ground. In another testing program in stiff clay, Ghionna et al. (1983) also reported differences between the lateral stresses measured by the three arms but in part, they attributed this phenomenon to a malfunction of the equipment. Finally, Benoit and Clough (1985) measured anisotropic stresses in a soft clay deposit. In none of the three cases describing anisotropic stresses, was a clear mechanism available to explain the reason for the condition. This subject is investigated further for the present testing in a subsequent section of this chapter.

6.4.2 Lateral stresses in terms of coefficient of lateral earth pressure

It is common in geotechnical engineering literature to calculate the ratio of the effective lateral pressure to the vertical effective pressure. This is referred to as the coefficient of lateral earth pressure, K_o. In the present case, neither of the Richmond sites evidenced a ground water table, and thus the stresses shown in Fig. 6.6 are both total and effective. The ratio of the lateral stresses to the vertical overburden stresses is the coefficient of lateral earth pressure. In Tab. 6.2, the K_o values for each of the arms for each of the tests are presented. The K_o values tend to decrease with depth, with those in the shallowest tests ranging from 7.4 to 18.6. The test performed at the depth of 15 M (50.4 ft) at the Coliseum site gave K_o values from 3.0 to 4.9.

The finding that the lateral stresses are higher than the vertical stresses in the Richmond clay (and hence, K_o greater than one), is not surprizing. Such conditions are commonly associated with stiff clays, and are usually explained in terms of the fact that the soils are

TABLE 6.2 EFFECTIVE STRESSES

Test	Horizontal Effective Stress, KN/M2 (psi) σ_h'			Vertical Effective Stress, KN/M2 (psi) σ_v'	Ko = $\frac{\sigma_h'}{\sigma_v'}$		
	Arm1	Arm2	Arm3		Arm1	Arm2	Arm3
R1	353 (51.2)	891 (129.1)	484 (70.1)	48 (7.0)	7.4	18.6	10.1
R2	413 (59.9)	1034 (149.9)	565 (81.9)	62 (9.0)	6.7	16.7	9.1
R3	390 (56.5)	997 (144.5)	542 (78.6)	74 (10.7)	5.3	13.5	7.3
R4	472 (68.4)	1176 (170.4)	624 (90.4)	90 (13.0)	5.2	13.1	6.9
R5	498 (72.2)	1443 (209.1)	705 (102.2)	106 (15.4)	4.7	13.6	6.7
R6	915 (132.6)	1184 (171.6)	1467 (212.6)	302 (43.8)	3.0	3.9	4.9

overconsolidated. An overconsolidated clay has undergone a vertical stress relief during its existence, and while this is accompanied by a lateral stress relief, the lateral stresses are reduced at a slower rate. Under a suitable amount of stress relief, the lateral stresses can become larger than the vertical stresses. Experiments to quantify the degree of this effect have often been done in the controlled laboratory environment. Brooker and Ireland (1965) published what is probably the definitive work in this vein. Notably, the soils they worked with were consolidated from slurries, and were subjected to only one simple cycle of unloading. Their data would suggest that for a soil such as the Richmond clay with an OCR of 5, the K_o should be 1.2, a value considerably less than that from the pressuremeter tests.

Other self-boring pressuremeter tests in stiff clay deposits have shown K_o values which are higher than those of Brooker and Ireland (1965). Most of the tests were done with first generation pressuremeter equipment which was capable of only determining the average lift-off pressure for the three measuring arms. Windle and Wroth (1977) report K_o values in stiff Gault and London clays on the order of 3. Also, Denby et al. (1981) give a K_o of 2 for Seattle clay, and Ghionna et al. (1983) determined values between 1.5 and 3 for Taranto clay. These soils have OCR values comparable to that for the Miocene clay and were tested at similar depth ranges to those of this program of study.

While other investigations show high K_o values in stiff clays, none of them have yielded values as high as those in this program. The reason for this is not entirely clear, and further study and testing is advisable before firm conclusions are drawn. However, it is possible to suggest a mechanism for the finding based only on the present results. In comparison to other self-boring pressuremeter testing programs in stiff clays, the Richmond clay is unique. All of the other clay deposits are characteristically shot through by fissures. This is an indication that the clay deposit has been unloaded to the point that the lateral stresses are large enough to cause passive failure in the soil. As the failure takes place, and the fissures are formed, it seems logical to expect that some degree of lateral stress relief occurs. Thus, the measured K_o value would be lowered from that which may have existed at one time.

The Richmond clay differs from the others in that the unloading process has not caused fissures to form in it. This suggests that a higher level of lateral stress is locked into this deposit. Evidence for this is obtained through the fact that the Richmond clay is often seen to disc after removal from a sample tube. Discing is common in rock core taken in areas of high lateral stresses, but it is not common in soils. Contacts with collegues[1] who have worked in the very stiff clays of Seattle have stated that discing is not observed in this case. Future research into the Richmond clay is certainly deserved, but in terms of present results, it would appear that the measured lateral stresses have a rational basis.

6.4.3 Further consideration of the anisotropy of measured lateral stresses

It is useful to probe the reasons that might exist for the anisotropy observed in the measured lateral stresses. To do this the concept of the ellipsoid of stress is introduced. Dalton and Hawkins (1982) were able to derive expressions to compute the magnitude and the orientation of the principal lateral pressures from the Mohr circle passing through the three points corresponding to the lateral pressures measured by the three arms.

The following slightly different method is proposed as it gives a closed form solution to determine the lateral pressure in any direction from the magnitude and orientation of the principal lateral pressures. The idea comes from the fact that when a plane is rotated around any point in a continuum subjected to stresses in three dimensions, the component of stress normal to the plane describes an ellipsoid which has the principal stresses for principal axis. If the state of stress is isotropic, the ellipsoid degenerates in a sphere. A detailed demonstration of this statement can be found in "Theory of Elasticity" by Timoshenko and Goodier (1970). Furthermore, if the vertical stress is a principal stress, the two other principal stresses

---

[1] Professor G. W. Clough, Dr G. M. Denby

are the principal axes of the ellipse which lies in the horizontal plane. This ellipse is shown in Fig. 6.7. It is entirely determined from the lateral pressures measured by the three arms. The figure gives the steps to follow in order to determine σ_1 and σ_2, the major and minor principal lateral pressures and α, the angle between the major principal axis and x, an arbitrary axis chosen parallel to the measuring direction of Arm1.

At the Coliseum site, the vertical stress is a principal stress as the soil is level around the site. The two other principal stresses must lie in the horizontal plane and can be determined according to the method given in Fig. 6.7.

The results of a parametric study of cuts in stiff clays made by Duncan and Dunlop (1969) with the finite element technique are used to assess the influence of the slope at the Schnabel Center site on the orientation of the principal stresses at the location of the tests R1 to R5. The case of the parametric study which approximatively simulates the conditions encountered at the site is shown in Fig. 6.8. It consists in a 1.5:1 cut in a clay characterized by a total stress pressure coefficient K equal to 1.6. Before the cut, the major principal stress is horizontal and the minor one is vertical. The orientation of the principal stresses in the soil mass after the cut is illustrated in Fig. 6.8 by crosses, the longer segment of the cross representing the major principal stress and the shorter representing the minor one. The results shown in Fig. 6.8 indicate that the rotation of the principal stresses due to the cut is limited in depth to the height of the cut, H and laterally, to the toe of the cut. Consequently, it is reasonable to consider that the principal stresses are vertical and horizontal at the location of the tests R1 to R5 which is situated at a distance 1.8H from the toe of the slope.

The approach given in Fig. 6.7 was used to interpret the data of the tests R1 to R6. The results of the interpretation are summarized in Tab. 6.3 and a profile of the principal stresses is given in Fig. 6.9. The interpretation indicates that the magnitude of the principal lateral pressures increases with depth at t he Schnabel Center site with values varying from 1287 to 1679 KN/M2 (186.5 to 243 psi) for σ_1 and from 344 to 486 KN/M2 (49.9 to 70.4 psi) for σ_2 but that the ratio of σ_1 by σ_2 is nearly constant for the five tests with values varying between 3.4 and

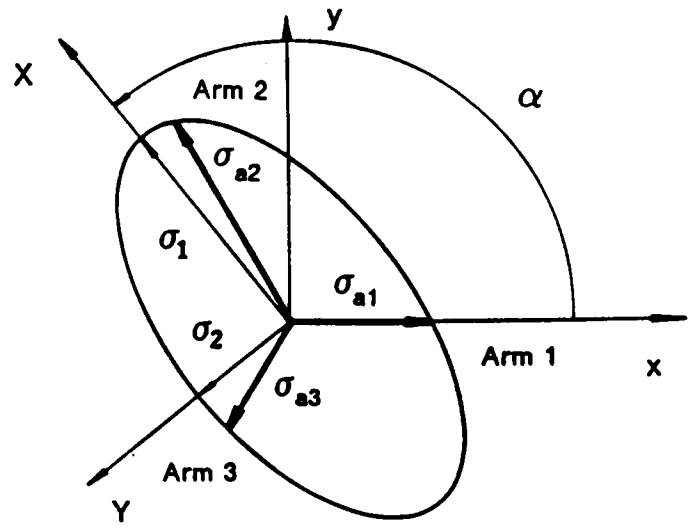

(x,y) coordinate system with x chosen arbitratily parallel to Arm 1.
(X,Y) coordinate system with X and Y respectively parallel to σ_1 and σ_2 , the major and the minor principal total lateral soil pressures in the horizontal plane.
Equation of the ellipse in the (X,Y) coordinate system

$$\frac{X^2}{\sigma_1^2} + \frac{Y^2}{\sigma_2^2} = 1$$

Equation of the ellipse in the (x,y) coordinate system

$$x^2\left(\frac{\cos^2\alpha}{\sigma_1^2} + \frac{\sin^2\alpha}{\sigma_2^2}\right) + y^2\left(\frac{\sin^2\alpha}{\sigma_1^2} + \frac{\cos^2\alpha}{\sigma_2^2}\right) + 2xy\cos\alpha \sin\alpha\left(\frac{1}{\sigma_1^2} - \frac{1}{\sigma_2^2}\right) = 1$$

or

$$Ax^2 + By^2 + Cxy = 1$$

$$\begin{bmatrix} x_1^2 & y_1^2 & x_1y_1 \\ x_2^2 & y_2^2 & x_2y_2 \\ x_3^2 & y_3^2 & x_3y_3 \end{bmatrix} \begin{Bmatrix} A \\ B \\ C \end{Bmatrix} = \begin{Bmatrix} 1 \\ 1 \\ 1 \end{Bmatrix}$$

where (x_1, y_1), (x_2, y_2) and (x_3, y_3) are the coordinates of the total lateral pressures measured by Arm 1, Arm 2 and Arm 3 respectively.

Solve for A, B and C

Then, solve for α, σ_1 and σ_2 with:

$$\tan 2\alpha = \frac{C}{A - B}$$

$$\frac{1}{\sigma_2^2} = A\cos^2\alpha + C\sin\alpha\cos\alpha + B\sin^2\alpha$$

$$\frac{1}{\sigma_1^2} = A\sin^2\alpha - C\sin\alpha\cos\alpha + B\cos^2\alpha$$

FIGURE 6.7 DETERMINATION OF THE ELLIPSE OF TOTAL LATERAL PRESSURES

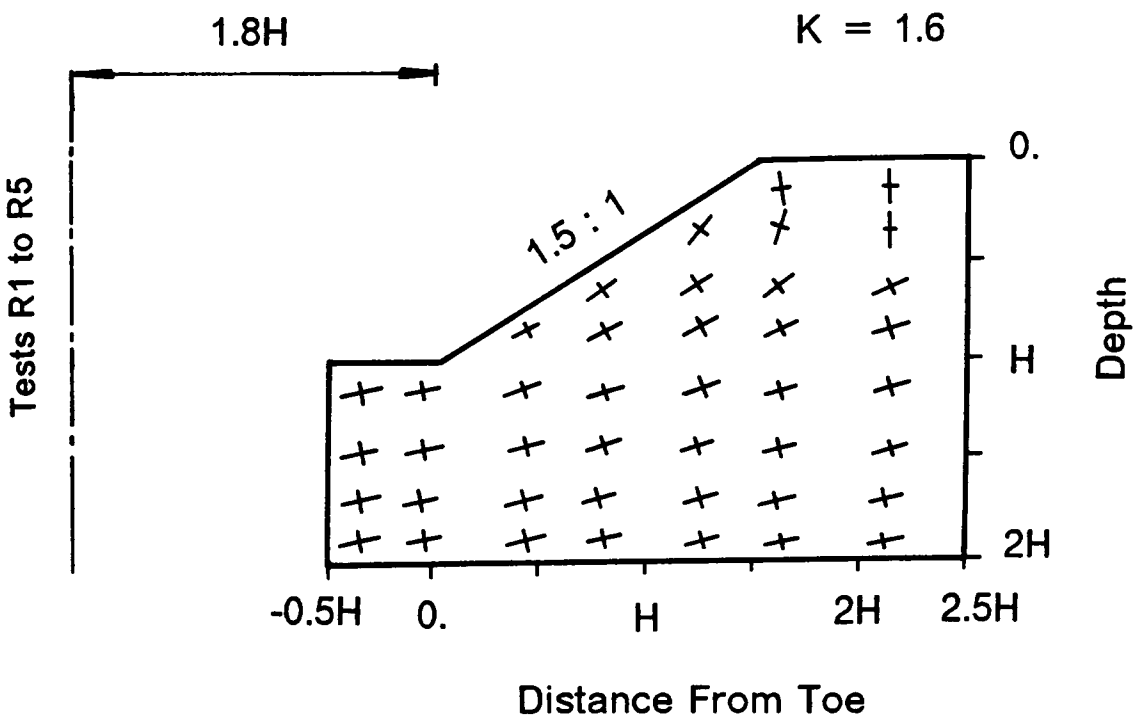

FIGURE 6.8 PRINCIPAL STRESS ORIENTATION IN CUTS IN STIFF CLAYS (AFTER DUNCAN AND DUNLOP, 1969)

TABLE 6.3 LATERAL PRINCIPAL STRESSES INTERPRETED FROM THE TEST RESULTS

Test	Site	σ_1 KN/M2 (psi)	σ_2 KN/M2 (psi)	$\frac{\sigma_1}{\sigma_2}$	α degrees
R1	Schnabel C.	1287 (186.5)	344 (49.9)	3.74	77
R2	Schnabel C.	1475 (213.8)	403 (58.4)	3.66	77
R3	Schnabel C.	1514 (219.4)	381 (55.2)	3.97	77
R4	Schnabel C.	1545 (223.9)	458 (66.4)	3.37	75
R5	Schnabel C.	1679 (243.3)	486 (70.4)	3.45	77
R6	Coliseum	1661 (240.7)	906 (131.3)	1.83	100

Note:

σ_1 the major principal stress in the lateral plane.

σ_2 the minor principal stress in the lateral plane.

α the angle between σ_1 and Arm1.

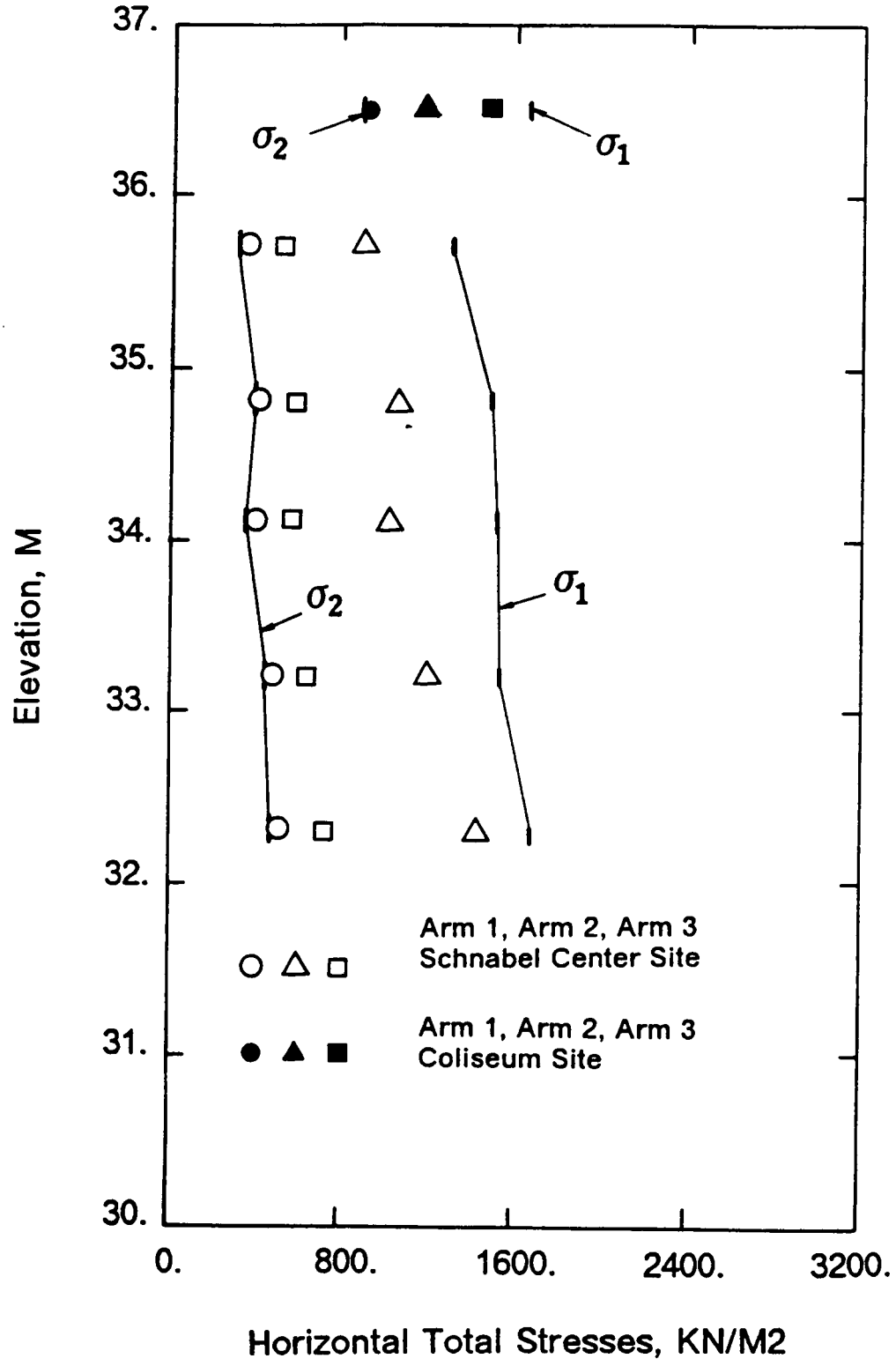

FIGURE 6.9 PROFILE OF THE PRINCIPAL LATERAL PRESSURES

4. The major and minor principal lateral pressures interpreted from the results of the test R6 are respectively 1661 KN/M2 (240.7 psi) and 906 KN/M2 (131.3 psi) and their ratio is 1.8.

The interpretation of the test results indicate that the major lateral stress at the Schnabel Center site has an orientation with the north which varies between 75 and 77 degrees for the tests R1 to R5. At the Coliseum site, the angle between the major principal lateral pressure and the north is 100 degrees. A close up of the Schnabel Center site with the orientation of the principal lateral pressures is shown at the bottom of Fig. 6.10. There is no correlation of the principal stress and the local slope at this site. As expected from the Duncan and Dunlop report, the tests were performed at enough distance not to be influenced by the slope.

At the top of the same figure, the orientation of the principal lateral pressures at the two sites are indicated on a regional topographic map of downtown Richmond. The regional map showes that the minor principal lateral pressures are oriented towards the James River at the two sites. This suggests that the high lateral stresses built up in the Miocene clay by pre-consolidation were released in the direction perpendicular to the bed of the river when the river cut through the different formations. The major principal lateral pressure is parallel to the river bed as the confinement of the soil remains the largest in that direction. Thus, the topography of the region can be readily used to explain the stress anisotropy.

6.5 UNDRAINED SHEAR STRENGTH

Two methods are used to interpret the undrained shear strength of the soil from the SBPM test results. The first one was proposed by Gibson and Anderson (1961). The second was developed simultaneously by different groups of workers: Baguelin et al. (1972), Ladanyi (1973) and Palmer (1972). The two methods assume that σ_r is the major principal stress and the minor principal stress during the expansion test. This stress condition leads to a failure

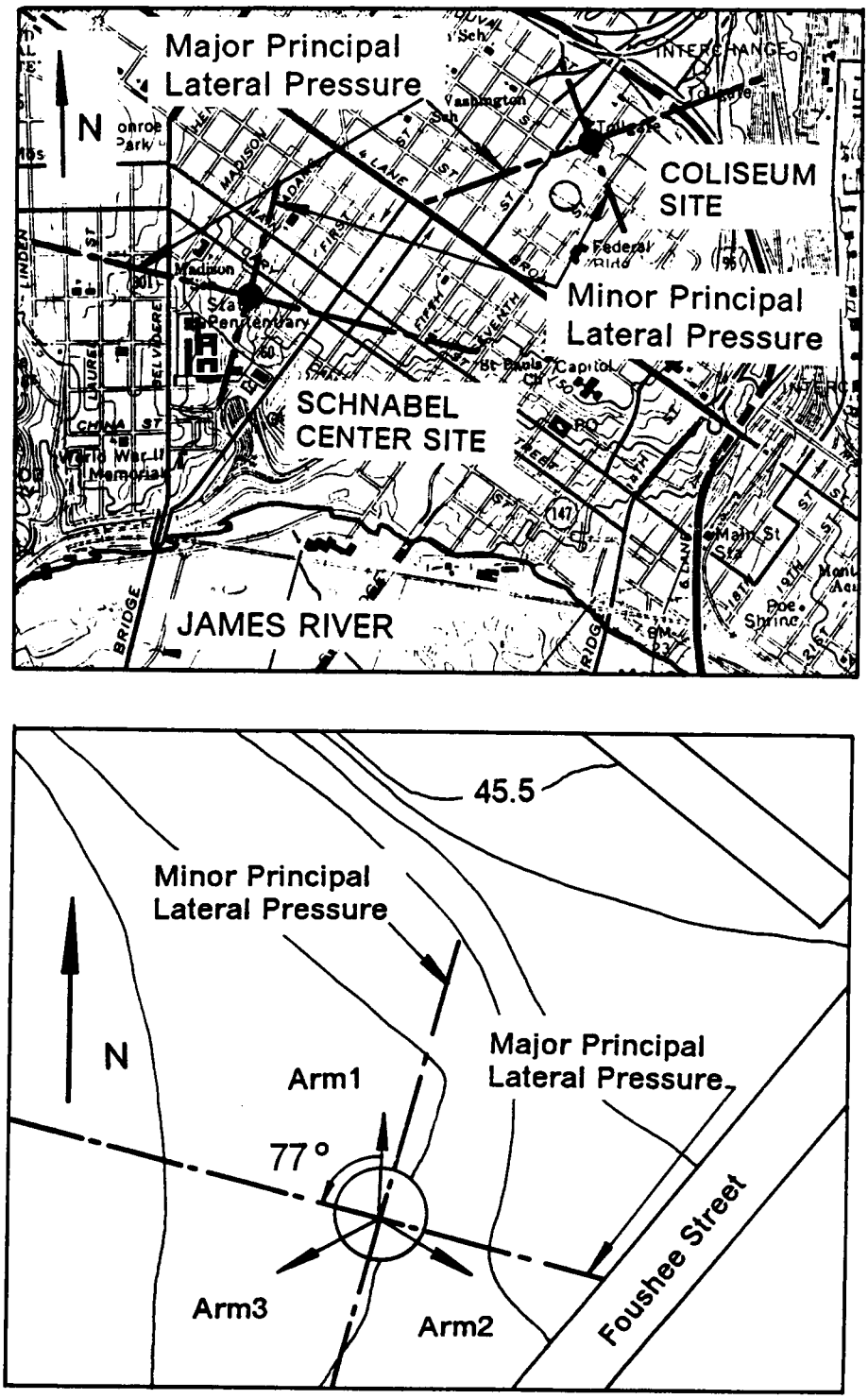

FIGURE 6.10 ORIENTATION OF THE PRINCIPAL LATERAL PRESSURES

in vertical planes which radiate outwards from the contact soil-probe with an angle of $\frac{\pi}{4} + \frac{\Phi}{2}$ with the tangent to the edge of the probe.

6.5.1 The Gibson Anderson interpretation

The Gibson Anderson interpretation considers the soil as an elastic perfectly plastic material characterized by an undrained Young's modulus, a Poisson ratio and an undrained shear strength su. The basic assumption of a perfectly plastic material leads generally to the determination of an average undrained shear strength for the soil which exhibit a stress softening behavior during shear. From the experience he gained in a large number of sites, Wroth (1982) considers the Gibson Anderson analysis as entirely satisfactory for design purposes in geotechnical engineering since it leads to conservative results.

Applying the cavity expansion theory to an elastic perfectly plastic material with the hypothesis that radial plane strain prevails and that no volume change occurs leads to the expression:

$$p = p_L + s_u \ln(\frac{\Delta V}{V} - 3(1 - \Delta V/V)\frac{\sigma_H}{E})$$

with

p	the pressure in the cavity
p_L	the limit pressure, pressure corresponding to an infinite expansion
s_u	the undrained shear strength of the soil
σ_H	the total lateral pressure of in the soil

E — the Young's modulus of the soil

$\Delta V = V - Vo$ — where Vo is the initial volume of the cavity and V the current volume corresponding to p.

If $\frac{\sigma_H}{E}$ is small in comparison to $\frac{\Delta V}{V}$, the expression of p has a nearly linear portion when represented in a semi-log diagram with p expressed in an arithmetic scale and $\frac{\Delta V}{V}$ expressed in a natural log scale. As an example, the results of the test R 5 are represented in such a manner in Fig. 6.11. They indicate a nearly linear portion of the curve for volumetric strains $\frac{\Delta V}{V}$ varying between 10^{-2} and 10^{-1}. The undrained shear strength of the clay can be determined from the expression:

$$s_u = \frac{p_2 - p_1}{\ln \dfrac{\varepsilon_{v2} - 3(1 - \varepsilon_{v2})\dfrac{\sigma_H}{E}}{\varepsilon_{v1} - 3(1 - \varepsilon_{v1})\dfrac{\sigma_H}{E}}}$$

where $(p_1, \varepsilon_{v1} = \frac{\Delta V1}{V1})$ and $(p_2, \varepsilon_{v2} = \frac{\Delta V2}{V2})$ are coordinates of two points chosen on the linear part of the curve. In this particular case, the calculated undrained shear strength is equal to 394, 299 and 315 KN/M2 (57.1, 43.3 and 45.7 psi) for Arm1, Arm2 and Arm3 respectively.

6.5.2 The Baguelin, Ladanyi and Palmer interpretation

The interpretations developed by Baguelin et al. (1972), Ladanyi (1973) and Palmer (1972) lead to the same expression for the derivation of the stress strain curve from the pressuremeter curve. The analyses are restricted to saturated soils which deform under undrained and radial plane strain conditions, symmetrically about the pressuremeter axis. In

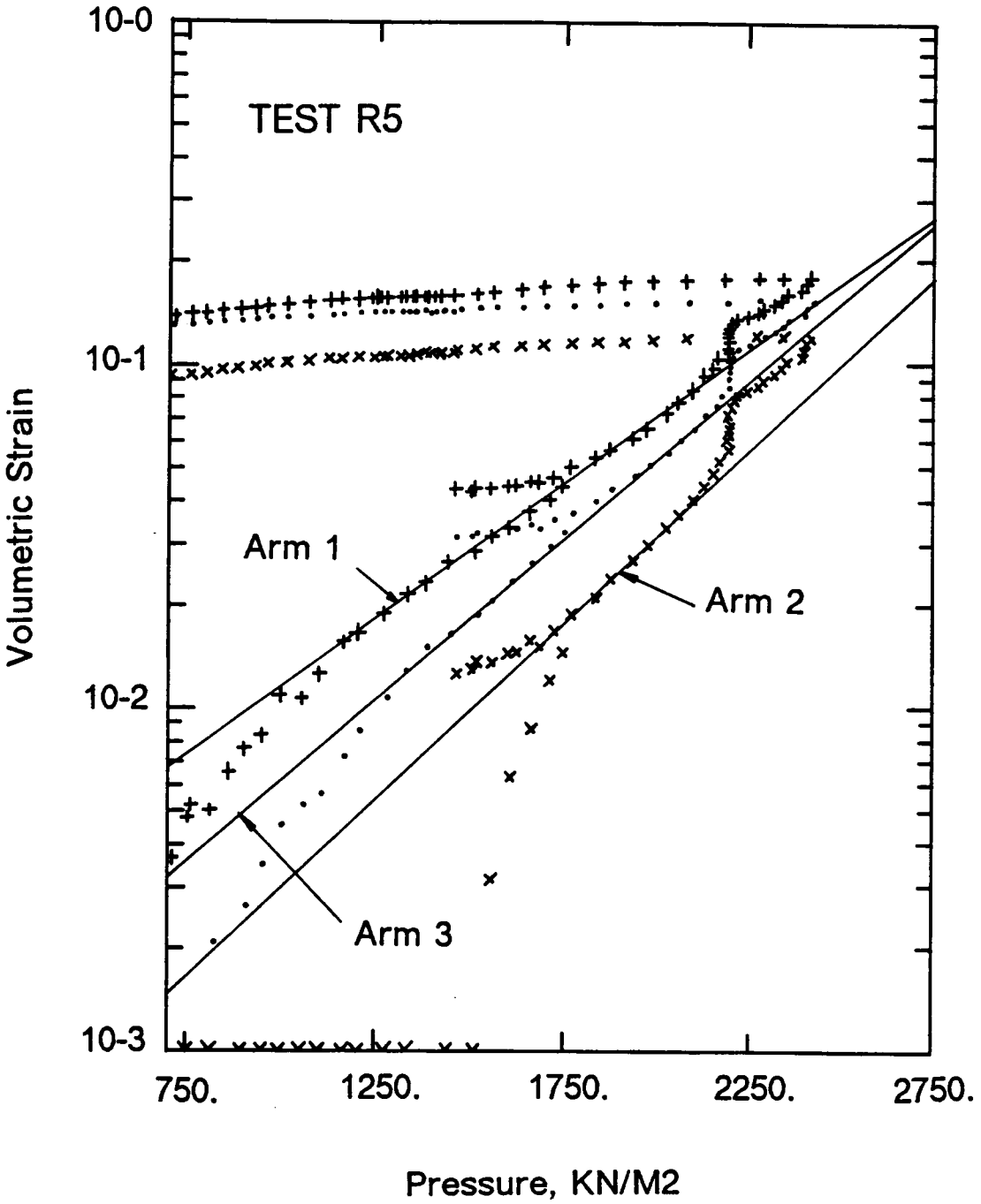

FIGURE 6.11 INTERPRETATION ACCORDING TO GIBSON ANDERSON

contrast to the Gibson Anderson interpretation, no assumption is made on the shape of the stress strain curve. The theoretical development leads to the final equation:

$$\Phi(\varepsilon_r) = \sigma_r - \sigma_\theta = \varepsilon_r(1 + \varepsilon_r)(2 + \varepsilon_r)\Psi'(\varepsilon_r)$$

with

σ_r the radial total stress

σ_θ the total tangential stress

ε_r the radial strain

$\Psi'(\varepsilon_r)$ the slope of the pressuremeter curve

For small strains, the equation can be approximated by

$$\frac{\sigma_r - \sigma_\theta}{2} = \varepsilon_r\Psi'(\varepsilon_r)$$

Details on the development which leads to these expressions are found in the original publications.

As an example, the undrained shear strength interpreted from the pressuremeter curve monitored by Arm1 of the test R6 is given in Fig. 6.12. A computer program which uses a spline fitting through the data points was written and the undrained shear strength was evaluated on the spline every 0.05% increments of the radial strain. The shape of the undrained shear shown at the bottom of the figure is characteristic of most of the interpretations performed on the results of the tests R1 to R6. In this case, it indicates a peak value of strength of 450 KN/M2 (65 psi) at 1% radial strain.

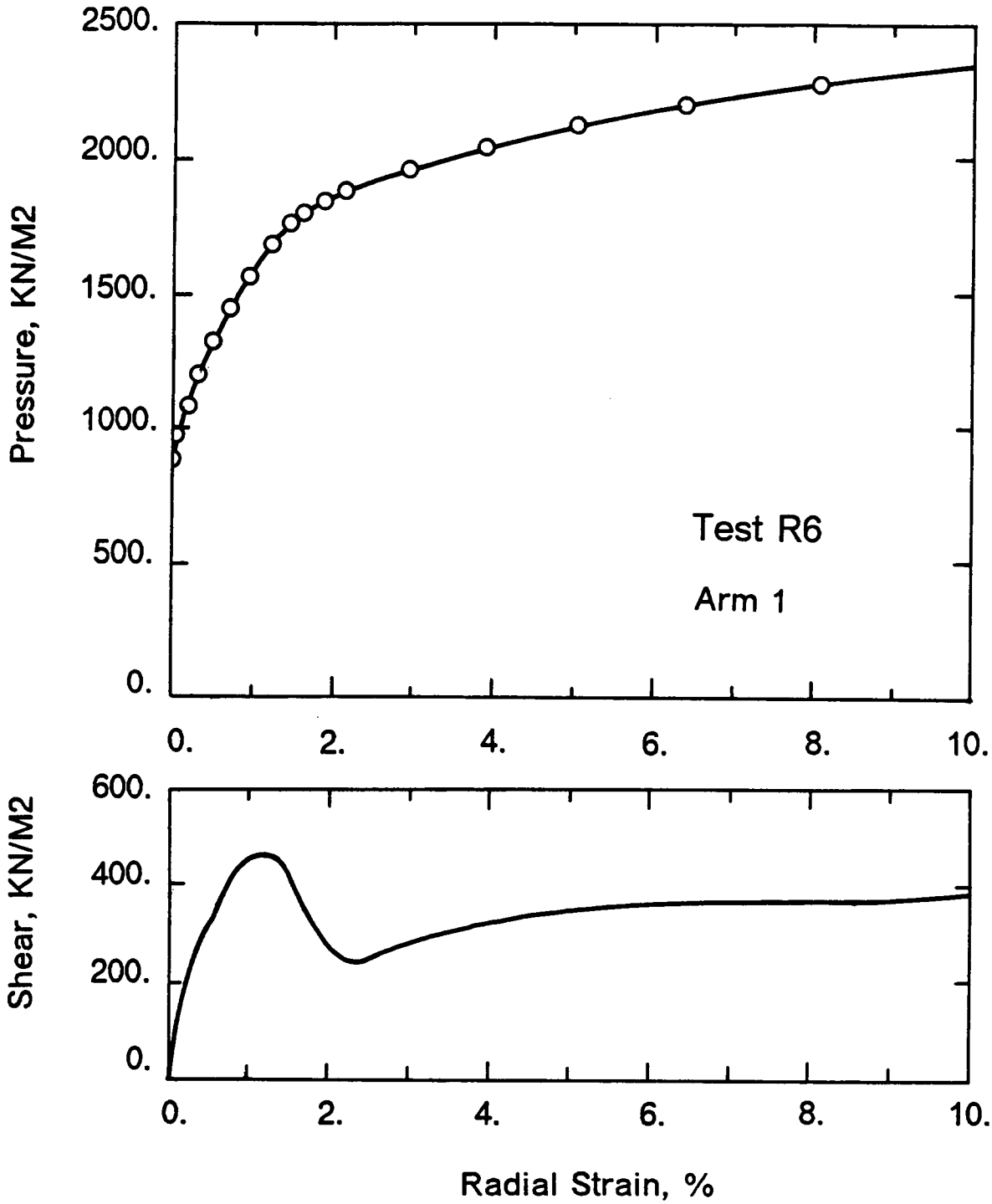

FIGURE 6.12 INTERPRETATION ACCORDING TO BAGUELIN LADANYI AND PALMER

6.6 UNDRAINED SHEAR STRENGTH VALUES

6.6.1 Gibson Anderson Interpretation

The undrained shear strength profile using the Gibson Anderson interpretation is plotted against the elevation in Fig. 6.13 for the tests R1 to R6. Typical values show a slight but steady increase as the elevation decreases from 200 KN/M2 (29 psi) at El. 36.5 to 300 KN/M2 (43.5 psi) at El. 32.3. The interpreted values for a given test are generally identical for the three arms or they fall in a narrow range except for the tests R4 and R5 for which the ratio between the largest and the smallest value is 1.5.

6.6.2 Baguelin, Ladanyi and Palmer interpretation

The undrained shear strength profile using the Baguelin, Ladanyi and Palmer interpretation is plotted against elevation and depth in Fig. 6.14 and 6.15 respectively for the tests R1 to R6. The following remarks can be drawn from these profiles:

1. There is a consistent difference between the magnitude of the undrained shear strength values interpreted from the pressuremeter curves monitored by Arm1, Arm2 and Arm3 in the tests R1 to R5. Arm1 indicates the highest undrained shear strength among the three arms with values varying between 366 and 560 KN/M2 (53 and 81 psi) from El. 35.8 to El. 32.2. Arm2 gives the lowest undrained shear strength values among the three arms with values varying between 110 and 421 KN/M2 (16 and 61 psi) from El. 35.8 to El. 32.2.

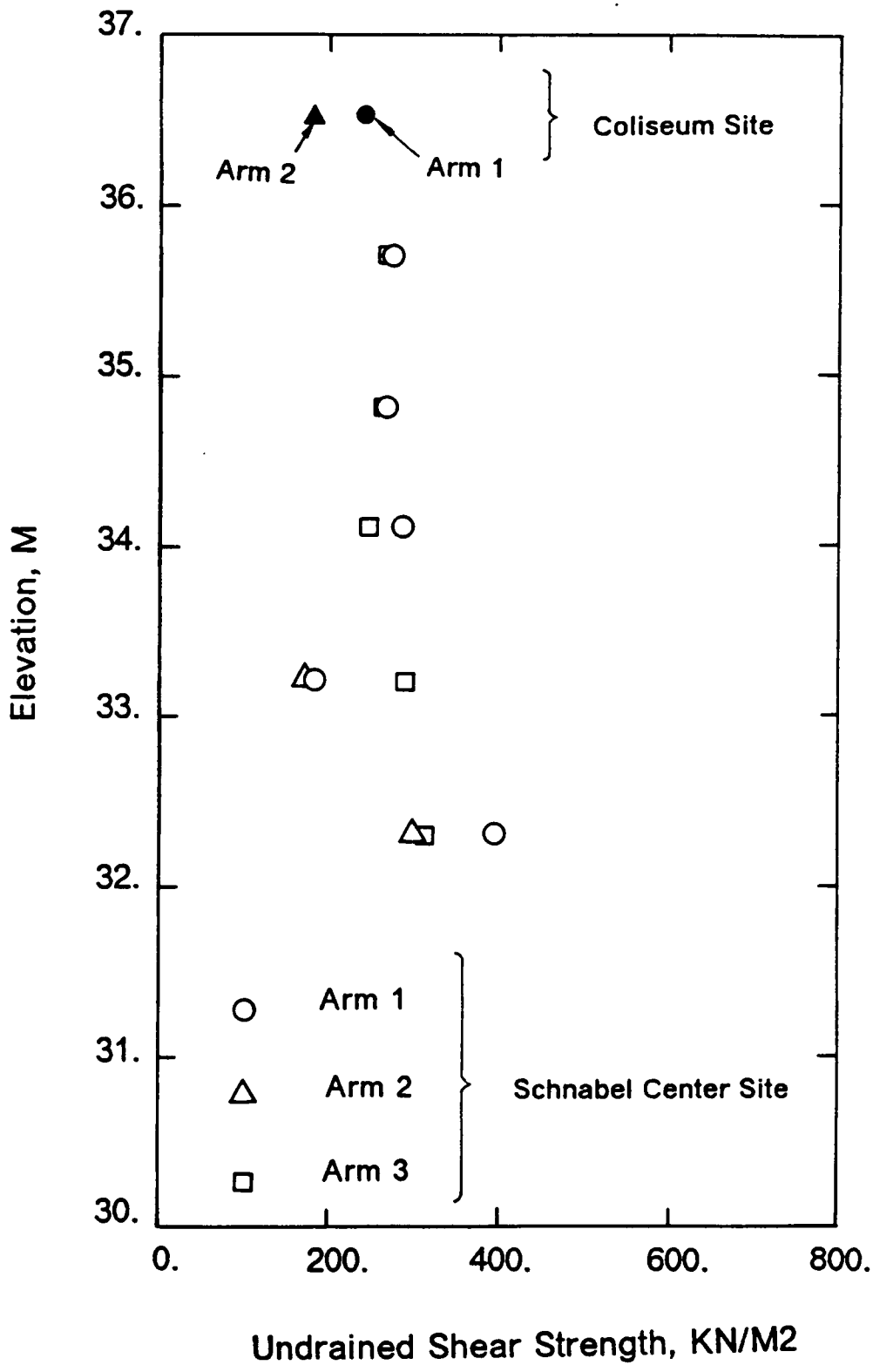

FIGURE 6.13 UNDRAINED SHEAR STRENGTH VALUES WITH ELEVATION FROM THE GIBSON ANDERSON INTERPRETATION

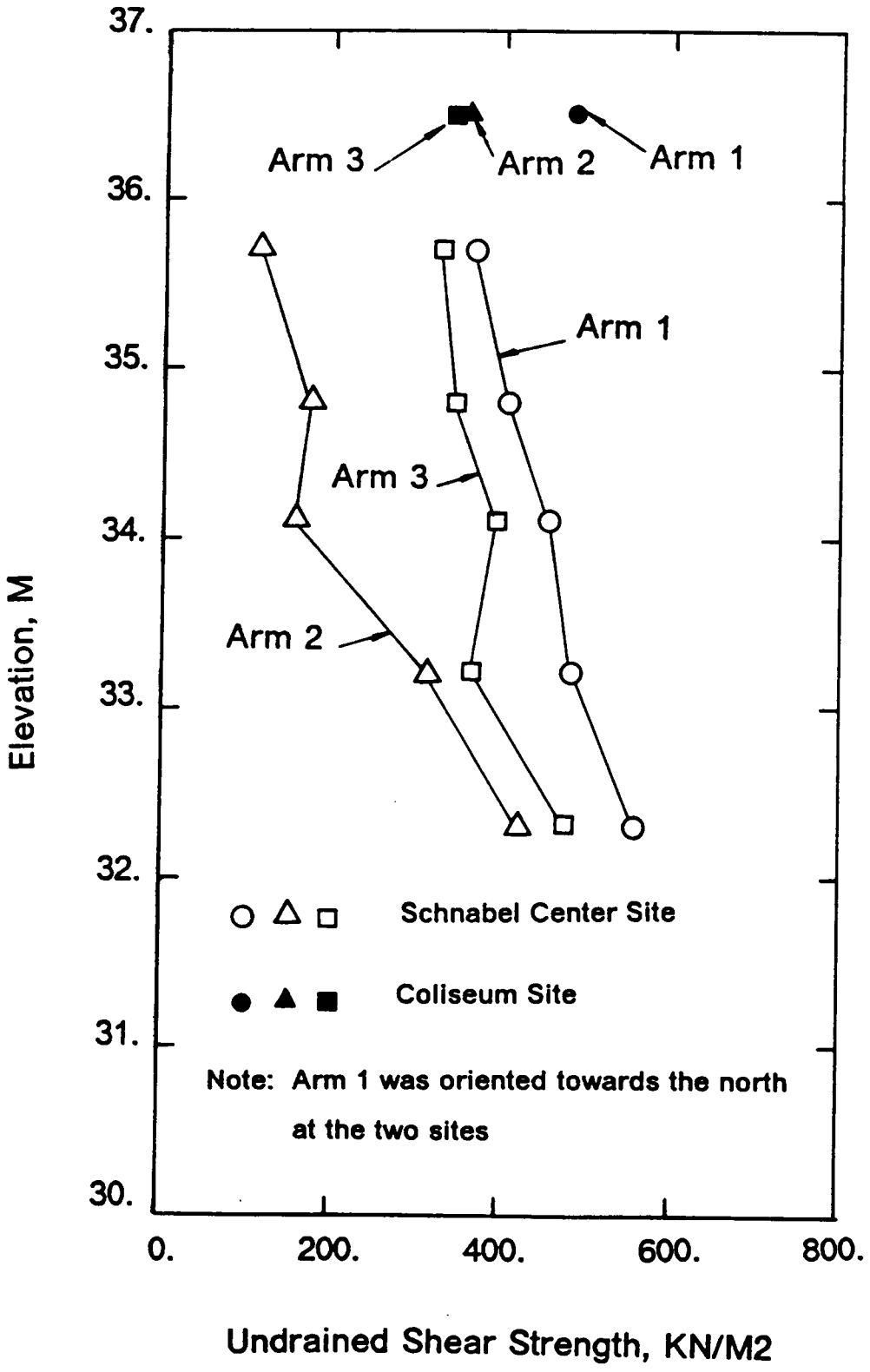

FIGURE 6.14 UNDRAINED SHEAR STRENGTH VALUES WITH ELEVATION FROM THE BAGUELIN, LADANYI AND PALMER INTERPRETATION

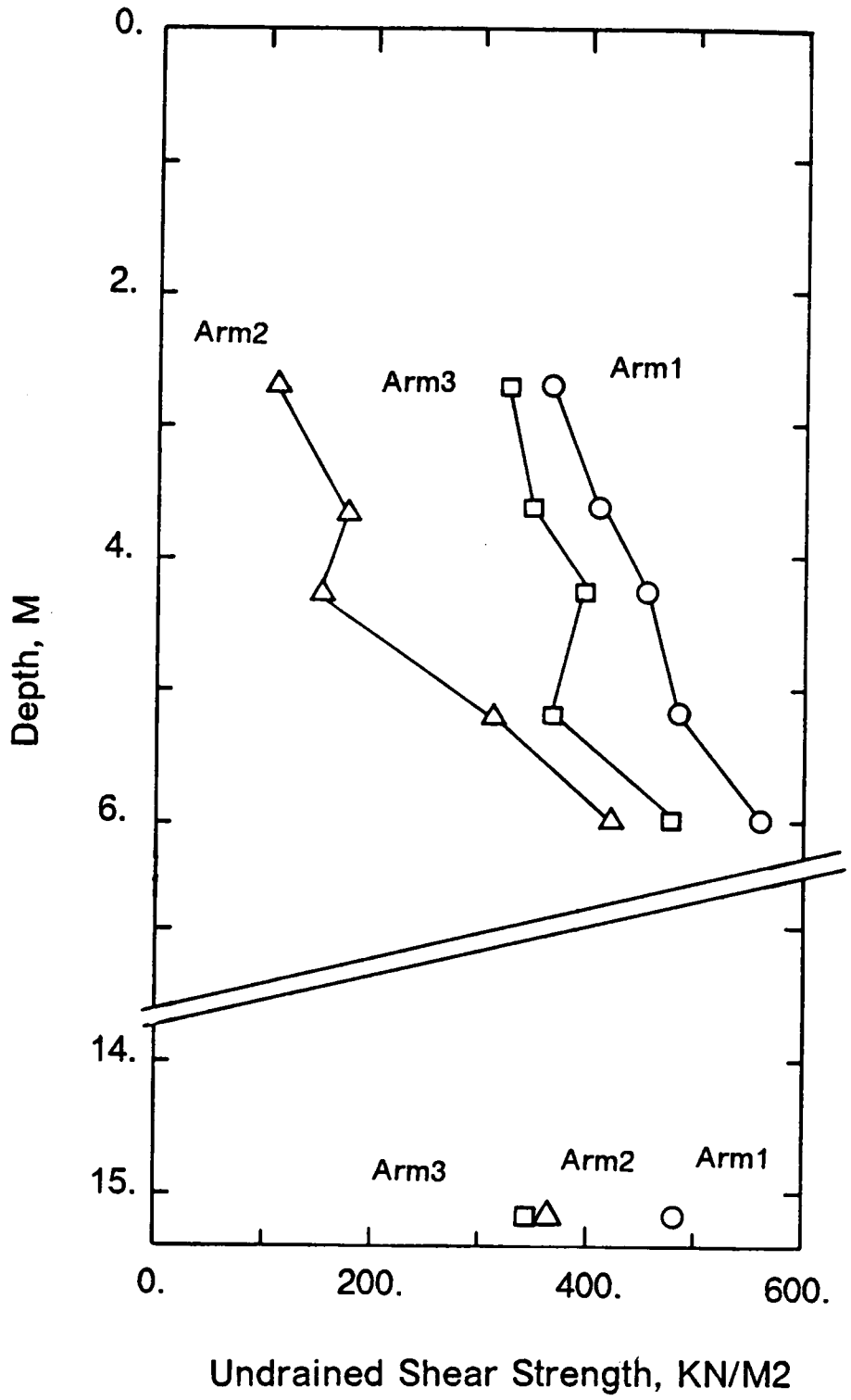

FIGURE 6.15 UNDRAINED SHEAR STRENGTH VALUES WITH DEPTH FROM THE BAGUELIN, LADANYI AND PALMER INTERPRETATION

2. When plotted against depth, the test R6 gives undrained shear strength values varying between 345 KN/M2 (50 psi) for Arm3 and 483 KN/M2 (70 psi) for Arm3 which follow the same trend as the values given by the tests R1 to R5.

3. Arm1 which measures consistently the lowest lateral pressures in the tests R1 to R6 gives systematically the highest interpreted undrained shear strength values. Similarily, Arm2 which measures the largest lateral pressures for the tests R1 to R5 gives the lowest interpreted undrained shear strength values of the three arms. The preceeding observation suggests that the undrained shear strength mobilized when expansion occurs in the direction of the largest lateral pressure is smaller than than the undrained shear strength mobilized when expansion occurs in the direction of the lowest lateral pressure. To avoid introducing specific studies at that stage of the analysis of the results, the interpretation of the relationship between the lateral pressures and the undrained shear strength is presented later in this chapter.

The low undrained shear strength values interpreted from Arm2 in the tests R1 to R3 situated between El. 36 and El. 34 suggest that the passive failure mentioned previously in the analysis of the lateral stresses has effectively occured and that the undrained shear strength values interpreted from Arm2 of these tests are post peak values.

6.6.3 Comparison between the different interpretations

The results of the two interpretations are plotted against depth in Fig. 6.16. Except for the test R1 for which the two interpretations give similar average undrained shear strength values, the values given by the Gibson Anderson (GA) interpretation are systematically lower than the values given by the Baguelin, Ladanyi and Palmer (BLP) interpretation . Typically, the ratio

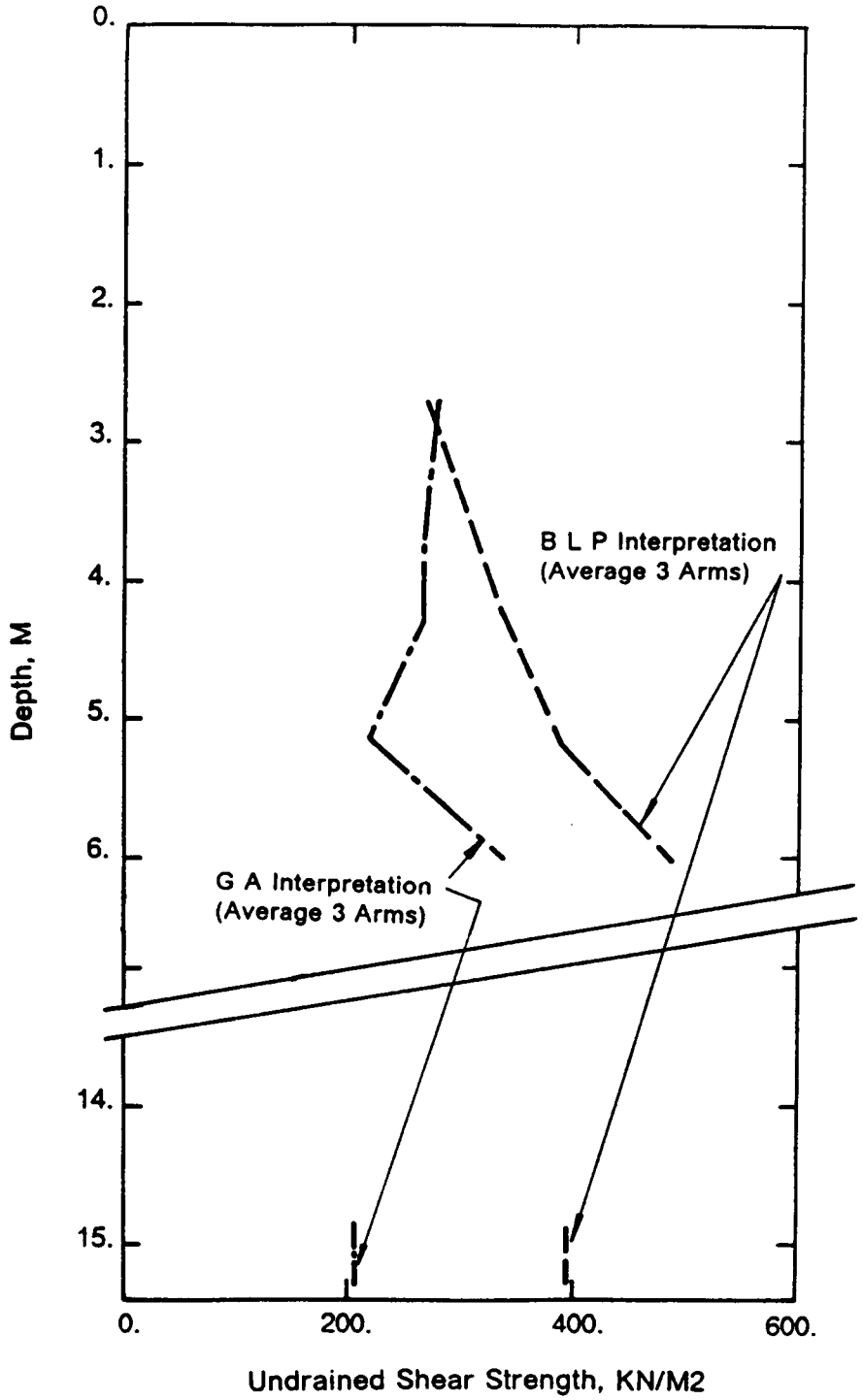

FIGURE 6.16 GIBSON ANDERSON VERSUS BAGUELIN, LADANYI AND PALMER INTERPRETATIONS

between the average values of the BLP interpretation and those of the GA one varies between 1.0 to 1.5 for the tests R1 to R5 and is approximatively 2.0 for the test R6.

In the case of strain hardening materials, the GA and the BLP interpretations give generally values similar to each others as the real stress strain curve of the material is close to the assumption of an elastic perfectly plastic material. The difference between the values of the two interpretations increases with brittle materials like the Miocene clay as the BLP interpretation is able to record the peak of strength and the GA interpretation gives only average values over the range of strains used for the interpretation.

6.6.4 Comparison between different test values

The undrained shear strength values interpreted from the SBPM tests are compared to values obtained in Menard pressuremeter testing and in the laboratory testing program given in Chapter 3 in Fig. 6.17 and Fig. 6.18 where they are plotted against depth and elevation respectively. The Menard pressuremeter test results were published recently by Martin and Drahos (1986). The tests were carried out the last few years to to determine the design parameters for the foundations of some of the major projects recently developed in the Richmond downtown area. The undrained shear strength is interpreted empirically from the results of the Menard pressuremeter test using the expression:

$$s_u = (p_L - p_o)/K_b$$

with

p_o	the total lateral pressure in the ground
s_u	the undrained shear strength of the soil
K_b	an empirical coefficient which ranges typically between 2.7 and 3.5.
p_L	the limit pressure

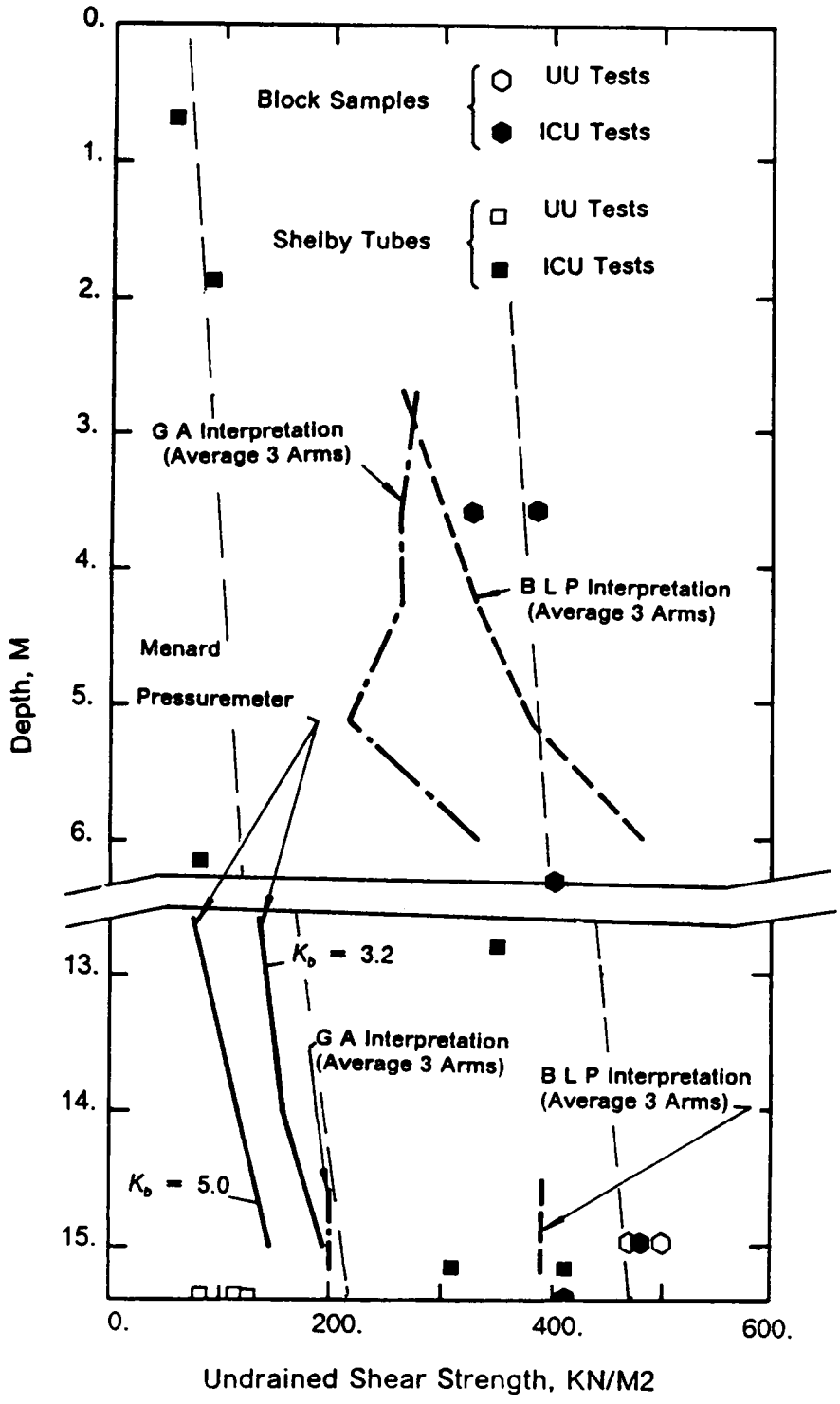

FIGURE 6.17 UNDRAINED SHEAR STRENGTHS VERSUS DEPTH

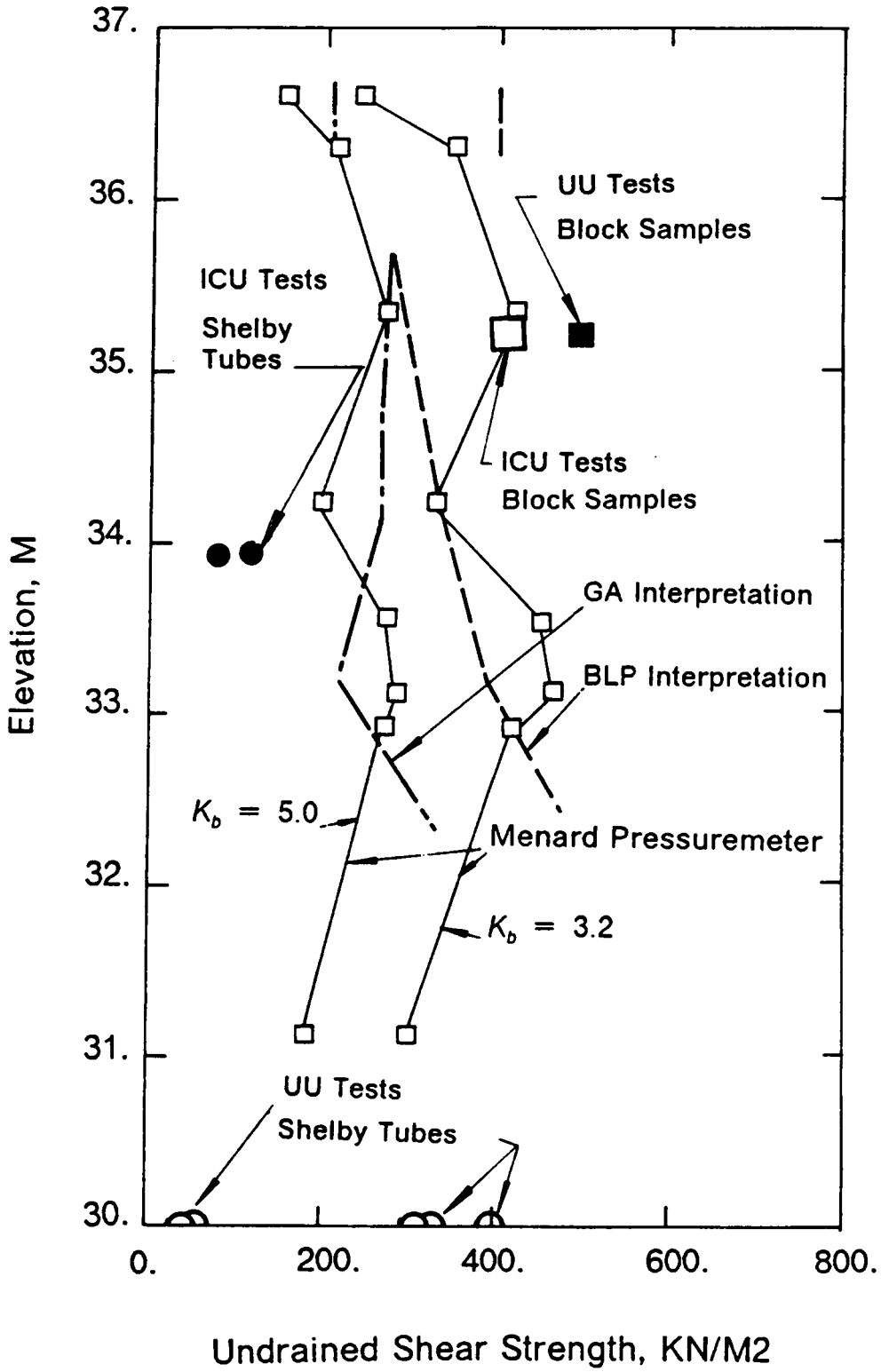

FIGURE 6.18 UNDRAINED SHEAR STRENGTHS VERSUS ELEVATION

In the figure, the undrained shear strength values are given for K_b equal to 3.2 as recommended by Menard for stiff soils and for K_b equal to 5.0 to match the local undrained shear strength values obtained by testing Shelby tube samples in the laboratory.

In Fig. 6.18 where the values are plotted against elevation, the average values obtained from the SBPM test results by the BLP interpretations of the same order of magnitude as the Menard pressuremeter values interpreted with K_b equal to 3.2. When interpreted with K_b equal to 5.0, the Menard pressuremeter values are comparable to the values obtained from the SBPM tests results using the GA interpretation.

The laboratory test results are of the order of 30% larger than the average of the SBPM test values at the same elevation using the BLP interpretation. They are very similar to the average value given by the BLP interpretation at the test R6 which is situated at a similar depth and two blocks away from the block samples. When plotted against depth in Fig. 6.17, the average value given by the BLP interpretation are in good agreement with the laboratory test results on the block samples but they are nearly twice the average value of the laboratory test results performed on the Shelby tube samples.

6.7 FAILURE MODES AND EFFECTIVE STRESSES

6.7.1 Failure modes

Among the two pore pressure cells PPA and PPB installed in the probe, only PPA which is placed on the same generating line as Arm1 recorded pore pressure measurements during the performance of the six tests R1 to R6. As a typical example, the variation of the effective stresses σ'_r, σ'_θ and σ'_v with the radial strain during the test R4 are given in Fig. 6.19 for Arm1 and Arm2. The stresses at Arm1 are computed as follows: The initial tangential stresses are both the solution of the equation of the ellipse of lateral pressures in the direction perpendic-

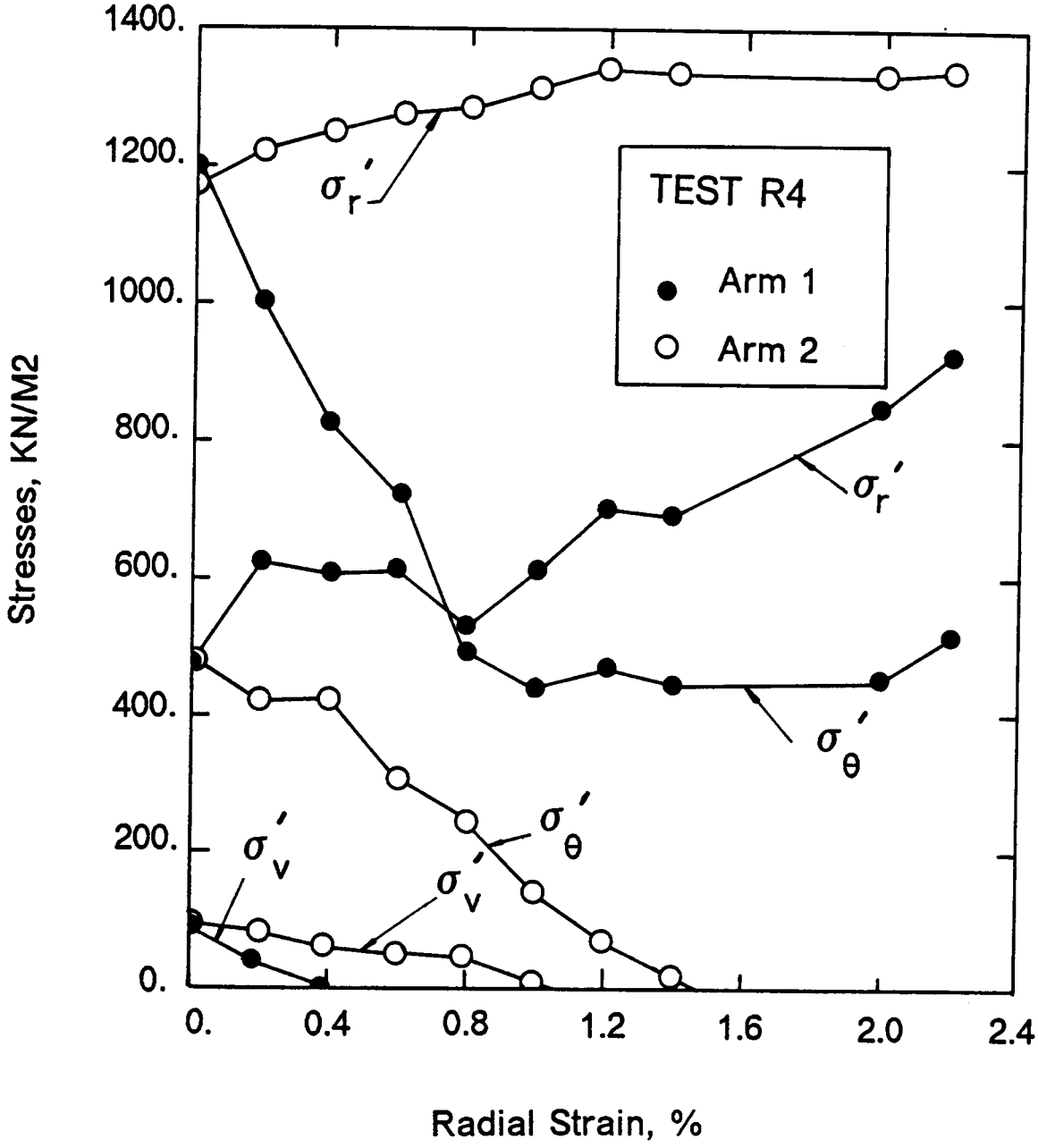

FIGURE 6.19 VARIATIONS OF THE EFFECTIVE STRESSES DURING THE SBPM TEST

ular to Arm1. The initial vertical stresses and are both equal to the overburden pressure. The total radial pressure during the expansion test is the probe pressure corrected for the stiffness of the membrane and chinese lantern system. The total tangential stress σ_θ is determined from the stress stain curve obtained by the Baguelin Ladanyi and Palmer interpretation of the pressuremeter curve of Arm1 and from σ_r. The total vertical stress, σ_v, does not vary with time. The effective stresses are determined by substracting from the total stresses the pore pressures recorded by the pore pressure cell PPA as this cell is on the same generatrice line as Arm1. A similar procedure is used to determine the total stresses in the direction of Arm2. To determine the pore pressures in other directions than Arm1, it is assumed that the pore pressure generation is controlled by the change of total radial stress after lift-off and that the distribution of pore pressure versus total radial stress after lift-off recorded by PPA is applicable in any radial direction around the probe.

From Fig. 6.19, the following can be drawn:

1. At the begining of the test, σ'_r and σ_r are both equal to the lift-off pressure measured by Arm1 corrected for membrane and chinese lantern stiffness.

2. The effective vertical stress is the minor stress at the beginning of the test and remains the minor stress throughout the test. This situation results from the large initial lateral stresses compared to the vertical stresses existing at the two sites.

3. At Arm1, the rotation of σ'_r and σ'_θ occurs as σ'_θ is larger than σ'_r at the beginning of the test.

4. A first failure in the plane (σ'_r,σ'_v) preceeds a second failure in the plane $(\sigma'_r,\sigma'_\theta)$.

5. As anticipated, σ'_r becomes constant when σ'_θ drops to zero.

The two failures are expected to develop as shown in Fig. 6.20. for the stress conditions prevailing at Arm2 (σ'_r larger than σ'_θ). The first failure occurs when the Mohr circle in the

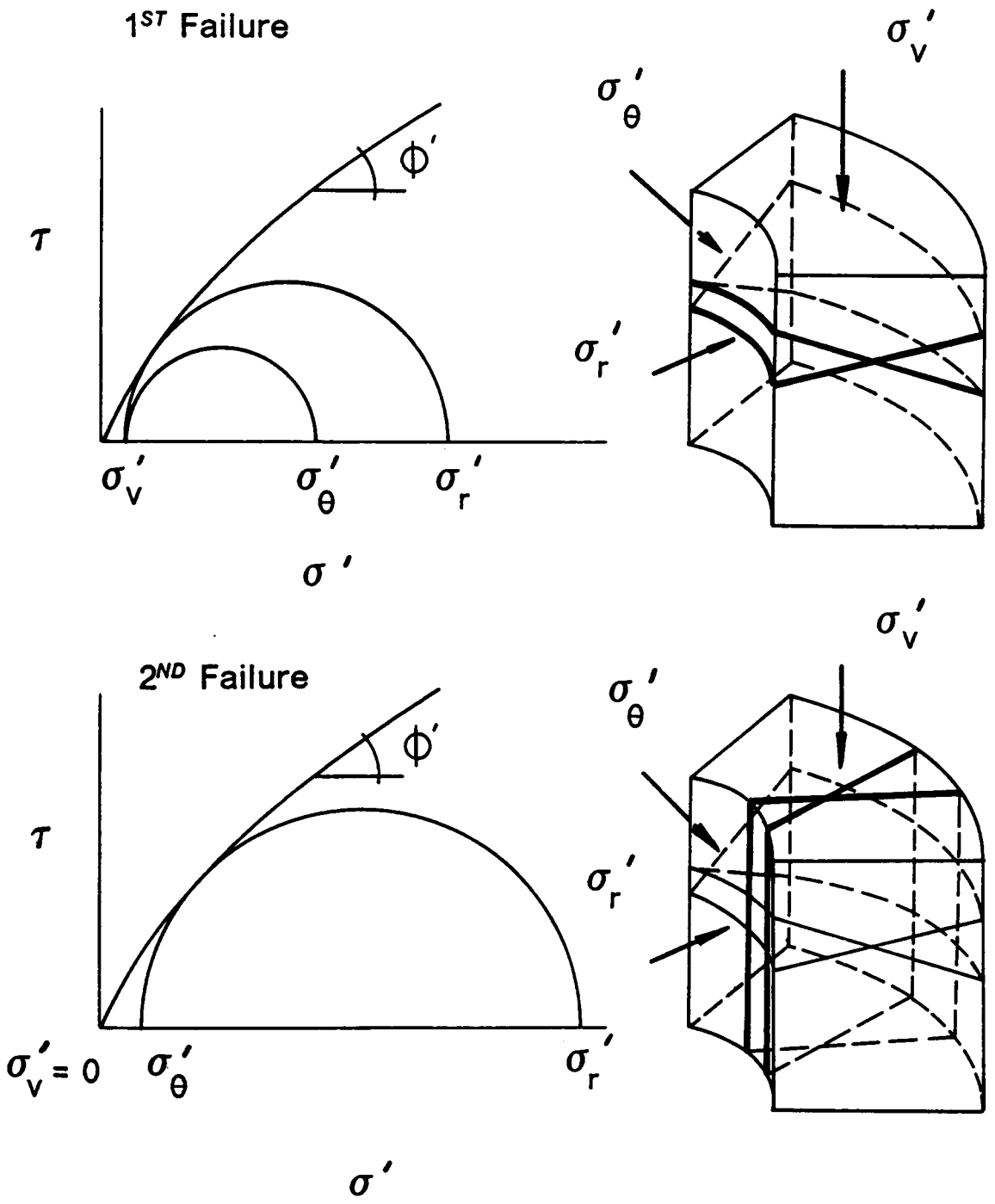

FIGURE 6.20 FAILURE MODES DURING THE SBPM TEST

plane σ'_v,σ'_r) touches the failure envelope. The failure planes which develop are nearly horizontal. They propagate away from the probe and extend as the pressure pressure in the probe is increased. As σ'_v is reduced to zero, an open cracks must propagate along the failure planes. At that time, shear in the plane $(\sigma'_r,\sigma'_\theta)$ increases until the second failure occurs when the Mohr circle $(\sigma'_r, \sigma'_\theta)$ touches the failure envelope. New failure planes develop. They are vertical and radiate outwards from the contact probe-soil. In normally consolidated soils and slightly overconsolidated soils, only the second failure mode occurs and it is legitimately the assumed mode of failure in the Gibson Anderson and Baguelin Ladanyi and Palmer interpretations of the undrained shear strength. As these interpretations assume plane strain conditions during the expansion tests, the effect of the first failure mode on the interpreted undrained shear strength should be addressed.

In the opinion of the author, for this particular case, the first failure mode has a limited effect on the interpreted undrained shear strength values. The reasons are:

1. Due to the brittleness of the soil, the second failure mode occurs between 1 and 25 radial strain which indicates that the overall strains at which the two failure modes occur are small.

2. The first failure planes being nearly horizontal, the vertical component of strain is limited.

3. As the failure planes of the second failure mode are nearly perpendicular to the failure planes of the first failure mode, their mutual influence on the measurement of the shear stresses is minimum.

The Baguelin, Ladanyi and Palmer interpretation allows the detection of the first failure mode for several tests. It is characterized by a small and sharp peak on the interpreted shear stress strain curve at strains varying between 0.4 to 0.6%. This peak does not show any significant influence on the overall shape of the stress strain curve.

6.7.2 Effective stresses

The effective stress paths during the SBPM tests are shown in Fig. 6.21 for the case where the initial effective radial stress σ'_r is smaller than the initial effective tangential stress σ'_θ (Arm1 in the tests R1 to R6). The pore pressures are directly read from the pore pressure cell PPA as it is placed on the same generating line as Arm1.

To take into account the three dimensional state of stress, the stress paths are derived in terms of the octahedral effective stresses σ'_{oct} and τ_{oct} which can be expressed as follows:

$$\sigma'_{oct} = \frac{1}{3}(\sigma'_r + \sigma'_\theta + \sigma'_v)$$

and

$$\tau_{oct} = \frac{1}{3}\sqrt{(\sigma_r - \sigma_v)^2 + (\sigma_\theta - \sigma_v)^2 + (\sigma_r - \sigma_\theta)^2 + (\tau_{r\theta})^2 + (\tau_{\theta v})^2 + (\tau_{vr})^2}$$

where σ'_r, σ'_θ and σ'_v are respectively the radial, tangential and vertical effective normal components of stress. τ_{oct} is given in terms of the total stresses as the deviatoric stresses ($\sigma_r - \sigma_\theta$), $(\sigma_r - \sigma_v)$ and $(\sigma_r - \sigma_\theta)$ and t he shear stresses $\tau_{r\theta}$, $\tau_{\theta v}$ and τ_{rv} have the same magnitude when expressed in terms of effective or total stresses.

In Fig. 6.21, the tests R1 to R5 performed at the Schnabel Center site indicate a consistent failure envelope. The test R6 which was performed at the Coliseum site under different initial stresses reaches the same failure envelope as the tests R1 to R5.

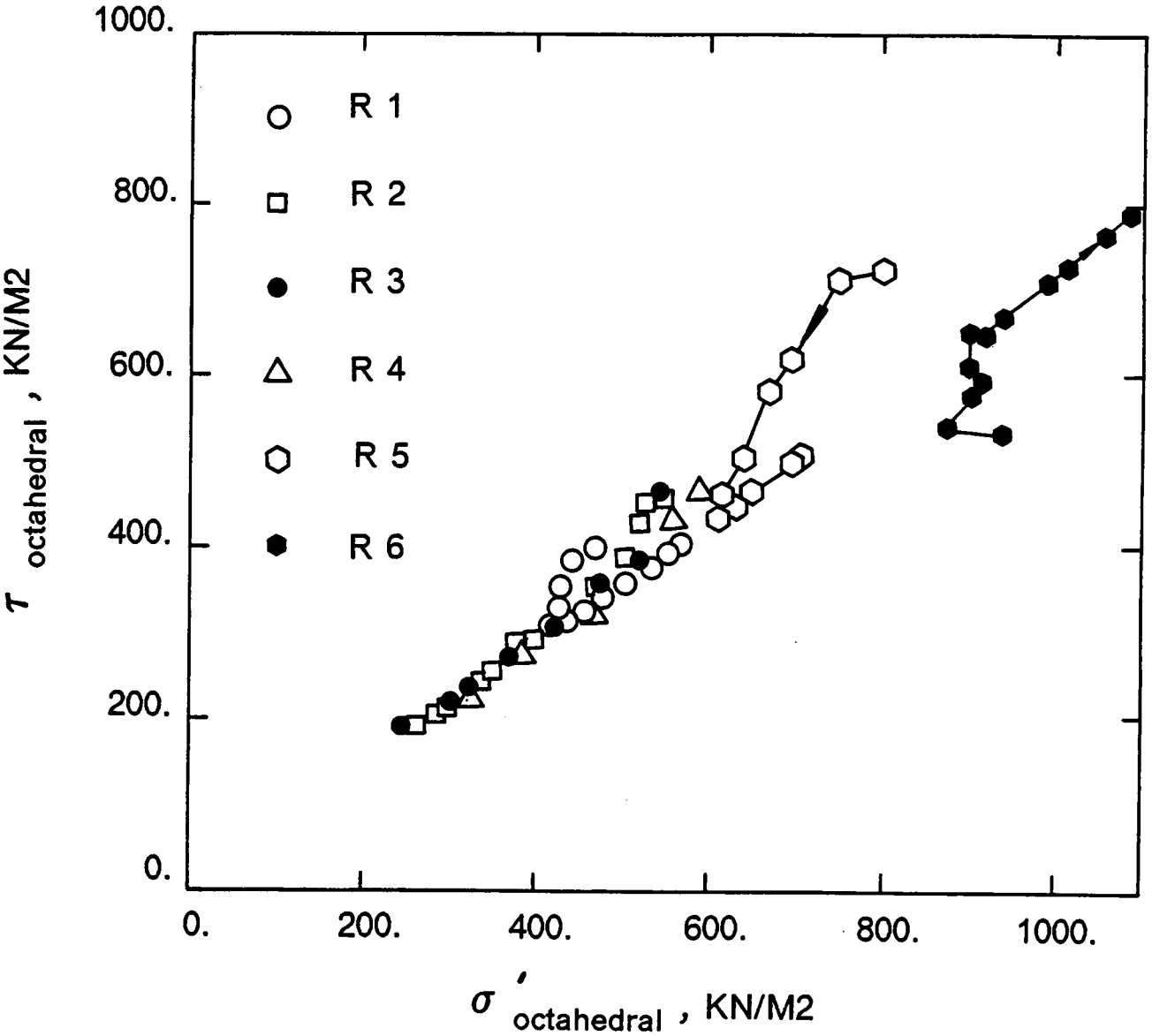

FIGURE 6.21 EFFECTIVE STRESS PATH DURING THE SBPM TESTS

6.7.3 Comparison with laboratory tests

The effective stress paths in terms of the octahedral stresses are shown in Fig. 6.22 for the laboratory tests and the SBPM tests. A comparison of the two envelopes is difficult as the strain and pore pressure conditions for the two tests are different once the peak of strength is reached. In the case of the laboratory tests, as the soil is very brittle at low confining pressures, the sample does not behaves like a mass of soil yielding uniformly but rather like a composite material where slipage occurs in a narrow band of yielding material situated between two elastic bodies. In this case, the pore pressure developed is approximatively proportional to the deviatoric stress applied to the sample. Once the peak of strength is reached, the true strain of the soil and the deviatoric stress drop simultaneously as they are controlled at that time by the post peak strength on the failure plane. Tracking a yield envelope in that case is not possible as fracture of the soil follows immediately yield. In the contrary, from the confinment of the soil in the case of the SBPM test, the strain develops throughout the soil mass as well as the pore pressures increases monotonically to the end of the test. The figure indicates however the tendancy for the envelope of the laboratory test results to bend towards the envelope of the SBPM tests for σ'_{oct} larger than 800 KN/M2 (116 psi).

6.8 MODULUS VALUES

6.8.1 Method

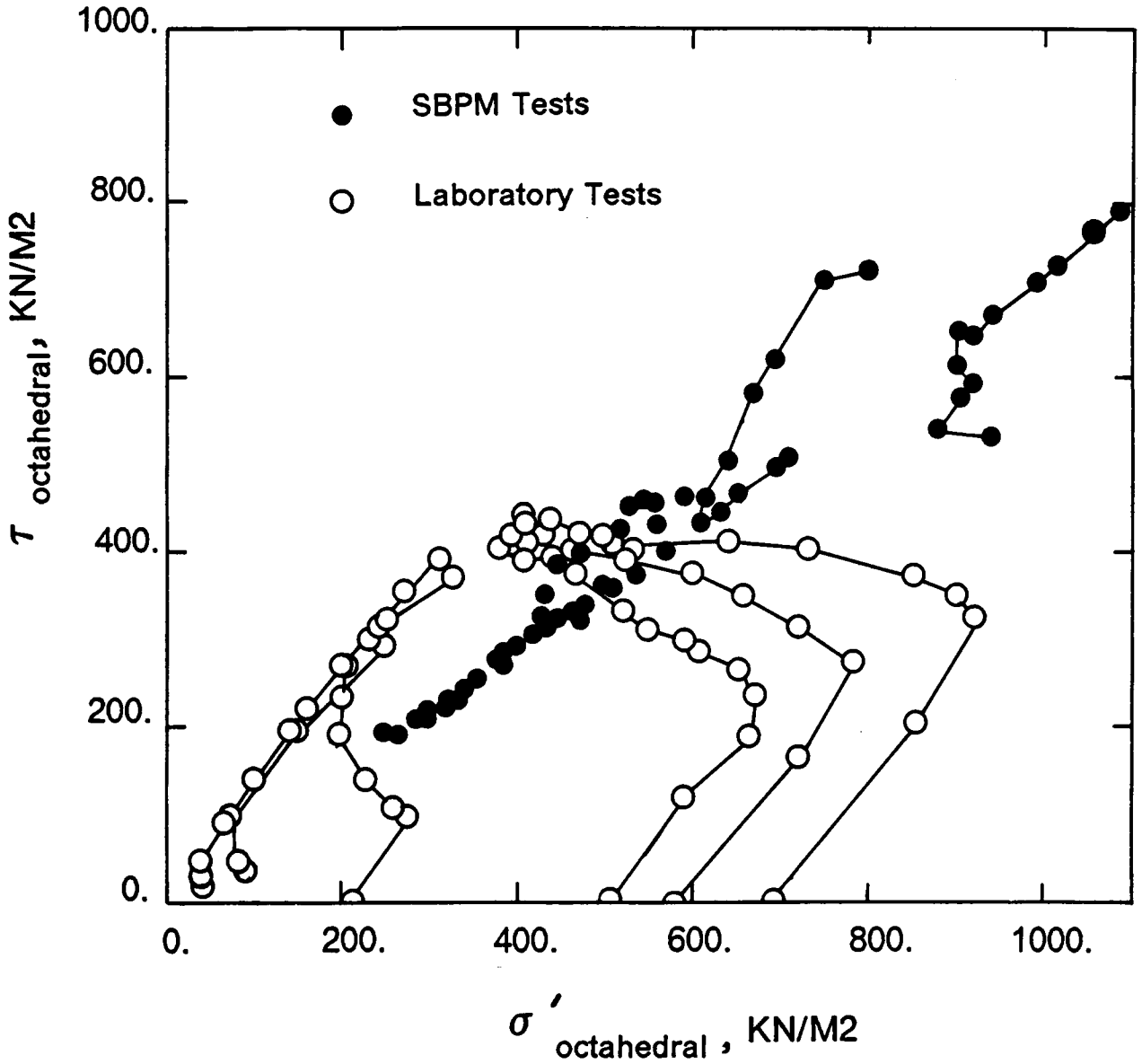

FIGURE 6.22 EFFECTIVE STRESS PATHS IN ICU AND SBPM TESTS

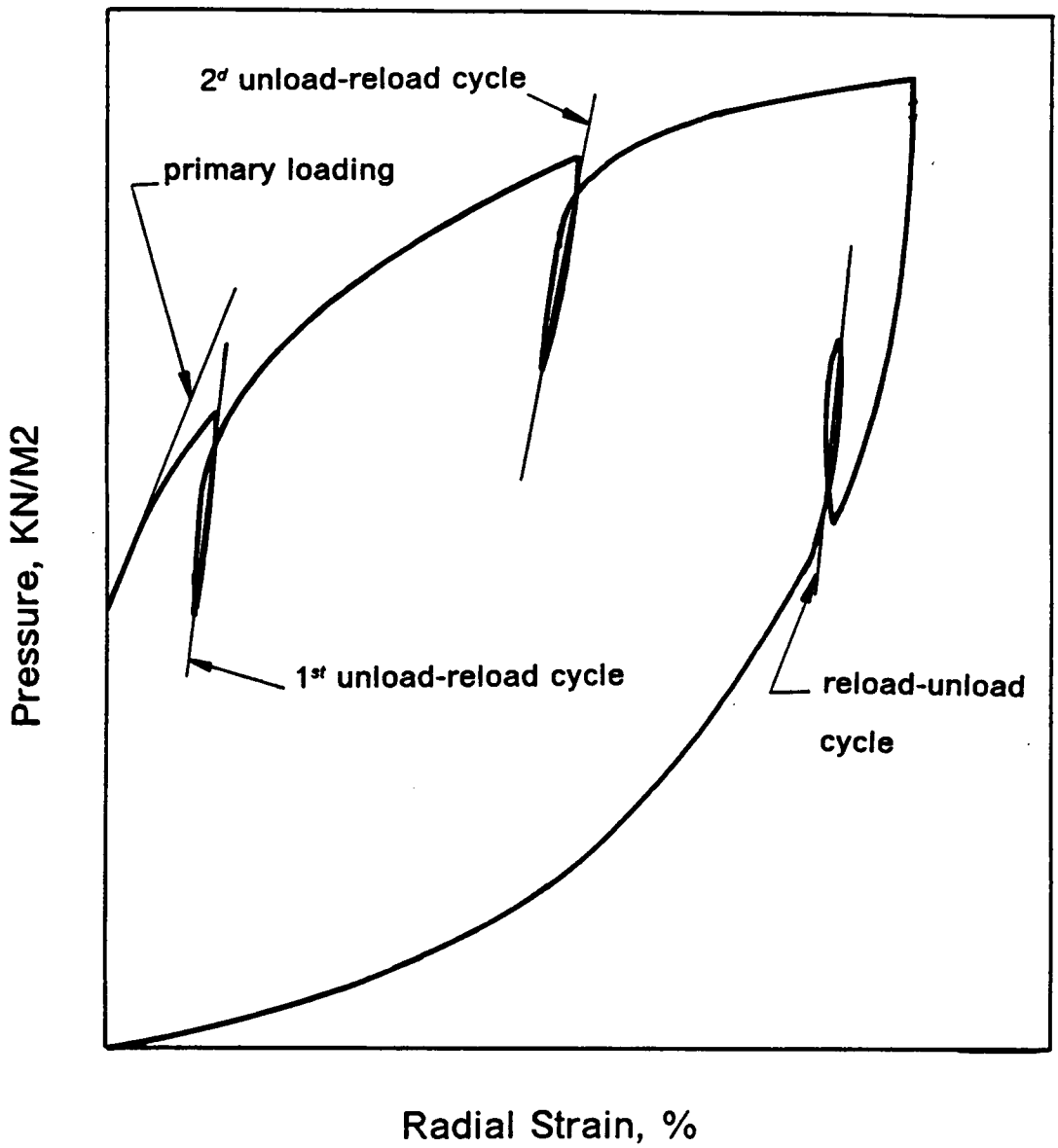

FIGURE 6.23 MODULUS MEASUREMENT ON THE SBPM CURVE

A typical pressuremeter curve is shown in Fig. 6.23 with the unload-reload and reload-unload cycles which are normally performed during the test to estimate the shear modulus of the soil.

The determination of the shear modulus of the soil is done as follows: From Baguelin, Ladanyi and Palmer,

$$\frac{1}{2}(\sigma_r - \sigma_\theta) = \varepsilon_r \Psi'(\varepsilon_r)$$

with

σ_r the radial stress

σ_θ the tangential stress

ε_r the radial strain

$\Psi'(\varepsilon_r)$ the slope of the pressuremeter curve

$$\Psi'(\varepsilon_r) = \frac{1}{2}(\sigma_r - \sigma_\theta)\varepsilon_r = \frac{\tau}{\varepsilon_r}$$

but

$$\varepsilon_r = \frac{\gamma}{2} \text{ as } \gamma = \varepsilon_r - \varepsilon_\theta \text{ and } \varepsilon_r = -\varepsilon_\theta$$

then

$$\Psi'(\varepsilon_r) = \frac{2\tau}{\gamma} = 2G$$

The slope of the pressuremeter curve is twice the shear modulus of the soil. If the soil behaves elastically at the primary loading following lift-off and during the unload-reload and reload-unload cycles, elastic shear modulus values can be determined at the different locations.

Generally, the modulus values determined at the primary loading location on the curve is smaller than the modulus values determined from the subsequent cycles as some unavoidable disturbance of the soil takes place at the contact with the probe during the self boring operation and affects therefore the initial slope of the expansion curve. Law and Eden (1980) performed intentionally tests in Leda clay with a probe equipped with an undersized and an oversized cutting shoe. The initial modulus values from the tests performed with an oversized and an undersized cutting shoe were respectively 30 % larger and 20 to 50 % smaller than the tests results performed with a probe equipped with a cutting shoe of the same diameter as the body of the probe.

6.8.2 SBPM values

A profile of the shear modulus values determined from the primary loading and the first unload-reload cycle on the pressuremeter curves of the tests R1 to R5 are presented in Fig. 6.24. Modulus values were not interpreted from the test R6 as no unload reload cycles were performed during that test. The following remarks may be made:

1. The modulus values increase with depth. If the values determined from the first unload-reload cycle are considered, the modulus values vary typically from 4 MN/M2 (580 psi) at El. 35.7 to 6.5 MN/M2 (940 psi) at El. 32.2.

2. The primary loading modulus at Arm2 was not determined as yield occurs immediately after lift-off in that direction and the determination of an initial slope is arbitrary.

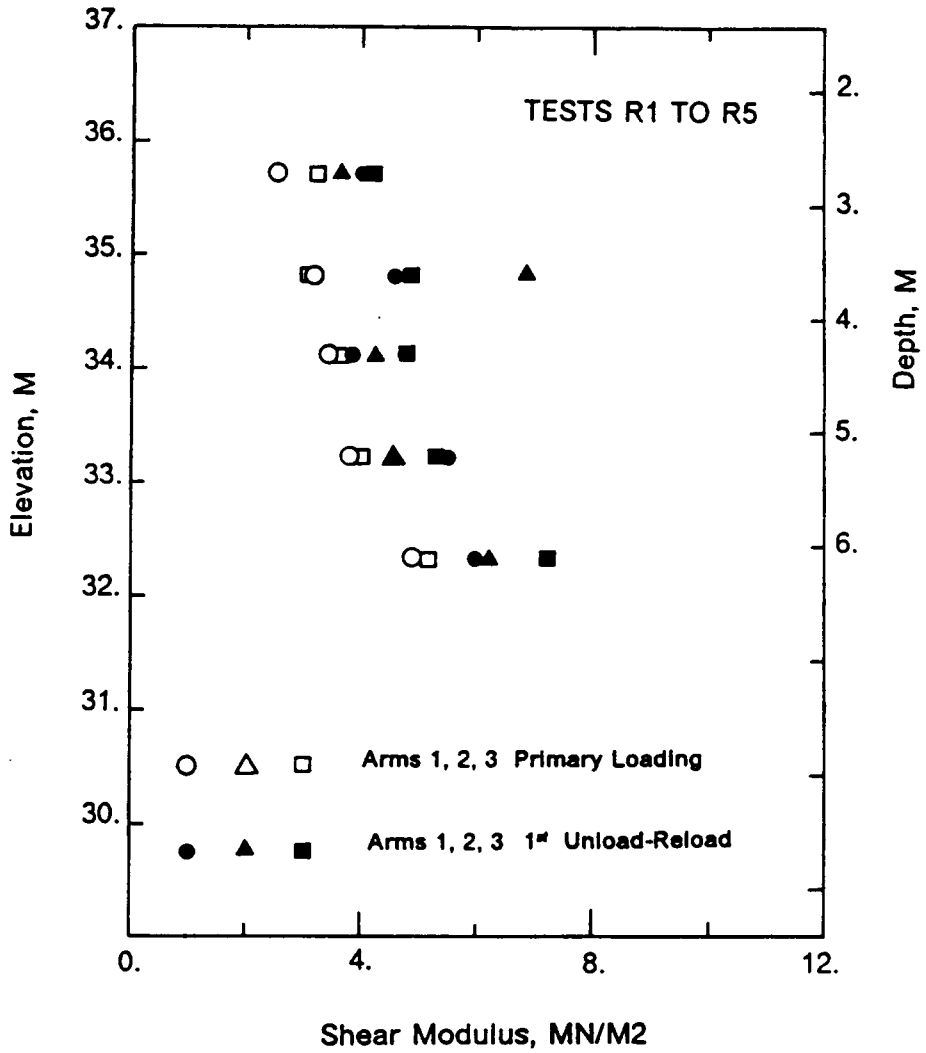

FIGURE 6.24 SHEAR MODULUS VALUES FROM PRIMARY LOADING AND FROM THE FIRST UNLOAD RELOAD CYCLE

3. The modulus values determined from the first unload-reload cycle are only 20% higher than the values determined from the primary loading at Arms 1 and 3 . In the author's opinion, this is a sign of a good placement of the probe as it suggests that the disturbance of the soil around is minimum.

4. For each test, very similar unload reload modulus values are determined from the three arms.

A profile of the modulus values determined from the unload-reload cycles and reload-unload cycles of the tests R1 to R5 is given in Fig. 6.25. The modulus values determined from the reload-unload cycles are generally 20% larger than those obtained from the unload-reload cycles.

Two unload-reload cycles were performed during the test R3 situated at El. 34.1. The second unload reload cycle gives modulus values 20% lower than the first unload-reload cycle.

6.8.3 Comparison with the Menard pressuremeter test results

The Menard pressuremeter modulus values published by Martin and Drahos (1986) are compared in Fig. 6.26 and Fig. 6.27 to the elastic modulus values determined with a Poisson ratio of 0.5 from the shear modulus values given in Fig. 6.24. In both figures, the average SBPM values are about twice the average Menard pressuremeter values. It seems that the prehole technique in soils where high lateral pressures exist cause disturbance by over-stressing the soil in the annulus zone of stress concentration around the hole.

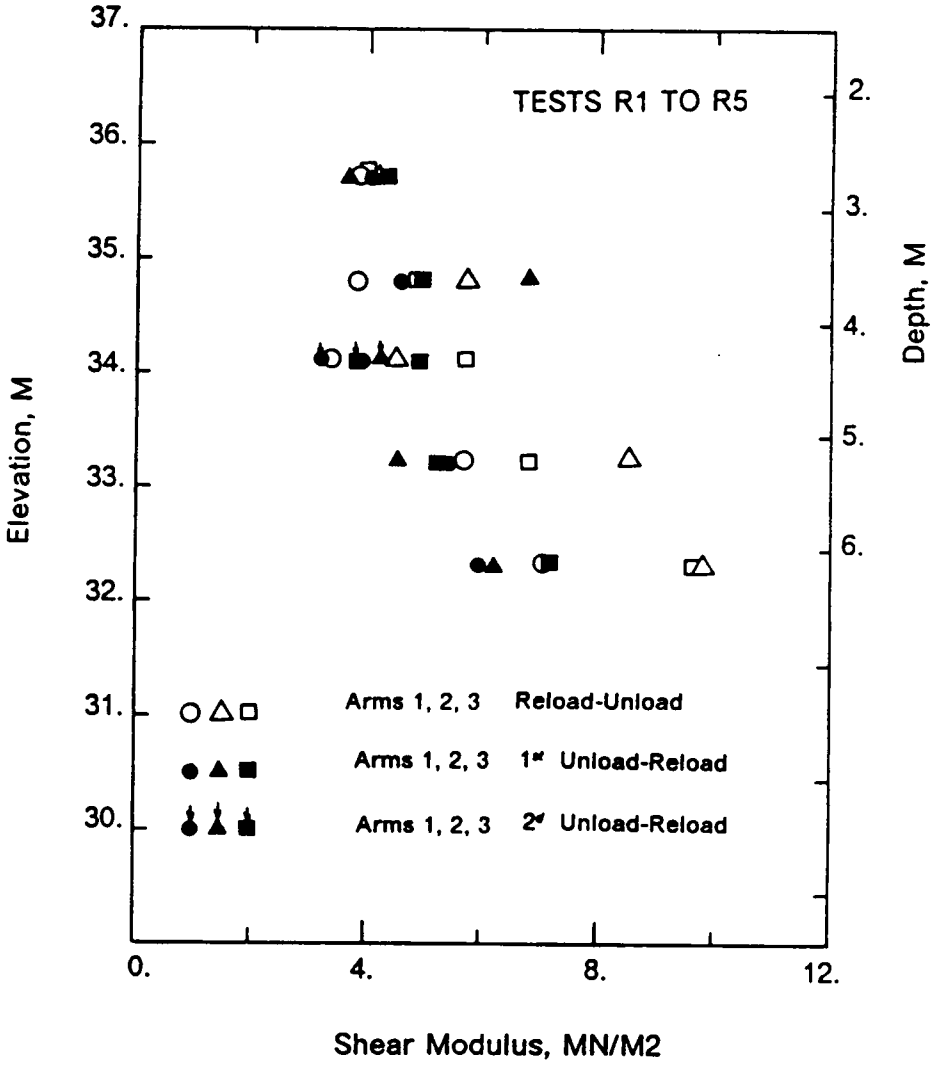

FIGURE 6.25 SHEAR MODULUS FROM UNLOAD RELOAD AND RELOAD UNLOAD CYCLES

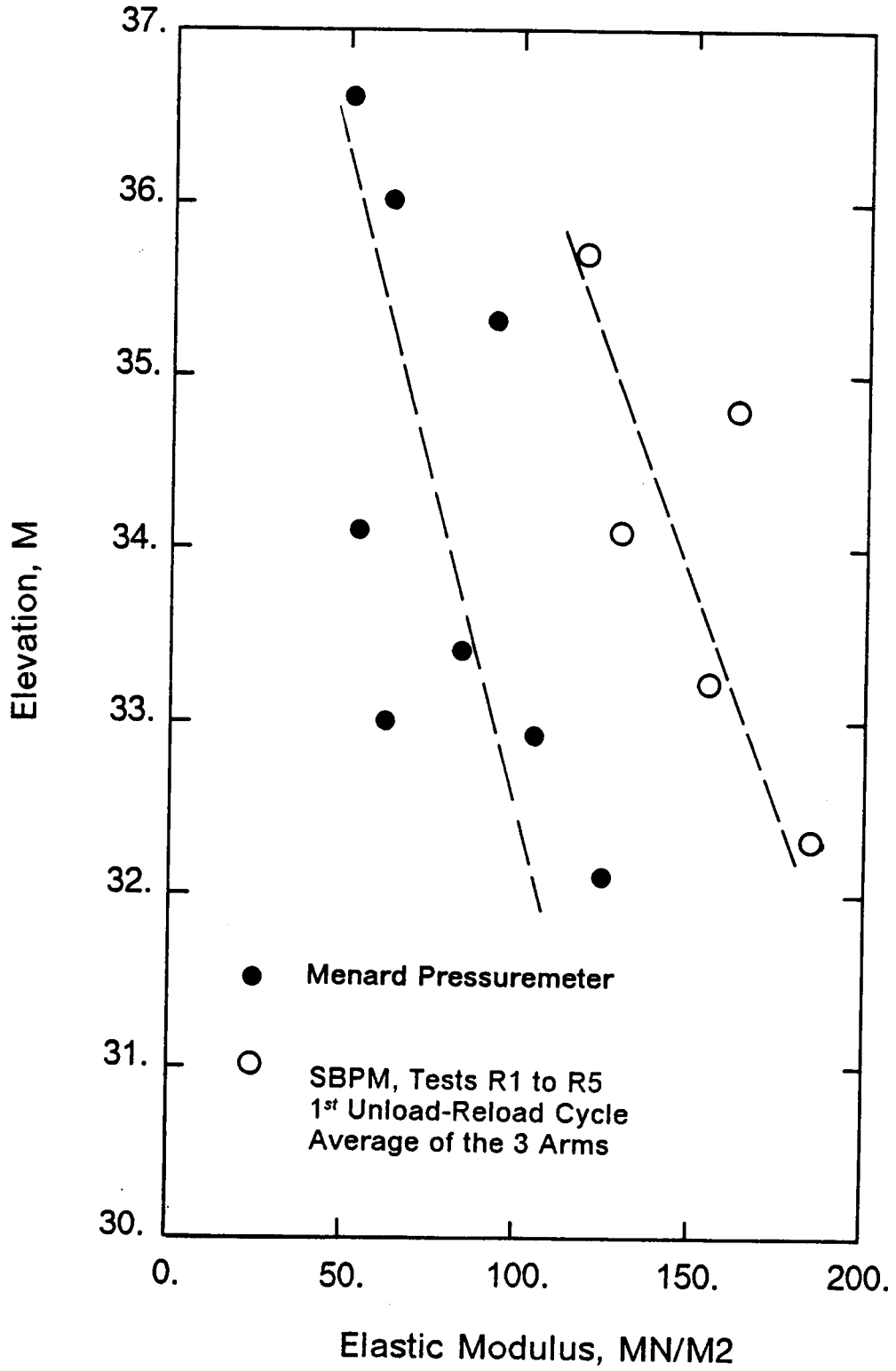

FIGURE 6.26 SBPM AND MENARD PRESSUREMETER ELASTIC MODULUS VALUES WITH ELEVATION

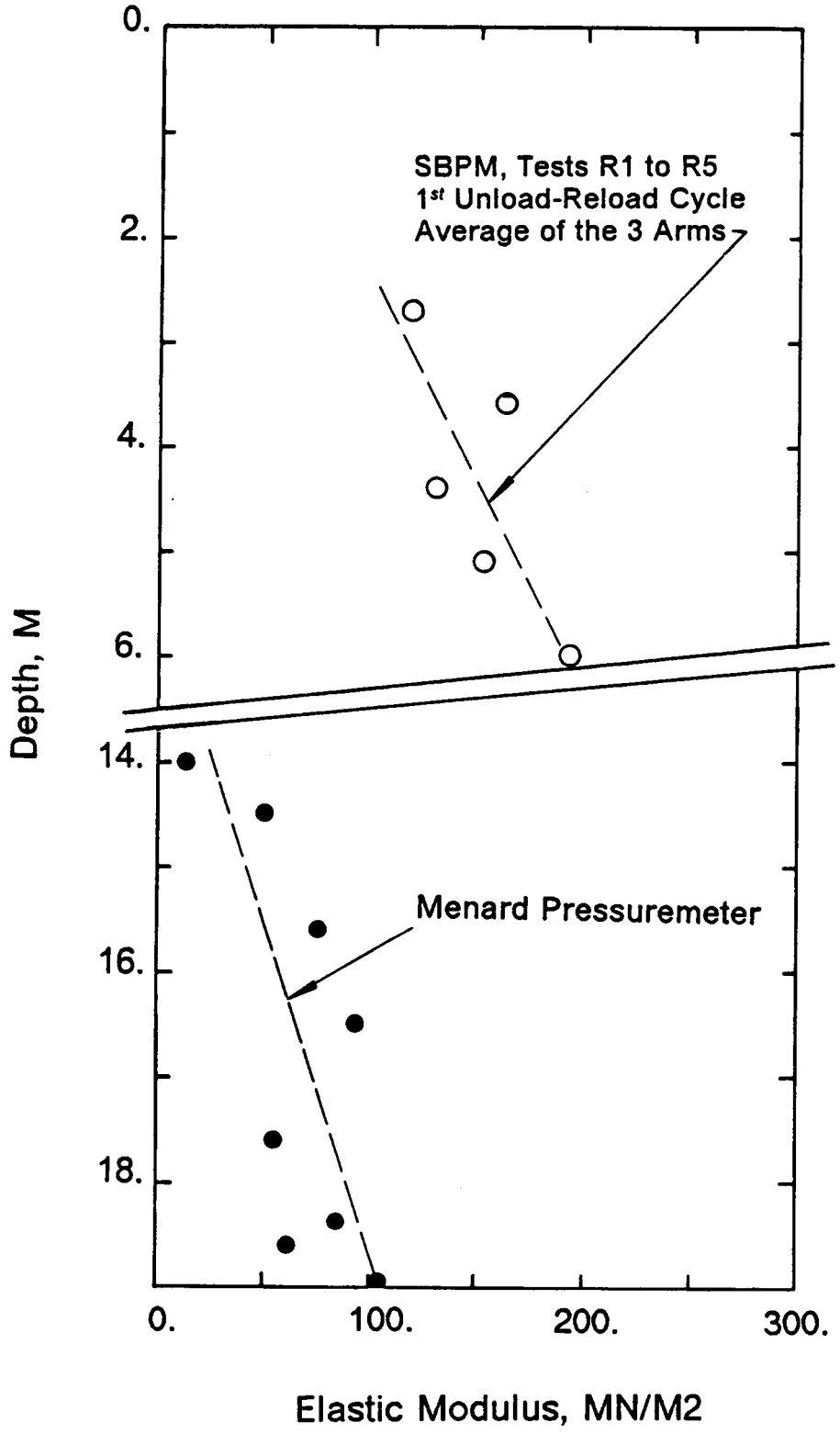

FIGURE 6.27 SBPM AND MENARD PRESSUREMETER ELASTIC MODULUS VALUES WITH DEPTH

6.8.4 Comparison with the laboratory tests

Modulus values from the laboratory tests on block samples and from the field are shown in Fig. 6.28 in terms of the initial effective octahedral stress σ'_{oct}. The laboratory modulus is a vertical modulus calculated at 50% of the peak deviatoric stress from the results of the UU and ICU triaxial tests performed on the block samples. Typical values vary between 35 MN/M2 (364 tsf) at no confinement to 120 MN/M2 (1250 tsf) for an initial effective octahedral stress of 600 KN/M2 (6.3 tsf).

The SBPM modulus values are calculated from the average slope of the unload-reload cycles of the three arms for a Poisson ratio equal to 0.5. They vary from 120 MN/M2 (1250 tsf) at 550 KN/M2 (5.7 tsf) initial octahedral stress to 195 MN/M2 (2028 tsf) at 950 KN/M2 (9.9 tsf) initial octahedral stress. These values are in good agreement with the laboratory values. Both follow similar trends with modulus values increasing with the initial effective octahedral stress. The scatter of the laboratory values could be reduced if the axial strains were computed from the relative displacements of two points situated on the soil sample itelf. This would eliminate from the computed strain the contribution of the contact sample plattens which is introduced when the strains are computed from the displacements of the piston.

6.9 SUMMARY

In this chapter, the properties of the Miocene clay were interpreted from the self boring pressuremeter test results. When possible, they were compared to the properties of the soil determined in the laboratory and from the Menard pressuremeter test results. The following points can be drawnfrom this study:

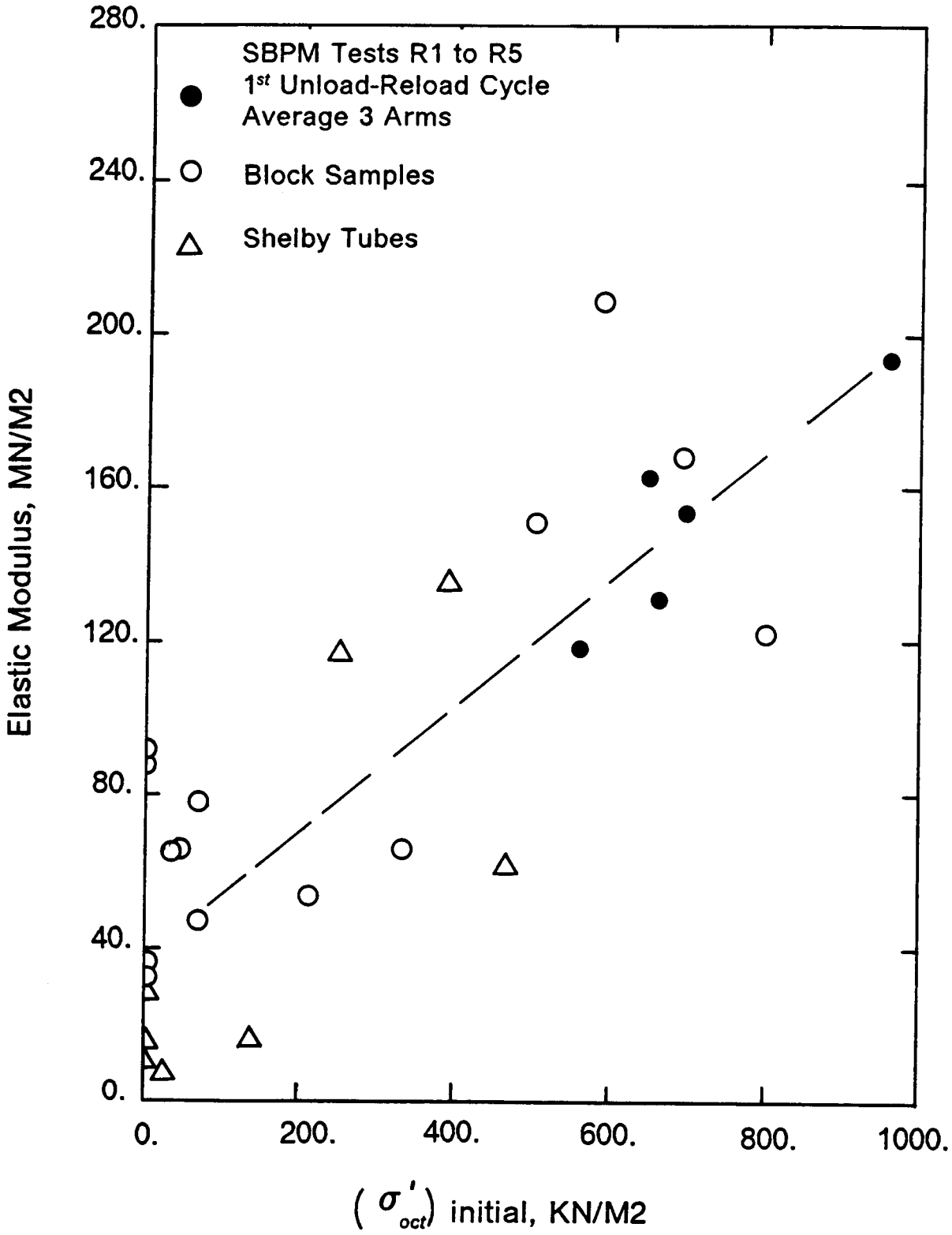

FIGURE 6.28 ELASTIC MODULUS VALUES FROM SBPM AND LABORATORY TESTS

1. The Miocene clay exhibits high lateral pressures with K_o values between 3 and 5 at a depth of 15 M. These values are larger than the ones normally found at similar depths in stiff clays with a same OCR. It is thought that the absence of fissures in the clay is at the origin of this potential for high lateral pressures.

2. The undrained shear strength obtained from the Baguelin Ladanyi and Palmer (BLP) interpretation compares well to the laboratory test values on block samples. As expected for brittle type of materials, the Gibson Anderson (GA) interpretation leads to lower values of undrained shear strength than the (BLP) interpretation.

   Undrained shear strength values interpreted from the Menard pressuremeter test results with the empirical factor K_b equal to 3.2 agree well with the SBPM values from the BLP interpretation. When using K_b, the undrained shear strength values interpretated from the Menard pressuremeter are comparable to the SBPM values from the GA interpretation.

3. Effective stress paths determined from the SBPM test results show a consistent trend at failure when plotted in the octahedral plane. A direct comparison with the stress paths from the laboratory tests is not possible as the boundary conditions are different in the two cases.

4. The modulus values interpreted from the Menard pressuremeter tests are typically half the ones interpreted from the SBPM tests. The high lateral pressures associated to the prehole technique used with the Menard pressuremeter seem to overstress the soil around the hole and cause a significant disturbance.

   Modulus values from the SBPM tests compare well with the laboratory values when they are expressed in terms of the octahedral effective stress.

Chapter 7

SELF-BORING TESTS IN THE RESIDUAL SOIL

7.1 INTRODUCTION

The prime objective of the testing program in the residual soil was to get acquainted to the equipment and to solve the technical problems encountered when self-boring in stiff soils. The site is situated approximatively three miles south west from the Virginia Tech campus (Fig. 7.1). The testing program consisted of fourty four SBPM tests performed between 1 and 9 M (3 and 30 ft) depth in nine holes. The probe oriented so that Arm1 was systematically towards the north. Many of the tests were conducted to sort out equipment problems. On the other hand, the final twenty two tests, termed T1 to T22, were performed in a manner to determine the characteristics of the residual soil and provide a data base for comparison with other in-situ tests to be performed in the future at the same location.

The raw data of the twenty two SBPM tests are given in Appendix F. The lateral pressures, the shear modulus and the friction and the dilation angles interpreted from the test results are presented in this chapter.

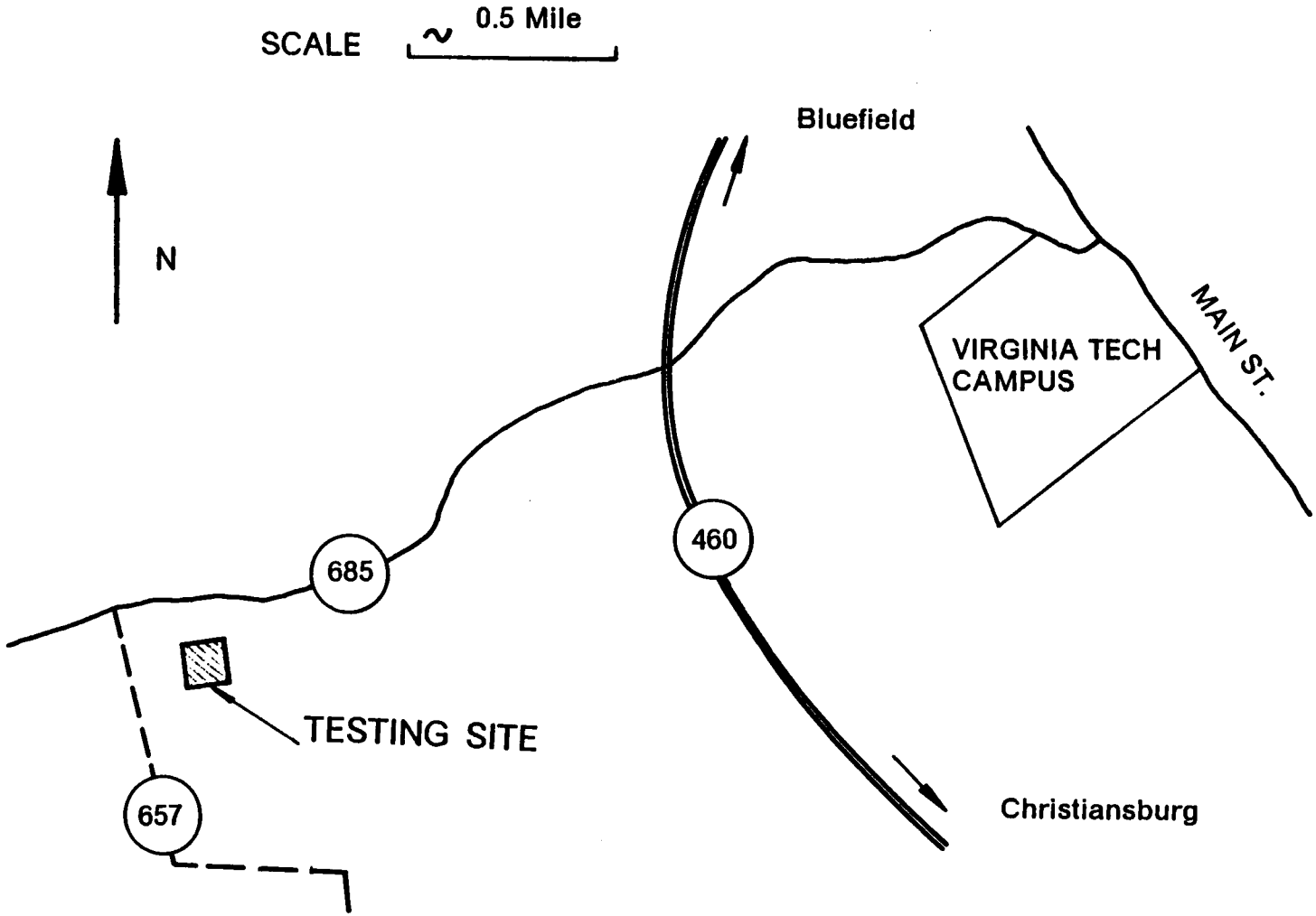

FIGURE 7.1 SBPM TESTING SITE

7.2 LATERAL PRESSURES

The lateral pressures are plotted against depth in Fig. 7.2 for the borings B4 and B5 and in Fig. 7.3 for the borings B6 and B8. The borings B1 to B3 and B9 are not represented as less than three tests per boring were performed in each of them. The two figures indicate for each test the lateral pressure interpreted for each arm as well as the average value for the three arms. For reference, the vertical effective pressure computed with a total unit weight of 15.5 KN/M3 (99 pcf) is also indicated.

In contrast to the results observed in the Miocene clay, the arms of each individual test give values of lateral pressures which are generally close to each other, and they do not indicate any systematic sequence of lift off among the three arms. This suggests that there is no anisotropy in the lateral stress field in the residual soil.

The profile of the average lateral pressure per test is plotted against depth in Fig. 7.4 for the tests T1 to T22. The lateral stresses exceed the vertical stresses, although there is a tendancy for the two profiles to converge with depth.

The at rest coefficient of lateral pressure calculated from the lateral and vertical effective stresses, K_o, is plotted against depth in Fig. 7.5. Values measured by individual arms and average values per test are both indicated. The K_o values are high near the ground surface, with values that decrease from 5 at 2 M (6.6 ft) to values between 1 and 2 at 5 M (16.4 ft) depth. From 5 to 9 M (16.4 to 30 ft), K_o is approximatively constant with depth with values of the order of 1 to 1.5.

The K_o profile is characteristic of a soil which has been subjected to dessication and drying, hence, the high values near the surface. This seems reasonable given that the area of the test is an agricultural area and is regularily aerated and allowed to loose moisture in this process.

Given K_o values of the order of 5 to be found in the soil at 2 M depth, the soil theoretically should a cohesion intercept of 25 KN/M2 (3.6 psi) under drained conditions, assuming that the

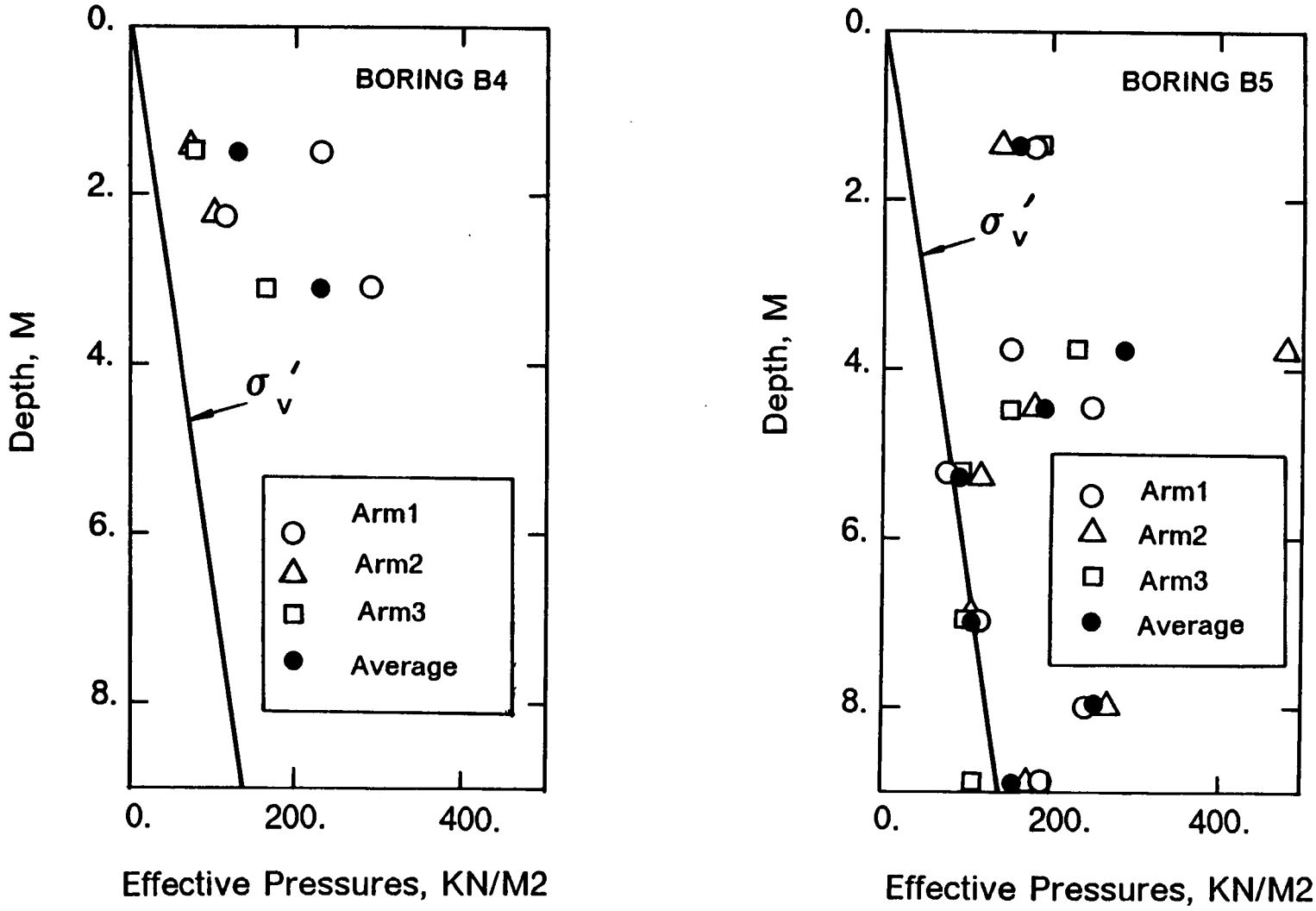

FIGURE 7.2 LATERAL PRESSURES MEASURED IN BORINGS B4 AND B5

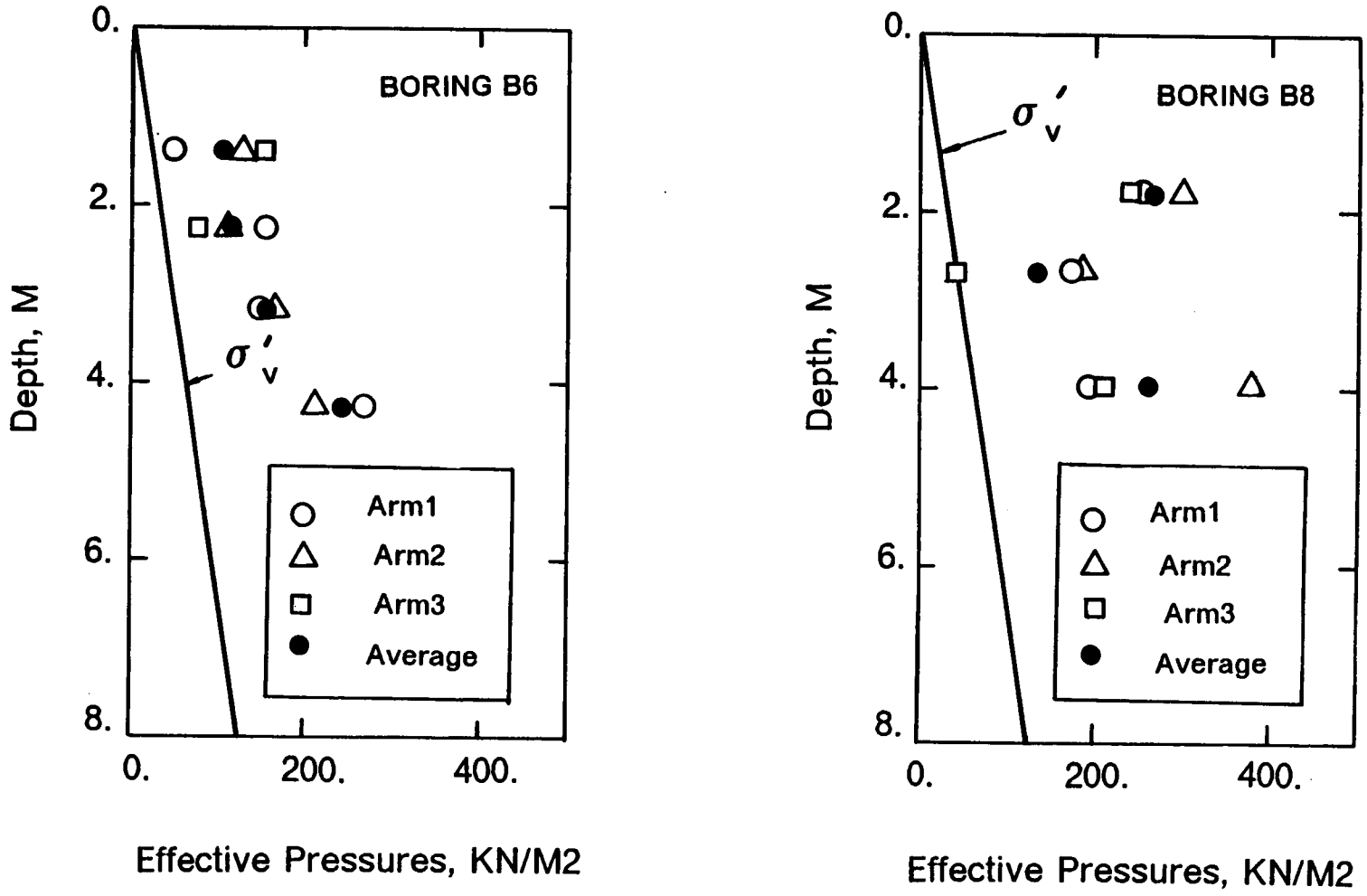

FIGURE 7.3 LATERAL PRESSURES MEASURED IN BORINGS B6 AND B8

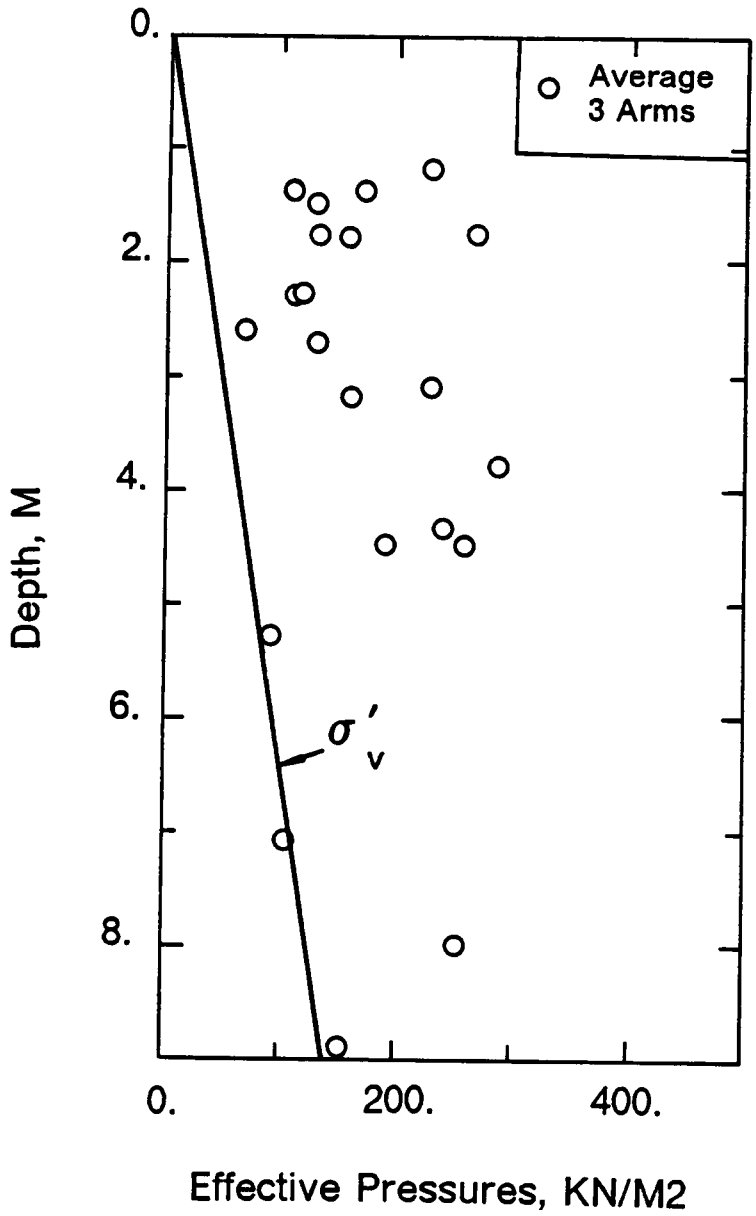

FIGURE 7.4 PROFILE OF AVERAGE LATERAL PRESSURES

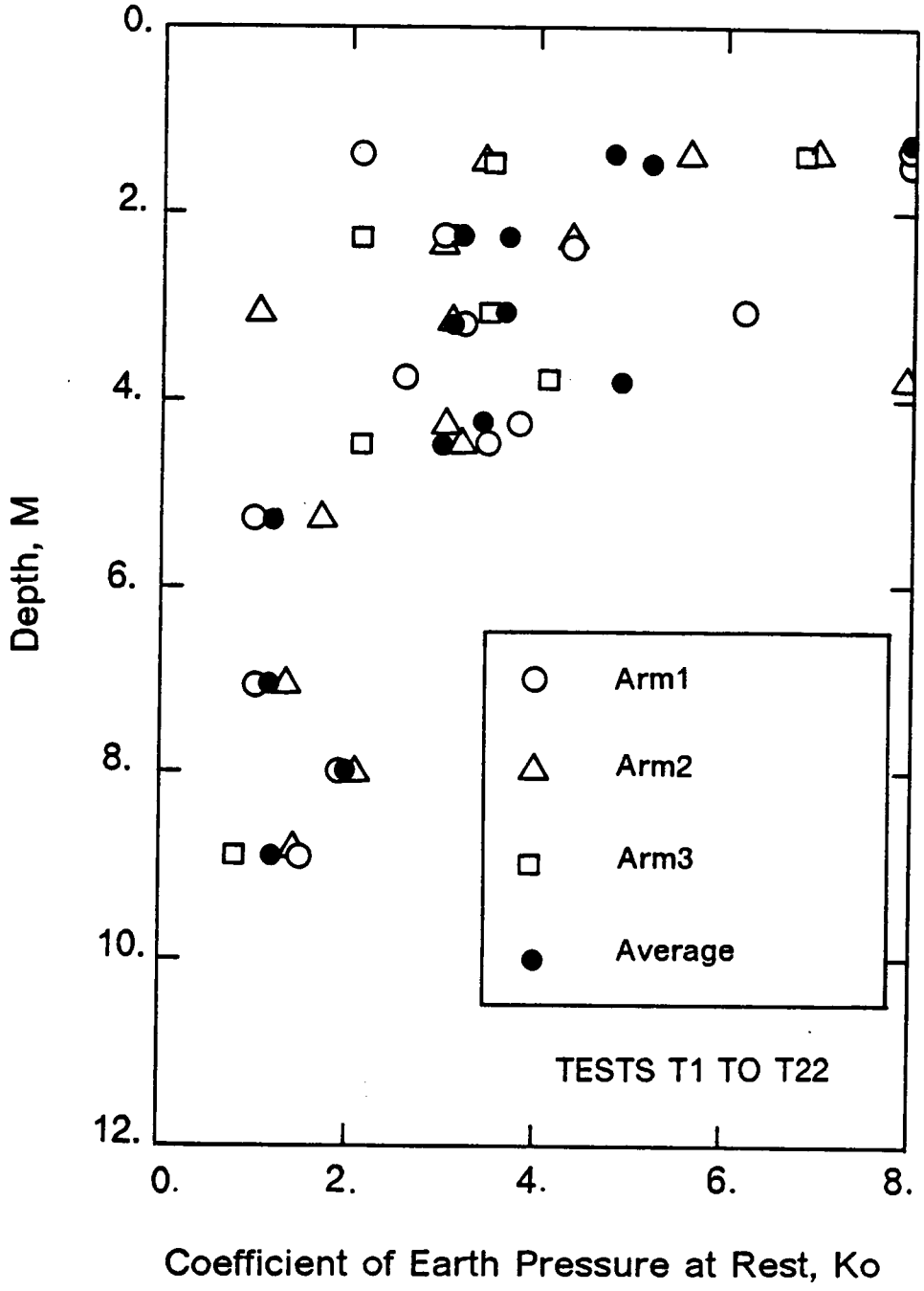

FIGURE 7.5 PROFILE OF THE COEFFICIENT OF EARTH PRESSURE AT REST, Ko

friction angle is 26 and that the soil has reached an impending passive state of failure ($K_o = K_p$ with K_p being the coefficient of passive earth pressure). It is likely that such a cohesion exists in the top few meters where the residual soil since it is a stiff to very stiff silt of high plasticity.

7.3 MODULUS VALUES

The initial shear modulus of the residual soil was determined from the slope of the pressuremeter curve at lift-off, and from the slope of the unload-reload cycles performed during the expansion part of the tests. A profile of the shear modulus values determined from initial loading is shown in Fig. 7.6 based on results for each of the data from the three pressuremeter strain arms as well as for the average test values. Little variation of the modulus values is observed with depth, and there is general agreement between the moduli determined from the different arms. Typical values range between 10 and 25 MN/M2 (104 and 261 tsf).

A similar profile for the modulus values calculated from the slope of the unload-reload cycles is presented in Fig. 7.7. The values in this case are more scattered than in the initial loading case.

The average modulus values per test at lift-off and from the unload-reload cycles are compared in Fig. 7.8. The modulus values from the unload-reload cycles are typically 1.5 to 3 times larger than the modulus values at lift-off.

The shear modulus values determined in the residual soil are similar to the values determined in the miocene clay.

Barksdale et al. (1986) report Menard pressuremeter modulus values varying between 5.6 and 19.4 MN/M2 (58 and 202 tsf) from tests performed at similar depths in the residual soil found in downtown Atlanta. These values are approximatively four times smaller than the

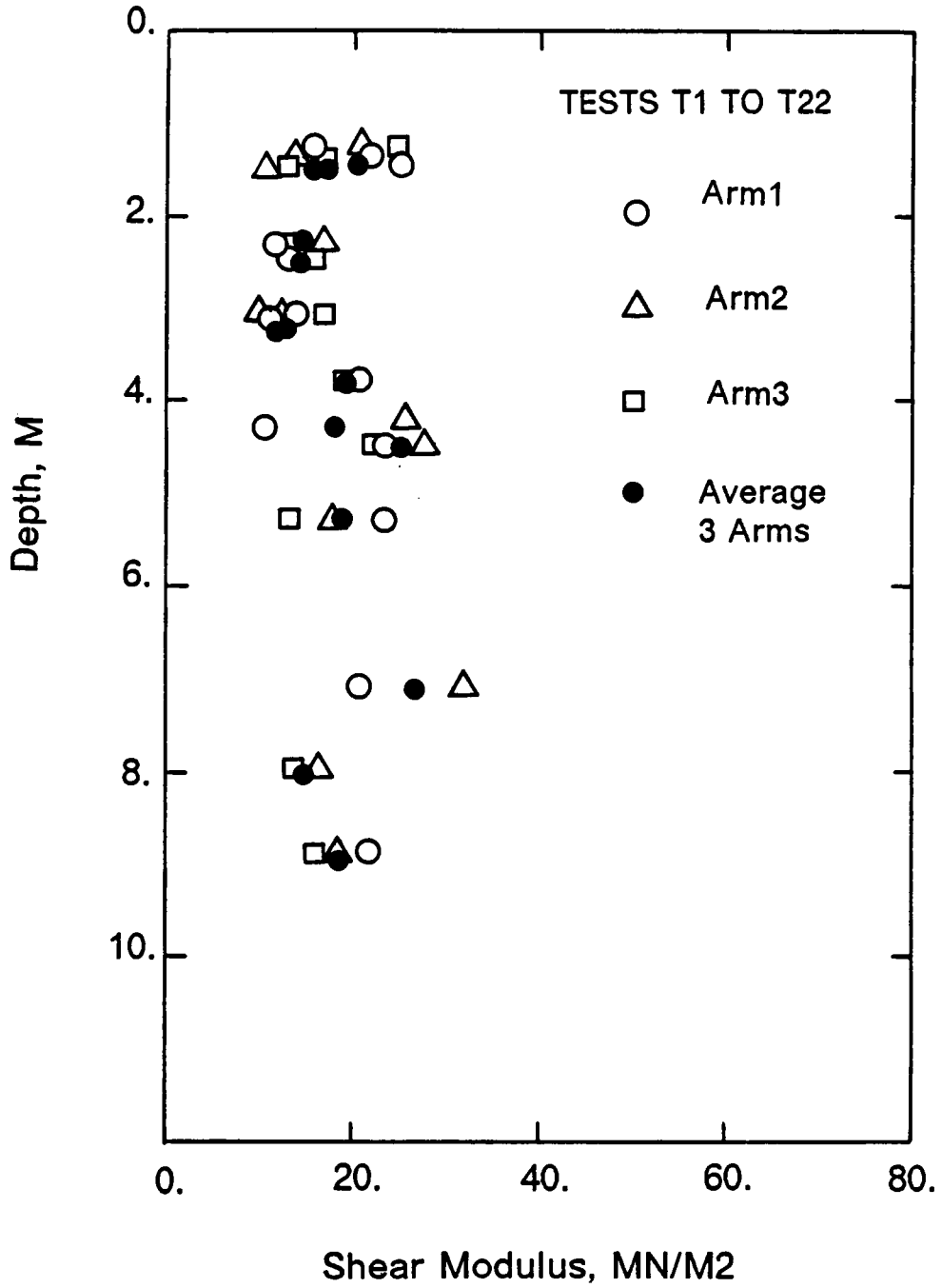

FIGURE 7.6 SHEAR MODULUS VALUES FROM PRIMARY LOADING

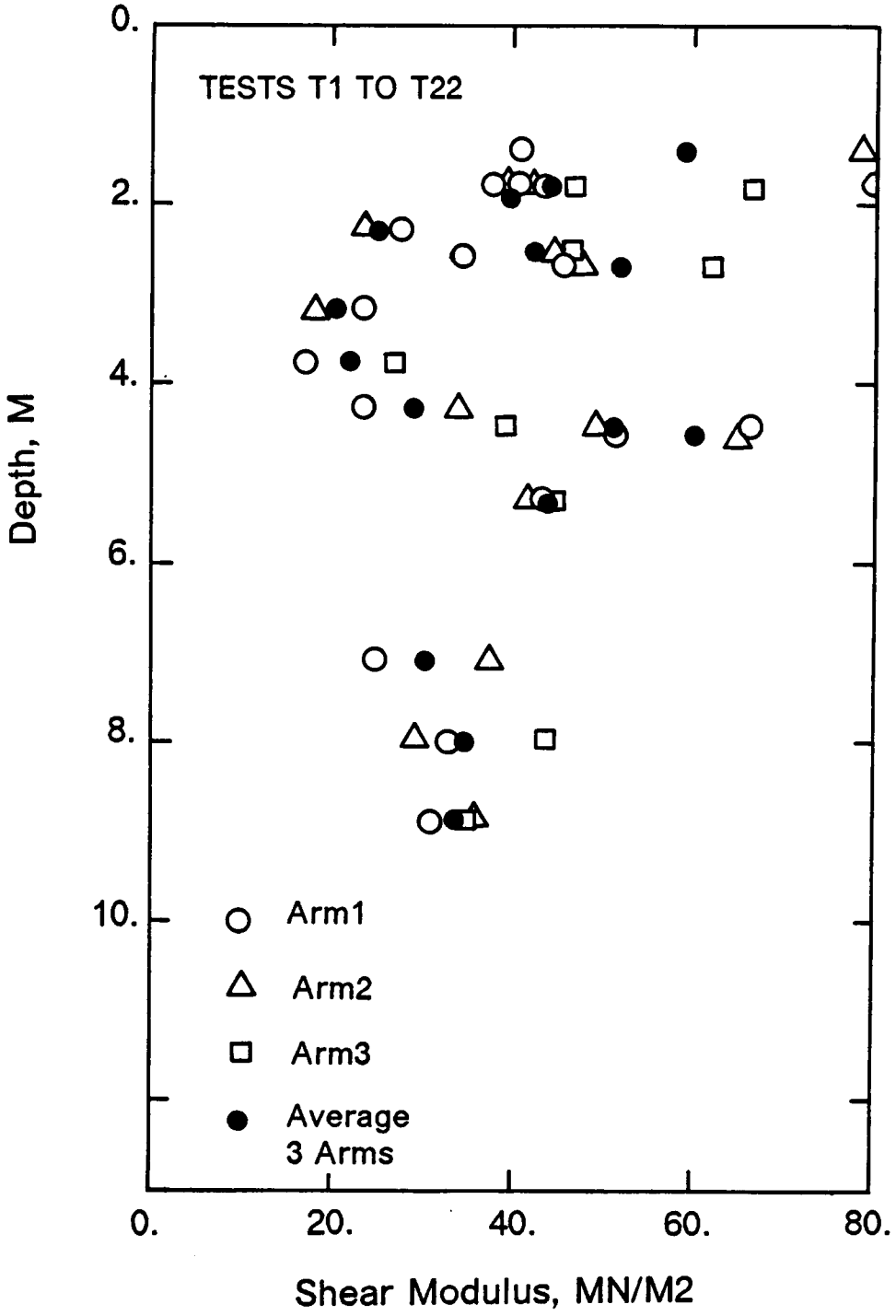

FIGURE 7.7 SHEAR MODULUS VALUES FROM UNLOAD-RELOAD CYCLES

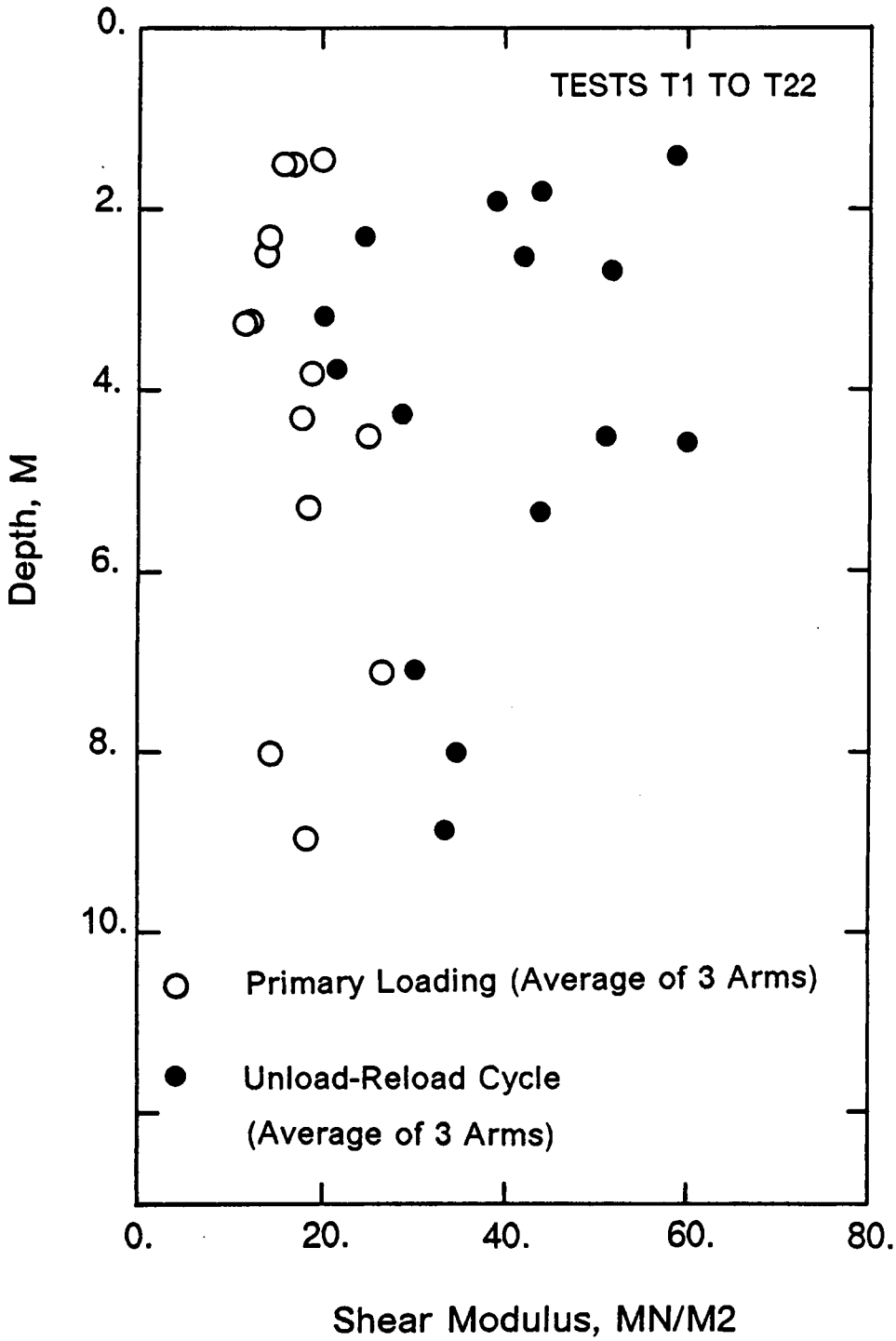

FIGURE 7.8 COMPARISON BETWEEN MODULUS VALUES BETWEEN PRIMARY LOADING AND UNLOAD-RELOAD CYCLES

average values reported in this study if the elastic modulus of the soil is computed from the shear modulus with a Poisson ratio equal to 0.2.

Robertson and Hughes (1986) report SBPM shear modulus values varying from 5 to 20 MN/M2 (52 to 208 tsf) from tests performed at similar depths in a loose to dense sand. These values are typically four times smaller than the SBPM values presented in Fig. 7.7.

Repeated unload-reload cycles were performed in the tests T20, T21 and T22 to observe if the shear modulus degrades under this loading condition. Ten cycles were performed during the test T20 and five cycles were during the tests T21 and T22. The results are presented in Fig. 7.9 where the ratio between the shear modulus G_i of the unload-reload cycle i and the shear modulus of the first unload-reload cycle G_1 is plotted against the cycle number. The results do not show any sign of degradation of the shear modulus with the number of cycles. The modulus G_i never differs more than 20% from the modulus G_1, the difference between the two being either positive or negative.

7.4 DILATION AND FRICTION ANGLES

7.4.1 Method

The method proposed by Hughes et al. (1977) was used to determine the maximum angles of dilation and friction of the residual soil from the SBPM test data. The method considers that the angle of friction is proportional to the rate of volume change during shear as suggested by Rowe (1962).

Assuming that the soil behaves as indicated in Fig. 7.10 (b), the method proposed by Hughes et al. (1977) leads to the expression:

$$\log\left(\frac{\Delta R}{R_o} + \frac{c}{2}\right) = \frac{n+1}{1-N}\log(p - u_o) + constant$$

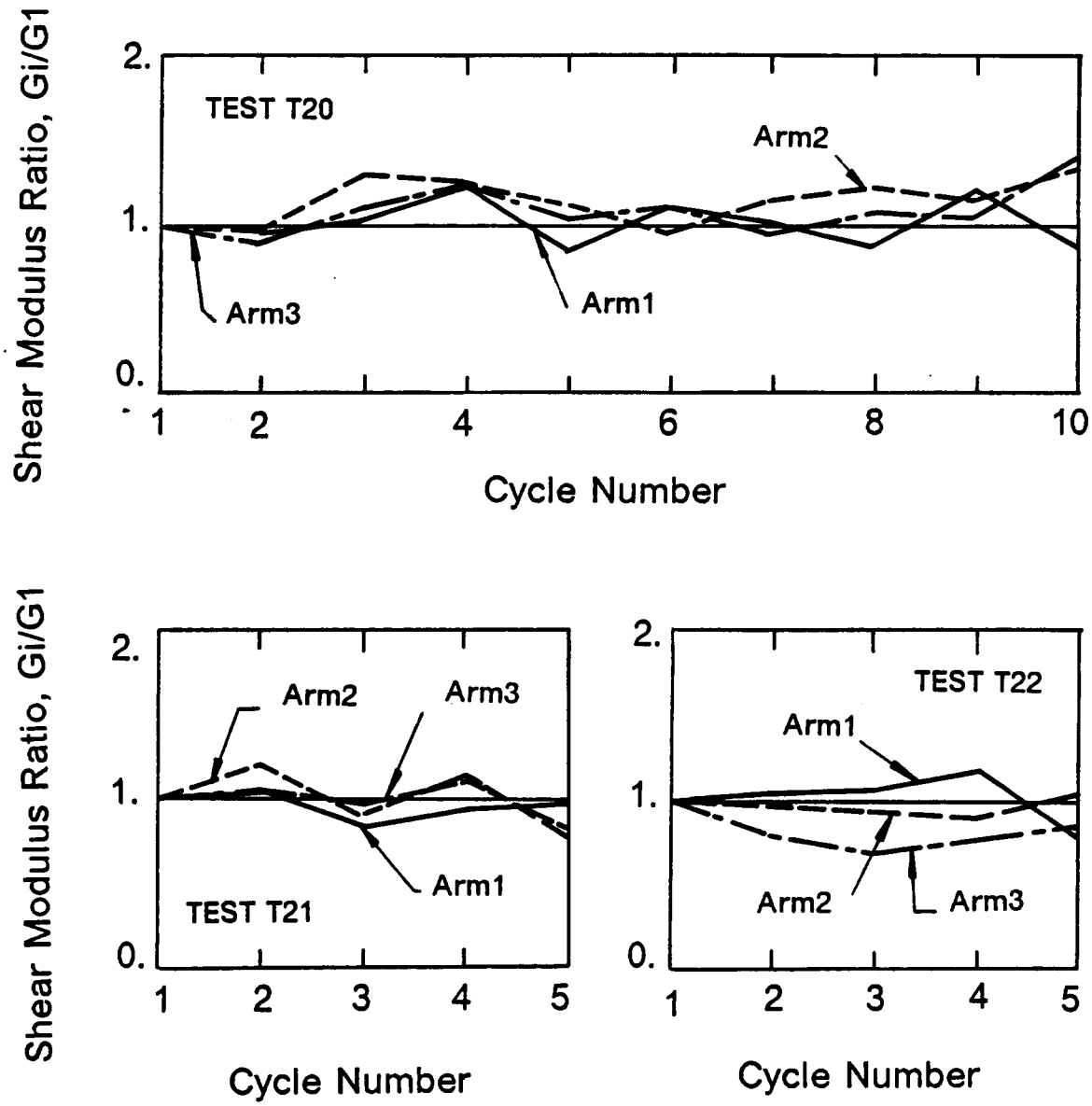

FIGURE 7.9 VARIATIONS OF THE SHEAR MODULUS WITH THE NUMBER OF UNLOAD-RELOAD CYCLES

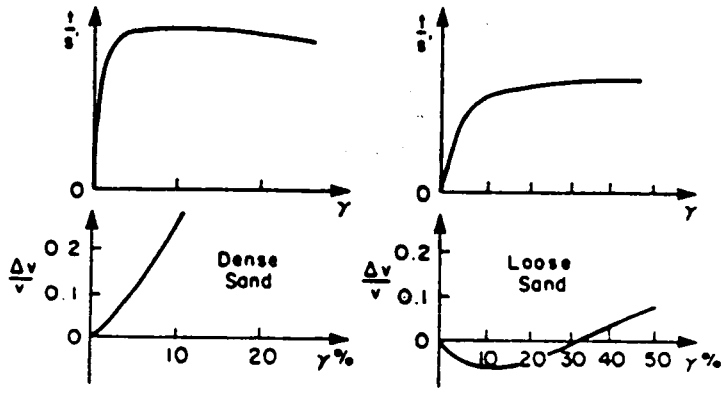

(a) Results of Simple Shear Tests (after Stroud, 1971)

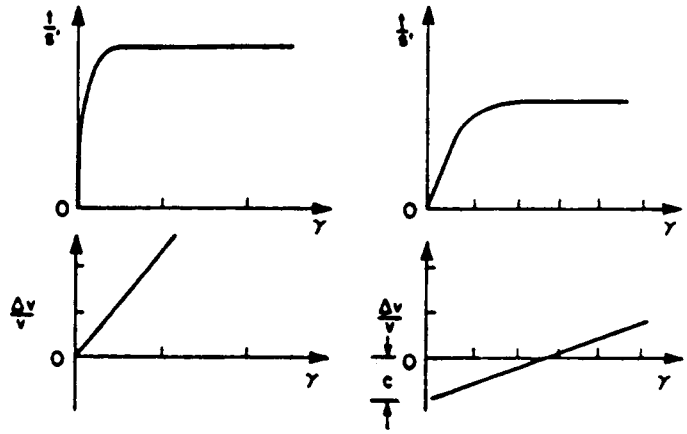

(b) Simplified Model assumed by Hughes et al. (1977)

FIGURE 7.10 SHEAR STRAIN AND VOLUMETRIC SHEAR STRAIN CURVES (AFTER ROBERTSON AND HUGHES, 1985)

with

R_o initial radius of the SBPM

ΔR change in radius of the SBPM

$\Delta R/R_o$ radial strain

c intercept shown in Fig. 7.10 (b)

P total pressuremeter pressure

u_o pore water pressure

$$\frac{1 - N}{1 + n} = \frac{1 + \sin v}{1 + \sin \Phi'} \sin \Phi' = slope\ s$$

$\sin v$ = maximum dilation rate

The preceeding expression indicates that the diagram of the radial strain versus the effective pressuremeter pressure tends towards a straight line of slope, s, when plotted on a log-log scale.

For dense sands, as indicated in Fig. 7.10, the rate of volume change is practically independant of the strain level and the relationship between the volume change and the shear strain proposed by Hughes et al. (1977) describes the volume changes occuring during shear. On the contrary, for loose to medium dense sands, the rate of volume change varies with the shear strain as indicated in Fig. 7.10. At 10% shear strain which represents the average shear strain in the soil around the SBPM when the membrane is fully expanded, the trend of volume change with the shear strain observed in Fig. 7.10 (a) is different from the one assumed by Hughes et al. (1977) in Fig.7.10 (b). This fact led Robertson and Hughes (1985) to propose a new correlations between the slope s, the friction angle at constant volume Φ_{cv} and the maximum angles of dilation and friction.

7.4.2 Results

The angle Φ_{cv} and the slope s are the input parameters for the correlation charts proposed by Robertson and Hughes (1985). The angle Φ_{cv} determined in Chapter 4 from the direct shear test results is 36 degrees.

A typical plot of the radial strain versus the effective pressuremeter pressure is shown in Fig. 7.11 in a log-log scale. In this example, the relationship between the two parameters tends towards a straight line of slope s equal to 0.29. Similar plots were developed from the data monitored by each arm in every test. A profile of the maximum angles of dilation and friction with depth is given in Fig. 7.12. The individual arm values and the average value per test are shown in the figure. The maximum dilation angle is in the range of -1 to +3 degrees. Friction angles determined from the results show little scatter, and indicate an average of 36 degrees. That this angle is the same as Φ_{cv} reflects the fact that the dilation angle is very small.

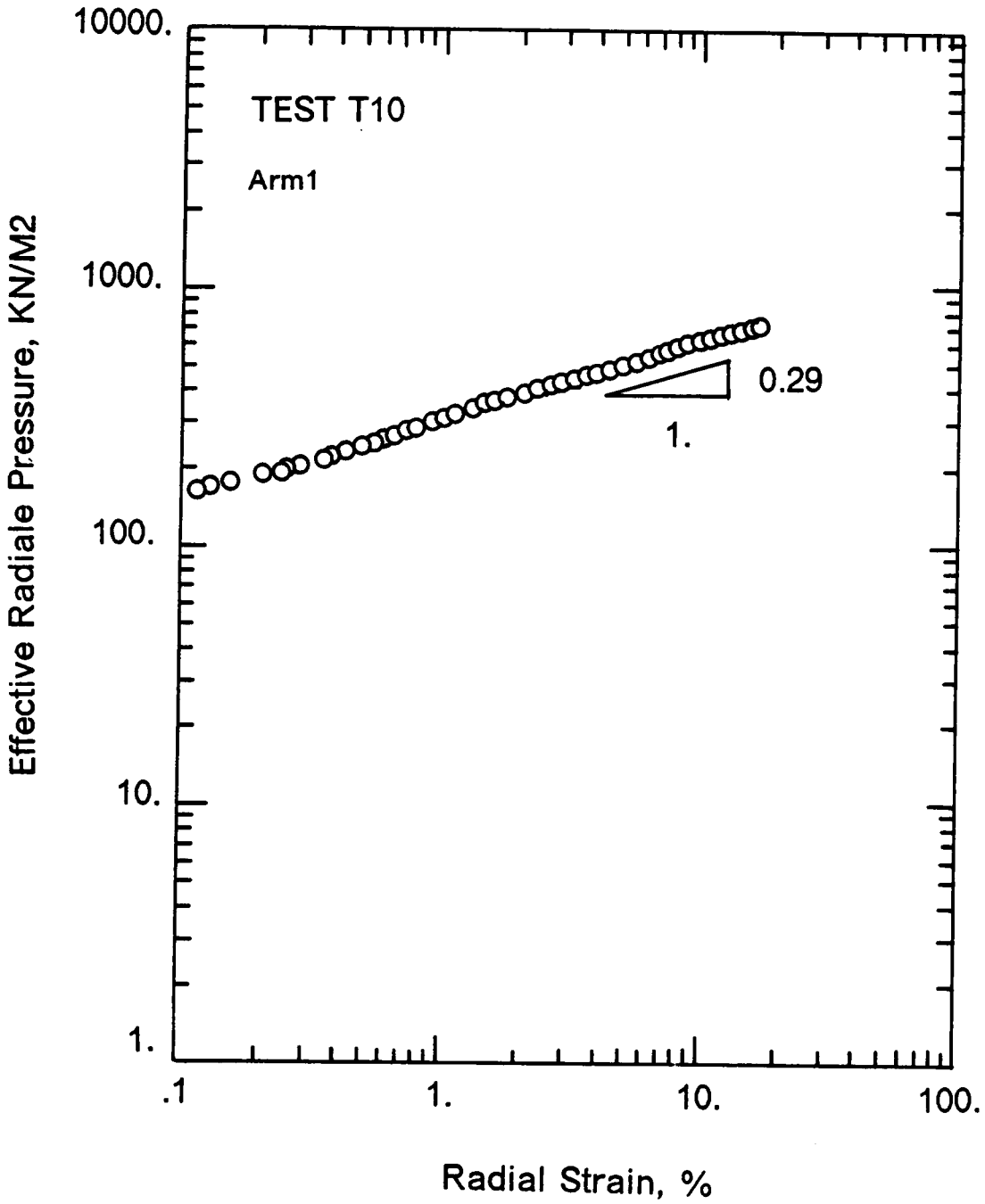

FIGURE 7.11 RADIAL STRAIN VERSUS EFFECTIVE RADIAL PRESSURE

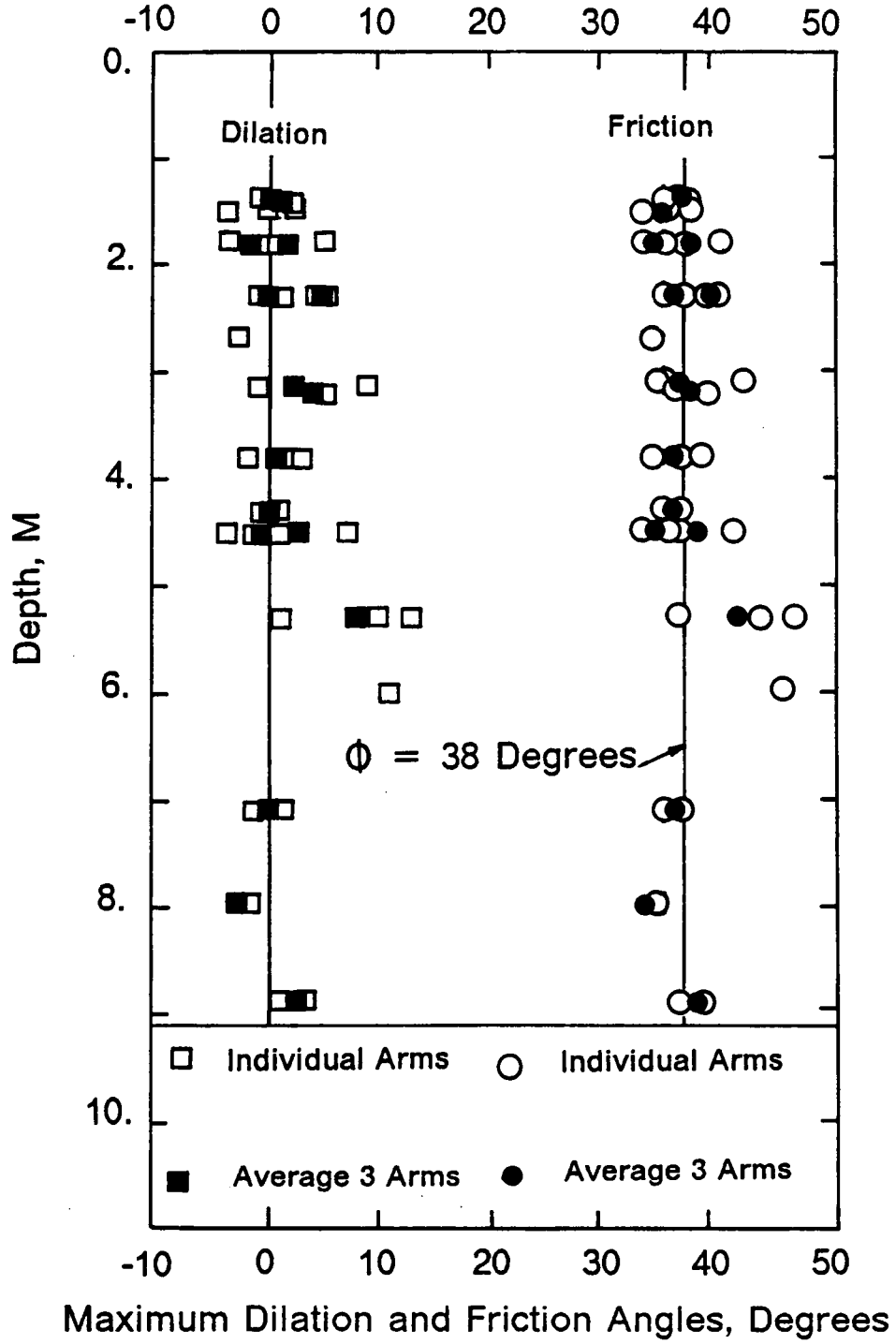

Note: Φ determined with Φ_{cv} = 36 degrees

FIGURE 7.12 PROFILE OF MAXIMUM DILATION AND FRICTION ANGLES

Chapter 8

SUMMARY AND CONCLUSIONS

8.1 SUMMARY

The prediction of geotechnical performance in stiff soils has been prone to a considerable amount of guess work and empiricism as the conventional approach of sampling and testing in the laboratory leads to information which is not consistent with the field performance. Generally, the structure of the soil and the fissures which are often present in the stiff soils and these features lead to failure in the laboratory tests which is inappropriate to field conditions.

In-situ testing offers an alternative for testing in stiff soils, and the pressuremeter has generated a particular interest. The Menard pressuremeter is the simplest form of this class of devices. It is placed in a predrilled hole and a cylindrical membrane is expanded against the sides of the hole. The resulting cavity expansion curve from the test is used to determine the lateral pressures in the soil, the soil stiffness, and the strength of the soil. In spite of its appealing nature and its widening use to determining design parameters for stiff soils, the

Menard pressuremeter has important drawbacks particularily through disturbance to the surrounding soil by the hole preparation and the lateral stress relief. The self-boring pressuremeter (SBPM) was developed to obviate these drawbacks. It drills itself into the ground while keeping intimate contact with the soil and avoiding the stress relief.

Experience to date with the SBPM in stiff soils has been limited. Results with the SBPM have generally shown stiffness and strength values that are higher than those obtained in conventional laboratory testing. It remains to establish if the parameters obtained from the SBPM tests are realistic, and this research was undertaken as a step in this direction.

This research is primarily experimental in nature and involves two sites in the Commonwealth of Virginia: A residual soil just outside Blacksburg and a stiff clay deposit in the downtown Richmond area. Testing at Blacksburg site allowed the investigator to gain experience with the equipment, to solve many of the special problems associated self-boring pressuremeter testing in stiff soils, and to develop an efficient data acquisition system to store the test data. This work also led to the generation of a valuable data base on the properties of the residual soils.

At Richmond site, a comparative study was performed between the soil parameters determined in the laboratory and those determined in situ. In the laboratory, tests were performed on samples taken from conventional pushed Shelby tubes and on high quality block samples. The test results were compared to the SBPM test results of this study and to Menard pressuremeter test results available in the literature. The comparison allows for important conclusions to be drawn relative to the impact of sample and test quality on design parameters for the Miocene clay and on the magnitude and orientation of the lateral stresses in the clay.

8.2 RESULTS AND CONCLUSIONS

The Miocene clay is classified as a medium gray, hard and non fissured clay of high plasticity. Sampling technique proved to be of primary importance in the determination of the soil parameters in the laboratory. The conventional procedure used in practice where Shelby tubes are pushed in led to significant disturbance. The results of the tests on the Shelby tube samples give lower modulus and strength values than the tests on the block samples, and the attendant data from the Shelby tube samples are scattered and often yield to inconsistent trends. On the contrary, the tests on high quality block samples indicate consistency in the results and in the behavior patterns.

Results of oedometer tests on the Miocene clay indicate that the field compression index, C_c, varies between 1.2 and 1.5, and the recompression index, C_r, between 0.14 and 0.16. Pre-consolidation pressures are determined between 1.3 and 1.6 MN/M2 (13 and 16 tsf) leading to overconsolidation ratio between 4 and 5. The undrained shear strength determined from UU tests performed on the block samples is of the order of 500 KN/M2 (73 psi). Tests results performed on Shelby tube samples are typically four times lower than the ones on the block samples. Full remolding of the soil lowers the strength well below that of the Shelby tube samples; average sensitivities are seven.

The residual soil situated near Blacksburg is heterogeneous by nature. It is generally a silty fine sand with blocks of weathered rock , except near the ground surface where the soil is classified as MH according to USCS. Sampling by pushing Shelby tubes was not found possible beyond 1 M (3.3 ft) deep as the soil is very stiff and nearly without plasicity. Standard Penetration Tests were performed continuously over a depth of 7 M (23 ft). Typical N values were found to vary between 10 and 30 blows/ft over the top 3 M (10 ft) and to remain constant and equal to 30 blows/ft below that depth.

Only a few tests were performed in the laboratory on the residual soils as quality sampling could not be obtained. The results of the tests which were conducted indicate that the preconsolidation pressure and the overconsolidation ratio are 200 to 300 KN/M2 (2 to 3 tsf) and 11 to 16 respectively at 1 M (3.3 ft) depth. Unconfined compression tests performed on disturbed soil samples taken from the cohesive layers indicate strength values which vary from 300 KN/M2 (3 tsf) at the ground surface to 150 KN/M2 (1.5 tsf) at 6 M (20 ft) depth. Direct shear tests carried out on dry non plastic silty sand indicate a friction angle at constant volume equal to 36 degrees.

Testing with the SBPM both of the stiff soils led to a number of new operational approaches to the work:

1. After experience showed that the normal, unreinforced pressuremeter membrane was frequently damaged during insertion, all subsequent testing was conducted using a flexible steel sheathed protective covering over the membrane known as a "Chinese lantern".

2. As the weight of the insertion equipment proved inadequate to advance the probe, a new adjustable frame was devised which could be connected to anchors drilled into the ground. The new frame served to hold the insertion equipment down and allow the probe to advance properly. This equipment was used to test the residual soil. In Richmond, a drill rig was used for the insertion of the probe in the ground as a matter of convenience, although the reaction frame could have served to advance the probe there as well.

3. Concern over the high pressures found necessary to expand the probe in stiff soils led to the development of a special calibration unit where it could be expanded under high pressures, and thus calibrated under conditions more like those encountered in the field. Test results in the new calibration unit indicate that no compliance of the strain arms of the probe occurs before lift-off, and that all the arms follow the same calibration response.

They also indicate that the calibration of the total pressure and pore pressure cells in the calibration sleeve supplied by the manufacturer of the probe is adequate.

4. Testing was performed with a new high pressure panel control unit for the pressuremeter and a new high capacity computarized data acquisition system.

The properties of the Miocene clay were interpreted from the SBPM test results. They can be summarized as follows:

1. Lateral pressures:

   The clay exhibits high lateral pressures with K_o values varying between 3 and 5 at 15 M (50 ft) depth. These values are larger than the ones normally found at similar depth in stiff soils with a same overconsolidation ratio. The absence of fissures in the clay seems to be at the origin of this potential for high lateral stresses. The test results indicate also that there is an anisotropic state of lateral stress which can be explained from the regional topography.

2. Undrained shear strength: The undrained shear strength obtained from the Baguelin, Ladanyi and Palmer (BLP) interpretation of the SBPM test results compare well to the laboratory values on the block samples.

   The Gibson Anderson (GA) interpretation of the SBPM test results provides a lower bound estimate of the undrained shear strength by a factor of 1 to 2.

   When expressed in terms of depth, the undrained shear strength values interpreted from the Menard pressuremeter test results with the empirical factor K_b equal to 3.2 agree well with the SBPM values obtained from the GA interpretation but they are approximatively half the strength values using the BLP interpretation.

3. Effective stresses: The effective stress paths determined from the SBPM test results show a consistent trend at failure when plotted in the octahedral plane. A direct comparison

with the stress paths from the laboratory tests is not possible as the boundary conditions are different in the two cases.

4. Modulus:

   The Menard pressuremeter modulus values are typically half the ones interpreted from the SBPM tests. The lateral stress relief ssociated to the prehole technique seems to disturbe the surrounding soil by overstressing.

   Modulus values from the SBPM compare well with the laboratory values when they are expressed in terms of the octahedral effective stress.

The interpretation of the SBPM tests performed in the residual soil indicate:

1. Lateral pressures:

   The residual soil exhibits high lateral pressures near the ground surface with K_o values of the order of 5. K_o decreases with depth and reaches values between 1 and 2 at 5 M (17 ft) depth and remains constant below that depth.

   The individual arm measurements indicate that, contrarily to the case of the Miocene clay, no anisotropy exists in the lateral stress field.

2. Modulus:

   The shear modulus values are of the same magnitude as as the shear modulus values of the Miocene clay. The elastic modulus computed from the shear modulus assuming a Poisson ratio equal to 0.2 are four times the modulus values determined from Menard pressuremeter tests performed in similar soils at other sites.

3. Friction angle:

   The maximum angle of friction interpreted from the SBPM tests show little scatter and indicate an average value of 36 degrees. This agrees with the Φ_{cv} value obtained in laboratory direct shear tests on reconstituted soil.

Appendix A

LOGS OF THE BORINGS IN THE MIOCENE CLAY

SCHNABEL ENGINEERING ASSOCIATES CONSULTING ENGINEERS	TEST BORING LOG	BORING NO.: B-203
PROJECT: 6TH STREET FESTIVAL MARKETPLACE, RICHMOND, VIRGINIA		SHEET NO. 1 OF 2
CLIENT: CHILTON ENGINEERING INC.		JOB NO.: V83742
BORING CONTRACTOR: AYER & AYERS INC	DRILL: CME 55	ELEVATION: 180.0±
WATER LEVEL DATA	DRIVE SAMPLER	CASING SIZE 3½"
DATE / TIME / DEPTH / CAVED	TYPE S.S.	DATE START: 1/27/84
ENCOUNTERED 1/27 / 9:37 / 34' / -	DIA. 2" OD	DATE FINISHED: 1/27/84
AFTER CASING PULLED 1/27 / 11:27 / MUD / 21.5'	WT. 140 #	DRILLER: J.T. STONE
___HR. READING BACKFILLED UPON COMPLETION	FALL 30"	INSPECTOR: S. COPLEY

STRATUM	DEPTH FT.	ELEV.	BLOWS ON SAMPLE SPOON, PER 6"	SYMBOL	IDENTIFICATION	REMARKS
	1.0	180.0±			ASPHALT CONCRETE	
A			3+4+6	S	CLAYEY SILT, FILL, SOME FINE SAND, MOIST-REDDISH BROWN (MH)	
			5+6+8	S		
			6+7+10	S	do, TRACE FINE SAND	FILL
	8.5		4+5+9	S	CLAYEY SILT, FILL, SOME FINE SAND, MOIST-REDDISH BROWN (ML)	
B		170	4+5+8	S	FINE CLAYEY SILTY SAND, MOIST-REDDISH BROWN (SM)	
			3+2+3	S	do, SOME CLAYEY SILT	
	18.0					
C		160	4+4+3	S	FINE TO MEDIUM SAND, SOME SILT, WITH FINE GRAVEL, MOIST-REDDISH BROWN (SM)	
			5+19+34	S	do, FINE TO COARSE SAND WITH FINE TO COARSE GRAVEL-BROWN	
		150	14+22+19	S	do, FINE TO COARSE GRAVELLY SAND	
			13+18+21	S	do, WET	
	40.0	140	8+6+4	S	SILTY CLAY, SOME FINE SAND, MOIST-MOTTLED BROWN & GRAY (CL)	MIOCENE
D			3+3+4	S		
	48.0				CLAY, TRACE FINE SAND, MOIST-DARK GRAY (CH)	
		130	3+3+4	S		
E				3"		Tube pushed 24" 24" Recovery
			4+5+8	S	do, TRACE ORGANIC MATTER	
				3"		Tube pushed 24" 24" Recovery
		120	4+4+5	S	do, SOME FINE SAND	
				3"		Tube pushed 24" 24" Recovery
			4+5+9	S	do, TRACE FINE SAND	

SCHNABEL ENGINEERING ASSOCIATES CONSULTING ENGINEERS	TEST BORING LOG	BORING NO.: B-203
PROJECT: 6TH STREET FESTIVAL MARKETPLACE, RICHMOND, VIRGINIA		SHEET NO 2 OF 2
CLIENT: CHILTON ENGINEERING INC.		JOB NO: V83742
BORING CONTRACTOR: AYERS & AYERS INC.		ELEVATION: 180.0±

DEPTH FT.	ELEV.	BLOWS ON SAMPLE SPOON PER 6"	SYMBOL	IDENTIFICATION	REMARKS
				BORING TERMINATED AT 65.5 FEET	

SCHNABEL ENGINEERING ASSOCIATES CONSULTING ENGINEERS	TEST BORING LOG	BORING NO.: B-202
PROJECT: 6TH STREET FESTIVAL MARKETPLACE, RICHMOND, VIRGINIA		SHEET NO. 1 OF 2
CLIENT: CHILTON ENGINEERING INC.		JOB NO. V83742
BORING CONTRACTOR: AYERS & AYERS INC.	DRILL: CME 55	ELEVATION: 178.4±
WATER LEVEL DATA	DRIVE SAMPLER	CASING SIZE: 3½"
DATE TIME DEPTH CAVED	TYPE S.S.	DATE START: 1/26/84
ENCOUNTERED 1/26 10:05 34' -	DIA. 2" OD	DATE FINISHED: 1/26/84
AFTER CASING PULLED 1/26 3:02 MD 18'	WT. 140#	DRILLER: J.T. STONE
___HR. READING BACKFILLED UPON COMPLETION	FALL 30"	INSPECTOR: S. COPLEY

STRATUM	DEPTH FT.	ELEV. 178.4+	BLOWS ON SAMPLE SPOON, PER 6"	SYMBOL	IDENTIFICATION	REMARKS
					12"± ASPHALT, CRUSHED STONE & SAND	
A			2+4+4	S	CLAY, FILL, SOME FINE SAND, MOIST-REDDISH BROWN (CH)	
			2+2+4	S		
			2+3+5	S	do, SOME FINE TO MEDIUM SAND	
		170	3+5+5	S	do, SOME FINE SAND	FILL
			3+4+4	S		
	13.0					
B			2+4+7	S	FINE TO MEDIUM CLAYEY SILTY SAND, MOIST-REDDISH BROWN (SM)	
	17.0					
C		160	4+7+8	S	FINE TO MEDIUM SAND, SOME SILTY CLAY, MOIST-REDDISH BROWN (SC)	PLEISTOCENE
			7+6+8	S		
			5+11+13	S	do, FINE TO COARSE SAND	
		150				
	30.0		2+6+8	S	do, SOME FINE GRAVEL-BROWN	
B					FINE CLAYEY SILTY SAND, MOIST-LIGHT GRAY (SM)	
	33.0					
C			13+12+11	S	FINE TO COARSE SANDY GRAVEL, SOME SILTY CLAY, WET-BROWN (GC)	
		140	28+27+26	S		
	42.0					
D			3+3+6	S	SILTY CLAY, SOME FINE SAND, MOIST-MOTTLED BROWN & GRAY (CL)	MIOCENE
	47.0					
E		130		3"	CLAY, TRACE FINE SAND, MOIST-DARK GRAY (CH)	Tube pushed 24" 24" Recovery
			3+4+4	S		
			3+4+4	S		
		120				
			5+6+10	S		
			4+6+11	S		

SCHNABEL ENGINEERING ASSOCIATES CONSULTING ENGINEERS	TEST BORING LOG	BORING NO.: B-202
PROJECT: 6TH STREET FESTIVAL MARKETPLACE, RICHMOND, VIRGINIA		SHEET NO 2 OF 2
CLIENT: CHILTON ENGINEERING INC		JOB NO : V83742
BORING CONTRACTOR: AYERS & AYERS INC		ELEVATION: 178.4+

DEPTH FT.	ELEV.	BLOWS ON SAMPLE SPOON PER 6"	SYMBOL	IDENTIFICATION	REMARKS
	110		3"	CLAY, TRACE FINE SAND, MOIST-DARK GRAY (CH)	Tube pushed 24" 24" Recovery
			S		
			3"		Tube pushed 24" 24" Recovery
75.5			S		
				BORING TERMINATED AT 75.5 FEET	

SCHNABEL ENGINEERING ASSOCIATES
CONSULTING ENGINEERS

TEST BORING LOG

BORING NO: B-181

PROJECT: EXHIBITION CENTER, 5TH & MARSHALL STS., RICHMOND, VIRGINIA
SHEET NO: 1 OF 2
CLIENT: MARRIOTT CORPORATION
JOB NO: 884406
BORING CONTRACTOR: AYERS & AYERS, INC.
DRILL: CME-55
ELEVATION: 171.5
CASING SIZE: 3-1/2"
DATE START: 6/15/84
DATE FINISHED: 6/15/84
DRILLER: C. JAMERSON
INSPECTOR: T. MASON

WATER LEVEL DATA	DATE	TIME	DEPTH	CAVED
ENCOUNTERED	6/15	9:30	19.0'	-
AFTER CASING PULLED	6/15	11:45	19.8'	19.8'
HR. READING	BACKFILLED UPON COMPLETION			

DRIVE SAMPLER	S.S.
TYPE	
DIA.	2" O.D.
WT.	140#
FALL	30"

STRATUM	DEPTH FT.	ELEV.	BLOWS ON SAMPLE SPOON PER 6"	SYMBOL	IDENTIFICATION	REMARKS
		171.5			GRAVEL PARKING LOT	
			4+3+3	S	FINE TO COARSE SILTY SAND, FILL, WITH ROCK AND	FILL
A	2.0	170			BRICK FRAGMENTS AND GRAVEL, MOIST - DARK BROWN	
			3+5+7	S	(SM)	
					SILTY CLAY, PROBABLE FILL, SOME FINE TO COARSE	PROBABLE FILL
A1			2+3+4	S	SAND, MOIST - BROWN (CL)	
	7.0					
B			2+5+9	S	SILTY CLAY, SOME FINE TO COARSE SAND, TRACE	
	9.0				GRAVEL, MOIST - RED TO YELLOW (CL)	
			11+16+19	S	FINE TO COARSE SANDY GRAVEL, SOME SILTY CLAY,	
C		160			MOIST - MOTTLED GRAY AND TAN (GC)	
	14.0					
			7+9+10	S	FINE TO COARSE SAND, SOME SILTY CLAY, WITH	
					GRAVEL, MOIST - LIGHT BROWN (SC)	
B			3+3+5	S	DO, FINE TO MEDIUM, WET	
		150				PLEISTOCENE
						TERRACE DEPOSITS
	24.0					
			2+3+1	S	FINE TO COARSE SAND, SOME CLAYEY SILT, WITH	
					GRAVEL, WET - LIGHT TAN (SM)	
	29.0					
			12+15+25	S	FINE TO COARSE SANDY GRAVEL, SOME SILT, WET -	
C					BROWN (GM)	
		140				
	34.0					
			3+4+5	S	SILTY CLAY, TRACE FINE SAND, MOIST - MOTTLED	
					LIGHT GRAY AND LIGHT BROWN (CL)	
			2+3+3	S	DO, FINE SANDY - DARK GRAY	
D						MIOCENE
		130				
	44.0					
			2+3+4	S	FINE SILTY CLAYEY SAND, MOIST - DARK GRAY (SC)	
	49.0					
E			3+3+4	S	CLAY, TRACE FINE SAND, MOIST - DARK GRAY (CH)	

SCHNABEL ENGINEERING ASSOCIATES CONSULTING ENGINEERS	TEST BORING LOG	BORING NO: B-101
PROJECT: EXHIBITION CENTER, 5TH & MARSHALL STS., RICHMOND, VIRGINIA		SHEET NO: 2 OF 2
CLIENT: MARRIOTT CORPORATION		JOB NO: V84406
BORING CONTRACTOR: AYERS & AYERS, INC.	DRILL: CME-55	ELEVATION: 171.5
WATER LEVEL DATA	DRIVE SAMPLER	CASING SIZE: 3-1/2"
DATE: 6/15	TYPE: S.S.	DATE START: 6/15/84
ENCOUNTERED: TIME: 9:30	DIA.: 2" O.D.	DATE FINISHED: 6/15/84
AFTER CASING PULLED: DEPTH: 19.0'	WT.: 140#	DRILLER: C. JAMERSON
HR. READING: CAVED: -	FALL: 30"	INSPECTOR: J. MASON
BACKFILLED UPON COMPLETION		

STRATUM	DEPTH FT.	ELEV.	BLOWS ON SAMPLE SPOON, PER 6"	SYMBOL	IDENTIFICATION	REMARKS
		120			CLAY, TRACE FINE SAND, MOIST - DARK GRAY (CH)	
			REC=73%	3"		
			5+9+12	S		
E			REC=100%	3"		MIOCENE
		110	6+6+14	S		
			REC=100%	3"		
	70.0		6+7+14	S		
					BORING TERMINATED AT 70.0 FT	

SCHNABEL ENGINEERING ASSOCIATES CONSULTING ENGINEERS	TEST BORING LOG	BORING NO: B-114
PROJECT: EXHIBITION CENTER, 5TH & MARSHALL STS., RICHMOND, VIRGINIA		SHEET NO: 2 OF 2
CLIENT: MARRIOTT CORPORATION		JOB NO: VR4406
BORING CONTRACTOR: AYERS & AYERS, INC.	DRILL: CME-55	ELEVATION: 170.5
WATER LEVEL DATA	DRIVE SAMPLER	CASING SIZE: 3-1/8"
DATE: 6/11	TIME: 10:00	DEPTH: 20.0'	CAVED: -	TYPE: S.S.	DATE START: 6/11/84
ENCOUNTERED				DIA.: 2" O.D.	DATE FINISHED: 6/11/84
AFTER CASING PULLED: 6/11	2:30	DRY	7.0'	WT.: 140#	DRILLER: T. AYERS, SR.
24 HR. READING: 6/12	2:30	16.5'	24.7'	FALL: 30"	INSPECTOR: T. MASON

STRATUM	DEPTH FT.	ELEV.	BLOWS ON SAMPLE SPOON, PER 6"	SYMBOL	IDENTIFICATION	REMARKS
D	52.0	120			CLAY, SOME FINE SAND, MOIST - DARK GRAY (CH)	
			6+7+22	S	CLAY, TRACE FINE SAND, MOIST - DARK GRAY (CH)	
			REC=100%	3"		
E			6+8+20	S		MIOCENE
		110				
			REC=5%	3"		
			5+6+13	S		
			REC=100%	3"	DO, SOME FINE SAND	
			5+7+10	S		
		100				
			REC=100%	3"		
	72.5				BORING TERMINATED AT 72.5 FT	

SCHNABEL ENGINEERING ASSOCIATES
CONSULTING ENGINEERS

TEST BORING LOG

BORING NO: B-114

PROJECT: EXHIBITION CENTER, 5TH & MARSHALL STS., RICHMOND, VIRGINIA
SHEET NO: 1 OF 2
CLIENT: MARRIOTT CORPORATION
JOB NO: V84486
BORING CONTRACTOR: AYERS & AYERS, INC.
DRILL: CME-55
ELEVATION: 170.5
CASING SIZE: 3-1/4"
DRIVE SAMPLER
DATE START: 6/11/84
DATE FINISHED: 6/11/84
DRILLER: J. AYERS, SR.
INSPECTOR: J. MASON

WATER LEVEL DATA

	DATE	TIME	DEPTH	CAVED
ENCOUNTERED	6/11	10:00	20.0'	-
AFTER CASING PULLED	6/11	2:30	DRY	7.0'
24 HR. READING	6/12	2:30	16.5'	24.7'

TYPE	S.S.
DIA.	2" O.D.
WT.	140#
FALL	30"

STRATUM	DEPTH FT.	ELEV.	BLOWS ON SAMPLE SPOON PER 6"	SYMBOL	IDENTIFICATION	REMARKS
		170.5			GRAVEL PARKING LOT	
		170	4+4+3	S	FINE TO COARSE SANDY SILTY CLAY, FILL, WITH BRICK, GRAVEL AND ROCK FRAGMENTS, MOIST - DARK	FILL
A	2.0		2+2+4	S	BROWN AND ORANGE-BROWN (CL)	
A1			2+2+4	S	SILTY CLAY, PROBABLE FILL, SOME FINE TO MEDIUM SAND, MOIST - TAN TO BROWN (CL)	PROBABLE FILL
	7.0				DO, MOTTLED DARK BROWN AND BROWN	
			2+6+7	S	FINE TO COARSE SANDY SILTY CLAY, WITH FINE GRAVEL, MOIST - MOTTLED LIGHT GRAY AND TAN (CL)	
	9.0		7+9+14	S	FINE TO COARSE SILTY CLAYEY SAND, WITH GRAVEL, MOIST - MOTTLED LIGHT GRAY AND TAN (SC)	
		160				
B			3+4+11	S		PLEISTOCENE TERRACE DEPOSITS
	19.0				FINE TO COARSE SANDY GRAVEL, SOME SILTY CLAY,	
			9+17+17	S	MOIST - LIGHT GRAY (GC)	
		150				
C	24.0					
			3+23+32	S	FINE TO COARSE SAND, TRACE SILT AND GRAVEL, WET - BROWN (SM)	
	29.0					
			3+3+4	S	SILTY CLAY, TRACE FINE SAND, WET - MOTTLED BROWN AND LIGHT GRAY (CL)	
		140				
	34.5		3+4+5	S		
D					CLAY, TRACE FINE SAND, MOIST - DARK GRAY (CH)	MIOCENE
			REC=100%	3"		
			2+3+3	S		
		130				
			3+3+5	S	DO, SOME FINE SAND	
			5+4+8	S		

Appendix B

OEDOMETER TEST RESULTS IN THE MIOCENE CLAY

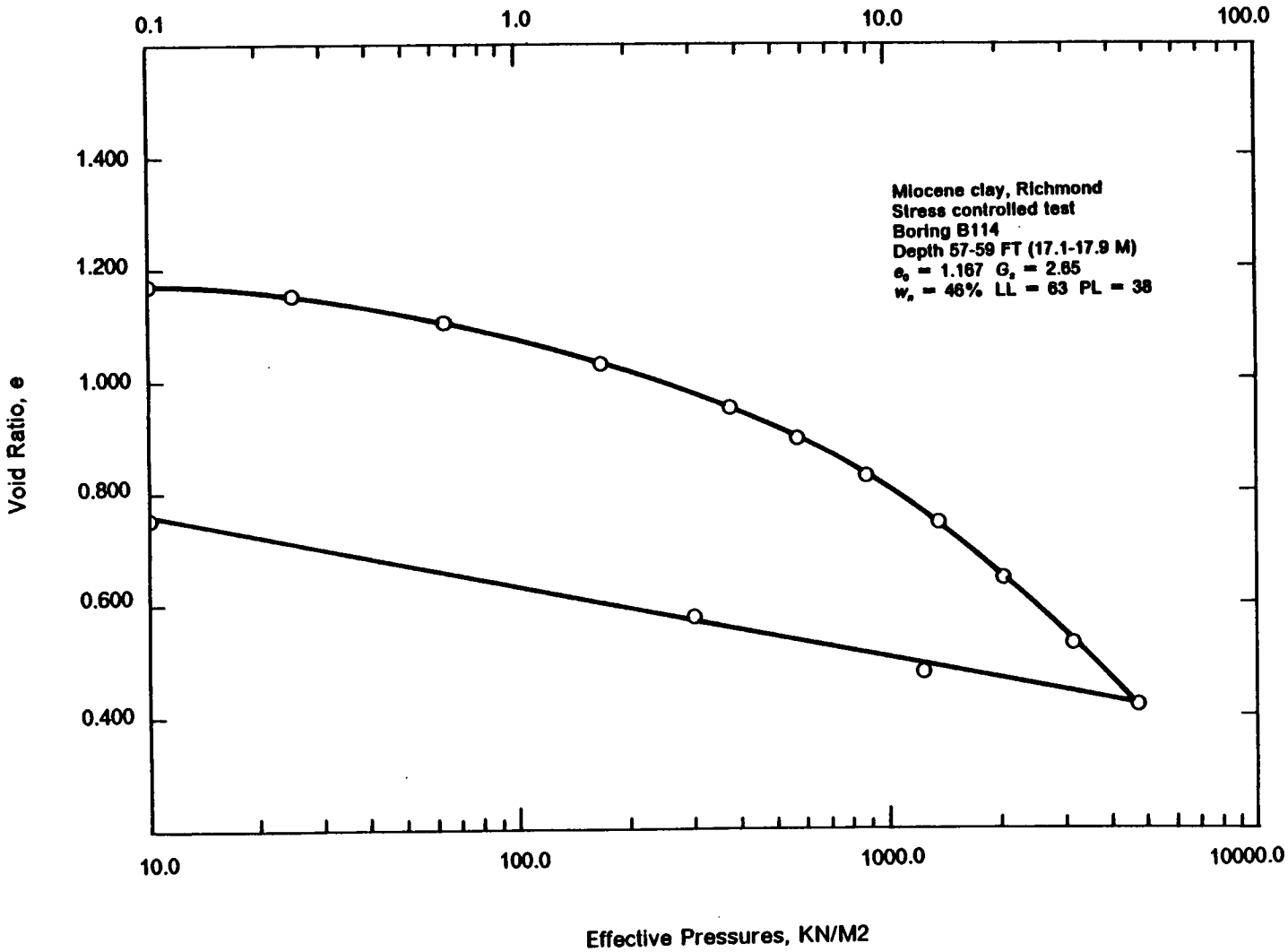
Effective Pressures, TSF
0.1
1.0
10.0
100.0
1.400
1.200
1.000
0.800
0.600
0.400
Void Ratio, e
Miocene clay, Richmond
Stress controlled test
Boring B114
Depth 57-59 FT (17.1-17.9 M)
e_o = 1.167 G_s = 2.65
w_n = 46% LL = 63 PL = 38
10.0
100.0
1000.0
10000.0
Effective Pressures, KN/M2

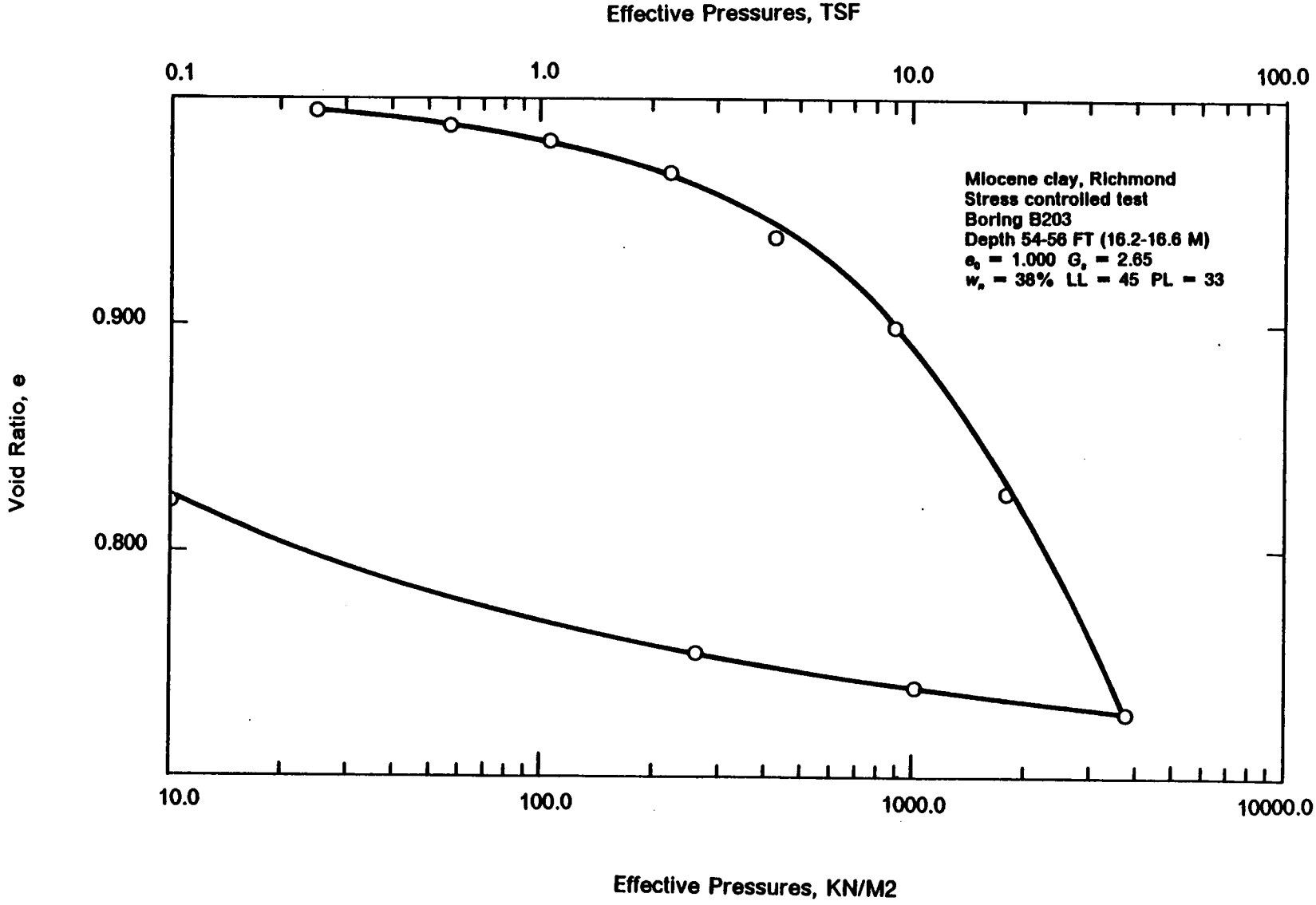
Effective Pressures, TSF
0.1
1.0
10.0
100.0
Miocene clay, Richmond
Stress controlled test
Boring B203
Depth 54-56 FT (16.2-16.6 M)
e_0 = 1.000 G_s = 2.65
w_n = 38% LL = 45 PL = 33
0.900
0.800
Void Ratio, e
10.0
100.0
1000.0
10000.0
Effective Pressures, KN/M2

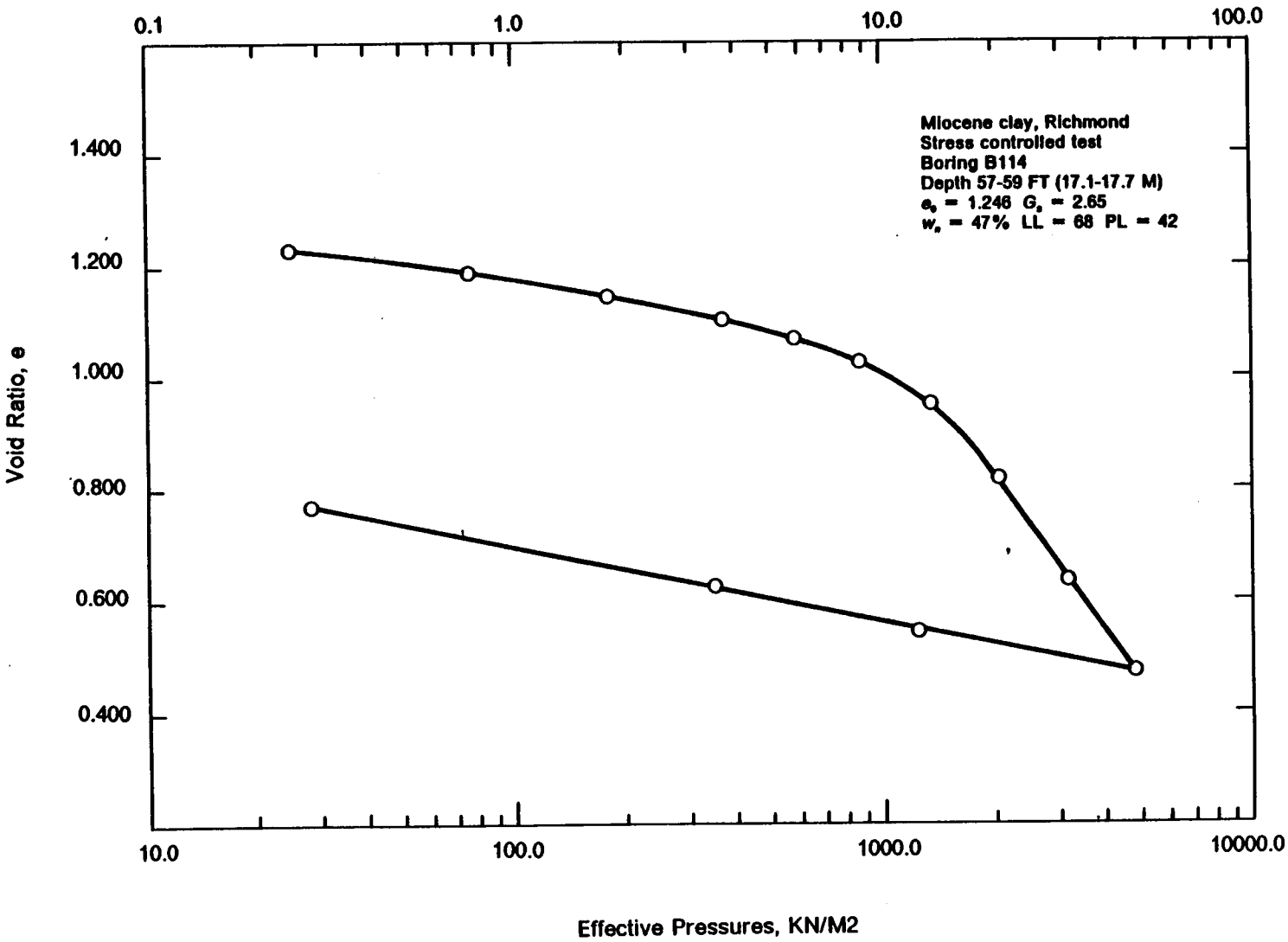
Effective Pressures, TSF
0.1
1.0
10.0
100.0
Miocene clay, Richmond
Stress controlled test
Boring B114
Depth 57-59 FT (17.1-17.7 M)
e_o = 1.246 G_s = 2.65
w_n = 47% LL = 68 PL = 42
Void Ratio, e
1.400
1.200
1.000
0.800
0.600
0.400
10.0
100.0
1000.0
10000.0
Effective Pressures, KN/M2

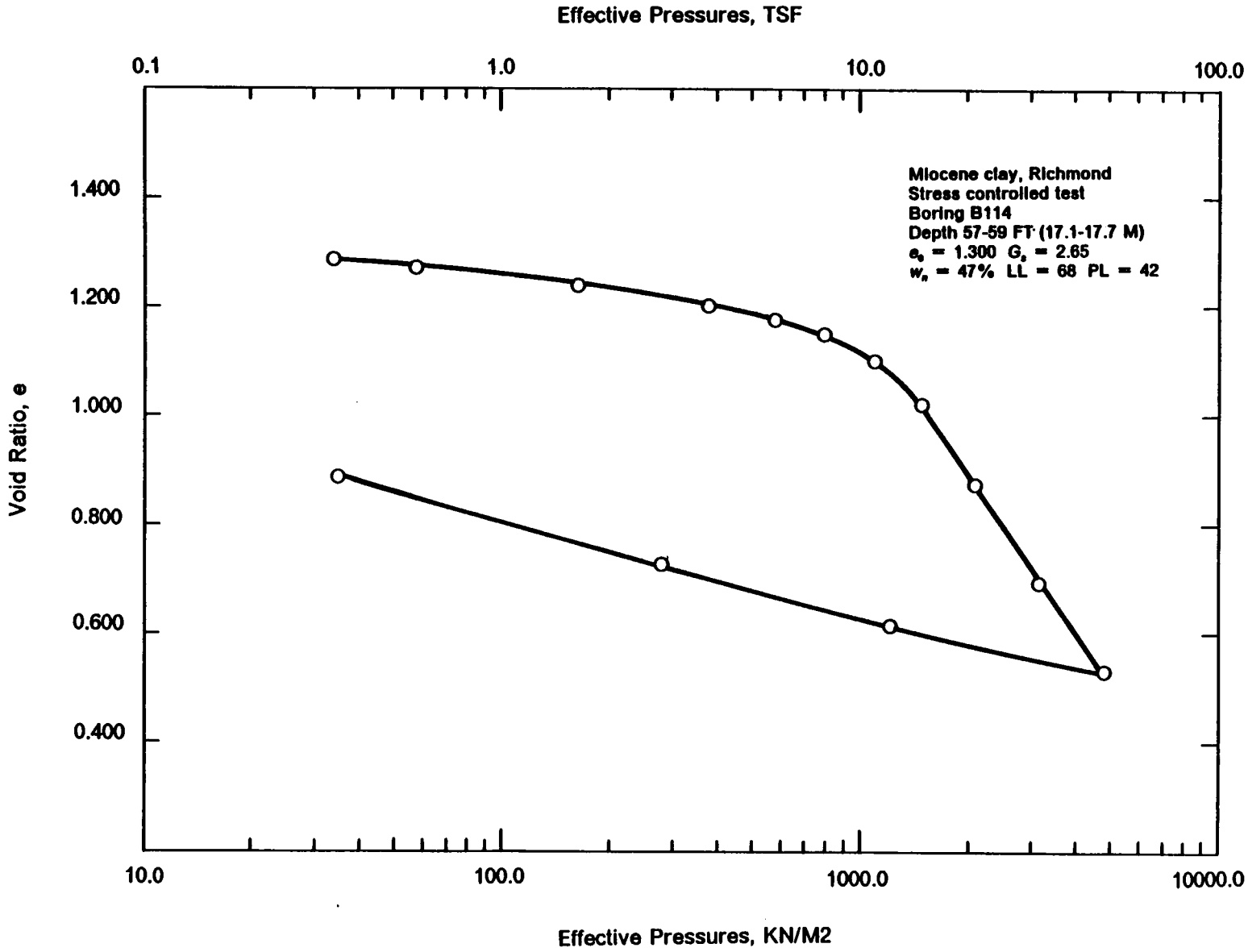
Effective Pressures, TSF
0.1
1.0
10.0
100.0
Miocene clay, Richmond
Stress controlled test
Boring B114
Depth 57-59 FT (17.1-17.7 M)
e_o = 1.300 G_s = 2.65
w_n = 47% LL = 68 PL = 42
Void Ratio, e
1.400
1.200
1.000
0.800
0.600
0.400
10.0
100.0
1000.0
10000.0
Effective Pressures, KN/M2

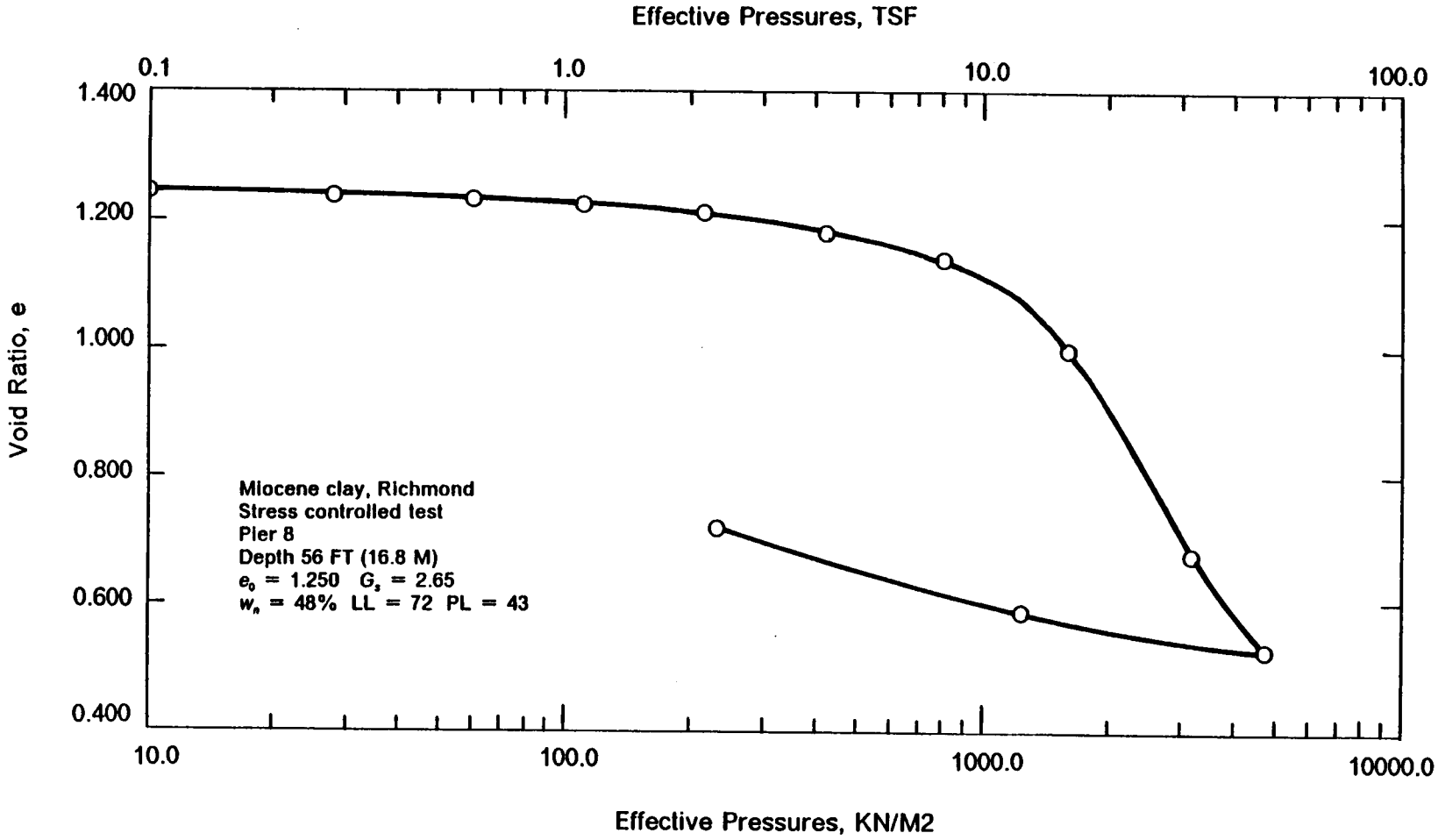
Effective Pressures, TSF
0.1
1.0
10.0
100.0
1.400
1.200
1.000
0.800
0.600
0.400
Void Ratio, e
Miocene clay, Richmond
Stress controlled test
Pier 8
Depth 56 FT (16.8 M)
e_0 = 1.250 G_s = 2.65
w_n = 48% LL = 72 PL = 43
10.0
100.0
1000.0
10000.0
Effective Pressures, KN/M2

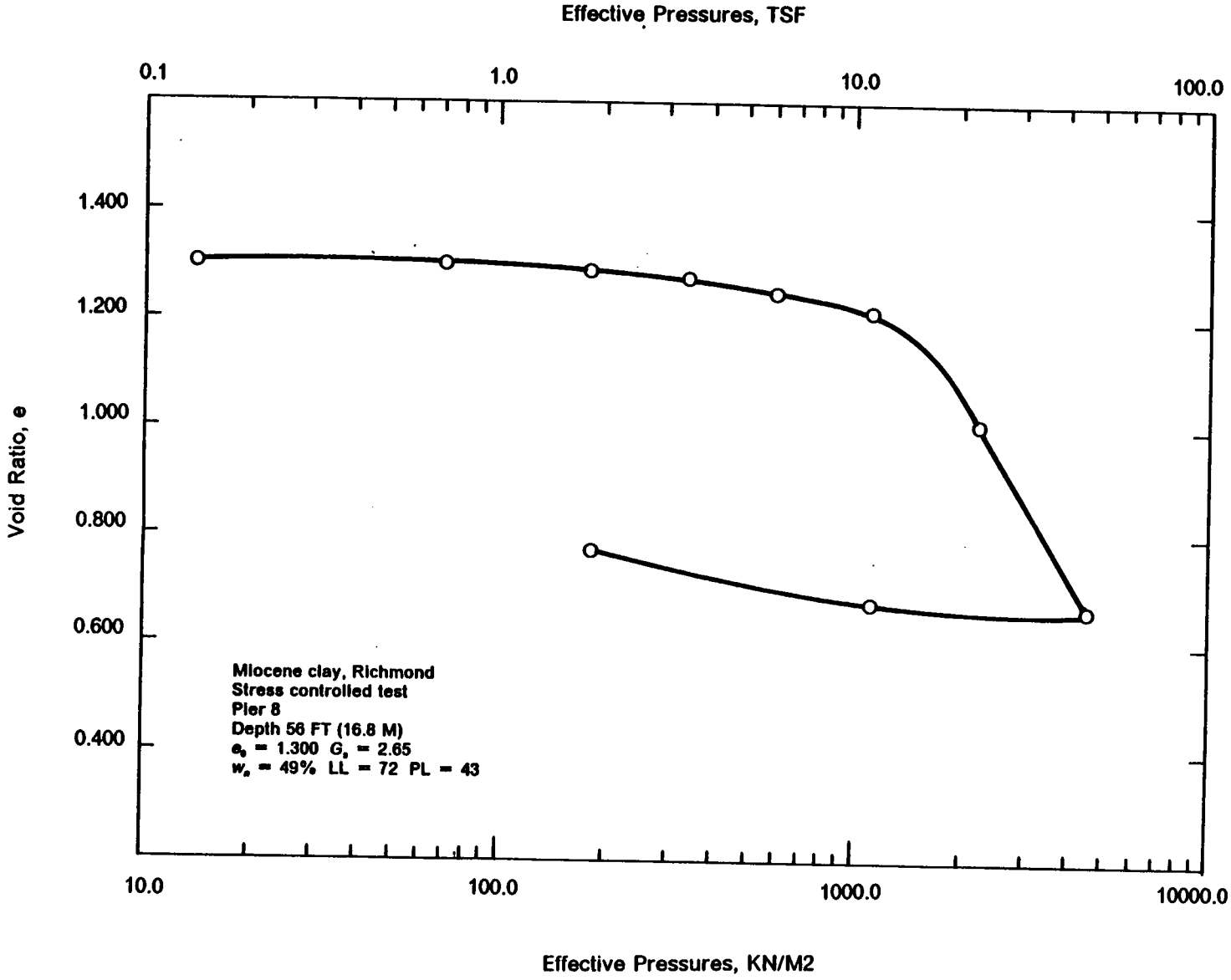
Effective Pressures, TSF
0.1
1.0
10.0
100.0
1.400
1.200
1.000
0.800
0.600
0.400
Void Ratio, e
Miocene clay, Richmond
Stress controlled test
Pier 8
Depth 56 FT (16.8 M)
e_o = 1.300 G_s = 2.65
w_o = 49% LL = 72 PL = 43
10.0
100.0
1000.0
10000.0
Effective Pressures, KN/M2

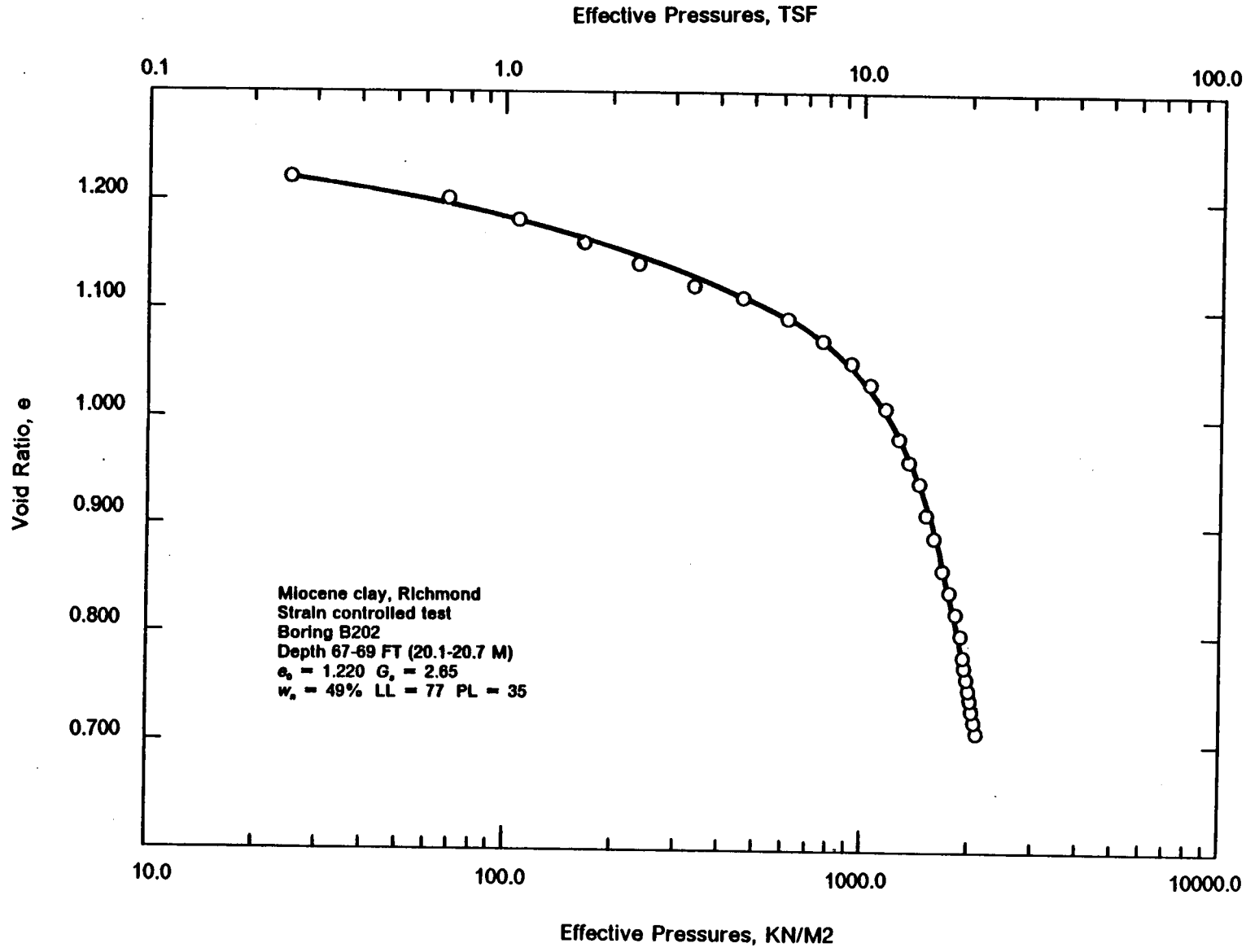
Effective Pressures, TSF
0.1
1.0
10.0
100.0
1.200
1.100
1.000
0.900
0.800
0.700
Void Ratio, e
Miocene clay, Richmond
Strain controlled test
Boring B202
Depth 67-69 FT (20.1-20.7 M)
e_o = 1.220 G_s = 2.65
w_n = 49% LL = 77 PL = 35
10.0
100.0
1000.0
10000.0
Effective Pressures, KN/M2

Appendix C

UU TRIXIAL TEST RESULTS IN THE MIOCENE CLAY

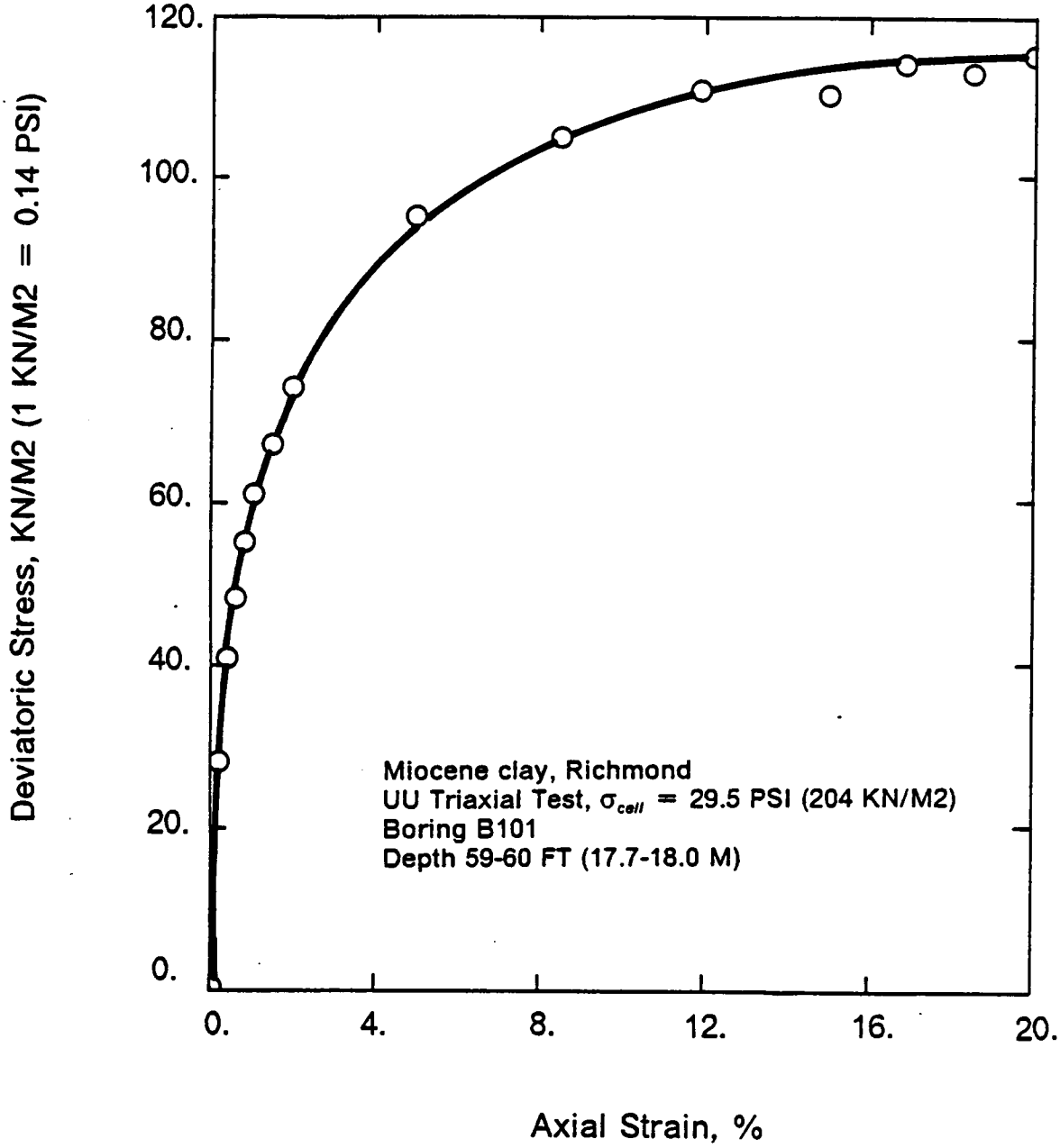
Deviatoric Stress, KN/M2 (1 KN/M2 = 0.14 PSI)
120.
100.
80.
60.
40.
20.
0.
0.
4.
8.
12.
16.
20.
Axial Strain, %
Miocene clay, Richmond
UU Triaxial Test, σ_{cell} = 29.5 PSI (204 KN/M2)
Boring B101
Depth 59-60 FT (17.7-18.0 M)

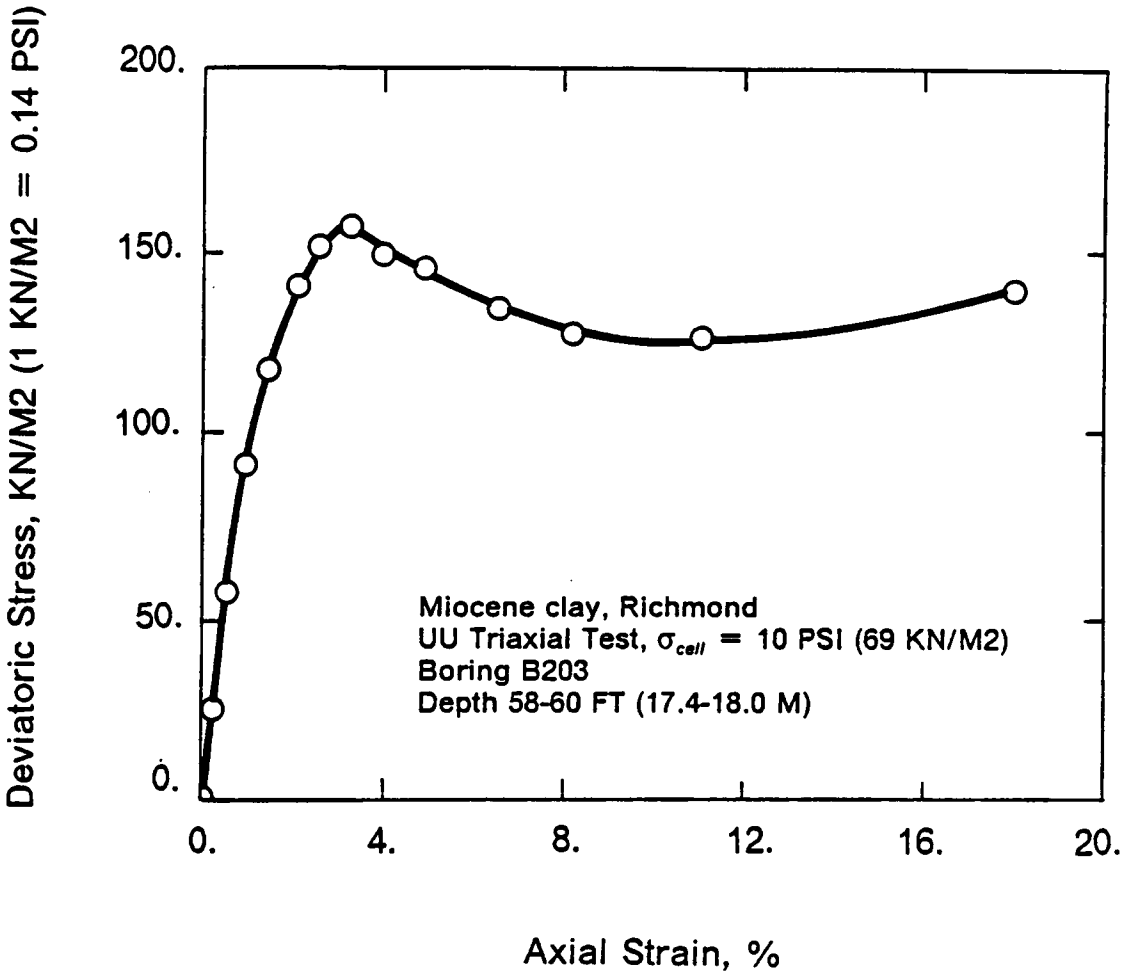
Deviatoric Stress, KN/M2 (1 KN/M2 = 0.14 PSI)
200.
150.
100.
50.
0.
0.
4.
8.
12.
16.
20.
Axial Strain, %
Miocene clay, Richmond
UU Triaxial Test, σ_{cell} = 10 PSI (69 KN/M2)
Boring B203
Depth 58-60 FT (17.4-18.0 M)

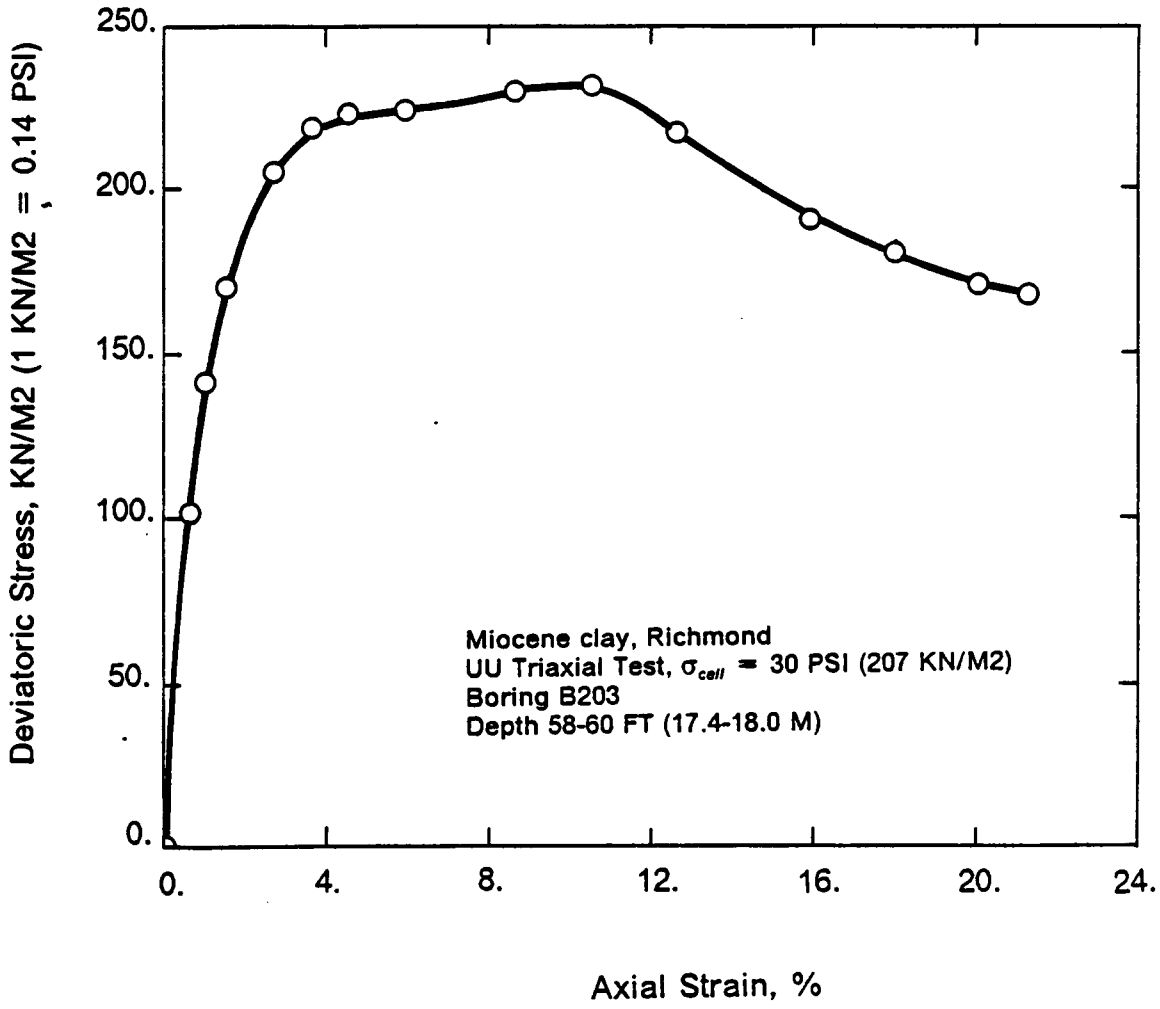
Deviatoric Stress, KN/M2 (1 KN/M2 = 0.14 PSI)
250.
200.
150.
100.
50.
0.
0.
4.
8.
12.
16.
20.
24.
Axial Strain, %
Miocene clay, Richmond
UU Triaxial Test, σ_{cell} = 30 PSI (207 KN/M2)
Boring B203
Depth 58-60 FT (17.4-18.0 M)

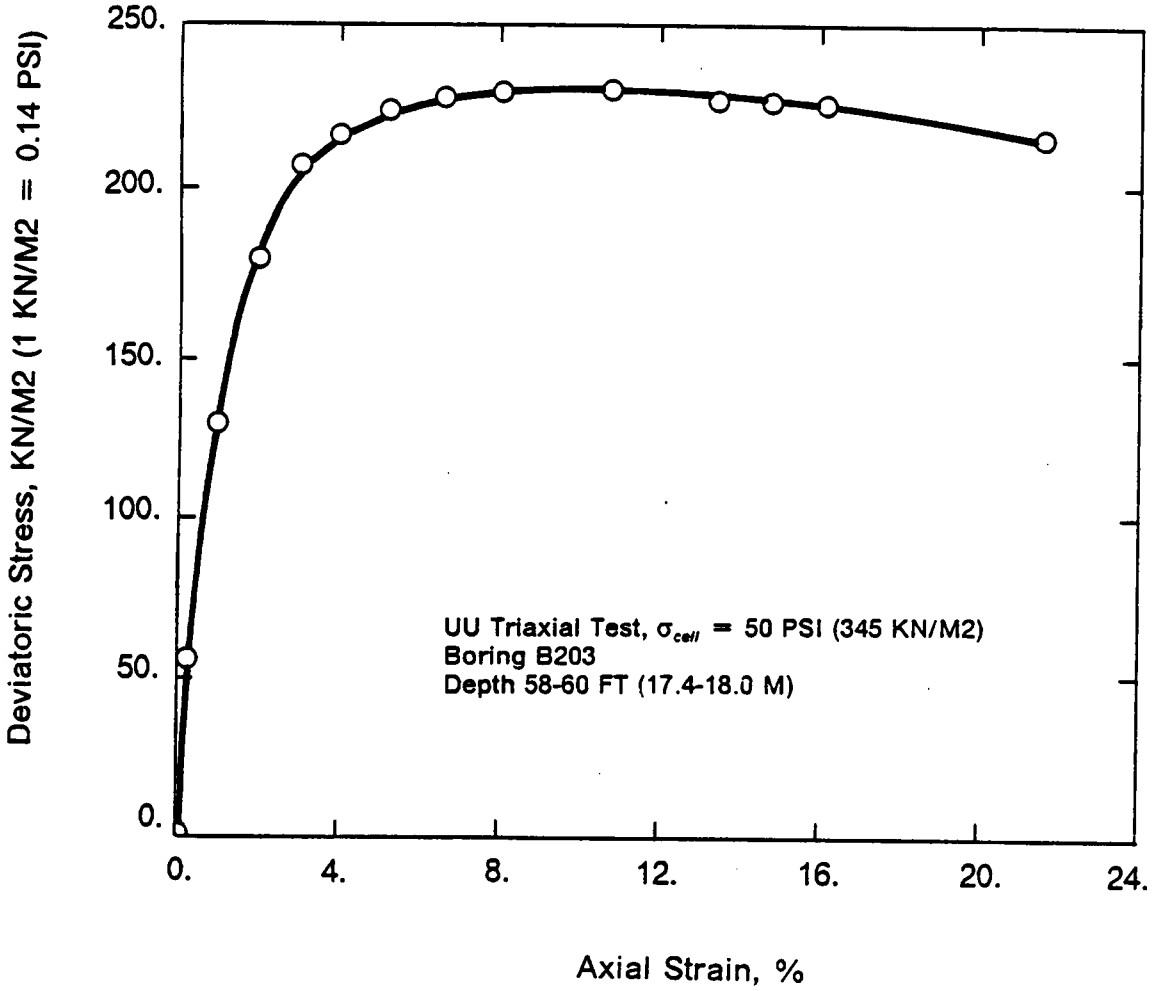
Deviatoric Stress, KN/M2 (1 KN/M2 = 0.14 PSI)
250.
200.
150.
100.
50.
0.
0.
4.
8.
12.
16.
20.
24.
Axial Strain, %
UU Triaxial Test, σ_{cell} = 50 PSI (345 KN/M2)
Boring B203
Depth 58-60 FT (17.4-18.0 M)

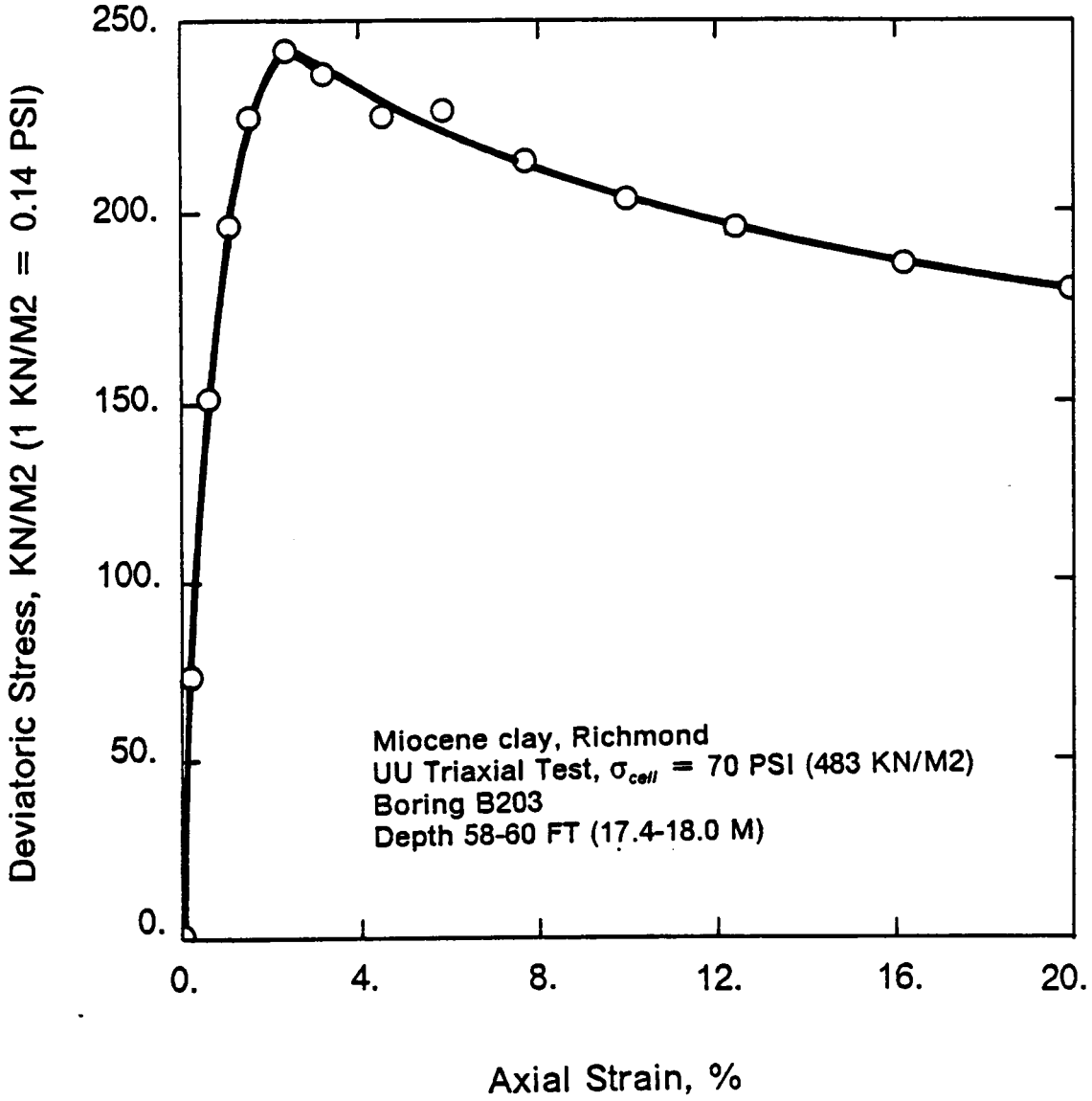
250.
200.
150.
100.
50.
0.
Deviatoric Stress, KN/M2 (1 KN/M2 = 0.14 PSI)
Miocene clay, Richmond
UU Triaxial Test, σ_{cell} = 70 PSI (483 KN/M2)
Boring B203
Depth 58-60 FT (17.4-18.0 M)
0.
4.
8.
12.
16.
20.
Axial Strain, %

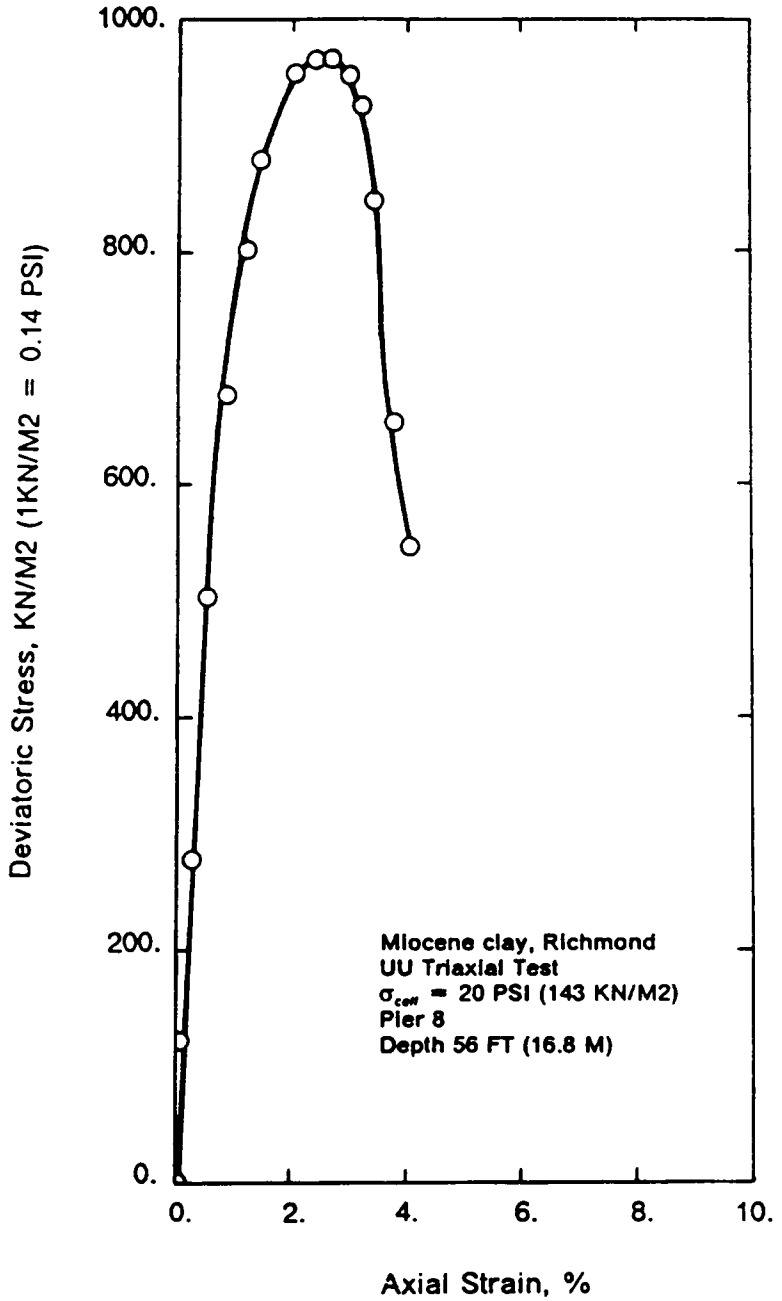
1000.
800.
600.
400.
200.
0.
0.
2.
4.
6.
8.
10.
Deviatoric Stress, KN/M2 (1KN/M2 = 0.14 PSI)
Axial Strain, %
Miocene clay, Richmond
UU Triaxial Test
σ_{cell} = 20 PSI (143 KN/M2)
Pier 8
Depth 56 FT (16.8 M)

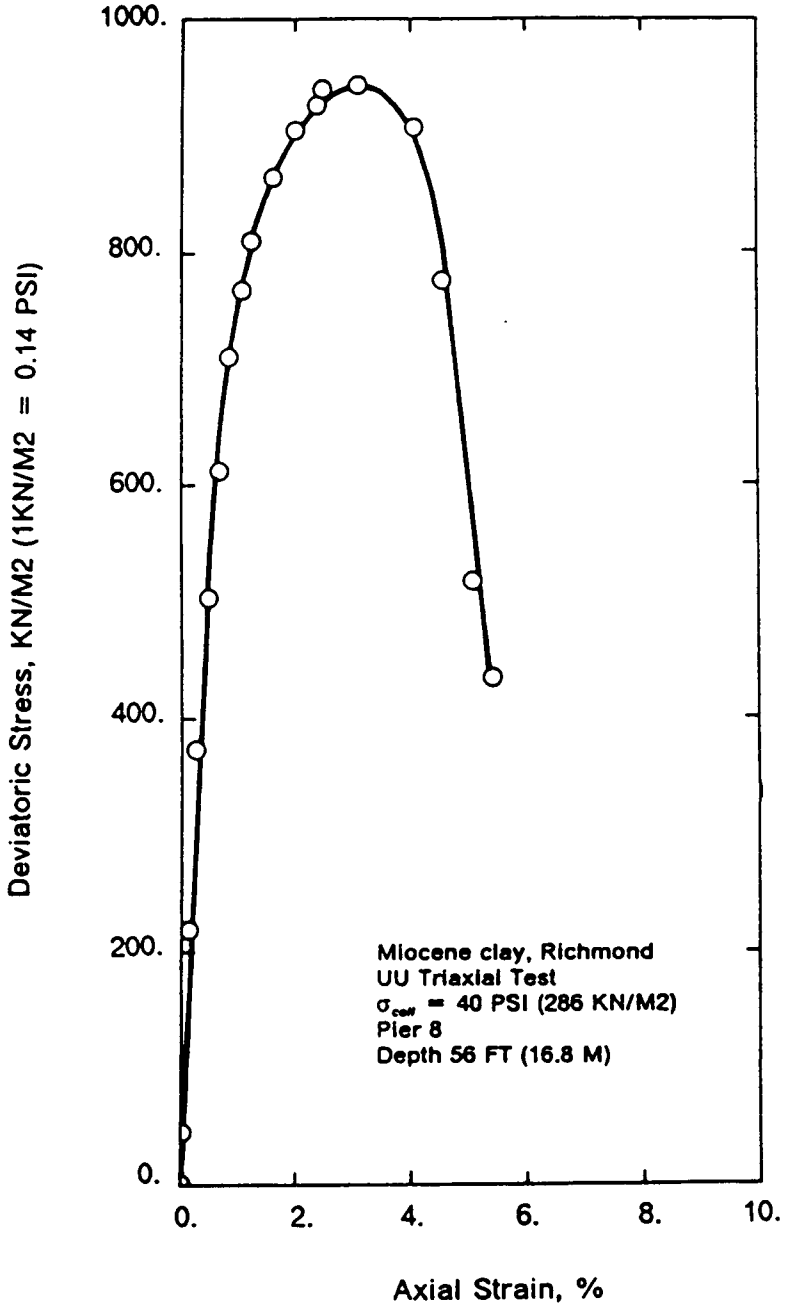
1000.
800.
600.
400.
200.
0.
0.
2.
4.
6.
8.
10.
Deviatoric Stress, KN/M2 (1KN/M2 = 0.14 PSI)
Axial Strain, %
Miocene clay, Richmond
UU Triaxial Test
σcell = 40 PSI (286 KN/M2)
Pier 8
Depth 56 FT (16.8 M)

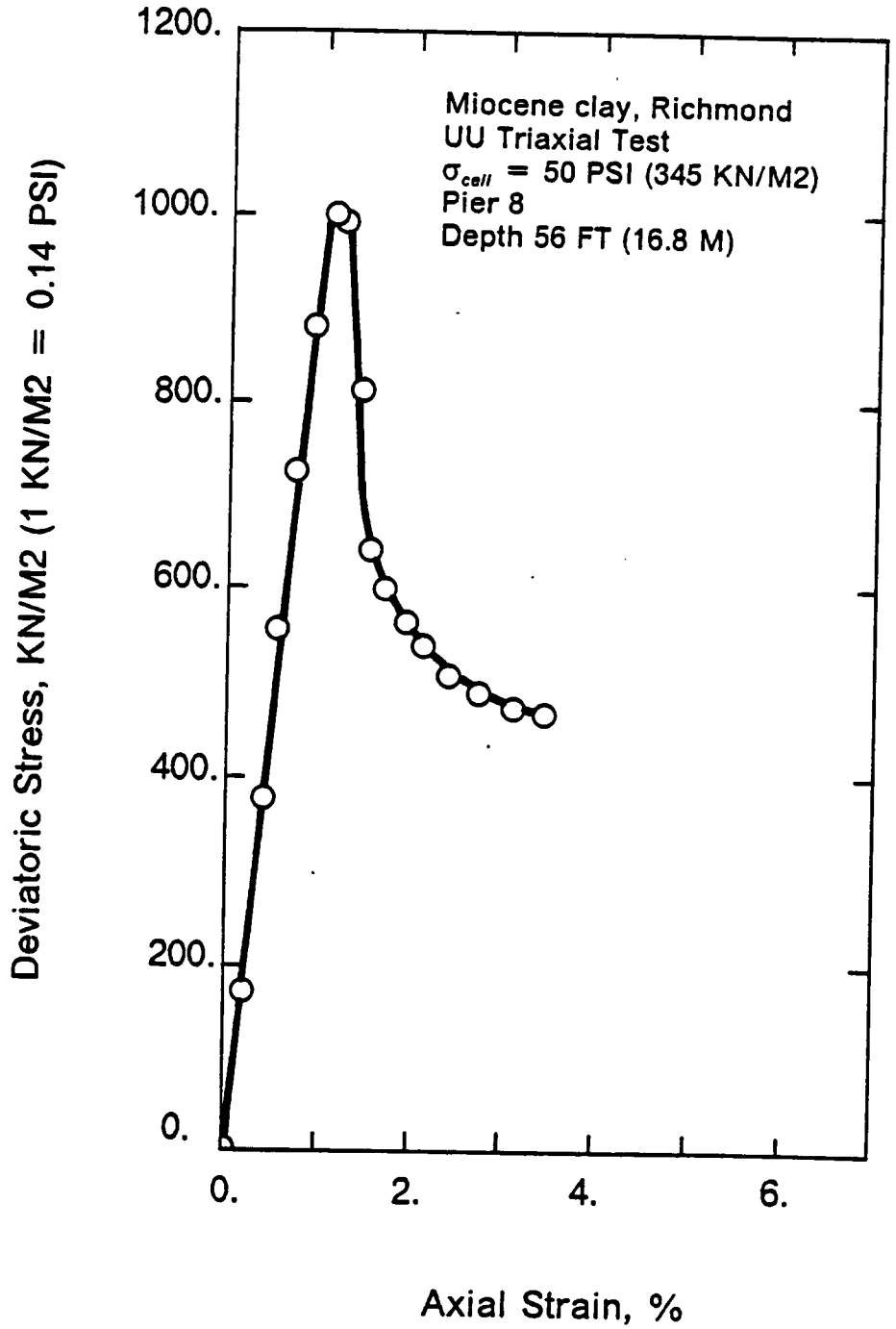
Miocene clay, Richmond
UU Triaxial Test
σ_{cell} = 50 PSI (345 KN/M2)
Pier 8
Depth 56 FT (16.8 M)
Deviatoric Stress, KN/M2 (1 KN/M2 = 0.14 PSI)
1200.
1000.
800.
600.
400.
200.
0.
0.
2.
4.
6.
Axial Strain, %

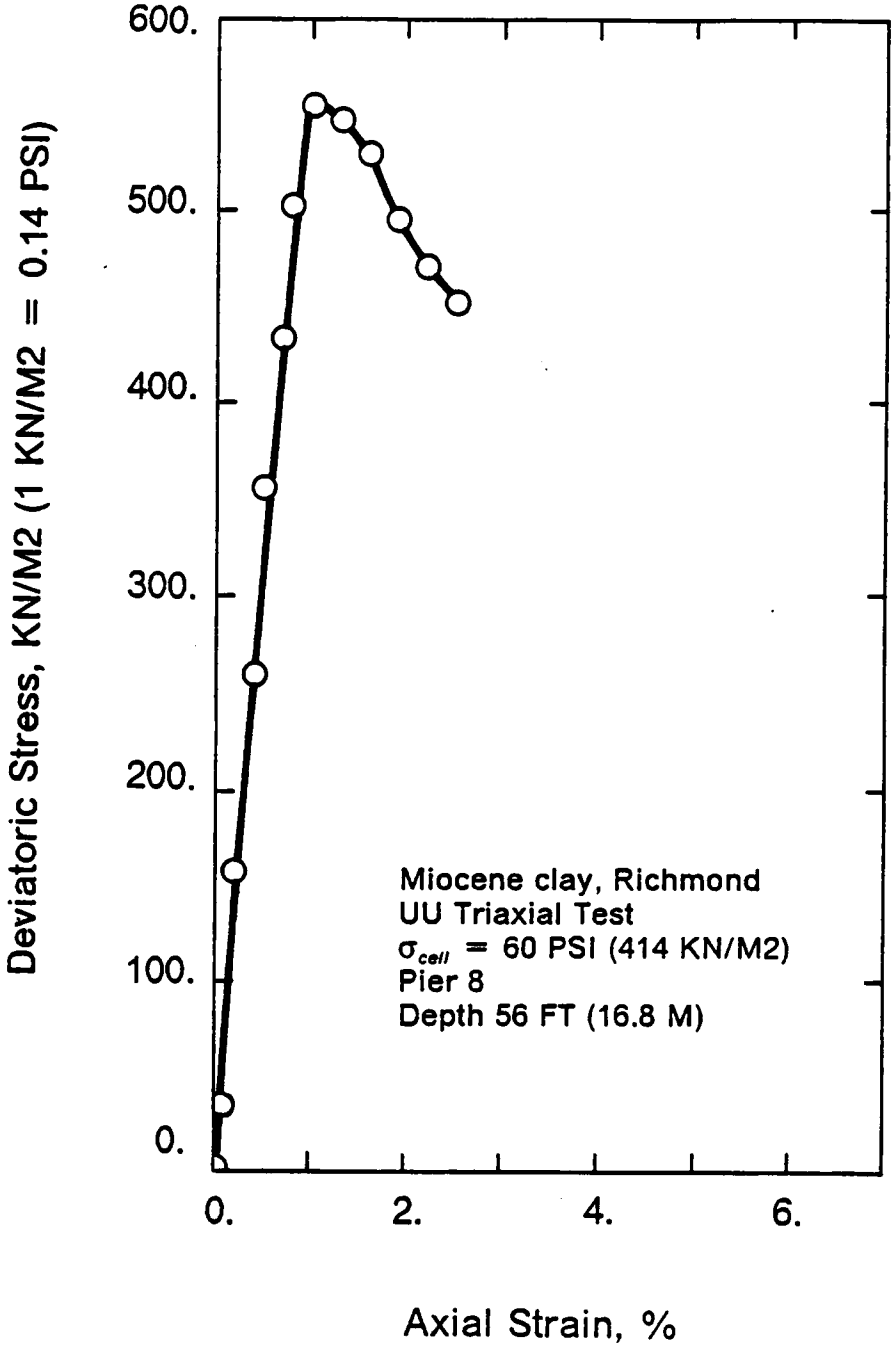
600.
500.
400.
300.
200.
100.
0.
0.
2.
4.
6.
Deviatoric Stress, KN/M2 (1 KN/M2 = 0.14 PSI)
Axial Strain, %
Miocene clay, Richmond
UU Triaxial Test
σ_{cell} = 60 PSI (414 KN/M2)
Pier 8
Depth 56 FT (16.8 M)

Appendix D

ICU TRIAXIAL TEST RESULTS IN THE MIOCENE CLAY

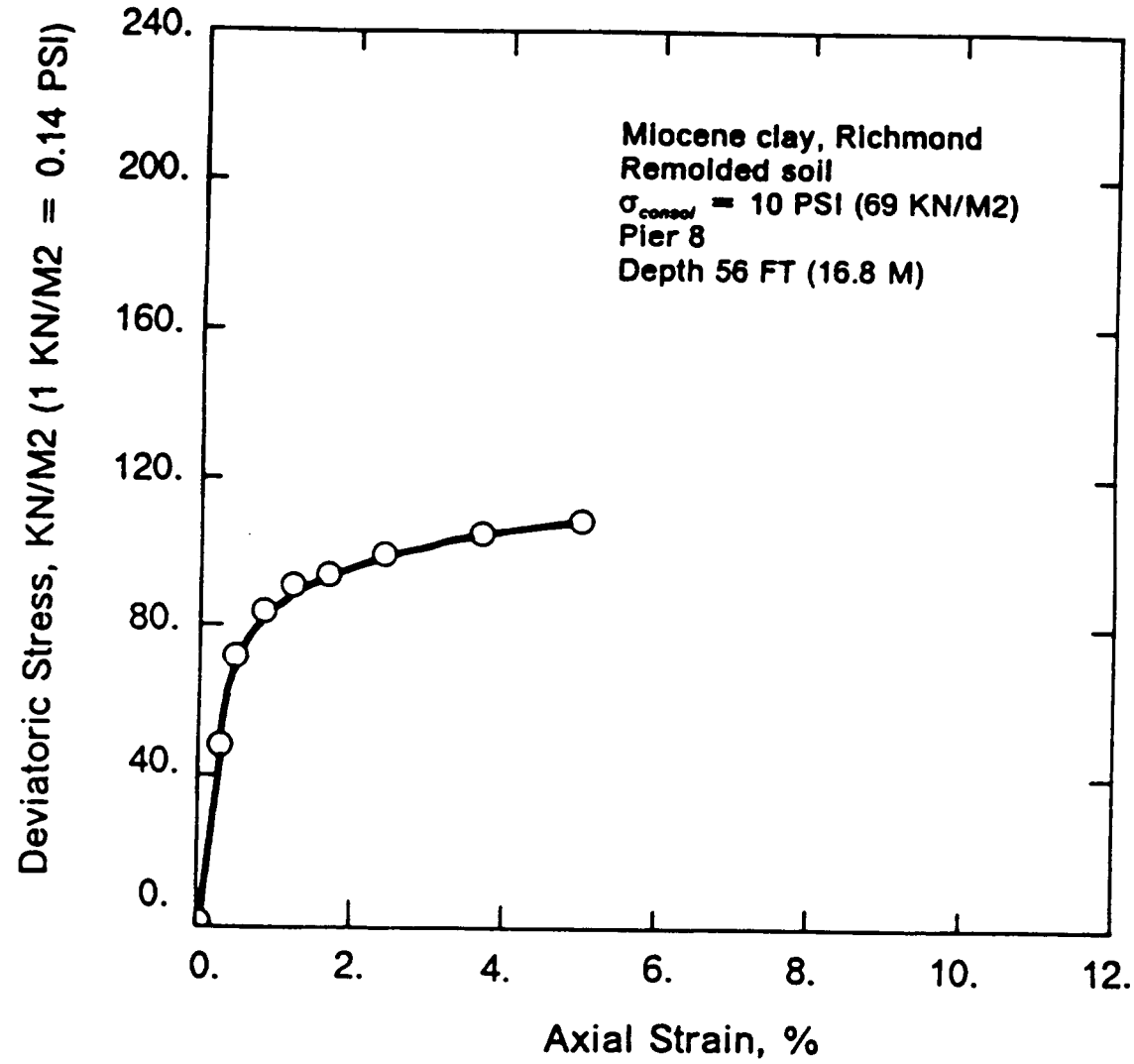
Deviatoric Stress, KN/M2 (1 KN/M2 = 0.14 PSI)
240.
200.
160.
120.
80.
40.
0.
0.
2.
4.
6.
8.
10.
12.
Axial Strain, %
Miocene clay, Richmond
Remolded soil
σconsol = 10 PSI (69 KN/M2)
Pier 8
Depth 56 FT (16.8 M)

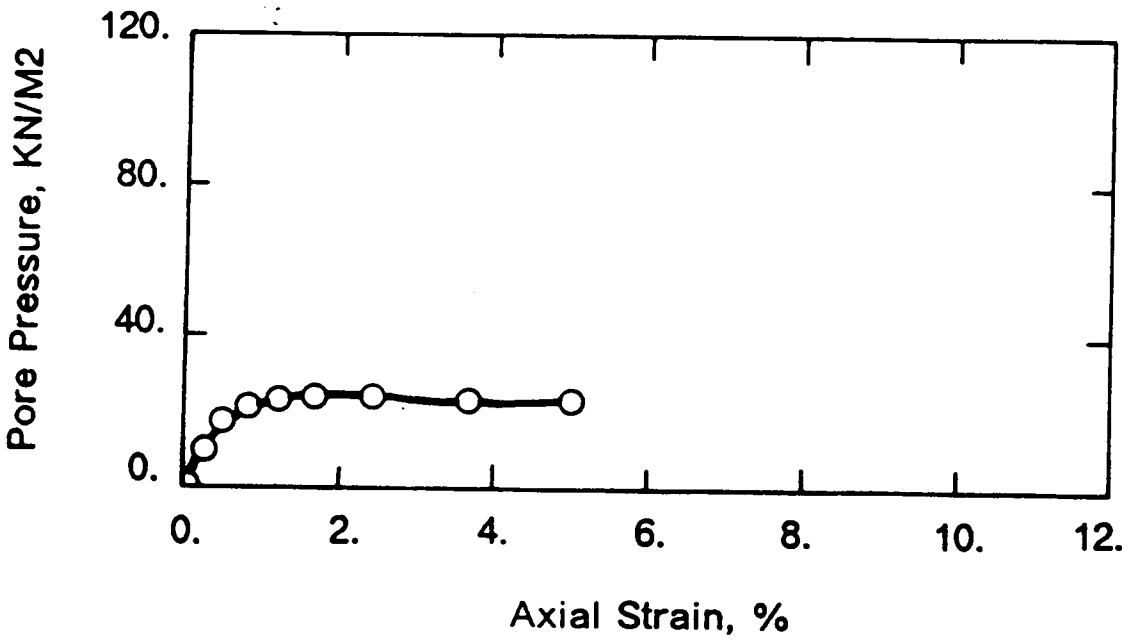
Pore Pressure, KN/M2
120.
80.
40.
0.
0.
2.
4.
6.
8.
10.
12.
Axial Strain, %

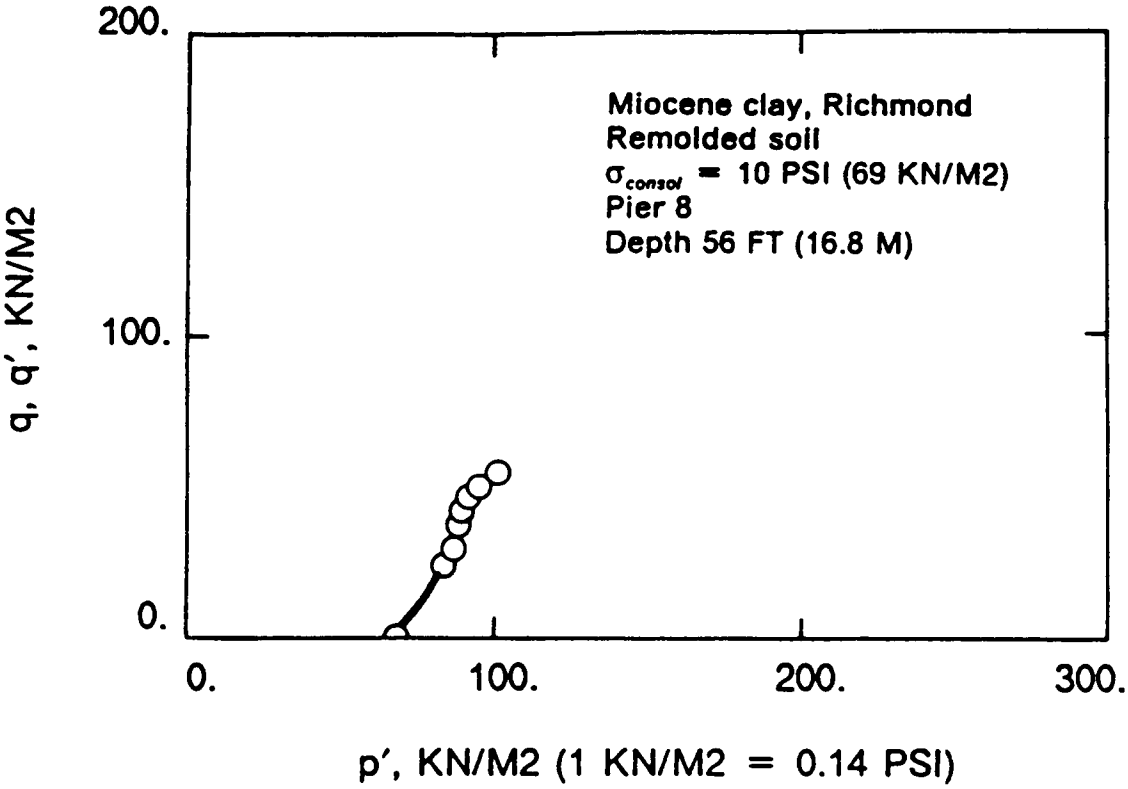
Miocene clay, Richmond
Remolded soil
σ_{consol} = 10 PSI (69 KN/M2)
Pier 8
Depth 56 FT (16.8 M)
q, q', KN/M2
200.
100.
0.
0.
100.
200.
300.
p', KN/M2 (1 KN/M2 = 0.14 PSI)

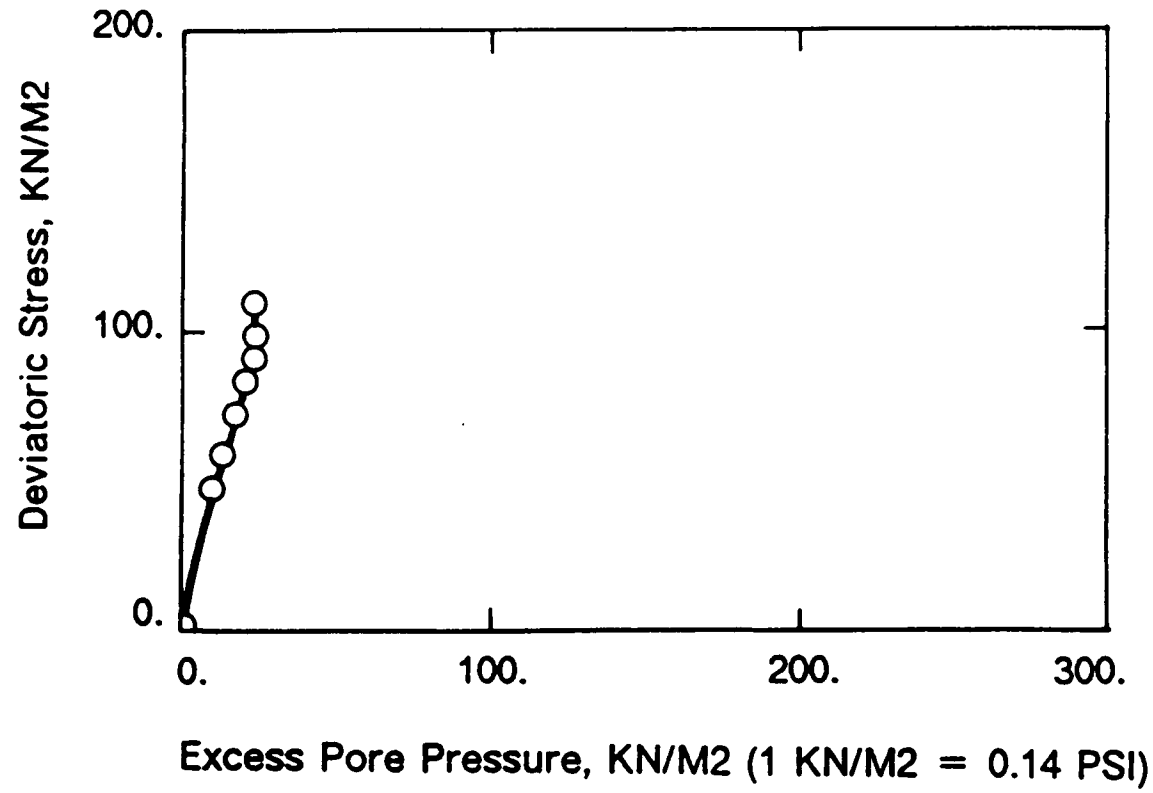
Deviatoric Stress, KN/M2
200.
100.
0.
0.
100.
200.
300.
Excess Pore Pressure, KN/M2 (1 KN/M2 = 0.14 PSI)

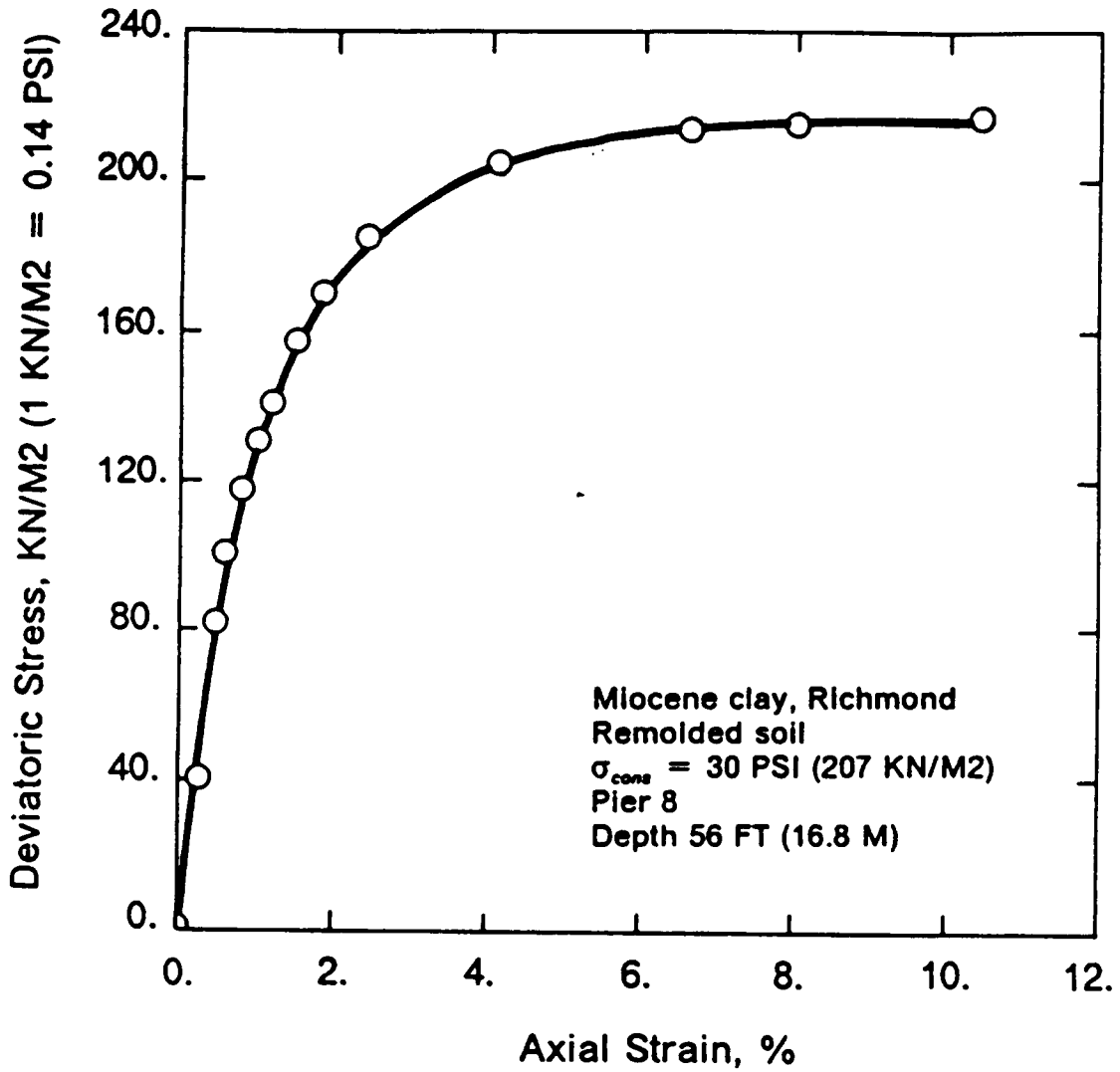
Deviatoric Stress, KN/M2 (1 KN/M2 = 0.14 PSI)
240.
200.
160.
120.
80.
40.
0.
0.
2.
4.
6.
8.
10.
12.
Axial Strain, %
Miocene clay, Richmond
Remolded soil
σ_{cons} = 30 PSI (207 KN/M2)
Pier 8
Depth 56 FT (16.8 M)

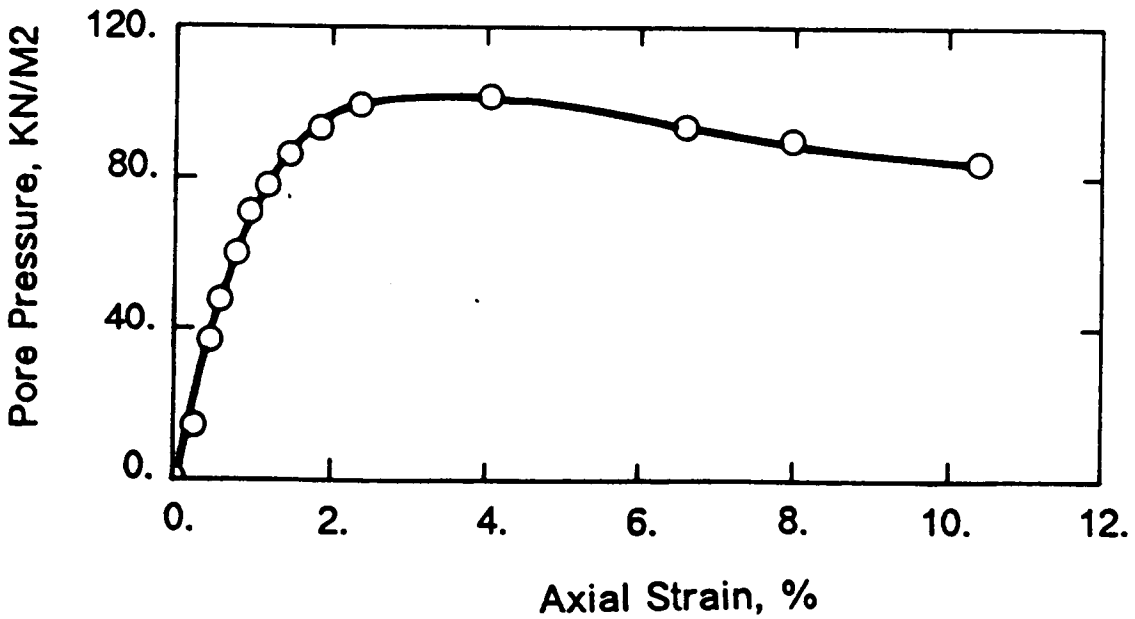
Pore Pressure, KN/M2
120.
80.
40.
0.
0.
2.
4.
6.
8.
10.
12.
Axial Strain, %

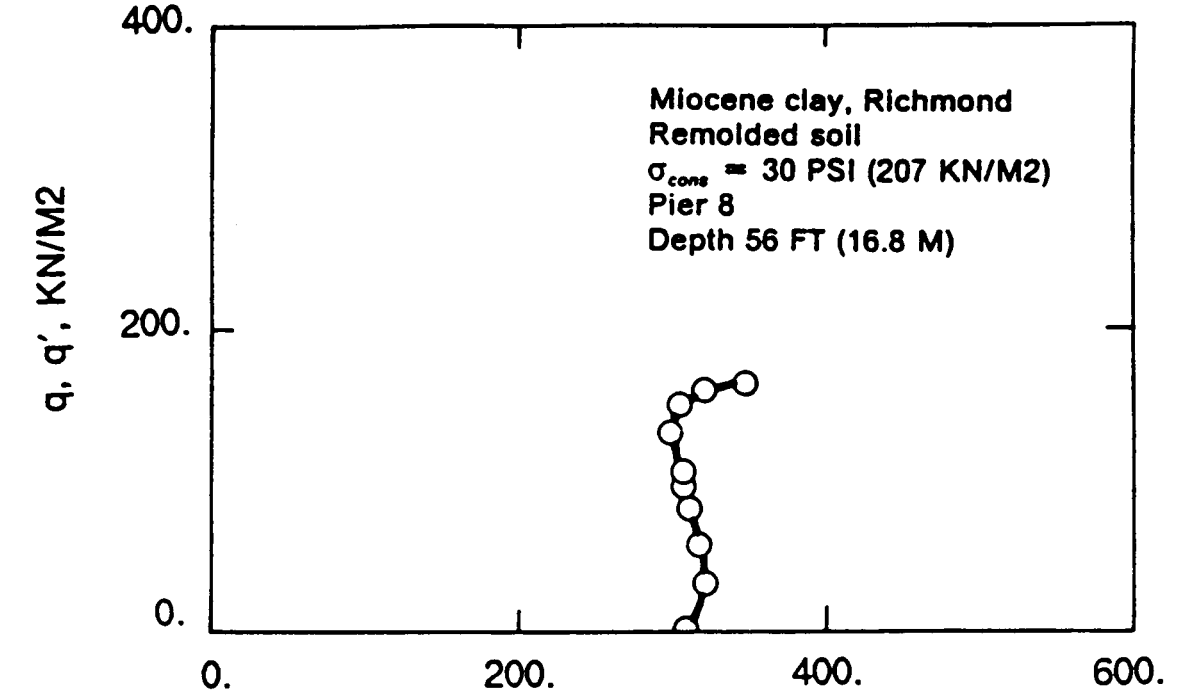
400.
200.
0.
0.
200.
400.
600.
q, q', KN/M2
Miocene clay, Richmond
Remolded soil
σ_{cons} = 30 PSI (207 KN/M2)
Pier 8
Depth 56 FT (16.8 M)
p', KN/M2 (1 KN/M2 = 0.14 PSI)

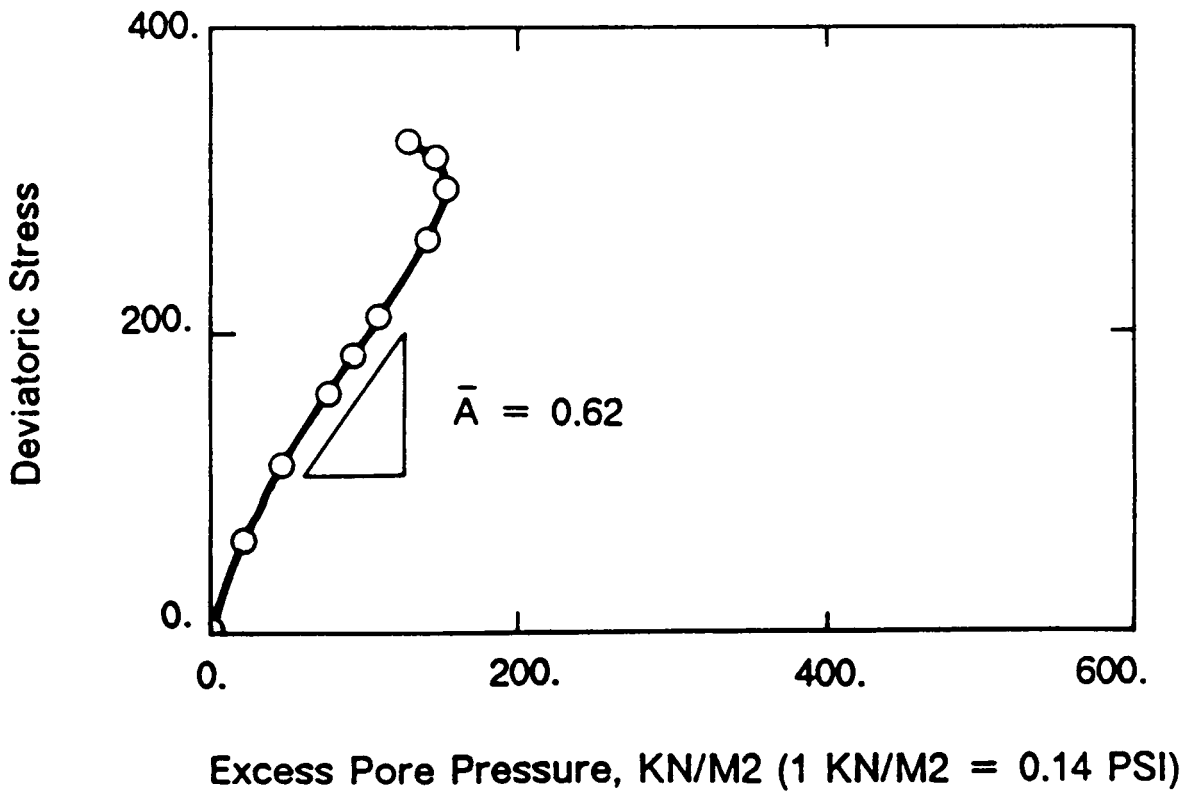
400.
200.
0.
0.
200.
400.
600.
Deviatoric Stress
$\bar{A}$ = 0.62
Excess Pore Pressure, KN/M2 (1 KN/M2 = 0.14 PSI)

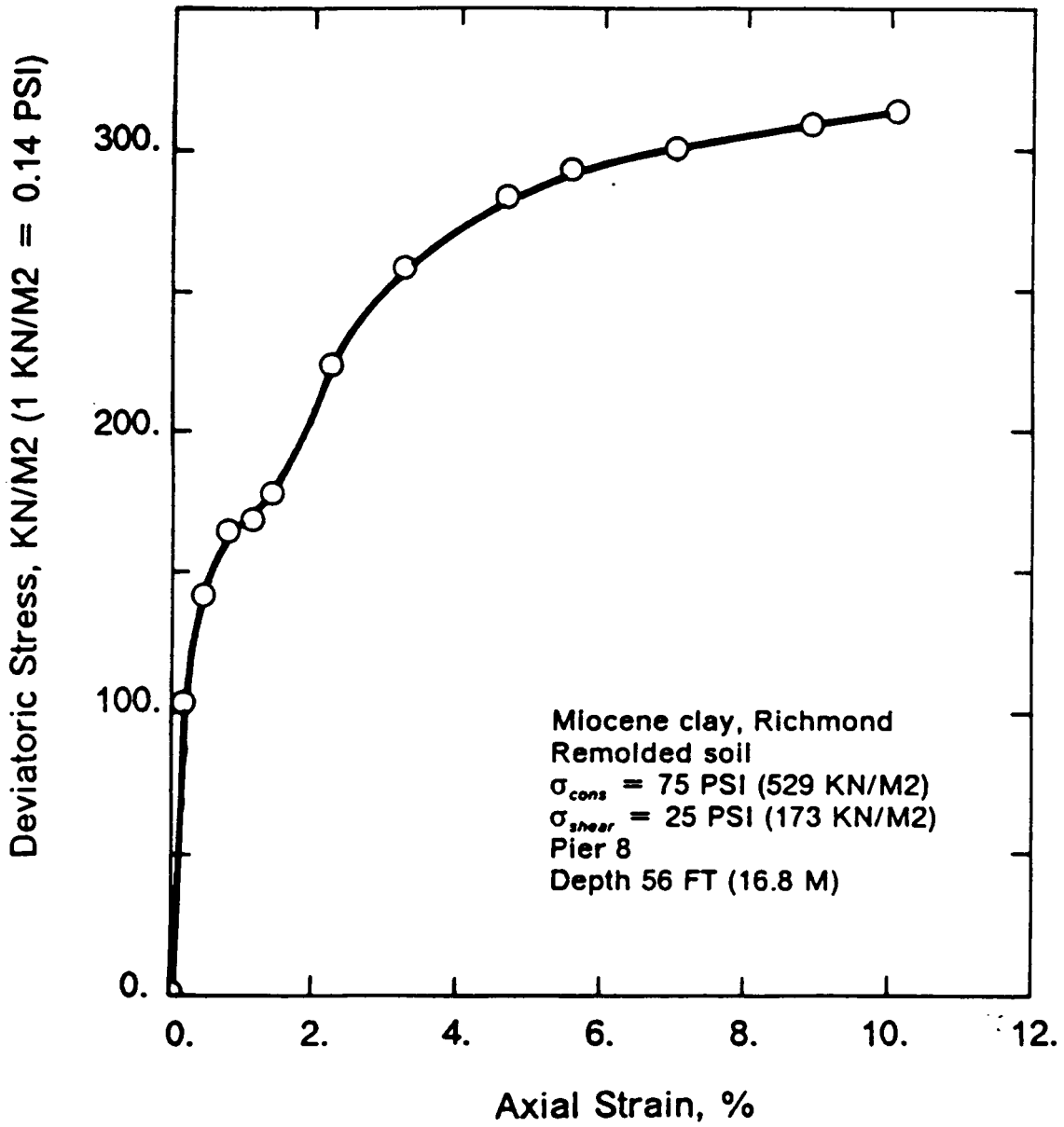
Deviatoric Stress, KN/M2 (1 KN/M2 = 0.14 PSI)
300.
200.
100.
0.
0.
2.
4.
6.
8.
10.
12.
Axial Strain, %
Miocene clay, Richmond
Remolded soil
σcons = 75 PSI (529 KN/M2)
σshear = 25 PSI (173 KN/M2)
Pier 8
Depth 56 FT (16.8 M)

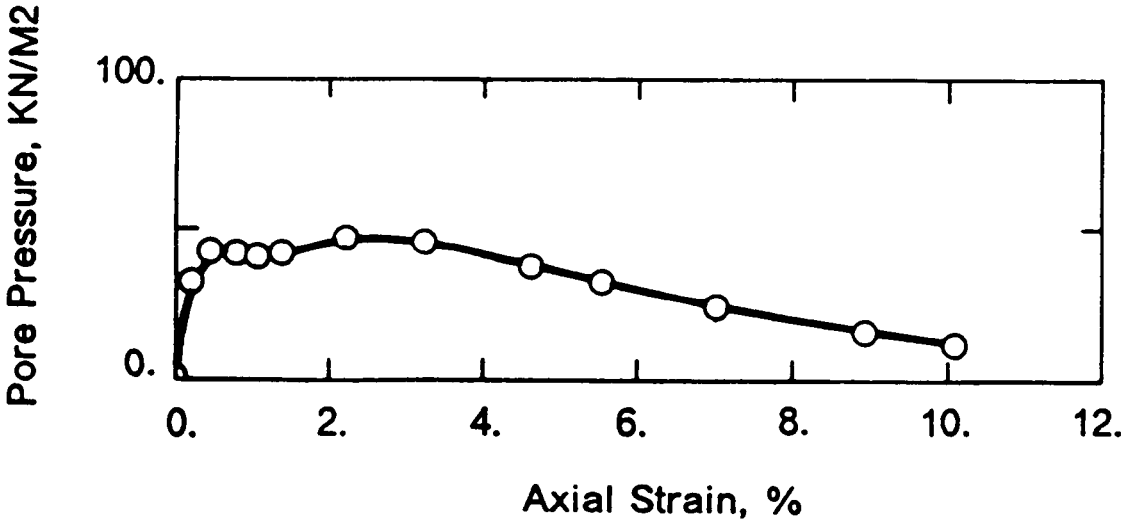
Pore Pressure, KN/M2
100.
0.
0.
2.
4.
6.
8.
10.
12.
Axial Strain, %

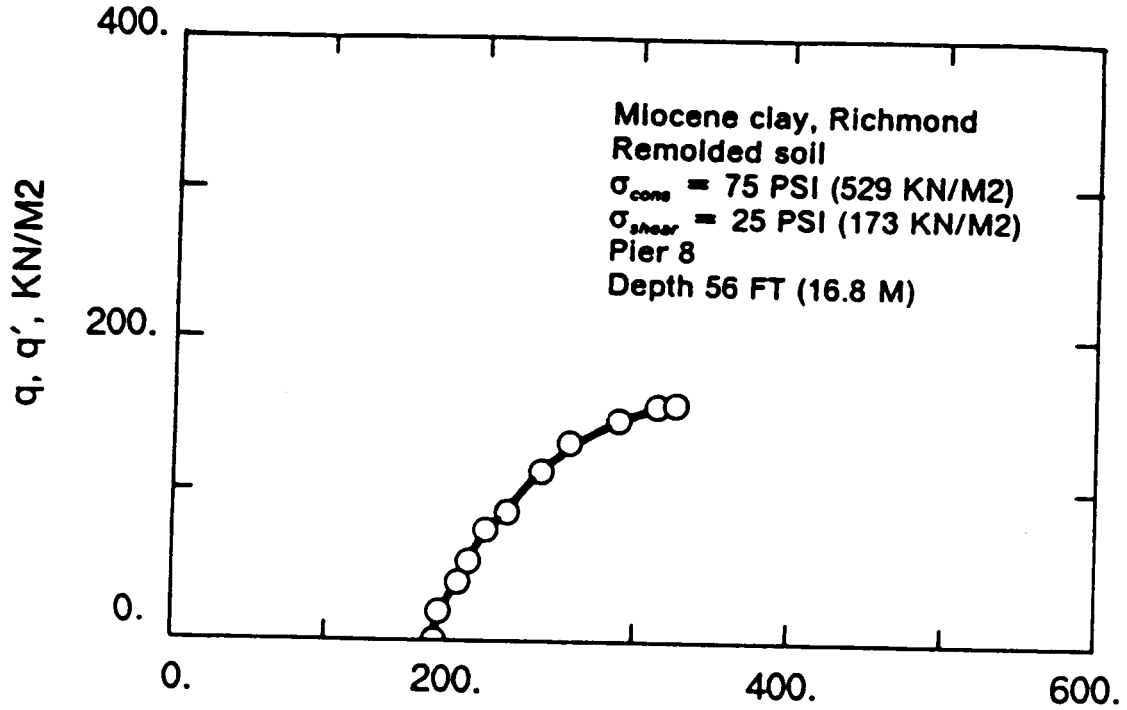
400.
200.
0.
q, q', KN/M2
Miocene clay, Richmond
Remolded soil
σcons = 75 PSI (529 KN/M2)
σshear = 25 PSI (173 KN/M2)
Pier 8
Depth 56 FT (16.8 M)
0.
200.
400.
600.
p', KN/M2 (1 KN/M2 = 0.14 PSI)

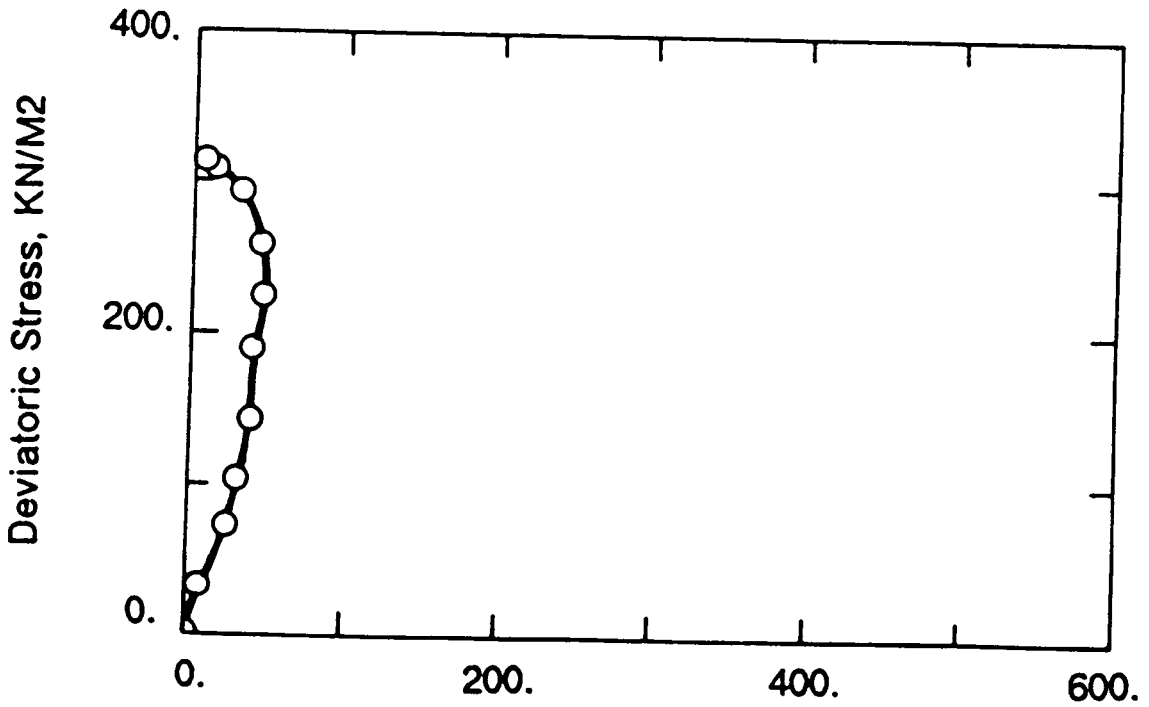
400.
200.
0.
Deviatoric Stress, KN/M2
0.
200.
400.
600.
Excess Pore Pressure, KN/M2 (1 KN/M2 = 0.14 PSI)

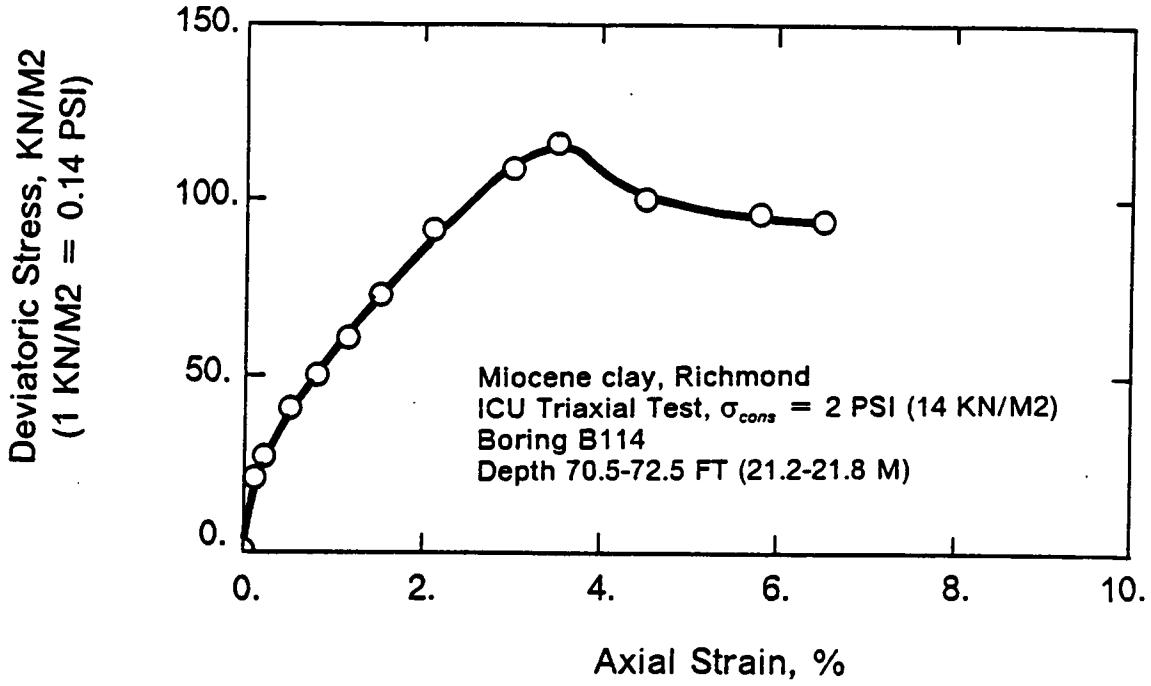
Deviatoric Stress, KN/M2
(1 KN/M2 = 0.14 PSI)
150.
100.
50.
0.
0.
2.
4.
6.
8.
10.
Axial Strain, %
Miocene clay, Richmond
ICU Triaxial Test, σ_{cons} = 2 PSI (14 KN/M2)
Boring B114
Depth 70.5-72.5 FT (21.2-21.8 M)

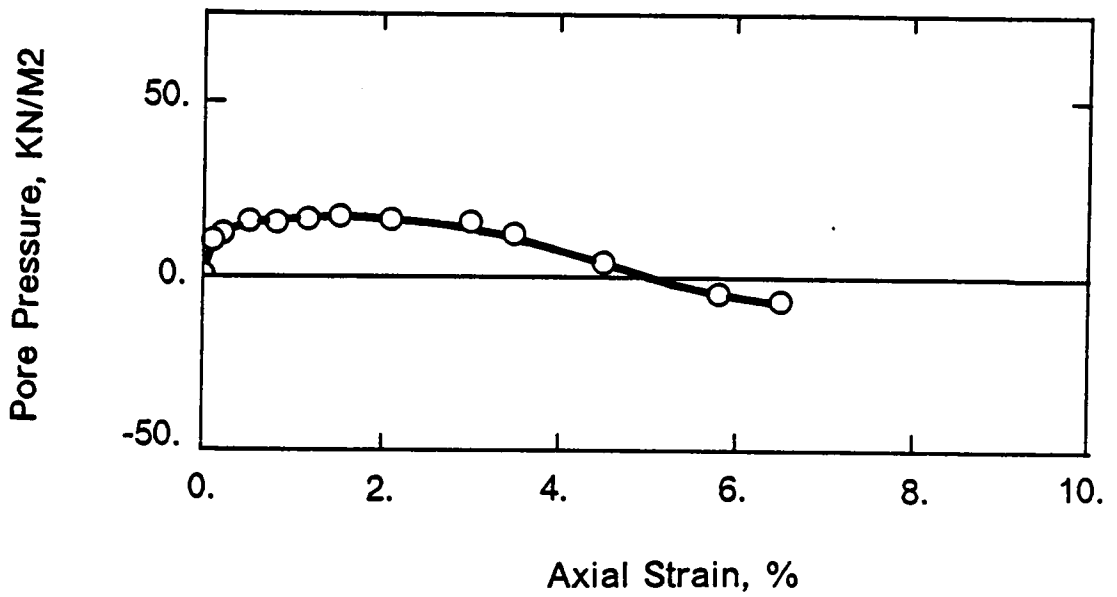
Pore Pressure, KN/M2
50.
0.
-50.
0.
2.
4.
6.
8.
10.
Axial Strain, %

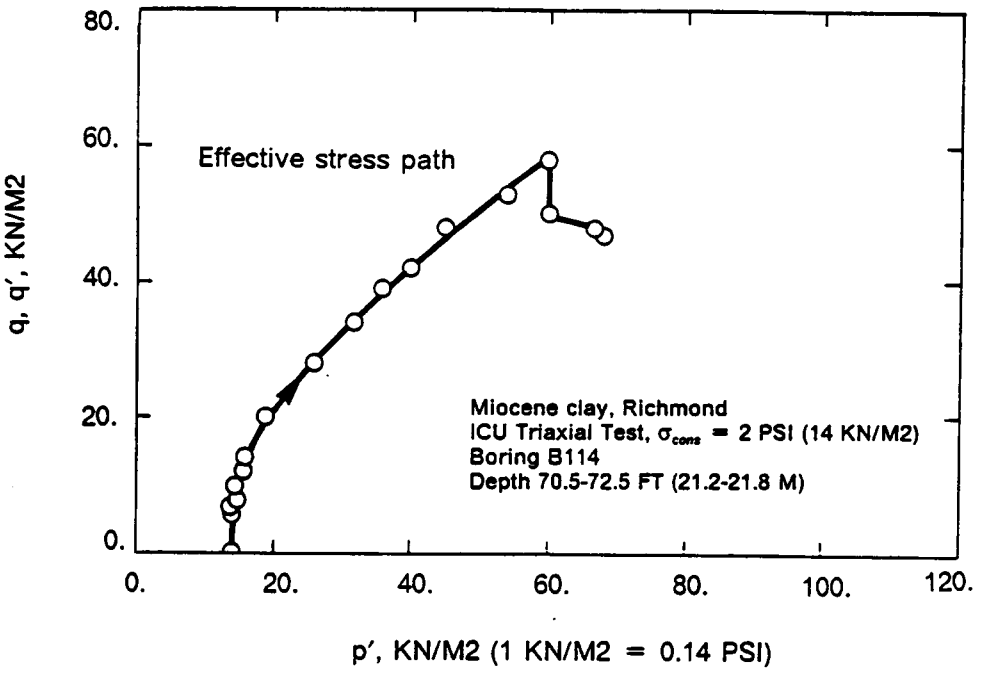
Effective stress path
Miocene clay, Richmond
ICU Triaxial Test, σ_{cons} = 2 PSI (14 KN/M2)
Boring B114
Depth 70.5-72.5 FT (21.2-21.8 M)
q, q', KN/M2
p', KN/M2 (1 KN/M2 = 0.14 PSI)
0.
20.
40.
60.
80.
100.
120.

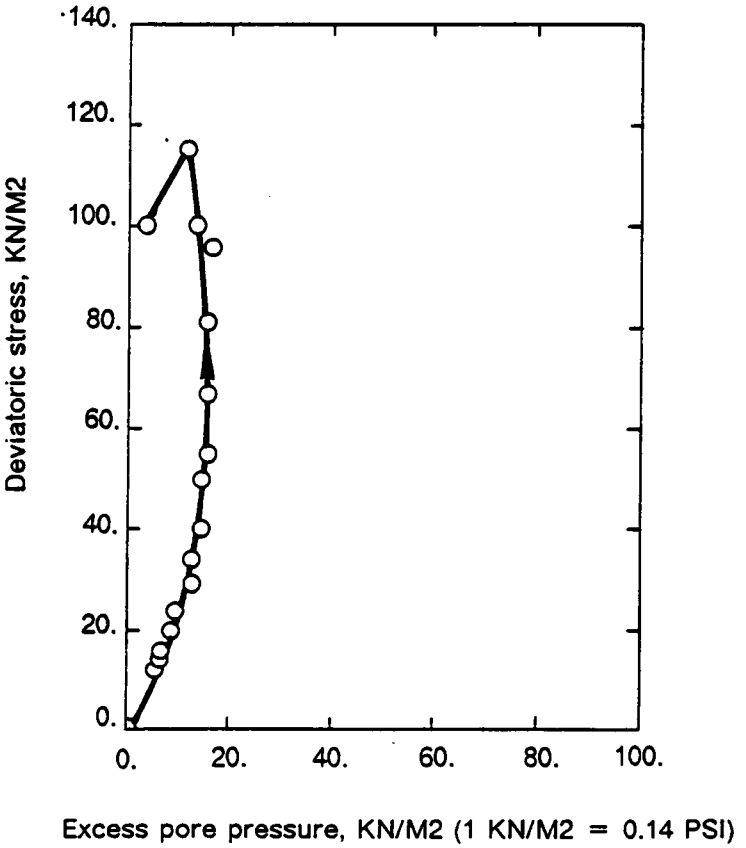
Deviatoric stress, KN/M2
Excess pore pressure, KN/M2 (1 KN/M2 = 0.14 PSI)
0.
20.
40.
60.
80.
100.
120.
140.

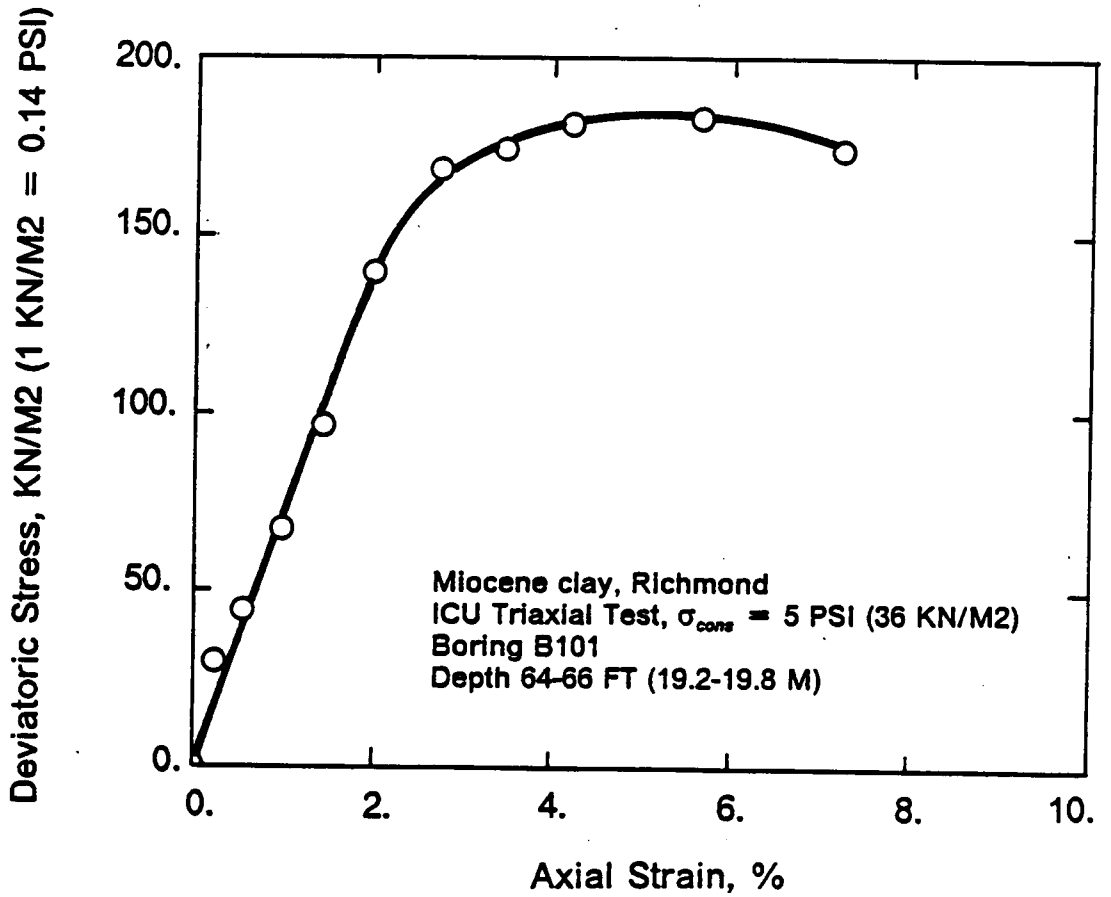
Deviatoric Stress, KN/M2 (1 KN/M2 = 0.14 PSI)
200.
150.
100.
50.
0.
0.
2.
4.
6.
8.
10.
Axial Strain, %
Miocene clay, Richmond
ICU Triaxial Test, σcons = 5 PSI (36 KN/M2)
Boring B101
Depth 64-66 FT (19.2-19.8 M)

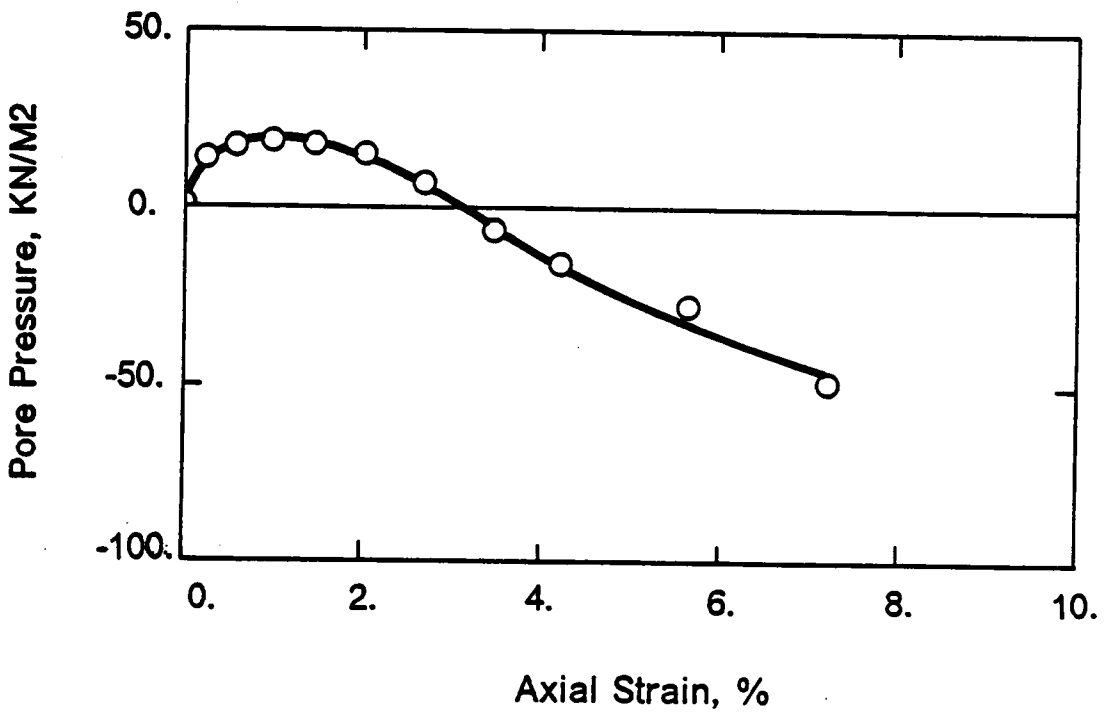
Pore Pressure, KN/M2
50.
0.
-50.
-100.
0.
2.
4.
6.
8.
10.
Axial Strain, %

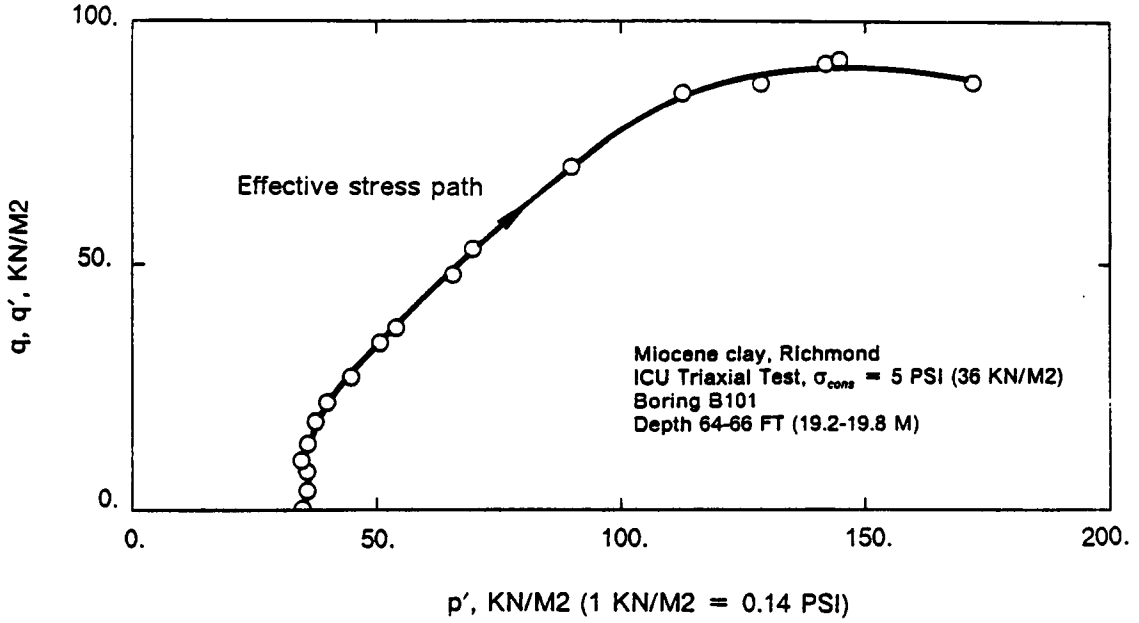
100.
50.
0.
q, q', KN/M2
Effective stress path
Miocene clay, Richmond
ICU Triaxial Test, σ_{cons} = 5 PSI (36 KN/M2)
Boring B101
Depth 64-66 FT (19.2-19.8 M)
0.
50.
100.
150.
200.
p', KN/M2 (1 KN/M2 = 0.14 PSI)

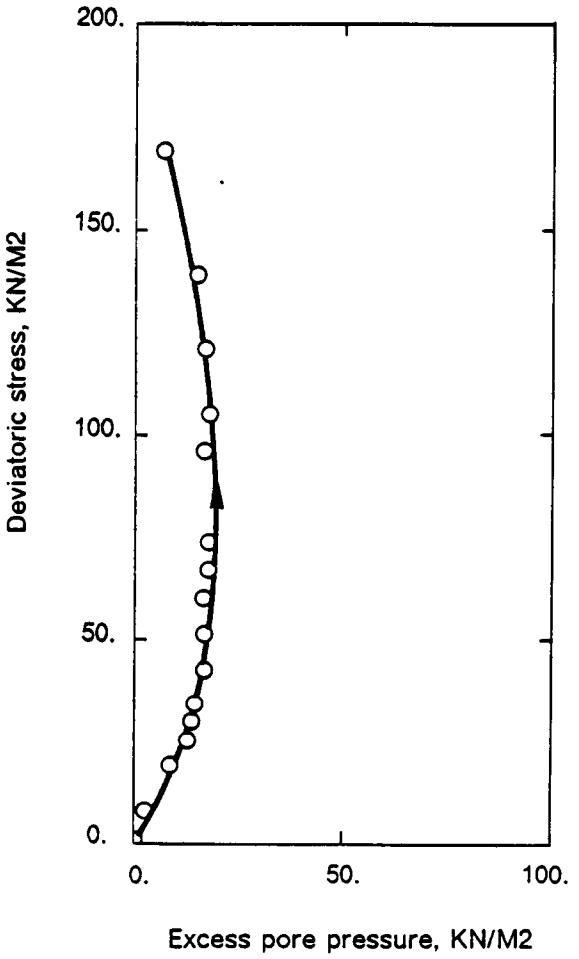
200.
150.
100.
50.
0.
Deviatoric stress, KN/M2
0.
50.
100.
Excess pore pressure, KN/M2

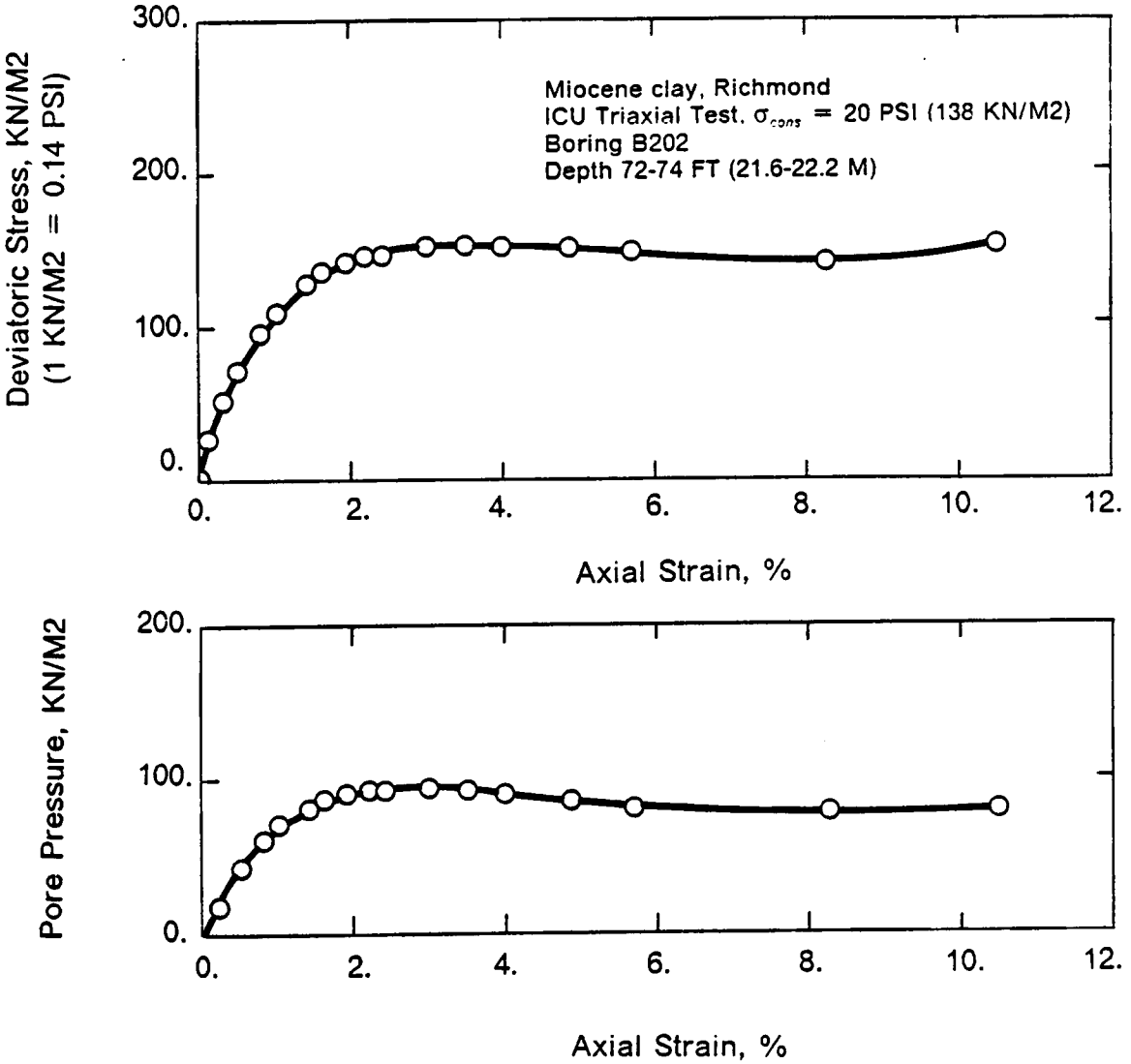
Deviatoric Stress, KN/M2
(1 KN/M2 = 0.14 PSI)
300.
200.
100.
0.
Miocene clay, Richmond
ICU Triaxial Test, σ_{cons} = 20 PSI (138 KN/M2)
Boring B202
Depth 72-74 FT (21.6-22.2 M)
0.
2.
4.
6.
8.
10.
12.
Axial Strain, %
Pore Pressure, KN/M2
200.
100.
0.
0.
2.
4.
6.
8.
10.
12.
Axial Strain, %

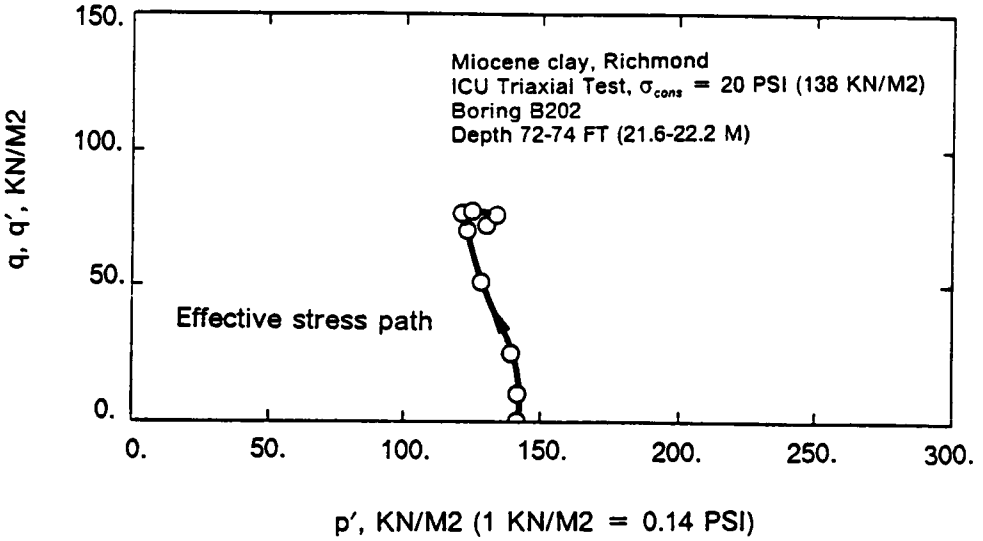
Miocene clay, Richmond
ICU Triaxial Test, σ_{cons} = 20 PSI (138 KN/M2)
Boring B202
Depth 72-74 FT (21.6-22.2 M)
Effective stress path
q, q', KN/M2
150.
100.
50.
0.
0.
50.
100.
150.
200.
250.
300.
p', KN/M2 (1 KN/M2 = 0.14 PSI)

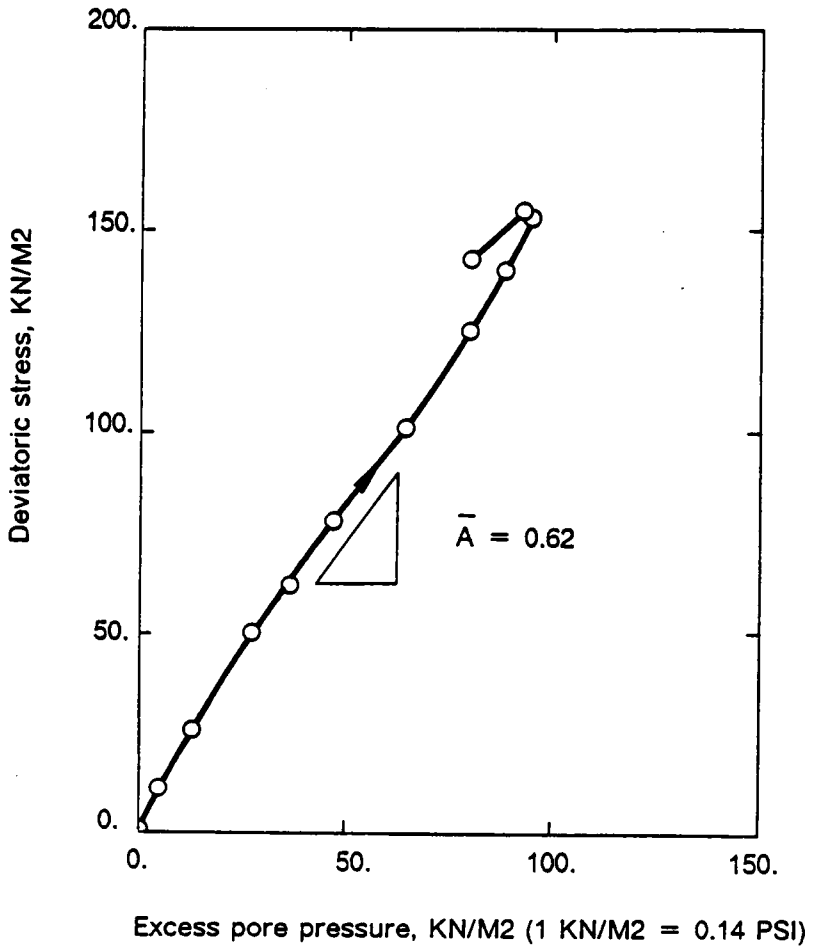
Deviatoric stress, KN/M2
200.
150.
100.
50.
0.
$\bar{A}$ = 0.62
0.
50.
100.
150.
Excess pore pressure, KN/M2 (1 KN/M2 = 0.14 PSI)

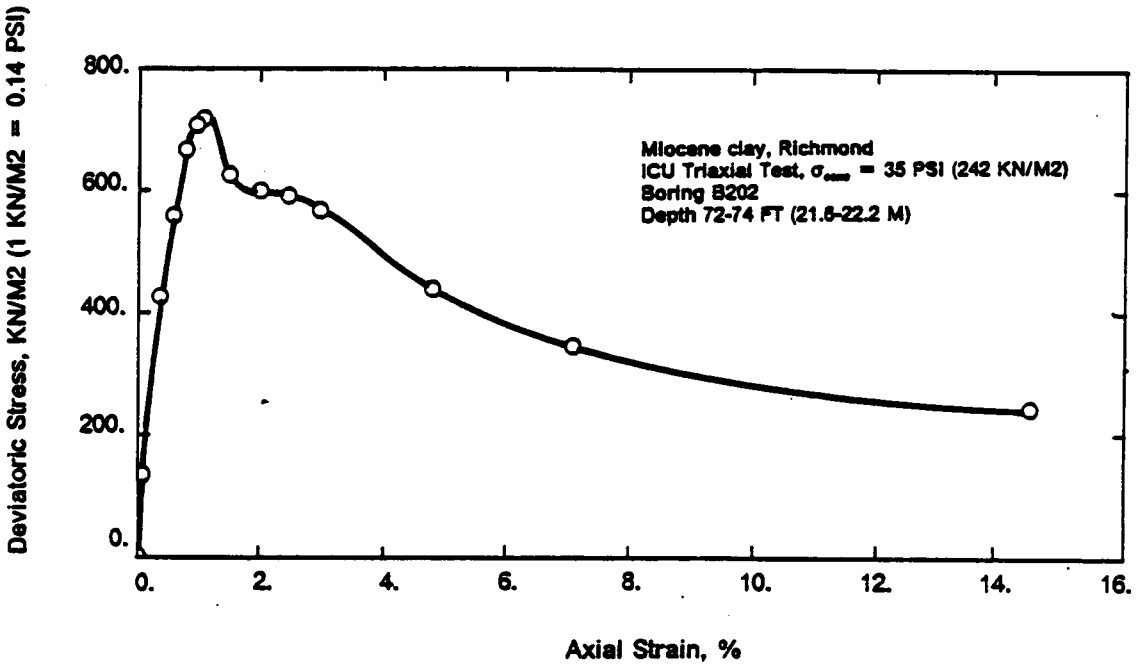
Deviatoric Stress, KN/M2 (1 KN/M2 = 0.14 PSI)
800.
600.
400.
200.
0.
0.
2.
4.
6.
8.
10.
12.
14.
16.
Miocene clay, Richmond
ICU Triaxial Test, σ_{cons} = 35 PSI (242 KN/M2)
Boring B202
Depth 72-74 FT (21.8-22.2 M)
Axial Strain, %

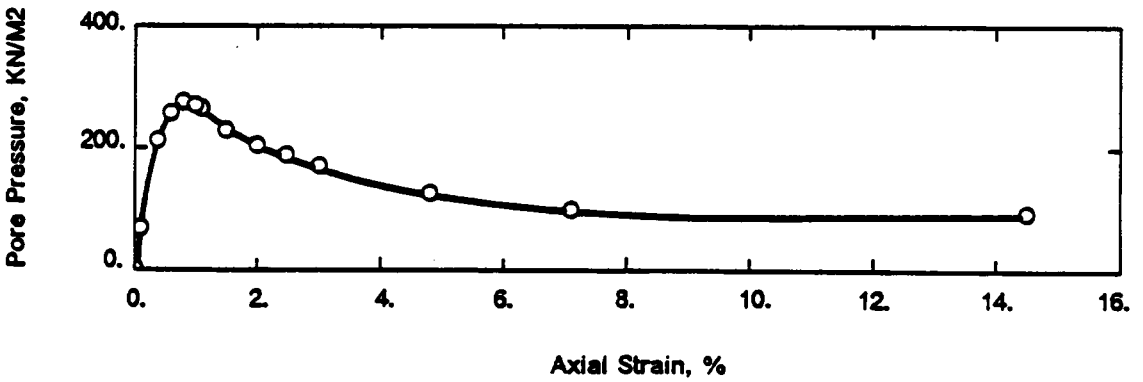
Pore Pressure, KN/M2
400.
200.
0.
0.
2.
4.
6.
8.
10.
12.
14.
16.
Axial Strain, %

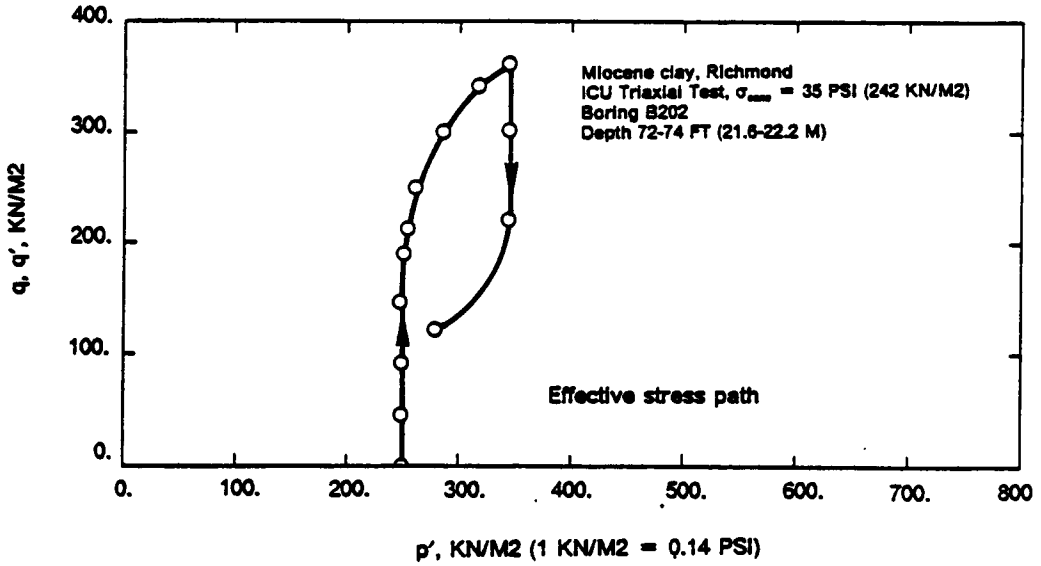
Miocene clay, Richmond
ICU Triaxial Test, σ_{cons} = 35 PSI (242 KN/M2)
Boring B202
Depth 72-74 FT (21.6-22.2 M)
Effective stress path
q, q', KN/M2
0.
100.
200.
300.
400.
0.
100.
200.
300.
400.
500.
600.
700.
800
p', KN/M2 (1 KN/M2 = 0.14 PSI)

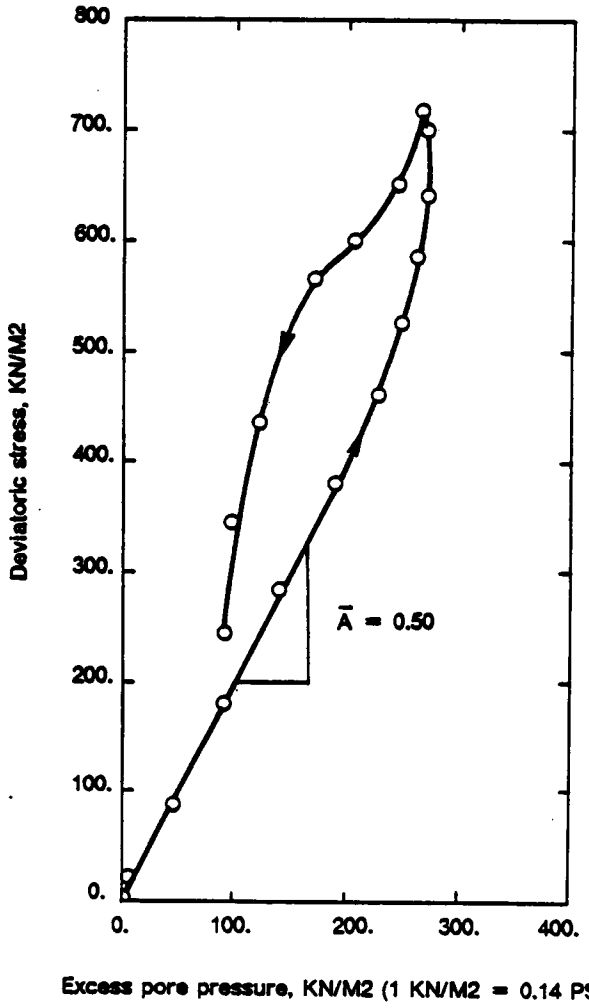
Deviatoric stress, KN/M2
800
700.
600.
500.
400.
300.
200.
100.
0.
$\bar{A}$ = 0.50
0.
100.
200.
300.
400.
Excess pore pressure, KN/M2 (1 KN/M2 = 0.14 PSI)

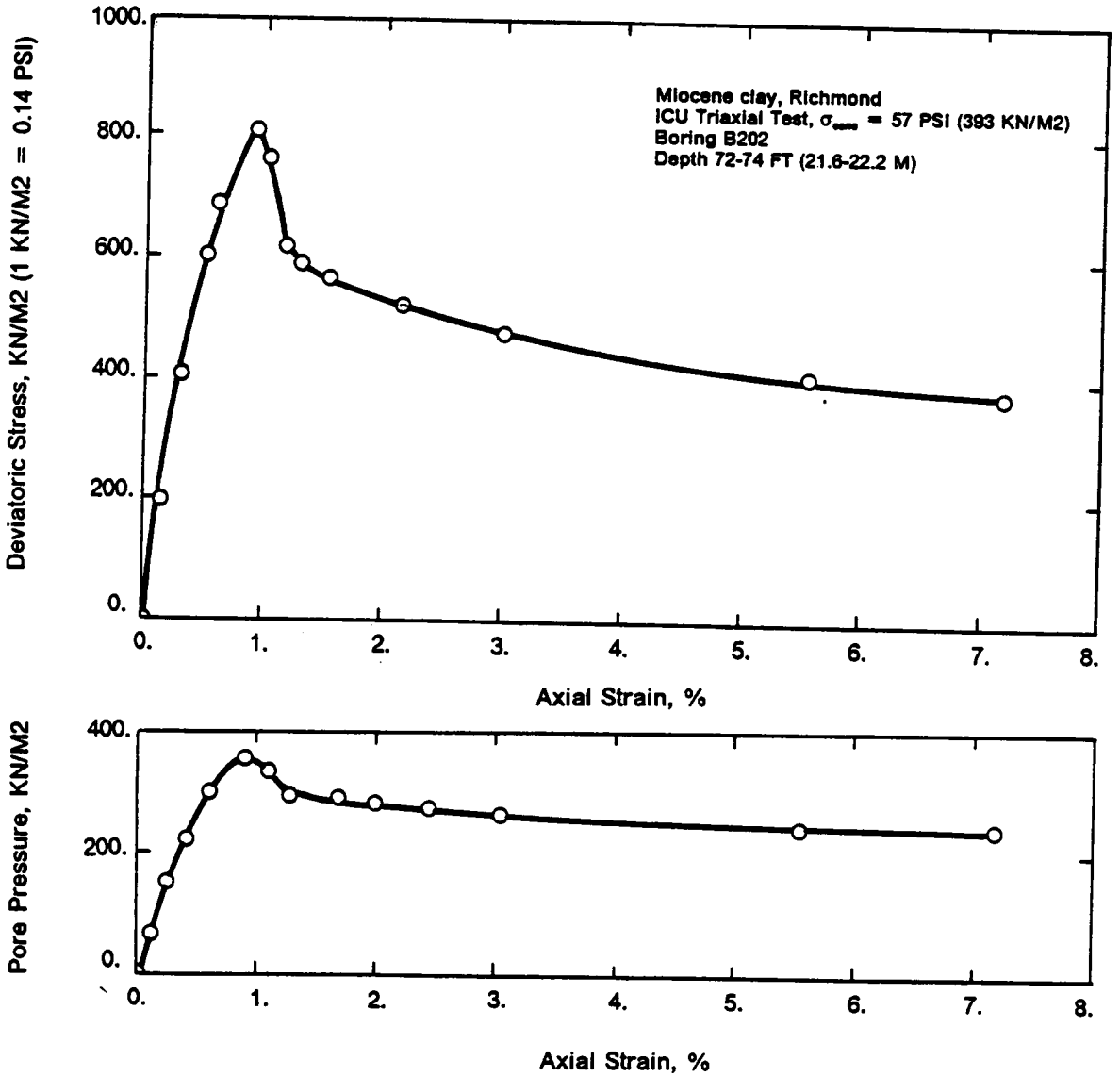
Miocene clay, Richmond
ICU Triaxial Test, σ_{cmp} = 57 PSI (393 KN/M2)
Boring B202
Depth 72-74 FT (21.6-22.2 M)
Deviatoric Stress, KN/M2 (1 KN/M2 = 0.14 PSI)
1000.
800.
600.
400.
200.
0.
0.
1.
2.
3.
4.
5.
6.
7.
8.
Axial Strain, %
Pore Pressure, KN/M2
400.
200.
0.
0.
1.
2.
3.
4.
5.
6.
7.
8.
Axial Strain, %

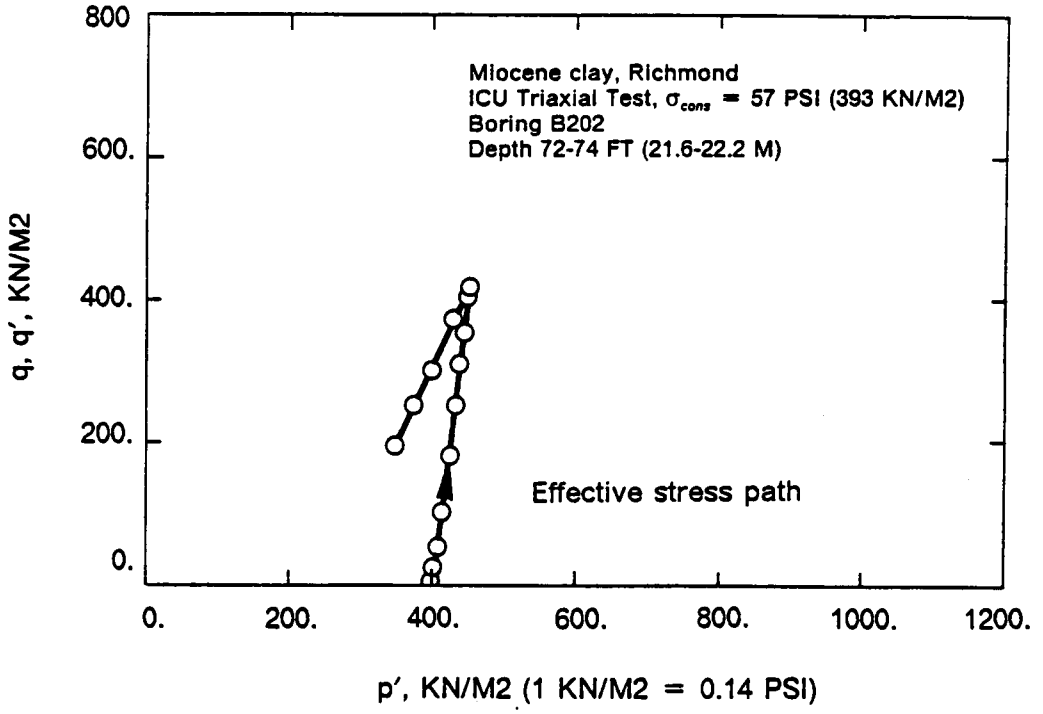
Miocene clay, Richmond
ICU Triaxial Test, σ_{cons} = 57 PSI (393 KN/M2)
Boring B202
Depth 72-74 FT (21.6-22.2 M)
Effective stress path
q, q', KN/M2
800
600.
400.
200.
0.
0.
200.
400.
600.
800.
1000.
1200.
p', KN/M2 (1 KN/M2 = 0.14 PSI)

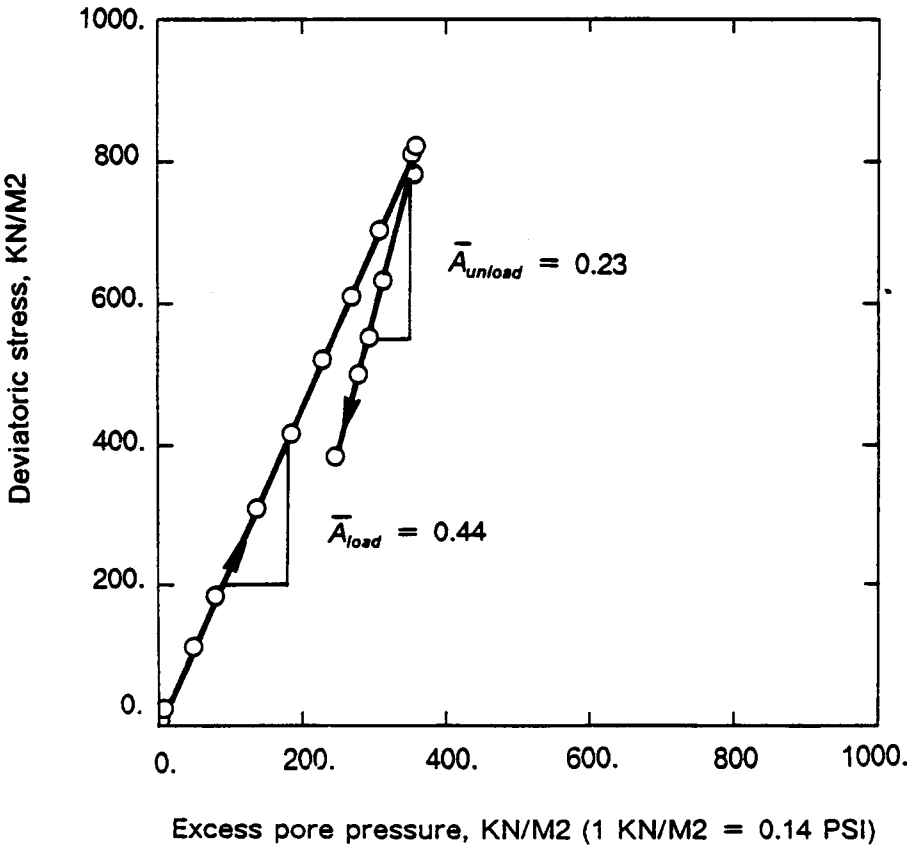
$\bar{A}_{unload}$ = 0.23
$\bar{A}_{load}$ = 0.44
Deviatoric stress, KN/M2
1000.
800
600.
400.
200.
0.
0.
200.
400.
600.
800
1000.
Excess pore pressure, KN/M2 (1 KN/M2 = 0.14 PSI)

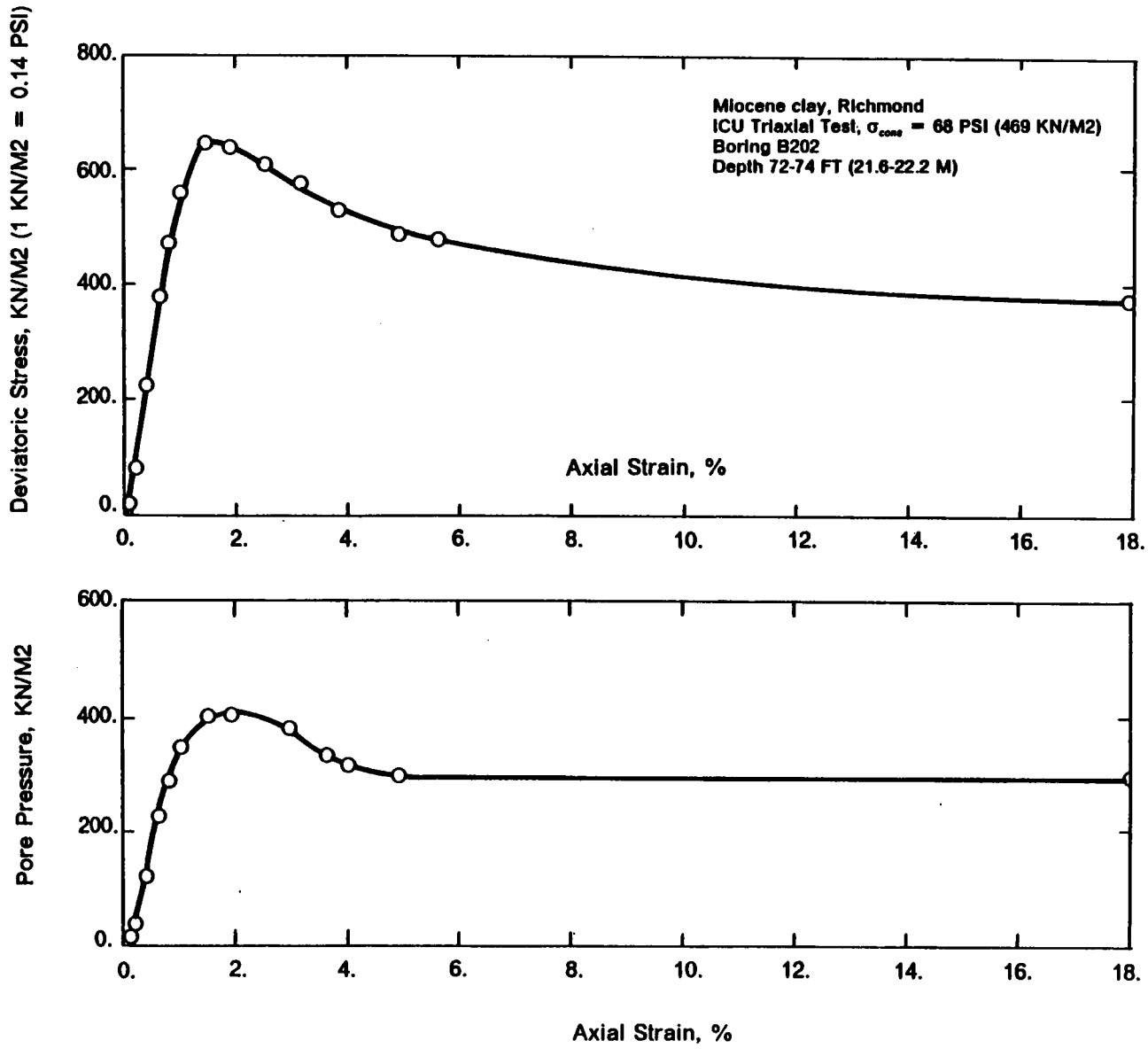
Miocene clay, Richmond
ICU Triaxial Test, σ_{cons} = 68 PSI (469 KN/M2)
Boring B202
Depth 72-74 FT (21.6-22.2 M)
Deviatoric Stress, KN/M2 (1 KN/M2 = 0.14 PSI)
800.
600.
400.
200.
0.
Axial Strain, %
0. 2. 4. 6. 8. 10. 12. 14. 16. 18.
Pore Pressure, KN/M2
600.
400.
200.
0.
0. 2. 4. 6. 8. 10. 12. 14. 16. 18.
Axial Strain, %

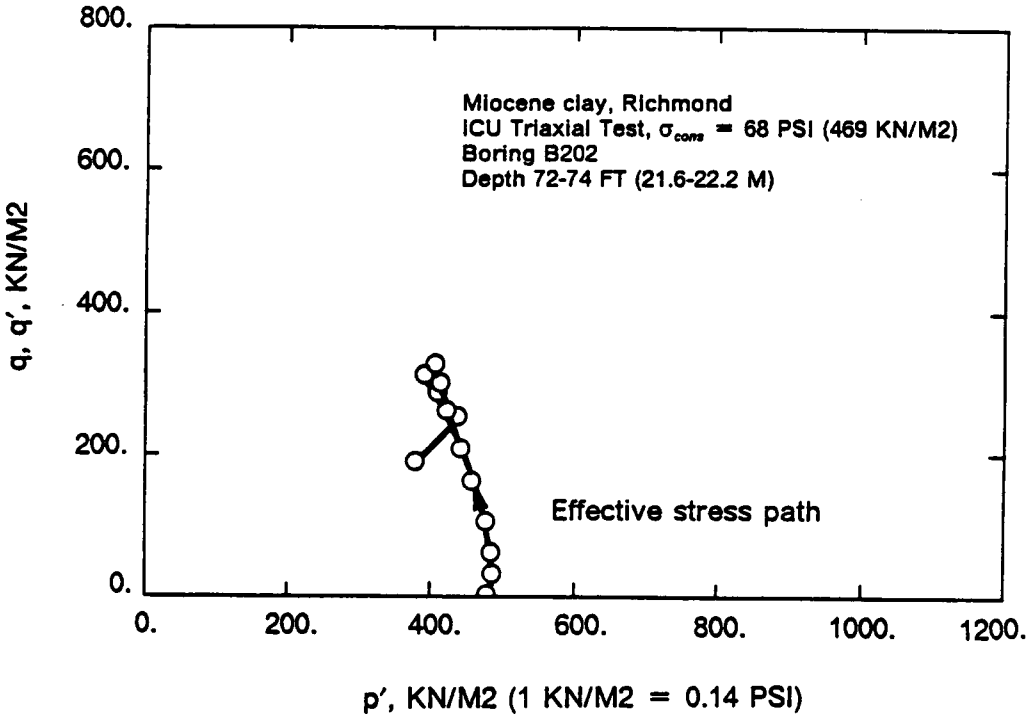
Miocene clay, Richmond
ICU Triaxial Test, σ_{cons} = 68 PSI (469 KN/M2)
Boring B202
Depth 72-74 FT (21.6-22.2 M)
Effective stress path
q, q', KN/M2
0.
200.
400.
600.
800.
0.
200.
400.
600.
800.
1000.
1200.
p', KN/M2 (1 KN/M2 = 0.14 PSI)

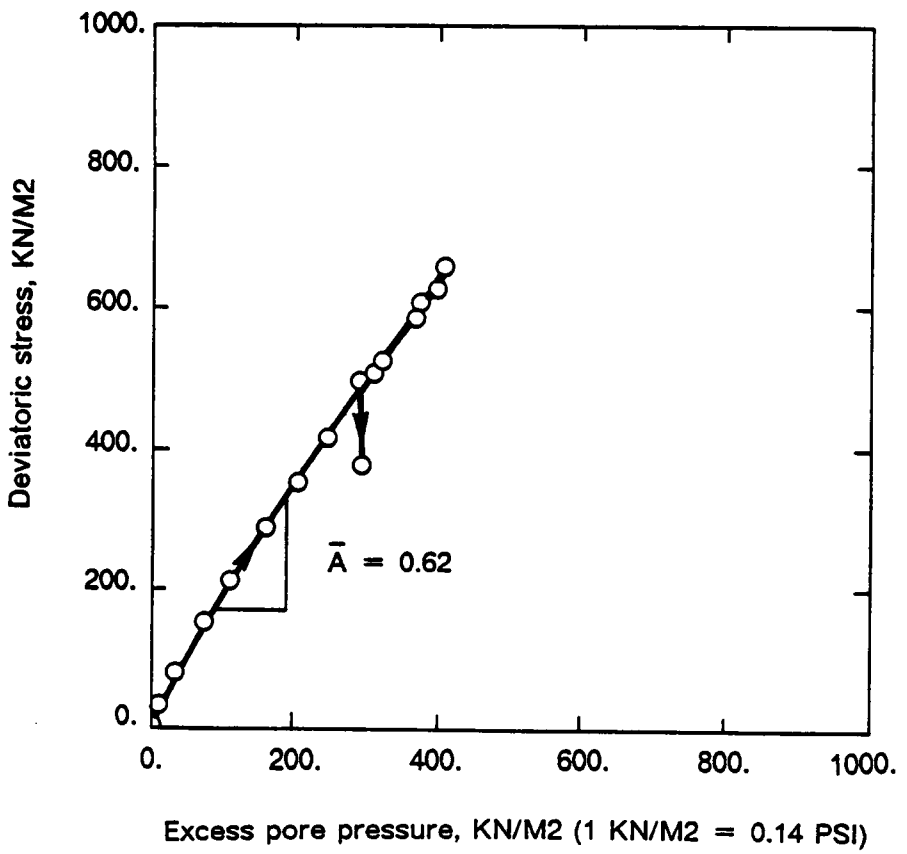
Deviatoric stress, KN/M2
$\bar{A}$ = 0.62
0.
200.
400.
600.
800.
1000.
Excess pore pressure, KN/M2 (1 KN/M2 = 0.14 PSI)

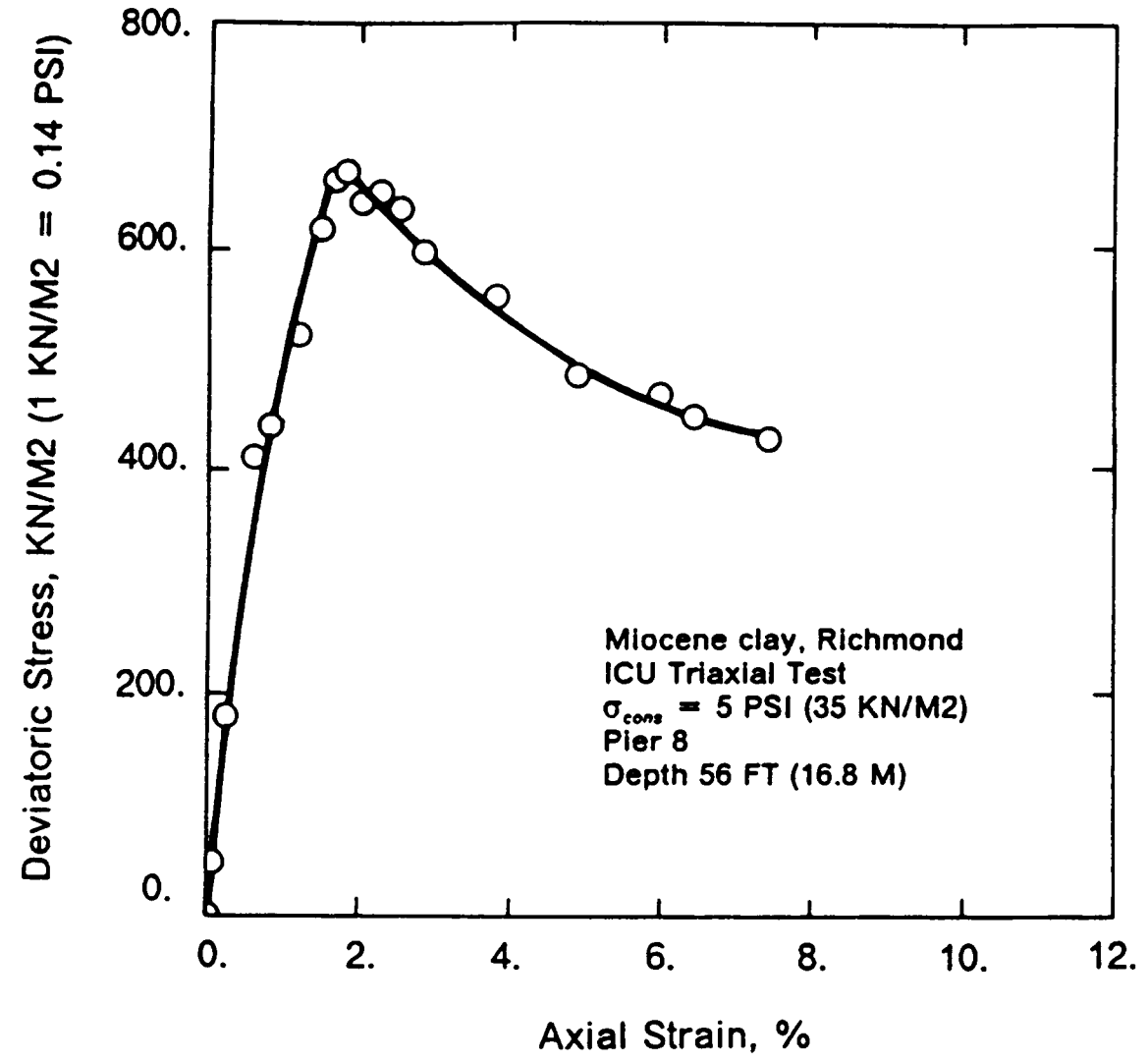
800.
600.
400.
200.
0.
Deviatoric Stress, KN/M2 (1 KN/M2 = 0.14 PSI)
Miocene clay, Richmond
ICU Triaxial Test
σ_{cons} = 5 PSI (35 KN/M2)
Pier 8
Depth 56 FT (16.8 M)
0.
2.
4.
6.
8.
10.
12.
Axial Strain, %

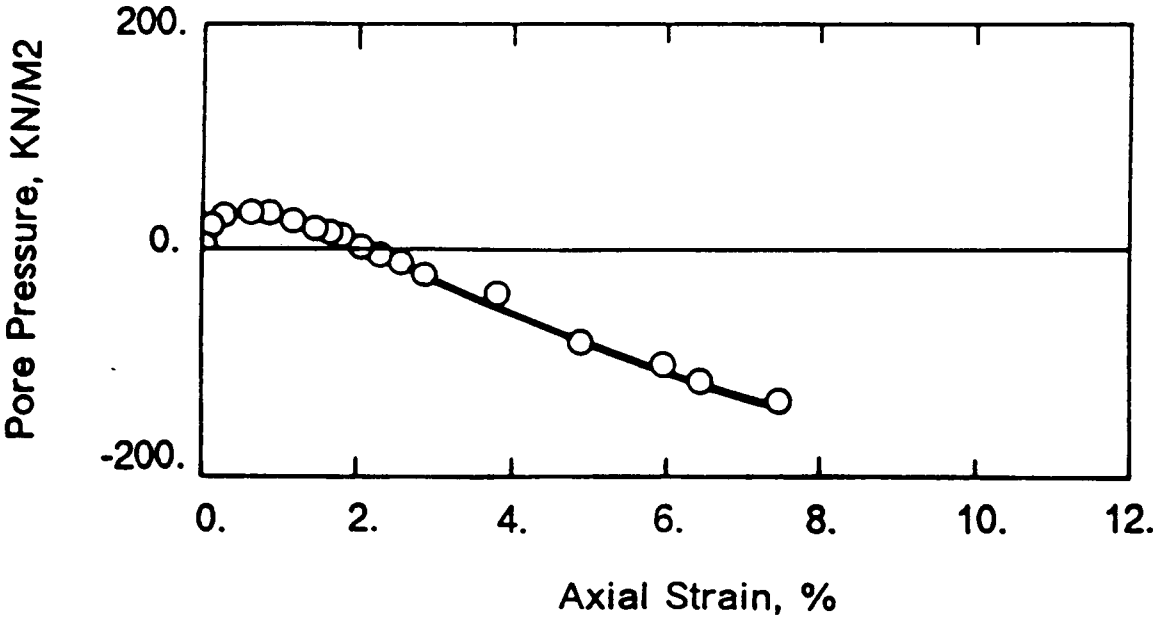
200.
0.
-200.
Pore Pressure, KN/M2
0.
2.
4.
6.
8.
10.
12.
Axial Strain, %

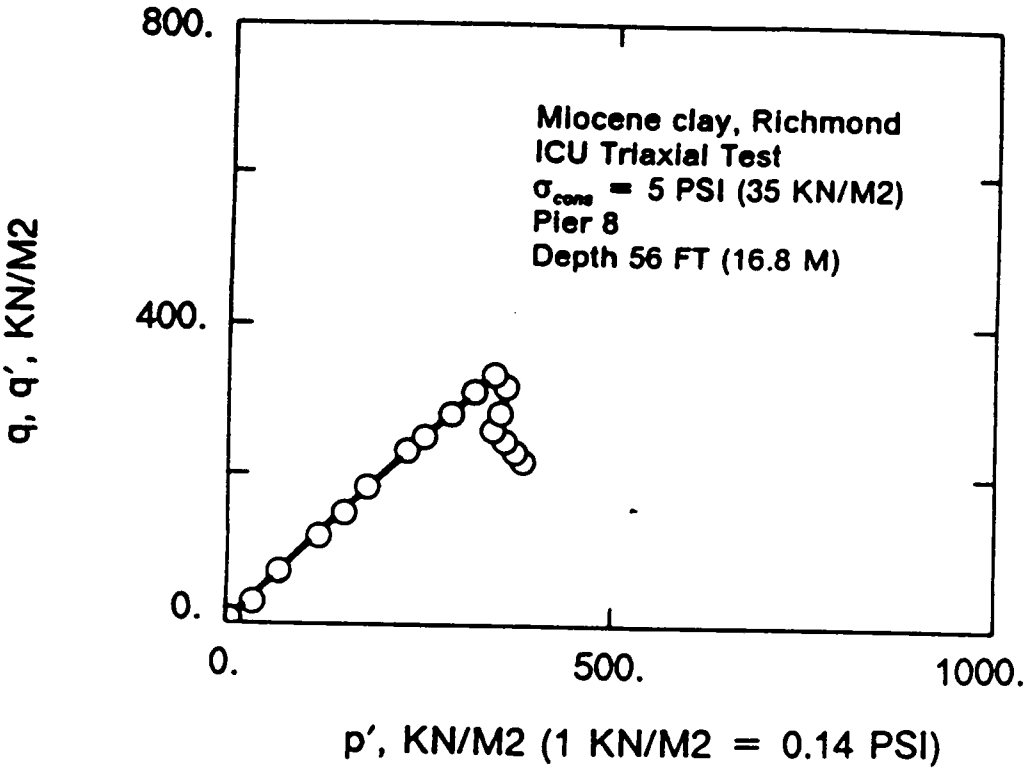
800.
400.
0.
0.
500.
1000.
q, q', KN/M2
p', KN/M2 (1 KN/M2 = 0.14 PSI)
Miocene clay, Richmond
ICU Triaxial Test
σcons = 5 PSI (35 KN/M2)
Pier 8
Depth 56 FT (16.8 M)

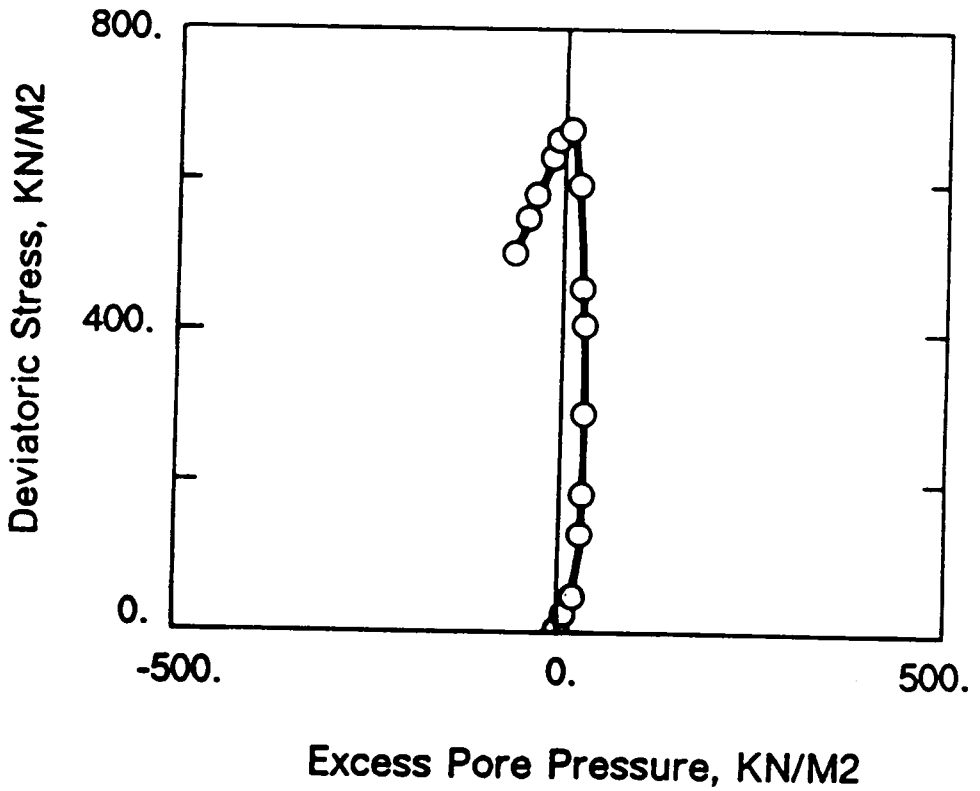
800.
400.
0.
-500.
0.
500.
Deviatoric Stress, KN/M2
Excess Pore Pressure, KN/M2

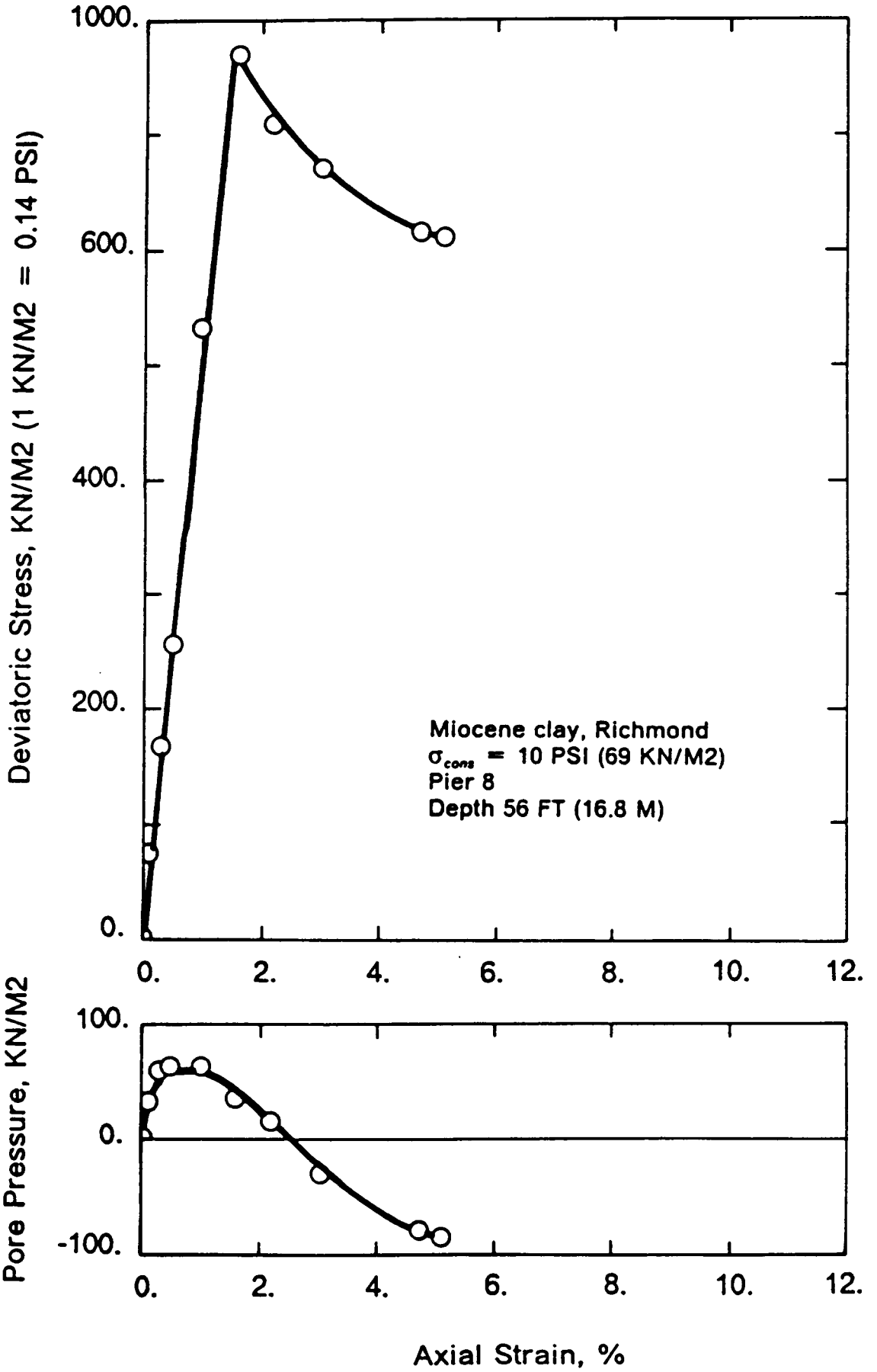
1000.
600.
400.
200.
0.
Deviatoric Stress, KN/M2 (1 KN/M2 = 0.14 PSI)
Miocene clay, Richmond
σcons = 10 PSI (69 KN/M2)
Pier 8
Depth 56 FT (16.8 M)
0.
2.
4.
6.
8.
10.
12.
100.
0.
-100.
Pore Pressure, KN/M2
0.
2.
4.
6.
8.
10.
12.
Axial Strain, %

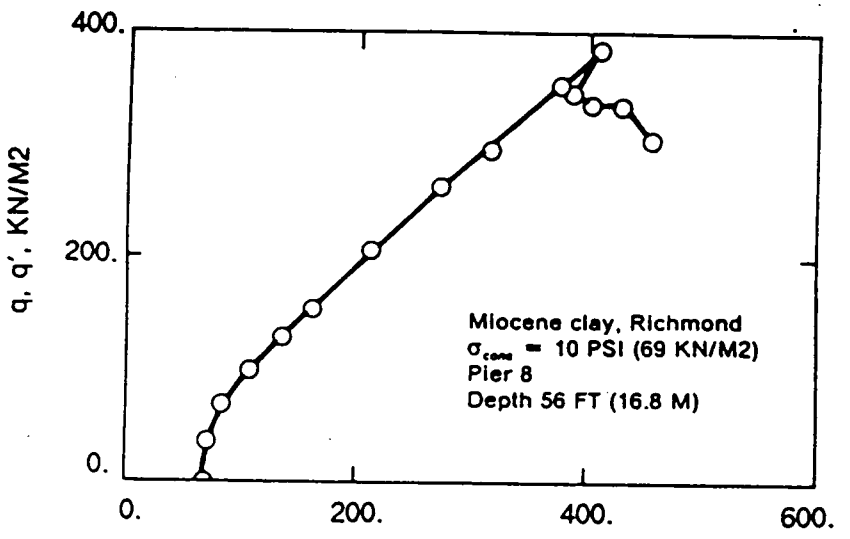
400.
200.
0.
q, q', KN/M2
0.
200.
400.
600.
Miocene clay, Richmond
σ_{cons} = 10 PSI (69 KN/M2)
Pier 8
Depth 56 FT (16.8 M)
p', KN/M2 (1 KN/M2 = 0.14 PSI)

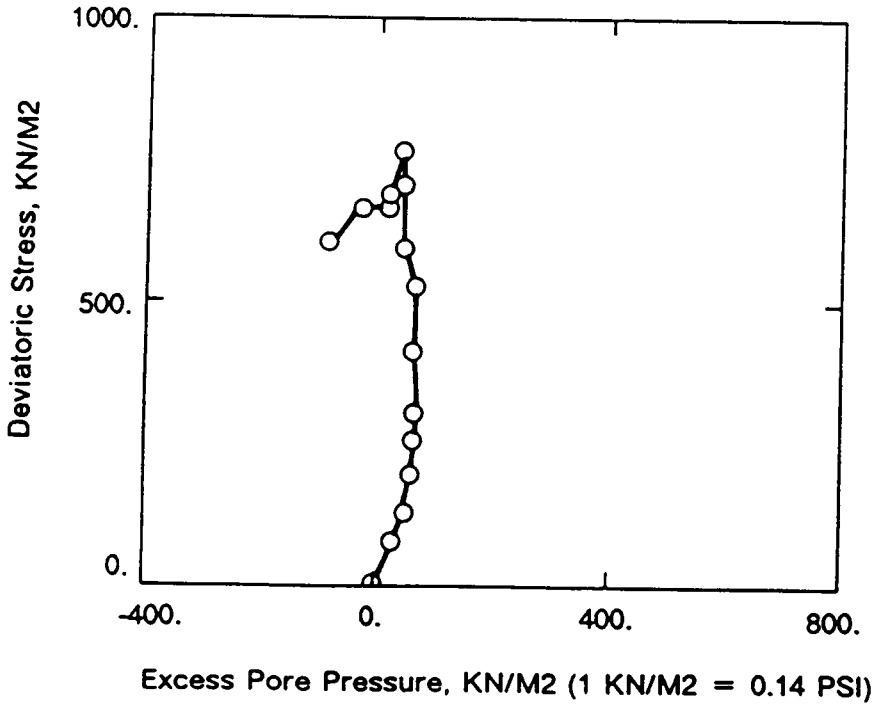
1000.
500.
0.
Deviatoric Stress, KN/M2
-400.
0.
400.
800.
Excess Pore Pressure, KN/M2 (1 KN/M2 = 0.14 PSI)

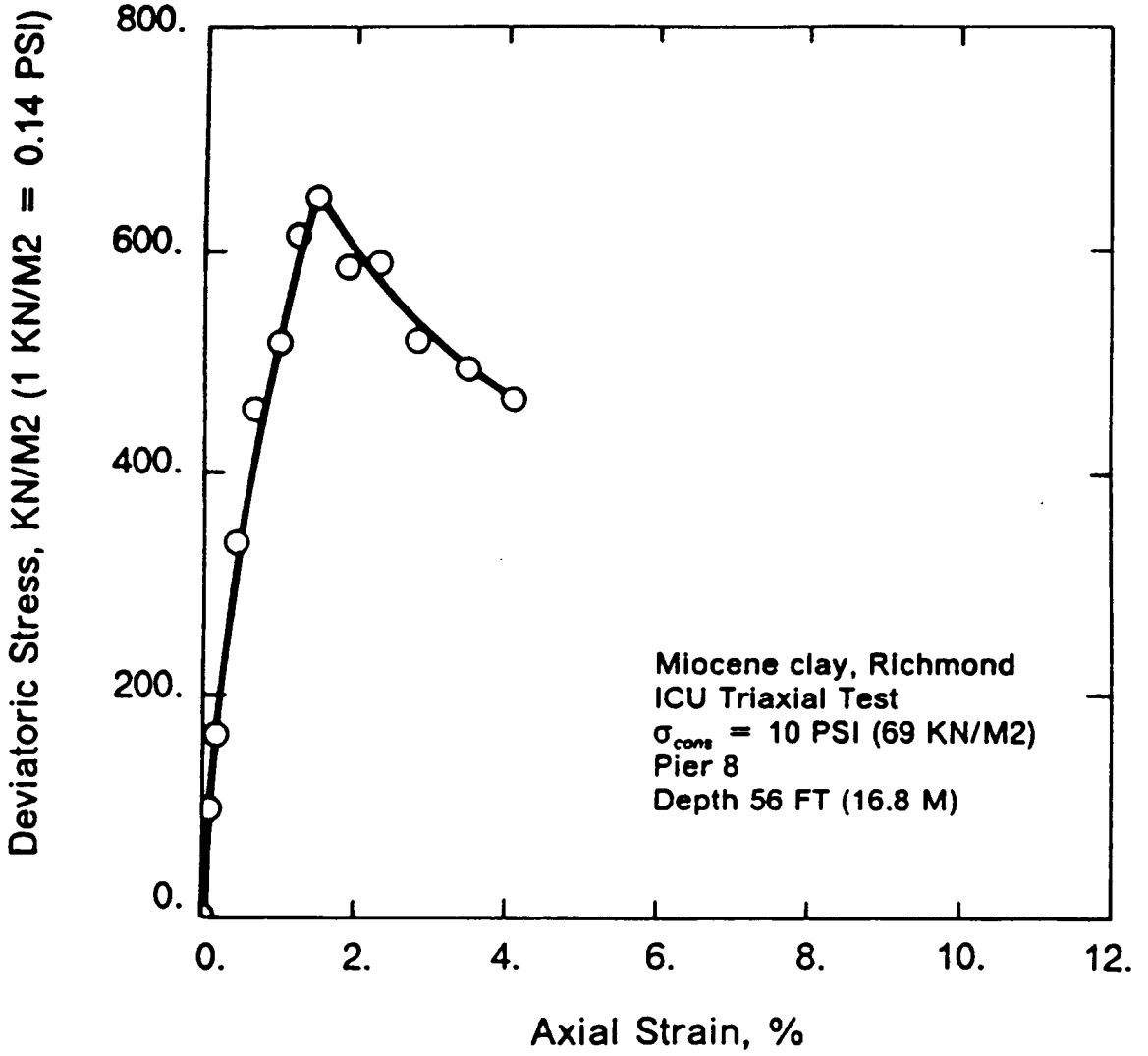
Deviatoric Stress, KN/M2 (1 KN/M2 = 0.14 PSI)
800.
600.
400.
200.
0.
0.
2.
4.
6.
8.
10.
12.
Axial Strain, %
Miocene clay, Richmond
ICU Triaxial Test
σcons = 10 PSI (69 KN/M2)
Pier 8
Depth 56 FT (16.8 M)

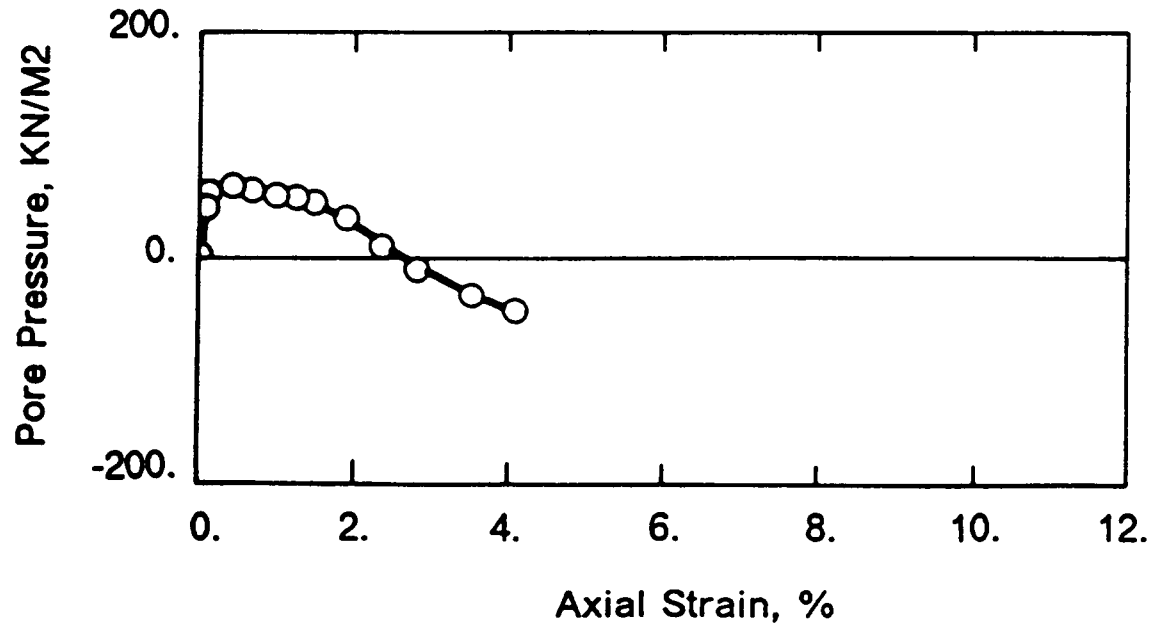
Pore Pressure, KN/M2
200.
0.
-200.
0.
2.
4.
6.
8.
10.
12.
Axial Strain, %

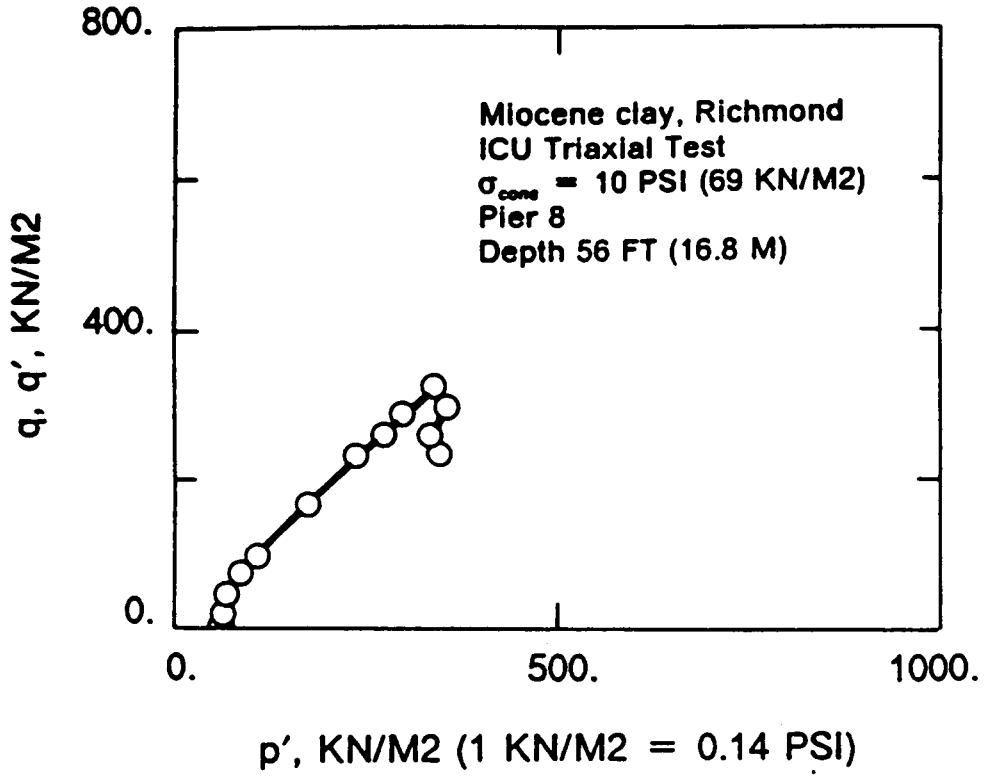
800.
400.
0.
0.
500.
1000.
q, q', KN/M2
p', KN/M2 (1 KN/M2 = 0.14 PSI)
Miocene clay, Richmond
ICU Triaxial Test
σcons = 10 PSI (69 KN/M2)
Pier 8
Depth 56 FT (16.8 M)

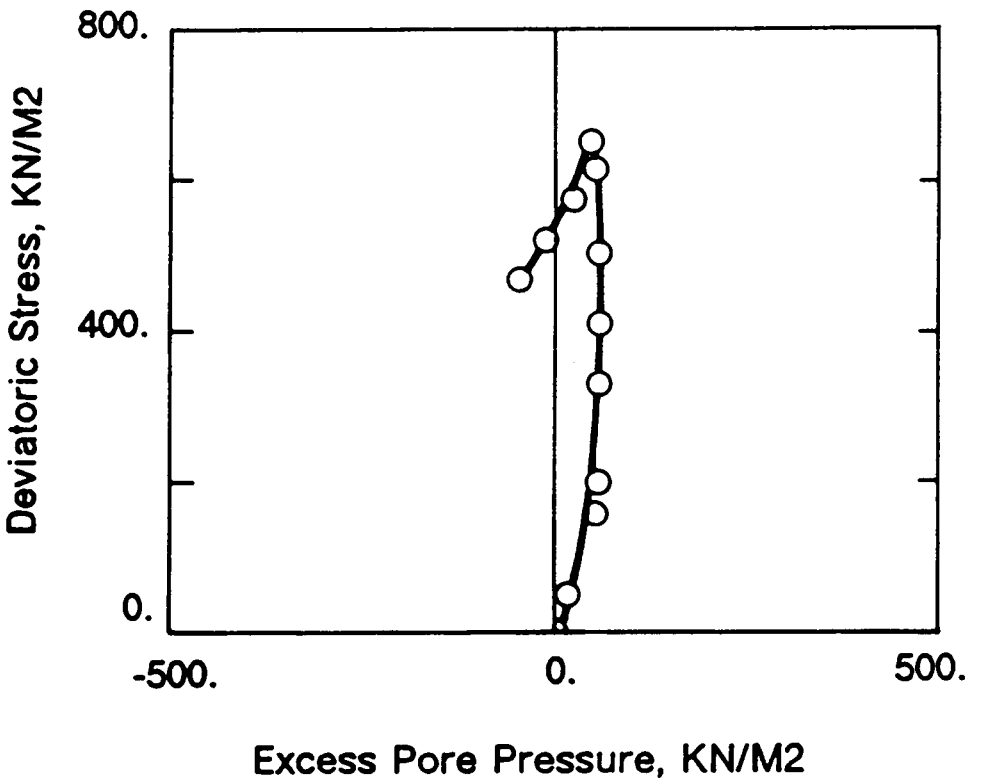
800.
400.
0.
-500.
0.
500.
Deviatoric Stress, KN/M2
Excess Pore Pressure, KN/M2

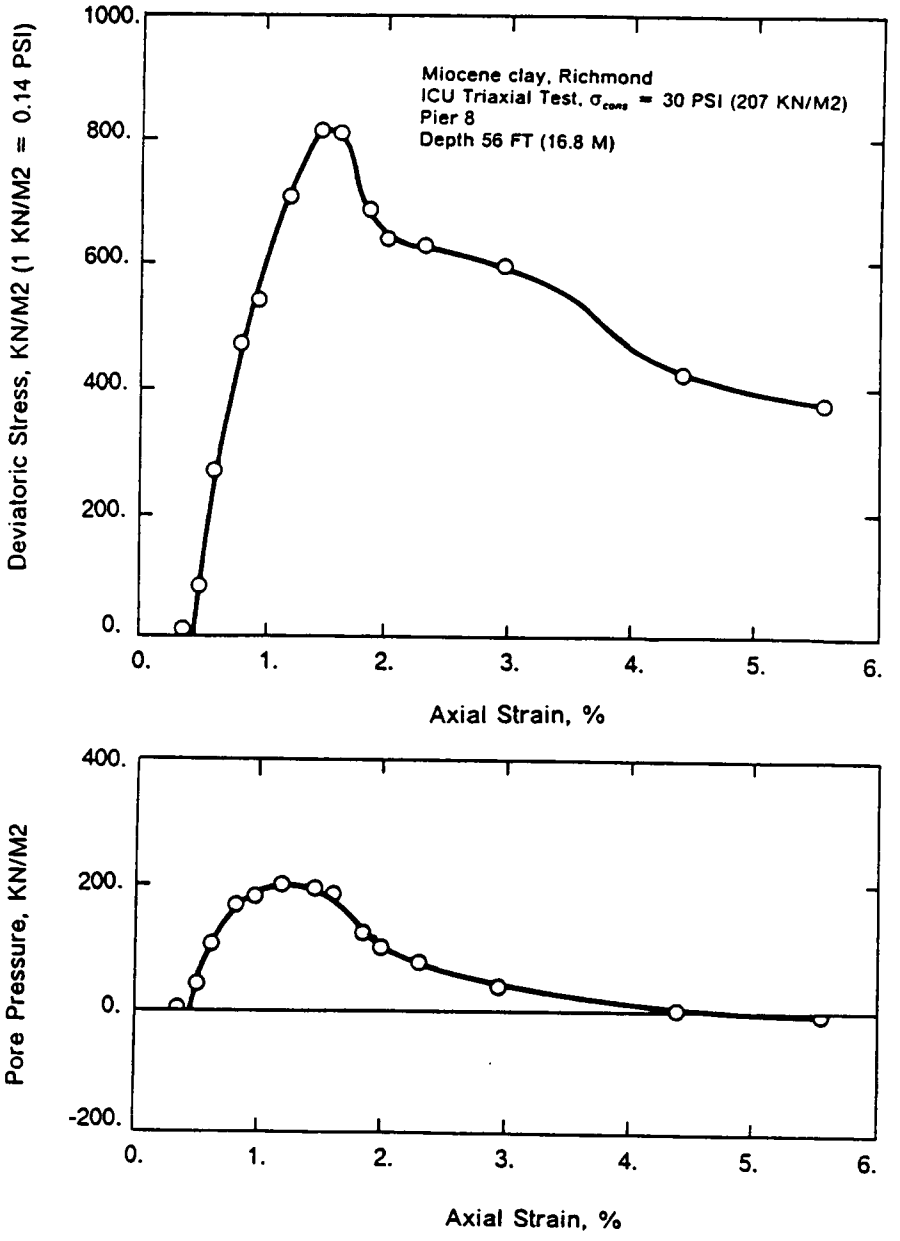
Miocene clay, Richmond
ICU Triaxial Test, σ_{cons} = 30 PSI (207 KN/M2)
Pier 8
Depth 56 FT (16.8 M)
Deviatoric Stress, KN/M2 (1 KN/M2 = 0.14 PSI)
1000.
800.
600.
400.
200.
0.
0.
1.
2.
3.
4.
5.
6.
Axial Strain, %
Pore Pressure, KN/M2
400.
200.
0.
-200.
0.
1.
2.
3.
4.
5.
6.
Axial Strain, %

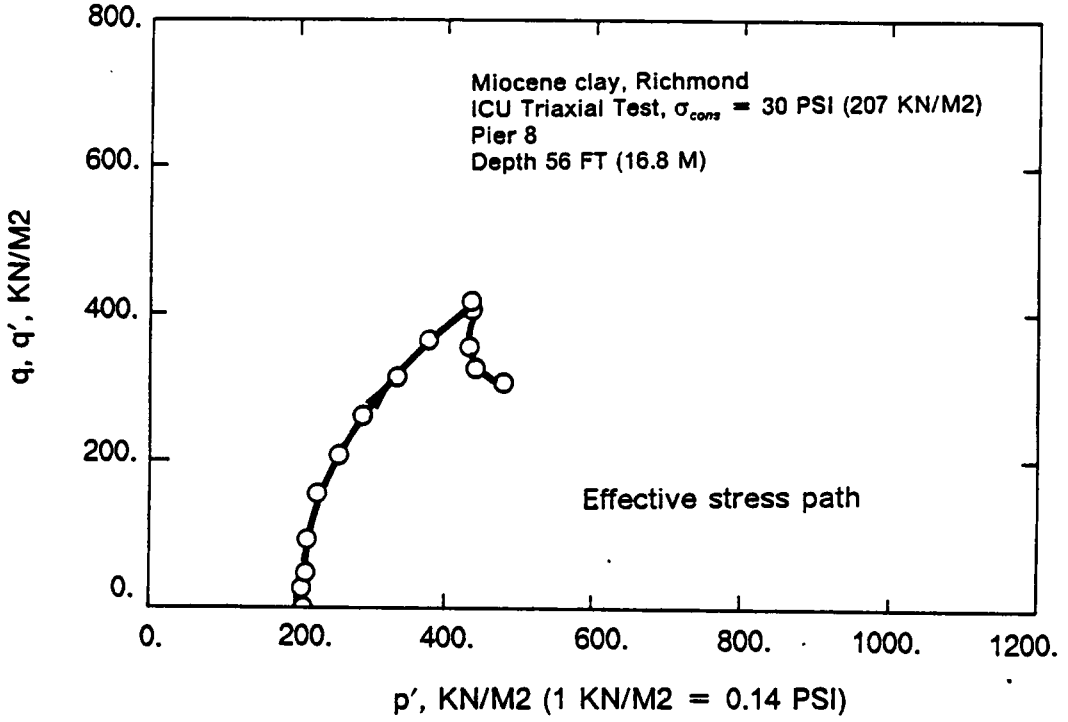
Miocene clay, Richmond
ICU Triaxial Test, σ_{cons} = 30 PSI (207 KN/M2)
Pier 8
Depth 56 FT (16.8 M)
Effective stress path
q, q', KN/M2
800.
600.
400.
200.
0.
0.
200.
400.
600.
800.
1000.
1200.
p', KN/M2 (1 KN/M2 = 0.14 PSI)

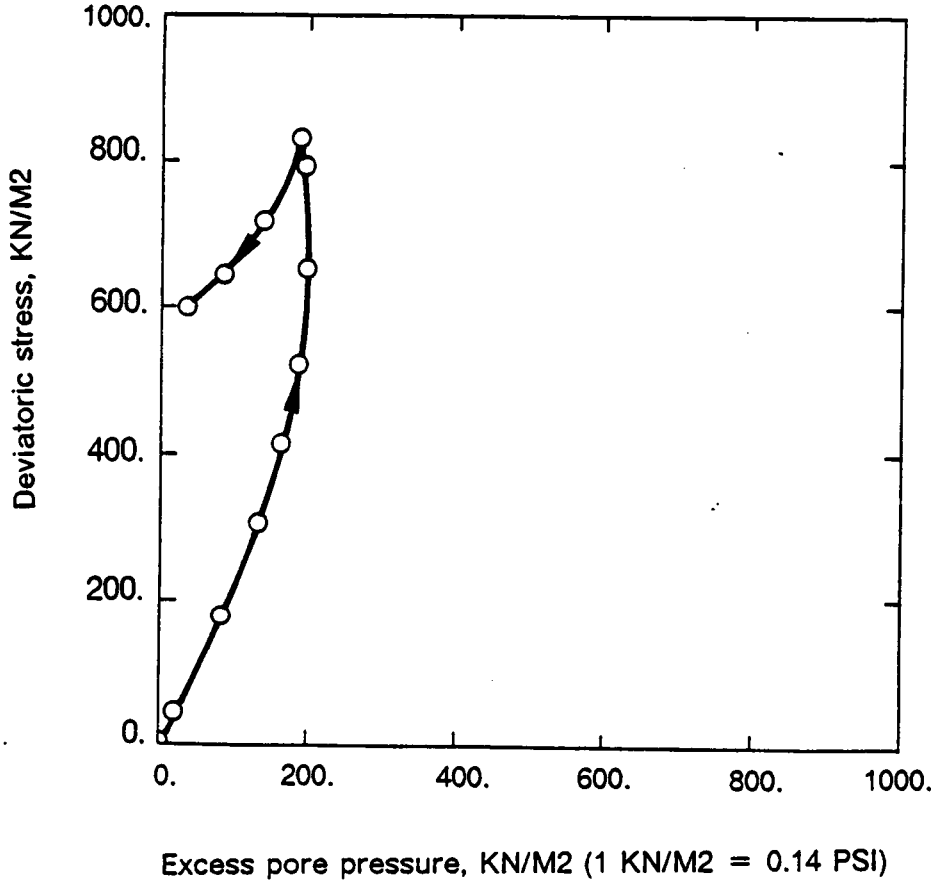
Deviatoric stress, KN/M2
1000.
800.
600.
400.
200.
0.
0.
200.
400.
600.
800.
1000.
Excess pore pressure, KN/M2 (1 KN/M2 = 0.14 PSI)

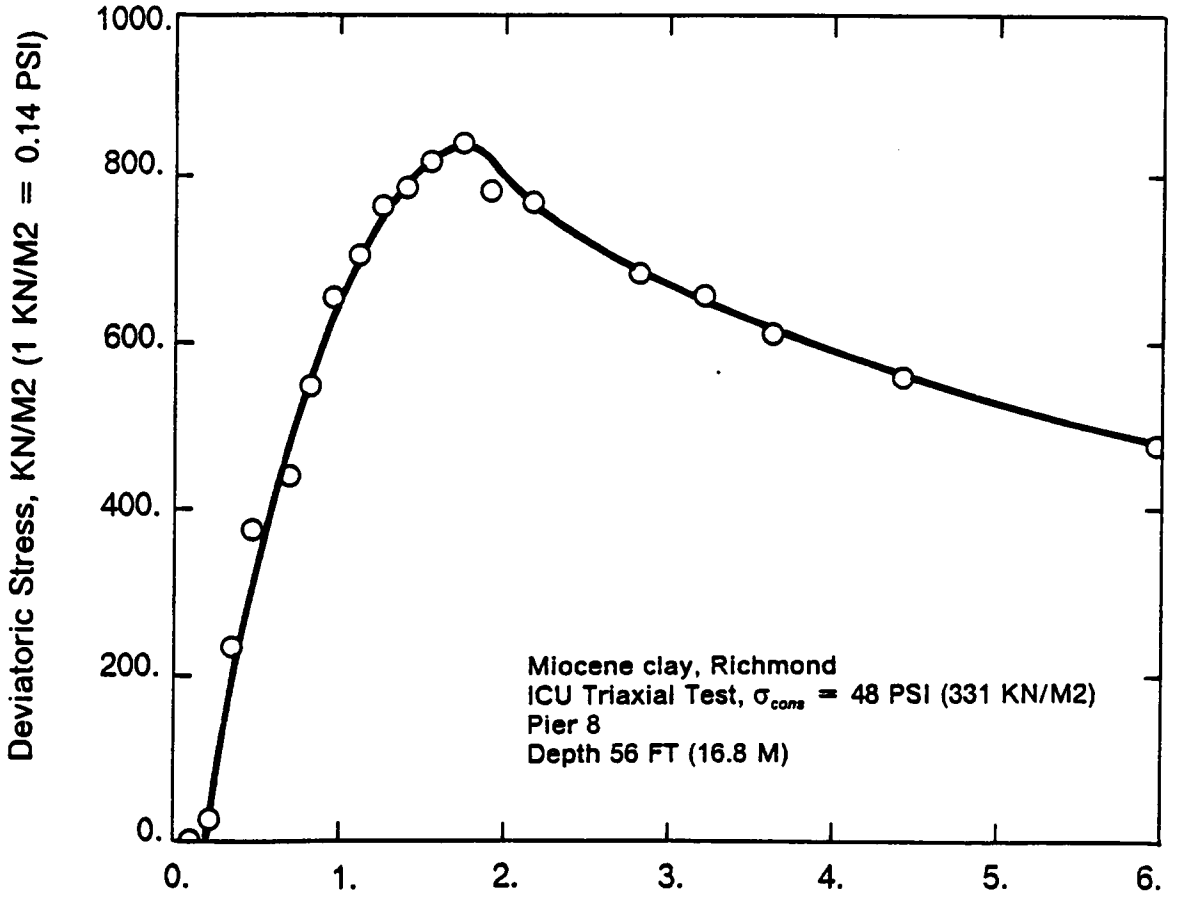
Deviatoric Stress, KN/M2 (1 KN/M2 = 0.14 PSI)
1000.
800.
600.
400.
200.
0.
0.
1.
2.
3.
4.
5.
6.
Axial Strain, %
Miocene clay, Richmond
ICU Triaxial Test, σ_{cons} = 48 PSI (331 KN/M2)
Pier 8
Depth 56 FT (16.8 M)

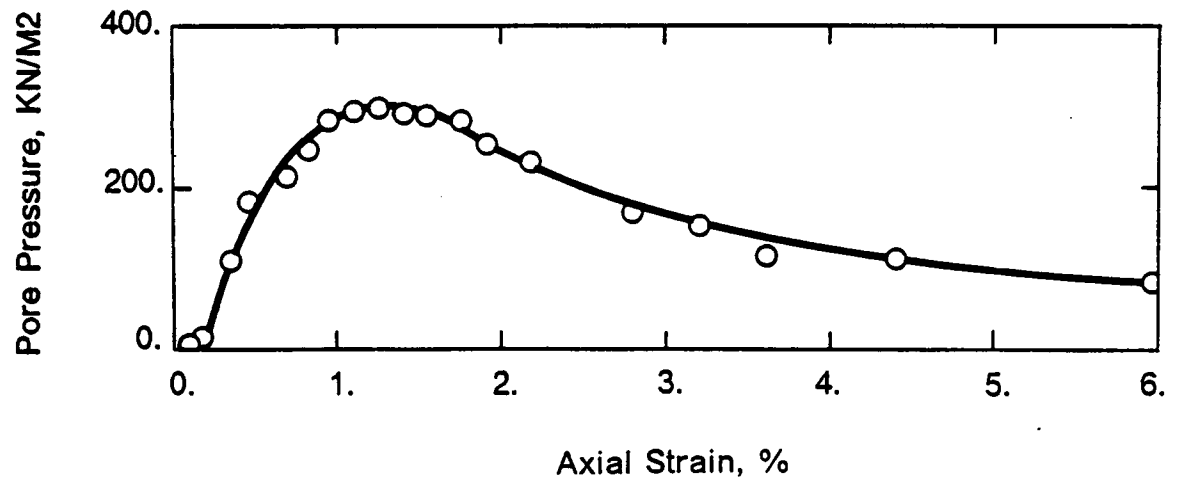
Pore Pressure, KN/M2
400.
200.
0.
0.
1.
2.
3.
4.
5.
6.
Axial Strain, %

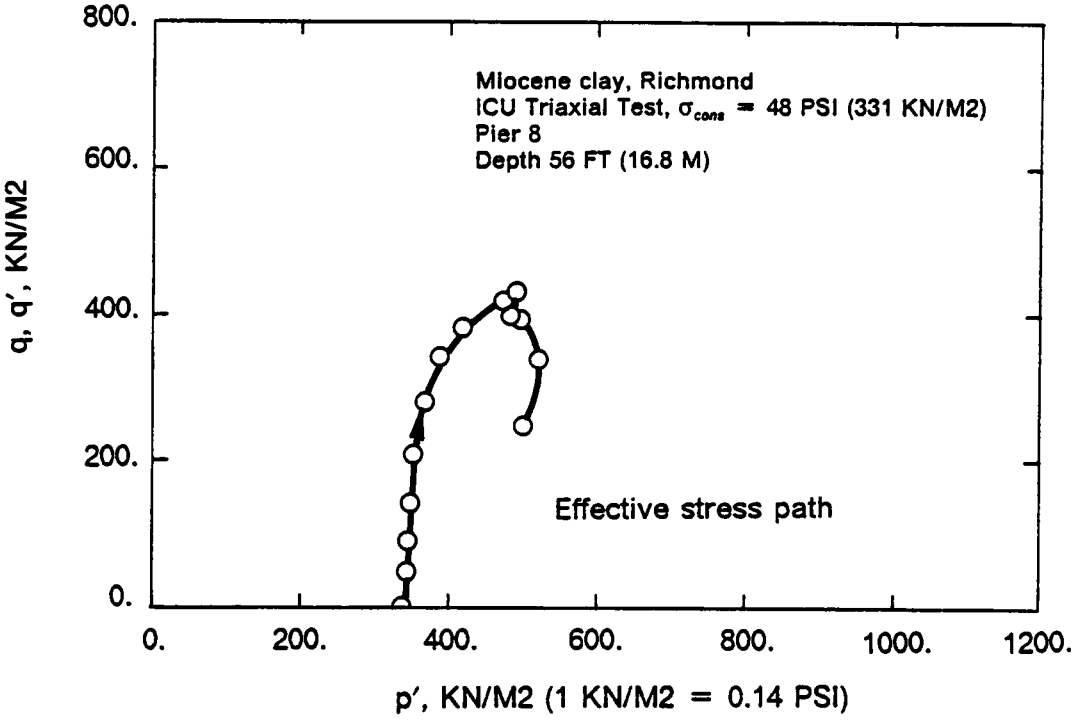
Miocene clay, Richmond
ICU Triaxial Test, σ_{cons} = 48 PSI (331 KN/M2)
Pier 8
Depth 56 FT (16.8 M)
Effective stress path
q, q', KN/M2
p', KN/M2 (1 KN/M2 = 0.14 PSI)
0.
200.
400.
600.
800.
1000.
1200.

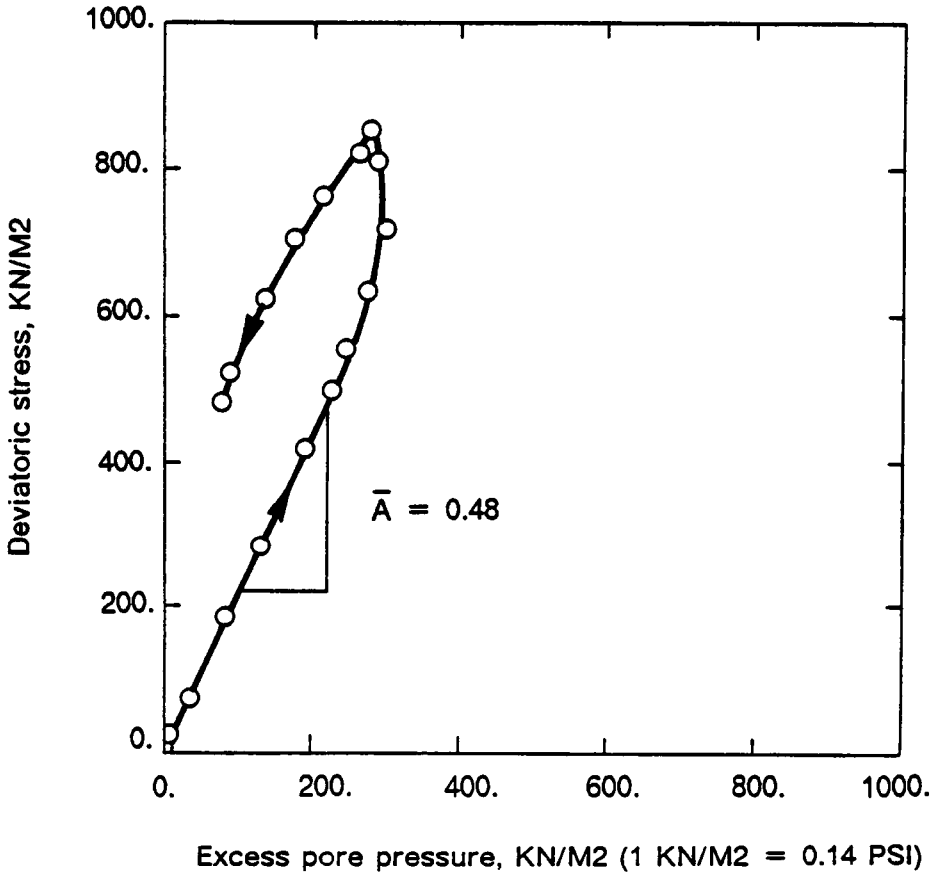
$\bar{A}$ = 0.48
Deviatoric stress, KN/M2
Excess pore pressure, KN/M2 (1 KN/M2 = 0.14 PSI)
0.
200.
400.
600.
800.
1000.

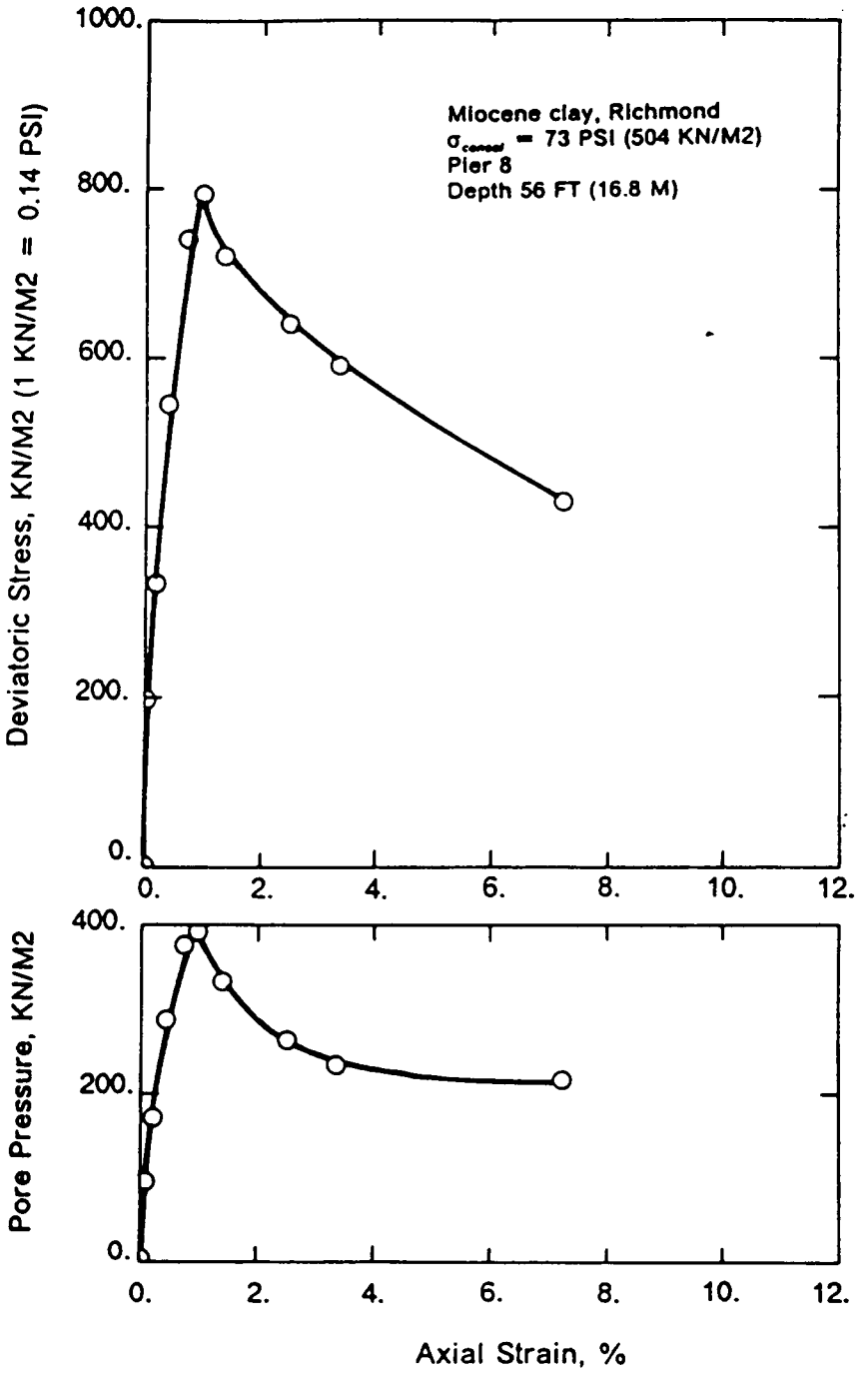
Miocene clay, Richmond
σ_{consol} = 73 PSI (504 KN/M2)
Pier 8
Depth 56 FT (16.8 M)
Deviatoric Stress, KN/M2 (1 KN/M2 = 0.14 PSI)
1000.
800.
600.
400.
200.
0.
0.
2.
4.
6.
8.
10.
12.
Pore Pressure, KN/M2
400.
200.
0.
0.
2.
4.
6.
8.
10.
12.
Axial Strain, %

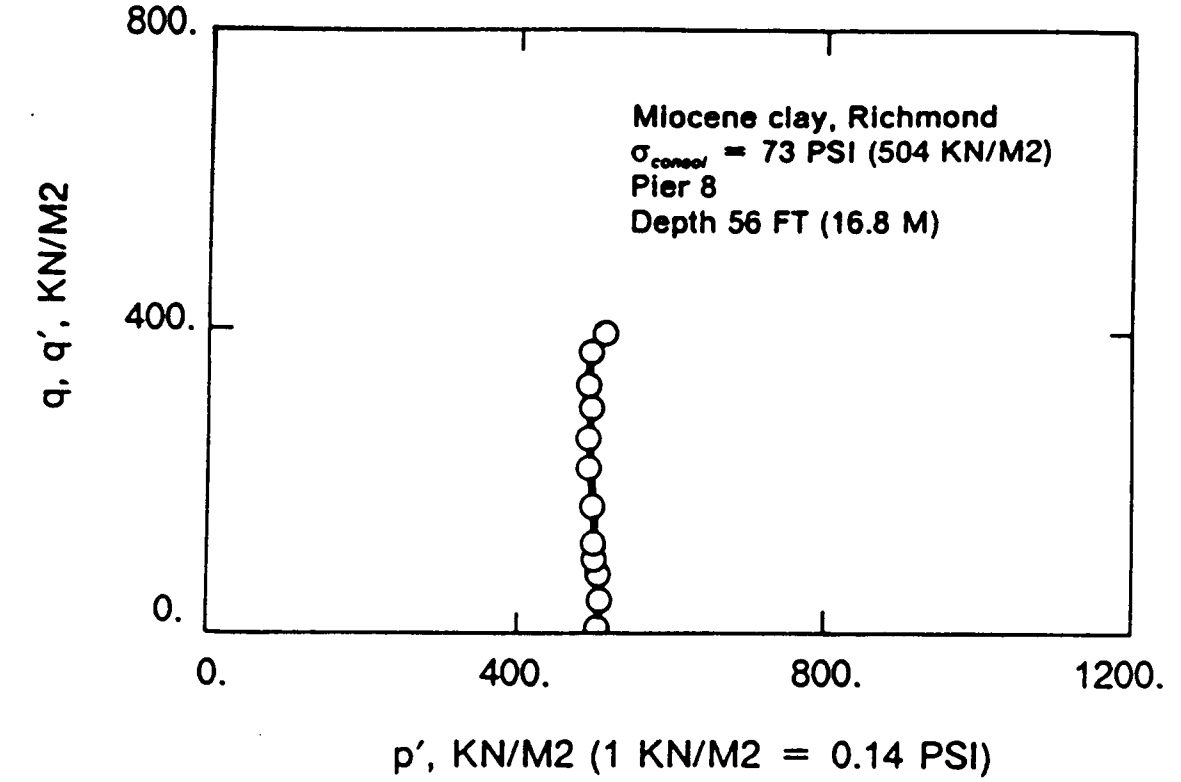
800.
400.
0.
q, q', KN/M2
Miocene clay, Richmond
σ_{consol} = 73 PSI (504 KN/M2)
Pier 8
Depth 56 FT (16.8 M)
0.
400.
800.
1200.
p', KN/M2 (1 KN/M2 = 0.14 PSI)

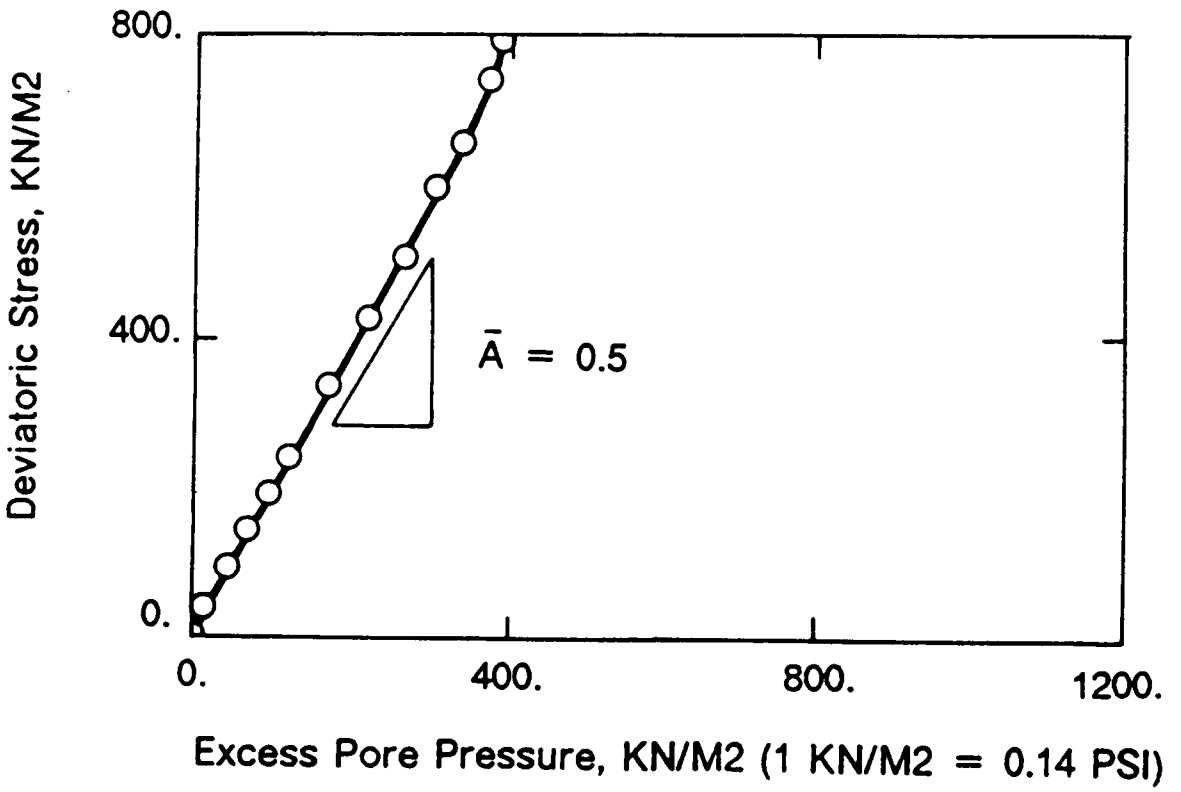
800.
400.
0.
Deviatoric Stress, KN/M2
$\bar{A}$ = 0.5
0.
400.
800.
1200.
Excess Pore Pressure, KN/M2 (1 KN/M2 = 0.14 PSI)

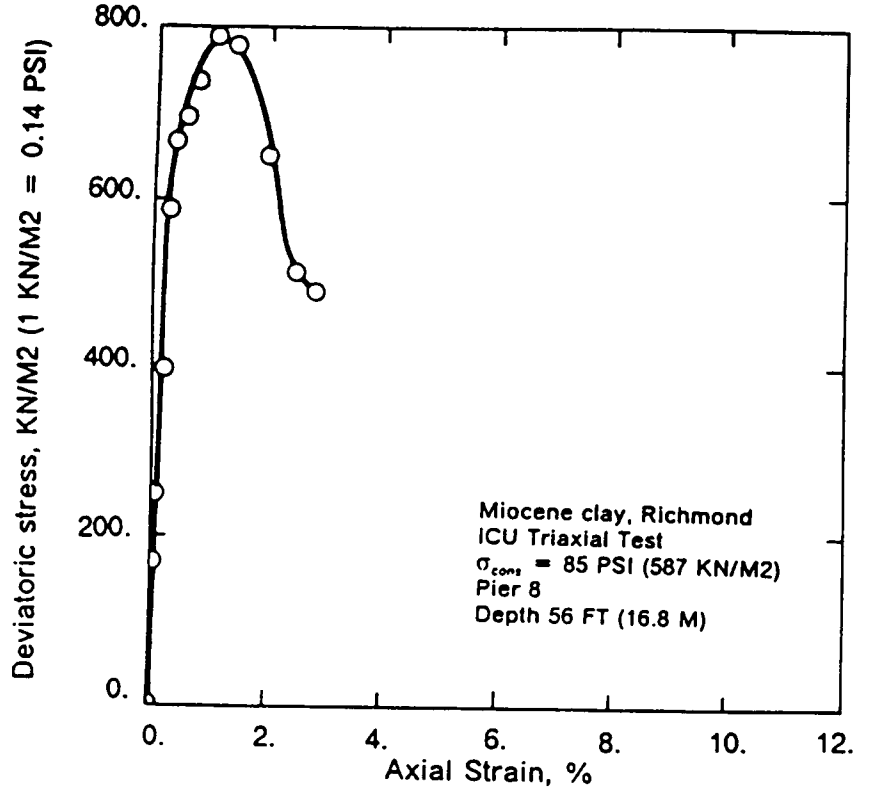
Deviatoric stress, KN/M2 (1 KN/M2 = 0.14 PSI)
800.
600.
400.
200.
0.
0.
2.
4.
6.
8.
10.
12.
Axial Strain, %
Miocene clay, Richmond
ICU Triaxial Test
σ_{cons} = 85 PSI (587 KN/M2)
Pier 8
Depth 56 FT (16.8 M)

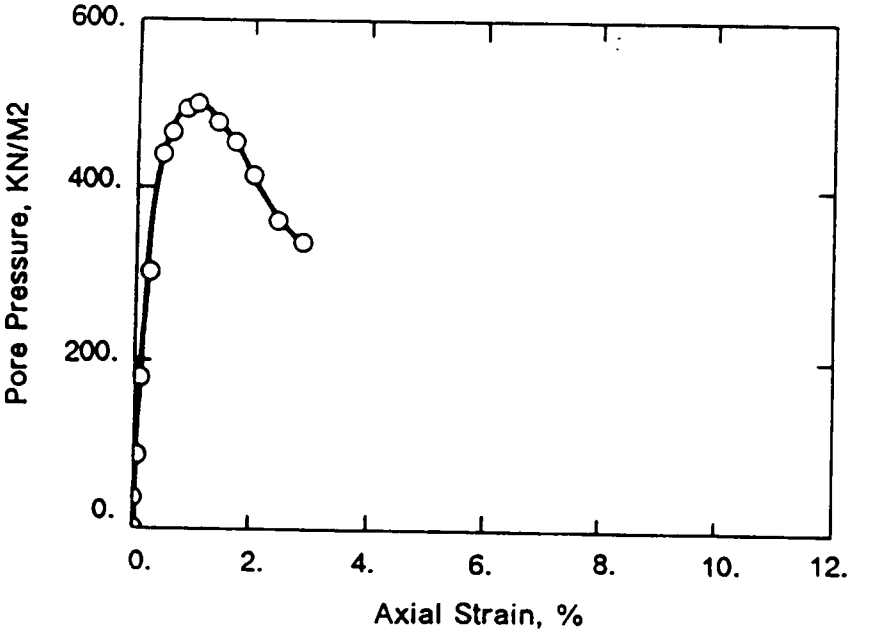
Pore Pressure, KN/M2
600.
400.
200.
0.
0.
2.
4.
6.
8.
10.
12.
Axial Strain, %

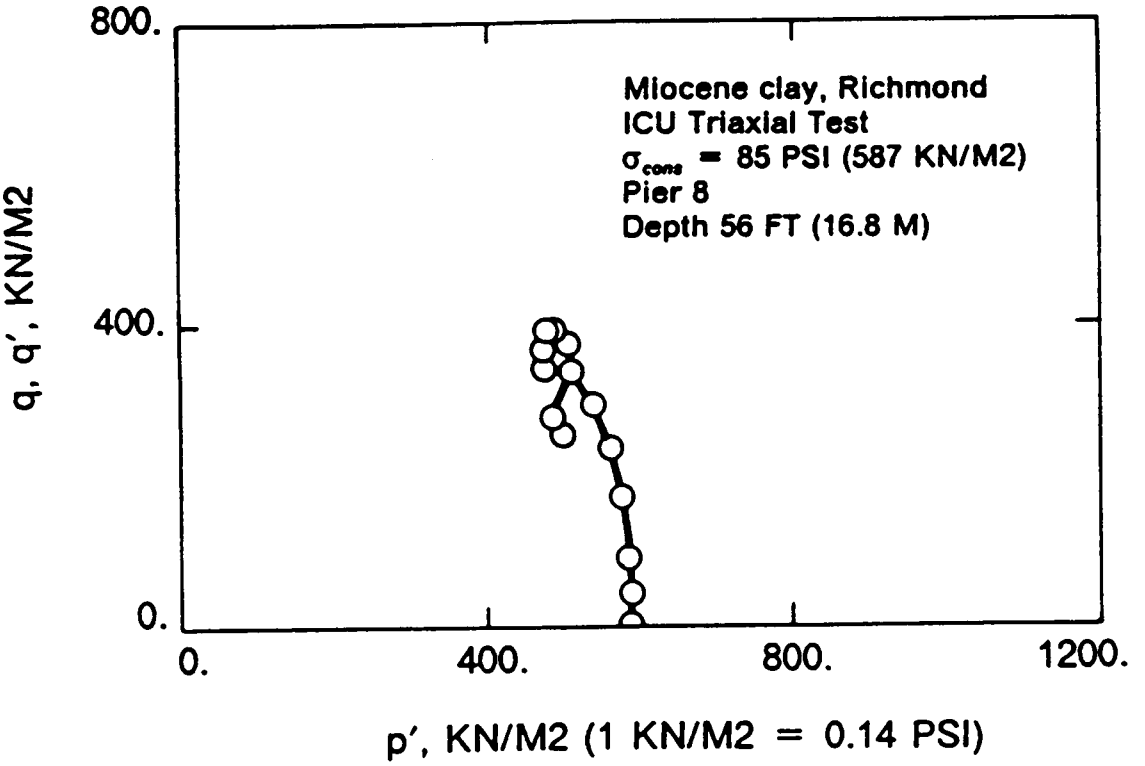
800.
400.
0.
0.
400.
800.
1200.
q, q', KN/M2
p', KN/M2 (1 KN/M2 = 0.14 PSI)
Miocene clay, Richmond
ICU Triaxial Test
σ_{cons} = 85 PSI (587 KN/M2)
Pier 8
Depth 56 FT (16.8 M)

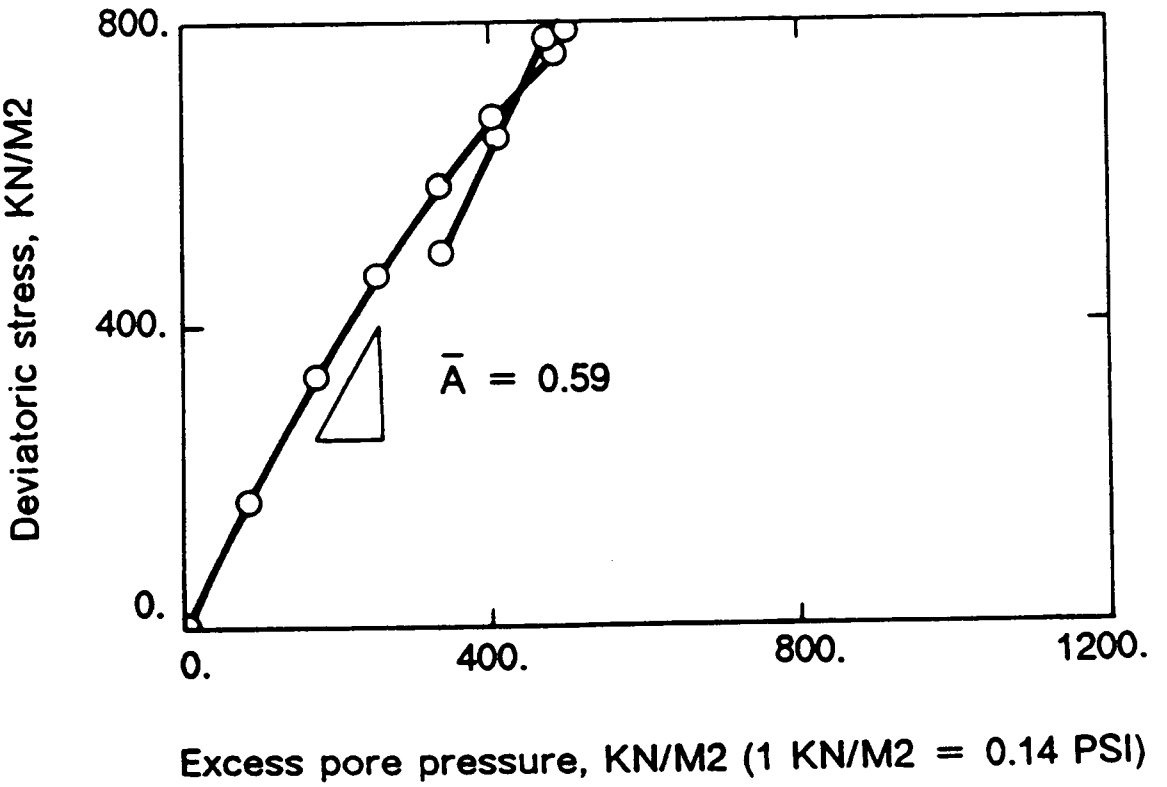
800.
400.
0.
0.
400.
800.
1200.
Deviatoric stress, KN/M2
$\bar{A}$ = 0.59
Excess pore pressure, KN/M2 (1 KN/M2 = 0.14 PSI)

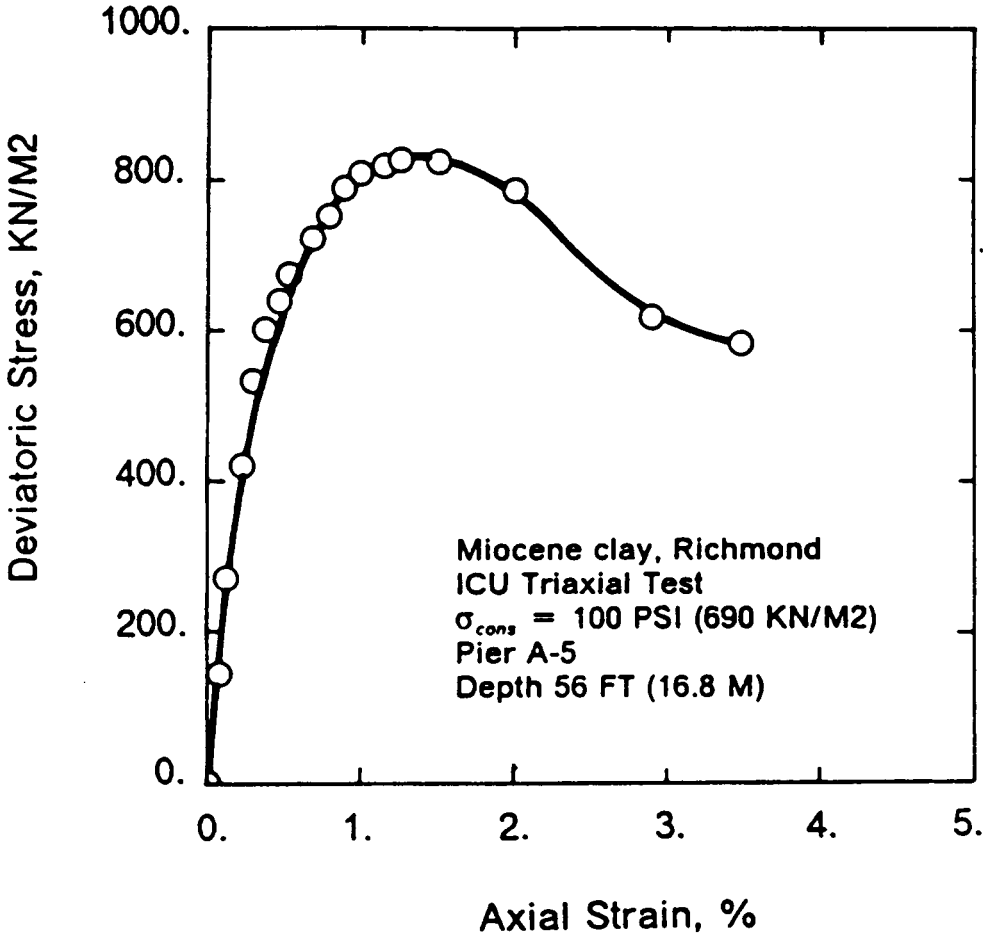
1000.
800.
600.
400.
200.
0.
Deviatoric Stress, KN/M2
0.
1.
2.
3.
4.
5.
Axial Strain, %
Miocene clay, Richmond
ICU Triaxial Test
σcons = 100 PSI (690 KN/M2)
Pier A-5
Depth 56 FT (16.8 M)

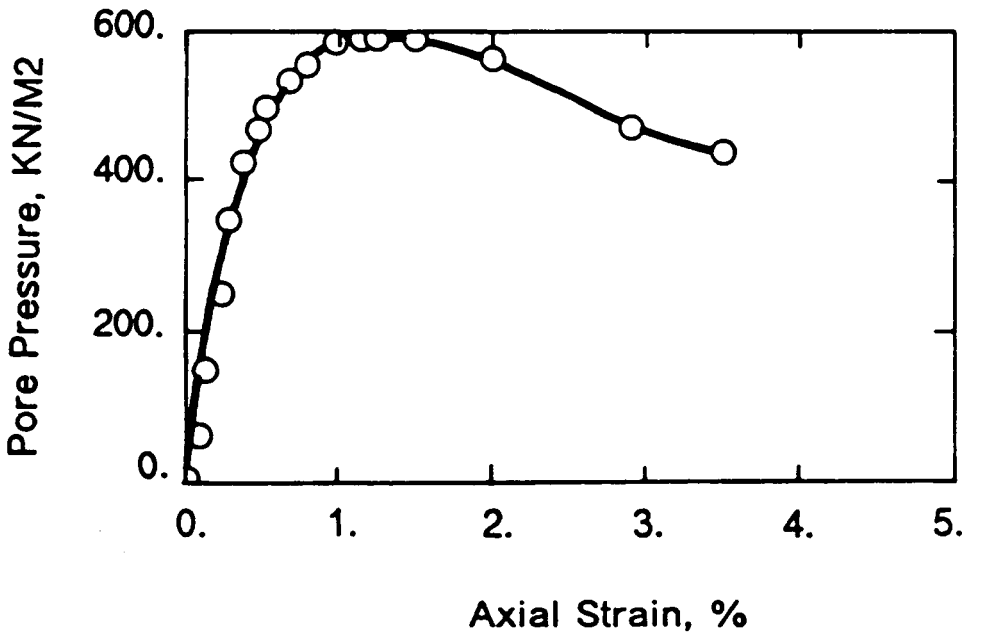
600.
400.
200.
0.
Pore Pressure, KN/M2
0.
1.
2.
3.
4.
5.
Axial Strain, %

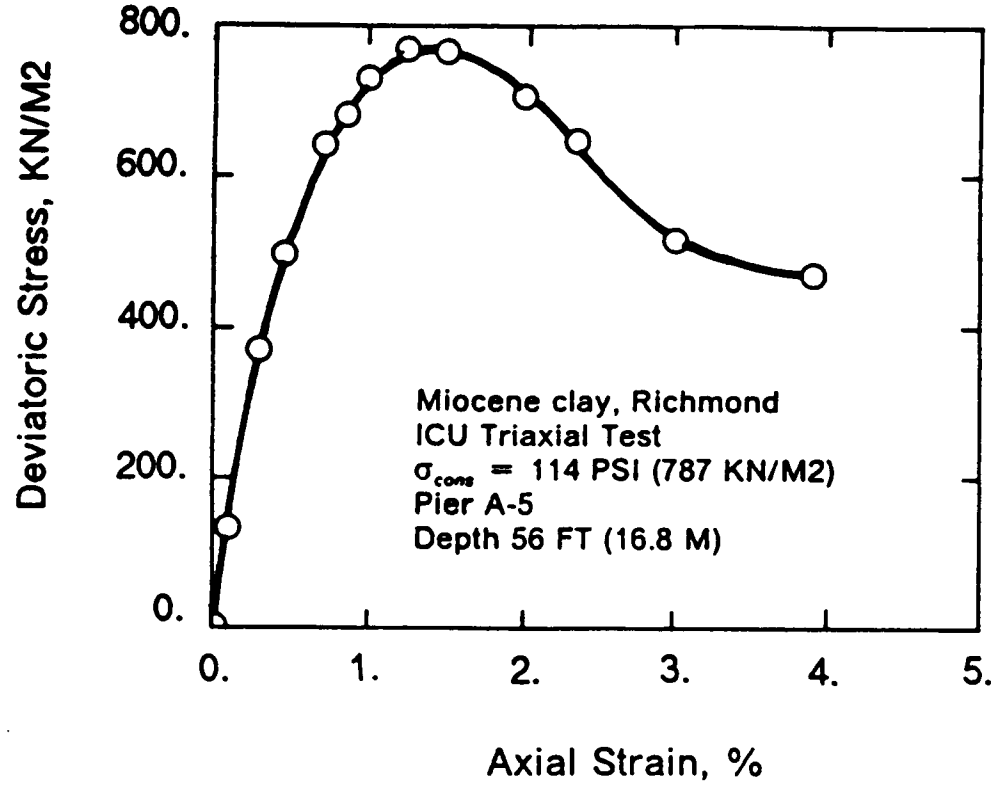
Deviatoric Stress, KN/M2
800.
600.
400.
200.
0.
0.
1.
2.
3.
4.
5.
Axial Strain, %
Miocene clay, Richmond
ICU Triaxial Test
σ_{cons} = 114 PSI (787 KN/M2)
Pier A-5
Depth 56 FT (16.8 M)

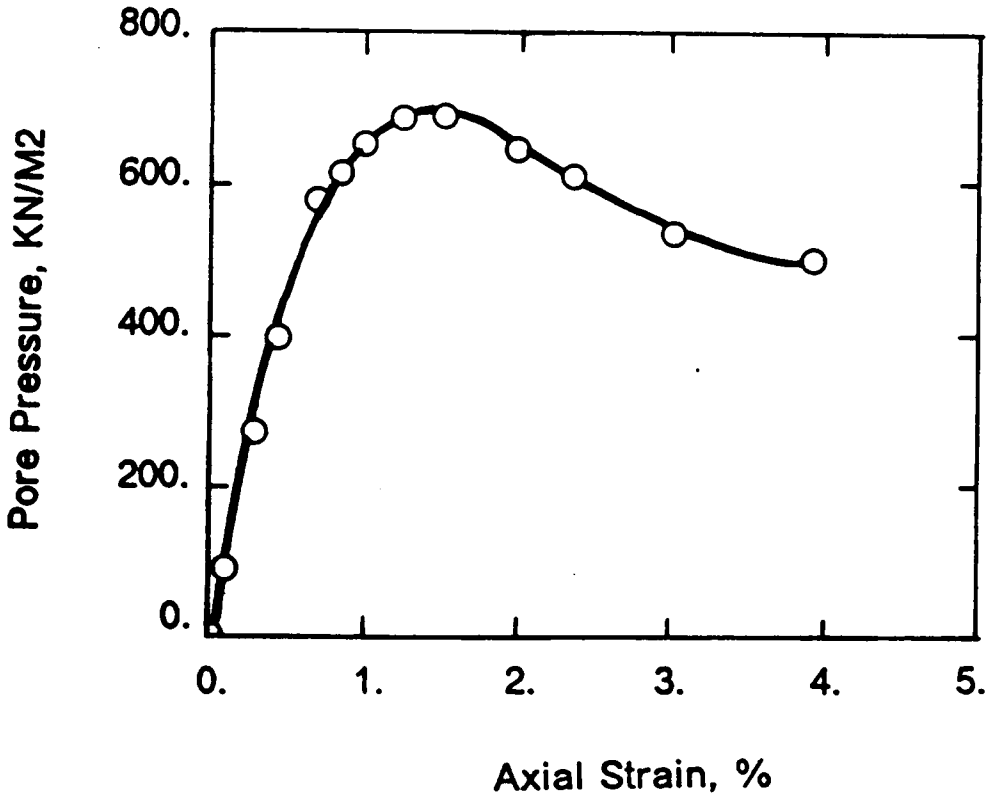
Pore Pressure, KN/M2
800.
600.
400.
200.
0.
0.
1.
2.
3.
4.
5.
Axial Strain, %

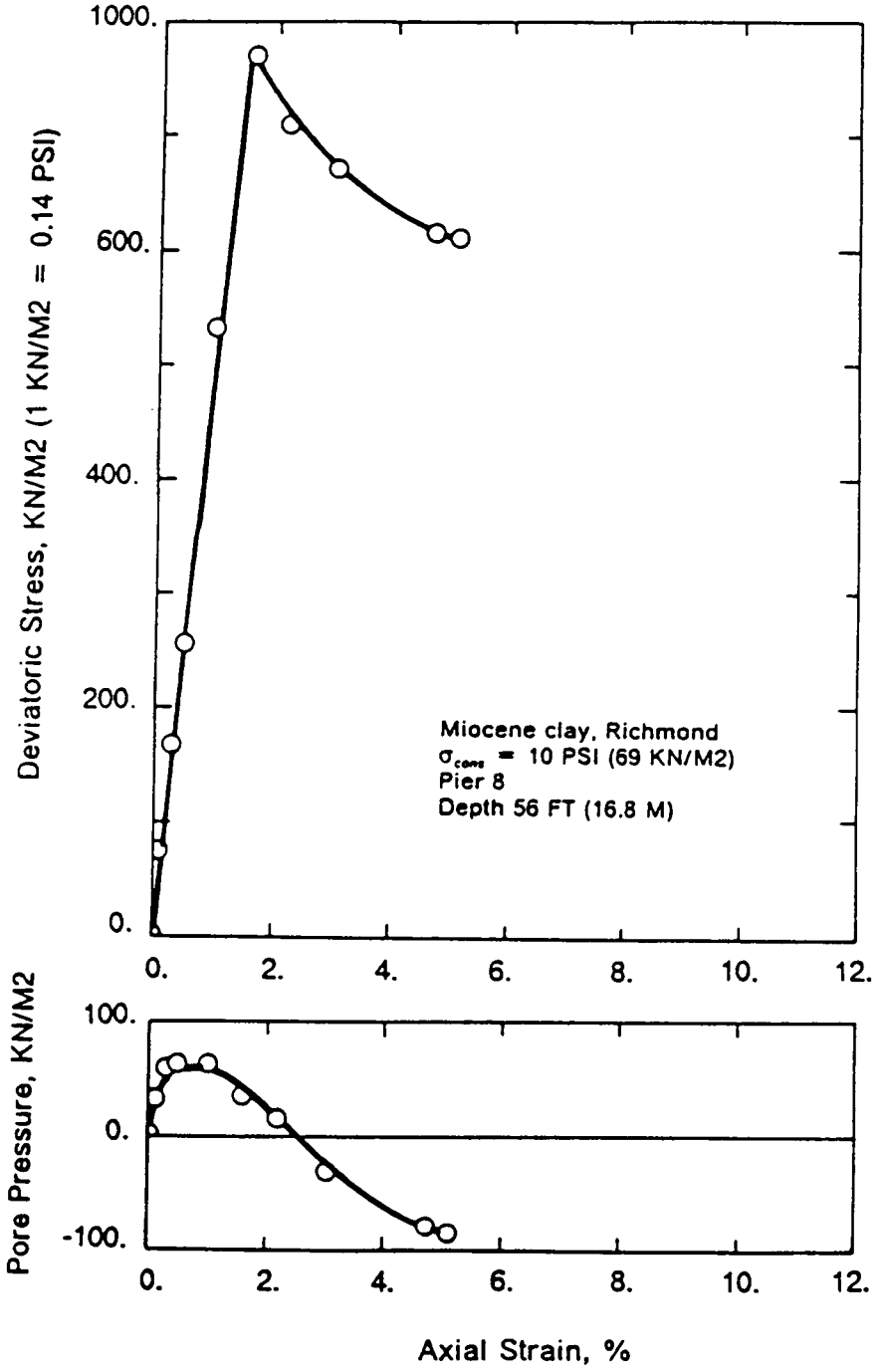
1000.
600.
400.
200.
0.
Deviatoric Stress, KN/M2 (1 KN/M2 = 0.14 PSI)
Miocene clay, Richmond
σ_{cons} = 10 PSI (69 KN/M2)
Pier 8
Depth 56 FT (16.8 M)
0.
2.
4.
6.
8.
10.
12.
100.
0.
-100.
Pore Pressure, KN/M2
0.
2.
4.
6.
8.
10.
12.
Axial Strain, %

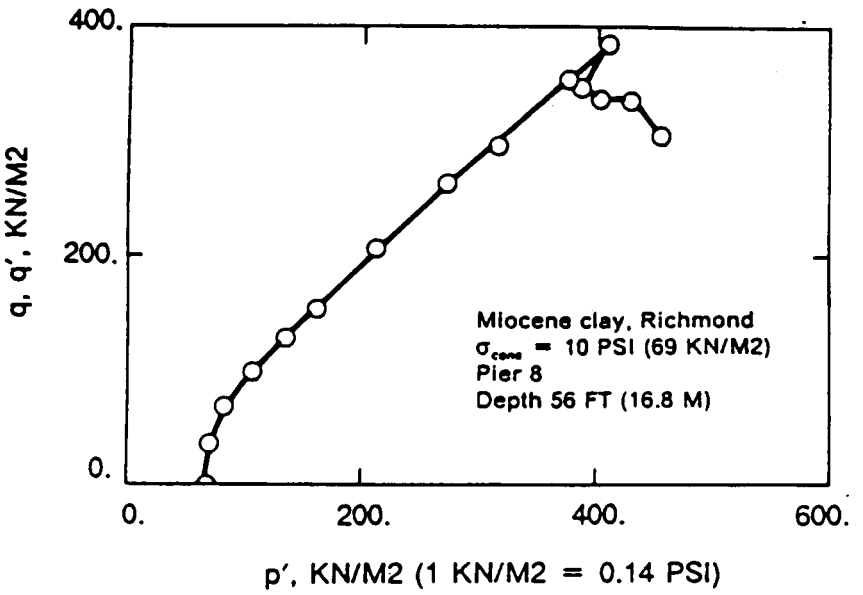
400.
200.
0.
q, q', KN/M2
0.
200.
400.
600.
Miocene clay, Richmond
σ_{cons} = 10 PSI (69 KN/M2)
Pier 8
Depth 56 FT (16.8 M)
p', KN/M2 (1 KN/M2 = 0.14 PSI)

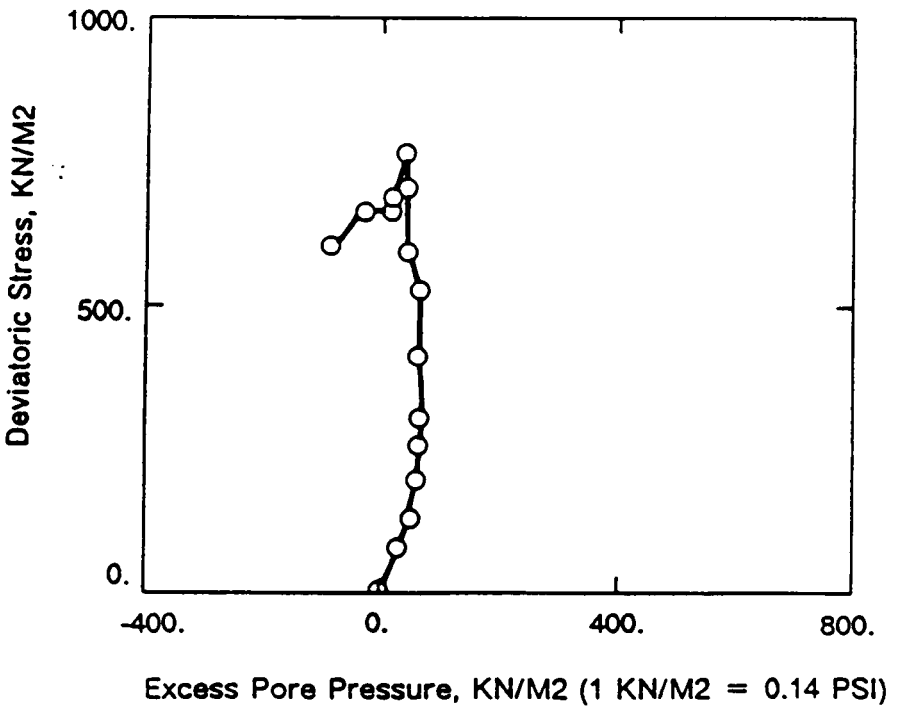
1000.
500.
0.
Deviatoric Stress, KN/M2
-400.
0.
400.
800.
Excess Pore Pressure, KN/M2 (1 KN/M2 = 0.14 PSI)

Appendix E

SBPM TEST RESULTS IN THE MIOCENE CLAY

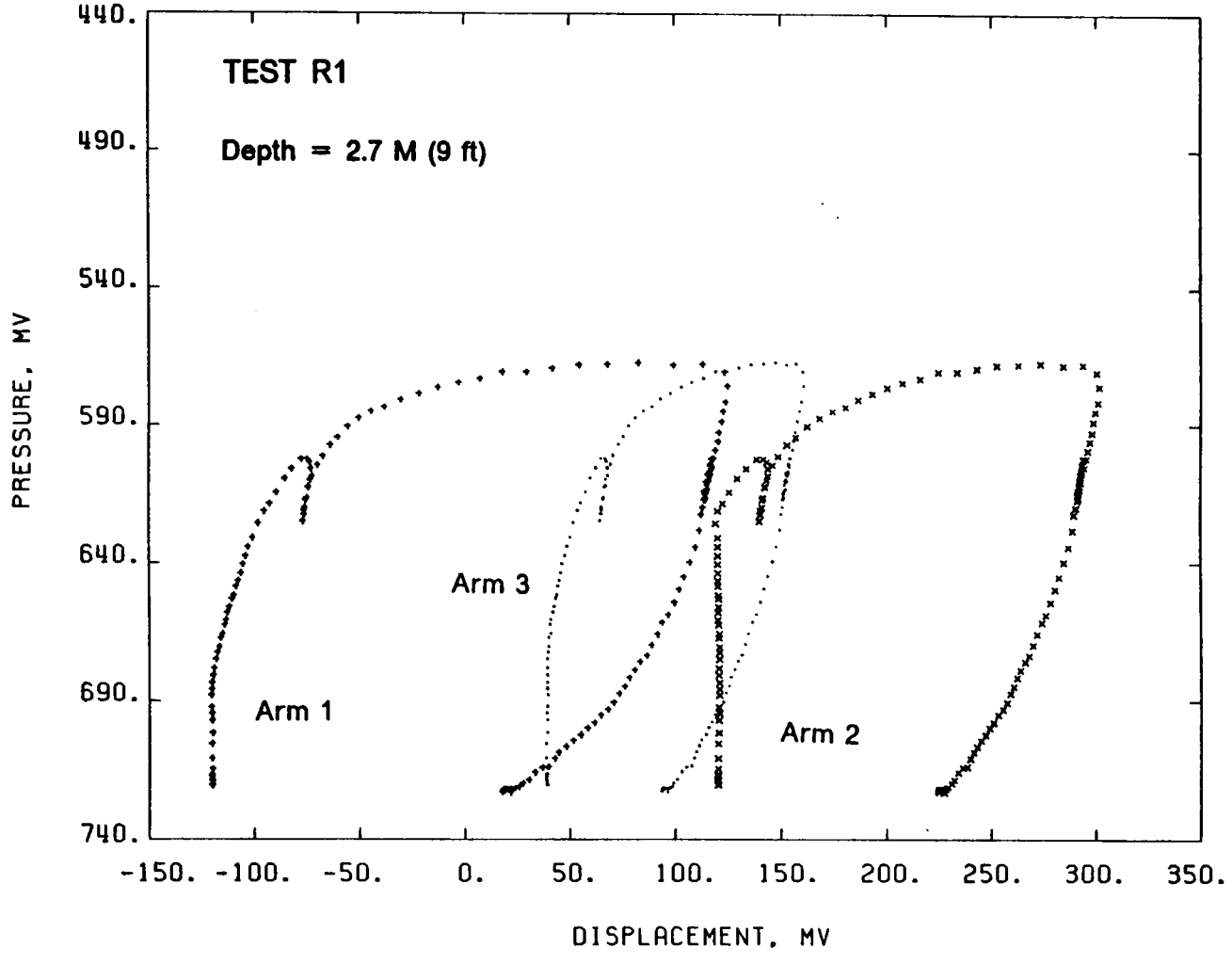
TEST R1
Depth = 2.7 M (9 ft)
Arm 1
Arm 3
Arm 2
PRESSURE, MV
DISPLACEMENT, MV
440.
490.
540.
590.
640.
690.
740.
-150.
-100.
-50.
0.
50.
100.
150.
200.
250.
300.
350.

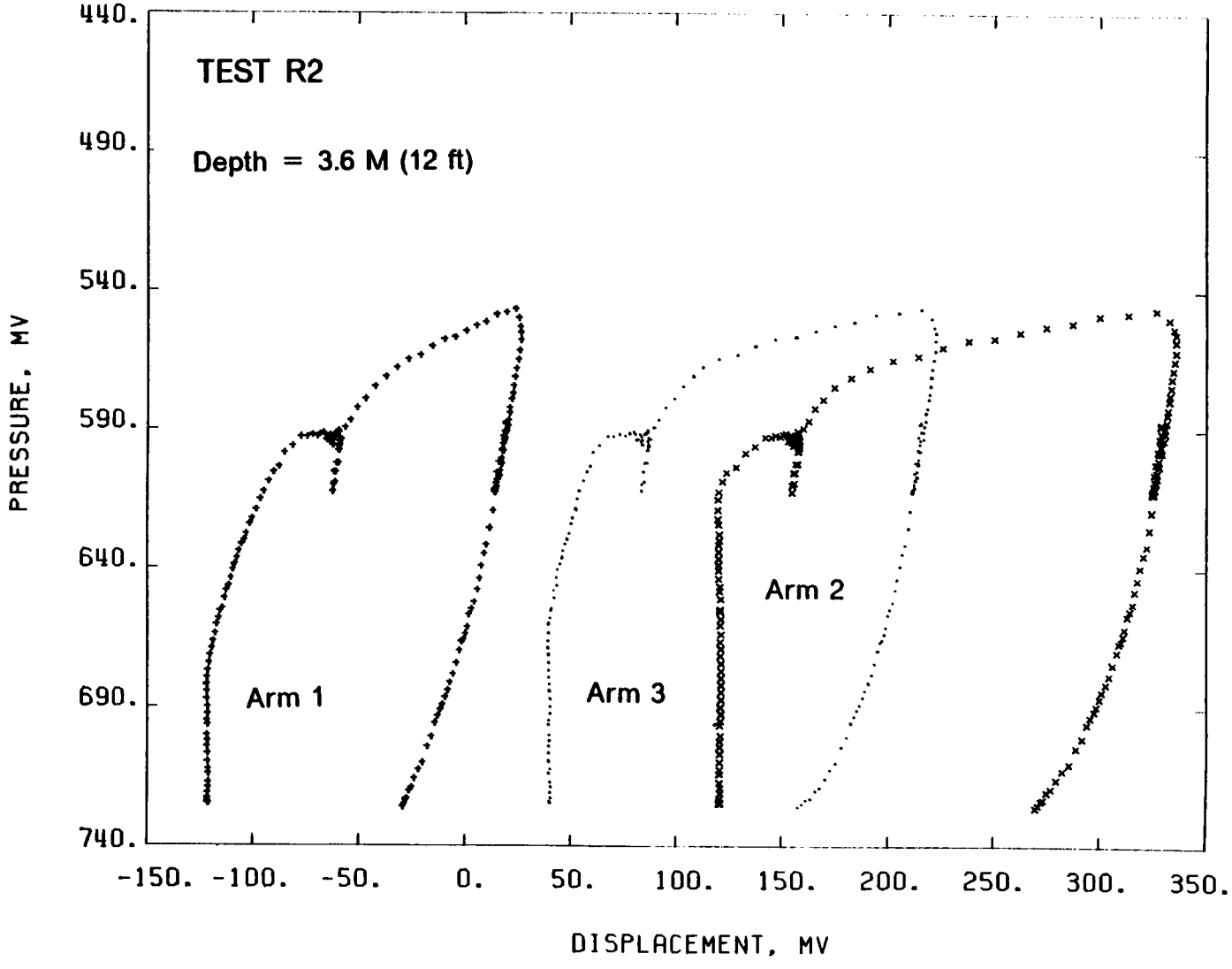
TEST R2
Depth = 3.6 M (12 ft)
Arm 1
Arm 2
Arm 3
PRESSURE, MV
440.
490.
540.
590.
640.
690.
740.
-150.
-100.
-50.
0.
50.
100.
150.
200.
250.
300.
350.
DISPLACEMENT, MV

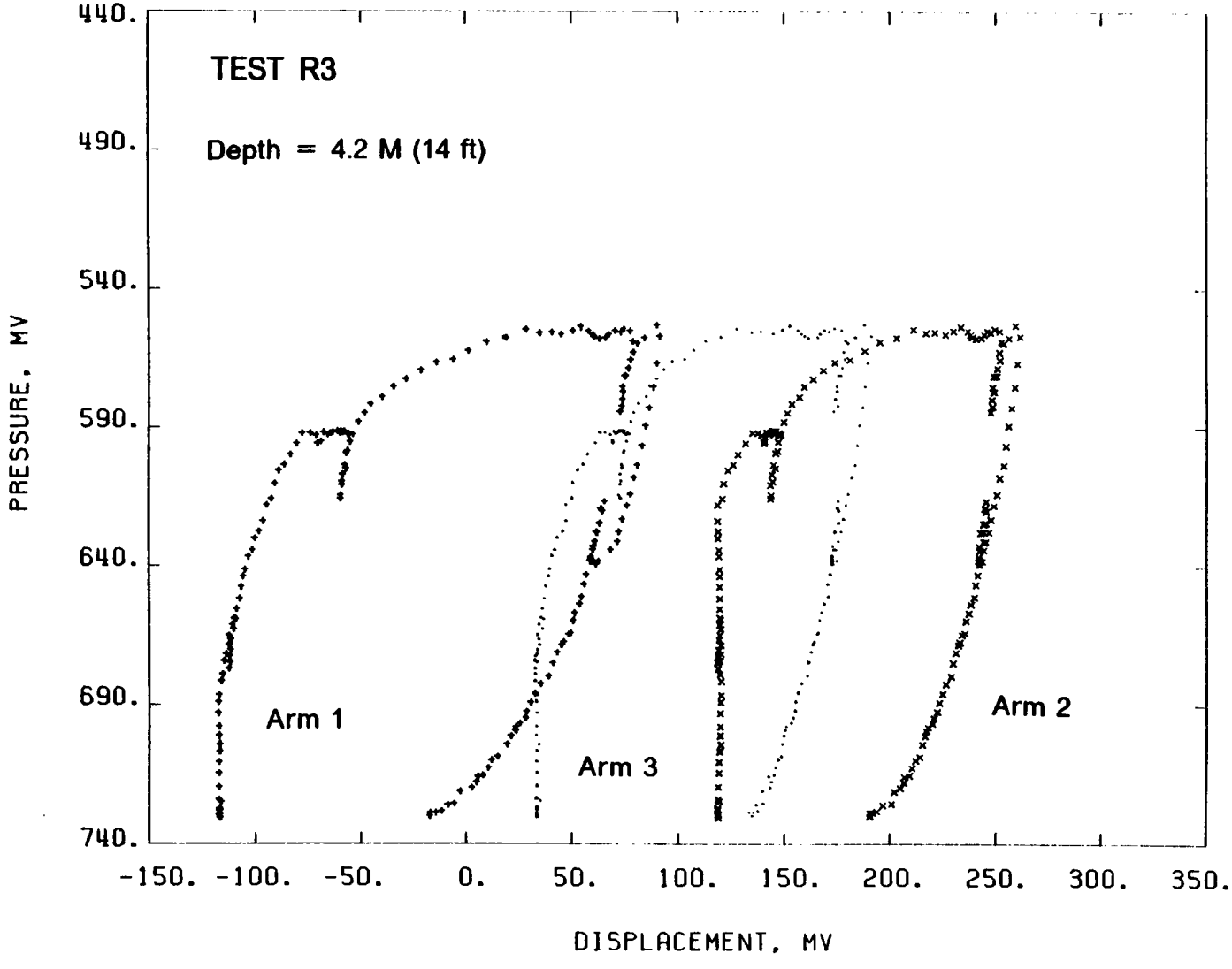
TEST R3
Depth = 4.2 M (14 ft)
Arm 1
Arm 3
Arm 2
PRESSURE, MV
DISPLACEMENT, MV
440.
490.
540.
590.
640.
690.
740.
-150.
-100.
-50.
0.
50.
100.
150.
200.
250.
300.
350.

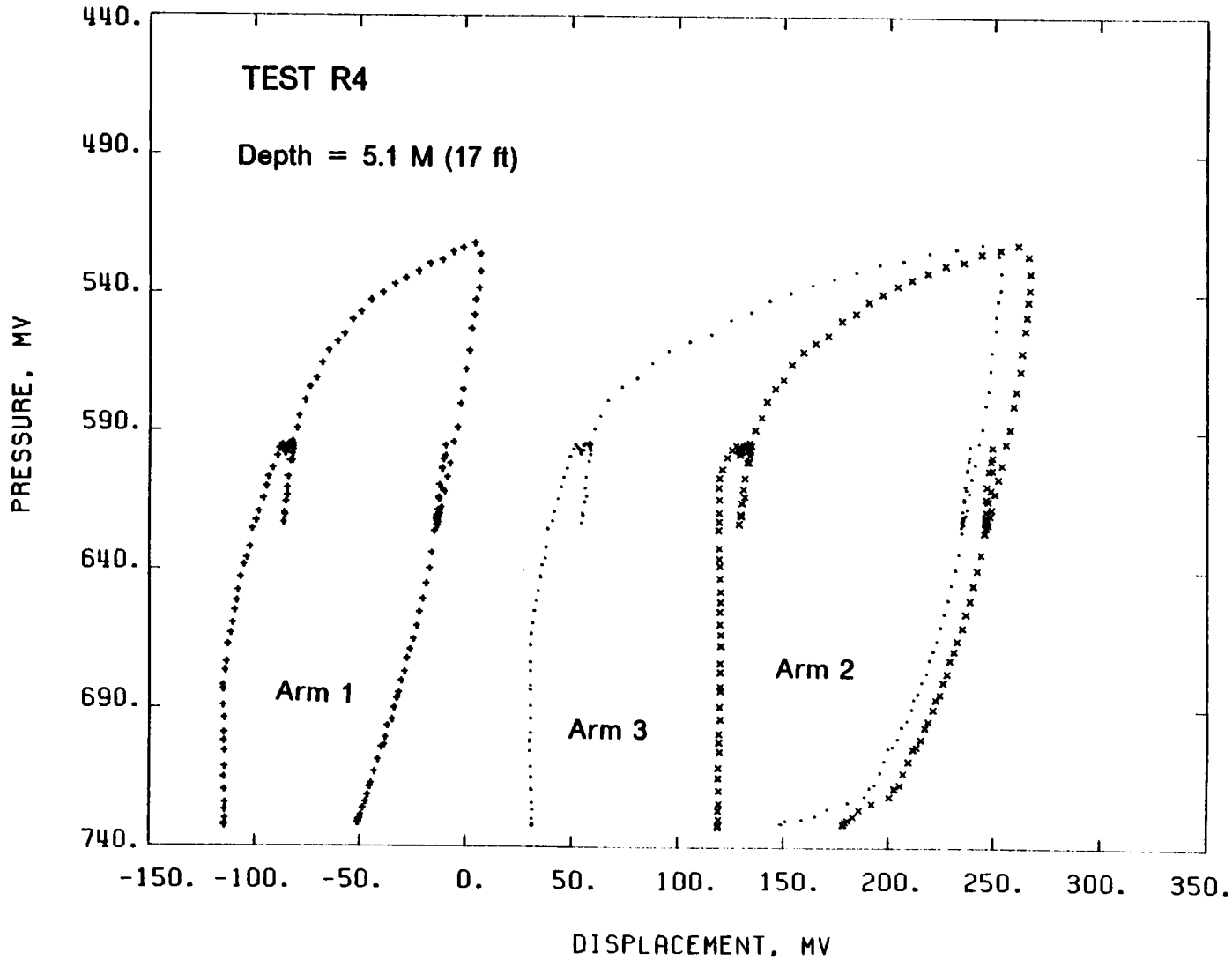
TEST R4
Depth = 5.1 M (17 ft)
Arm 1
Arm 3
Arm 2
PRESSURE, MV
DISPLACEMENT, MV
440.
490.
540.
590.
640.
690.
740.
-150.
-100.
-50.
0.
50.
100.
150.
200.
250.
300.
350.

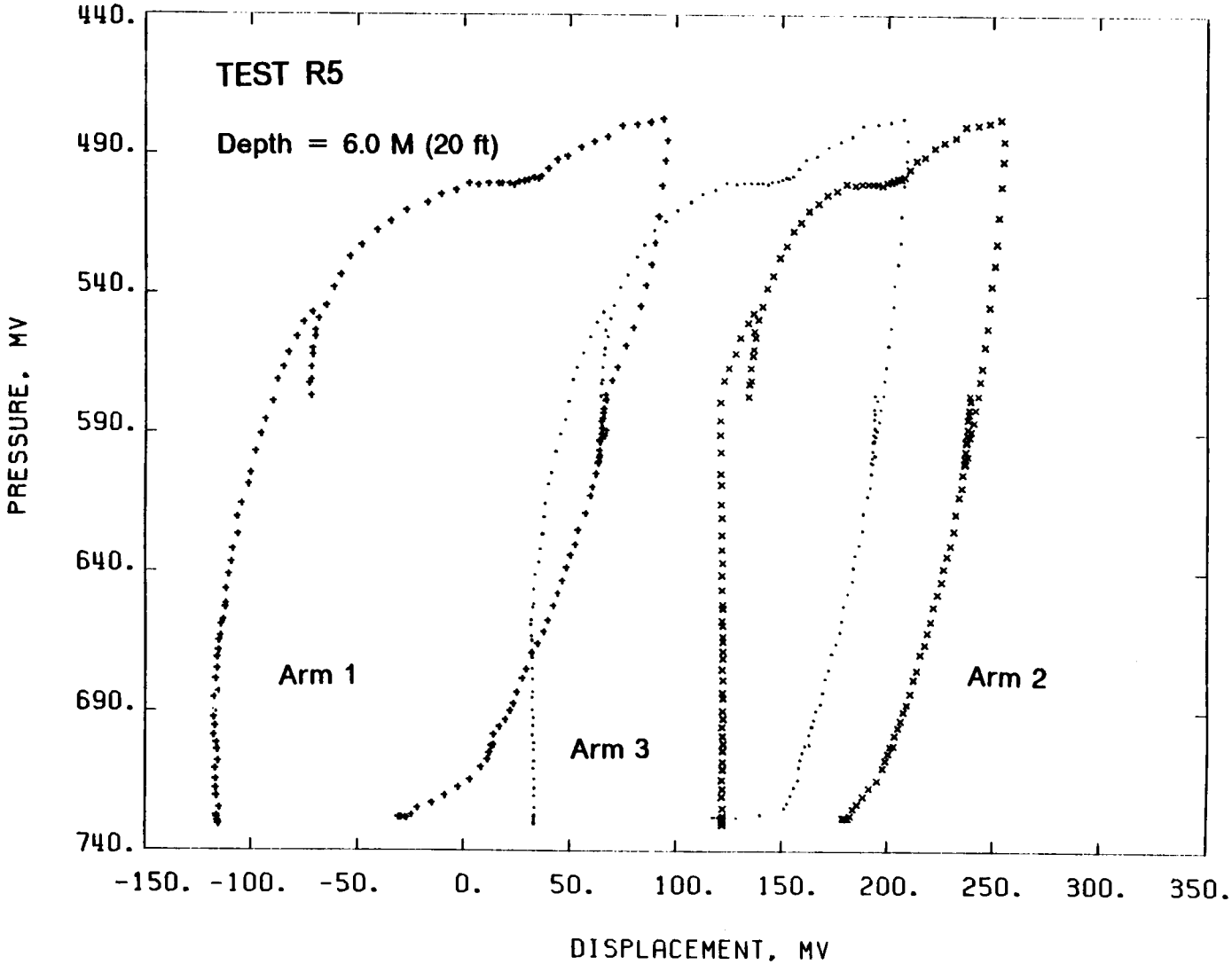
TEST R5
Depth = 6.0 M (20 ft)
Arm 1
Arm 2
Arm 3
PRESSURE, MV
DISPLACEMENT, MV
440.
490.
540.
590.
640.
690.
740.
-150.
-100.
-50.
0.
50.
100.
150.
200.
250.
300.
350.

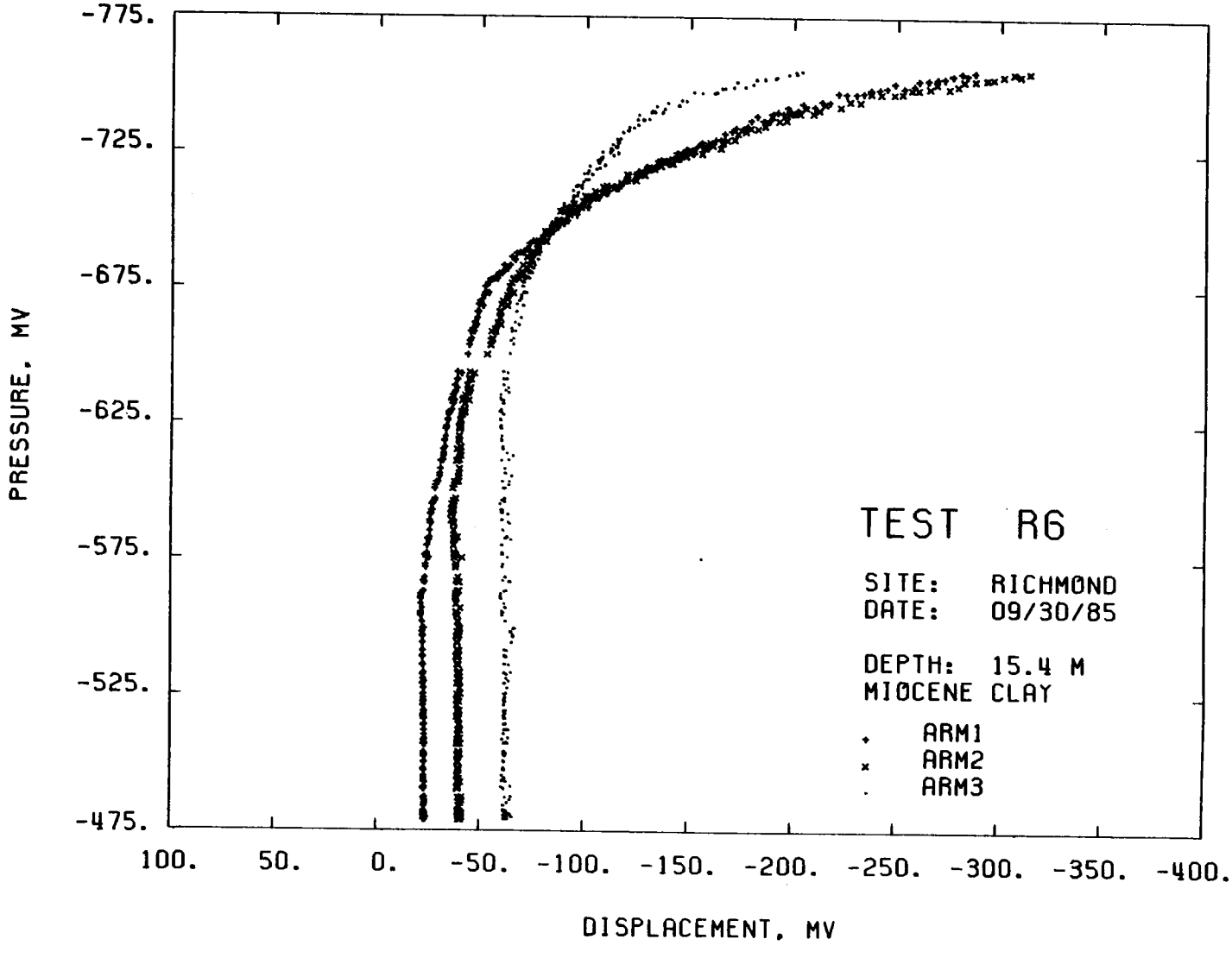
-775.
-725.
-675.
-625.
-575.
-525.
-475.
PRESSURE, MV
100.
50.
0.
-50.
-100.
-150.
-200.
-250.
-300.
-350.
-400.
DISPLACEMENT, MV
TEST R6
SITE: RICHMOND
DATE: 09/30/85
DEPTH: 15.4 M
MIOCENE CLAY
ARM1
ARM2
ARM3

Appendix F

SBPM TEST RESULTS IN THE RESIDUAL SOIL

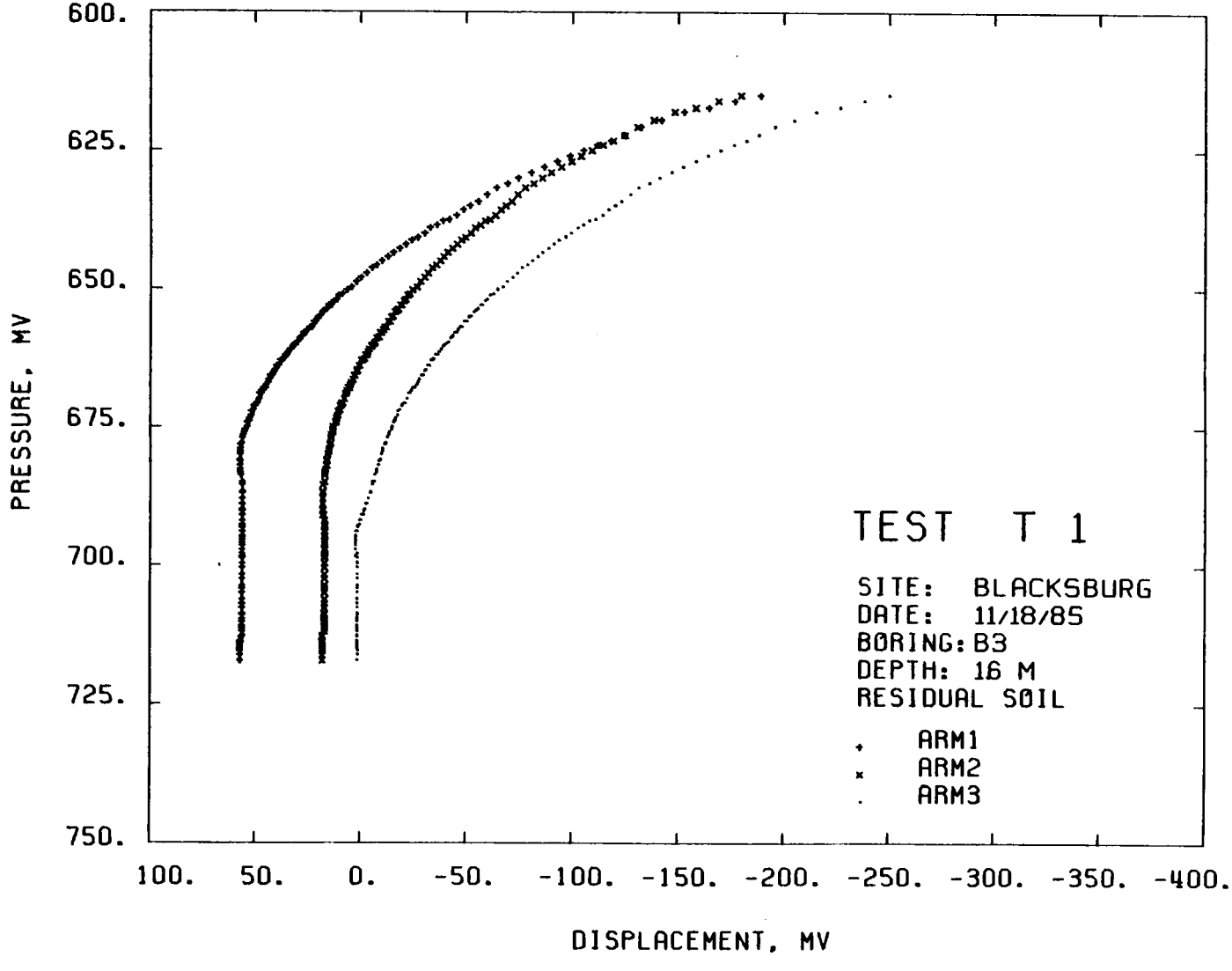
600.
625.
650.
675.
700.
725.
750.
PRESSURE, MV
100.
50.
0.
-50.
-100.
-150.
-200.
-250.
-300.
-350.
-400.
DISPLACEMENT, MV
TEST T 1
SITE: BLACKSBURG
DATE: 11/18/85
BORING: B3
DEPTH: 16 M
RESIDUAL SOIL
ARM1
ARM2
ARM3

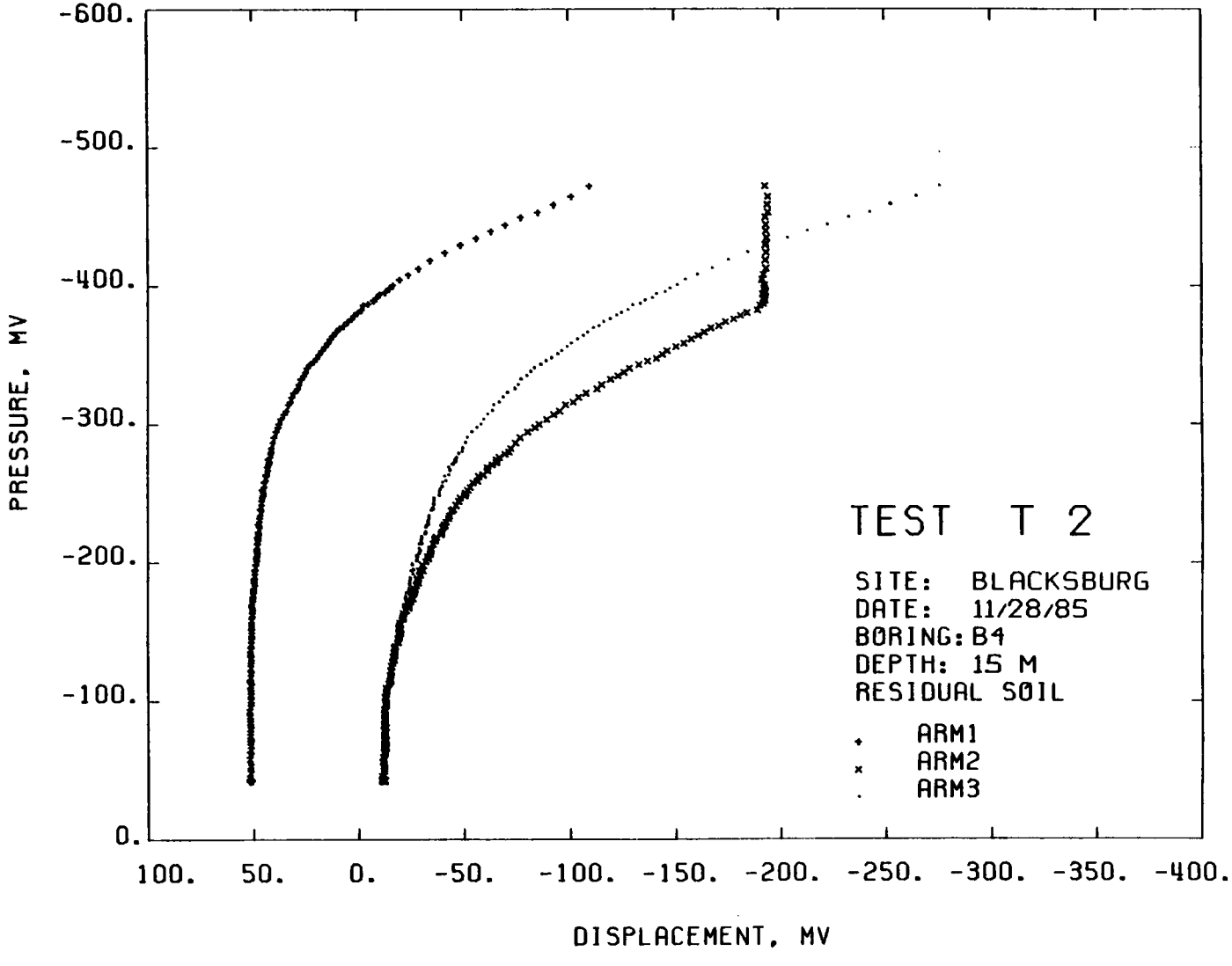
-600.
-500.
-400.
-300.
-200.
-100.
0.
PRESSURE, MV
100.
50.
0.
-50.
-100.
-150.
-200.
-250.
-300.
-350.
-400.
DISPLACEMENT, MV
TEST T 2
SITE: BLACKSBURG
DATE: 11/28/85
BORING: B4
DEPTH: 15 M
RESIDUAL SOIL
ARM1
ARM2
ARM3

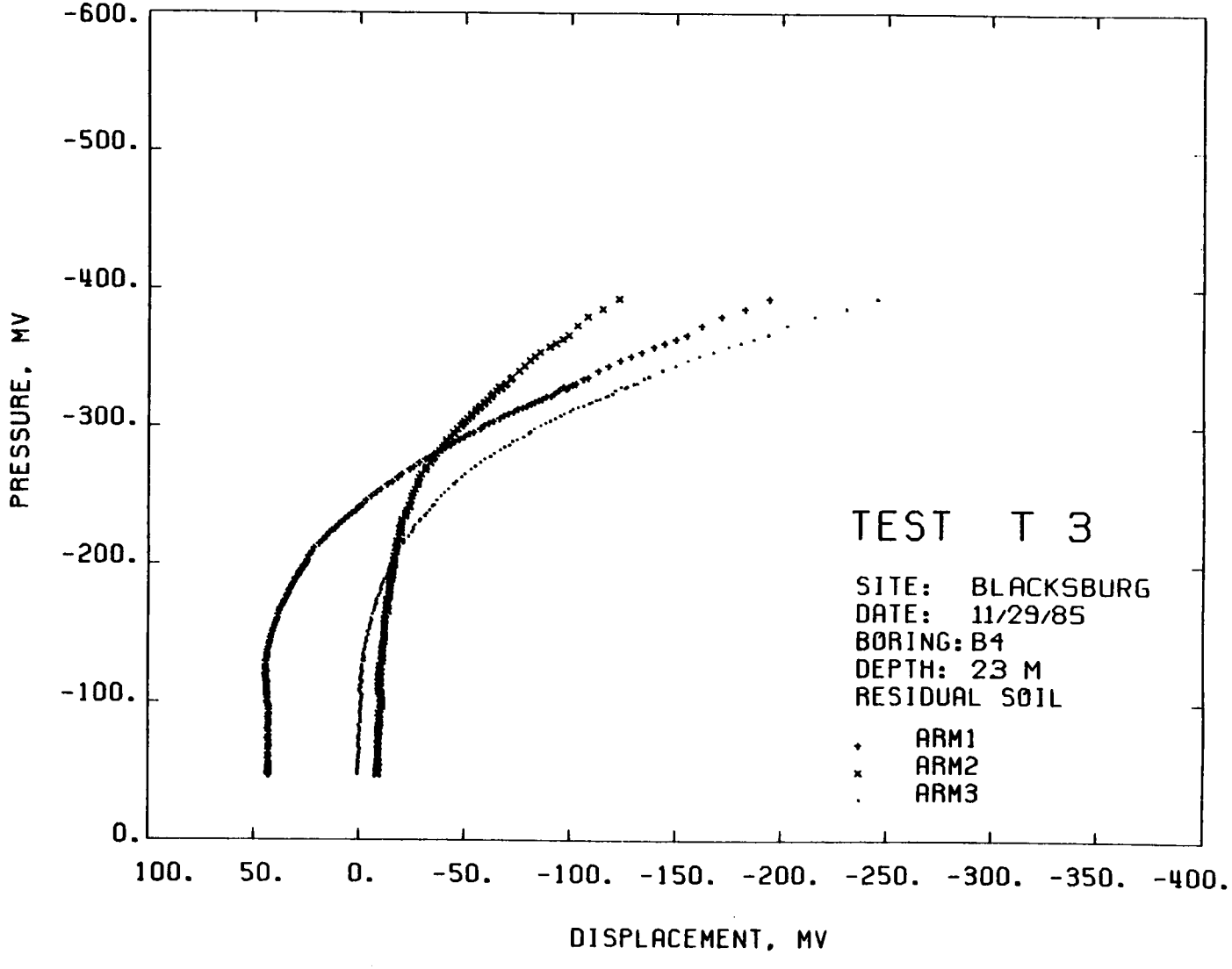
-600.
-500.
-400.
-300.
-200.
-100.
0.
PRESSURE, MV
100.
50.
0.
-50.
-100.
-150.
-200.
-250.
-300.
-350.
-400.
DISPLACEMENT, MV
TEST T 3
SITE: BLACKSBURG
DATE: 11/29/85
BORING: B4
DEPTH: 23 M
RESIDUAL SOIL
ARM1
ARM2
ARM3

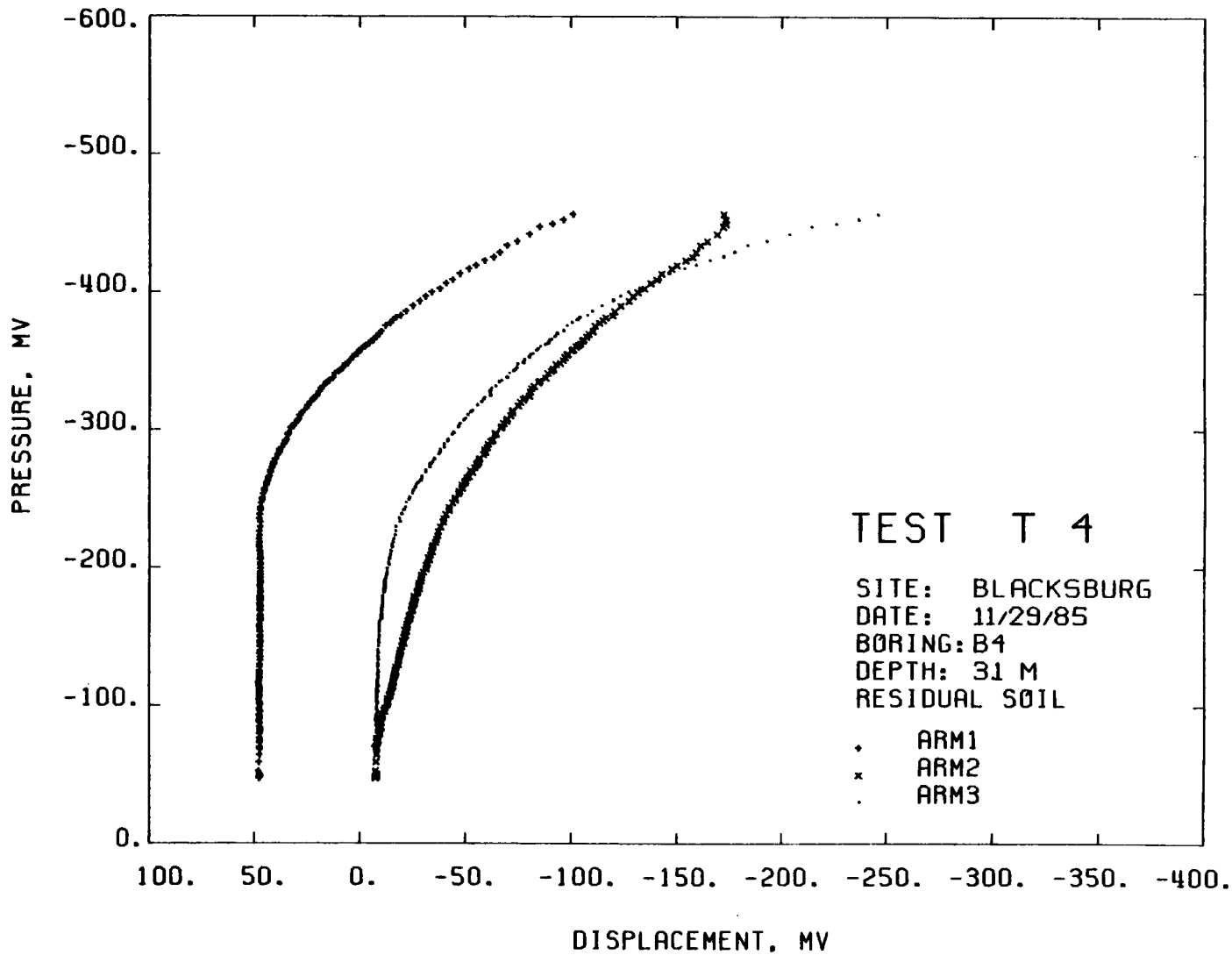
-600.
-500.
-400.
-300.
-200.
-100.
0.
PRESSURE, MV
100.
50.
0.
-50.
-100.
-150.
-200.
-250.
-300.
-350.
-400.
DISPLACEMENT, MV
TEST T 4
SITE: BLACKSBURG
DATE: 11/29/85
BORING: B4
DEPTH: 31 M
RESIDUAL SOIL
ARM1
ARM2
ARM3

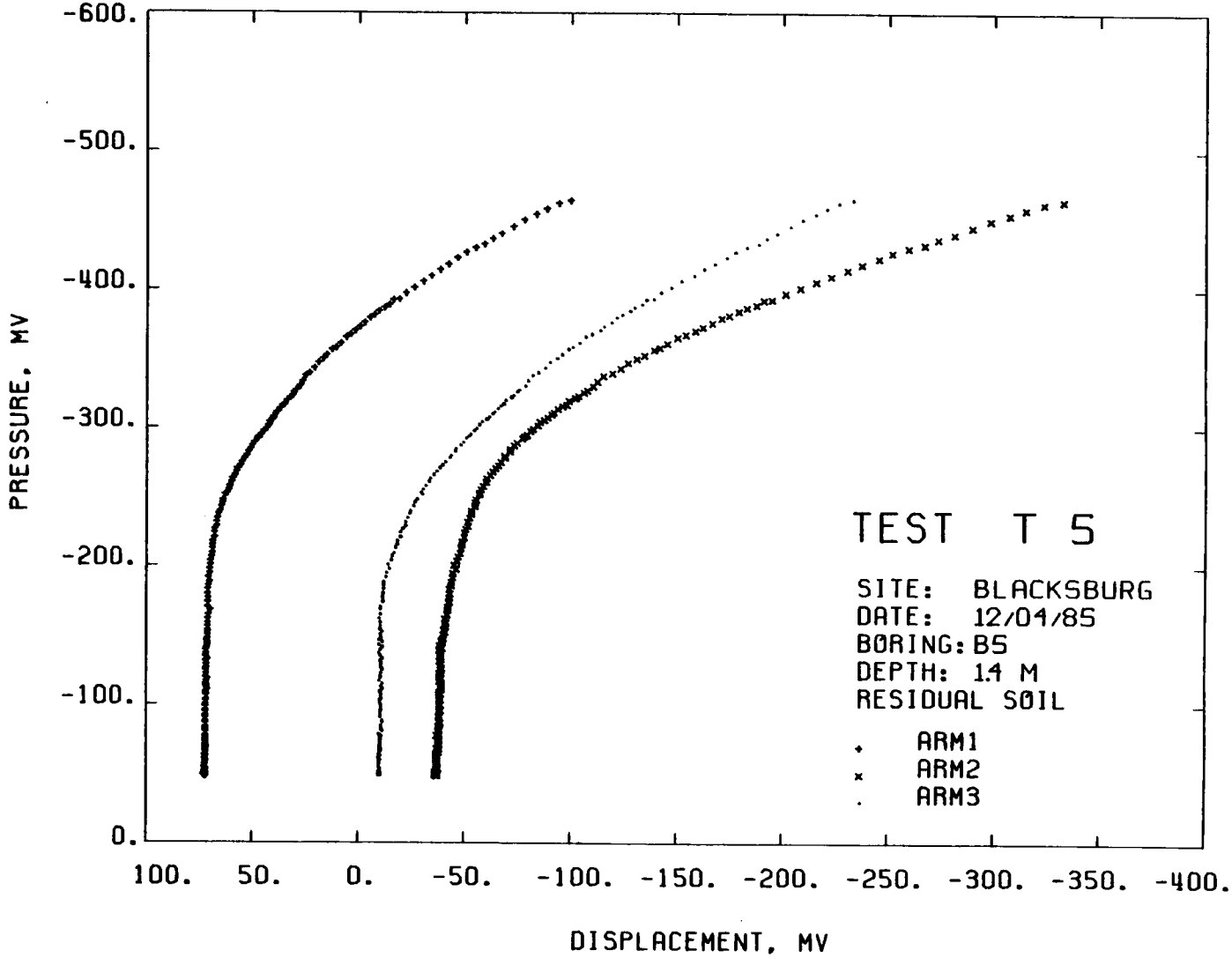
-600.
-500.
-400.
-300.
-200.
-100.
0.
PRESSURE, MV
100.
50.
0.
-50.
-100.
-150.
-200.
-250.
-300.
-350.
-400.
DISPLACEMENT, MV
TEST T 5
SITE: BLACKSBURG
DATE: 12/04/85
BORING: B5
DEPTH: 1.4 M
RESIDUAL SOIL
ARM1
ARM2
ARM3

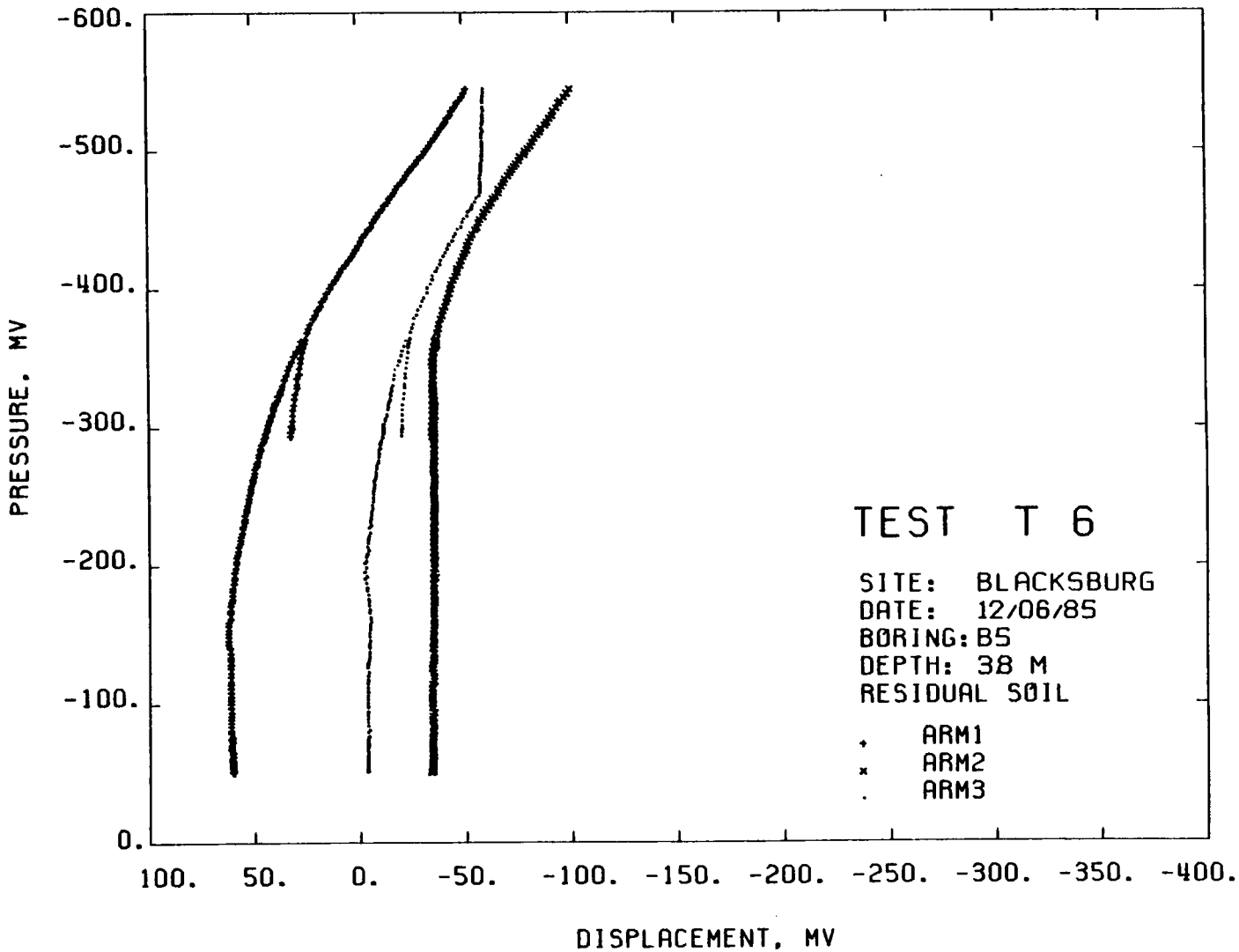
-600.
-500.
-400.
-300.
-200.
-100.
0.
PRESSURE, MV
100.
50.
0.
-50.
-100.
-150.
-200.
-250.
-300.
-350.
-400.
DISPLACEMENT, MV
TEST T 6
SITE: BLACKSBURG
DATE: 12/06/85
BORING: B5
DEPTH: 38 M
RESIDUAL SOIL
ARM1
ARM2
ARM3

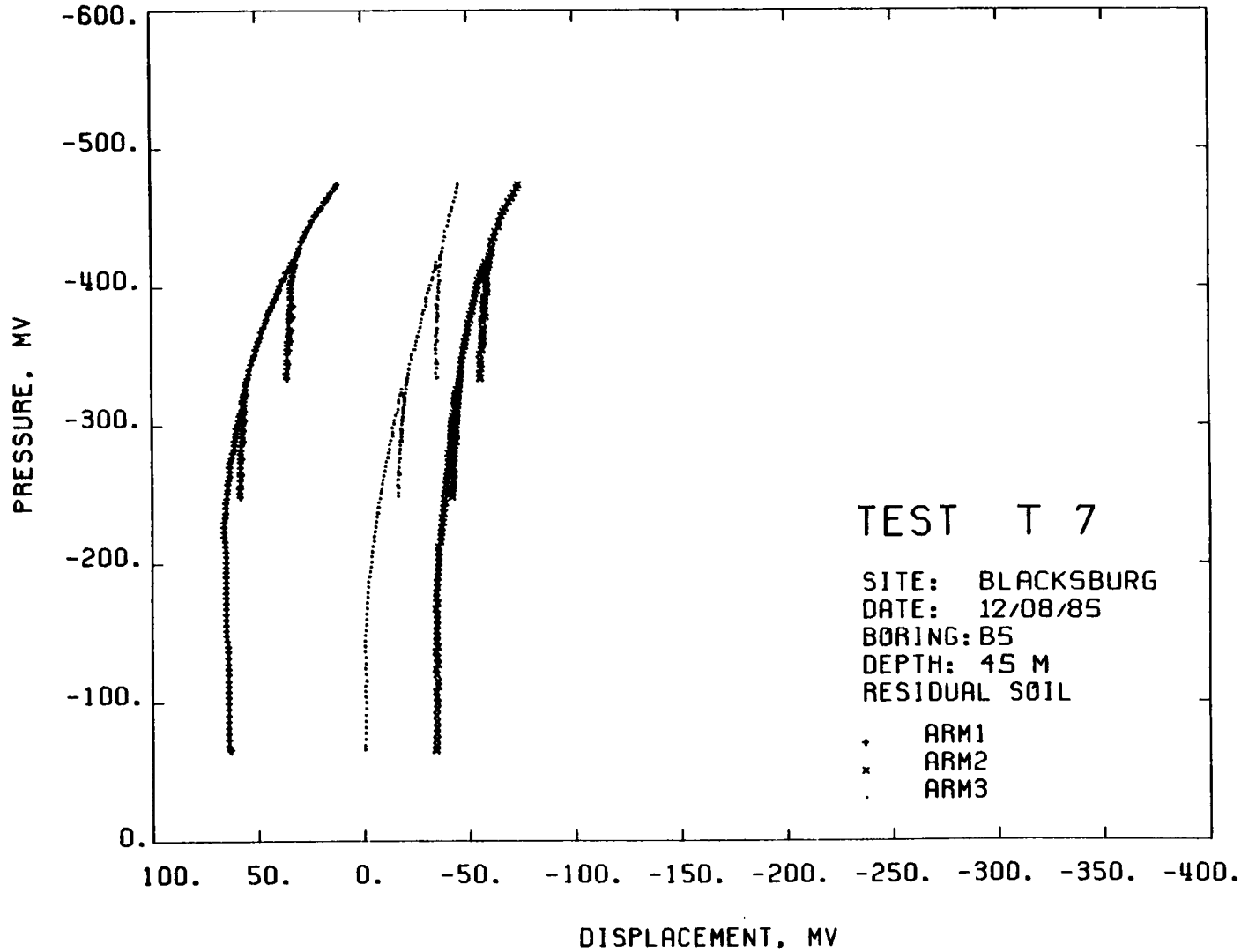
-600.
-500.
-400.
-300.
-200.
-100.
0.
PRESSURE, MV
100.
50.
0.
-50.
-100.
-150.
-200.
-250.
-300.
-350.
-400.
DISPLACEMENT, MV
TEST T 7
SITE: BLACKSBURG
DATE: 12/08/85
BORING: B5
DEPTH: 45 M
RESIDUAL SOIL
ARM1
ARM2
ARM3

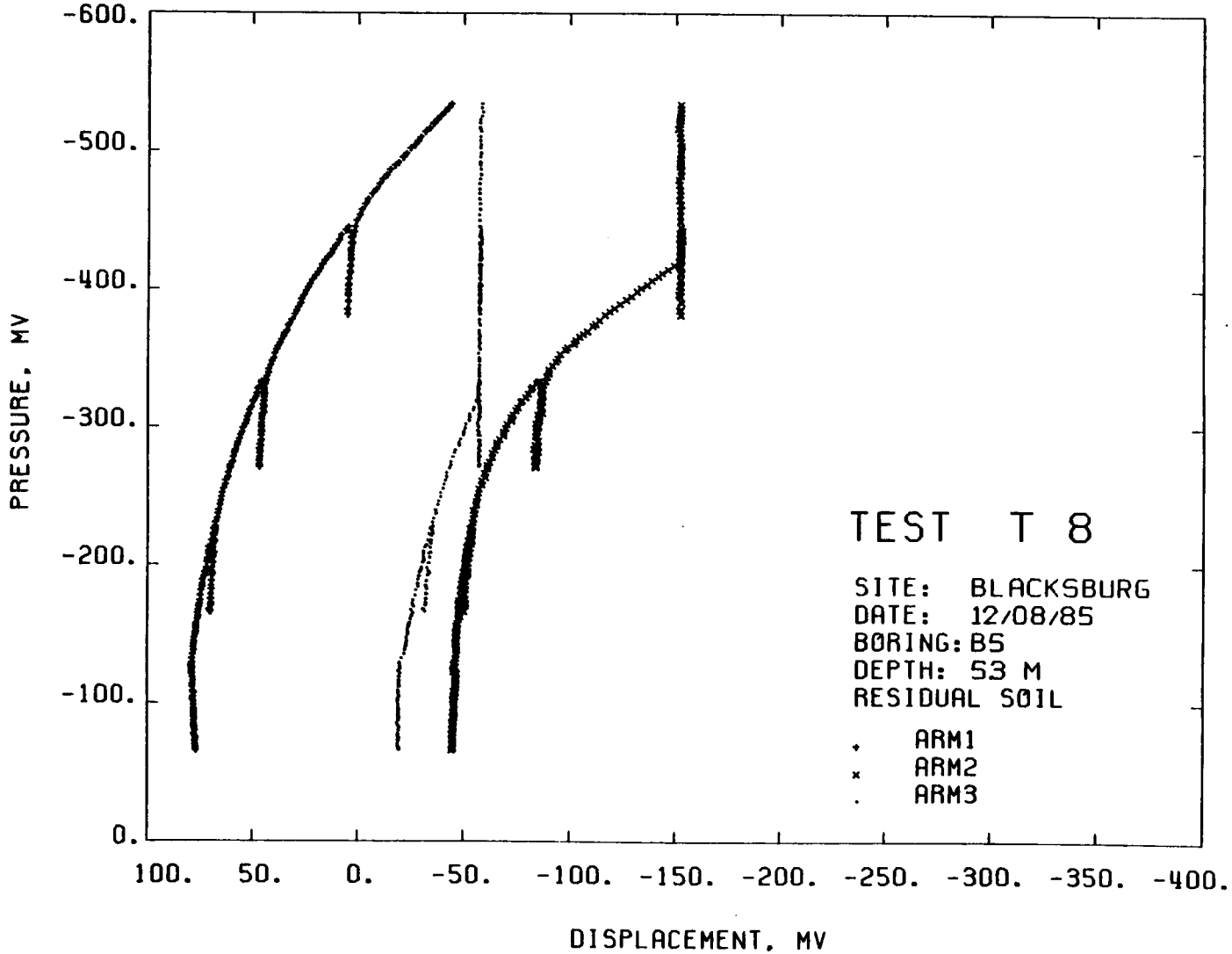
-600.
-500.
-400.
-300.
-200.
-100.
0.
PRESSURE, MV
100.
50.
0.
-50.
-100.
-150.
-200.
-250.
-300.
-350.
-400.
DISPLACEMENT, MV
TEST T 8
SITE: BLACKSBURG
DATE: 12/08/85
BORING: B5
DEPTH: 53 M
RESIDUAL SOIL
+ ARM1
x ARM2
. ARM3

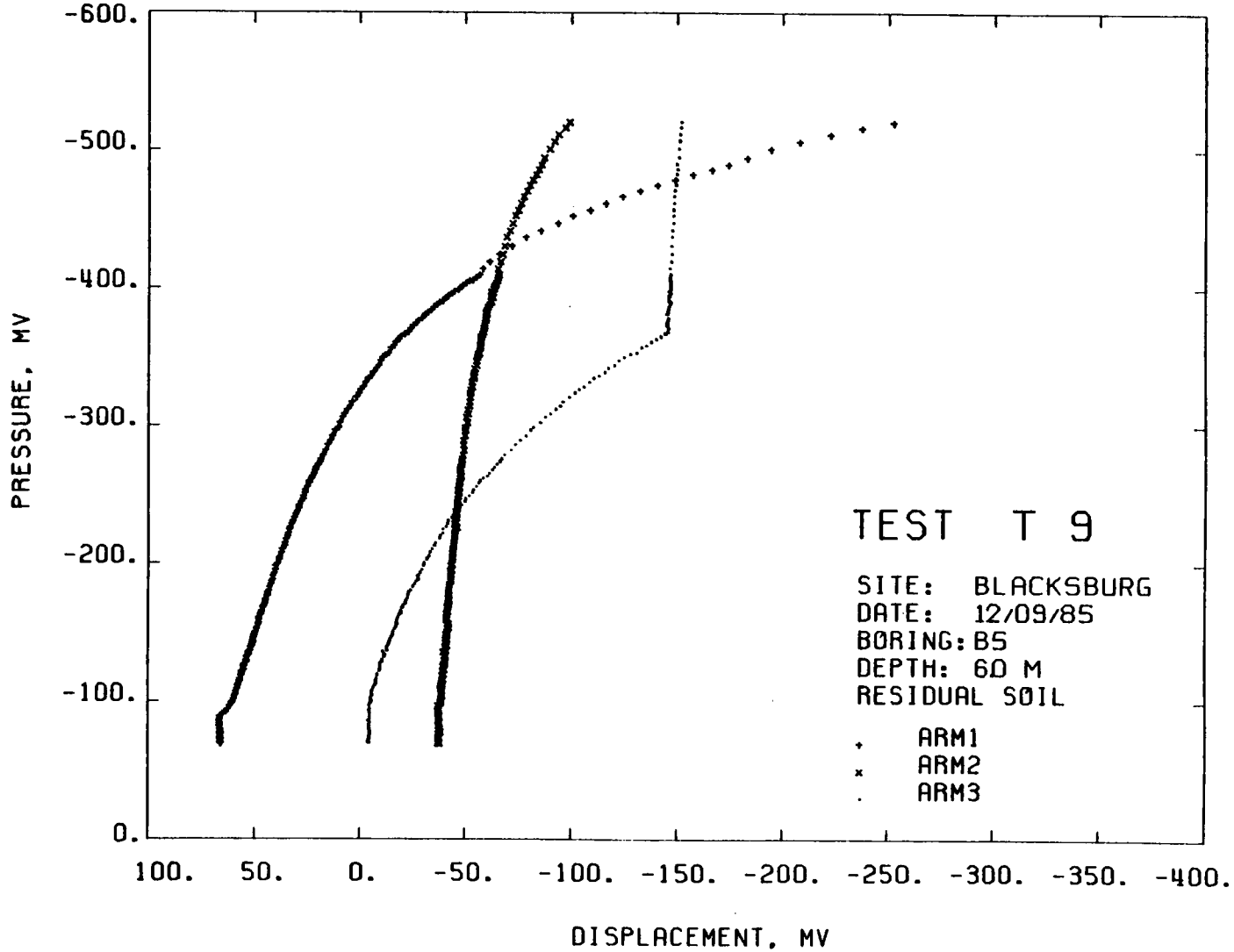
-600.
-500.
-400.
-300.
-200.
-100.
0.
PRESSURE, MV
100.
50.
0.
-50.
-100.
-150.
-200.
-250.
-300.
-350.
-400.
DISPLACEMENT, MV
TEST T 9
SITE: BLACKSBURG
DATE: 12/09/85
BORING: B5
DEPTH: 60 M
RESIDUAL SOIL
ARM1
ARM2
ARM3

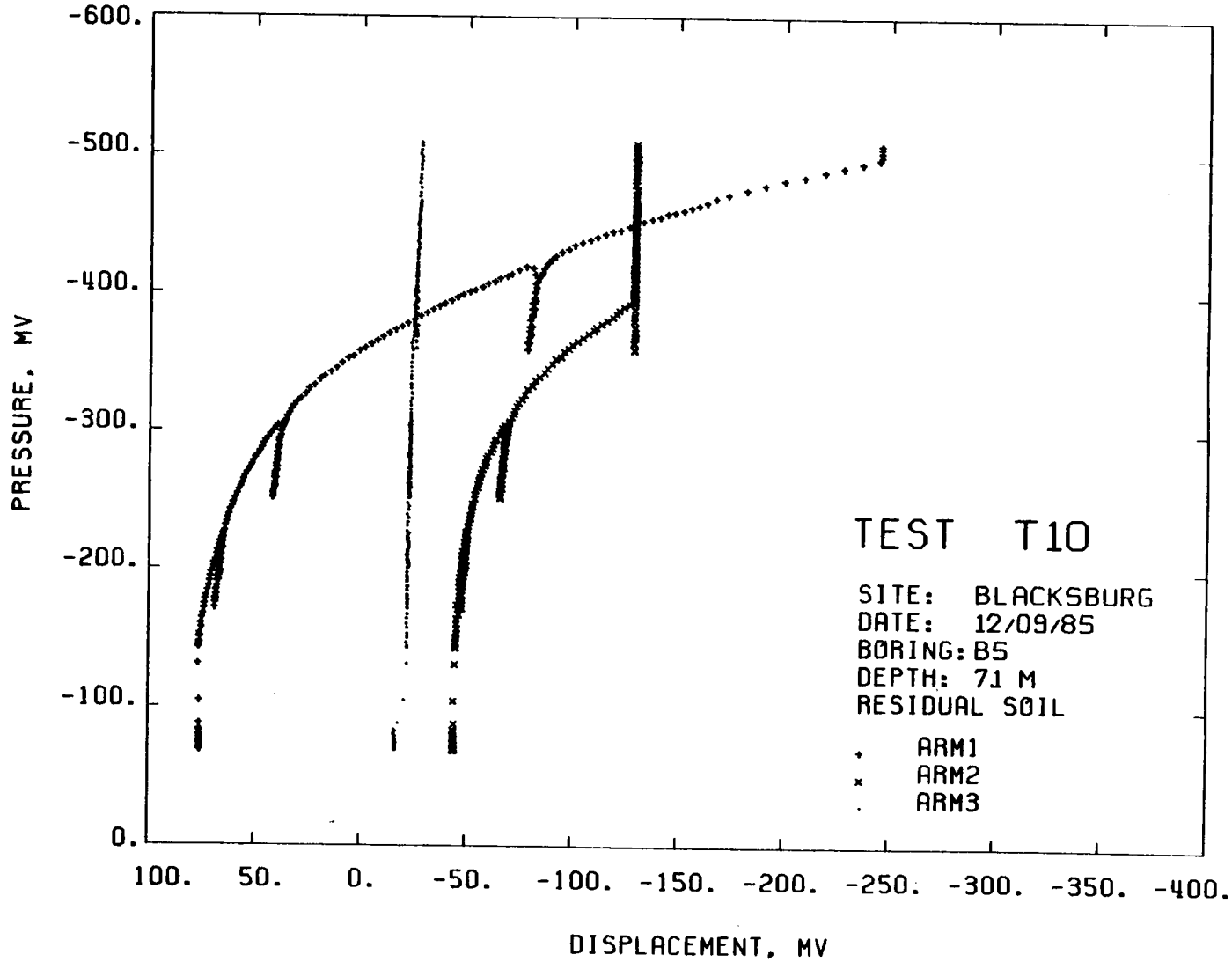
-600.
-500.
-400.
-300.
-200.
-100.
0.
PRESSURE, MV
100.
50.
0.
-50.
-100.
-150.
-200.
-250.
-300.
-350.
-400.
DISPLACEMENT, MV
TEST T10
SITE: BLACKSBURG
DATE: 12/09/85
BORING: B5
DEPTH: 71 M
RESIDUAL SOIL
ARM1
ARM2
ARM3

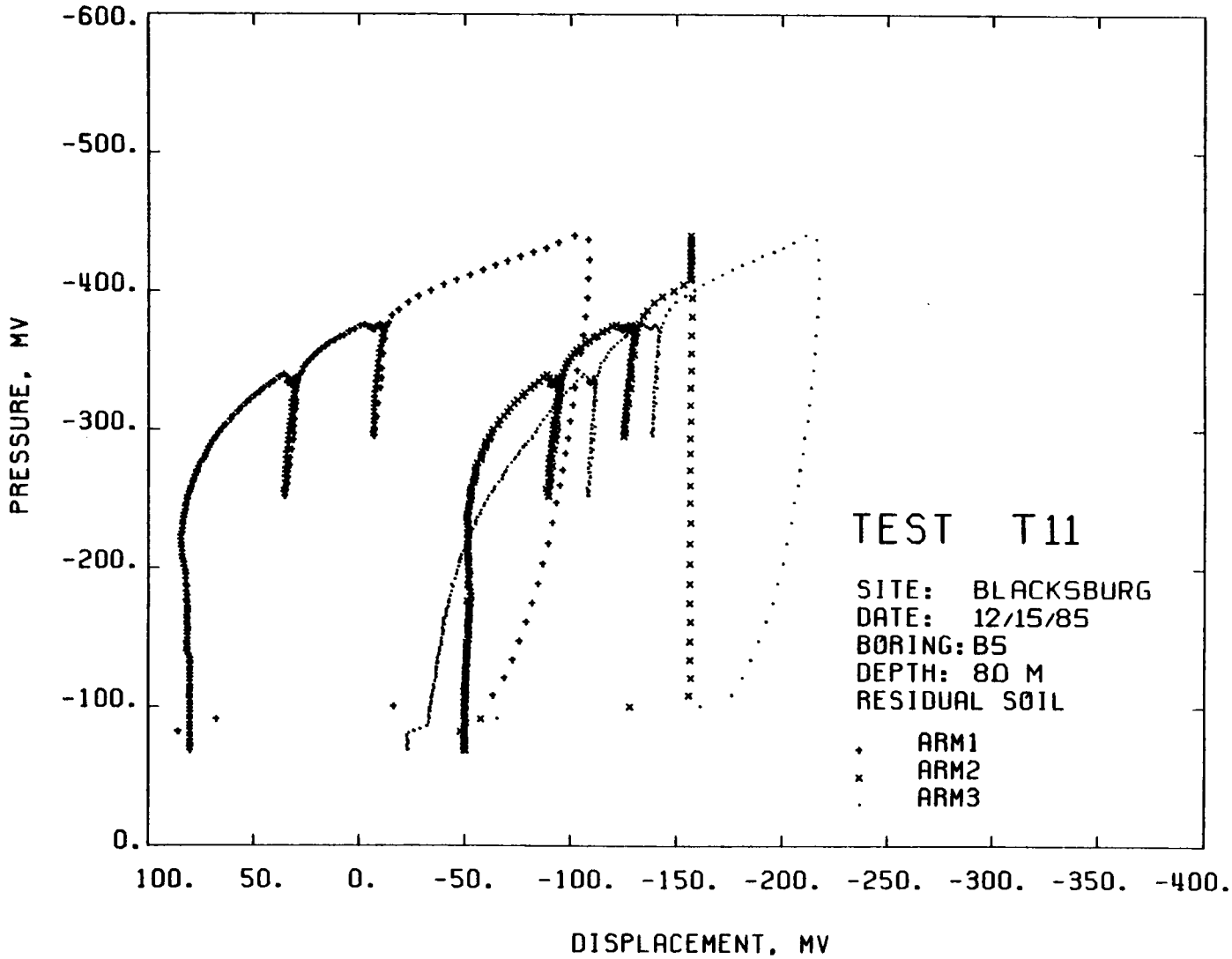
-600.
-500.
-400.
-300.
-200.
-100.
0.
PRESSURE, MV
100.
50.
0.
-50.
-100.
-150.
-200.
-250.
-300.
-350.
-400.
DISPLACEMENT, MV
TEST T11
SITE: BLACKSBURG
DATE: 12/15/85
BORING: B5
DEPTH: 80 M
RESIDUAL SOIL
ARM1
ARM2
ARM3

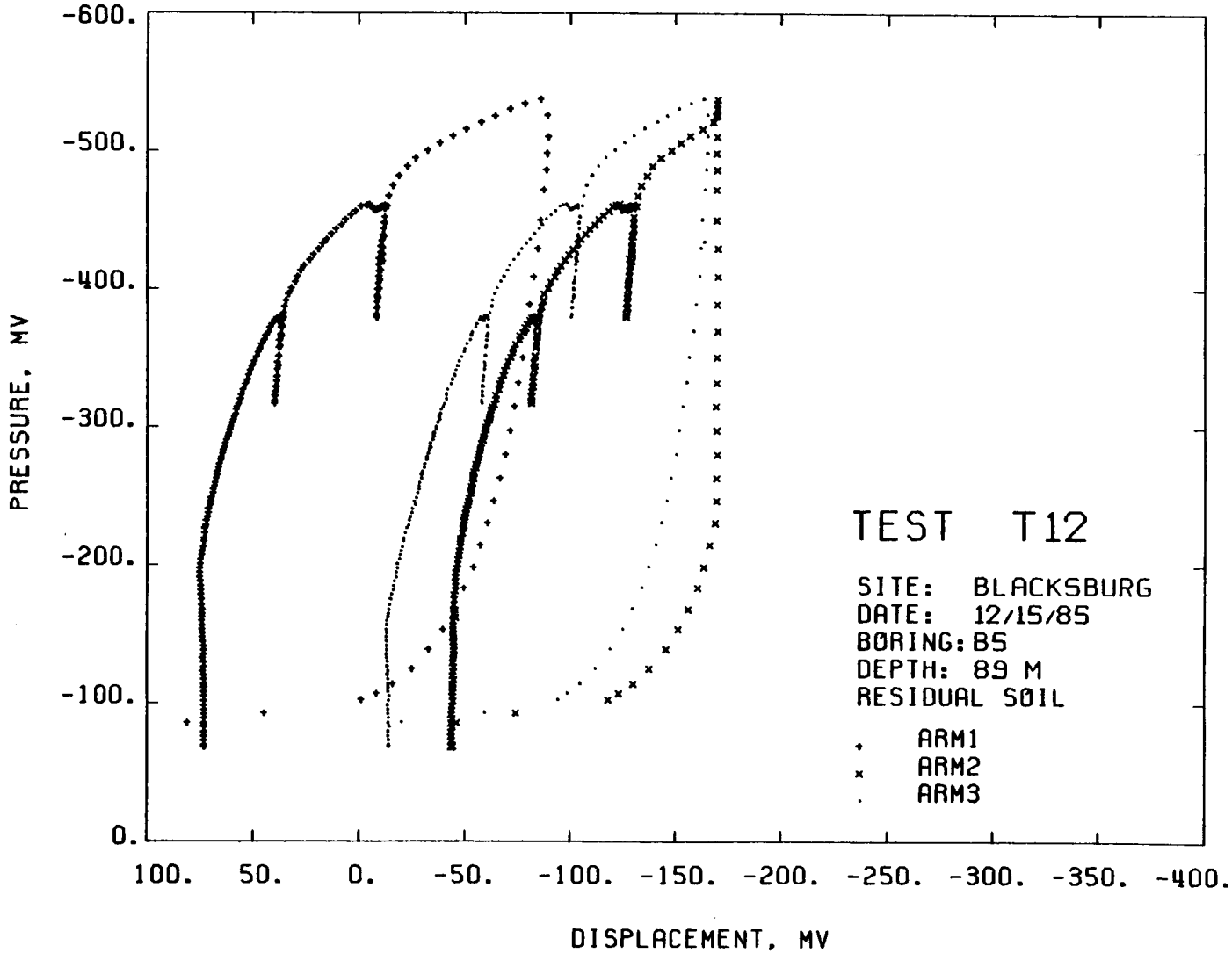
-600.
-500.
-400.
-300.
-200.
-100.
0.
PRESSURE, MV
100.
50.
0.
-50.
-100.
-150.
-200.
-250.
-300.
-350.
-400.
DISPLACEMENT, MV
TEST T12
SITE: BLACKSBURG
DATE: 12/15/85
BORING: B5
DEPTH: 89 M
RESIDUAL SOIL
ARM1
ARM2
ARM3

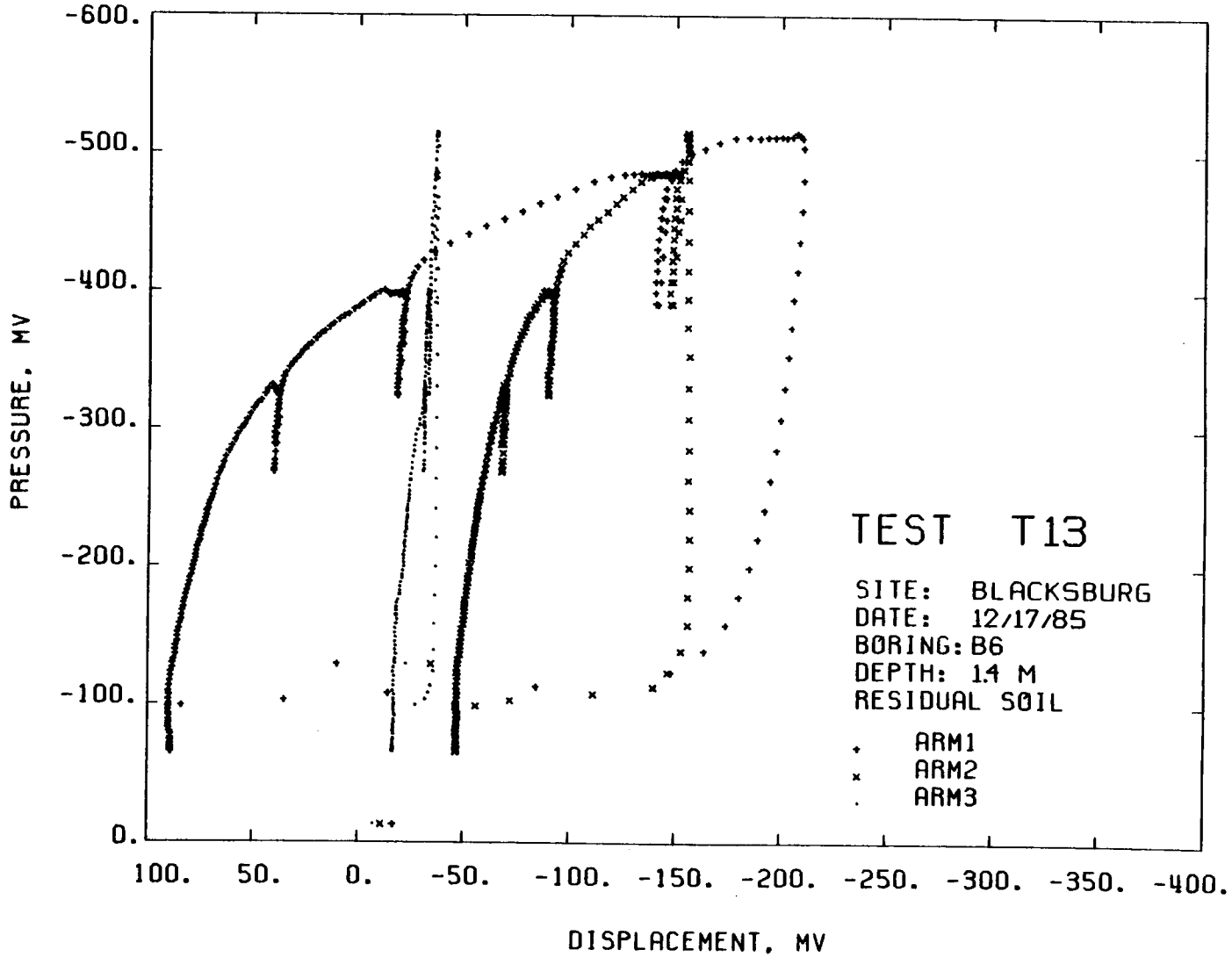
-600.
-500.
-400.
-300.
-200.
-100.
0.
PRESSURE, MV
100.
50.
0.
-50.
-100.
-150.
-200.
-250.
-300.
-350.
-400.
DISPLACEMENT, MV
TEST T13
SITE: BLACKSBURG
DATE: 12/17/85
BORING: B6
DEPTH: 1.4 M
RESIDUAL SOIL
ARM1
ARM2
ARM3

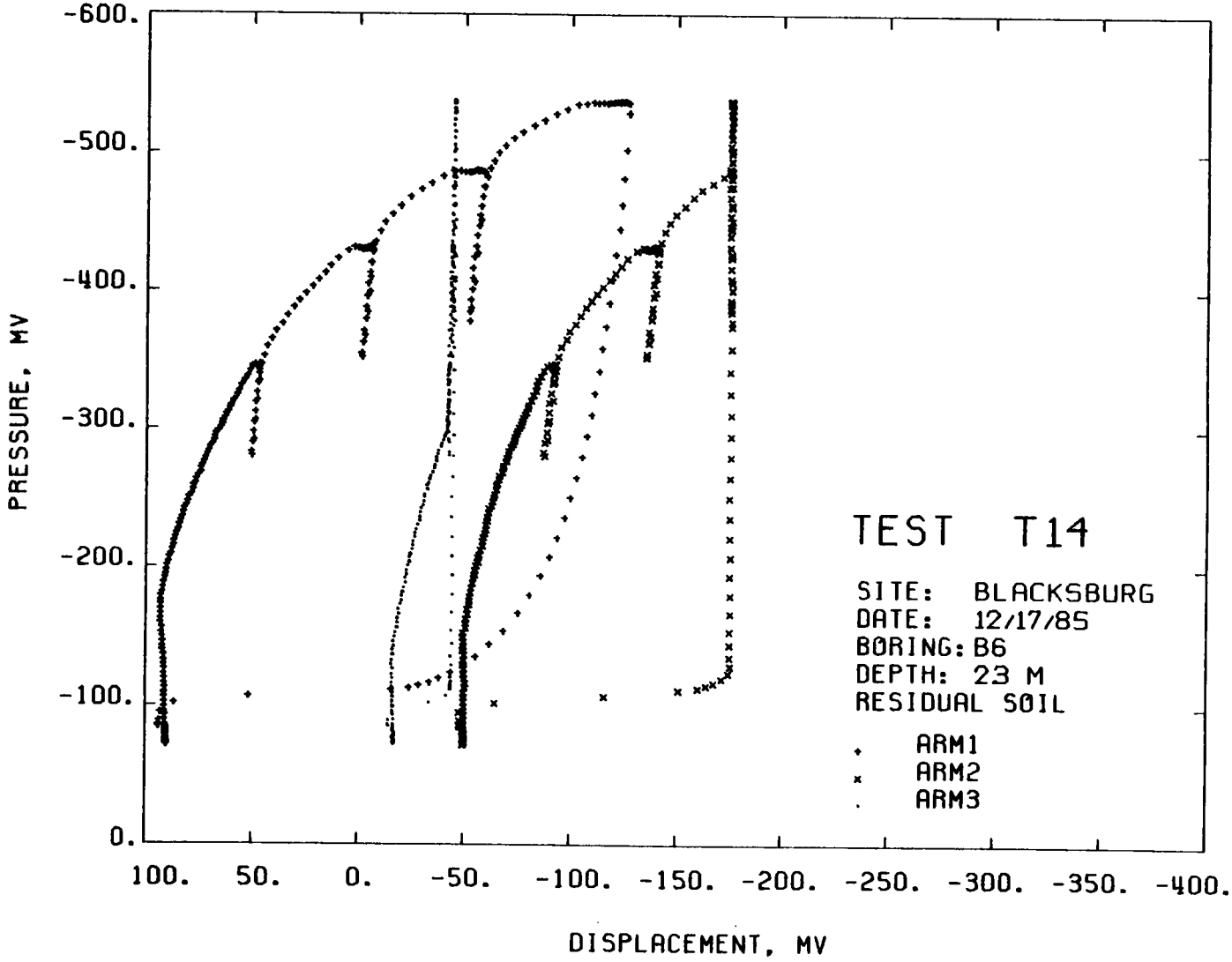
-600.
-500.
-400.
-300.
-200.
-100.
0.
PRESSURE, MV
100.
50.
0.
-50.
-100.
-150.
-200.
-250.
-300.
-350.
-400.
DISPLACEMENT, MV
TEST T14
SITE: BLACKSBURG
DATE: 12/17/85
BORING: B6
DEPTH: 23 M
RESIDUAL SOIL
ARM1
ARM2
ARM3

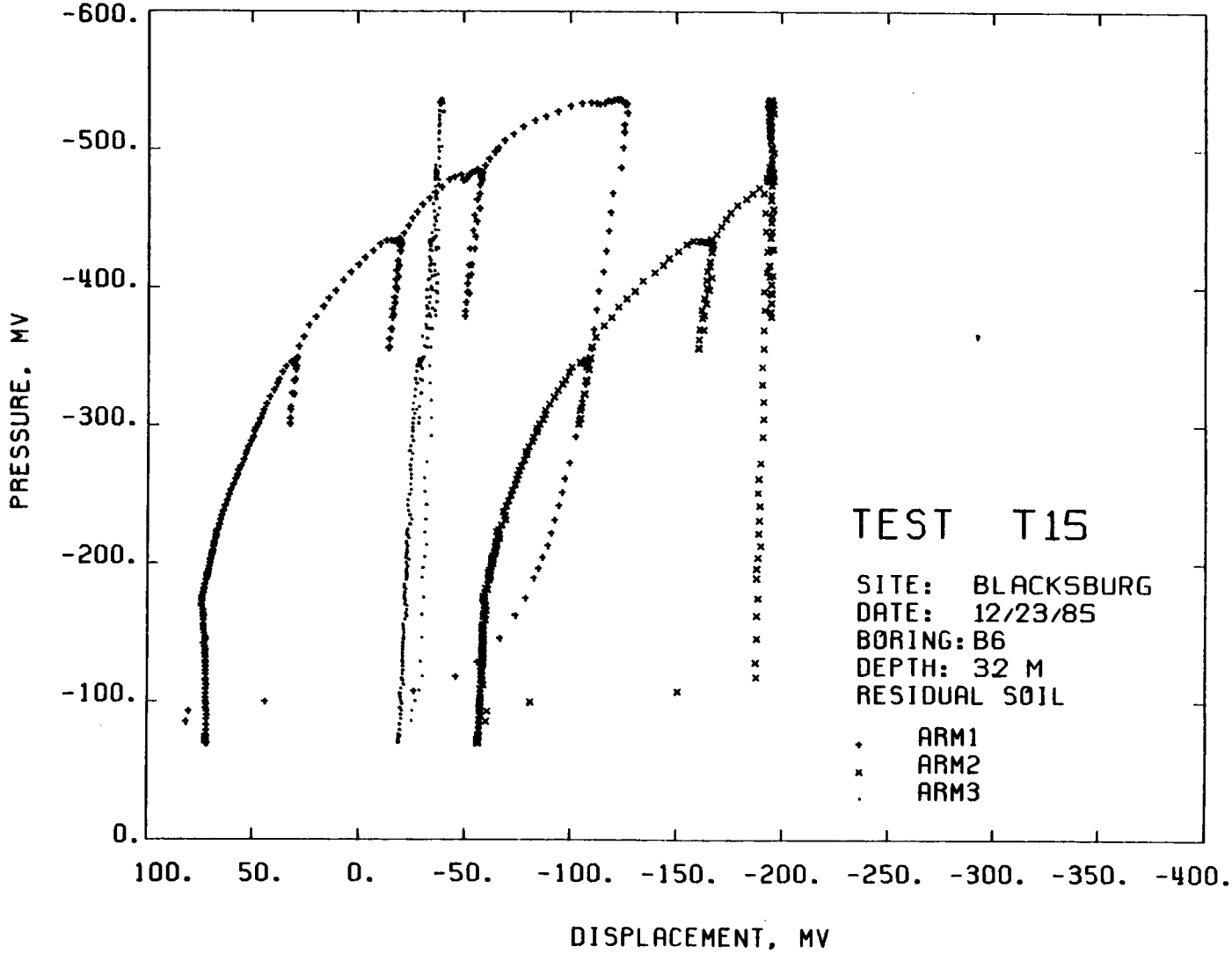
-600.
-500.
-400.
-300.
-200.
-100.
0.
PRESSURE, MV
100.
50.
0.
-50.
-100.
-150.
-200.
-250.
-300.
-350.
-400.
DISPLACEMENT, MV
TEST T15
SITE: BLACKSBURG
DATE: 12/23/85
BORING: B6
DEPTH: 32 M
RESIDUAL SOIL
ARM1
ARM2
ARM3

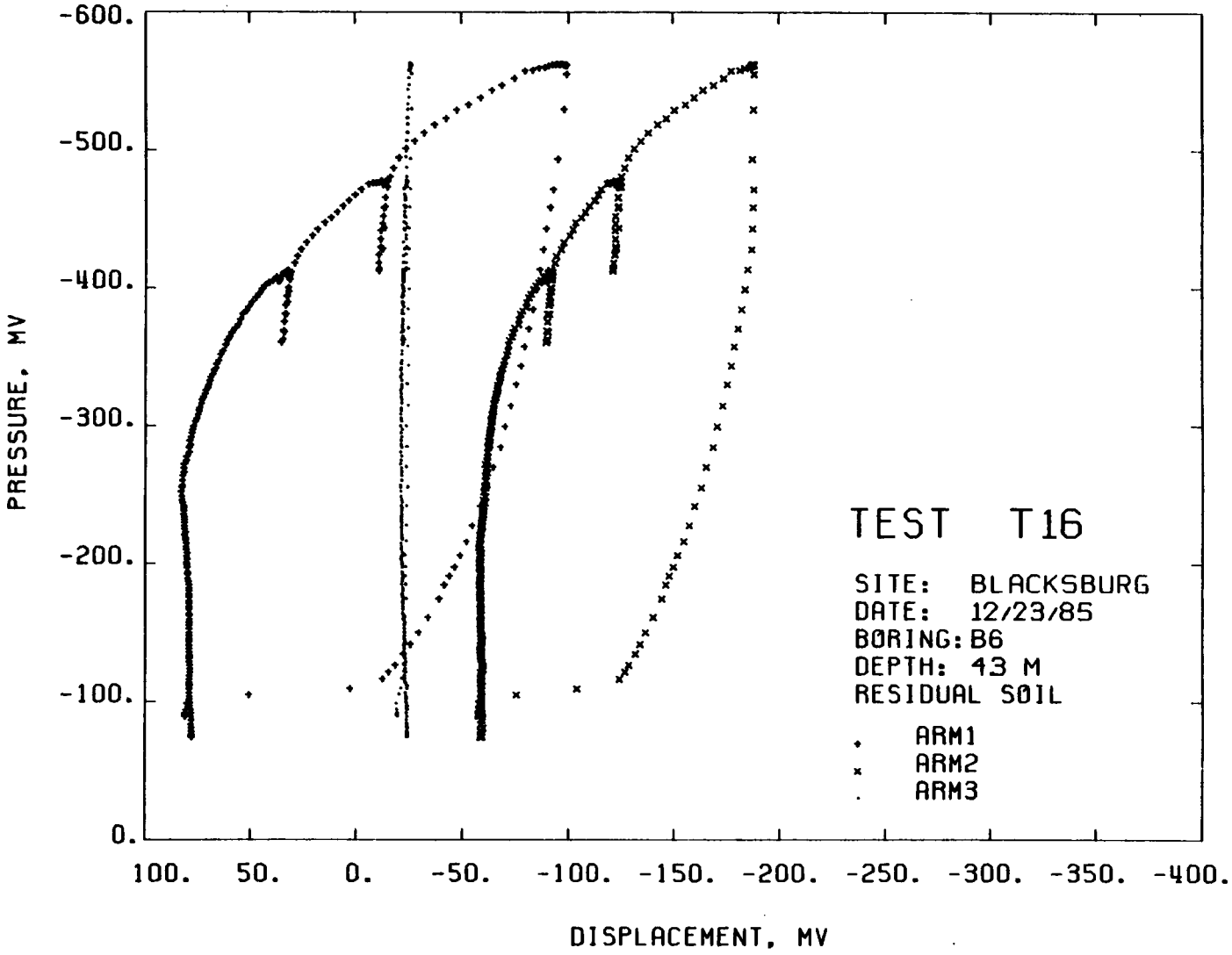
-600.
-500.
-400.
-300.
-200.
-100.
0.
PRESSURE, MV
100.
50.
0.
-50.
-100.
-150.
-200.
-250.
-300.
-350.
-400.
DISPLACEMENT, MV
TEST T16
SITE: BLACKSBURG
DATE: 12/23/85
BORING: B6
DEPTH: 43 M
RESIDUAL SOIL
ARM1
ARM2
ARM3

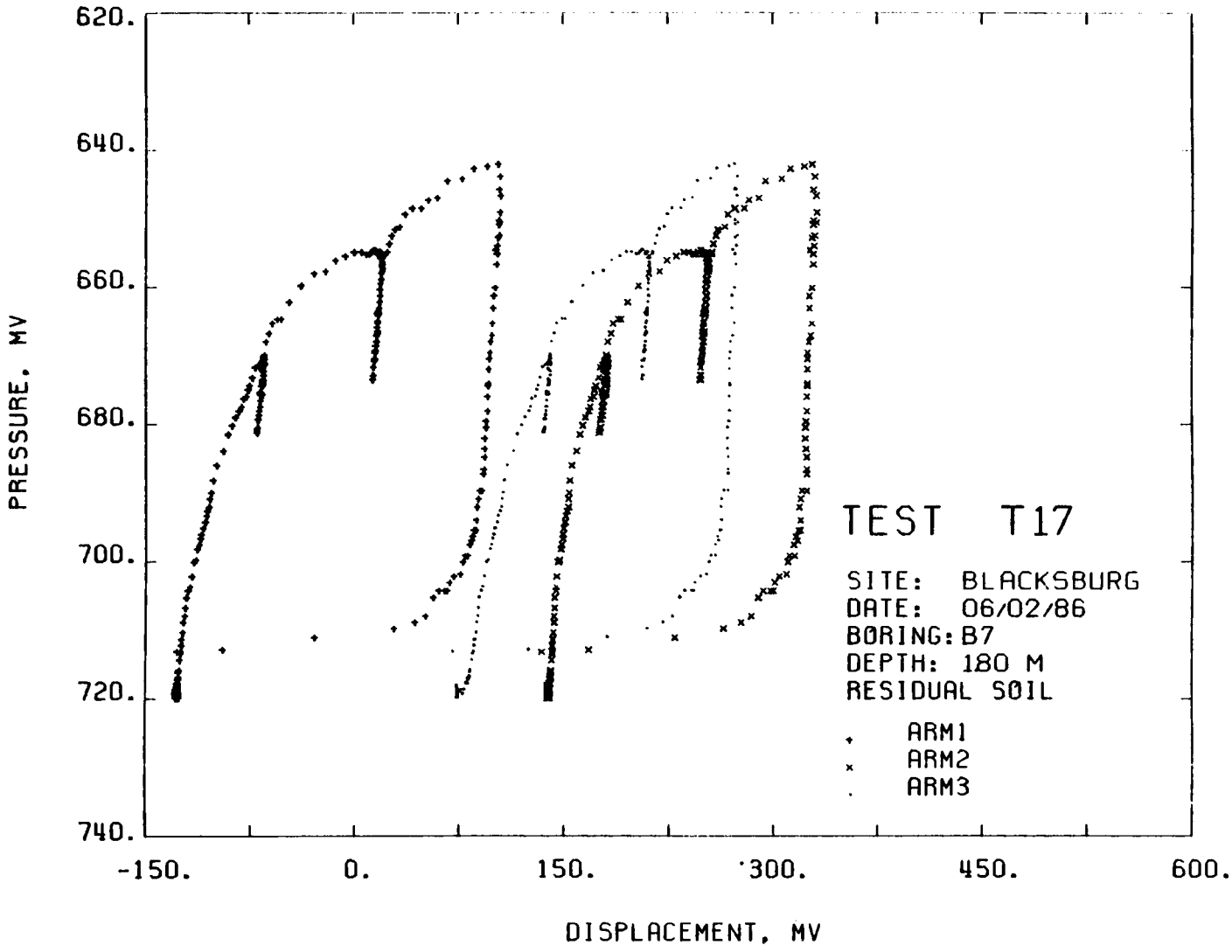
620.
640.
660.
680.
700.
720.
740.
PRESSURE, MV
-150.
0.
150.
300.
450.
600.
DISPLACEMENT, MV
TEST T17
SITE: BLACKSBURG
DATE: 06/02/86
BORING: B7
DEPTH: 180 M
RESIDUAL SOIL
ARM1
ARM2
ARM3

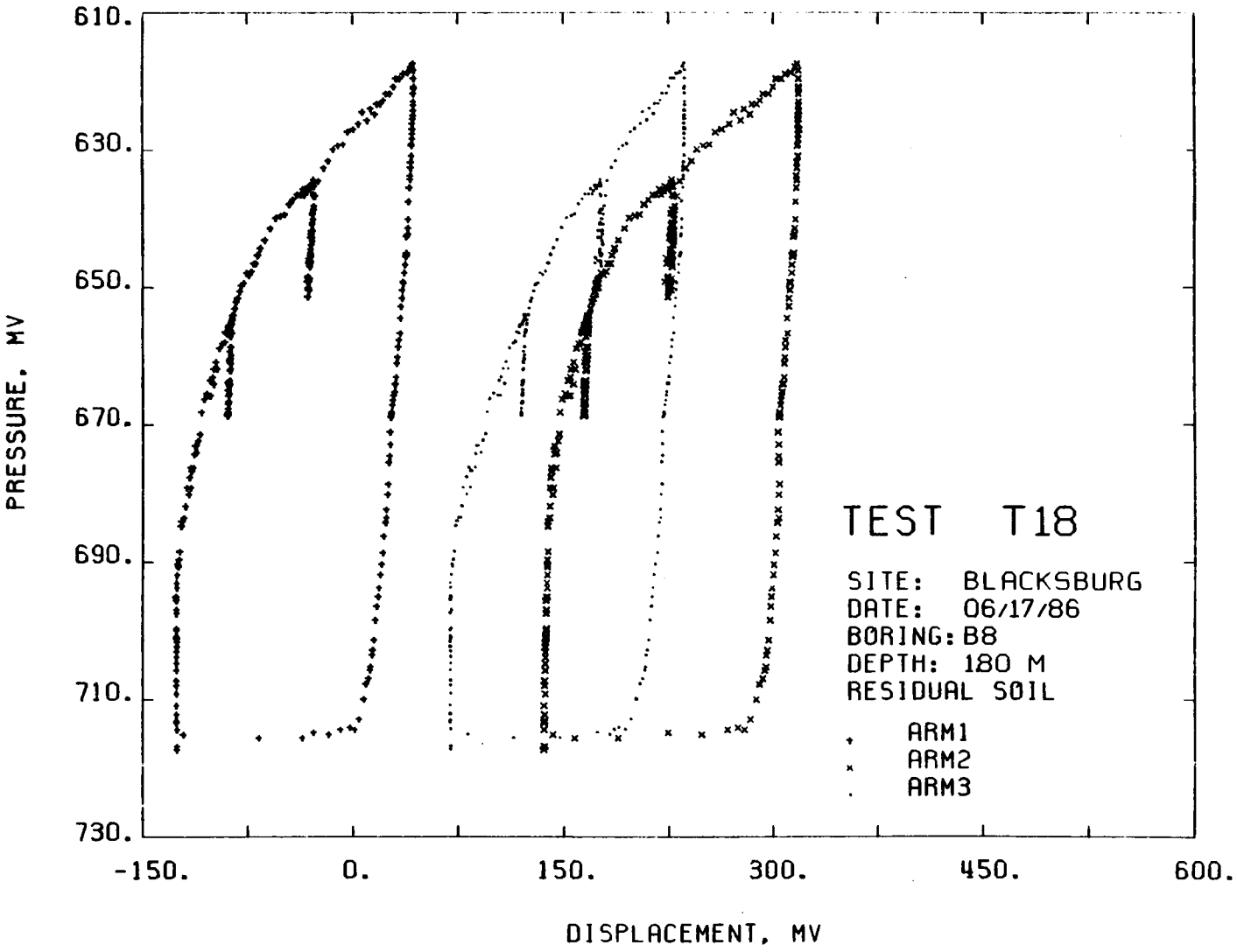
610.
630.
650.
670.
690.
710.
730.
PRESSURE, MV
-150.
0.
150.
300.
450.
600.
DISPLACEMENT, MV
TEST T18
SITE: BLACKSBURG
DATE: 06/17/86
BORING: B8
DEPTH: 180 M
RESIDUAL SOIL
ARM1
ARM2
ARM3

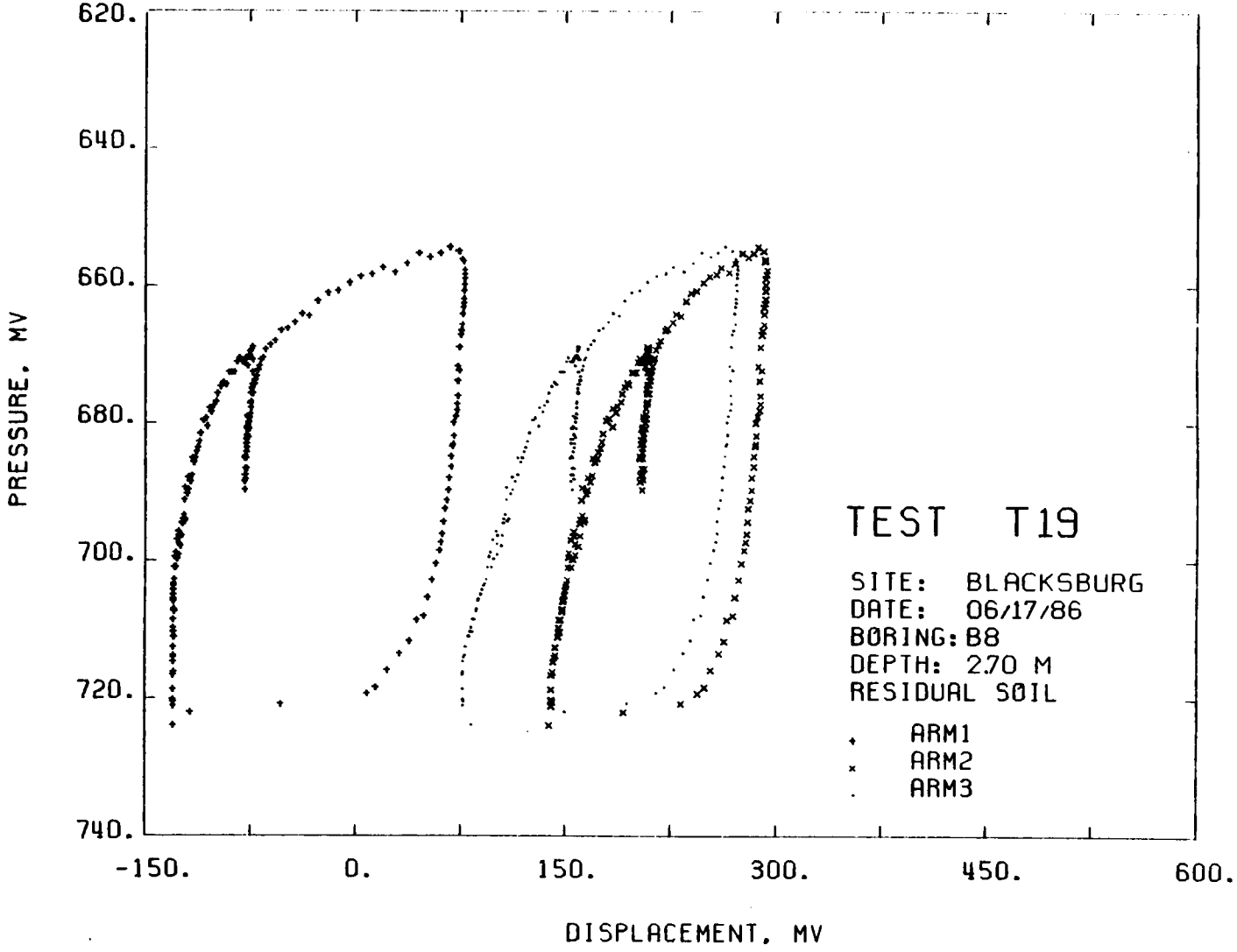
620.
640.
660.
680.
700.
720.
740.
PRESSURE, MV
-150.
0.
150.
300.
450.
600.
DISPLACEMENT, MV
TEST T19
SITE: BLACKSBURG
DATE: 06/17/86
BORING: B8
DEPTH: 2.70 M
RESIDUAL SOIL
ARM1
ARM2
ARM3

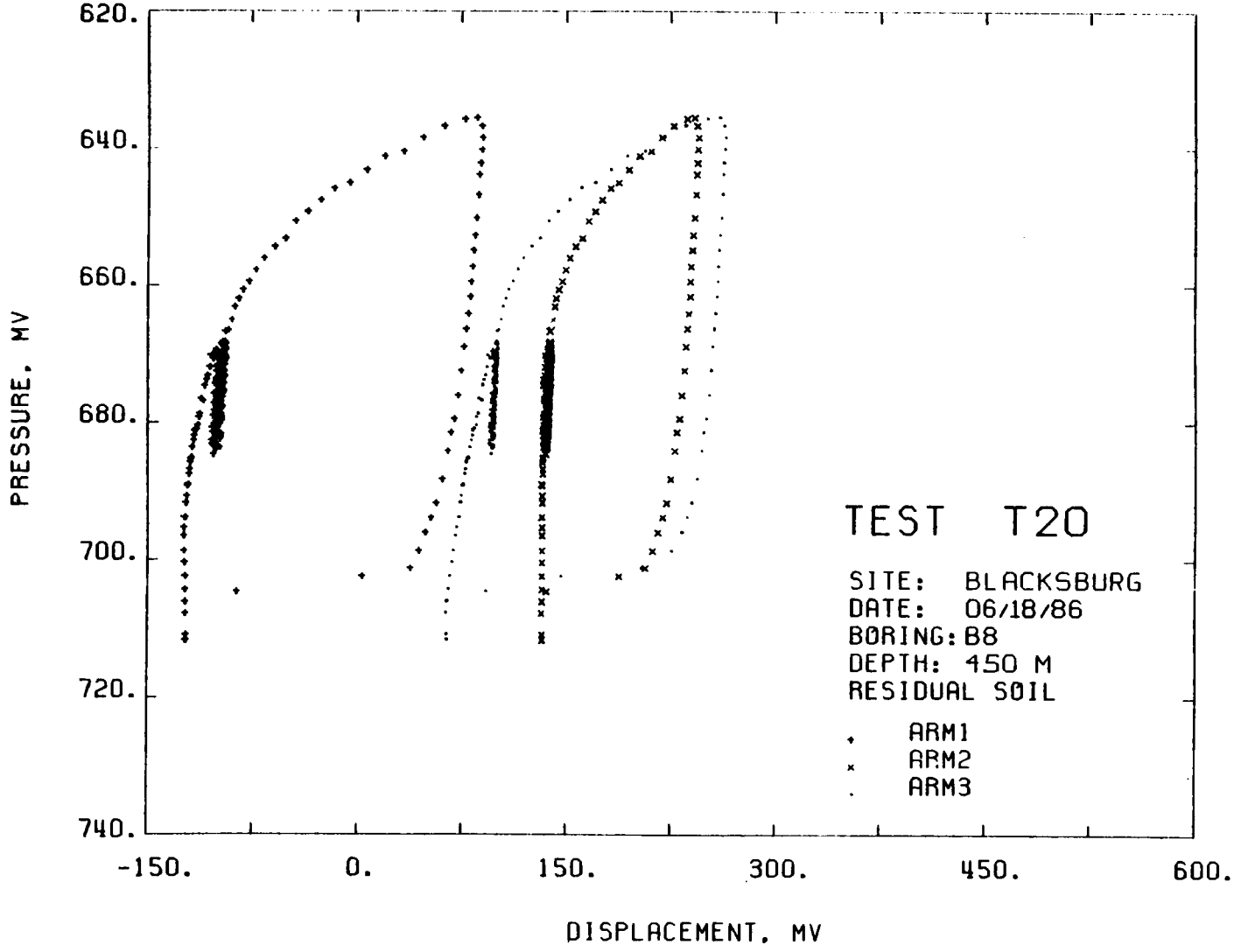
620.
640.
660.
680.
700.
720.
740.
PRESSURE, MV
-150.
0.
150.
300.
450.
600.
DISPLACEMENT, MV
TEST T20
SITE: BLACKSBURG
DATE: 06/18/86
BORING: B8
DEPTH: 450 M
RESIDUAL SOIL
ARM1
ARM2
ARM3

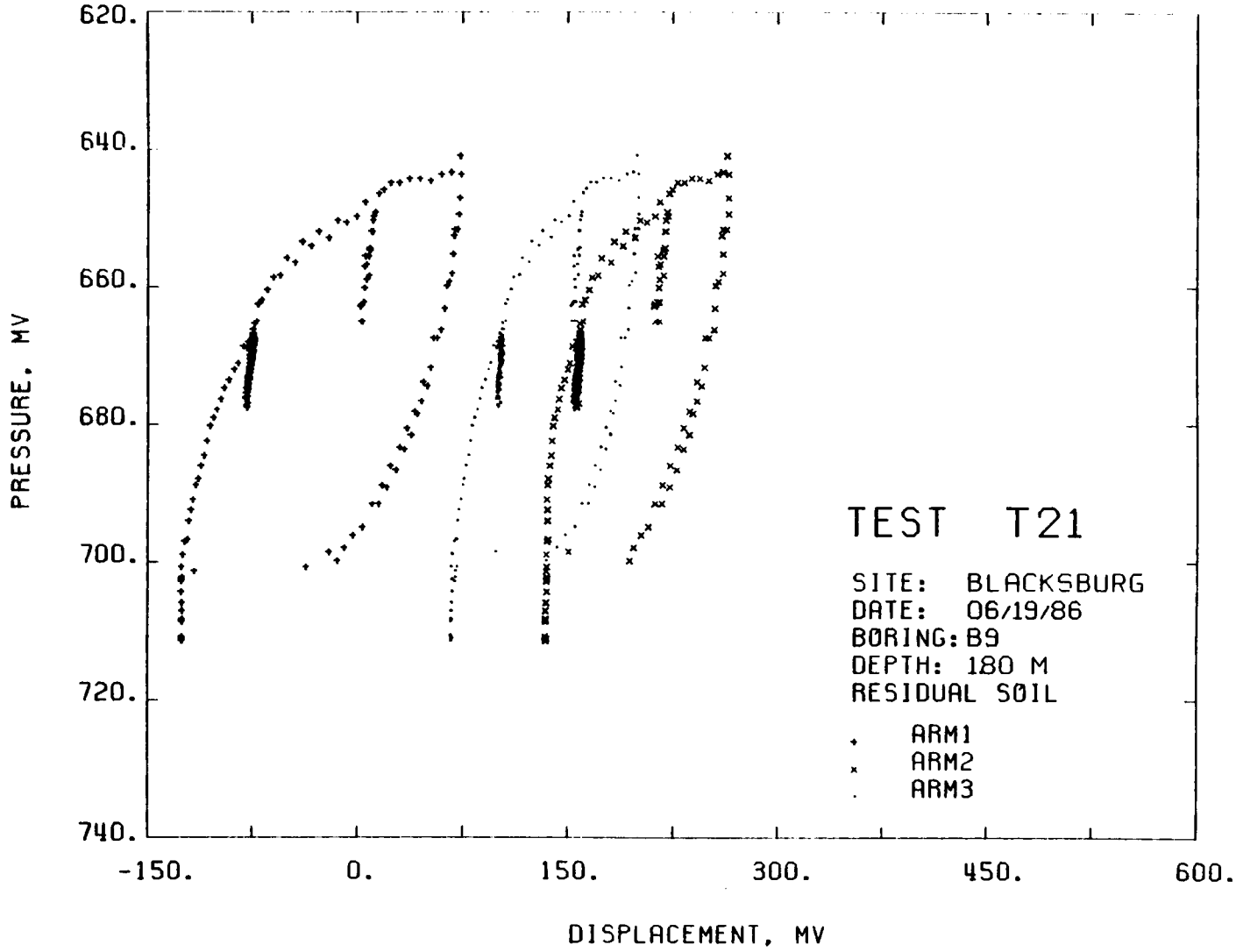
620.
640.
660.
680.
700.
720.
740.
PRESSURE, MV
-150.
0.
150.
300.
450.
600.
DISPLACEMENT, MV
TEST T21
SITE: BLACKSBURG
DATE: 06/19/86
BORING: B9
DEPTH: 180 M
RESIDUAL SOIL
ARM1
ARM2
ARM3

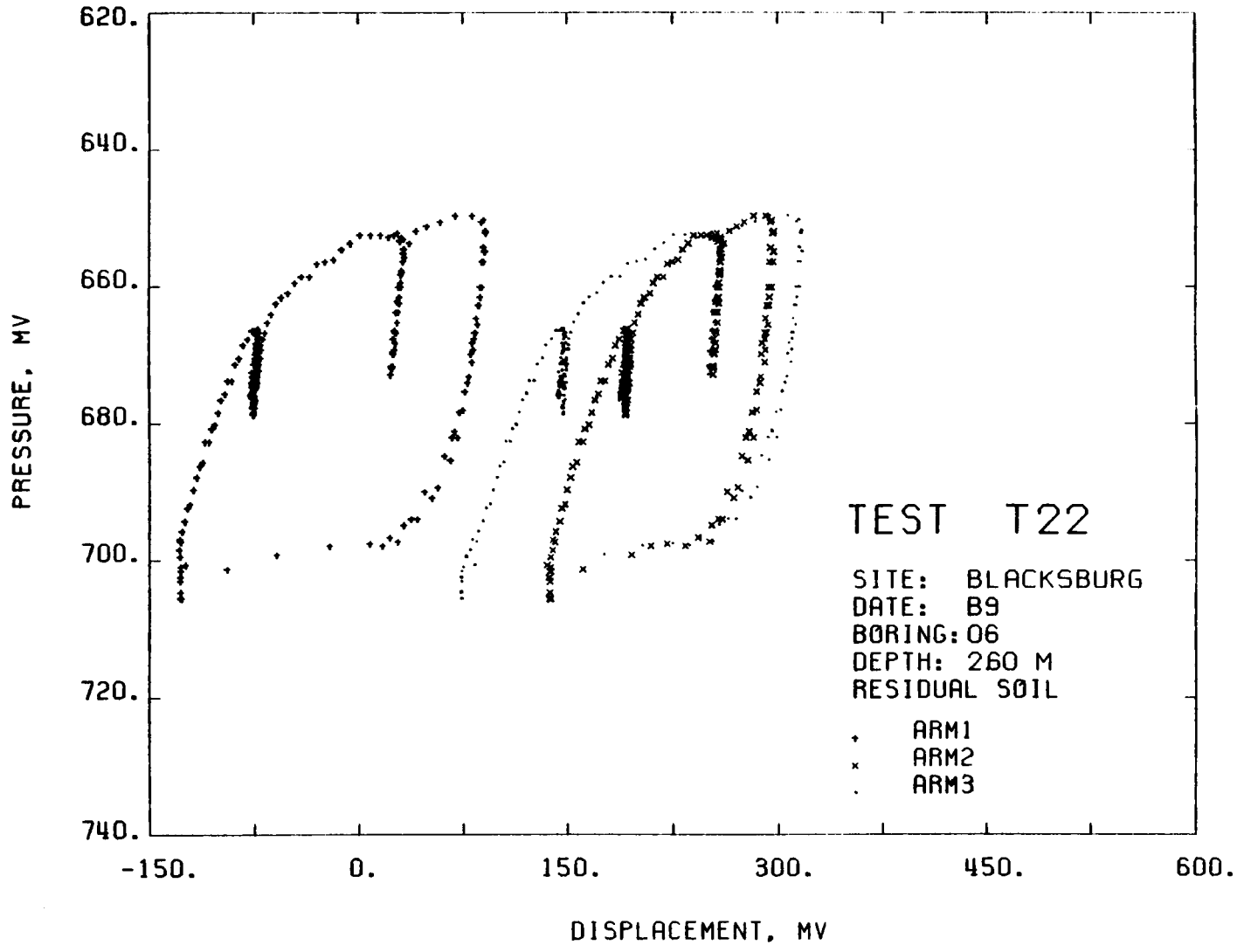
620.
640.
660.
680.
700.
720.
740.
PRESSURE, MV
-150.
0.
150.
300.
450.
600.
DISPLACEMENT, MV
TEST T22
SITE: BLACKSBURG
DATE: B9
BORING: 06
DEPTH: 260 M
RESIDUAL SOIL
ARM1
ARM2
ARM3

REFERENCES

Baguelin, F., Jezequel, J. F., Le Mee, E., and Le Mehaute, A., "Expansion of Cylindrical Probes in Cohesive Soils," Journal of the Soil Mechanics and Foundation Engineering Division, ASCE, Vol. 98, No. SM11, 1972, pp.1129-1142.

Barksdale, R. D., Ferry, C. T., and Lawrence, J. D., "Residual Soil Settlement from Pressuremeter Moduli," Use of In Situ Tests in Geotechnical Engineering, In Situ 86, ASCE Geotechnical Special Publication No. 6, Blacksburg 1986.

Benoit, J., "Analysis of Self-Boring Pressuremeter Tests in Soft Clay," A Dissertation Submitted to the Department of Civil Engineering and the Committee on Graduate Studies of Stanford University in Partial Fulfillement of the Requirements of the Degree of Doctor of Philosophy, 1983.

Benoit, J., and Clough, G. W., "Principal Stresses Derived from the Self-Boring Pressuremeter Tests in Soft Clays," The Pressuremeter and its Marine Applications, 2nd International Symposium, 1985.

Benoit, J., and Clough, G. W.,"Self-Boring Pressuremeter Tests in Soft Clays," Journal of Geotechnical Engineering, ASCE, Vol. 112, No. 1, 1986.

Bishop, A. W., and Henkel, D. J., "The Measurement of Soil Properties in the Triaxial Test," Edward Arnold Publishers Ltd, London, Second Edition, 1962.

Bishop, A. W., Webb, D. L., and Lewin, P. I., "Undisturbed Samples of London Clay from the Ashford Common Shaft: Strength-Effective Stress Relationship," Geotechnique, Vol. 15, No. 1, 1965, pp. 1-31.

Brooker, E. W., and Ireland, H. O., "Earth Pressures at Rest Related to Stress History," Canadian Geotechnical Journal, Vol. II, Number 1, February 1965, pp. 1-15.

Bruzzi, D., Ghionna, V., Jamiolkowski M., Lancellotta, R., and Manfredini, G., "Self-Boring Pressuremeter in Po River Sand," 2nd International Symposium on The Pressuremeter and its Marine Applications, 1986.

Casagrande, A., "The Determination of the Preconsolidation Load and its Practical Significance," Proceedings of the 1st International Conference on Soil Mechanics, Cambridge, Mass., 1936, 3, pp. 60-64. Casagrande, L., "Subsoils and Foundation Design in Richmond, Virginia," Journal of Soil Mechanics and Foundation Engineering Division, ASCE, SM5, September 1966, pp. 109-126.

Clarke, B. G., Carter, J. P., and Wroth, C. P., "In Situ Determination of Consolidation Characteristics of Saturated Clays," Design Parameters in Geotechnical Engineering, VII ECSMFE, Brighton, Vol. 2, 1979, pp. 207-211.

Clarke, B. G., "In Situ Testing of Clay Using Cambridge Self-Boring Pressuremeter," PhD Thesis, Cambridge University, 1981.

Clough, G. W., and Silver, M. L., Eds., Proceedings, "Workshop on Research Needs in Experimental Geotechnical Engineering," Virginia Polytechnic Institute and State University, April, 1984.

Crawford, C. B., and Eden, W. J., "A Comparision of Laboratory Results with In Situ Properties of Leda Clay," Proc. 6th Int. Conf. Soil Mech. Found. Eng., 1, 1965, pp. 31-35.

Dalton, J. C. P., and Hawkins, P. G., "Some Measurements of the In Situ Stress in a Meadow in the Cambridgeshire Countryside," Ground Engineering, Vol.15, No. 4, May 1982.

Denby, G. M., "Self-Boring Pressuremeter in the San Francisco Bay Mud," A Dissertation Submitted to the Department of Civil Engineering and the Committee on Graduate Studies of Stanford University in Partial Fulfillment of the Requirements for the Degree of Doctor of Philosophy, 1978.

Denby, G. M., Costa, C. A., Clough, G. W., and Davidson R. R., "Laboratory and Pressuremeter Tests in Stiff Clay," Proceedings of the Tenth International Conference on Soil Mechanics and Foundation Engineering, Stockholm, Sweden, 1981.

Deere, D. U., and Patton, F. D., "Slope Stability in Residual Soils," Proceedings of the Fourth Panamerican Conference on Soil Mechanics and Foundation Eng., Vol. I, 1971, pp. 87-170.

Duncan, J. M., and Dunlop, P., "Slope in Stiff-Fissured Clays and Shales," Journal of the Soil Mechanics and Foundation Division, Vol. 95, No. SM2, Mars 1969.

Eden, W. J., and Law, K. T., "Comparison of Undrained Shear Strength Results Obtained by Different Test Methods in Soft Clays," Canadian Geotechnical Journal, Vol. 17, 1980.

Ghionna, V., Jamiolkowski, M., Lacasse, S., Ladd, C. C., Lancellotta, R., and Lunne, T., "Evaluation of Self-Boring Pressuremeter," Symposium International, Vol. 2, Paris, 1983.

Ghionna, V. N., Jamiolkowski, M., and Lancellotta, R., "Characteristics of Saturated Clays as Obtained from SBP tests," Technical University of Turin (Politechnico), Italy.

Gibson, R. E., and Anderson, W. F., "In Situ Measurement of Soil Properties with the Pressuremeter," Civil Engineering Works Review, Vol. 56, May 1961, pp. 615-618.

Henkel, D. J., "The Effect of Overconsolidation on the Behaviour of Clays During Shear," Geotechnique, Vol. 6, 1956, pp. 139-150.

Henkel, D. J., "The Shear Strength of Saturated Remoulded Clays," Proceedings, ASCE Specialty Conference on Shear Strength of Cohesive Soils, University of Boulder, Colorado, June 13-17, 1960, pp. 533-554.

Hughes, J. M. O., Wroth, C. P., and Windle, D., "Pressuremeter Tests in Sands," Geotechnique, No. 4, 1977, pp. 455-477.

Jezequel, J. F., Le Mehaute, A., and Le Mee, E., "Etude du Developpement et de la Dissipation des Surpressions Intersticielles Creees dans les Sols Naturels par l'Expansion des Sondes Pressiometriques ," 1970.

Johnson, G. W., "Use of Self-Boring Pressuremeter in Obtaining In Situ Shear Moduli of Clays," Geotechnical Engineering Thesis GT82-1, Geotechnical Eng. Center, Civil Engineering Department, The University of Texas at Austin, Austin, Texas, 1982.

Jamiolkowski, M., and Lancellotta, R., "Remarks on the Use of Self-Boring Pressuremeter in Three Italian Clays," Rivista Italiana di Geotechnica, Organo dell'Associazione Geotechnica Italiana, Anno XI-N. 3 - Luglio-Settembre 1977.

Lacasse, S., and Lunne T., "In Situ Horizontal Stress from Pressuremeter Tests," Proc. of the Symp. on the Pressuremeter and its Marine Applications, Paris 1982.

Ladanyi, B., "Expansion of a Cavity in a Saturated Clay Medium," Journal of the Soil Mechanics and Foundation Engineering Division, ASCE, Vol. 89, No. SM4, Proc. Paper 3577, July 1973, pp. 127-161.

Law, K. T., and Eden, W. J., "Influence of the cutting shoe size in Self-Boring Pressuremeter Tests in Sensitive Clays," Canadian Geotechnical Journal, Vol. 17, 1980.

Ladd, C. C., and Foott, R., "New Design Procedure for Stability of Soft Clays," Journal of the Soil Mechanics and Foundation Division, ASCE, Vol. 100, No. GT7., July 1974, pp. 763-785.

Ladd, C. C., Foott, R., Ishihara, K., Schlosser, F., and Poulos, H. G., "Stress-Deformation and Strength Characteristics," Proceedings of the Ninth ICSMFE, Vol. 2, Tokyo, Japan, 1977, pp. 421-494.

Lo, K. Y., "The Operational Strength of Fissured Clays," Geotechnique, Vol. XX, Number 1, March 1970, pp. 57-74.

Lo, K. Y., and Morin, J. P., "Strength Anisotropy and Time Effects of Two Sensitive Clays," Canadian Geotechnical Journal, Vol. 9(3), 1972, pp. 261-277.

Mahar, L. J., and O'Neill, M. W., "Geotechnical Characterization of Dessicated Clays," Journal of Geotechnical Engineering Division, ASCE, Jan. 1983.

Marsland, A., and Randolph, M. F., "Comparisons of the Results from Pressuremeter Tests and Large In Situ Plate Tests in London Clay," Geotechnique 27, 1977.

Martin, R. E., and De Stephen, R. A., "Large Diameter Double Underreamed Drill Shafts," Journal of Geotechnical Engineering, ASCE, Vol. 109, No. 8, Aug. 1983, pp. 1082-1098.

Martin, R. E., and Drahos, E. G., "Pressuremeter Correlations for Preconsolidated Clay," Proceedings of In Situ 86, a Specialty Conference Sponsored by the Geotechnical Engineering Division of the American Society of Civil Engineers, June 23-25, 1986, pp. 206-220.

Menard, L., "An Apparatus for Measuring the Strength of Soils in Place," MSc Thesis, University of Illinois, 1957.

Palmer, A. C., "Undrained Plane Strain Expansion of a Cylindrical Cavity in Clay: A Simple Interpretation of the Pressuremeter Test," Geotechnique, Vol. 22, No. 3, 1972, pp. 451-457.

Parry, R. H. G., "Triaxial Compression and Extension Tests on Remolded Saturated Clay," Geotechnique, London, England, Vol. 10, No. 4, 1960, pp. 166-180.

Prevost, J. H., and Hoeg, K., "Analysis of Pressuremeter in Strain- Softening Soil," Journal of the Geotechnical Engineering Division, Proceedings of the ASCE, Vol. 101, No. GT8, August 1975, pp. 717-732.

Robertson, P. K., and Hughes, J. M. O., "Determination of Properties of Sand from Self-Boring Pressuremeter Tests," The Pressuremeter and Its Marine Applications, Second International Symposium, 1985.

Rowe, P. W., "The Stress Dilatancy Relation for Static Equilibrium of an Assembly of Particles in Contact," Proceedings of the Royal Society , Vol. 269, Series A, 1962, pp. 500-527.

Schmertmann, J. H., "Estimating the True Consolidation Behavior of Clay from Laboratory Test Results," Proc. ASCE 79, Separate 311, 1953.

Schmertmann, J. H., "The Undisturbed Consolidation Behavior of Clay," Trans. ASCE, 120, 1955, pp. 1201-1227.

Simpson, B., Calabresi, G., Sommer, H., and Wallays, M., "Design Parameters for Stiff Clays," Proceedings of the Seventh European Conference on Soil Mechanics and Foundation Engineering, Brighton, 1979, Vol. 5, pp. 91-125.

Skempton, A. W., "Notes on Compressibility of Clays," Quart. J. Geol. Soc., London, 1944, C, pp. 119-135.

Skempton, A. W., "Horizontal Stresses in an Overconsolidated Eocene Clay," Proc. Fifth Int. Conf. Soil Mech. and Found. Eng., Paris, 1, 1961, pp. 351-357.

Skempton, A. W., "Slope Stability of Cuttings in Brown London Clay," Proc. ninth Int. Conf. on Soil Mech. and Found. Eng., Vol. 3, Tokyo, Japan, 1977, pp. 261-270.

Smith, R. E., and Wahls, H. E., "Consolidation Under Constant Rates of Strain," Journal of Soil Mechanics and Foundation Engineering Division, ASCE, SM2, March 1969, pp. 519-539.

Sowers, G. F., "Engineering Properties of Residual Soils Derivated From Igneous and Metamorphic Rocks," Proceedings, 2nd Pan American Congres on Soil Mechanics and Foundation Eng., Brazil, 1963.

Sowers, G. F., and Richardson, T. L., "Residual Soils of the Piedmont and Blue Ridge," Transportation Research Board, Research Record No. 919, 1983, pp. 10-16.

Stroud, M. A., "Sand at Low Stress Levels in the Simple Shear Apparatus," PhD Thesis, University of Cambridge, 1971.

Sylvestri, V., Yong, R. N., Soulie, M., and Gabriel, F., "Controlled- Strain, Controlled Gradient, and Standard Consolidation Testing in Sensitive Clays," Consolidation in Soils: Testing and Evaluation, Ft Lauderdale, 1985, pp. 433-450.

Tavenas, F., and Leroueil, S., "Effets du Temps et des Contraintes sur l'Etat Limite des Argiles," Proceedings of the Ninth International Conference on Soil Mechanics and Foundation Engineering, Tokyo, Japan, Vol. 1, 1977, pp. 319-326.

Taylor, D. W., "Review of Research on Shearing Strength of Clay, 1948-1953," Report to Waterways Experimental Station, Soil Mechanics Laboratory, Massachussetts Institute of Technology, Cambridge, Mass., 1955.

Terzaghi, K., and Peck, R. B., "Soil Mechanics in Engineering Practice," John Wiley and Sons, Second Edition, 1967.

Timoshenko, S. P., and Goodier, J. N., "Theory of Elasticity," Mac Graw-Hill Book Company, 3d Edition, 1970.

Windle, D., and Wroth, C. P., "The Use of a Self-Boring Pressuremeter to Determine the Undrained Properties of Clays," Ground Engineering, September 1977.

Windle, D., "In Situ Testing of Soils with a Self-Boring Pressuremeter," A Dissertation Submitted for the Degree of Doctor of Philosophy at Cambridge University, 1976.

Windle, D., and Wroth, C. P., "In Situ Measurement of the Properties of Stiff Clays," Proceedings of the Ninth International Conference on Soil Mechanics and Foundation Engineering, Tokyo, Japan, 1977.

Wroth, C. P., "The Interpretation of In Situ Soil Tests," Twenty Fourth Rankine Lecture, Geotechnique 34, No. 4, 1984, pp. 449-489.

Wroth, C. P., "British Experience with the Self-Boring Pressuremeter," Proc. Symp. Pressuremeter and Its Marine Applications, Paris, 1982, pp. 143-164.

Wroth, C. P., "In Situ Measurement of Initial Stresses and Deformation Characteristics," Proceedings of the Conference on In Situ Measurement of Soil Properties, Raleigh, 1975, pp.181-230.

Wroth, C. P., and Hughes, J. M. O., "An Instrument for the In Situ Measurement of the Properties of Soft Clays," Report of Department of Engineering, University of Cambridge, CUED/C, Soils TR13.

Wroth, C. P., and Hughes, J. M. O., "Development of a Special Instrument for the In Situ Measurement of the Strength and Stiffness of Soils," Proceedings of the Conference on Subsurface Exploration for Underground Excavation and Heavy Construction, ASCE, Henniker, N. H., August 11-16 1974, pp. 295-311.

The vita has been removed from the scanned document